ARO
ADVANCES IN RADIOLOGY AND ONCOLOGY

Editors
Tomaž Benulič
Gregor Serša
Viljem Kovač

ADVANCES IN RADIOLOGY AND ONCOLOGY

Editors
Tomaž Benulič
Gregor Serša
Viljem Kovač

ADVANCES IN RADIOLOGY AND ONCOLOGY

Editors

Tomaž Benulič, M. D.
Department of Radiotherapy
Institute of Oncology
Ljubljana, Slovenia

Gregor Serša, Ph. D.
Department of Tumor Biology and Biotherapy
Institute of Oncology
Ljubljana, Slovenia

Viljem Kovač, M. D.
Department of Nuclear Medicine and
Department of Radiotherapy
Institue of Oncology
Ljubljana, Slovenia

Research and review papers
contributed on the 25th anniversary of
publishing Radiologia Iugoslavica.

All rights reserved

Radiologia Iugoslavica, Založka 2,
61000 Ljubljana, Slovenia

Reader of English language
Olga Shrestha

Design
Monika Fink-Serša *dipl. ing. arch.*

UDC and Key words
dr. ***Eva Klemenčić***

Secretary
Milica Harisch, Betka Savski

Printed by
Tipograf, *Rijeka, Croatia*

CIP – katalogizacija v knjigi
Narodna in univerzitetna knjižnica, Ljubljana

615.849(082)
616-006-073.75(082)

ADVANCES in radiology and oncology / (uredniki, editors Tomaž Benulič, Gregor Serša, Viljem Kovač). – Ljubljana : Radiologia Iugoslavica, 1992

1. Benulič, Tomaž 2. Serša, Gregor
28392960

SCIENTIFIC BOARD

Sonja Bebar,
Ljubljana, Slovenia

Tomaž Benulič,
Ljubljana, Slovenia

Matija Bistrović,
Zagreb, Croatia

Erika Brenčič,
Ljubljana, Slovenia

Ivo Drinković,
Zagreb, Croatia

Jure Fettich,
Ljubljana, Slovenia

Đurđa Horvat,
Zagreb, Croatia

Berta Jereb,
Ljubljana, Slovenia

Vladimir Jevtić,
Ljubljana, Slovenia

Viljem Kovač,
Ljubljana, Slovenia

Ivan Lovasić,
Rijeka, Croatia

Miljenko Marotti,
Zagreb, Croatia

Dušan Pavčnik,
Ljubljana, Slovenia

Stojan Plesničar,
Ljubljana, Slovenia

Miran Porenta,
Ljubljana, Slovenia

Gregor Serša,
Ljubljana, Slovenia

Josip Stojanović,
Zagreb, Croatia

Slavko Šimunić,
Zagreb, Croatia

Janez Škrk,
Ljubljana, Slovenia

FOREWORD

The book »Advances in Radiology and Oncology« has been published by the journal »Radiologia Iugoslavica« to celebrate the appearance of the 25th volume.

Since its founding in 1964, the journal has featured scientific papers dealing with X-ray diagnosis, nuclear medicine, radiotherapy, oncology, radiobiology, radiophysics, radiation protection as well as with recently developed fields including interventional radiology, computed tomography, magnetic resonance imaging, ultrasound and experimental oncology. With continuing publication of the results of increasingly comprehensive scope of research conducted at home and abroad, the journal succeeded in keeping abreast with the latest achievements in these branches of medicine.

The fact that the papers published were not restricted to just a few topics or even a single subject, inevitably led to fragmentation of particular topics which were dealt with in several different issues or even entire volumes.

For the sake of consistency, and to give a more comprehensive overview of formerly published materials, we decided on the occasion of the 25th anniversary of the journal to issue a comprehensive book which would combine both topic-related papers and specific thematic fields.

Many authors from Slovenia and abroad responded to our invitation by contributing their papers for this issue.

The book has been created over a longer period of time, during the years when the links between the former Yugoslav republics were beginning to break up. Nevertheless, thanks to the joint efforts of the authors, institutions and sponsoring producers of medical equipment we finally overcame all obstacles to the publication of this book. We trust that it will be greeted with interest by a large reading public.

Despite the rapid progress made in medical technology, it must be admitted that human distress, anxiety and pain related to disease have unfortunately remained unchanged. Nevertheless, a number of modern diagnostic and treatment devices and modalities enable us to help the patient in a faster, much more effective and less painful way that was possible in the past. If in these times of highly developed technology involving complex graphs and figures, we have also succeeded in directing due attention to the patient, the purpose of this book will have been fully justified.

T. Benulič, MD

TABLE OF CONTENTS

Chapter I. INTERVENTIONAL AND DIAGNOSTIC RADIOLOGY

Percutaneous transcatheter placement of the aortic valve
Pavčnik D, Wright K, Wallace S **15**

An injection technique for repositioning subcvlavian catheters
Mahon T, Lawrence D, Sr. **22**

Properties of biodegradable polymers for 5-fluorouracil and tamoxifen microcapsules
Yang DJ, Byun HS, Kuang LR, Yamashita Y, Moult RG, Tansey W, Wright KC, Wallace S **25**

Intravenous trombolysis of acute coronary occlusion after percutaneous transluminal angioplasty
Kranjec I, Cijan A, Pavčnik D **30**

Current diagnostic of pituitary disorders by CT
Lovrenčić M **35**

Chest CT in sarcoidosis
Dalagija F, Dizdarević Z, Bešlić Š **41**

Computed tomography during arterial portography of the liver without interslice gap
Yasumori K, Hasuo K, Baba H, Yoshida K, Mizushima A, Hirakata R, Kuroiwa T, Onitsuka H, Masuda K **47**

CT – guided percutaneous drainages of abdominal abscesses
Lincender L **51**

Computerized tomography of the spine
Papa J **56**

Magnetic resonance imaging of kidney diseases
Marotti M, Hricak H, Kovačević D **60**

Magnetic resonance imaging of hand joints in patients with rheumatoid arthritis, psoriatic arthritis and nondifferentiated seronegative polyarthritis
Jevtić V, Rozman B, Kos-Golja M, Jarh O, Demšar F **66**

Preoperative evaluation of long bone osteosarcomas with magnetic resonance imaging
Poleksić Lj, Zdravković Đ, Atanacković M, Mitrović M, Bačić G **72**

Chapter II. ULTRASONOGRAPHY

Ultrasound diagnostic of the neck: A ROC study
Pichler E, Breyer B, Mihajlović L, Boko H, Kralj Z **81**

Position of nodules in echographically multinodular thyroid in comparison with patohistologic nature of nodules
Brkljačić B, Drinković I, Delić-Brkljačić D, Boko H, Vidjak V **86**

Parameters for echographic evaluation of gallbladder contractions
Mirić S, Sabljak I **90**

The treatment of appendiceal abscess by ultrasonically guided drainage
Drinković I, Brkljačić B, Boko H, Odak D, Vidjak V, Anić P **96**

Ultrasound in diagnostics of muscular injuries
Vidjak V, Drinković I, Brkljačić B, Krmpotić T, Boko H, Odak D **99**

Ultrasound as a diagnostic tool in malignant bone tumours
Babić M, Matovinović D **102**

Chapter III. NUCLEAR MEDICINE

Labelling leucocytes with Tc-99m HMPAO for imaging inflammation
Peters AM **111**

COST B2 – Cooperation in science and technology: A european programme on the quality assurance of nuclear medicine software
Britton KE **116**

New aspects in nuclear cardiology – PET, NMR and SPECT
Henze E, Milčinski M, Lietzenmayer R, Clausen M **123**

Reflections on immunoscintigraphy and radioimmunotherapy
Roos JC, van Lingen A, Teule GJJ **135**

Interlaboratory comparison study on quality performance of nuclear medicine imaging devices
Karanfilski B **142**

Chapter IV. CLINICAL ONCOLOGY

Radiosurgery: A review of clinical aspects
Souhami L, Podgoršak EB **151**

Medulloblastoma, results of treatment at the Institute of Oncology, Ljubljana
Petrič-Grabnar G, Župančić N, Klun B, Umek B, Stare J, Kopač Š, Kragelj B, Cindro L, Škrbec M, Jereb B **167**

Intrapleural application of human leukocyte interferon (IFN-α) in breast cancer patients with pleural carcinosis
Jereb B, Štabuc B, Us-Krašovec M, Cerar O, Stare J 175

Soft tissue sarcomas in childhood. Experience of the Austrian cooperative rhabdomyosarcoma study (A-RMS 82). A final report
Ladenstein R, Grümayer ER, Hawliczek R, Krepler R, Fink FM, Haas H, Mutz I, Ploier R, Stölinger O, Thun-Hohenstein L, Tulzer W, Urban C, Gadner H 181

Our experience in treating children with osteogenic sarcoma
Benedik-Dolničar M 196

Recent strategies in the treatment of malignant germ cell tumour
Clemm Ch 202

Thyroid status following irradiation for laryngeal cancer
Dimitrovska A, Karanfilski B, Georgieva B, Velkov K, Jovanovski D, Nikolova L 208

Tumour markers in clinical oncology
Novaković S, Serša G 214

The predictive significance of CA 15-3 for the first relapse in early breast cancer patients
Nešković-Konstantinović Z, Vuletić L, Tasić S, Ogrizović N, Šušnjar S 221

Chapter V. EXPERIMENTAL ONCOLOGY

Prostaglandins in malignant tumours: Role in tumour growth and therapy
Milas L 229

Problems in tumour cell repopulation during irradiation treatment of squamous cell carcinoma of head and neck
Budihna M, Škrk J 236

Dipyridamole enhances the cytotoxicity of drugs and radiation in HeLa and V-79 cells *in vitro*
Ban J, Sorić J, Bistrović M, Dujmović I, Miletić Z 241

Stress, tumour metastasis and antitumour chemotherapy in mice
Giraldi T, Perissin L, Rapozzi V, Zorzet S 249

Combining photodynamic therapy with immunotherapy: Will it work?
Krošl G, Korbelik M 261

Role of DNA flow cytometry and cytomorphology in the search of effective chemotherapy for chemoresistant tumours (Renal cell carcinoma)
Auersperg M, Us-Krašovec M, Stanovnik M, Čufer T, Bešić N, Goehde W 268

Flow-cytometric DNA ploidy and clinicopathologic variables in primary breast carcinoma
Us-Krašovec M, Bračko M, Ćufer T, Goehde W, Košmelj K, Lamovec J, Pogačnik A **275**

Correlation of DNA-ploidy and estrogene and progesterone receptor content in primary breast cancer
Ćufer T, Bračko M, Goehde W, Lamovec J, Košmelj K, Pogačnik A, Us-Krašovec M **280**

Potentials of hyperthermia in clinical use
Lešničar H, Budihna M **284**

Chapter VI. RADIOPHYSICS

Radiosurgery: A review of physical aspects
Podgoršak EB, Souhami L **301**

A survey of radiation biophysics for the radiotherapist
Bistrović M **311**

A practical method of TBI *in vivo* dosimetry based on real scatter contributions
Vrtar M **323**

Subtotal-skin electron irradiation of the torso
Umek B, Habič M, Jereb B, Štabuc B **330**

Scanning slit radiography apparatus with a radiographic grid
Miklavčič L **335**

Chapter VII. RADIATION PROTECTION

Incidence of structural chromosome aberrations in medical staff occupationally exposed to ionizing radiation
Horvat Đ **343**

The effect of ionizing radiation on the peripheral blood flow of occupationally exposed medical personnel
Brumen V, Bonić I **348**

Biological effects of microwave radiation
Garaj-Vrhovac V **356**

Chapter I.
INTERVENTIONAL AND DIAGNOSTIC RADIOLOGY

Adv Radiol Oncol 1992; 15–21.

Percutaneous transcatheter placement of the aortic valve

Pavčnik D, Wright K and Wallace S

From the John S. Dunn Research Foundation Center for Radiological Sciences, University of Texas, M.D. Anderson Cancer Center and from the Institute Diagnostic and Interventional Radiology, University Medical Center, the University of Ljubljana, Slovenia.

Twelve adult mongrel dogs have received prosthetic aortic valves consisting of a ring, cage and ball. All valves were percutaneously placed in the ascending aorta as the first step in the investigation of transcatheter delivered prosthetic aortic valves for the treatment of aortic insufficiency. Results of these studies have led to several design modifications. At present, prosthetic valve is a ball-in-cage design which functions as a simple one-way ball valve. Competency of the valves was tested by injecting contrast media. The ultimate goal of this project is to construct and experimentally evaluate an alternative device which can be placed percutaneously, obviating the need for general anesthesia and open heart surgery. Additional studies are now in progress to evaluate the current design wiht regard to thrombogenicity, hemodinamic function, durability and biocompatibility.

Key words: aortic valve-surgery, heart valve prosthesis, catheterization, percutaneous

Introduction

As a result of trauma, disease, or congenital abnormalities, the valves of the heart may become incompetent and blood can either regurgitate or leak back against the normal direction of the circulation. Prosthetic valves are now manufactured which can be used to replace the natural valves of the heart.

Heart valve replacement began thirty–seven years ago when Hufnagel surgically implanted the first valve prosthesis in the descending aorta.[1] Since then, over twenty different mechanical and biological valves have been developed.[2-4] However, all of the prosthetic cardiac valves used clinically have to be implanted surgically. Our objective in this project is to construct and experimentally (canine model) evaluate an alternative valve which can be placed percutaneously, obviating the need for general anesthesia and open heart surgery.

Correspondence to: Dr. Dušan Pavčnik, M.D. Associate Professor of Radiology Institute for Diagnostic and Interventional of Radiology, University Medical Center, Zaloška 7, 61000 Ljubljana, Slovenia.

Supported in part by a grant from the John S. Dunn Research Foundation and the George A. Cook Memorial Fund.

UDC: 616.126.52-089.28

Materials and methods

Device description

The prosthetic aortic valve for percutaneous insertion includes a cage, a ring and a ball (Figure 1). The cage consists of a Gianturco self-expanding stainless stell stent[5] with barbs and four to six lenghts of flat, flexible stainless steel wire attached at one end to form the top of the cage.

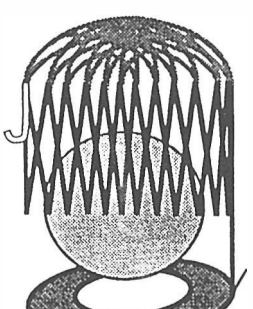

Figure 1. Prosthetic aortic valves – cross section

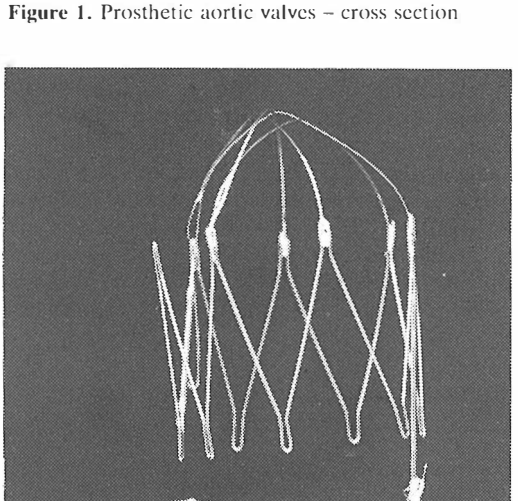

Figure 2. Cage and ring fully expanded after being pushed from a 12-F sheat.

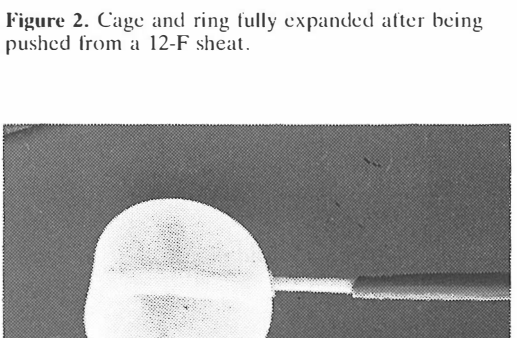

Figure 3. Inflated detachable latey balloon placed at the tip of a 5 French catheter.

The ring is constructed of two stainless steel wires coiled together in a spring like configuration and covered with nylon mesh. Barbs are located at various points around the ring for stabilization following placement. The ring is attached to the cage assembly with a length of stainless steel tubing (Figure 2).

The ball is a detechable latex balloon made out of the front part of 6 or 8 Foley catheters with a 3 cc balloon placed at the tip of a 5–French high–flow catheter. It is filled with liquid silicone rubber[6] after placement in the cage assembly (Figure 2).

For placement in dogs, the valve was made in different sizes. The cage was either 2.8 or 3.0 cm. in diameter, the outside diameter of the ring varied in 2 mm incriments from 2.4 cm. to 3.4 cm. For each valve the size of the ball was predetermined as well as the required volume of silicone (Table 1).

The valve system can be collapsed and pushed through an 11-12 French catheter system (Figure 4).

Table 1. Predetermined volume of silicone.

CM Balloon	Air ml		Silicone ml
1.0	3.0	1.8	1+0.8
1.2	3.2	2.1	1.3+0.8
1.3	3.4	2.6	1.8+0.8
1.4	3.8	2.8	2.0+0.8
1.5	4.0	3.0	2.2+0.8
1.6	4.2	3.2	2.4+0.8
1.7	4.5	3.3	2.5+0.8
1.8	5.0	3.6	2.8+0.8
1.9	5.5	3.8	3.0+0.8
2.0	6.0	4.1	3.3+0.8

Animal studies

Initial *in vivo* testing of the valve has been carried out in twelve dogs. After induction of general anesthesia, the right common carotid artery was surgically isolated and an 11-12 French Teflon sheath was introduced. This sheath was advanced into the ascending aorta under fluoroscopic monitoring.

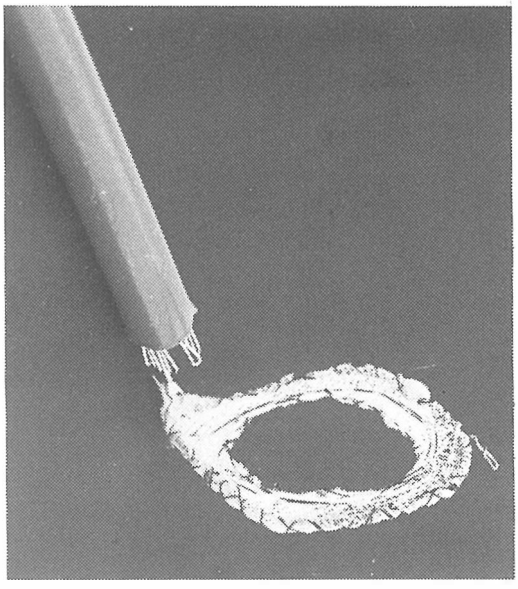

Figure 4. Collapsed prosthetic aortic valve within a distal end of a 12-F sheath.

With the animal in the left lateral position, an aortogram was performed to determine the diameter of the sinus Valsalva and ascending aorta (Figure 5). This is necessary in order to select the proper size of the prosthetic valve.

Following the aortogram, the tip of the delivery sheath was positioned in the posterior non cornonary cusp. A small amount of contrast materal was hand injected to check the position of the sheath, and this was marked by placement of a needle in the overlying skin. The prosthetic valve was then delivered through the sheath using a pusher catheter. As the ring exited the sheath, it opened and was anchored against the annulus by the barbs. Once certain that the ring was positioned correctly, the entire device was extruded into the aorta. The ring was placed below the ostia of the coronary arteries in such

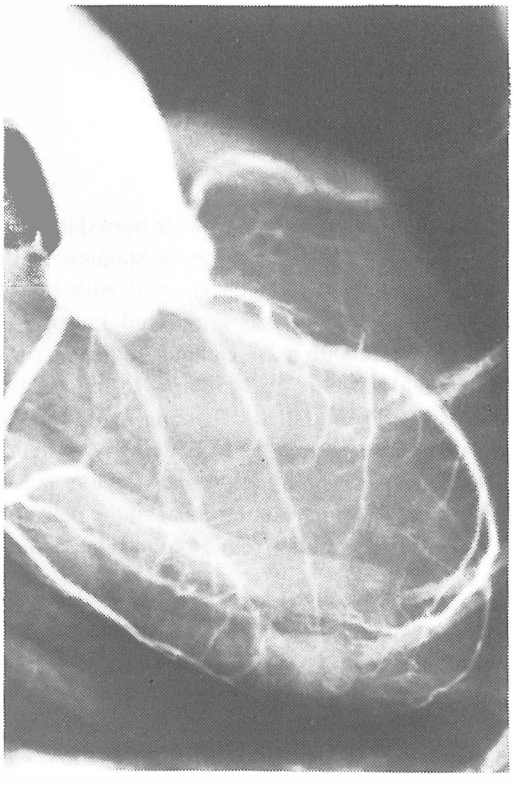

Figure 5. Normal aortogram = left lateral position.

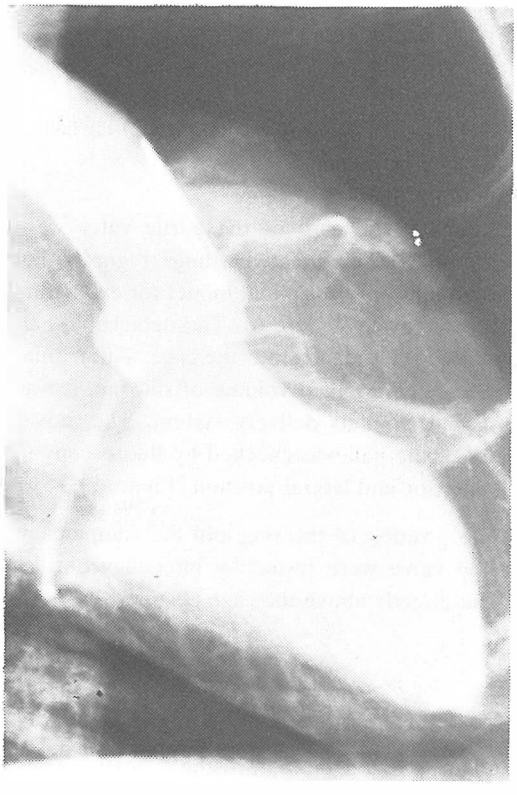

Figure 6. Aortic regurgitation after ring and cage placement–Right anterior oblique position.

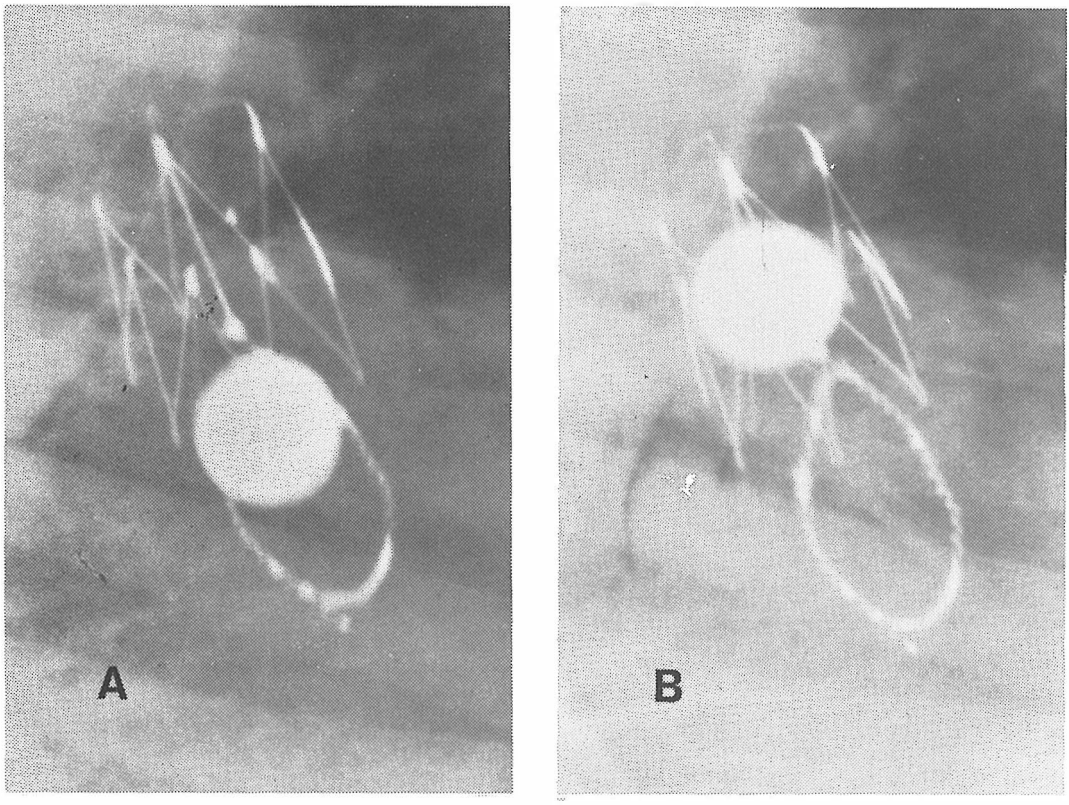

Figure 7. a) Movement of the ball – diastole b) Movement of the ball – sistole

a way that the cups of the aortic valve were compressed. This created a huge regurgitation and an appropriate animal model for evaluating the new device (Figure 6). The detachable balloon was then placed into the cage. After inflating a predetermined volume of silicone, it was detached from its delivery system. The movement of the ball was checked by fluoroscopy in an anterior and lateral position (Figure 7).

The position of the ring and the competency of the valve were tested by injecting contrast media directly above the cage (Figure 8).

Results

To date, we have placed prosthetic aortic valves in 12 dogs. Results of these studies have led to several design modifications.

The first four aortic valves were placed in dogs with the ring constructed out of stainless steel coil wire and latex tubing covered with nylon mesh. Latex tubing was connected through a one-way valve with a 2-F catheter to fill the ring with liquid silicone. All attempts to inflate the ring with silicone failed. The ring made out of latex tubing required a 14-F delivery system. The ring was simplified. A new nylon mesh design was developed and the size of the delivery system was decreased from 14 to an 11-F catheter.

In ten animals, the ring was successfully placed below the ostia of the coronary arteries. Postmorten examination showed that the ring was anchored against the annuls of the heart by the barbs in such a way that cusps of the aortic valve were compressed. This created a huge regurgitation and an appropriate model for evaluating the

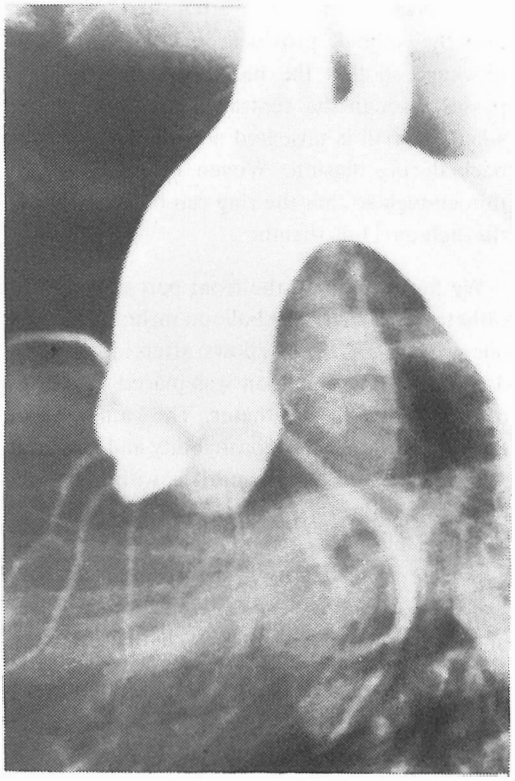

Figure 8. Competence of the prosthetic valve. Ring is placed below the ostia of the coronary arteries (filling defect).

new device. In all 12 cases, a huge insufficiency was created.

In the first two experiments the cage was constructed out of a Gianturco Z stent, 2.5 cm in lenght x 2.5 cm in diameter, from stainless steel wire (0.018 inch) bent in a zig zag pattern and two lengths of stainless steel guide wire soldered at one end to form the top of the cage. Animal experiments showed that the cage was too long and that the guide wire was not appropriate for the top of the cage. At necropsy, thrombus was found. It was attached to both lengths of the guiding wire.

To decrease the length of the cage, stents were constructed out of 0.014 stainless steel wire with 8–9 bends and 1.7 cm in length. Instead of guide wire, four lengths of flat, flexible stainless steel wire were attached to the bends.

Once the ring and cage assembly were in place, the balloon was inserted within the valve between the ring and cage. In the first nine experiments, the balloon was filled with air or contrast medium.

Several *in vitro* experiments were performed with a DOW CORNING 3110 R. T. V. silicone rubber to which barium sulfate (250% W/V, E–Z–Hd, E–2–EM Inc., Westbury, NY) Ethidiol (Savage Laboratories, New York), DOW CORNING 4 catalyst and DOW CORNING 200 silicone fluid were added. These experiments led to preparation of silicone formulation consisting of 5 ml of 3110 silicone, 1 ML of 200 silicone, 0.3 ml of barium sulfate and 0.20 ml of DOW CORNING 4 catalyst. This silicone formulation had low enough initial viscosity to be injected through a 60 cm long 5 French high flow P. E. catheter with a 1 ml syringe. Polymerisation of the mixture occurred within 25 minutes after mixing and, when fully cured, had the consistency of soft rubber.

The silicone mixture was used in three dogs for balloon inflation. In all three cases, a small amount of air stayed trapped in the balloon.

The three most recently placed valves showed excellent results for a short period of time. The ring and surrounding structures were sufficiently close together to prevent leakage of blood between them. In all cases, the coronary arteries were patent. In the last dog, the ball escaped out of the cage after three hours.

Migration of valves was noted in one animal.

Discussion

Mechanical heart valves are generally of two designs, either a ball–in–cage valve or a slim valve. At present, the ideal valve does not exist.[1] With regard to currently aviable prosthetic valves, the doctor and patient must weight the advantages and disadvantages of each type of prosthetic valve.

Currently, placement of prosthetic valves requires general anesthesia and open heart surgery before, and the recipient of the prosthetic valve

is subjected to the inherent risk of mortality associated with surgery.

A need therefore exists for a prosthetic heart valve which does not require surgery for installation and placement and, therefore, eliminates the risk associated with surgery.

When we started with construction of the prosthetic valve for the percutaneous transcatheter technique, we thought that the valve with the ball–in–cage design would be the best to reach te goal.

A factor which limits the construction of the prosthetic valve for the transcatheter technique the most is the size of the delivery system. All three parts of the valve, ring, cage and ball should be small enough to be collapsed and pushed through the catheter sheath of reasonable size.

At present, our prosthetic valve is a ball–in–cage design which functions as a simple one–way ball valve.

The valve can be collapsed and pushed through an 11-12 French Teflon sheath. Since the assembly is self–expanding, it opens as it exits the introducer. The final step is deployment of the ball. The essential feature of valve stability is mechanical fixation provided by the ring with the barbs and cage with the barbs. The ring and cage are attached by stainless steel tubings. Also assisting fixation of the valve is the stent. When fully extended, a combination presure/friction effect which tends to help the stent wires in contract with surrounding tissue. The tissue ingrowth may also occur to prevent migration of the valve.

For good hemodynamic function of the prosthetic valve, the position of the ring without regurgitation and periprosthetic leaks is important. The use of 4–5 barbs holds the ring in place below the ostia of the coronary arteries. The ring is covered with a fine mesh of a woven nylon material. Yoshioba et al.[7] and Uirich et al.[8] proved that nylon mesh can provide a framework for neointimal encasement. Our experiments demonstrated that nylon mesh with film deposits, which occur immediately after valve placement into the animal, provides effective blood flow blockage so that the blood flow in the sistoli passes through the central opening of the ring when the ball is unseated and prevents leakage back during diastoli. Woven nylon material is thin enough so that the ring can be easily passed through an 11–F sheath.

We have modified the front part of the Foley catheter for a ball. The balloon includes a simple one–way valve which allows after–inflation for detachment. The balloon was placed at the top of a 5–F high flow catheter. The catheter contains mandril for better pushability and insertion. After placement, the mandril is withdrawn and the air within the catheter and balloon was removed by a 20 cc syringe. Then the balloon was filled with a silicone mixture and detached from the catheter. Once the silicone has been injected and the balloon detached, a one way valve sealed the silicone within the latex balloon to maintain the ballon's spherical shape. In all cases, we had a problem. A small balloon of air always stayed trapped in the ball.

Conclusion

The limited experience reported prevents conclusive opinions. However, encouraging initial results from the animal trials have been one more step toward transcatheter valve replacement in humans.

Additional studies are now in progress to evaluate the current design with regard to thrombogenicity, haemodinamic function, durability, and biocompatibility.

Acknowledgments

The authors wish to thank Raquel Collins, B.S. and Irene Szwarc, R. T., for their invaluable technical assistance and Peggy Bergmanson for her secretarial help in the preparation of this manuscript.

References

1. Hufnagel CA, Harvey WP, Rabil PJ, McDermott TF, Washington D. C. Surgical correction of aortic insufficiency. *Surgery* 1954;**35:**673-83.
2. Rabago G. A worldwide overview of valve usage. In: Rabago G,Cooley DA, eds. *Heart valve replacement and future trends in cardiac surgery*. New York, Futura Publishing Co., Inc. 1987;3-9.
3. Morse D, Steiner RM, Fernandez J. *Guide to Prosthetic Cardiac Valves*. New York, Springer-Verlag, 1985;24-69.
4. Cooley DA. *Technique in Cardiac Surgery*. Philadelphia, Saunders, 1986:11.
5. Wright K, Wallace S, Charnsangavej C, Carrasco CH, Gianturco C. Percutaneous endovascular stents: An experimental evaluation: *Radiology* 1985;**156:**68-72.
6. Mahon TG, Wright KC, Armeniades CD. Injection of a silicone prepolymer system into the gallbladder of rabbits. *Investigative Radiology* 1991; (in press).
7. Yoshioka T, Wright K, Wallace S, Lawrence Jr. D, Gianturco C. Self expanding endovascular graft: An experimental study in dogs. *AJR* 1988;**151:**673-6.
8. Mirich D, Wright K, Wallace S, Yoshioka T, Lawrence Jr. D, Charnsangavej C, Gianturco C. Percutaneously placed endovascular grafts for aortic aneurisms: Feasibility study. *Radiology* 1989;**170:**1033-7.

Adv Radiol Oncol 1992; 22-4.

An injection technique for repositioning subclavian catheters

Mahon T and Lawrence D, Sr.

Department of Diagnostic Radiology The University of Texas M.D. Anderson Cancer Center 1515 Holcombe Blvd. Houston, TX 77030

Malpositioned central venous catheters need to be repositioned so as to avoid local toxicity from chemotherapeutic and other agents and to prevent venous thrombosis.
We describe a simple safe and effective technique for repositioning silicone central venous catheters, by using a hand injection of sterile saline. It was successful in all 9 patients in whom it was attempted, with no complications. Five catheters were single lumen and 4 were double lumen.
We feel that this method should be attempted prior to the use of more invasive techniques.

Key words: catheterization central venous, catheters, indwelling, injections

Introduction

The insertion of central venous catheters is a common procedure, particularly in patients requiring chemotherapy, total parenteral nutrition or long term intravenous antibiotics. Occasionally the catheter may be malpositioned, most often into the ipsilateral internal jugular vein. The catheter can be repositioned using a variety of invasive techniques. We assessed a new minimally invasive method to reposition silicone catheters.

Methods

Ten patients presented between April 9, 1990 and June 30th, 1990 for repositioning of central venous catheters. A limited venogram was performed by injecting 10 to 20 mls of Angiovist–292 (diatrizoate meglumine and diatrizoate sodium, Berlex Laboratories) through the catheter. In one patient the catheter tip was in a tributary of the internal jugular vein and the patient was excluded from the study. Nine patients were studied, in whom venography demonstrated intraluminal placement of the catheter tip and a patent superior vena cava.

Two catheters were inserted via the left subclavian vein. The tip was in the left internal jugular vein in 1 patient and in the right internal jugular vein in the other patient. The former was a single lumen catheter and the latter a double lumen catheter.

Seven central venous catheters were inserted into the right subclavian vein. The tip was in the right internal jugular vein in 3 patients, the left subclavian vein in 2, the left internal jugular vein in 1, and the azygos vein in 1 patient. The two catheters in the left subclavian vein and one in the right internal jugular vein were 7 French

Correspondence to: Dr. Thomas Mahon, New England Deaconess Hospital, Harvard Medical School Department Diagnostic Radiology, 185 Pilgrim Rd. Boston, MA 02215.

UDC: 616.141-072.2

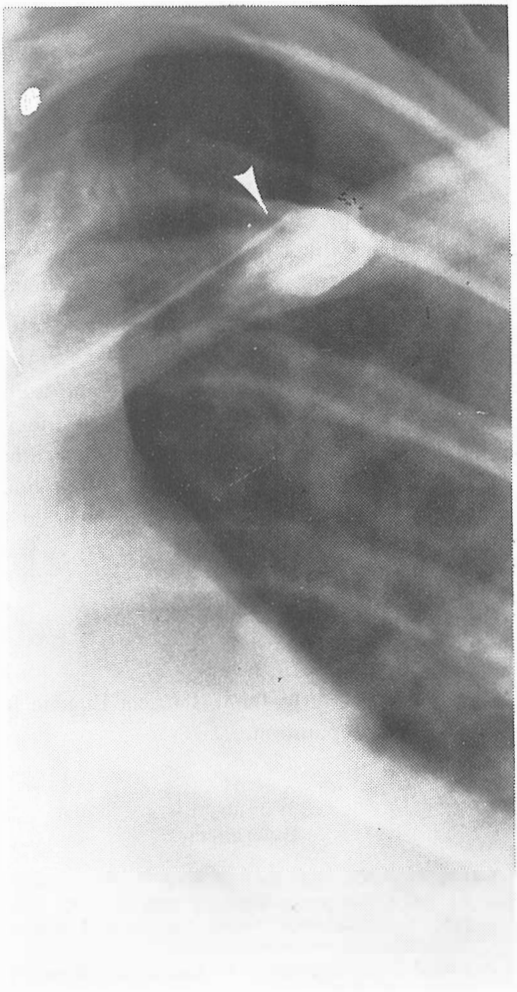

Figure 1(a). Double lumen right subclavian catheter (arrowheads) with tip in left subclavian vein.

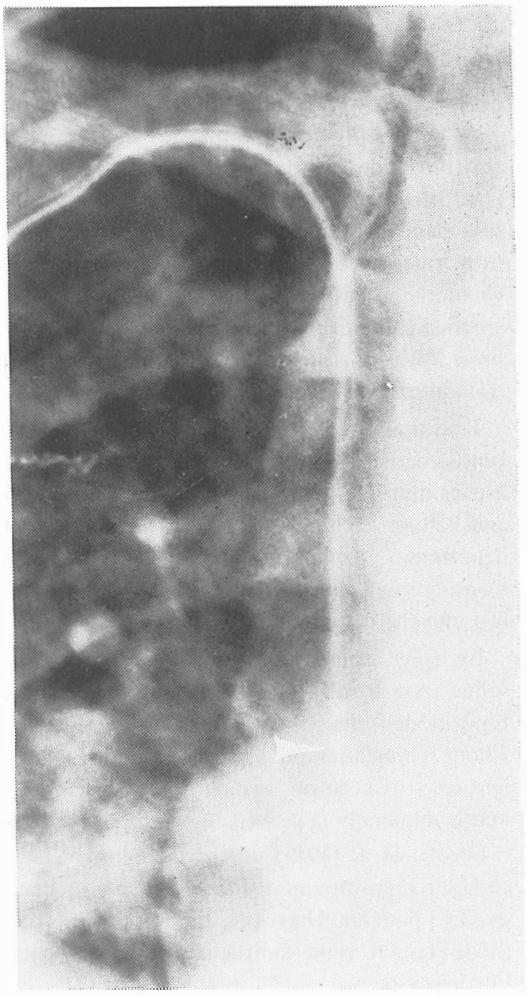

Figure 1(b). After a single injection of saline the tip (arrowhead) is in the right atrium.

double lumen silicone catheters (Cook Inc.) the others were 5 French single lumen silicone catheters (Davol Inc.)

Following the venogram, the catheter was flushed with a brisk hand injection of 5 mls of normal saline in a 5 ml syringe. Moderate effort was used over about 1 second. This was done in the erect position in 6 patients, and in the supine or semi–erect position in 3 patients. A repeat venogram was then performed to confirm satisfactory position of the catheter.

Results

In all 9 cases the catheter was repositioned, with its tip in the superior vena cava or right atrium. In 2 patients a second injection of saline was necessary. One was a single lumen right subclavian catheter with the tip in the left internal jugular vein, the other was a double lumen left subclavian catheter with the tip in the right internal jugular vein.

There was no evidence of any complications, patient discomfort or trauma to the catheters.

Discussion

It is important that central venous catheters are properly sited with their tips in a major central vein. The optimal position we feel is in the superior vena cava below the azygos vein. This is so as to provide maximum concentration on first pass of chemotherapy and to have a high flow rate so as to avoid local toxicity from chemotherapeutic and other agents. The malpositioned catheter may also initiate venous thrombosis if it is in a minor vein or is in a position to traumatize the vessel wall.

Traditional methods for repositioning central venous catheters are invasive and may entail the use of multiple guide wires, tip–deflector wires and balloon catheters (Lois et al, 1987). In our department, catheters were often repositioned by using a deflector guidewire which was introduced into the catheter.

By using a hand injection of 5 mls of normal saline in a 5 ml syringe, we have successfully repositioned the catheter in all 9 patients in whom it was attempted. The technique is quick and easy to perform, avoids patient discomfort and is minimally invasive.

Olcott, et al (1989) describes central venous catheter repositioning using an injection technique in 3 patients. However, all their patients had single lumen right subclavian catheters only. Furthermore, we placed the patient in the erect position, when possible, so as to use gravity to aid in repositioning. We also believe that performing an initial venogram is essential. This will confirm satisfactory intraluminal position of the catheter, the absence of thrombus and normal venous anatomy.

Due to the possible risk of intravascular trauma, only floppy silicone catheters were injected and patients with triple lumen catheters were excluded from the study. Similarly no attempt was made to reposition long venous lines, as injection of these may traumatize the catheter.

We feel that this method is a safe and useful technique for the treatment of malpositioned single or double lumen silicone subclavian catheters. While it was successful in all our patients, if it fails, other methods may then be used to reposition the catheter.

Acknowledgement

The authors wish to thank Patricia Eugene for manuscript preparation.

References

1. Olcott E, Gordon R, and Ring E. The injection technique for repositioning central venous catheters: Technical note. *Cardiovascular and Interventional Radiology* 1989;**12**:292-93.
2. Lois J, Gomes A, Pusey E. Nonsurgical Repositioning of Central Venous Catheters.*Radiology* 1987;**165**:329-33.

Adv Radiol Oncol 1992; 25–9.

Properties of biodegradable polymers for 5-fluorouracil and tamoxifen microcapsules

Yang DJ, Byun HS, Kuang LR, Yamashita Y, Moult RG, Tansey W, Wright KC and Wallace S

Division of Diagnostic Imaging, Box 57, 1515 Holcombe Boulevard, University of Texas M. D. Anderson Cancer Center Houston, Texas 77030 U.S.A.

Selective intraarterial infusion of microcapsules exerts therapeutic effects through both infarction and sustained drug activity; such use of microcapsules has also been applied to chemoembolization use. This study is aimed at developing biodegradable microcapsules which contain the widely used tumor chemotherapeutic agents such as 5-fluorouracil (5-FU) and tamoxifen (TX) for drug delivery. Poly-d, l-lactic acid (PLA), polycaprolactone (PCL), and polycaprolactone diol (PCLD) were the polymers chosen for preliminary evaluation. Drug to polymer ratios of 1:1 and 1:3 were prepared with mean capsule size of 100 μm. We then compared the effects of the drug: polymer ratios and incubation time on in vitro *dissolution rate. Our study demonstrated that the type of polymer used had a direct relationship to the amount of drug released. The following polymers are listed in descending order according to the effectiveness of each in facilitating the release of contents at 48 h incubation from TX-loaded microcapsules: PLA > PCL > PCLD, with 5-FU loaded microcapsules, efficacy of polymers was also rated: PCL > PCLD > PLA. The percent drug yield compared to drug: polymer ratios were, on average (W/W): from TX microcapsules, 14% at 1:3 and 30% at 1:1; from 5-FU microcapsules, 8% at 1:3 and 10% at 1:1. The results indicate that 5-FU and TX microcapsules produce sustained release properties and are useful in tumor chemotherapy.*

Key words: fluorouracil; tamoxifen; capsules; infusions, intra-arterial; biodegradation

Introduction

The development of microencapsulation as a technique for administering sustained release dosages has been successfully applied to tumor chemotherapy.[1-4] Selective intraarterial infusion of ethylcellulose microcapsules loaded with mitomycin C has been used in the treatment of primary or secondary carcinoma of the kidney, liver, bone, intrapelvic and retroperitoneal organs. These capsules exert therapeutic effects through both infarction and sustained local drug activity during the chemoembolization process. Furthermore, microcapsules also alter the systemic toxicity that is produced by the parent drugs.[5-7] In this study, we will provide information on sustained release properties as they apply to different biodegradable polymers. Such information which will facilitate tumor chemotherapy evaluation (e. g. reduce toxic effects on non-target tissues).

5-fluorouracil (5-FU), a fluorinated primidine analog, shows a close correlation with metabolism of nucleic acid and has been used in primary breast and metastatic liver chemotherapy.[8] Ta-

Correspondence to: Yang DJ. Ph. D.
UDC: 615.277.3.014.6.032.13

moxifen (TX), a potent nonsteroidal antiestrogen, which is more lipophilic than 5-FU has also been used in treatment of breast tumor.[9] Both drugs were chosen as model drugs in this evaluation. The use of biodegradable polymers for a drug delivery system has been reported.[10-13] Because they are non-toxic, biodegradable polymers provide the ideal coating for the preparation of microcapsules. Anticancer drugs can then be sent to the target site in sustained dosages released by microcapsules. The release patterns for these loaded microcapsules vary according to the different polymers used. However, little is known about the release rates of various polymers. For that reason, three commonly used biodegradable polymers, each with different chemical structures and properties, were chosen for preliminary evaluation: poly-d, l-lactic acid (PLA), polycaprolactone (PCL), and polycaprolactone-diol (PCLD). PLA is a weakly ionic polymer, whereas PCL and PCLD are more non-ionic in character. In order to examine the release properties of these polymers, we used drug: polymer ratios of 1:1 and 1:3 (w/w) and a mean capsule size of 100 μm.

Materials

Poly-d, l-lactic acid (M. W. 2000-50000), polycaprolactone (M. W. 35000-45000), polyvinyl alcohol and polycaprolactone diol (M. W. 3000) were purchased from Polysciences Inc. (Warrington, PA). Tamoxifen and 5-FU were purchased from Sigma Chemical Company (St. Louis, MO).

Preparation of microcapsules

The microcapsules were prepared using the solvent evaporation method, with drug: polymer ratios of 1:1 and 1:3 (W/W) and polyvinyl alcohol as an emulsifier. Drugs were dissolved in methylene chloride, then added with the emulsifier to a stirred at emulsifier 400 rpm water solution. After 6 h, the capsules were washed with water and dried in air. The capsules ranging in size from 106 to 212 μm in diameter were collected from mesh screens.

Microscopic examination

The microcapsules were observed with a binocular research microscope (Zeiss, Germany). The microcapsule's size was measured by an eyepiece micrometer. Following the observation by the light microscope, microcapsules (100 μm) were scanned with a scanning electron microscope to evaluate the surface characters of microcapsules.

Assay of the drug content

Microcapsules (5 mg) were weighed and dissolved in 5 ml of methanol. The solution was centrifuged and the supernatant (100 μl) was diluted with methanol (3 ml) and analyzed spectrophotometrically at 238 nm by a single beam spectrometer. A standard curve was produced using the same procedure by adding known amounts (2 mg) of both TX and 5-FU. The drug content was calculated as a percent of the total capsule weight. The experiment was performed in triplicate.

Dissolution studies

A set of capped test tubes was filled with 5 ml phosphate buffered saline solution of pH 7.4 (0.05 M) and placed in a water bath shaker set at 100 rpm with a constant temperature of 37°C.

Microcapsules (5 mg) were added to each test tube, and sample solutions of 3 ml were collected at different time intervals during centrifugation.

After each determination, the sample solutions were returned to each test tube. The concentrations of the drug released from microcapsules were determined by comparison with the standard drug (2 mg) in the same dissolution solution for the controls and measured spectrophotometrically at 238 nm. The experiment was performed in triplicate.

Statistical analysis

A student's t-test[14] was used to compare the significant difference ($p < 0.05$ level) between the sample at 1 h and the corresponding sample at different incubation time interval.

Results and discussion

In general, the encapsulated yield from the TX microcapsules was 30 to 36% for the 1:1 group and 13 to 23% for the 1:3 group; yield for 5-FU microcapsules was 8 to 10% for the 1:1 group and 6 to 9% for the 1:3 group (Table 1). Since 5-fluorouracil is hygroscopic and hydrophilic, some drugs may diffuse into water from the capsules during the encapsulation process. Therefore, the yield of 5-FU loaded microcapsules is lower than that of TX microcapsules. Scanning electron microscopy showed that all the microcapsules prepared were spherical in shape with smooth outer surfaces (Figure 1). Although the release rate of TX from the PCLD capsules at 48 h the different drug: polymer, there is a similar pattern of release. The release rate of TX at 48h incubation time was found to decrease in the order: PLA > PCL > PCLD (1:1) (Figure 3). The release rate for PCL capsules was slightly faster than PLA in 1:3 group at 24 and 48 h. The release rate of TX from the PCLD capsules at 48h incubation time was 10% which remained significantly ($p < 0.05$) lower than for PLA and PCL microcapsules. In general, TX was released from PLA capsules at a rate of 35% at 48 h incubation time for both 1:1 and 1:3 ratios. The drugs in the standard had already dissolved by that time. The release rate of 5-FU microcapsules at 48h incubation time was found to decrease in the order: PCL > PCLD > PLA (Figure 4). 5-FU was released from PCL capsules by 45% for the 1:1 and 60% for the 1:3, a yield that was significantly higher ($p < 0.05$) than the yield for PLA and PCLD capsules. The differences among the release rates of the capsules could be attributed to the lipophilic character of the drugs; TX is more lipophilic than is 5-FU. The properties of various polymers also my alter the release rates.

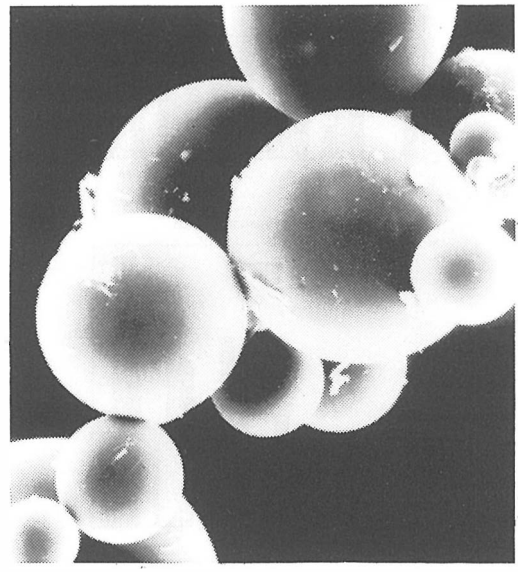

Figure 1. Scanning electron microscope PCL microcapsules loaded with 5-FU at the rations of 1:1.

Our preliminary studies indicate that biodegradable polymers can be used to prepare sustained release microcapsules of hydrophobic – and hydrophilic-type drugs. A lipophilic drug coated with PLA showed a faster release rate than did the same drug coated with other polymers; a hydrophilic drug coated with PCL similarly showed a faster release rate pattern than when other polymers were used. This faster release rate would be appropriate when administering the initial dose of the sustained release formulation.

Table 1. % of drug contents in microcapsules.

DRUG	POLYMER	DRUG: 1:1	POLYMER 1:3
Tamoxifen	Polylactic acid	30.0	22.5
	Polycaprolactone	30.7	13.0
	Polycaprolactone diol	36.4	14.9
5-Fluorouracil	Polylactic acid	8.8	8.5
	Polycaprolactone	9.9	6.6
	Polycaprolactone diol	7.6	7.6

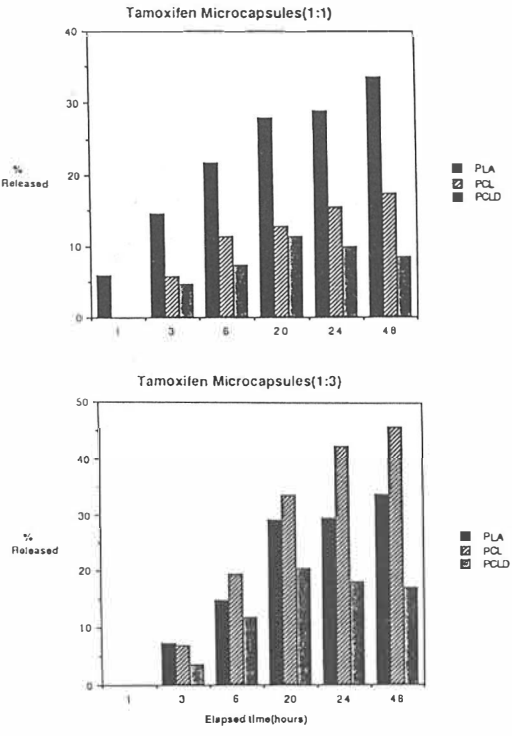

Figure 2. Release rate of microcapsules loaded with tamoxifen.

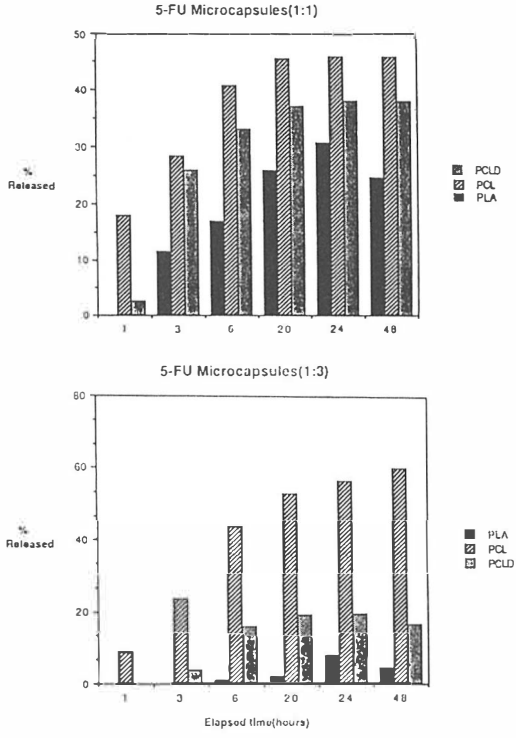

Figure 3. Release rate of microcapsules loaded with 5-FU.

We believe that the sustained release properties of both 5-FU and TX microcapsules demonstrate potential for use in tumor chemotherapy. The information in this study would be useful in predicting the sustained release properties of drugs and reducing the toxic effects on non-target tissues.

Acknowledgements

This work is supported in part by John S. Dunn Chair in Diagnostic Radiology, John S. Dunn Foundation and Cancer Fighters of Houston. We thank Dianne Perez Onuogu for preparing the manuscript.

References

1. Bechtel W, Wright KC, Wallace S, Mosier B, Mosier D, Mir S, Kudo S. An experimental evaluation of microcapsules for arterial chemoembolization. *Radiology* 1986; **161**:601-4.
2. Brunning JL, Kintz, BL. In: *Computational Handbook of Statistics*. Scott, Foresman and Company, Glenview, Illi., 1977; 13-5.
3. Jalil R, Nixon, JR. Microencapsulation using poly (l-lactic acid) I: Microcapsule properties affected by the preparative technique. *J Microencapsulation* 1989; **6**(4):473-84.
4. Kato T, Nemoto R, Mori H, Kumagai I. Sustained-release properties of microencapsulated mitomycin C with ethylcellulose infused into the renal artery of the dog. *Cancer* 1980; **46**:14-21.
5. Kato T, Nemoto R, Mori H, Takahashi M, Harada M. Arterial chemoembolization with mitomycin C microcapsules in the treatment of primary or secondary carcinoma of the kidney, liver, bone and intrapelvic organs. *Cancer* 1981; **48**:674-80.
6. Kato T, Nemoto R. Preparation and properties of microencapsulated mitomycin C. *IRCS Medical Science* 1978; **6**:311.
7. Leelarsamee N, Howard SA, Malanga CJ, Ma JKH. A method for the preparation of polylactic acid microcapsules of controlled particle size and drug loading. *J Microencapsulation* 1988; **5**(2):147-57.
8. Leelarsamee N, Howard SA, Ma JKH. Effect of surface active agents on drug release from polylactic acid hydrocortisone microcapsules. *J Microencapsulation* 1988; **5**(1):37-46.

9. Loser R, Seibel K, Roos W, Eppnberger U. In vivo and in vitro antiestrogenic action of 3-hydroxytamoxifen, tamoxifen and 4-hydroxytamoxifen. *Eur J Cancer Clin Oncol* 1988; **21**(8):988-90.
10. Miyazaki S, Hashiguchi N, Sugiyama M, Takada M, Morimoto Y. Fibrinogen microspheres as novel drug delivery systems for anticancer drugs. *Chem Pharm Bull* 1986; **34**:1370-75.
11. Spenlehauer G, Veilland M, Benoit J-P. Formation and characterization of cisplatin loaded poly-d, l-lactide microspheres for chemoembolization. *J Pharm Sci* 1986; **75**:750-5.
12. Tsurumi Y, Kameyama M, Ishiwata K, Katakura R, Monma M, Ido T, Suzuki J. F-18-Fluoro-2-deoxyuridine as a tracer of nucleic acid metabolism in brain tumors. *J Neurosurg* 1990; **72**:110-3.
13. Wallace S, Chung VP, Carrasco CH, Charnsangavej C, Bechtel W, Wright KC, Gianturco C. Physio-anatomic concepts and radiologic techniques for intraarterial delivery of therapeutic agents. *Cancer Bull* 1984; **36**:6-14.
14. Wright KC, Wallace S, Mosier B, Mosier D. Microcapsules for arterial chemoembolization: appearance and *in vitro* drug release characteristics. *J Microencapsulation* 1988; **5**(1):13-20.

Adv Radiol Oncol 1992; 30-4.

Intravenous thrombolysis of acute coronary occlusion after percutaneous transluminal agnioplasty

Kranjec I, Cijan A, Pavčnik D

Department of Cardiology, University Medical Centre, Ljubljana
Institute for Diagnostic and Interventional Radiology, Ljubljana

Thrombolytic therapy can restore vessel patency in some patients with acute coronary occlusion after percutaneous transluminal coronary angioplasty. A case is presented in which prolonged intravenous application of thrombolytic agent appeared as effective and safe as intracoronary treatment. The potential use of fibrin-specific enzymes in similar circumstances is discussed.

Key words: coronary thrombosis, angioplasty, transluminal, percutaneous coronary thrombolytic therapy

Introduction

Acute coronary occlusion (ACO) of the dilated vessel is the most apprehended complication after percutaneous transluminal coronary angioplasty (PTCA) as it may lead to myocardial infarction or even death. ACO develops mostly within the first 24 hours after the procedure. In a recent series at the University Hospital of Geneva it occured in 4% of PTCA procedures,[1] compared to a rate of 5% seen in our last 100 patients. A variable combination of coronary wall dissection, thrombosis and vasoconstriction is involved in the pathogenesis of ACO. Therefore, mechanical recanalization, thrombolytic therapy and nitrate administration have been proposed as measures to improve the jeopardized coronary perfusion. Repeated PTCA is considered the treatment of choice, especially if the guide wire is still in position. Intracoronary application of thrombolytic agents may prove effective if PTCA or other mechanical means fail to achieve durable patency and when rapid transfer for bypass surgery is not necessary. However, this type of therapy is time consuming,[1] the success may be difficult to assess,[2] and a significant haemostatic defect with a bleeding potential is often induced.[3] Despite the aforementioned disadvantages several published articles have confirmed the efficacy of the intracoronary streptokinase[4] or urokinase[5] in restoring patency of the occluded coronary artery. In this report we describe a case with ACO after PTCA in which the thrombolytic agent was applied first into the coronary artery and then also intravenously.

Correspondence to: Igor Kranjec M.D. Kotnikova 19, 61000 Ljubljana, Slovenia.

UDC: 616.132.2-005.6-089

Case report

A 58-year-old man was referred to our hospital for coronary angiography. Five months before the admission he began to experience a chest discomfort occuring initially with physical activity and in the last two weeks also at rest. His

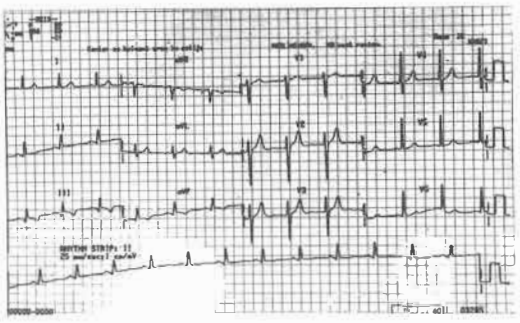

Figure 1. ECG tracing at the hospital admission showing Q-waves and inversion of T-waves in inferior leads.

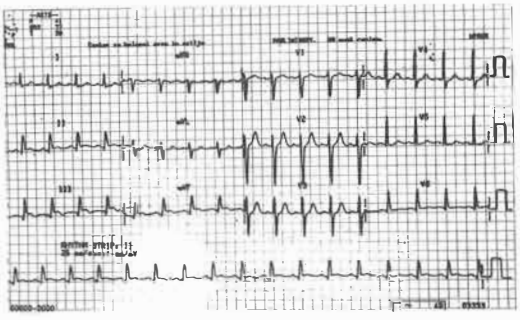

Figure 4. ECG tracing during the first episode of chest pain after PTCA showing elevation of ST-segment in inferior leads.

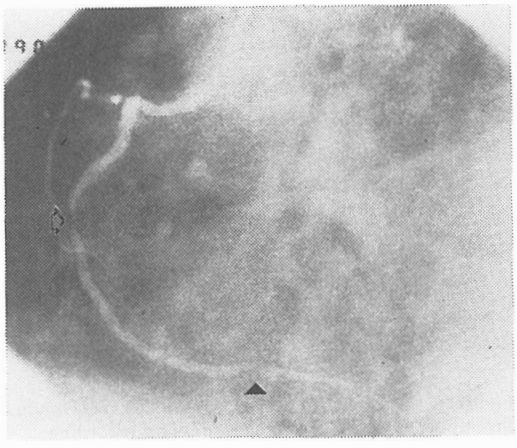

Figure 2. Left anterior oblique angiogram of the right coronary artery before the PTCA. There is 83% stenosis in the midportion (arrow) and 76% in the distal segment (arrowhead).

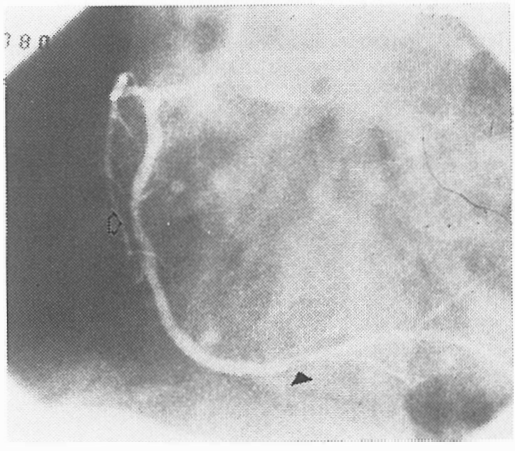

Figure 3. Left anterior oblique angiogram of the right coronary artery after the PTCA. The proximal stenosis is reduced to 38% (arrow) and the distal stenosis to 50% (arrowhead).

symptoms were always completely relieved by sublingual nitroglycerin. Yet his ECG on admission revealed new Q-waves and T-wave inversion in inferior leads (Figure 1). He was stabilized with oral nitrates, metoprolol, nifedipine and aspirin. A left ventriculogram showed severe hypokinesia of the inferior wall. Coronary angiography demonstrated two successive narrowings of the dominant RCA, the first (83%) in the midportion and the second (76%) in the distal segment (Figure 2). Subsequently, PTCA was performed using an 8F Judkins right guiding catheter, an 0.014 in. ACS high-torque floppy guide wire, and a 2.5mm Cordis Scimed balloon dilatation catheter. At first the medial RCA was dilated twice using 7 and 10 atm of pressure; afterwards the distal RCA was dilated four times with 4–6 atm of pressure. The primary success of PTCA was considered satisfactory, the proximal stenosis having been reduced to 38% and the distal one to 50% (Figure 3). The patient was transferred to the CCU with the arterial and venous sheaths left in place and he was put on intravenous heparin. One hour after the procedure, the patient complained of a sudden chest discomfort and the ECG showed ST-segment elevation in the inferior leads (Figure 4). On control coronary angiography the residual proximal stenosis was

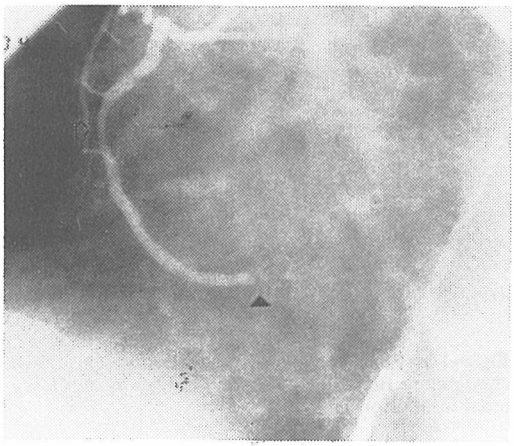

Figure 5. Left anterior oblique angiogram of the right coronary artery during the first episode of spontaneous myocardial ischemia after PTCA. The proximal stenosis in now 57% (arrow) and there is total occlusion of the distal segment (arrowhead). Thin vertical dissection line is not visible in this view.

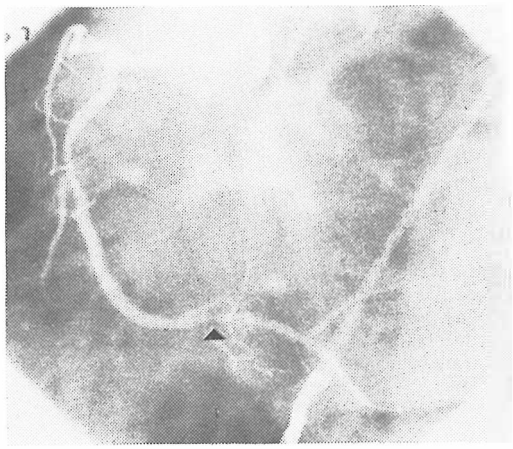

Figure 6. Left anterior oblique angiogram of the right coronary artery after intracoronary thromobolysis. Vessel patency is restored with remaining 62% stenosis of distal segment (arrowhead).

worse (57%) and was accompanied by a thin vertical nonocclusive dissection, while an ACO was evident in the distal RCA (Figure 5). Intracoronary injection of nitroglycerin 200 μg did not relieve the ACO. A repeat PTCA was avoided as the introduction of the coronary guide wire was undesirable in the presence of the dissection. The insertion of a perfusion catheter was avoided for the same reasons. Emergency

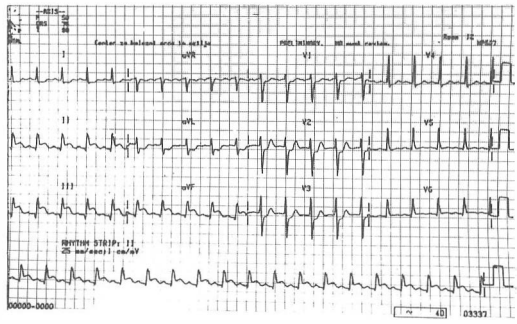

Figure 7. ECG tracing during the second episode of chest pain after PTCA showing even greater elevation of ST-segment in inferior leads and depression of ST-segment in leads V1.3.

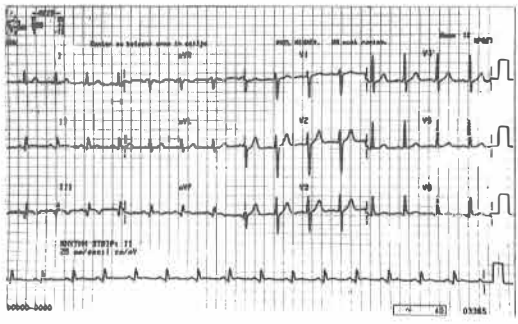

Figure 8. ECG tracing after completed intravenous thrombolysis is similar to the admission recording.

coronary artery bypass surgery was not requested because of haemodynamic stability, peripheral location of the ACO and previous occurrence of a myocardial infarction in the same area. Therefore, an attempt at intracoronary thrombolysis was made, using streptokinase in a total dose of 100,000 IU delivered through the diagnostic right coronary catheter over 25 min. Patency of the distal RCA was restored, but a residual stenosis of 62% persisted (Figure 6). The patient was transported back to the CCU and a continuous intravenous infusion of heparin (1,000 IU/h) and nitroglycerin (3 mg/h) was started. The ECG pattern reverted to the one before the PTCA. Half an hour later, the patient again developed an intense chest discomfort associated with ST segment elevation in the ECG (Figure 7). A reocclusion of the RCA was suspected but

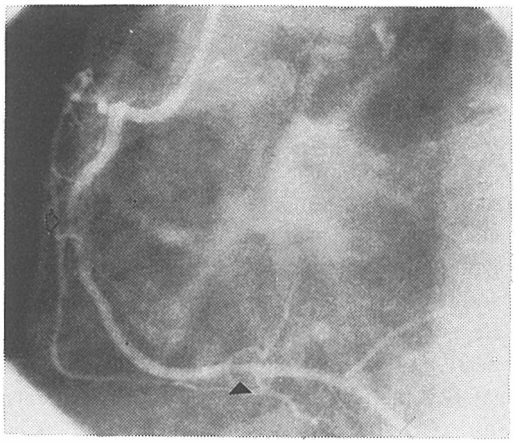

Figure 9. Left anterior oblique angiogram of the right coronary artery after completed intravenous thrombolysis. A 57% proximal stenosis (arrow) and 47% distal stenosis (arrowhead) remained.

coronary angiography was not repeated. Intravenous thrombolytic therapy was applied, using streptokinase in a total dose of 1,750,000 IU, administered slowly over the next 16 hr. There was no evidence of bleeding around the femoral sheaths though the thrombin time was elevated to >120 sec (normal values 7–11 sec) and fibrinogen was unmeasurable toward the end of thrombolysis (normal values 1.6-4.5 g/l). The chest discomfort soon disappeared and the ECG tracing reverted to the previous pattern again (Figure 8). However, the total plasma CK activity rose to 7.61 μkat/l (normal values 0.17–2.08 μkat/l) with 8% of the MB-CK fraction. These findings indicated a small inferior wall reinfarction. The final coronary angiography performed next day revealed a patent RCA with narrowings of 57% and 47% in its medial and distal segments, respectively (Figure 9). The patient remained asymptomatic. At a predischarge stress test administered 10 days later, he exercised to 7 MET without symptoms of ECG signs of myocardial ischaemia.

Discussion

ACO is a serious complication directly related to PTCA. It still continues to occur in spite of increased safety of the equipment and increased operator experience. Extensive arterial damage with medial dissection and creation of an occlusive intimal flap may be caused during the procedure by the guiding catheter, the guidewire, or the balloon catheter.[6, 7] The tip of the guiding catheter has a greater potential to produce arterial trauma than routine diagnostic catheters when advancing into the target artery. However, we can exclude this mechanism in our patient because the ACO occurred at the site of the distal stenosis. Guide wires 0.014 in. or less in diameter with flexible tips are very unlikely to damage the vessel wall. Yet even these inherently safe quide wire systems can get under an atherosclerotic plaque.[7] The goal of PTCA is to achieve a controlled injury to the artery during balloon inflation. In some cases a significant dissection of the intima occurs, especially if an oversized balloon is used. In our case, the lumen diameter behind the distal narrowing was estimated to be 2.8 mm and the balloon we used was thought to fit well. Nevertheless, guide wire manipulation or balloon inflation might have produced the ACO.

However, it is most frequently thrombosis, brought about by the sluggish flow in the dissected area, that converts an obstructive dissection into an occlusive one.[1] Apparently, this occurred also in our patient. Reported cases with spontaneous[8] or thrombolytic[4, 5] recanalization of ACO, along with our example, support the important role of thrombus in the development of abrupt vessel closure following PTCA. In our patient, the ACO occurred unfortunately after complete removal of the dilatation system. In the presence of proximal wall dissection, we were unable to recross the area of the abrupt ACO with the guiding wire in order to repeat the PTCA or insert a perfusion catheter. Emergency bypass surgery was not considered necessary because the endangered myocardial area was estimated to be relatively small. Thus, a trial of thrombolytic therapy was thought to be the most reasonable approach. The minimum effective dosage of intracoronary streptokinase or urokinase that results in angiographic evidence of

recanalization (100,000–360,000 U) is usually administered.[5] This low dosage regimen proved effective in our patient.

The recurrence of clinical and ECG manifestations of acute myocardial ischaemia half an hour after successful intracoronary thrombolysis suggested reocclusion at the same distal site but this was not confirmed by a repeat coronary angiography. The rather unexpected development of an occlusive thrombus, despite the adequate heparinization, was probably related to the low dosage of thrombolytic agent. As the trombolytic therapy had previously turned out to be reasonable and in order to avoid further transportation of the patient from the CCU to the catheterization laboratory, we decided on the intravenous mode of therapy. A high-dose infusion of brief duration is usually applied if streptokinase or urokinase is chosen as the thrombolytic agent in acute myocardial infarction. However, a significant haemostatic defect is induced in most patients. Moreover, haemorrhage is a major hazard in patients after a catheterization procedure, especially when sheaths are left in vessels. Therefore, we decided on the prolonged infusion regimen. Though definite coagulation changes were demonstrated toward the end of the streptokinase infusion, no bleeding complications were observed. In this regard, the safety of the described intravenous regimen appears to be comparable with that of intracoronary thrombolysis.[5]

It has been suggested that the success of thrombolytic therapy might be difficult to assess in patients with ACO after PTCA.[2] With the aid of coronary angiography, we found that intracoronary and also intravenous streptokinase could restore patency in the occluded artery. From this point of view, thrombolysis may be effective in some patients with this complication. On the other hand, the time to reperfusion is longer with thrombolysis compared to repeated PTCA. A rise in total plasma CK activity is common after PTCA because of tissue trauma[1, 9] but an MB–CK fraction exceeding 5% of total activity is diagnostic of a myocardial infarction.[9] In our patient a small additional myocardial necrosis occurred despite the thrombolytic treatment.

In conclusion, coronary thrombus has an important role in the development of ACO after PTCA. Thrombolytic therapy can restore vessel patency in some patients with this complication, yet minor myocardial necrosis may not be completely prevented. Prolonged intravenous application of thrombolytic agent is as effective and safe as intracoronary treatment. Intravenous application of fibrin–specific thrombolytic enzymes may become the treatment of choice in patients with ACO after PTCA when repeated PTCA in not possible and prompt coronary bypass surgery is not necessary.

References

1. Meier B. Complications and management. In Meier B ed. *Coronary Angioplasty*. Orlando: Grune & Stratton, Inc., 1987, pp 107-49.
2. Vlietstra RE: Management of acute occlusion after percutaneous transluminal coronary angioplasty. *Europ Heart J* 1989;**10** (Suppl H): 101-3.
3. Tiefenbrunn AJ. Tissue–type plasminogen activator: Intracoronary applications. *Cathet Cardiovasc Diagn* 1990;**19:**108-15.
4. Schoffer J, Krebber H, Bleifeld W, Matthey DG.. Acute coronary artery occlusion during percutaneous transluminal coronary angioplasty: Reopening by intracoronary streptokinase before emergency coronary artery surgery to prevent myocardial infarction. *Circulation* 1982;**66:**1325-31.
5. Verna E, Repetto S, Boscarini M, Onofri M, Qing LG, Binaghi G. Management of complicated coronary angioplasty by intracoronary urokinase and immediate re–angioplsty. *Cathet Cardiovasc Diagn* 1990;**19:**116-22.
6. Ryan TJ, Faxon DP, Gunnar RM, Kennedy JW, King SB, Loop FD, Peterson KL, Reeves TJ, Williams DO, Winters WL. Guideliness for percutaneous transluminal coronary angioplasty. A report of the American College of Cardiology (American Heart Association Task Force on assessment of diagnostic and therapeutic cardiovascular procedures). *J Am Coll Cardiol* 1988;**12:**529-45.
7. Clark DA. Complications of coronary angioplasty. In Clark DA. *Coronary Angioplasty*. New York: Alan R. Liss, Inc., 1987;99-102.
8. Slack JD, Pinkerton CA, VanTassel JW. Late recanalization at the site of failed percutaneous transluminal coronary angioplasty. *Cathet Cardiovasc Diagn* 1985;**11:**615-21.
9. Roberts R. Enzymatic diagnosis of acute myocardial infarction. *Chest* 1988;**93:**3-6.

Adv Radiol Oncol 1992; 35-40.

Current diagnostic of pituitary disorders by CT

Lovrenčić M

University Hospital, Dr. M. Stojanović, Institute of Radiology and Oncology, Zagreb

High resolution CT has been established as a method for the evaluation of sellar morphology. It has yielded valuable results in the investigation of patients with pituitary-secreting and non-secreting adenomas. CT with intravenous administration of a water-soluble contrast medium is useful in establishing size and localization of the lesion as well as in the evaluation of suprasellar and parasellar growth. Small adenomas and isodense lesions represent a limitation of the method.

Key words: pituitary disease, tomography, X-ray computed.

Introduction

While early experiences with CT in pituitary tumours diagnosis were satisfactory in the diagnostics of macroadenomas, the method was not reliable in the diagnosis of hormone–secreting microadenomas.[1] Poor contrast and spatial resolution of the available machines, thick sections and inadequate technique of examination reduced diagnostic accuracy. Progress in technology and the construction of high resolution CT scanners as well as sophisticated software programs increased the clinical application of the method and improved the diagnosis of sellar pathology.[2,3]

The pituitary gland can be evaluated by means of high resolution CT scans.[4] It is best demostrated either directly on coronal scans or indirectly from data obtained in the axial plane and reformatted into coronal and sagittal images.[5, 6] The use of high resolution CT scans for the diagnosis of pituitary microadenomas is currentlly well established.[7, 8]

Correspondence to: Prof. Dr. M. Lovrenčić, Department of Radiology and Oncology, Dr. M. Stojanović, University Hospital 41000 Zagreb, Vinogradska 29. Croatia.

UDC: 616.432-002-073.756.8

Technique

Axial sections are made in the supine position and are easy to perform, except in patients with major kyphosis. They can be done in elderly people or in patients in whom the prone position, required for direct coronal sections, is not feasible due to obesity, respiratory failure, pregnancy etc. CT scans in axial projection are generally acceptable in large lesions but do not provide sufficient information about the relation of the tumour to the pituitary gland.[9] Surrounding structures like the base of the skull, cisterns and vessels can make linear artefacts and reduce diagnostic ability.[10] The thickness of the slices should be adequate to the size of the lesion. In some cases axial sections must be performed in addition to coronal slices i. e. anteriorly or posteriorly located lesions, or poorly defined lesion in the coronal plane.[11] Partial volume

effect by axial section can usually obscure the visualization of a small lesion such as microadenoma. For this reason direct coronal sections are preferred in the exploration of the pituitary gland.

Coronal and sagittal images can be reformated from data obtained in the axial plane.[5, 6] Sagittal or coronal reconstruction requires thin axial slices because they improve visualization of intrasselar content. For larger lesions with supra– and parasellar extension, scans from the sphenoid sinus to the third ventricle, with slice thickness 2 to 4 mm, should be obtained. Sagittal reformated images can be very useful in the analysis of the topography of those lesions with extrasellar spread or existence of intrasellar pathology for up to 5 mm in diameter.[12]

Direct coronal scans are absolutely imperative in the diagnosis of intrasellar pathology. Application of this modality has led to an increase in the diagnosis of pituitary pathology and to an increase in the number of published reports.[2, 3, 7, 8, 13] Direct coronal CT scans require an appropriate cooperation of the patient. Hyperextension of the head in the prone position is not comfortable and requires a very rapid study. A metalic dental prosthesis can cause linear artefacts and obscure the exact visualization of the pituitary gland. Using scoutview and lateral digital localizer, artefacts can be avoided by appropriate angulation of the gantry. Coronal sections are performed from planum sphenoidale to the interpeduncular cisterns. The sellar floor is studied on coronal sections whereas the anterior wall and dorsum sellae are better visualized in the axial plane.

Contrast medium

A study of the pituitary gland is generally performed after intravenous administration of a water–soluble contrast medium. Either ionic or non–ionic contrast media may be injected intravenously. In routine scanning the contrast medium may be given slowly, whereas dinamic CT direct coronal sections require rapid injection.[14] In a majority of cases native scans can be omitted and only contrast study performed to shorten the duration of examination and avoid uncomfortable position of the patient, necessary to carry out direct coronal section.

A native scan allows analysis of the volume of the pituitary gland and suprasellar cisterns in patients with contrast medium or drug allergy, as well as the intrasellar or suprasellar calcifications. The use of intrathecal administration of a non–ionic contrast medium has not been very common in the diagnosis of intrasellar tumours[15, 16] since the introduction of high resolutions scaners. It is only performed in the differential diagnosis of empty sella and cystic or necrotic pituitary adenomas.

Anatomy

Enhanced pituitary gland in CT scans is visible as a homogenious structure.[17] The lateral borders of the gland are in contact wiht cavernous sinus, but not always clearly separated. The superior border of the gland can be flat or slightly concave.[11] Between the central part of the gland and the infundibular recess of the third ventricle the pituitary stalk is visible. Anatomical variants of the sellar floor, such as the sphenoid sinus may lead to an asymmetry of the pituitary gland. In coronal section the posterior lobe of the pituitary gland is not seen clearly.[18] The pituitary gland is less well defined in axial section due to the partial volume effect. Exceptionally, the posterior lobe of the pituitary gland is visible in more than 50% of the cases.[12]

Pathology

Pituitary macroadenomas may be limited to the sella turcica, or grow and present with suprasellar spread. At first, tumours fill up the sella, entirely but a part is visble in the suprasellar cisterns separated from the optic chiasma (Figure 1). Larger adenomas with major suprasellar spread completelly fill the chiasmatic cisterns. The tumour can be symmetric and located me-

dially; tumours located laterally reveal asymmetry. At the later stage the entire cisterns are filled by tumours. They extend to the anterior horn of the lateral ventricles. Very large tumours present polycyclic contours. The adenomas with inferior extension can cause osseous deformity. The sellar floor can be excavated or depressed while the volume of the sphenoid sinus is reduced. The lateral extension of adenomas into the cavernous sinus is not very common. Simple lateral extension displaces either one or both cavernous sinuses. True invasion of the cavernous sinus bends its lateral wall.

The most common pituitary microadenomas are prolactin-secreting adenomas (Figure 1) The hyperprolactinemia causes endocrinological disorders e. g. amenorrhoea with or without galactorrhoea and libido loss in men.[19, 20] The size of the pituitary, expressed as height of the gland is increased. The superior pole of the gland presents upward convexity with asymmetrical bulging (Figure 1C).[21] A localized erosion of the bone with thinning can be sometimes visible in tumours larger than 5 mm on the sellar floor. Some adenomas reveal calcifications. The adenomas are visible as rounded, oval areas, less dense than the normal enhanced pituitary tissue. The pituitary stalk is frequently inclined from the vertical axis (Figure 1A). The sensitivity rate of correct localization in prolactin-secreting microadenomas has been very high i. e. 91,9%.[22] The growth-hormone (GH) secreting adenomas appear clinically as acromegaly. Skeletal deformities can be a common cause of technical difficulties in CT scanning particulary in the coronal plane. It results in a blurred pattern of the lesion in coronal and sagittal planes. Intrasellar GH adenomas are not allways clearly demarcated from pituitary tissue (Figure 2). These tumours commonly present a depression of the sellar floor, but the bone cortex is no eroded.[21] The areas of partial or total intratumoral necrosis may be observed on CT scans as small hypodensities or ring enhanced lesions. Reliable differentiation between prolactin-secreting and GH-secreting adenomas only from CT scans has not been possible. Diagnostic accuracy of tumour localization and size estimation on CT scans in GH adenomas has been 90%.[23]

Cushing's disease is usually due to a pituitary corticotropic-cell adenoma. Detection of the tumour by CT is not allways easy because adenomas are often very small. The buffalo neck and the kyphosis of the thoracic spine, characteristic of Cushing's disease, render coronal sections difficult. The corticotropic-cell adenomas are rather small, most frequently located intrasellary and are visible on CT scan as round or oval low density areas (Figure 3A). Exceptionally, the enhanced adenomas may be of the same density as

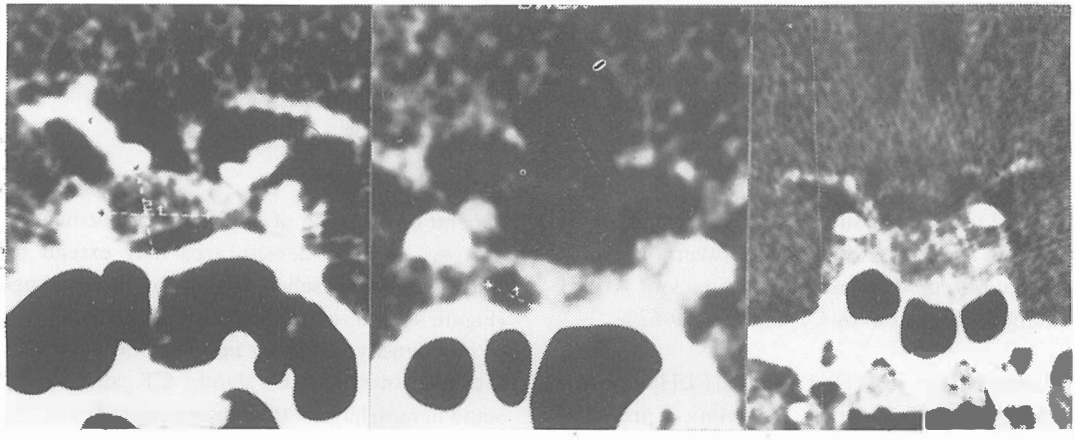

Figure 1. Prolactin-secreting adenomas. A. Coronal scan: Hypodense macroadenoma 10 x 13 mm. Pituitary stalk is inclined ant the gland pushed to the left. B. Coronal scan: A microadenoma 5 mm in size in the left part of gland. C. Coronal scan: A macroadenoma 15 x 15 mm with cranial extension.

Figure 2. GH-secreting adenoma. Coronal scan: Intrasellar adenoma with depression of the sella floor.

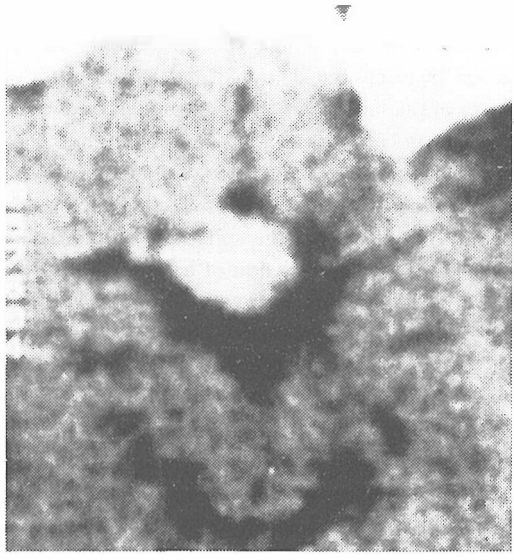

Figure 4. Pituitary apoplexy. Native axial scan: Increased density in suprasellar cisterns due to haemorrhage.

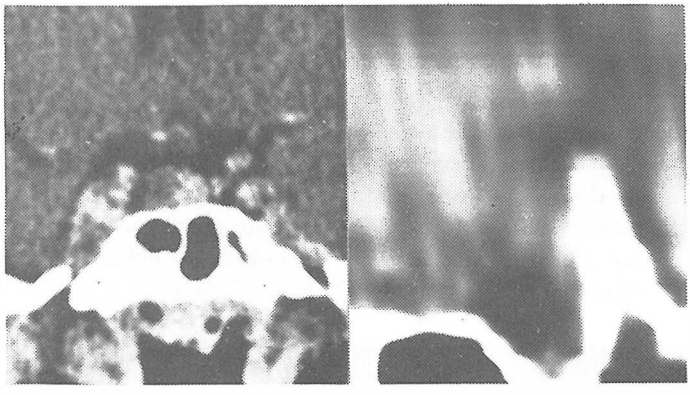

Figure 3. ACTH-secreting adenomas. A. Coronal scan: A 7 mm hypodeense adenoma demarcated by fat laterally to the cavernous sinus. B. Sagital reconstruction: Increased fat deposits in the sella.

normal pituitary tissue. Sometimes a fat deposit (Figure 3 A, B) whithin the cavernous sinus can be observed. Diagnostic accuracy of ACTH secreting adenomas by CT has been 39-62%.[24,25]

Other types like TSH and FSH-LH secreting adenomas are quite rare. The clinical presentation of pituitary apoplexy comprises headache, nausea, visual disorders, stiffness of the neck and ophthalmoplegia.[26] The CT appearances depend on the type of the lesion-hemorrhage or necrosis. A high density area may extend towards the suprasellar region by hemorrhage (Figure 4). An ischemic lesion presents as an area of low density. Pituitary apoplexy occurs within a normal or neoplastic gland.[5] CT can visualize acute hemorrhage within approximatelly the first 3 days, but subacute and chronic hemorrhage may be confused with cystic degeneration or an abscess.[27]

The appearance of rare intrasellar lesions is nonspecific.[1,28] Some lesions are presented by low attenuation areas like cysts, epidermoids, abscesses, while others are enhancing lesions such as metastases, infundibulomas, germinomas and granulomas. In some lesions calcification can be observed e.g. craniopharyngeomas, chondromas and chordomas.

In pituitary dwarfism CT demonstrates a small gland with aplastic or hypoplastic pituitary stalk.[29] This forms can be better visualized by MRI due to improved spatial resolution.[30]

CT is also helpfull in visualization of surgical changes, complications and residual or recurrent tumours. CT is also an established method after surgery in the sellar region[31] using transphenoidal approach in the intrasellar lesion or the subfrontal approach in large tumours with suprasellar extension. After complete transsphenoidal removal of the tumour a mass is visible which does not return to normal size immediately after surgery, but gradually reverts to normal after 3 or 4 months.[32]

Gaps on the sphenoid bone, osseous grafts placed to reconstitute the sellar floor are presented on CT scans after transphenoidal surgery. The sellar content may be partially or completely emptied, and the pituitary stalk inclined to the remnant stump of the pituitary tissue. The cavity may be filled with muscle fat, gelfoam or surgical. Sometimes it is not possible to differentiate this material from a recurrent tumour. Diagnosis of pituitary gland or a recurrent tumour is easier if fat has been used for packing.

Acknowledgement

I would like to express my gratitute to Mrs. Tuckwell for her effort and help in preparing of English manuscript.

References

1. Naidich TP, Pinto RS, Kushner MJ, Lin JP, Kricheff II, Leeds NE, Chase NE. Evaluation of sellar and parasellar masses by CT. *Radiology* 1976; **120:**91-9.
2. Syvertsen A, Haughton VM, Williams AL, Cusick JF. The computed tomographic appearance of the normal pituitary gland and pituitary microadenomas. *Radiology* 1979; **133:**385-91.
3. Wolpert SM, Post KP, Biller BJ, Molitch ME. The value of CT in evaluating patients with prolactinomas. *Radiology* 1979; **131:**117-20.
4. Roppolo HMN, Latchaw RE, Meyer JD, Curtin HD. Normal pituitary gland: Macroscopic-anatomy CT correlation. *AJNR* 1984; **4:**927-36.
5. Maravilla KR. Computer reconstructed sagittal and coronal computed tomography head scans: Clinical applications. *J Comp Assis Tom* 1978; **2:**189-98.
6. Marotti M, Lovrenčić M, Kalousek M, Klarić R, Krolo I, Klanfar Z, Sekso M. Vrijednost frontalne i sagitalne rekonstrukcije u dijagnostici hipofiznih tumora. *Lij Vjes* 1984; **106:**429-34.
7. Hemminghytt HS, Kolnhoff RK, Daniels DL, Williams AL, Grogan JP, Haughton VM. Computed tomographic study of hormone-secreting microadenomas. *Radiology* 1983; **146:**65-8.
8. Davis PC, Hoffman JC jr, Tindall GT, Braun IR. Prolactinsecreting pituitary microadenomas: Inaccuracy of high-resolution CT imaging. *AJNR* 1984; **5:**721-6.
9. Daniels DL, Willliams AL, Thornton RS, Meyer GA, Cusick JF, Haughton VM: Differential diagnosis of intrasellar tumours by computed tomography. *Radiology* 1981; **141:**693-701.
10. Earnest F, Mc Cullough EC, Frank DA. Fact or artifact: an analysis of artifact in high-resolution computed tomographic scanning of the sella. *Radiology* 1981; **140:**109-13.
11. Lovrenčić M, Kalousek M, Klarić R, Sekso M. Computertomographie des Inhaltes der Sella turcica in transversaler und frontaler Ebene. *Fortschr Röntgenstr* 1984; **141:**417-22.
12. Boneville JF, Cattin F, Dietemann JL. *Computed tomography of the pituitary gland,* Springer, 1986 Berlin, Heidelberg.
13. Irnberger Th. Die hochauflösende koronare Computertomographie bei endokrin aktiven Mikroadenomen der Hypophyse unter besonderer Berücksichtigung ihrer Kontrastmitteldynamik. Fortschr *Röntgenstr* 1985; **143:**315-21.
14. Bonneville JF, Cattin F, Moussa-Bacha K, Portha C. Dynamic computed tomography of the pituitary gland. The tuft sign. *Neuroradiology* 1983; **149:**145-8.
15. Drayer BP, Rosenbaum AE, Kennerdell JS, Robinson AG, Bank WO, Deeb ZL. Computed tomographic diagnosis of suprasellar masses by intrathecal enhancement. *Radiology* 1977; **123:**339-44.
16. Kalousek M. Usporedba nalaza kompjutorizirane tomografije i neurološke simptomatologije tumora selarnog i periselarnog područja. *RAD JAZU* 1985; **20:**109-27.

17. Peyster RG, Hoover ED, Viscarello RR, Moshang Th, Hasnia ME. CT appearance of the adolescent and preadolescent pituitary gland. *AJNR* 1983; **4:**411-14.
18. Roppolo HMN, Latchaw RE. Normal pituitary gland; Microscopic anatomy – CT correlation. *AJNR* 1983; **4:**937-44.
19. Davis PC, Hoffman JC jr, Tindall GT, Braun IF. CT surgical correlation in pituitary adenomas. Evaluation in 113 patients. *AJNR* 1985; **6:**711-6.
20. Jung RT, White MC, Bowley NB, Bydder G, Mashiter K, Joplin GF. CT abnormalities of the pituitary in hyperprolactinemic women with normal or equivocal sellae radiologically. *Med Jour* 1982; **285:**1078-81.
21. Lovrenčić M, Kalousek M, Sekso M, Vizner B, Gnjidić Ž. CT in pituitary tumours with emphasis on prolactinomas and growth-hormone secreting adenomas in Calabro A, Leonardi M: *Computer aided neuroradiology*. CID Ediz Inter 1987 Roma, 431-4.
22. Marcovitz S, Wee R, Chan J, Hardy J. Diagnostic accuracy of preoperative CT scanning of pituitary prolactinomas. *AJNR* 1988; **9:**13-7.
23. Marcovitz S, Wee R, Chan J, Hardy J. Diagnostic accuracy of preoperative CT scanning of pituitary somatotroph adenomas. *AJNR* 1988; **9:**19-22.
24. Marcovitz S, Wee R, Chan J, Hardy J. The diagnostic accuracy of preoperative CT scanning in the evaluation of pituitary ACTH – secreting adenomas. *AJNR* 1988; **9:**23-6.
25. Savis SC, Patronas NJ, Doppmann JL, Loriaux DL, Cutlet GB, Hieman LK, Chronsos GP, Olfield ED. Cushing syndrom: Pituitary CT scanning. *Radiology* 1987; **162:**775-7.
26. Post JD, David NJ, Glaser JS, Safran A: Pituitary apoplexy: diagnosis by computed tomography. *Radiology* 1980; **134:**665-70.
27. Ostrov SG, Quencer RM, Hoffman JC, Davis PC, Hasso AN, David NJ. Haemorrhage within pituitary adenomas: How often associated with pituitary apoplexy syndrome. *AJNR* 1989; **10:**503-10.
28. Miller JH, Peña AM, Segall HD. Radiological investigation of sellar region in children. *Radiology* 1980; **134:**81-7.
29. Lovrenčić M, Kalousek M, Kadrnka-Lovrenčić M. CT analysis of the pituitary gland and stalk in pituitary dwarfism and in children without pituitary disorders. *Neuroradiology* supp 1991; **33:**270-2.
30. Kelly WM, Kucharczyk J, Kjos B, Peck WW, Norman D, Newton TH. Posterior pituitary ectopia: an MR feature of pituitary dwarfism. *AJNR* 1988; **9:**453-60.
31. Dolinskas CA, Simeone FA. Transsphenoidal hypophysectomy: Postsurgical CT findings. *AJR* 1985; **144:**487-92.
32. Teng MMH, Huang ChI, Chang T. The pituitary mass after transsphenoidal hypophysectomy. *AJNR* 1988; **9:**23-6.

Adv Radiol Oncol 1992; 41-6.

Chest CT in sarcoidosis

Dalagija F, Dizdarević Z, Bešlić Š

University Medical Center Sarajevo
Institute of Radiology and Oncology

The findings of chest CT in 52 patients with intrathoracic sarcoidosis have been analysed retrospectivelly and compared with the appropriate findings of the conventional chest radiographs.
The obtained results, agreeing with the attitudes in literature, confirmed the superiority of CT over the chest radiography. CT provides the accurate and safe detection, evaluation and follow-up of changes in hila, lung parenchyma, pleura and particularely in mediastinum.
However, besides all qualities and advantages, CT should be performed after chest radiography, which is considered to be the main radiologic diagnostic method for thoracic organs.

Key words: thoracic diseases, sarcoidosis, tomography, x-ray computed

Introduction

Sarcoidosis is a systemic granulomatous disease of unclear etiology.[11] Although it can affect any organ, mediastinal and hilar lymphnodes and lung parenchyma are involved in more than 90% of patients.[2] The changes can spontaneously regress, or progress to fibrosis.[3]

Therefore, adenopathy with or without parenchymatous disease is a radiographic hallmark of sarcoidosis.[4] Most frequently, in about 90%, bilateral symmetric hilar adenopathy is present and it is often associated with the paratracheal adenopathy.[1]

Besides clinical, laboratory, endoscopic and bioptic and conventional radiologic methods (plain radiography in two positions, fluoroscopy, esophageal passage, conventional tomography in three projections), computed tomography (CT) has been used in the diagnosis of intrathoracic sarcoidosis, during the last ten years.

Although CT cannot replace conventional radiography, it is believed to represent an improvement in the investigation of intrathoracic sarcoidosis.[5,6,7,8,9,10]

Correspondence to: dr. Faruk Dalagija, Institut za radiologiju i onkologiju UMC-a Sarajevo, Ul. Moše Pijade 25.

UDC: 616.2-002.582-076.756.8

Materials and methods

With the aim to analyse the possibilities of CT in the diagnosis of intrathoracic sarcoidosis, the authors have presented a retrospective analysis of chest radiographs and chest CT in 52 patients with this disease. There were 36 (69%) females and 16 (31%) males, aged 17-60 years (mean 35 yrs); 70% of patients were aged 25-40 years. Twenty patients (38%) had nodose erythema of the lower leg skin with elevated erythrocyte sedimentation values.

CT examinations were performed on Somaton SF and DR Siemens units with 8 and 4 slice thickness, before and after i.v. administration of contrast media in the form of bolus and/or

infusion. Both windows (mediastinum and lung parenchyma) were used.

The evaluation of the expresiveness and quality of the presentation of changes in hila, mediastinum and lung parenchyma was performed by two experienced radiologists independently. Four marks were used to classify the changes as slight (±), medium (+), marked (++) and extremely pronounced (+++).

Hilar and mediastinal lymphnodes were considered as enlarged when their diameter exceeded 5 and 10 mm, respectively.[3]

Lung changes included nodular opacification in lung parenchyma, pleural thickening and fibrosis.

Results

The analysis of hilar adenopathy

Hilar adenopathy was detected in all 52 (100%) patients by conventional radiography and confirmed by CT.

Whereas on chest radiographs bilateral hilar adenopathy was present in 43 (82.7%) patients, and unilateral, in 9 (17.3%) CT detected bilateral hilar adenopathy in all 52 (100%) patients. On chest radiographs, it appeared symmetric in 27 (51,9%) patients, CT defined it in 43 (82,7%) patients, while 7 (13,5%) patients had enlarged right, and 2 (3,8%) enlarged left hilus.

More than a half of the patients had medium hilar adenopathy (+) on chest radiograph, on CT it was marked (++).

The analysis of mediastinal adenopathy

Whereas on chest radiographs the involvement of mediastinum was present in 22 (42,3%) patients, CT detected mediastinal adenopathy in 49 (94,2%) patients. Chest radiographs showed bilateral adenopathy only in 5 (9,6%) patients, CT detected it even in 44 (84,6%) patients. Out of that, symmetric bilateral mediastinal adenopathy was detected in 29 (55,7%) patients, and asymmetric in 15 (28,8%) patients, in all these it was situated more to the right. Unilateral right-sided mediastinal adenopathy, as apparent in 17 (32.7%) on chest radiograms, was confirmed by CT only in 5 (9,6%) patients. Unilateral left sided mediastinal adenopathy remained unconfirmed both by chest radiography and CT.

Chest radiographs evidenced slight (±) and medium (+) mediastinal involvement, CT scans mostly showed, medium (+) and marked (++) mediastinal adenopathy.

The analysis of parenchymal and pleural disease

Nodular opacifications on chest radiographs were confirmed in 15 (28,8%) patients – mostly slight (±) CT scan presented it in 29 (55,7%) patients mostly as medium (+) and marked.

Interstitial fibrosis was confirmed on chest radiographs in 5 (9,6%) patients mostly as slight (±), whereas CT scan presented it in 18 (34,6%) patients as medium (+).

In 6 (11,5%) patients, CT scans alone confirmed pleural changes (pleural thickening) mostly as slight (±), in 7 (13,5%) as bullous disease, and in one patient pneumothorax.

Discussion

Sarcoidosis has been known for over a hundred years. It is a systemic granulomatous disease of unclear etiology. According to two basic theories presented in literature, sarcoidosis is a syndrome of the immune response due to various causative agents or caused by, still undetected agent.[1]

Histologically, it is characterized by noncaseating granulomata in a number of body organs and tissues (liver, spleen, skin, eyes, bones, salivary glands); in over 90% of cases, mediastinal and hilar lymphnodes and lung parenchyma are involved.[2]

Therefore, adenopathy with or without parenchymatous disease is a radiographic hallmark of sarcoidosis. Most frequently, paratracheal, tracheo-bronchial and hilar lymphnodes are involved. Bilateral symmetric hilar adenopathy, usually with paratracheal adenopathy is presen-

ted in about 90% of patients.[1] However, differentiating it from hilar, paratracheal adenopathy can be also asymmetric.[11]

Unilateral hilar adenopathy is considered as rare, as the paratracheal without hilar adenopathy. Besides, subcarinal, anterior and posterior mediastinal lymphnodes may be affected.[11,12]

It has been asserted that parenchymal disease, as well as adenopathy is characteristically bilateral and asymmetric, but exceptions are seen during the growth or regression of the disease. There are four forms of those changes: reticulnodular is most frequent, acinous (rarely) and relatively rare large – nodular. The fourth form is interstitial fibrosis with consecutive lung arterial hypertension and hypertrophia of the right ventricle.[1,13]

As it has been confirmed, 25-30% of patients with sarcoidosis have non-typical radiographic appearance. 90-100% would have the changes in lung parenchyma, and almost 1/4 would have the respiratory insufficiency. 5-10% of patients would die of this disease–mostly because of the respiratory insufficiency and cor pulmonale. So, early recognition of those anomalies has been suggested.[10,14,15]

CT, which has been performed during the last ten years, confirmed its superiority over the chest radiography in diagnosis of intrathoracic sarcoidosis. Because of the presentation in transverse projection without superposition of anatomic structures, CT has the significantly increased sensitivity in the detection, evaluation and follow-up of parenchymatous and pleural changes and intrathoracic adenopathy.[5,10,11,16,17,18,19,20]

Most frequently, chest radiographs have presented hilar and right-sided paratracheal adenopathy, while subcarinal area, aorto-pulmonary window and azygo-esophageal recess, are considered as areas with unadequate radiographs for the detection of adenopathy.[16] However, CT enables the accurate detection and complete evaluation of the extent of lymphadenopathy, smaller sizes even in unusual localizations. It refers to the unsuspected anterior mediastinal adenopathy including internal mammary nodes, paratracheal (with or without calcifications) and subcranial nodes.[8,9,10,11,12,16,21]

Sarcoidosis is characterized by the presence of noncaseating microscopically sized granulomatas, which could take the form of macroscopic nodules. It has been confirmed that they are placed along the blood vessels and bronchi, subpleurally and along the interlobar septae, and that this distribution closely correlates with the biopsy findings. Fibrosis, occurring in sarcoidosis, mostly involves the peribronchovascular region.[22,23,24] Because of the superimposition of parenchymal shadows, chest radiography is insensitive for the presence of parenchymal changes. Patients without parenchymal anomalies on the chest radiographs have granulomatas on transbronchial biopsy in more than 60% of cases.[23,24]

However, CT is considered superior to chest radiography in the detection of the presence and the extent of lung changes.[1,5,10,11,23] It can demonstrate the presence or absence of inaccurate, unclear, suspected or unsuspected parenchymatous changes on chest radiography.

Micronodular and interstitial infiltrates, alveolar infiltrates with or without air-bronchograms and mass-like conglomerates can be found. In patients with clear infiltrations, CT would show the complete extent of disease, including the pleural involvement.[10,23]

Secondary findings, detected by CT, include pleural effusions, bulous disease, bronchiectases, cavitations with or without micetomas and fibrosing mediastinitis.[5,10] Besides, the information obtained by CT enables the choice of the most useful method for the tissue confirmation (bronchoscopy, transtracheal, transbronchial or percutaneous needle biopsy).[10]

Although CT demonstrates the unsuspected cystic changes, pleural disease and lung noduses, it is noted that there are limitations in the detection and characterization of minimal disease. In the detection of unsuspected lung parenchymatous and pleural disease, high resolution CT (HRCT) proved to be superior to conventional CT. It is believe that HRCT can demonstrate fine lung detail, including septal thickening,

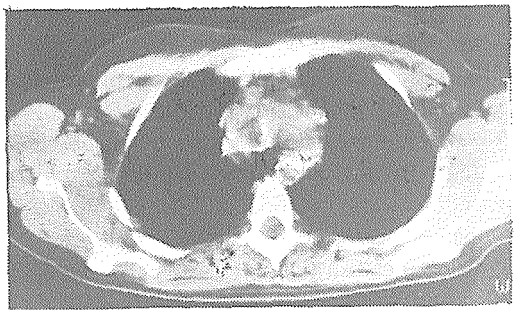

Figure 1. Anterior mediastinal and retrocaval lymphadenopathy.

Figure 2. Retrocaval and precarinal lymphadenopathy.

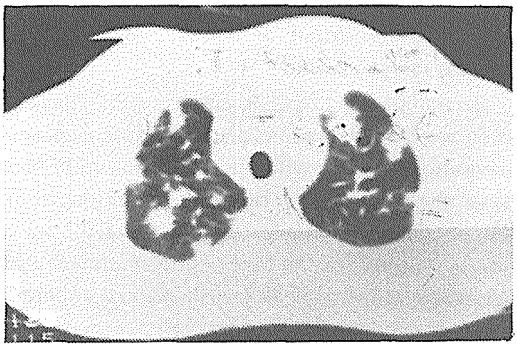

Figure 3. «Mass – like» infiltrates.

small nodular and focal areas of high density. Moreover, characterizing the extent of interstitial fibrosis, HRCT enables the selection of the appropriate biopsy site and follow-up of patients at therapy.[23,24,25]

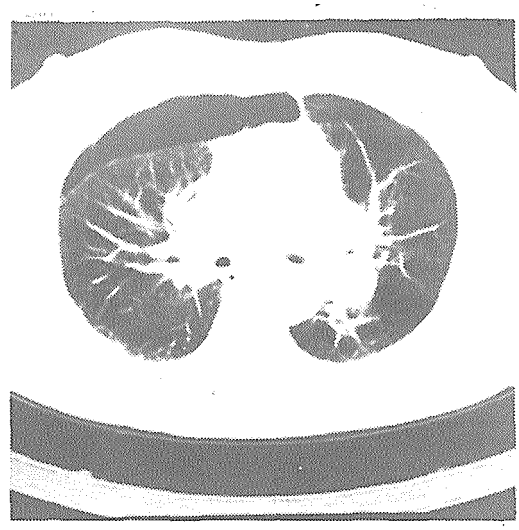

Figure 4. Pneumothorax of the right upper lobe.

The presented results in this study, and the experience of the cited authors have confirmed the superiority of CT over chest radiography.

Transverse presentation without superinposition of the particular structures with greater spatial and contrast resolution of CT enables a relativelly simple and safe evaluation of hilar and especially mediastinal lymphadenopathy, as well as changes in lung parenchyma and pleura. CT detected bilateral hilar adenopathy in 17,3%, symmetric hilar adenopathy in 30,7%, total mediastinal adenopathy in 51,9% and bilateral mediastinal adenopathy even in 75% of patients i.e. more than by chest radiography. The greatest diferences relate to unsuspected enlargement of the anterior mediastinal including internal mamary, retrocaval, subcarinal, para – aortal and lymphnodes in aortic window (Figure 1 and 2).

The same is true of nodular opacification in lung parenchyma, confirmed by CT in 26,9% and fibrous changes in 25% of patients more than by chest radiography. The changes in lung parenchyma included small single or diffuse and single medium nodular opacifications and the large »mass-like« infiltrates (Figure 3).

In 6 patients, only CT detected pleural changes, in 7 patients bulous disease and rightsided pneumothorax in one patient were found (Figure 4).

All parenchymal and pleural changes are mostly pesented only by the window for lung parenchyma. In most of the patients, all changes were more marked on CT scans than on chest radiographs. The greatest difference was found in unsuspected or slightly marked (±) changes on chest radiographs, while the tiny difference in marked (++) and sparse extremelly marked (+++) were found in chest radiographs and CT scans.

However, although superior over the conventional radiologic diagnostic methods, CT is not tissue-specific, so the tissue analysis of the disease is neccessary.

Since noncaseating granulomatas, as confirmed, may be present even when chest radiographs, conventional CT scans and HRCT scans are completely normal, it is considered that CT can not be used with the aim to exclude the diagnosis of lung sarcoidosis.[23]

Conventional tomography is considered superfluous when-ever CT can be performed. But, when there is no CT, conventional tomography remains a useful method.[6]

Finally, conventional chest radiography, an available, useful and inexpensive method, as part of the initial examination of the thoracic organs, remains the method of choice for routine detection, diagnosis and evaluation of intrathoracic sarcoidosis.[16]

Conclusion

On the basis of the obtained results, and according to the experiences of other authors, it is concluded that CT is superior to conventional radiologic diagnostic methods in the diagnosis of intrathoracic sarcoidosis. It enables more precise and safe detection, evaluation and follow-up of changes in the hila, lung parenchyma, pleura and particularly in mediastinum.

Since it is not tissue-specific, CT would provide the best results with other available diagnostic procedures including the endoscopic methods and biopsies with the tissue confirmation of sarcoidosis.

However, regardless all qualities and advantages, CT should be performed after conventional chest radiography which still remains the basic radiologic diagnostic examination of thoracic organs.

References

1. Miller BH, Putman CE. The radiographic manifestations of pulmonary sarcoid. *Postgraduate Radiology* 1985;**5:**291-318.
2. Crystal RG, Robert WC, Hunninghake GW, et al. Pulmonary sarcoidosis – A disease characterized and perpetuated by activated lung T-lymphocytes *Ann Inter Med* 1981; **94:**73-94.
3. Muller NL, Kulling P, Miller R. The CT findings of pulmonary sarcoidosis. Analysis of 25 patients. *AJR* 1989; **152:**1179-82.
4. Mc Loud TC, Eyler GR, Gaensler EA, et al. A radiographic classification of sarcoidosis: physiologic correlation. *Invest Radiol* 1982; **17:**129-38.
5. Soloman A, Kreel L, Mc Nicol M, Johnson N. Computer tomography in pulmonary sarcoidosis. *J Comput Assist Tomogr* 1979; **3:**754-8.
6. Heitzman ER. Computed tomography of the thorax: current perspectives. *AJR* 1981; **136:**2-12.
7. Stiris MG, Borthwick R. Computed tomography (CT) evaluation in pulmonary sarcoidosis. *Eur J Radiol* 1981; **1:**16-9.
8. Kreel IL. Computed tomography of interstitial pulmonary disease. *J Comput Assist Tomogr* 1982; **6:**181-99.
9. Gilman MJ, Laurens RG Jr, Somogy JW, Honig EG. CT attenuation values of lung density in sarcoidosis. *J Comput Assist Tomogr* 1983; **7:**407-10.
10. Hamper U, Fishman EK, Khouri NF, et al. Typical and atypical CT manifestations of pulmonary sarcoidosis. *J Comput Assist Tomogr* 1986; **10(6):**928-36.
11. Rodan BA, Putman CE. Radiologic alterations in sarcoidosis. In Fauburg BL, ed. *Sarcoidosis and other granulomatous diseases of the lung.* New York: Marcell Dekker, 1983:37-75.
12. Bein ME, Putman CE, Mc Loud TC, Mink JH. A reevaluaiton of intrathoracic lymphadenopathy in sarcoidosis. *AJR* 1978; **131:**409-15.
13. Kirks DR, Greenspan RH. Sarcoid. *Radiol Clin Norh Am* 1973; **11:**279-94.
14. Ellis K, Reenthal G. Pulmonary sarcoidosis. Roentgenographic observations on course of disease. *AJR* 1962; **88:**1070-83.
15. Stender HS. Roentgen diagnosis of sarcoidosis. *Prax Klin Pneumol* 1983; **37:**523-8.

16. Craig DA, Colletti PM, Ratto D, et al. MRI findings in pulmonary sarcoidosis. *Magnetic Resonance Imaging* 1988; **6(5):**567-73.
17. Bergin CJ, Muller NL. CT of interstitial lung disease: a diagnostic approach. *AJR* 1987; **148:**8-15.
18. Bergin CJ, Rogli V, Coblentz CL, Chiles C. The secondary lobule: normal and abnormal CT appearance. *AJR* 1988; **151:**21-5.
19. Webb WR, Stein MG, Finkbeiner WE, et al. Normal and diseased isolated lungs: high – resolution CT. *Radiology* 1988; **166:**81-7.
20. Bergin CJ, Coblentz CL, Chiles C, et al. Chronic lung diseases: Specific diagnosis by using CT. *AJR* 1989; **152:**1183-8.
21. Schnyder PA, Gamsu G. CT of the pretracheal retrocaval space. *AJR* 1981; **136:**303-8.
22. Thomas PD, Hunninghake GW. Current concepts of the pathogenesis of sarcoidosis. *Am Rev Respir Dis* 1987; **135:**747-60.
23. Muller NL, Mawson JB, Mathieson JR, et al. Sarcoidosis: Correlation of CT with clinical, functional, and radiological findings. *Radiology* 1989; 171-3.
24. Lynch DA, Webb WR, Gamsu G, et al. Computed tomography in pulmonary sarcoidosis. *J Comput Assist Tomogr* 1989; **13(3):**405-10.
25. Mayo JR, Webb WR, Gould R, et al. High resolution CT of the lungs: an optimal approach. *Radiology* 1987; **163:**507-10.

Adv Radiol Oncol 1992; 47–50.

Computed tomography during arterial portography of the liver without interslice gap

Yasumori K, Hasuo K, Baba H, Yoshida K, Mizushima A, Hirakata R, Kuroiwa T, Onitsuka H and Masuda K

Department of Radiology, Faculty of Medicine, Kyushu University, Japan

Computed tomography during arterial portography of the liver without any interslice gap was done using a rapid sequential CT scanner. A run of eight continuous scans of the liver was obtained during a single breathhold, which was followed by another run after about one minute interval for breathing. The examinations were judged to be adequate in 80 out of 91 patients. This method allows us to scan the entire liver without any interslice gap and to expect confident detection of a hepatic mass as small as 5 mm in diameter with a relatively small amount of contrast medium.

Key words: portography; tomography, x-ray computed

Introduction

Computed tomography during arterial portography (CTAP) is one of the most sensitive methods to detect hepatic tumours.[1,2,3,4] When a lesion is clinically suspected or when a hepatic tumour is evident and more lesions need to be searched to decide the surgical indication, CTAP is selected for this purpose. Theoritically, the entire liver should be scanned without any interslice gap. However, this has not been an easy task due to the restrictions of a conventional CT scanner. For instance, the conventional CT scanner requires longer scanning time and interscan delay. In this paper, we describe the use of a rapid sequential CT scanner for CTAP without any interslice gap.

Correspondence to: Dr. K. Yasumori, 3-1-1, Maidashi Higashi-ku, Fukuoka, Japan.

UDC: 616.149-076.73:616.36-076.756.8

Materials and methods

A TCT-900S scanner (Toshiba, Tokyo), equipped with a slip-ring system to eliminate interscan delay, was used. Scanning time was one second and the time for table movement was two seconds.

To assess the low-contrast object detection by the CT scanner, we used a phantom containing agar embedded with spheres. The spheres were prepared by polyphenylethylene-resin ranging 3, 5, and 10 mm in diameter. The difference of attenuation coefficients in Hounsfield units (HU) between agar and spheres was set at 40 HU. The phantom was scanned consecutively by means of the same technical factors as used in clinical practice (200 mA, 120 kVp and 10 mm slice thickness) except that overlapping scan technique with a table excursion of 0.5 mm was used.

Ninety one patients with known or suspected hepatic tumours underwent CTAP. A catheter was introduced into the superior mesenteric artery in the angiographic room and a patient was then transported to the CT room. The

cranial limit of the liver was determined from a digitized radiograph. Immediately after administering tolazoline (20 mg) through the catheter, contrast material (Omnipaque, Daiichi; iodine 220 mg/ml) was infused from a volume flow rate injector at a rate of 0.9 ml/sec for 45 seconds. Forty seconds after the beginning of the contrast injection, a run of eight scans with slice thickness and table excursion of 10 mm was obtained with automatic table incrementation. These scans were done under a single breathhold of 22 seconds. At about one minute interval for breathing, contrast material was infused at the same rate for 40 seconds. The second run of eight contiguous scans was obtained immediately after contrast injection under another single breathhold. The last slice of the first run of eight scans was overlapped with the first slice of the second run to keep gapless scanning of the liver. The total dose of iodine used was 16.8 g per patient.

An average attenuation coefficient with one standard deviation was obtained from the tumour, hepatic parenchyma and abdominal aorta of ten patients with hepatocellular carcinoma larger than two centimeters in diameter determined from surgical specimen. All the data were plotted against the order of slices.

Results

In the phantom study, the 10 mm sphere was detected in 36 consecutive slices, the 5 mm sphere in 26 slices and the 3 mm sphere in 18 slices, respectively (Figure 1).

In clinical study, no dislodgement of the catheter or other complication were observed. The 22 second rapid sequential scanning technique was short enough for all patients to hold their breath. No interslice gap was seen between the first and second runs of scanning. The entire liver was scanned in 89 patients as shown in Figure 2. In the remaining two patients, the liver was not completely scanned. One of them had marked hepatomegaly and the other had a large mass with exophytic growth. Inhomogenous enhancement of the hepatic parenchyma of nine patients was so prominent that the examinations were judged to be inadequate. The smallest nodule detected on CTAP and confirmed by surgery was 5 mm in diameter.

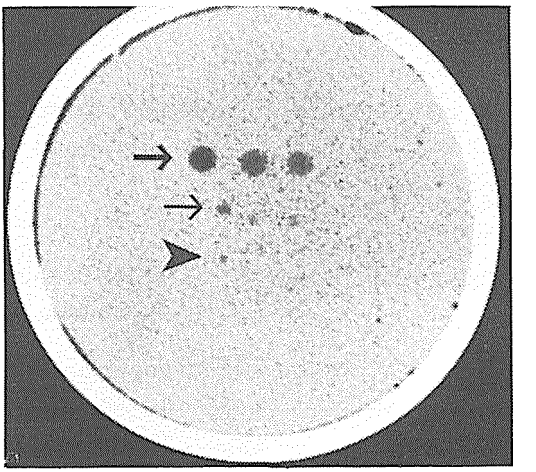

Figure 1. One of the slices obtained on scanning of the phantom. Spheres with three kinds of diameter are identified as low density areas in the leftmost row. (thick arrow: 10 mm, thin arrow: 5 mm, arrowhead: 3 mm in diameter).

The average attenuation coefficient was as follows: the hepatic parenchyma was between 116 and 134 HU, hepatocellular carcinoma was from 44 to 79 HU and the aorta progressively increased from 72 to 122 HU. The density difference between tumours and the liver ranging from 37 to 90 HU with the mean value of 67 HU was observed (Figure 3).

Discussion

Other reports have shown that the scanning time with usual CTAP technique is 2 to 3 minutes for the entire liver.[1-5] During this period, contrast medium is continuously injected with a total iodine load of 33.3 g (1), 25.4 to 28.2 g (2), 15,3 to 21.4 g (3), 28.2 to 30.0 g (4) or 25.5 g (5). Twelve to twenty scans are obtained and the patients need to hold their breath during each scan.

There are several weak points with these reported techniques. First, as respiratory excursion changes each time, there is a possibility to

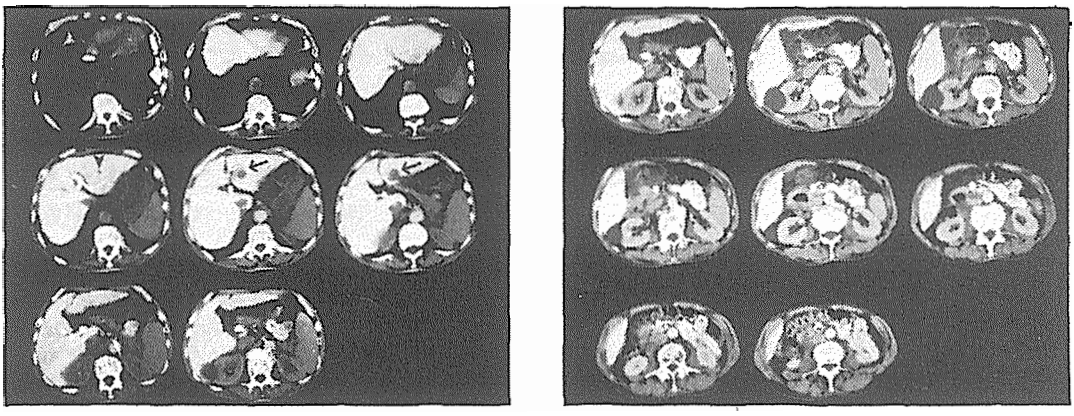

Figure 2. A representative case with two foci of hepatocellular carcinoma confirmed by surgery.
a – In the first run of eight continuous scans, two lesions in the left lobe of the liver (arrows and arrowhead) are evident. The smaller one (arrowhead) was one centimeter in diameter in the surgical specimen.
b – In the second run of another eight continuous scans, almost the entire liver is scanned. Note that there is no interslice gap between the last slice of the first run and the first slice of the second run.

miss small lesions. Second, continuous injection of contrast medium throughout the scanning results in large amounts of contrast medium. This is unfavorable because CTAP is usually carried out as a part of hepatic arteriography. Moreover, the difference in attenuation coefficients between the hepatic parenchyma and tumour remains smaller in a low dose rate infusion of contrast medium.

We have demonstrated an experiment to assess the theoretical low-contrast object detection by our clinical CTAP technique. Applying the result of our experiment to clinical practice, one must consider not only the difference of the table excursion between them, but also the attenuation coefficient difference between sphere-agar and tumour-hepatic parenchyma. In the experiment, the spheres larger than 5 mm in diameter could be visualized in more than 20 consecutive slices under the overlapping scan technique (slice thickness of 10 mm and table excursion of 0.5 mm), indicating that these spheres should be detected by 10 mm collimated continuous method as applied in our clinical practice. Moreover, in the experiment, the attenuation coefficient difference between the sphere and agar (40 HU) was set less than that of the average between the tumour and hepatic parenchyma (67 HU) seen in clinical practice.

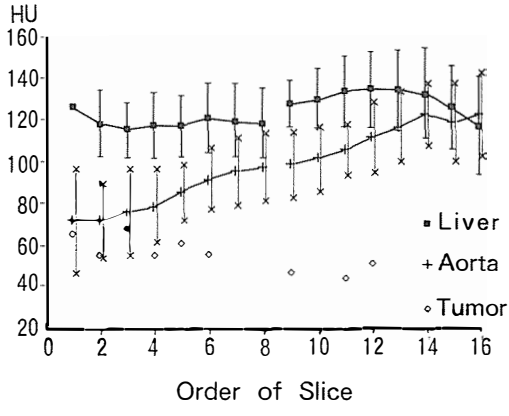

Figure 3. Changes of attenuation coefficients during CTAP. Attenuation coefficients of hepatic parenchyma, abdominal aorta and hepatocellular carcinoma are plotted against the order of slices (average of 10 patients with 1 SD). The density difference between the hepatic paranchyma and tumour ranged from 37 to 90 HU with the mean value of 67 HU.

The greater the attenuation coefficient difference is obtained, the more clearly the sphere or lesion is depicted. Based on these facts, lesions larger than 5 mm in diameter are expected to be constantly detected by our clinical CTAP method.

In clinical cases, 22 seconds was short enough for the patients to hold their breath and interslice gap was not seen between the first and second runs of scanning owing to overlapping by one

slice. The density difference between the tumour and liver, which was 67 HU on the average, was sufficient on the images. The amounts of contrast material used were far smaller compared with other reports. Although suboptimal studies seen in nine of our patients, all of whom showed inhomogenous enhancement of the hepatic parenchyma mainly caused by inflow of unopacified blood from the splenic vein[5], are inherent in CTAP, we believe our CTAP technique without interslice gap is a promising method. This technique should be performed along with angiography in patients who are potential candidates for hepatic resection.

Acknowledgement

‹We thank David J. Yang and Yoshiyuki Umezu for the preparation of this manuscript.›

References

1. Foley WD. Dynamic hepatic CT. *Radiology* 1989; **170:**617-22.
2. Heiken JP, Weyman PJ, Lee JKT, Balfe DM, Picus D, Brunt EM Flye MW. Detection of focal hepatic masses: prospective evaluation with CT, delayed CT, CT during arterial portography, and MR imaging. *Radiology* 1989; **171:**47-51.
3. Matsui O, Kadoya M, Suzuki M, Inoue K, Itoh H, Ida M, Takashima T. Sequential computed tomography during arterial portography in the detection of hepatic neoplasms. *Radiology* 1983; **146:**721-7.
4. Nelson RC, Chezmar JL, Sugarbaker PH, Murray DR Bernardino ME. Preoperative localization of focal liver lesions to specific liver segments: utility of CT during arterial portography. *Radiology* 1990; **176:**89-94.
5. Beers BV, Pringot J, Gigot JF, Dautrebande J, Mathurin P. Nontumorous attenuation differences on computed tomographic portography. *Gastrointest Radiol* 1990; **15:**107-11.

Adv Radiol Oncol 1992; 51–5.

CT-guided percutaneous drainages of abdominal abscesses

Lincender L

University Medical Center
Institute of Radiology and Oncology
Sarajevo

During the period of 6 years 98 CT-guided percutaneous drainages of abdominal abscesses and fluid collections were performed. The accurate CT guidance of drainage enabled a successful procedure in 90 (98%) patients whereas in 8 (8%) patients, drainage failed to result in a cure and 5 (5%) patients underwent an additional surgery. There were no complications. The importance of the percutaneous drainage of abdominal abscesses guided by CT has been discussed.

Key words: abscess, drainage, abdomen, tomography, x-ray computed

Introduction

Percutaneous drainage has become a method of choice in the treatment of a majority of abdominal and retroperitoneal abscesses and fluid collections.[1] For a successful percutaneous drainage it is important to define the origin of the abscess, its relationship to the surrounding anatomic structures, the nature of fluid content and presence of digestive fistulas. Apart from other radiologic methods, especially US[2,3], percutaneous drainages are successfully performed when guided by CT[4] or by the combination of US and CT.

The use of percutaneous drainage as a palliative procedure to decrease high morbidity and mortality, along with the surgical drainage in critical patients provides a significant success. Techniques such as CT and US facilitate localization, identification and extension that, is its septation. Dynamic CT suggests also the nature of the abscess wall, which is one of the factors that can increase the risk of bacteriological infection in the course of abscess drainage.[5]

Obrez[6] was one of our first authors, who reported on the percutaneous drainages of abdominal abscess.

Correspondence to: dr. Lidija Lincender, Institute of Radiology and Oncology, University Medical Center Sarajevo, Moše Pijade 25, 71000 Sarajevo, Yugoslavia.

UDC: 616-002.3-076.756.8

Material and methods

Percutaneous drainages in the abdomen under the guidance of CT have been performed since 1984. We performed the drainage after a detailed CT treatment and the analysis of clinical and laboratory findings. We analysed 98 drainages of the abdomen, among which 84 patients had only one drain, 12 had 2, and two patients had 3 drains. The duration of drainage was from one to 60 days. There were 60 (61%) males and 38 (39%) females. The patients were 10-70 years, old most of them – 27 (28%) were 61-70 years of age; 77 (79%) patients were hospitalized, and 21 (21%) underwent a CT-guided percutaneous

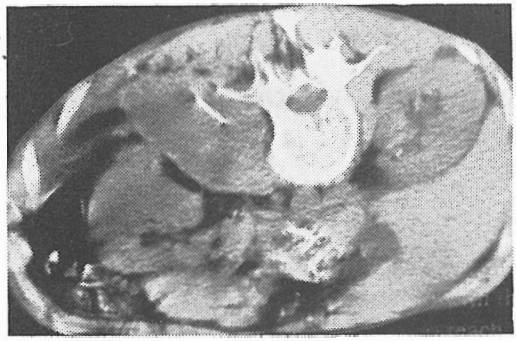

Figure 1. Biopsy of an abscess in the region of the left m. psoas with an 18 gauge needle.

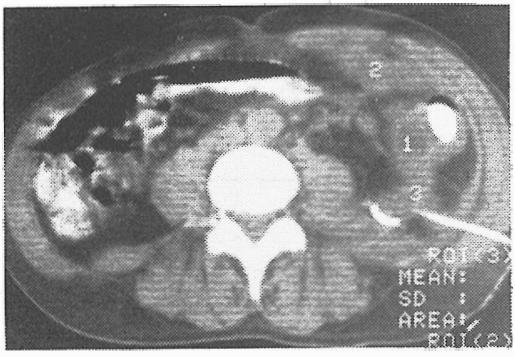

Figure 2. Drainage catheter placed into a retroperitoneal abscess by the left dorsal approach.

Figure 3. Abscessography – a retroperitoneal abscess with several pockets.

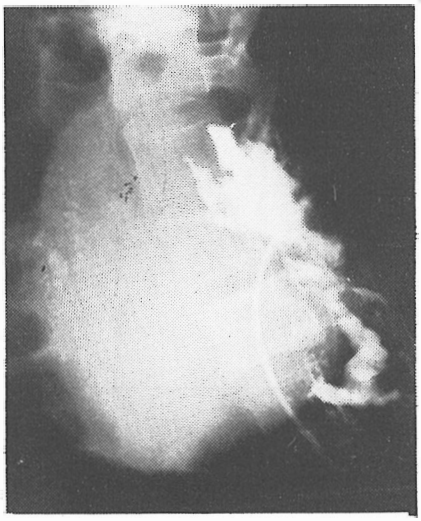

Figure 4. Abscessography – a retroperitoneal abscess in pancreatitis.

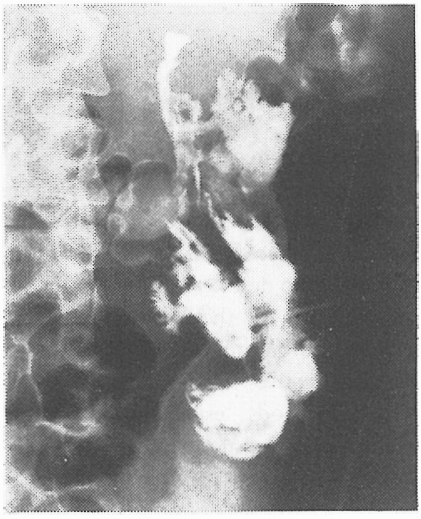

Figure 5. Follow-up abscessogram in an abscess at m. psoas.

drainage on the out-patient basis. Needle biopsy and aspiration of the abscess were done under the accurate CT localization of the needle-entering site. The aspirated content was taken immediately to the Institute of Microbiology for culture analysis and antibiogram. The abscess cavity was biopsied directly with a 18-gauge needle (Figure 1). Rarely we used first a 22 or 20 gauge

needle, and after the aspiration of contents the biopsy was continued with an 18 gauge needle, and after that a pig-tail catheter sized 8-12 was placed (Figure 2) using Seldinger's technique. For evaluation of the extent and septicity of the abscess cavity by diascopy, we applied a water-soluble iodine contrast medium (Figure 3,4), which was also used on the controle follow-up examinations to define a reduction or disappearance of the abscess cavity, i.e. to evaluate the success of therapy (Figure 5).

Results

Out of 98 percutaneous abdominal drainages, 57 (58%) patients had a bacterial infection whereas in 41(42%) the aspirates were sterile, even though 23 of them (24%) comprised inflammatory cellulary elements.

In the culture of 23 (24%) patients, anaerobic bacteria were isolated, and 34 (35%) patients had aerobic bacteria.

In the drainage contents of 18 (19%) patients neither bacteria nor cellulary elements were found (Table 1). Out of 98 percutaneous drainages of abscess collections, 90 (92%) drainages were successful, while 8 (8%) were not (Table 2).

Most of the patients with abdominal drainage had the collections around pancreas, which were sterile in 25 patients: 6 patients had some kind of anaerobic infection whereas 4 had an aerobic one.

Furthermore, most of the anaerobics were associated with retroperitoneal abscesses – in 5 patients (Table 3).

Of the patients with unsuccessful drainage, three had pancreatic and two retroperitoneal abscess (Table 4). They underwent additional surgery. The aspirated content in two patients with pancreatic abscess contained anaerobic bacteria in the culture, whereas aerobic bacteria were found in one patient. Anaerobic infection was found in the retroperitoneal abscess which required additional surgery.

Table 5 shows the duration of drainage (1-60 days), and the amount of drainage content ranging from 50 ml to 3 litres (Table 5).

Table 1. Microbiologic analysis of the aspirated material.

Culture +	No. of patients	Culture –	No. of patients
Aerobic infection	34 (35%)	Inflammatory cellular elements	23 (24%)
Anaerobic infection	23 (24%)	Without cellular elements	18 (19%)

Table 2. Abscess localization and results of percutaneous drainages.

Abscess localization	No. of patients	No. of successfully treated patients	No. of unsuccessfully treated patients
Pancreatic	35	32	3
Hepatic	9	8	1
Subphrenic	16	16	0
Subhepatic	6	6	0
Perirenal	4	4	0
Retro-peritoneal	13	11	2
Splenic	7	6	1
Ileocaecal	5	5	0
Interstitial	3	2	1

Table 3. Relationship between localization and abscess type in percutaneous drainage of abdominal abscess.

Localization	Type of abscess		
	Sterile content with cellular elements	Aerobic infect.	Anaerobic infect.
Pancreatic	25	4	6
Hepatic	2	5	2
Subphrenic	6	8	2
Subhepatic	3	3	0
Perirenal	0	2	2
Retro-peritoneal	3	5	5
Splenic	2	3	2
Ileocaecal	0	3	2
Interstitial	0	1	2
Total	41 (42%)	34 (35%)	23 (23%)

According to the localization and size of abscess, we used one catheter in 84 (86%) patients, two in 12 (12%) patients and 3 catheters in 2 (2%) patients. The catheters were from 5 F to 14 F (Table 6).

Discussion

Accurate determination of the direction in percutaneous drainage is one of the most important factors in the drainages of abdominal fluid collections, guided by the radiologic methods.[7]

Table 4. Unsucessful percutaneous drainages of abdominal abscesses with additional surgery.

Abscess localization	No. of treated patients	Additional surgery	Culture Aerobic	Culture Anaerobic
Pancreas	35	3	1	2
Retroperitoneum	13	2	0	2

Table 5. Duration of abdominal abscesses drainage and the amount of drainage content.

Abscess localization	Drainage duration of abdominal abscess	Amount od drainage content
Pancreatic	10–60 days	200–3000 ml
Hepatic	1–14 days	50– 250 ml
Subphrenic	7–21 days	500–2500 ml
Subhepatic	6–16 days	300–1500 ml
Perirenal	8–26 days	500–1200 ml
Retroperitoneal	21–45 days	200–2000 ml
Splenic	15–45 days	300–1500 ml
Ileocaecal	15–28 days	450– 600 ml
Interintestinal	13–21 days	750–1000 ml

Previously described contraindications for percutaneous drainages, gradually decrease. A successful drainage to a patient means cure. The reported literature has proved that these drainages provide good results together with a low rate of mortality.[4,6,8]

The ability to identify the agent and the culture of microorganisms in the aspirated contents helps to control the infection and to select an adequate therapy. The drainage process is completed when the abscess cavity is emptied, and when after 48 hours, catheter is closed and the content does not gather again.[5,9]

The analysis of material revealed that most of the abscesses and fluid collections that we had biopsed appeared after pancreatitis, though there were also subphrenic and retroperitoneal abscesses. The contents of 57 (58%) patients contained bacteria: 34 (35%) of these patients had aerobic and 23 (24%) anaerobic bacteria. Only 8 (8%) patients had unsuccessful drainage, and an additional surgery was performed in 5 (5%) patients.

Drainages are usually performed in hospitalized patients, but when the patient begins to recover during the course of drainage, he or she is being taught about the catheter hygiene and is

Table 6. Percutaneous abscess drainage with 1 or more catheters and their size in F.

Abscess localization	No. of patients	Catheter size in F	No. of catheters		
			one	two	more
Pancreatic and extraperitoneal fluid collection	35	5F – 12 F	30	3	2
Hepatic	9	6F – 12F	7	2	0
Subphrenic	16	7F – 12F	14	2	0
Subhepatic	6	8F – 12F	4	2	0
Perirenal	4	9F – 12F	4	0	0
Retroperitoneal	13	9F – 12F	11	2	0
Lien Splenic	7	7F – 12F	6	1	0
Ileocaecal	5	12F – 14F	5	0	0
Interstitial	3	6F	3	0	0
Total	98	5F – 14F	84 (86%)	12 (12%)	2 (2%)

discharged to home care with periodical follow-up checks. In a lesser number of patients, the drainage is performed in the out-patient basis.

Conclusion

According to our experience, the success of drainage depends on the type of agent; the greatest problem and the longest drainage was associated with anaerobic pancreatic abscesses. A good cooperation of the patient and the interventional radiologist, as well as the persistence in drainage duration make this procedure successful.

References

1. Mueller PR, van Sonnenberg E, Ferrucci JT. Percutaneous drainage of 250 abdominal abscesses and fluid collections. Part II: Current procedural concepts. *Radiology* 1984; **151:**343-7.
2. Otto R Ch. Interventional sonography for diagnosis and therapy. *Radiol Iugosl* 1990; **24:**341-5.
3. Frolich E, Striegel K, Heller Th, Frank U, Muhr T, Eberle S, Seeger G. Ultrasound guided percutaneous drainage of abdominal abscesses. *Radiol Iugosl* 1990; **24:**393-5.
4. Haaga Jh, Weinstein AJ. CT-guided percutaneous aspiration and drainage of abscesses. *AJR* 1980; **135:**1187-94.
5. Lang EK, Springer RM, Glorioso LW III, Cammarta CA. Abdominal abscesses drainage under radiologic guidance: Causes of failure. *Radiology* 1986; **159:**329-36.
6. Obrez I, Šurlan M, Pavčnik D, Klančar J. Perkutana drenaža apscesa u trbuhu. U: Mašković J, Boschi S, Stanić I. eds: *Intervencijska radiologija*. Split: ZLH 1986: 201-6.
7. Van Sonnenberg E, Ferrucci JT JR, M, Mueller PR, Wittenberg J, Simeone JF. Percutaneous drainage of abscesses and fluid collections. *Radiology* 1982; **142:**1-10.
8. Sones PJ. Percutaneous drainage of abdominal abscesses. *AJR* 1984; **142:**35-9.
9. Bernardino ME, Baumgartner BR. Abscesses drainage in the genitourinary tract. *Radiol Clin North Am* 1986: **24:**539-49.

Adv Radiol Oncol 1992; 56–9.

Computerized tomography of the spine

Papa J

Croatian Medical School, University of Zagreb, Clinical Medical Center Institute of Radiology, Zagreb

Within new trends in diagnostic radiology in which the concept of living pathology and imaging dominates, diagnostic possibilities of computer tomography of the spine are demonstrated. Indications and contraindications for CT of the spine are also shown as well as the comparison with other imaging methods.

Key words: spine, tomography, x-ray computed

The spine as well as other parts of the skeleton, have been interesting for clinicians and diagnostic radiology from the very beginning of the development of methods for visualizing human body. The specific structure of osseous tissue has presented, by means of classic radiologic methodology, the natural contrast towards other tissues, which has resulted in satisfactory imaging of the spine in a roentgenogram. Typical, functional, directed tomography of the spine has given the clinicians the first morphological information which have been very often insufficient for understanding the clinical manifestations of the spinal diseases. Thus, the concept od dynamic segment as the functional and morphological unit of the spine, created by vertebrologists, presents the first step in solving complex relationship between morphological changes and clinical symtpoms. This functional model is greatly simplified by getting into the focus of a pathologic process in the spinal canal, as a clearly defined space. If this space is endangered by any anatomic and pathologic structure, the pathologic symptoms occur. Computerized tomography of the spine (CT) perfectly fits into both mentioned clinical concepts. Simultaneous presentation of the osseous part of the spinal canal, paravertebral soft tissue and structures in the spinal canal in the antero–posterior dimen-

Correspondence to: dr. Papa J, Croatian Medical School, University of Zagreb, Institute of Radiology, Croatia.

UDC: 616.711-076.756.8

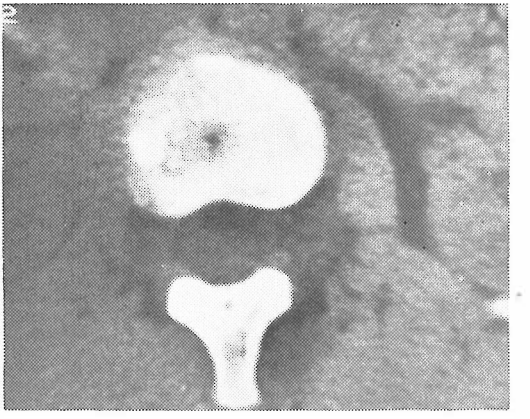

Figure 1. Transverse slice L1 in the intervertebral foramen.

sion does not enable only detailed visualization of the spine, but at the same time reveals the narrowest anterio-posterior diameter of the spinal canal (Figure 1).

From the radiological aspect, CT of the spine belongs to a large family of the so-called computerized radiology, thus subjected to all advantages and drawbacks attributed to tomography. This is particularly valid for the notion of partial volume effect due to which the measurement of absorption values in all parts of the spinal canal is not equally diagnostically reliable. On the other hand, visualization of the intraspinal structures is much better in lumbar part of the spine. This is due not only to the broader spinal canal in the lumbar part of the spine, but also to the natural contrasting quality which occurs because of the shape of the fatty tissue in the epidural space of the lumbar region. On these presumtpions are based the indications for spinal CT in which diagnosing of pathologic processes in the lumbar region has a dominant role compared to those in the cervical and thoracal parts. However, it must be mentioned that the application of spinal CT in diagnostics is limited by a conceptional problem and is closely connected with now already commonly accepted diagnostic strategy of imaging. In the algorithm of diagnostic visualization methods applicable to the spine, we nowadays have a whole series of methods varying not only in their scope, but also in the quality of morphologic information. Thus the clinician is faced with the problem of correct diagnostic and therapeutic procedure, in which knowledge of radiologic methodology has an important role.

Qualitatively new diagnostic results have been given by CT findings in patients with radicular compressive syndrome, thus enabling even closer collaboration with clinicians. This primarilly concerns the application of CT in the acute phase of disease, the possibilities of differentiating protrusion and prolapse of a disk, as well as the analysis of the radicular canal. The acute phase of the radicular compressive syndrome, although clinically easily recognizable in the case of bad

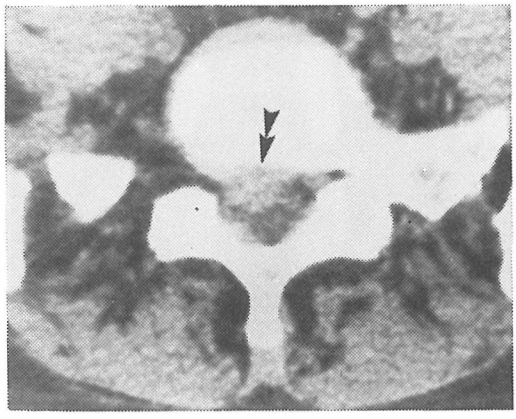

Figure 2. Dorsolateral prolapse of the L5-S1 disk.

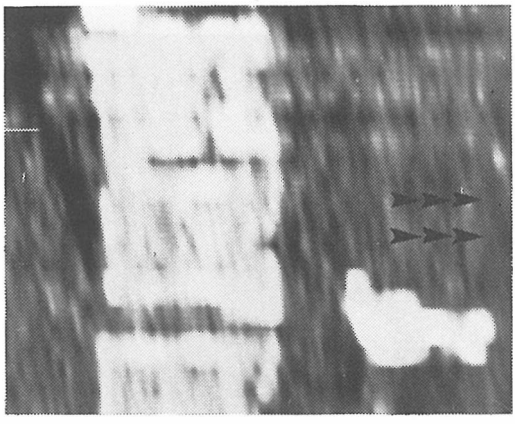

Figure 3. Sagittal reconstruction of the spinal canal after laminectomy.

treatment, can be the case of relapses during therapy. Repeated control CT examinations in this phase can give the clinicians very valuable information pointing to the size and site of a disk prolapse in the spinal canal, as well as the data about partial or complete withdrawal of the disk from the spinal canal. These data have a decisive role not only in the treatment of a patient, particularly in rehabilitation, but are very important for the prognosis of the disease. CT analysis of the dorsal part of a disk enables mutual differentiation of the disk protrusion or prolapse, and in this way it directly impacts the choice of conservative therapy and modalities of surgical treatment (Figure 2). In surgery, along with

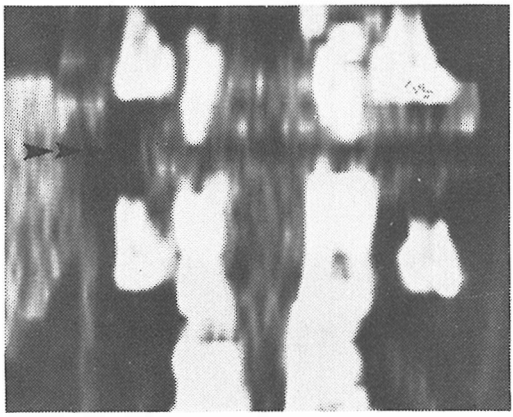

Figure 4. Coronal reconstruction of the spinal canal after laminectomy.

Figure 5. Condition after laminectomy. Infiltration of a tumorous process in the corpus. Tumorous enlargement of the soft paravertebral tissue on the left.

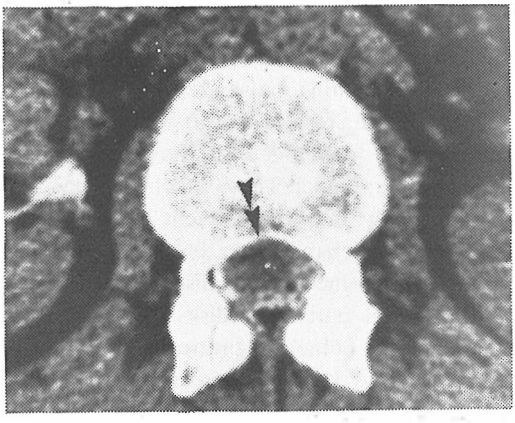

Figure 6. Cystic tumour in the lumbar spinal canal.

classic diskotomy, percutaneous approach to a disk has an important role as well. A completely new morphological entity is the finding of a bulging disk on CT. The basis of such a finding is the process of aging of a disk, which can very often be mistaken for a pathological process, and the patient with such a finding can sometimes be unjustifiably subjected to surgery. On the other hand, the insight into all parts of the spinal canal, through which the nerve root ends are passing on their way to the spinal ganglion, enables the CT investigation of localizations of root compression. Other methods do not offer possibilities for examining these localizations (lateral recessus stenosis, the condition of the vertebral canal, disk prolapses outside the spinal canal). The information obtained in such a way has a direct impact on the choice and size of surgical intervention (Figure 3, 4).

CT enables significant diagnostic achievements also in patients with an acute spinal injury. This is particularly valid for localizing longitudinal fractures in the area of the vertebral body, bony fragments in the spinal canal and pathological changes in the spinal cord, where CT myelography has an important role. These data are fully justified in cases of urgent surgical procedures, and often are more decisive for survival and lessening the degree of invalidity. Similar results are obtained in vertebral oncology, where CT helps in the estimation of the size of a neoplastic process, important for planning surgical and reconstructional intervention (Figure 5, 6).

Besides undoubtful diagnostic improvements achieved by means of CT in the analysis of the spine, it is necessary to mention disappointing results which have been obtained in the analysis of its cervical and thoracal parts. In these areas CT myelography has achieved additional diagnostic improvement, while magnetic resonance imaging has definitely established itself regarding the direct visualization of the spinal cord.

In the field of imaging methods, CT of the spine must be used rationally, according to the

clinically defined problem, knowing all its advantages and drawbacks. The clinician's knowledge of the achievements, dangers and faults of CT in comparison with other methods is the basis for building up the strategy of diagnostic procedure in the diseases of the spine. Here the patient and his disease are always the starting point and diagnostic method is only a tool for obtaining the diagnosis, but not at any price.

References

1. Genant, H K, Chafez N, Helms C A. *Computed tomography of the Lumbar Spine*. Univ. California, Press, San Francisco 1981.
2. Anderson R E. *Practical Aspects of CT Imaging of the Spine*. Year Book Med. Publ. Chicago 1982.
3. Post M J D. *Computed Tomography of the Spine*. Wiliams Wilkins, Baltimore 1984.
4. Papa J. Kompjutereizirana tomografija kralješnice. *Med enciklopedija*. Drugi dopunski svezak, 644-646, Zagreb MCMLXXXVI Jugoslavenski leksikografski zavod «Miroslav Krleža».

Adv Radiol Oncol 1992; 60–5.

Magnetic resonance imaging of kidney diseases

Marotti M[1], Hricak H[2], Kovačević D[1]

[1]Zavod za radiologiju kliničke bolnice «Sestre Milosrdnice», Zagreb, Department of Radiology and Urology,[2] University of California School of Medicine, San Francisco California

With the introduction of magnetic resonance imaging (MRI) in the abdominal region, the great diagnostic potential of the new technique has been clearly recognized. MRI has demonstrated outstanding anatomical view of retroperitoneal organs. With the improvements of contrast resolution and sensitivity, compared to exsisting modalities, MRI provide exstremelly usefull diagnostic informations of the genitourinary system. The article illustrates the potential values of MRI in displaying the normal renal anatomy and various pathological conditions. The brief introduction of the physical principals and some specific phenomena has been described.

Key words: kidney diseases, magnetic resonance imaging

Introduction

Magnetic resonance (MR) is a relatively new, noninvasive, nonionizing method of imaging which shortly after its introduction into clinical practice, gave a new dimension to the diagnostics of the uropoetic system. MR is comparable with computed tomography (CT) in representing anatomical details of the kidney, distingushing cystic from solid lesions, displaying a cause of obstructive disease as well as in the assesement of malignant tumour spread. MR showed promising results in the evaluation of kidney transplant rejection and kidney transplant function.[1, 2, 3] The main shortcoming of MR in the kidney disease evaluation, is in its inability to show small calcifications and distinguish them from fibrous tissue.[4] Calcifications are shown as areas void of signal.

The capability of MR to image pathological conditions in multiple planes improves the spatial orientation and visualization of tumour origin.[5] MR has a better contrast resolution than previous radiological imaging methods. With present improvement of MR hardware, its spatial resolution is near to the spatial resolution of CT.

Correspondence to: dr. Miljenko Marotti, Zavod za radiologiju kliničke bolnice »Sestre Milosrdnice«, Vinogradska 29, 41000 Zagreb, Croatia.

UDC: 616.2-073:539.143.43

Physical principles of MR

Potential MR is a new, potential diagnostic tool which displays the images in three planes. Transversal MR images are similar to CT images. CT is a method which forms images by the use of X-rays whereas MR is based on the interaction of radiofrequency (RF) waves and determined atomic nucleus of the body placed in the strong magnetic field. As in a CT picture, elements (pixel) are reconstructed by computer. In CT,

numerical value of every picture element displays the measured value of X-ray absorption in the determined tissue volume (voxel). In MR, the numerical value of every picture element, displays the MR signal strength of determined tissue volume. Signal is emitted from the body according to the principle of magnetic resonance.[6, 7] The strenght of the signal is determined by the number of resonance nuclei, blood flow, and by two chemical parametars i. e. T1 and T2 relaxation times.[8-13] Shortly after the body is placed in the strong external magnetic field, the magnetization of the body occurs. After a short exposure of the sample to RF impulse at the same frequency of preccessing hydrogen nuclei, the nuclei start to preccess in a coherent way. Reemission of RF signal occurs which is detectable with RF antenna.

By varying the strenght of magnetic field in various parts of the object imaged, nuclei preccess in different frequencies, enabling localization of different parts of the body. This is achieved by superimposing of «gradient» magnetic field on the main magnet.[11]

Blood flow fenomena

According to blood flow and lack of signal, MR has advantage of showing the vessels without contrast media. Signal intensity of flowing blood is a function of blood time relaxivity and the speed of flow.[1, 4] It also depends on the imaging parameters used, and plane position in multislice imaging method. The first slice in which the blood stream enters the imaging plane demonstrates a high intensity signal in the vessel lumen.

The hydrogen protons entering the first slice have not yet been exposed to radiofrequency excitation and therefore produce maximal signal.[14, 15] The folowing slices loose signal due to previous radiofrequency excitations. Transaxial slices show intraluminal artery signal in the most cranial slice, while intraluminal vein signal is shown in the most caudal one.

Renal anatomy

MR enables three dimensional dysplay of renal anatomic details in tranversal, sagittal and coronal view.[16] Renal pelvis on spin–echo technique images exhibited a high intensity signal due to too high fat content of the pelvic region. Fat had a relatively short T1 relaxation time and a long T2 relaxation time, with consequential high intensity signals on both T1 and T2 weighted images.

Renal arteries and veins are demonstrated as tubular structures void of signal due to fast blood flow.[14, 15, 17] Passing through the renal hilus, renal veins flow into the vena cava. The right renal vein has a short course to v. cava while the left renal vein passes anteriorly to aorta until the junction with v. cava.

The pelvis, calices and ureters demonstrated low signal intensity due to long T1 and T2 relaxation times of water, the main urine content. Urine signal intensity changes with various TR and TE parameters used for imaging. Spin–echo imaging wiht prolonged TR parameter increases magnetization recovery athus enhancing urine signal intensity which results in the change of pelvocalyceal system from black to gray. Increasing TE parameter also enhances the signal intensity of urine. Optimal display of the pelvicalyceal system is obtained using short TR and TE parameters. Slices obtained during increased diuresis showed mild widening of the pelvicalyceal system.

Magnetic resonance imaging distinguished kidney cortex from medulla.[1] Kidney cortex has a higher signal intensity than medulla but lower than surrounding perirenal fat. Medulla is seen as a triangular centrally placed area of lower signal intensity. Medulla signal intensity depands on the degree of hydration. During enhanced diuresis there is an intensified contrast between cortex and medulla. The best differentiation between cortex and medulla is achieved by short TR sequences (TR=500 msec). With prolongation of repetition time (TR=2000 msec) and echo time (TE=56, 60 msec) the contrast between cortex and medulla fades.

Perirenal fat tissue demonstrated high signal intensity due to relatively short T1 relaxation time and long T2 relaxation time.

Fascia Gerota is visualized as a low intensity linear structure dividing perirenal from pararenal space. The low signal intensity of fascia Gerota is due to high content of connective tissue with small amount of water and consequently small amount of hydrogen.

The psoas muscle has on magnetic resonance image low signal intensity and is easily distinguished from the bone, veins, arteries and surrounding fat tissue. Striated muscles have moderately long T1 relaxation value and short T2 relaxation time value. With a short TR (500 msec) striated muscles exibited low signal intensity. As a result of long T1 relaxation time value, which does not allow full recovery of magnetization between succesive excitation. With longer parameters (TR=2000 msec) there is a slight increase in signal intensity, but in spite of that striated muscles resemble low signal intensity than surrounding tissue. With prolongation of echo-time, (TE) parameter, striated muscles due to short T2 relaxation value, will show lower signal intensity than the surrounding soft tissue. The vertebra shows low signal intensity from cortical bone. The lack of signal is due to low mobile proton density. Change of imaging parameters, TR and TE, does not result in any change of signal from cortical bone. Bone marow exibits high signal intensity due to high fat content and therefore short T1 relaxation time.

On the gray scale of magnetic resonance image with spin-echo technique, air and cortical bone demonstrated the lowest signal intensity. These are folowed by ligament and tendons, striated muscles, smooth muscles, parenhimatous organs, brain, spinal cord, bone marow and fat with the highest signal intensity.[18,19]

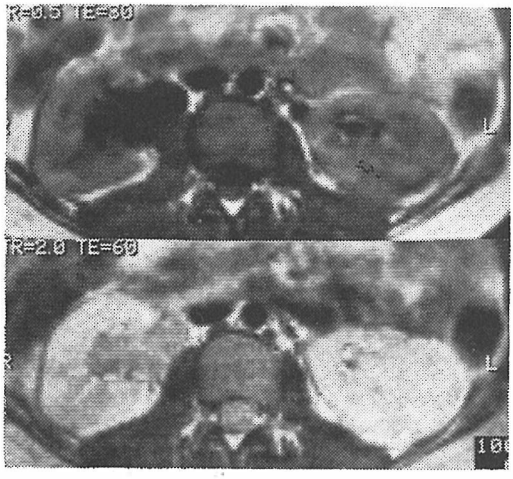

Figure 1a, 1b. Transverse, spin-echo T1 and T2 weighted images of the kidneys with mild hydronephrosis of the right kidney.

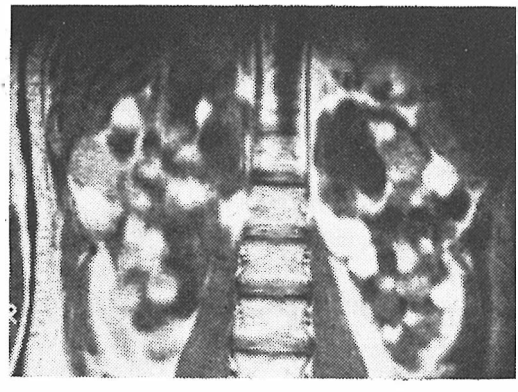

Figure 2. Coronal spin-echo T2 weighted image of the polycystic kidney disease.

Renal pathology – Renal hilus

Pelvicalyceal distention as well as ureter dilatation are readily recognized by magnetic resonance imaging. On spin-echo T1 weighted image (TR=500 msec, TE=30 msec) hydronephrosis and hydroureter demonstrated low signal intensity. Signal intensity increases with prolongation of TR and TE parameters. On spin-echo images, the ureters can be readily distinguished from the bowel, lymph nodes and vessels. Distinction between obstructive and non-obstructive hydronephrosis is possible with magnetic resonance imaging on T1 weighted images (TR=500 msec, TE=30 msec). In obstructive hydronephrosis there is a loss of cortico-medullary differentia-

tion. In the non-obstructive disease cortico-medullary differentiation is preserved.

Due to various relaxation parameters magnetic resonance imaging enables differentiation between peripelvic cyst and hilar lipomatosis. Water content is displayed due to long T1 relaxation time as an area of low signal intensity, whereas fat tissue due to short T1 relaxation time resembles high signal intensity. Differentiation between peripelvic cyst and hilar lipomatosis is better on magnetic resonance imaging than on computerised tomography because partial volume effect can result in false density values.

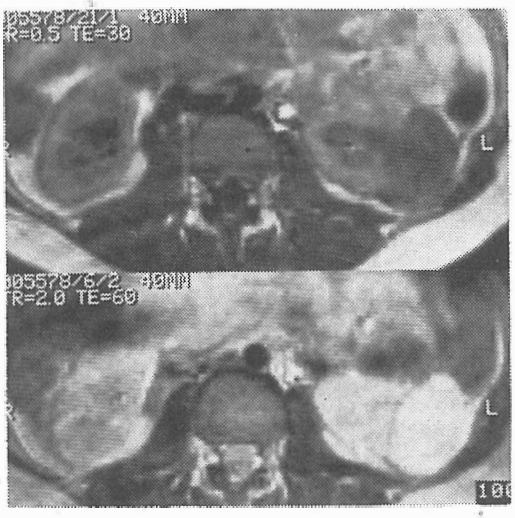

Figure 3a, 3b. Transverse, spin-echo T1 and T2 weighted images of a solid left kidney tumour.

Figure 4. Coronal spin-echo T1 weighted image of the inferior vena cava with tumour thrombus.

Parenchimal diseases

Spin-echo tehnique enables differentiation between the cortex and medulla in healthy kidneyes.[1, 2] A majority of kidneys involved with parenchymatous diseases have shown diminished or lost cortico-medulary contrast. Acute bacterial nephritis demonstrated enlarged kidney with diminished cortico-medullary contrast.

Acute obstructive disease has shown preserved cortico-medullary contrast. In chronic obstructive disease there is a loss of cortico-medullary contrast.

Radiation nephritis and chemotherapy induced nephritis have also shown the loss of cortico-medullary contrast wiht preserved kidney size.

Nephrotic syndrome and Wegener's granulomatosis demonstrated enlarged kidneyes with a loss of cortico-medullary contrast.

In chronic renal failure, the kidneys are small with loss of cortico-medullary contrast.

Diffuse infiltration of the kidneys in malignant lymphoma and in thrombosis of the renal vein results in kidney enlargement and a diminished or lost cortico-medullary contrast.

Trauma of the kidney with acute haematomas demonstrated localised loss of the cortico-medullary contrast. Patients after lithotripsy have shown enlarged kidneys with preserved cortico medullary contrast.

Magnetic resonance imaging has shown excelent results in the evaluation of renal allografts. Differentiation between acute allograft rejection anc cyclosporin nephrotoxicity is possible.

Volume measurement of kidney parenchyma and evaluation of kidney status is possible with MRI. The patients with end stage inflammatory disease demonstrated an increased incidence of cysts and kidney neoplasms. These patients have compromised renal function and are suitable for MRI examination, because there is no need for contrast media which is neccessary in computerised tomography examination.

Space occupying lesions – cysts

Capabillity of magnetic resonance imaging in differentiation of cystic from solid lesions is similar to that of computer tomography with contrast media. On magnetic resonance imaging, cysts demonstrated homogenous signal intensity, whit sharp edge toward kidney parenchyma. Cyst capsule is not visible. Simple cyst liquid content has identical relaxation parameters of water and therefore yields identical signal intensity on a magnetic resonance image. Cysts have long T1 relaxation time (longer than 2000 msec) and long T2 relaxation time (longer than 200 msec) and thus exibit a low intensity signal on T1 weighted images (TR=500 msec, TE=30 msec). Increasing of TR and TE parameters increases also cyst signal intensity. MRI demonstrated certain advantages in the characterization of cyst content as compared to ultrasound and computed tomography.[20] Hemorrhagic and infected cysts yield a different signal intensity compare to simple cysts.[20] Hemorrhagic cyst demonstrated a high intensity signal, due to short T1 relaxation time, whatever imaging spin-echo sequence used. Infected cyst demonstrated an inhomogenous lower signal intensity than hemorrhagic cyst.

Tumours

Renal demonstrated miscelaneous features on magnetic carcinomas resonance imaging. On spin-echo images, signal intensity, varies from medium to high. Usually carcinomas show an increased T1 relaxation time as compared to normal renal parenchyma. Unless changed by hemorrhage of infection, clear cell carcinomas demonstrated a higher signal intensity than normal renal cortex. Granular cell carcinomas yield a lower signal intensity as compared to the renal cortey. The reason is higher lipid content in the clear cell carcinomas than in granular cell carcinomas. Tumorous pseudocapsule exhibits a low signal intensity which separates tumour from normal renal parenchyma. Preliminary reports of renal cell carcinoma staging showed some advantages over other methods, mainly because of the exquisite demonstration of blood vessels.[21, 22, 23]

The main disadvantage of magnetic resonance imaging in the diagnosis of renal pathology is its inadequate demonstration of calcifications, whatever spin-echo sequence used. Calcifications yield no signal duo to small number of moving hydrogen protons. Calcifications are demonstrated as areas without signal and thus can not be differentiated from dense fibrous tissue.

References

1. Marotti M, Hricak H, Terrier F, Mcaninch JW, Thuroff JW. MR in renal disease: importance of cortical–medullary distinction. *Magnetic Resonance in Medicine* 1987;**5:**160-72.
2. Hricak H, Terrier F, Marotti M et al. Posttransplant renal rejection: comparison of quantitative scintigraphy, US and MR imaging. *Radiology* 1987;**162:**685-8.
3. Hricak H, Terrier F, Demas BE. Renal allografts: evaluation by magnetic resonance imaging. *Radiology* 1986;**159:**435-41.
4. Hricak H, Crooks LE, Sheldon P. Nuclear magnetic resonance of the kidney. *Radiology* 1983;**146:**425-32.
5. Steiner RE. Magnetic resonance imaging: its impact on diagnostic radiology. *Am J Roentegenol* 1985;**145:**883-93.
6. Bloch F. Nuclear induction. *Phys Rev* 1946;**70:**460-73.
7. Purcel EM, Torrey HC, Pound RV. Resonance absorbtion by nuclear magnetic moments in a solid. *Phys Rev* 1946;**69:**37-8.
8. Bradley W, Tosteson H, Basic principles of NMR. In: Kaufman L, Crooks LE, Margulis AR, ed *Nuclear Magnetic Resonance in Medicine*. New York, Tokio: Igaku–Shoin 1981;11-29.
9. Crooks LE, Grover TP, Kaufman L, Singer JR. Tomographic imaging with nuclear magnetic resonance. *Invest Radiol* 1978;**13:**63-6.
10. Crooks L, Hoenninger J, Arakawa M, i sur. Tomography of hydrogen with nuclear magnetic resonance. *Radiology* 1980;**136:**701-6.
11. Gore JC, Emery EW, Orr JS, Doyle FH. Medical nuclear magnetic resonance imaging: physical principles. *Magnetic Resonance Imaging* 1981;**4:**269-74.
12. Rosen BR, Brady TJ. Principles of nuclear magnetic resonance for medical application. *Sem Nucl Med* 1983;**4:**308-18.
13. Fullerton GD. Basic concepts for nuclear magnetic resonance imaging. Magnetic Resonance Imaging 1982;**1:**39-55. Interaction: examples employing nuclear magnetic resonance. *Nature* 1973;**242:**190-1.
14. Bradley WG, Waluch V. Blood flow: magnetic resonance imaging. *Radiology* 1985;**154:**443-50.
15. Von Schultes GK, Mcmurdo KK, Tscholakoff D. et al. Blood flow imaging with MR: spin-phase phenomena. *Radiology 1985;***157:**687-95.

16. Smith FW, Reid A, Mallard JR et al. Nuclear magnetic resonance tomographic imaging in renal disease. *Diagn Imaging* 1982;**51:**209-13.
17. Hricak H, Williams RD, Moon KK, et al. Nuclear magnetic resonance imaging of the kidney: renal masses. *Radiology* 1983;**147:**765-72.
18. Partain CL, James AE, Watson J, Price RR, Coulam CM, Rollo FD. Nuclear magnetic resonance and computed tomography. *Radiology* 1980;**136:**767-70.
19. James AE, Partain CL, Holland GN, et al. Nuclear magnetic resonance imaging: the current state. *Am J Roentgenol* 1981;**138:**201-10.
20. Marotti M, Hricak H, Fritzche P, Crooks LE, Hedgcock MW, Tanagho EA. Complex and simple renal cysts: comparative evaluation with MR imaging. *Radiology* 1987;**162:**679-84.
21. Hricak H, Demas BE, Williams RD et al. Magnetic resonance imaging in the diagnosis and staging of renal and perirenal neoplasms. *Radiology* 1985;**154:**709-15.
22. Choyke PI, Kressel HY, Pollack HM, Arger PM, Axel L, Manourian AC. Focal renal masses: magnetic resonance imaging. *Radiology* 1984;**152:**471-8.
23. Hricak H, Thoeni RF, Carrollpr, Demas BE, Marotti M, Tanagho EA. Detection and Staging of Renal Neoplasms: A Reassessment of MR Imaging. *Radiology* 1988;**166:**643-9.

Adv Radiol Oncol 1992; 66–71.

Magnetic resonance imaging of hand joints in patients with rheumatoid arthritis, psoriatic arthritis and nondifferentiated seronegative polyarthritis

Jevtić V, Rozman B, Kos – Golja M, Jarh O, Demšar F

Institute for Diagnostic and Interventional Radiology, UCC, Ljubljana

The purpose of our study was to compare diagnostic efficacy of magnetic resonance imaging (MRI) and conventional radiography in early and late rheumatoid arthritis, psoriatic arthritis and nondifferentiated seronegative polyarthritis. Our results suggest that MRI is more efficient in several respects. It proved to be more sensitive in diagnosing both, early and late rheumatoid arthritis, as well as psoriatic arthritis and nondifferentiated polyarthritis. Using MRI easier differential diagnosis between early rheumatoid arthritis on one side and psoriatic arthritis with some nondifferentiated seronegative polyarthritis, on the other side was possible. One of the most important practical advantages of MRI in comparison to classical radiology is its possibility to registrate the activity of inflammatory process at the beggining and during exacerbations of the disease with all therapeutical implications.

Key words: arthritis; hand; magnetic resonance imaging

Introduction

Conventional radiography is not a sensitive method of assessing subtle soft tissue changes in early rheumatoid arthritis, psoriatic arthritis and nondifferentiated seronegative polyarthritis. Even in advanced stages only the secondary effect of chronic synovial inflammation on the skeletal elements is detectable, while direct presentation of the early and late nonskeletal soft tissue inflammatory changes by means of noninvasive conventional radiology is not possible. However, precise morphologic demonstration of all inflammatory signs is important not only from the diagnostic standpoint, but as well as the criteria for assesing the activity and progression of the diseases. The latter means that they influence the beginning, the type and the response to treatment.[1] MRI, owing to its high contrast resolution, enables clear noninvasive presentation of the para- and intraarticular soft tissue structures.[2, 3]

In our study small peripheral hand joints of 28 patients with clinically suspect or proven early and late rheumatoid arthritis, psoriatic arhtritis and nondifferentiated seronegative polyarthritis were investigated by means of conventional radiography and MRI. The results were compared.

Correspondence to: doc. dr. Vlado Jevtić, Institute for Diagnosic and Interventional Radiology, UCC, Zaloška 4, 61000 Ljubljana, Slovenia.

UDC: 616.72-002-073:539.143.43

Material and methods

On the basis of routine radiographic, clinical and laboratory investigations, 16 patiens (12 females

and 4 males; mean age 47 years) were classified as having rheumatoid arthritis, 6 in stage I and 10 in stage II-III according to Steinbrocker. In 10 patients (7 males and 3 females; mean age 43 years) clinical diagnosis of early (5 patients) and late psoriatic arthritis (5 patients) was made. In 2 seronegative patients (middle-aged male and female) with early asymmetric polyarthritis deffinite clinical diagnosis was not possible. In one of them most probable diagnosis was that of Reiter's syndrome. For the determination of normal MRI criteria, small hand joints of 10 normal volunteers (mean age 35 years) were studied.

All the patients had standard anteroposterior hand and wrist radiographs taken. The next day MRI was performed on a 2.35 T BRUKER MR scanner. A spin echo sequence with T1 weighted images (TR 600 msec, TE 34 msec) and T2 weighted images (TR 2000 msec, TE 34/90 msec) was used. A field of view was 12 cm with data acquisition matrix of 256 x 256. In all the patients the images were performed in coronal plane with additional axial cuts in two of them. The joints of interest were presented in 3 mm thick consecutive slices. MR images were interpreted by radiologist and two rheumatologists and compared with the plain films.

Results

In 4 cases with early rheumatoid arthritis plain films of 2 were interpreted as normal, while all of them were estimated as pathological on MRI. In one patient with normal conventional radiogram of the 2nd metacarpophalangeal joint MRI (T2 weighted images) demonstrated intra and paraarticular soft tissue swelling of relatively high signal intensity localized on the radiovolar aspect which probably represented fluid accumulation in inflammatory edema. In the next patient with normal plain film MRI revealed marginal erosion of the metacarpal head filled with pannus. It was presented as a homogeneous low signal intensity area (T1 and T2 weighted images) which contrasted to the high signal intensity of the adjacent bone marrow. In this patient rheumatoid arthritis was estimated as stage II-III according to Steinbrocker only on the basis of MRI. In a case where typical fusiform soft tissue swelling was proved by both examinations, MRI showed that the area of increased intra – and paraarticular signal intensity (T2 weighted images) was limited to immediate vicinity of the proximal interphalangeal joint.

In 2 patients with clinical findings suggestive of very early rheumatoid arthritis plain radiography as well as MRI were negative.

In 10 patients with advanced rheumatoid arthritis the exact diagnosis and staging was made using both examinations. Yet, MRI proved to be more efficient in several respects. In 6 cases additional bone erosions and pseudocysts were demonstrated only by MRI. In every case of advanced rheumatoid arthritis where plain films showed pseudocysts, MRI proved that a majority of them were bone erosions filled with pannus of low (T1 and T2 weighted images) to moderate signal intensity (T2 weighted images) (Figure 1). In a patient with advanced rheumatoid arthritis plain film demonstrated a round radiolucency

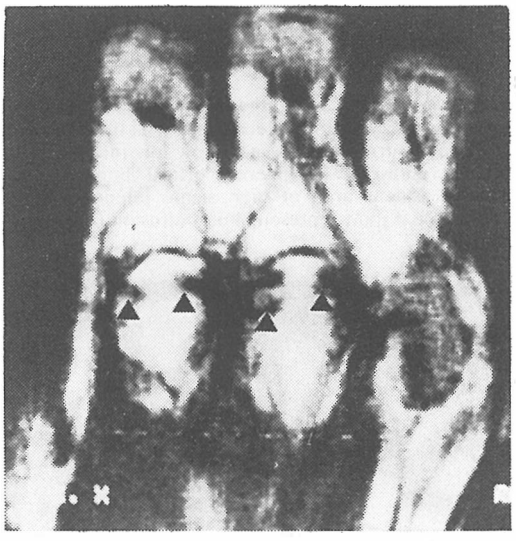

Figure 1. MRI (T1 weighted). Advanced R.A. Numerous bone erosions filled with low intensity pannus.

with thin cortical margin localized beneath the articular surface of the distal radial epiphysis typical for inflammatory pseudocyst (Figure 2). On

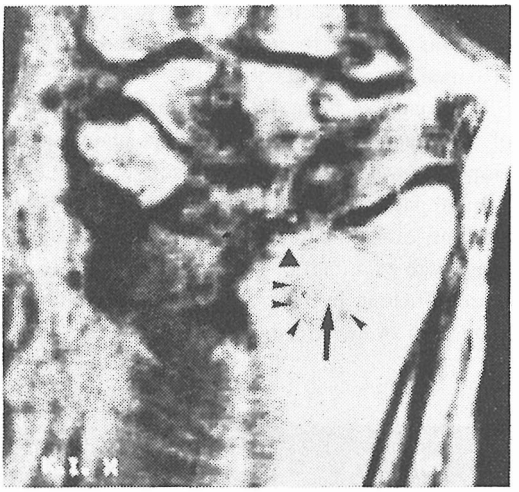

Figure 2. MRI (T2 weighted). Advanced R. A. Pseudocyst with high signal intensity synovial fluid inside of it (arrow) surrounded by a narrow low intensity area which represents peripheral cortical bone (arrowheads). Linear area of high signal intensity in the radio-carpal joint represents joint effusion (big arrowhead).

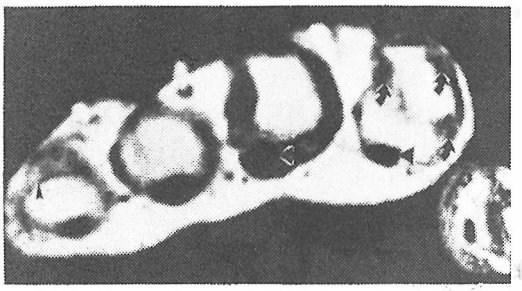

Figure 3. MRI (relatively T2 weighted). Advanced RA. Axial image of metacarpo-phalangeal joints shows pannus of moderate signal intensity (arrows). Good demonstration of medialization of the second and the third flexor digit tendon (big arrow heads). An area of high signal intensity of the fifth extensor digit tendon represents active tenosynovitis (small arrow head).

MRI (T2 weighted images) high and homogenous signal, consistent with synovial fluid, was registered in the central part, similar to intensive signal of the surrounding bone marrow. The border inbetween was a narrow area of low signal intensity corresponding to the peripheral cortical bone of longstanding pseudocyst. T2 weighted images demonstrated a linear area of high signal intensity in the radiocarpal joint, which repesented joint effusion. In a patient with typical ulnar deviations and volar subluxations, MR images of the metacarpophalangeal joints in an axial plane were obtained (Figure 3). Very good demonstration of spatial relationship of invading pannus to the 2nd metacarpal head was achieved. Besides, medialisation of the 2nd and the 3rd digit flexor tendons as well as the tenosynovitis of the 5th digit extensor tendon were discovered.

In 3 cases with early psoriatic arthritis both examinations were positive regarding the demonstration of paraarticular soft tissue swelling. Still, MRI enabled more accurate estimation of inflammatory soft tissue changes. In comparison to fusiform intra – and paraarticular swelling of the early rheumatoid arthritis, which was limitted only to joint capsule and the vicinity of the proximal interphalangeal joint, in early psoriatic arthritis T1 and T2 weighted images demonstrated low and high signal intensity affecting a wider area, which corresponded to thickened edematous and hyperemic collateral paraarticular ligaments. These typical changes were proved in all of the patients with early psoriatic arthritis. Only by means of MRI, (T2 weighted images), we were able to discover fluid effusions in 2 patients. On the contrary, a discrete periosteal reaction, demonstrated on plain films, was not presented by MRI.

Similar to rheumatoid arthritis, in two patients with clinical suspicion of very early psoriatic arthritis, plain films and MRI were negative.

In 5 patients with late psoriatic arthritis the results of MRI and conventional radiography were comparable to those in late rheumatoid arthritis.

In a male with early nondifferentiated seronegative polyarthritis, probably Reiter's syndrome, low and high signal intensity edematous collateral ligaments were presented on T1 and T2 weighted images, i.e. findings which were other-

wise in our series typical for psoriatic arthritis (Figure 4). The second female patient with early asymmetric seronegative polyarthritis had normal plain films. MRI proved a small pseudocyst in one of the metacarpal heads.

The results of MRI in a control group were similar to those described by some other authors (2,3,8).

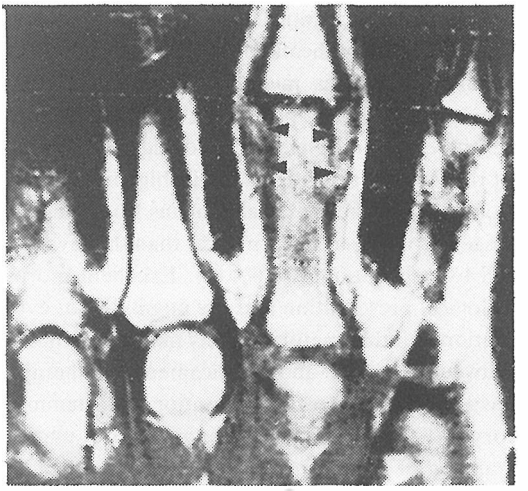

Figure 4. MRI (T2 weighted). Early nondifferentiated seronegative polyarthritis, probably Reiter's syndrome. Widespread high signal intensity area represents edematous and hyperemic collateral ligament (arrowheads), findings otherwise typical for psoriatic arthritis.

Discussion

In our study mainly soft tissue and bony changes of the small peripheral hand joints in rheumatoid arthritis, psoriatic arthritis and nondifferentiated seronegative polyarthritis (distal and proximal interphalangeal, metacarpophalangeal), which are usually affected at the beginning of rheumatic inflammatory disease, were evaluated by MRI. In most of the other similar studies, inflammatory changes in rheumatoid arthritis affecting the carpal and big peripheral joints[4,5] as well as cervical spine articulations[6] were demonstrated.

Our results are comparable to other similar studies[4,5] and prove that MRI is more sensitive in diagnosing both, early and late rheumatoid arthritis. According to our experience, the same is true of psoriatic and nondifferentiated seronegative polyarthritis. In early inflammatory disease this was the result of superior soft tissue contrast resolution of MRI. So, intra and paraarticular soft tissue changes were presented earlier and more accurately. T2 weighted images proved to be more efficient in the early diagnosis of all three types of polyarthritis. Accumulation of fluid (edema, hyperemia, synovial fluid) was presented as high signal intensity areas on T2 images.[4,7]

In late rheumatoid and psoriatic arthritis MRI was superior to conventional radiography only partially owing to its greater soft tissue resolution with better presentation of synovial proliferation invading bone. As a tomographic method, MRI enabled more efficient demonstration of erosions and pseudocysts on consecutive sections of the joint. Besides, using MRI we were able to prove that a majority of pseudocysts shown on conventional radiograms actually represented marginal erosions filled with pannus (Figure 1). In typical cases, the differentiation between marginal erosions and pseudocysts was not difficult. Typical erosion was presented as a localised oval or round area of homogenous low signal intensity on both T1 and T2 weighted images, which contrasted to the surrounding high signal intensity of the bone marrow. Communication of the erosion with joint cavity was relatively wide and localised somewhat away from the articular surface corresponding mainly to bare areas of the joint. Typical pseudocyst was demonstrated on MRI as a round, homogenous low to high signal intensity area on T1 and T2 weighted images. The high signal intensity of the synovial fluid within the cyst was similar to the bone marrow in the vicinity (Figure 2). The differentiation between them was possible only owing to narrow low signal intensity area of peripheral cortical bone, usually presented in long-standing pseudocysts. In comparison to marginal erosions, pseudocysts were localised in the subarticular region connected with narrow, communication with the joint cavity. Still, in some cases the differentiation between erosions and pseudocysts was not easy. Sometimes, bone deffect had all known

characteristics of bone erosions with one exception: registered signal intensity was relatively high on T2 weighted images. These cases corresponded to clinically more active joint inflammation. So, we believe that they represent edematous and hyperemic pannus which is probably more aggressive. Similar to this, in a majority of cases accumulation of fluid (edema, hyperemia, joint effusion), presented as high signal intensity correlated well with clinically more active inflammatory disease. Thus, one of the most important practical advantages of MRI in comparison to classical radiology is its possibility to registrate the activity of inflammatory process at the beginning and during exacerbations of the disease with all therapeutic implications.

In our study MRI showed an important differential diagnostic potential between early rheumatoid arthritis on one side and psoriatic arthritis together with some nondifferentiated seronegative types of polyarthritis on the other side. High signal intensity soft tissue inflammatory changes in early rheumatoid arthritis have been limited to the joint capsule of the proximal interphalangeal joints and its immediate vicinity. In early psoriatic arthritis, and probably in the case of Reiter's syndrome, wider area was affected, corresponding to edematous and hyperemic collateral ligaments (Figure 4). This difference could be of special interest in cases of early nondifferentiated inflammatory polyarthritis in which definite clinical diagnosis, important for adequate therapy, is not possible. So, the results of our study show that MRI enables more specific diagnosis between early rheumatoid arthritis, early psoriatic arthritis and probably early Reiter's syndrome. On the contrary, in advanced diseases no important differences have been noted.

Using MRI, much better anatomic presentation of soft tissue inflammatory changes, e.g. invading pannus, changed position of flexor tendons (Figure 3), relevant for the planning of eventual surgical procedure, was possible.

Although there are many advantages of MRI in comparison with classical radiography in the diagnosis of rheumatoid and psoriatic arthritis, both methods failed to prove clinical impression of very early inflammatory disease in 4 of 28 cases. One of known disadvantages of MRI is its low sensitivity for cortical bone changes. Discrete periosteal apposition in psoriatic arthritis was demonstrated only on plain films. Long examination time for T1 and T2 images caused in some of the patients motion artefacts with degradation of images.

The stated advantages of MRI have several therapeutical implications. Earlier diagnosis of rheumatic arthritis means earlier beginning of therapy and better prognosis. MRI as a more sensitive method enables more accurate staging of rheumatoid arthritis due to its higher sensitivity, which in practice usually means I or II higher stage according to Steinbrocker than that evaluated by conventional radiology. Excellent morphological presentation and the possibility of evaluation of inflammatory activity makes the choice between surgical and medicamentous therapy easier. Finally, direct visualisation of inflammatory soft tissue changes will enable better understanding of pathogenesis in rheumatoid arthritis, psoriatic and nondifferentiated seronegative polyarthritis.

Conclusion

In 28 patients with early and late rheumatoid arthrits (16), psoriatic arthritis (10) and nondifferentiated seronegative polyarthritis (2), the diagnostic efficacy of MRI and conventional radiography were compared. MRI proved to be more efficient in many respects. MRI has been more sensitive and enabled earlier diagnosis of all three types of polyarthritis. The most important advantage was the possibility to evaluate inflammatory activity at the beggining and during exacerbations of rheumatic disease. Using MRI, the differentation between early rheumatoid arthritis and early psoriatic arthritis together with some nondifferentiated seronegative polyarthritis was possible. MRI enables direct visualisation of inflammatory intra – and paraarticular soft tissue changes. All the enumerated advantages of MRI have important therapeutical implications.

References

1. Steinbrocker O, Traeger CH, Batterman RC. Therapeutic criteria in rheumatoid arthritis. *JAMA* 1949; **140:**659-62.
2. Weiss KL, Beltran J, Shamam OM, Stilla RF, Levey M. High-field MR surface-coil imaging of the hand and wrist. Part I. Normal anatomy. *Radiology* 1986; **160:**143-6.
3. Baker LL, Hajek PC, Björkengren A, Galbraith R, Sartoris DJ, Gelberman RH, Resnick D. High-resolution magnetic resonance imaging of the wrist: normal anatomy. *Skeletal Radiol* 1987; **16:**128-32.
4. Gilkeson G, Polisson R, Sinclair H, Vogler J, Rice J, Caldwell D, Spitzer C, Martinez S. Early detection of carpal erosions in patients with rheumatoid arthritis: A pilot study of magnetic resonance imaging. *J Rheumatol* 1988; **15:**1361-6.
5. Senac MO, Deutsch D, Bernstein BH, Stanley P, Crues III JV, Stoller DW, Mink J. MR imaging in juvenile rheumatoid arthritis. *AJR* 1988; **150:**873-8.
6. Bundschuh C, Modic MT, Kearney F, Morris R, Deal C. Rheumatoid arthritis of the cervical spine: surface-coil MR imagilng. *AJR* 1988; **151:**181-7.
7. Weiss KL, Beltran J, Lubbers LM. High-field MR surface coil imaging of the hand and wrist. Part II. Pathologic correlations and clinical relevance. *Radiology* 1986;**160:**147-52.
8. Krahe T, Schindler R, Landwehr P. MRI of the hand: tehnical requirements. *Medicamundi* 1989; **34:**20-3.

Adv Radiol Oncol 1992; 72–8.

Preoperative evaluation of long bone osteosarcomas with magnetic resonance imaging

Poleksić LJ[1], Zdravković Đ[1], Atanacković M[2], Mitrović M[3], Bačić G[1,4]

[1] UCC Belgrade, Magnetic Resonance Center,
[2]University of Belgrade, Faculty of Medicine, Institute of Pathology.
[3]Special Orthopaedic Hospital »Banjica«, Belgrade, [4]University of Belgrade, Department of Physical Chemistry

The magnetic resonance imaging (MRI) characteristics of long bone osteosarcomas were studied in order to evaluate the clinical usefulness of MRI in planning of surgical approach. Intra – and extraosseous tumour propagation, as well as muscle and blood vessel involvelment were determined and compared to intraoperative and surgically resected specimen findings. MRI delineation of tumour borders correlated well with surgical findings. An increased signal of surrounding muscles was noted on T2W images in all patients. Histological evaluation of these muscles showed various degrees of edema, atrophy and necrosis, but never a sign of tumour infiltration. No reliable criteria were found for distinguishing adhesions from infiltration when vessels were in close contact with tumour.

Key words: osteosarcoma, magnetic resonance imaging

Introduction

Amputation or limb salvage resection are standard surgical approaches in the multidisciplinary treatment of bone osteosarcomas. The preoperative decision for limb salvage surgery must be based on the precise anatomical localization of tumour, its extent and relationship to the surrounding structures.[1] Magnetic resonance imaging (MRI) has been found equal or superiror to computerized tomography (CT) in evaluating intramedullary tumour propagation.[2,3,4] Soft tissue extension usually present on diagnosis[5], is better visualized by MRI because of its inherent better soft tissue contrast resolution.[6,7,8] The possibility of direct multiplanar imaging with MRI enables better spatial orientation than CT.[9] On the other hand, CT has advantages in detecting calcification, ossified osteoid matrix, endosteal thinning and fine periostal reaction.[4] Consequently, in patients with biopsy proven long bone osteosarcoma staging should be done using MRI in order to choose candidates for limb salvage and CT examination is seldom needed.[4]

Recent publications show that both MRI and MR spectroscopy could play an important role in monitoring the effects of chemotherapy on bone sarcomas.[6,10,11] The purpose of this paper is to compare preoperative, post-chemotherapy MRI findings with intraoperative and surgically resected specimen findings in long bone osteosarcoma in order to improve staging and surgical planning.

Correspondence to: dr. Ljubomir Poleksić, University Clinical Center, Magnetic Resonance Center, 11000 Belgrade, Pasterova 2, Yugoslavia.

UDC: 616.7-006.34.04-073:539.143.43

Material and methods

Ten patients (3 males and 7 females) with histologically proven osteosarcomas were examined (Table 1). The mean age was 15.5 years (range 9-35). Tumours were located in femur (7 patients), proximal fibula, proximal tibia and proximal humerus.

All patients received preoperative chemotherapy prior to MR examination. Five patients received trans-catheter intraarterial medication and five patients were treated by systemic intravenous therapy (Table 1). Combination of several chemotherapeutic agents (adriamycin, cisplatin, methotrexate, vincristine) was used.

All patients were treated surgically: in 6 limb salvage procedure was done and 4 underwent amputation (Table 1). The period between MR examination and surgery ranged from 1 to 40 days (mean 18.4).

MR examination was performed with a 1.5T MR imager (Magnetom, Siemens). Two spin-echo imaging sequences were used: T1W (380-600/15) and T2W (1600-2000/90). Slice thickness was 5-8 mm with interslice distance 2-4 mm. Images were obtained using body coil (4 patients) or surface coil with the field-of-view = 17 cm (6 patients). Tumor propagation as delineated on MRI was compared with surgical and/or resected specimen findings in the following categories: intra – and extraosseous propagation, muscle and vascular involvement.

Results

MRI depicted the margins of intramedullary tumor completely and precisely in all patients. Tumor tissue had low signal intensity (SI) on

Table 1.

Type of osteosarcoma	Chemoth.	Cystic formations	Tumour necrosis	Type of surgery
fibroblastic gr. III	i.a.	haemorrhagic	90%	LS
fibroblastic gr. II	i.a.	serous	90%	LS
chondroblastic gr. II	i.v.	–	75%	A
osteoblastic gr. II	i.v.	–	75%	LS
osteoblastic gr. III	i.v.	–	80%	LS
osteoblastic gr. II	i.a.	haemorrhagic	70%	A
osteoblastic gr. II	i.a.	haemorrhagic	90%	LS
osteoblastic fibroblastic gr. III	i.v.	haemorrhagic	85%	LS
osteoblastic chondroblastic gr. III	i.v.	–	20%	A
osteoblastic teleangiectatic gr. III	i.a.	–	40%	A

i.a. – trans-catheter intrarterial, i.v. – systemic intravenous LS – limb salvage, A – amputation

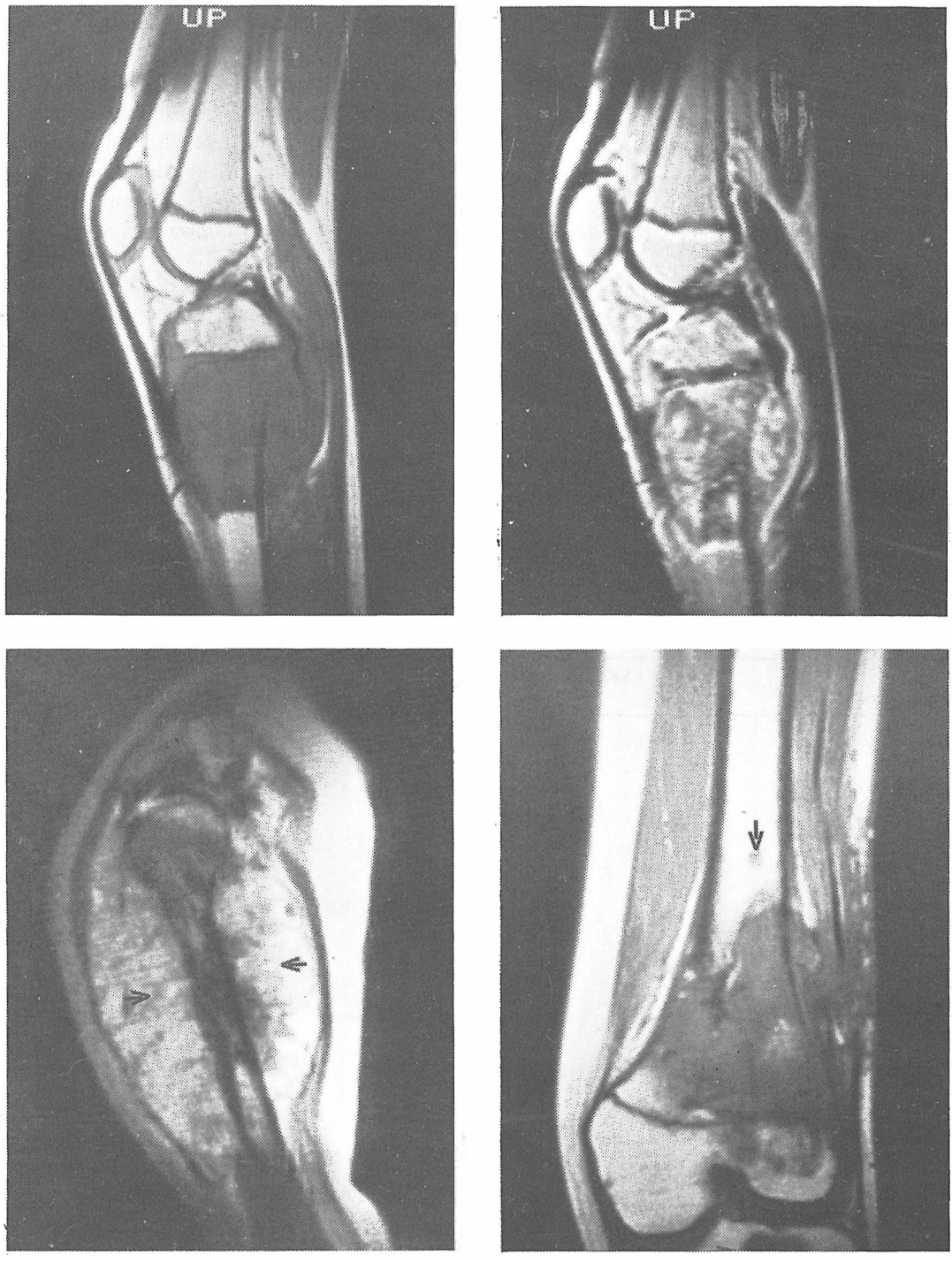

Figure 1. MR images of osteosarcoma: Sagittal T1W (a) and T2W (b) MR images of osteosarcoma of the proximal tibia. (c) T2W image of osteoblastic osteosarcoma of the humerus. Note low SI of intraosseous tumour and high SI of extraosseous tumour (arrows). (d) T1W image of osteosarcoma of the distal femur with one skip lesion in the femur and one in epiphisis of the protimal tibia (arrows).

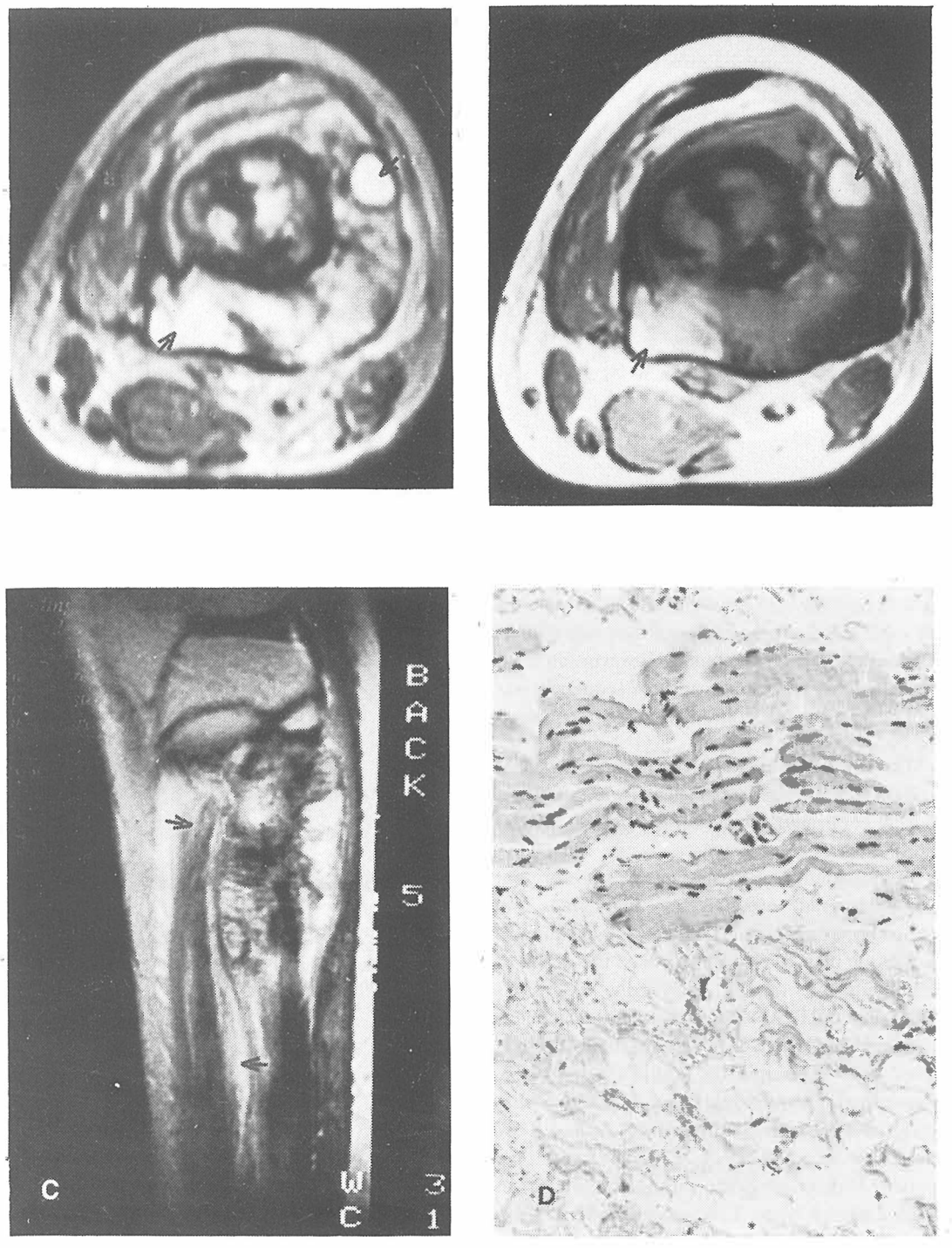

Figure 2. T1W (a) and T2W (b) axial images of hemorrhagic cystic formations in soft tissue part of the distal femoral osteosarcoma (arrows). (c) Coronal T2W image of the proximal fibular osteosarcoma showing increased SI of surrounding muscles (arrow). (d) Histological cross-section of the muscle, showing its edema and atrophy with marked interstitial proliferation of fat cells.

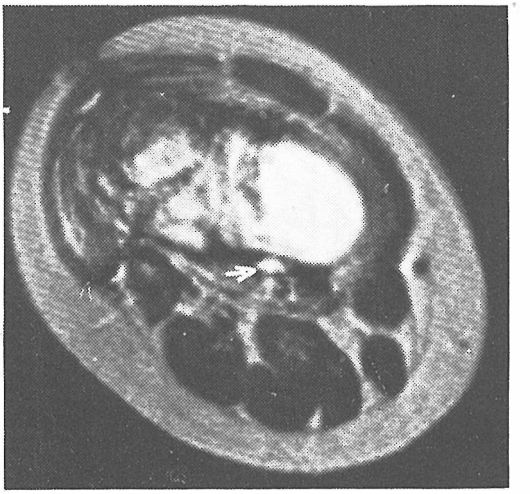

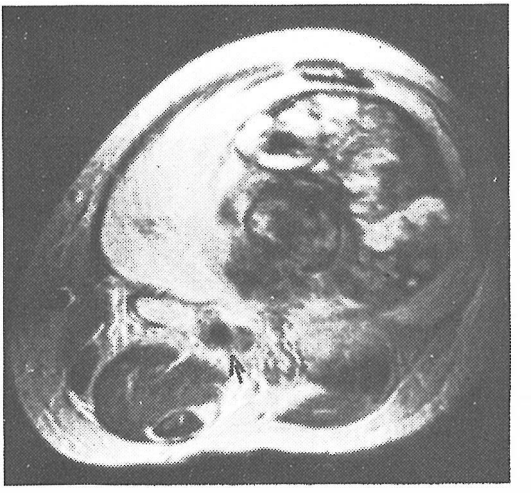

Figure 3. Blood vessels/tumour relationship in an osteosarcoma of the femur–axial T2W MR images. Arrows show femoral artey and vein. (a)Vessels separated from tumour by a layer of normal fat tissue. (b)Vessels in close contact with tumorous cystic formation (area of high SI). (c)Vessels surrounded by the tumour.

T1W sequences and intermediate to high SI on T2W sequences (Figure 1a,b). Only the intramedullary part of pure osteoblastic osteosarcoma had low SI on T2W sequences prior to chemotherapy (Figure 1c) as a consequence of increased content of calcium in these tumours.[3] However, after the therapy their appearance on T2W sequences was not distinguishable from other types of osteosarcoma.

The epiphyseal cartilage invovelment or penetration was seen in 8 cases, which was macroscopically confirmed. Four skip lesions were detected in 2 cases (Figure 1d).

In all patients soft-tissue masses were present and their grade was IIB (i.e. high grade and extracompartmental). The longitudinal extent of soft tissue mass in 6 cases exceeded the extent of intramedullary tumour. Soft-tissue extensions were seen on T2W sequences as inhomogeneous intermediate to high SI masses, partially incapsulated (low SI margin on both T1W and T2W sequences). Hemorrhagic cystic, formations characterized by high SI on both T1W and T2W images, were noted in 4 cases (Figure 2a, b). One patient had serous cystic formation (low SI on T2W and high SI on T2W images) following the pathologic bone fracture.

The increased SI of adjacent muscles was seen on T2W sequences in all cases (Figure 2c). Histological evaluation of these muscles was performed in 4 cases. The popliteal fat specimen in a case with increased SI on T2W image was also analysed. No signs of tumor infiltration were found; the various degrees of edema, atrophy, necrosis, and interstitial proliferation were registered (Figure 2d).

In 9 cases, the delineation of major blood vessels on MR images was sufficient to enable

evaluation of their relationship with soft tissue tumours. However, in tumours located below the knee (two cases), the delineation of vessels was poorer than in tumours located in the femur. In most cases axial images were more informative than sagittal or coronal (Figure 3). In a case of the tumour of the proximal humerus, major vessels were not delineated. The vessel encasement was seen in one case (Figure 3a). The close contact between the tumour and vessels was seen in 4 cases. Macroscopically, vessels were adherent to tumour in three cases (Figure 3b) and invaded in one case. A layer of normal or edematous tissue was seen in four cases (Figure 3c).

Discussion

Intraosseous tumor extent

Excellent tumour/marrow delineation is obtained using T1W sequences (Figure 1a) as a consequence of replacement of normal bone marrow with tumour tissue having long T1 relaxation time.[9] Sharp margin usually seen in the tumour/marrow interface is due to chemical shift-artifacts.[6] T2W sequences are less informative for evaluation of intramedullary extension of tumour. The margins of resected bone were tumour-free in all patients who underwent limb salvage procedure.

The use of surface coils improves the image quality (resolution), but there is a certain risk to skip lesions due to small field of view. In a case of tumour located in the femur, MRI examination skiped lesion in the proximal tibia (Figure 1d), which changed the initial surgical plan to a more radical approach.

Extraosseous propagation

T2W sequences were superior over T1W in demonstrating soft-tissue bulk owing to better contrast resolution. Inhomegeneous signal of the soft-tissue tumours on T2W sequences is due to mineralization, edematous zones, hemorrhages, necrotic areas and lipomatous elements.[12] It should be stressed that the inhomogeneous signal of soft-tissue tumours is not the criterion of malignancy per se.[13] Under chemotherapy 4 patients developed hemorrhagic cystic formations (Table 1). Interestingly the degree of tumour necrosis in these patients ranged between 70-90% (mean 83%), whereas in other patients the degree of tumour necrosis was lower, ranging between 20-90% (mean 63%).

Larger longitudinal extent of extraosseous parts of the tumour compared to intraosseous (6/10 cases) is possibly result of its faster growth (lower resistance of soft tissues and presence of malignant cells on the edges) and increased rate of proliferation of adjacent periosteum.

Muscle involvement

Increased SI on T2W sequences in adjacent muscles was observed in all patients. This raised the question of exact definition of the tumour borders, i.e. whether MRI overestimates actual tumour size. Histological examination showed no signs of tumour infiltration, which implies that the reactive zone of edematous tissue in osteosarcoma was free of disease after chemotherapy. It should be noted, however, that increased SI of the skeletal muscle around a soft-tissue mass has been found in all malignant tumours, regardless whether the muscle is only edematous or invaded by tumour.[14] Therefore, our conclusion about muscle involvement is limited to osteosarcomas and requires further investigation on a larger number of patients.

Vessel infiltration

MR examination was sufficient to make surgical planning when vessels are encased by tumour or when there is a layer of normal tissue between tumour and vessels. We were unable to find reliable criteria for distinguishing adhesions from infiltration when vessels were in close contact with tumour. Therefore, we propose that arteriography should be done in such cases.

In conclusion, MRI is an excellent method for in preoperative evaluation staging and planning the type of surgery of long bone osteosarcomas. Intramedullary and extraosseous components of bone tumours are delineated better than with

any other diagnostic modalities. MRI was found to be a method of low specificity in assessing the infiltration of surrounding muscles and vessels. Improved specificity is to be expected by introducing MRI procedures such as MR angiography, utilization of contrast agents and measurement of T1 and T2 values of different tissues into everydays practice.

References

1. Hudson TM, Schiebler M, Springfield DS, Hawkins IF Jr, Enneking WF, Spanier SS. Radiologic imaging of osteosarcoma: role in planning surgical treatment. *Skeletal Radiol* 1983;**10:**137-46.
2. Ehman RL, Berquist TH, McLeod RA. MR imaging of the musculoskeletal system: a 5 – year appraisal. *Radiology* 1988;**166:**313-20.
3. Zimmer WD, Berquist TH, McLeod RA, Sim FH, Pritchard DJ, Shives TC, Wold LE, May GR. Magnetic resonance imaging of osteosarcomas: comparison with computed tomography. *Clin Orthop* 1986;**208:**289-99.
4. Sunderam M, McGuire MH. Computed tomography or magnetic resonance for evaluating the solitary tumour or tumour-like lesion of bone? *Skeletal Radiol* 1988;**17:**393-401.
5. Simon MA, Aschliman MA, Thomas N, Mankin HJ. Limb-salvage treatment versus amputation for osteosarcoma of the distal end of the femur. *J Bone Joint Surg (Am)* 1986;**68A:**1331-7.
6. Redmond OM, Stack PJ, Dervan PA, Hurson BJ, Carney DN, Ennis JT. Osteosarcoma: use of MR imaging and MR spectroscopy in clinical decision making. *Radiology* 1989;**172:**811-5.
7. Totty WG, Murphy WA, Lee JKT. Soft-tissue tumours: MR imaging. *Radiology* 1986;**160:**135-141.
8. Petasnick JP, Turner DA, Charters JR, Gitelis S, Zacharias CE. Soft-tissue masses of the locomotor system: comparison of MR imaging with CT. *Radiology* 1986;**160:**125-33.
9. Boyko OB, Cory DA, Cohen MD, Provisor A, Mirkin D, DeRosa GP. MR imaging of osteogenic and Ewing's sarcoma. AJR 1987;**148:**317-22.
10. Holscher HC, Bloem JL, Nooy MA, Taminiau AHM, Eulderik F, Hermans J. The value of MR imaging in monitoring the effect of chemotherapy on bone sarcomas. *AJR* 1990;**154:**763-9.
11. Erlemann R, Scuik J, Bosse A, Ritter J, Kusnierz-Glaz CR, Peters P, Wuisman P. Response of osteosarcoma and Ewing sarcoma to preoperative chemoterapy: assessment with dynamic and static MR imaging and skeletal scintigraphy. *Radiology* 1990:**175:**791-6.
12. Bohndorf K, Reiser M, Lochner B, Feaux de Lacroix W, Steinbrich W. Magnetic resonance imaging of primary tumours and tumour-like lesions of bone. *Skeletal Radiol* 1986;**15:**511-7.
13. Poleksić Lj. Zdravković Đ, Atanacković M, Bačić G. Tumori mekih tkiva: vizuelizacija magnetnom rezonancijom. *Farm vestn* 1990;**41:**354-5.
14. Beltran J, Simon DC, Katz W, Weis LD. Increased MR signal intensity in skeletal muscle adjacent to malignant tumours: pathologic correlation and clinical relevance. *Radiology* 1987;**162:**251-5.

Chapter II. ULTRASONOGRAPHY

Adv Radiol Oncol 1992; 81–5.

Ultrasound diagnostics of the neck: A ROC study

Pichler E[1], Breyer B[2], Mihajlović L[1], Boko H[3], Kralj Z [1]

[1] *Institute for Tumours and Allied Diseases, Zagreb*
[2] *Gynaecological Cancer Centre, Zagreb*
[3] *University Hospital »Dr. O. Novosel«, Zagreb*

ROC analysis of the overall improvement of neck tumour diagnostics by addition of ultrasound echography to clinical examination was performed. Information content of clinical examination only in 62 patients and of clinical plus ultrasound diagnostics in 92 patients was compared using the ROC method. The results indicate an essential improvement of the overall performance because the content of information rises by 78.3%. The actual specificity and sensitivity values indicate that the method is not suitable for one step screening.

Key words: neck; neoplasms; ultrasonography

Introduction

The broad availability of high frequency probes for realtime ultrasound scanning made the lateral region of the neck amenable to ultrasound diagnostics. In this region, although amenable to physical examination, in some cases it is hard to decide about the nature of the process, especially when the morphology is changed. Metastatic lymph nodes in the region are sometimes hard to find.[1]

Some expansive processes are specific for this region i.e. branchiogenic cysts or salivary gland tumours which give characteristic ultrasonic finding[1,2,3], what makes the benign-malignant differentiation easier [4,5,6,7] (Figure 1,2).

The neck tumours are of special interest to the Institute of Tumours and Allied Diseases where the patients can undergo a variety of medical treatments. In particular, the incidence of malignant tumours of the neck is much larger than the prevalence in the population. The in-patients are referred to the ultrasonic department on a routine basis. Under such conditions we decided to assess the contribution of ultrasound echography to the information on the malignant nature of the tumours.

Correspondence to: Dr. Pichler E. Institute for tumours and allied diseases, 41000 Zagreb, Croatia.

UDC: 616.743-006.6-073:534-8

Materials and methods

Patients

There were 154 patients with clinical diagnosis of neck tumour examined during a continuous period of 2 years. The control group comprised 62 patients and the group which underwent ultrasound echography 92 patients. At the end of the study, malignancy or benign nature of the tumour was verified by cytology or histology in all the cases. Thus, the number of malignancies is an aposteriori knowledge not present at the time

of examination. The patients from the control group underwent a clinical and an ultrasound examination by two physicians, the ultrasound data not being included into the ROC study documentation. The study group patients underwent the same procedure, with the ultrasound data being implemented into the ROC study. Both, the clinical and the ultrasound examination were performed by the same physicians. Thus, the only difference between both groups was the presence or absence of ultrasound data. The patients with cytology alone were those with benign disease and no need for surgical treatment. They all have been followed up by repeated clinical and ultrasound examination.

Method

Ultrasound examinations were done using a 5 MHz-linear and sector probe with a delay bath. The patients were lying prone. All the referred patients had palpable masses. After the examination in all the patients an ultrasound guided aspiration biopsy was done. Patients with negative cytology or histology were subject to further follow up. The specific pathology in patients is given in Table 1.

The so called ROC analysis was applied in order to determine the improvement of our diagnostics by addition of ultrasound to the conventional clinical examination. It enables the comparison of information content of different diagnostical proceedings.

The ROC analysis[8,9] is an abbreviation for 'Receiver Operating Characteristic' and is mathematically based on the Bayes' theorem. The receiving operator characteristic (ROC) is a curve which characterizes the ability of an observer or operator (e.g. a diagnostician using ultrasound or X rays) to detect features of interest (e.g. a malignant tumour) in the image. The curve represents the functional interdependence of the sensitivity and the specificity for an observer using a particular method or instrument.

The sensitivity of a diagnostic test is defined as the probability p(TP) to guess the presence of a given feature if it is actually present. In other words, it is the ratio of the number of true positive answers and the number of all actually present features.

On the other hand, the specificity is the probability p(TN) to guess the absence of a given feature if it is actually absent, i.e. the ratio of the number of true negative answers and the number of all actually absent features.

A diagnostic test is good only if both, the sensitivity and the specificity are high (i.e. nearly 1 or 100%).

Our resulting ROC curves are shown in Figure 3. The sensitivity p(TP) is represented on the ordinate. On the other hand, the specificity is represented by abscissa, but expressed using the quantity p(FN)=1-p(TN), instead of the very p(TN). This quantity indeed is the probability of false negative answers and easier to calculate. Thus, the specificity p(TN)=1 at p(FN)=0 and, reversely, p(TN)=0 at p(FN)=1.

The ROC analysis can be carried out only when one can define a question which is to be answered by YES with varying percentage of confidence criteria, the answer YES with 0%

Table 1. Specific pathology found in 154 patients examined for palpable neck mass.

Disease	Ultrasound + Clinical	Clinical only
Sialadenitis	5	3
Hyperplastic salivary gland	3	2
Pleomorphic adenoma	5	5
Lymphomatous cystadenoma	3	2
Cylindroma		1
Lymphadenitis	13	7
Tuberculous lymphadenitis	1	
Hyperplastic lymphnodes	2	6
Metastatic lymph nodes	21	17
Planocellular carcinoma	5	6
Lymphoma	7	2
Liposarcoma		1
Cervical cysts	7	6
Glomus tumour	1	
Lipoma	7	2
Neurinoma	2	
Various anatomic variations	8	1
Atheroma	1	1
Supurative inflammation	1	
Total	92	62

confidence meaning the answer NO with 100%. For instance, in our study the question was – »Is there a malignancy in the patients neck?« There were five confidence levels: »Almost definitely YES« (80-100%), »Probably YES« (60-80%), »Unsure YES« (40-60%), »Probably not YES« (20-40%) and »Almost certainly not YES« (0-20%). Note that the confidence criteria should be reversely ordered if answer NO were graduated. The ROC analysis is the adequate instrument to process the given type of data.

In order to construct the ROC curve one has first to examine the patient and then write down the diagnosis in above terms. Later on, one must verify it by a direct method (in our case by

Table 2. Malignancy suspected (clinical examination only). Question answered: »Is there a malignant disease in the neck of this patients?«

	CATEGORY				
	Almost certainly YES (80-100%)	Probably YES (60-80%)	Unsure YES (40-60%)	Probably not YES 20-40%)	Almost certainly not YES (0-20%)
	TP ANSWERS:				
Number classified into the category	17	4	4	3	0
	total = 28 malignancies present				
Probability estimate	17/28= 0.61	4/28= 0.14	0.14	0.11	0
p(TP) Cumulative probability	0.61	0.75	0.89	1	1
	FN ANSWERS				
Number classified into the category	2	6	5	18	3
	total = 34 benign (malignancy absent)				
Probability estimate	0.059	0.176	0.147	0.529	0.088
p(FN) Cumulative probability	0.059	0.235	0.382	0.911	1

probability estimate = number in the category divided by total number of malignant or benign respectively
cumulative probability = sum of probability estimates

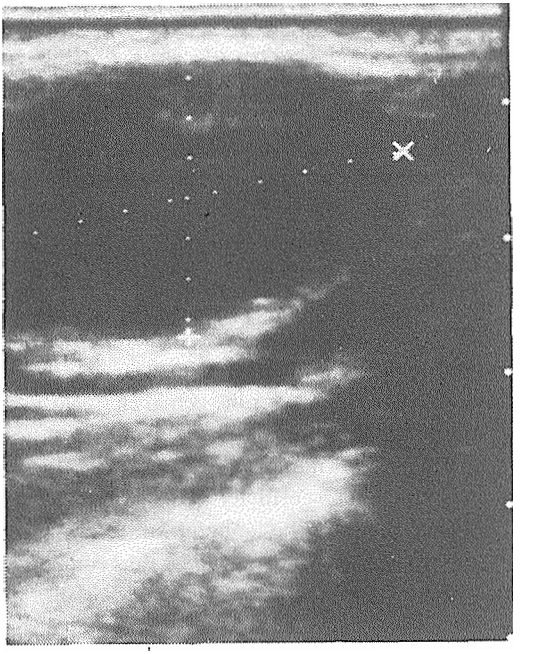

Figure 1. Ultrasound image of a branchogenic cyst is rather typical for benign expansive process of the neck.

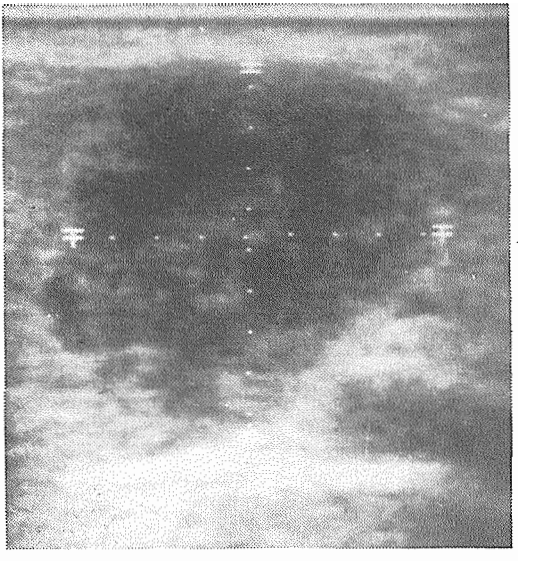

Figure 2. Metastatic lymph nodes when larger than 2 cm have a typical ultrasound appearance. Irregular, not sharply delineated borders and inhomogeneous echo distribution.

cytology or histology). After having been collected, data were processed as shown in Table 2. Indeed, Table 2 was derived from the documentation of patients where a line was reserved with choices of answer YES at various criteria. The answers were filled in at the time of examination and the final outcome after the cytological or histological verification. The ROC curve belonging to the data in Table 2 is the lower curve in Figure 3.

The 45° line represents the characteristic ROC curve of an ideally useless test carrying no information. The further the actual characteristic from the 45° line, the better the diagnostics. For an ideally useful method the curve would jump directly to 100% sensitivity at 100% specificity, i.e. zero p(FN). The amount of information carried by one ROC curve can be thus compared to another one. In reality it is not possible to work without previous (a priori) knowledge, be it from other clinical tests or from general clinical knowledge. The ROC curve shows how the sensitivity increases with decreasing specificity when the observer's (the sonologist's in our case) criteria are changing. A particular observer or person necessarily moves along his own ROC curve. Namely, if the observer decides to become more sensitive (for example due to some serious pitfall), the specificity will be reduced according to the ROC curve. Thus, the ROC curve shows the relationship of specificity versus sensitivity for a specific diagnostical proceeding or method. It is far more detailed than a rough estimate of bulk sensitivity and specificity.

The size of the area between the curve and the 45° line is proportional to the information content for the given proceeding. If two diagnostical methods (diagnosticians) are compared, the one with larger area will represent the better method.

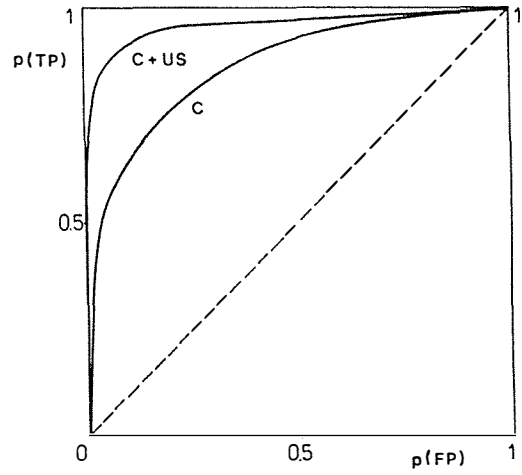

Figure 3. ROC curves showing the receiving operator characteristics for the clinical examination only (C) and for the clinical examination supplemented with ultrasound scanning (C+US). The difference between the surfaces below the two curves indicates the difference between the information contents. The sensitivity is represented on ordinate by p(TP). The specificity p(Tn) is represented using a reversed scale p(FN)1-p(TN) so that specificity = 1 at p(FN)=0 and, reversely, specificity = 0 at p(FN) = 1.

Results

Ultrasonic appearance of different expansive lesions and pitfalls

Sialadenitis and hyperplastic salivary glands were recognized both clinically and ultrasonographically. They appeared as a diffusely enlarged gland. Echogenicity has been dependent on the stage of the disease. One case of an abscess in a chronically inflamed gland caused the following diagnostical problem: On the ultrasound, as well as clinically it was considered as equivocal, namely a 'probably YES'. The abscess appeared ultrasonographically irregular in shape, partly unsharply delineated circumscribed mass within the submandibular gland. On ultrasonically guided fine needle biopsy it was proved to be an abscess. The clinicians insisted on histology because the mass was fixed and they regarded it to be probably malignant. The diagnosis was proved by histology.

In patients with known primary carcinoma in the head and neck region, small lymph nodes up to 1.5 cm in diameter were the most problematic, both clinically and ultrasonographically. These lymph nodes appeared as regular, ovally shaped, hypoechoic, with uniform echo distribution regardless of pathology. In two such cases we

pronounced lymph nodes 1 cm of size to be probably benign, whereas ultrasonically guided aspiration biopsy and subsequent histology proved them to be metastases.

In another patient, a 3 cm large lymph node was ultrasonically diagnosed as malignant because of inhomogeneous internal echo distribution and irregular borders. The same node was clinically judged probably malignant because it was fixed. Subsequent histology revealed it to be lymphadenitis with necrosis.

Patients with malignant lymphomas were correctly recognized as malignant, both clinically and ultrasonographically. However, in a case of a young man who presented with clinically and ultrasonographically typical findings for lymphoma, a tuberculous lymphadenitis was found on histology. Ultrasonography showed regular, multiple enlarged hypoechoic nodes. This was a 100% diagnostic miss.

Cervical cysts were always recognized by ultrasonography as benign. In two of the cases, inflamed cysts were clinically judged as probably malignant, but were ultrasonically correctly assesed as benign. In one (rare) case of cystic metastasis without known primary tumour at the time of examination, the ultrasonic diagnosis was correct due to the irregular and thickened lower wall. Clinical diagnosis missed this metastasis because the lesion appeared palpatorily cystic. Later on, the primary tumour was discovered as a small lesion at the base of the tongue.

One of the cases of neurinoma was regularly shaped with hyperechoic regular capsule. It was correctly diagnosed as benign. In another case of neurinoma the capsule was irregular and it was ultrasonically misinterpreted as malignant.

The final results of ROC analysis are shown in Figure 3. The lower curve represents the clinical assessment alone, and the upper curve the clinical + ultrasound assessment. The information content of the two curves was calculated by Shannon and Weaver theorem and results with 0.9 binary information units for clinical and 1.65 binary units for clinical + ultrasound method. After addition of ultrasound a 78.3% improvement of the diagnostic efficiency has been obtained.

Discussion

The results shown in Figure 3 and the information content calculation indicate an essential contribution of ultrasound to the ability of differentiating benign and malignant tumours of the neck. The flattened curve for a clinical diagnostics only indicates an increased number of indecisive (50/50) cases which become potentially decisive with the addition of ultrasound. This result is important for a specialized oncological institution with a high incidence of malignancies as the one presented in Table 1. Namely, the curves show that whichever specificity cutoff point we choose, the addition of ultrasound echography significantly improves the sensitivity of the conventional approach.

References

1. Bruneton JN, Roux P, Caramella E, Demard F, Valliconi J, Chauvel F. Ear nose and throat cancer: Ultrasound diagnosis of metastasis to cervical lymph nodes. *Radiology* 1984; **152:**771-2.
2. Badami JP, Athey PA. Sonography in the diagnosis of bronchial cysts. *AJR* **137:**1981;1245-
3. Ballerini G, Mantero M, Sbrocca M. Ultrasound patterns of parotid masses. *J Clin Ultrasound* 1984; **12:**273-74.
4. Bruneton JN. *Ultrasonography of the neck*. Springer Verlag, 1987.
5. Evans AL. *The evaluation of medical images*. A. Hilger Ltd, Bristol, 1981.
6. Gritzmann N, Czembirek H, Hajek P, Karnel F, Freuhwald F. Sonographische Halsanatomie und ihre Bedeutung beim Lymphknotenstaging von Kopf-Hals-Malignomen. *Roentgenstrahlen*, 1987; **138:**1-2.
7. Kuhn FP, Mika M, Schiuld H, Klose K. Spektrum der Sonographie von lateralen Kopf und Halsweichteilen. *Fortschr Roentgenst* 1983, **138:**435-436.
8. Metz GE, Starr SJ, Lausted LB. Quantitative evaluation of visual detection performance in medicine: ROC analysis and determination of diagnostic benefit. In GA Hay, ed. Medical Images: *Formation Perception and Measurement*. London: Willey, 1977; 220-221.
9. Metz CE, Goodenough DJ, Rossmann K. Evaluation of receiver operating characteristic curve data in terms of information theory with applications in radiography. *Radiology* 1973; **109:**297-298.

Adv Radiol Oncol 1992; 86–9.

Position of nodules in echographically multinodular thyroid in comparison with patohistologic nature of nodules

Brkljačić B, Drinković I, Delić-Brkljačić D, Boko H, Vidjak V

University Hospital »Dr. O. Novosel« Zagreb
Center for Ultrasound

Intrathyroid positions of nodules, with respect to their patohistologic nature, in 160 patients having echographically multinodular thyroid were investigated. Patohistologic findings were categorized as malignant and benign, and nodules divided into 7 categories in relation with their intrathyroid position. 414 nodules were surgically removed; 67 were malignant (16.2%) and 347 benign (83.8%). Among all positions, the lower pole of lobe was the most cammon site of nodules. Relative proportion of malignant nodules is the highest in the upper pole of lobes (27%), while in other observed positions it is not significantly different from the proportion of malignant nodules among all removed nodules (16.2%). The observed difference is statistically significant (Hi–square = 6,86; p<0,01). The authors conclude that probability of malignancy in echographically multinodular thyroid is higher if nodule is positioned in the upper pole of lobe. Position of nodules in echographically multinodular thyroid should be taken in account when deciding in which nodule to perform fine needle aspiration biopsy.

Key words: thyroid neoplasms; ultrasonography; biopsy

Introduction

Although multinodular thyroids are considered to be bening changes, it is not so rare to see malignant nodules in multinodular thyroid.[1,2] Introduction of ultrasound in diagnostics of thyroid diseases has enabled us to visualize small occult, nonpalpable thyroid nodules, measuring only few millimeters. Many nodules that cannot be palpated or seen on scintigraphy can therefore be discovered by ultrasound. Consequently, ultrasonic of thyroid multinodularity is, appart from patohistologic, the most accurate one.[3]

Correspondence to: Dr. Boris Brkljačić, mr. sci, Zavod za radiologiju, KB »Dr O. Novosel«, 41000 Zagreb, Zajčeva 19, Croatia.

UDC: 616.441-006.6-073:534-8

Hence it is desirable to have estabiliched echographic indicators for determination of nodules that carry higher risk of malignancy and in which fine needle aspiration biopsy (FNAB) should be performed. Such indicators are e.g. echostructure of nodules, irregular nodular contours, hypoechoic limb (»halo–effect«), cystic changes, intranodular clacifications.[2,3]

Position of nodules within the thyroid gland, with regard to their patohistologic nature should also be of interest to ultrasonographers. Data about this matter in literature are not abundant. Some studies on patohistologic specimens indicate that medullary thyroid cancer is more often situated in upper and middle parts of thyroid lobes,[4] and that papillary cancer is more common in upper pole of lobes.[5] As far as authors are aware, studies concerning position

of nodules in echographically multinodular thyroid, in respect to their patohistologic nature, were not performed.

Material and methods

We investigated 160 patients with echographic findings of multinodular thyroids. All patients underwent resection of thyroid, either total, or lobectomy. We compared patohistologic findings of removed nodules with preoperative ultrasonic findings, considering position of nodules within the thyroid.

Patohistologic findings of nodules were categorized as malignant and benign. Positions of nodules were categorized as follows: upper pole (for nodules situated in the upper half of thyroid lobe on longitudinal ultrasonic scan); lower pole (nodules situated in the lower half of lobe); middle part (nodules situated in the middle portion of lobe, partially occupying both halves of lobe); isthmus (nodules situated in isthmus); upper two thirds; lower two thirds; and the whole lobe (larger nodules, measuring more than half of lobe length).

Ultrasonic examination was performed using Aloka SSD 256 machine having 5 MHz linear probe and G.E.–CGR Radius CF machine having 7.5 MHz convex probe.

In statistical analysis we used Hi–square test for determination analysis of statistical significance of differences between obtained data.

For graphical processing of data we have used standard computors programme Harward Graphics.

Results

In 160 examined patients with echographically multinodular thyroids were found 476 nodules; 230 in the right lobe, 197 in the left lobe and 46 in the isthmus. 414 nodules were surgically removed. Of these nodules 67 were malignant (16,2%) and 347 benign (83,8%).

Among malignant nodules (all carcinomas) we found 48 papillary, 12 follicular, 4 Huerthle–cell and 3 medullary carcinomas. Among benign nodules we found 216 colloid goiter nodules, 105

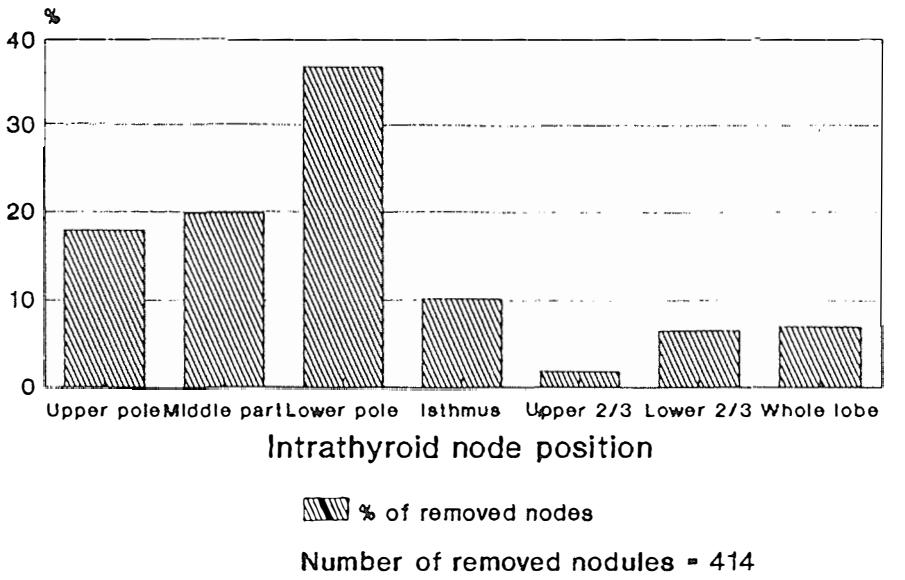

Figure 1. Position of removed nodules in thyroid

follicular adenomas, 11 Huerthle-cell adenomas and 15 lymphocytis thyroiditis nodules.

Distribution of removed nodules in relation to their position in thyroid is shown in Figure 1. It can be seen that of all positions, lower pole is by far the most common site of thyroid nodules. Only 64 nodules (15,4%) were larger, i.e. measuring more than half length of lobe (Figure 1).

Figure 2 shows distributions of nodules in different positions in relation to their patohistologic nature. It is visible that compared to other positions, relative proportion of malignant nodules is the highest in the upper pole of thyroid lobe. Proportion of malignant nodules among romoved nodules was 16,2%, while their proportion in upper pole was 27.0%. The difference is statistically significant (Hi-square=6,86; $p<0.01$).

Distribution of nodules categorized upon their patohistologic nature in relation to their position in thyroid is shown in Figure 3. Among carcinomas, 29.8% of nodules were situated in the

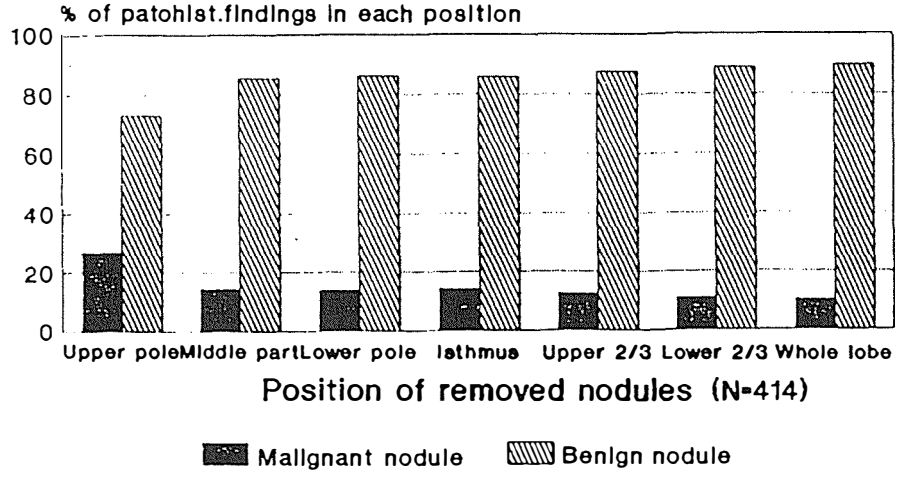

Figure 2. Intrathyroid position of nodules in relation to patohistologic findings.

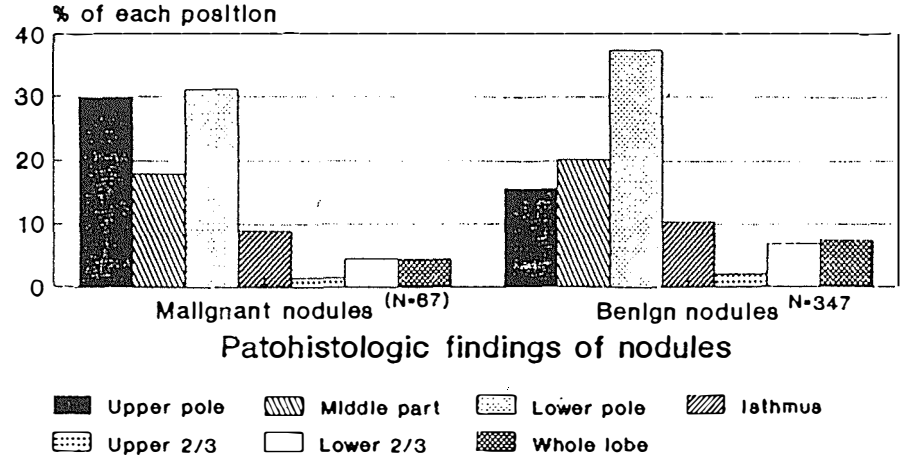

Figure 3. Patohistologic findings of nodules in relation to intrathyroid positions.

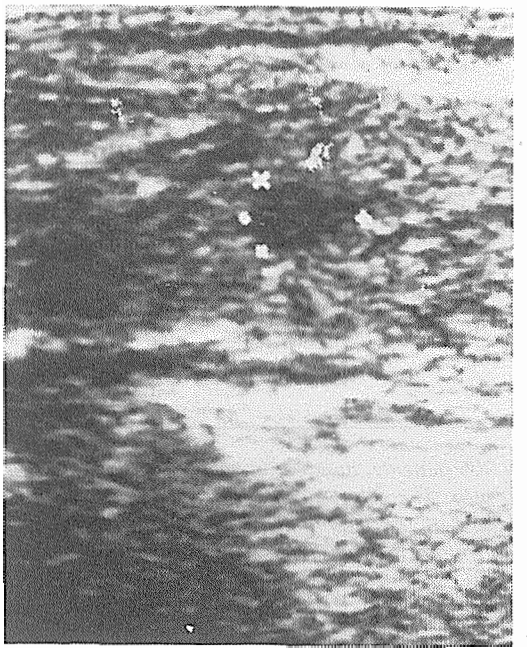

Figure 4. Ultrasonic image of hypoechoic nodule positioned in the upper pole of left (LR) thyroid lobe. Patohistologic finding: medullary carcinoma.

upper pole, almost as much as in lower pole, although nodules regardless of their patohistologic nature were twice as often situated in lower pole, as in comparison with the upper pole.

Hypoechoic nodule, measuring only 9x6 mm, positioned in the upper pole of thyroid is shown in Figure 4. Pathohistologic finding was medullary carcinoma.

Discussion

Analysis of results enables us to conclude that among all positions of nodules, lower pole is is the most common site in multinodular thyroid, since 36.7% of removed nodules were positioned there.

Relative proportion of malignant nodules in individual positions was almost equal to the proportion of malignant nodules among removed nodules (16.2%). The only exception is upper pole of thyroid lobe, where proportion of malignant nodules in statistically singificantly higher ($p<0.01$), compaired to their proportion among removed nodules.

Therefore, we can conclude that probability of malignancy is higher if nodule is positioned in the upper pole of multinodular thyroid, attention should be given to the nodules in upper poles of lobes, and FNAB should be performed upon them with priority. When performing FNAB in echographically multinodular thyroid, position of thyroid nodules should be taken in account altogether with other echographic indicators of malignancy.

References

1. De Groot LJ, Larsen PR, Refetoff S, Stanbury JB. *The thyroid and its diseases.* 5th edition. New York–Chicester–Brisbane–Toronto–Singapore: J Wiley&Sons Inc, 1984: 732-830.
2. Brkljačić B. Značenje ultrazvuka i ciljane citološke punkcije u dijagnostici tumora u multinodozno promijenjenim štitnjačama (Magisterij). Zagreb: Medicinski fakultet Sveučilišta u Zagrebu, 1991.
3. Tomić–Brzac, Bence–Žigman Z. Štitnjača U: Kurjak A, Ur. *Ultrazvuk u kliničkoj medicini*, Naprijed, Zagreb, 1989; 660-71.
4. Ingbar SH, Braverman LE ed. Werner's The Thyroid. *A fundamental and clinical text.* Philadelphia, London, New York, Sao Paolo, Mexico City, St Louis, Sydney: JB Lippincott Company, 1986.
5. Melliere D, Massin JP, Calmettes C, Chigot JP, Savoire JC, Garnier H. Le risque de malignite des nodules froids thyroidiens. *La Presse Medicale* 1970;**78**:311.

Adv Radiol Oncol 1992; 90–5.

Parameters for echographic evaluation of gallbladder contractions

Mirić S and Sabljak I

University Medical Center
Institute of Radiology and Oncology,
Sarajevo

The degree of gallbladder contraction was evaluated in 306 patients, divided into four groups according to the type of the stimulatory meal after 30,45 and 60 min. The echographic evaluation of changes of the gallbladder diameter was obtained by the correlation of the gallbladder image before and after ingestion, as well as measuring the width and lenght of the diameter. The best contractions were obtained after the ingestion of two dried fresh egg yolks. The most optimal time for evaluation of the degree of contractions was 45 min. after stimulatory meal ingestion.

Key words: gallbladder; ultrasonography

Introduction

Gallbladder, ductus cysticus, choledochus and Oddi's sphincter function is an entity with reciprocal intervention of gallbladder and Oddi's sphincter. Therefore, the changes in emptying of the gallbladder are indicative for the diagnosis of pathologic and functional changes of the gallbladder and biliary ducts. Doyden (1926), Sussman (1937), Ivy (1947) et al. described changes in gallbladder size after ingestion of a fatty meal as the stimulation for contractions during peroral cholecystography.[1,2,3]

The development of real-time ultrasonographic units enables rapid and successful diagnosis of all types of structural pathologic changes of the gallbladder, as well as changes in contractions, which can reflect the organic and functional conditions of the gallbladder and biliary ducts.[4-12]

According to our previous investigation by the correlative follow-up of gallbladder contractions during peroral cholecystography and echography, echographic evaluation of contractions agrees with the information provided by peroral cholecystography.[13]

During the investigation and later on it is noted that gallbladder contraction is averagely less marked in stimulation by two dried eggs after 30 min. So, the new investigation was performed in order to determine the optimal time of gallbladder contractions and an applicable type of stimulatory meal.

Correspondence to: Prof. dr Slavica Mirić, Institute of Radiology and Oncology, University Medical Center, 71000 Sarajevo, Moše Pijade 25.

UDC: 616.366-073:534-8

Materials and methods

The investigation was performed on 306 patients distributed into four groups according to the

type of stimulatory meal. Group I included 78 patients who ingested two dried eggs. Group II also included 78 patients who ingested two fresh egg yolks. Group III comprised 75 patients who ingested 25 gr of »Eurocreme«. In group in IV 75 patients, who ingested 10 gr of chocolate. Echographically, all patients had normal morphologic findings of the gallbladder.

The evaluation of gallbladder contractions was performed according to the roentgenologic standards, correlating visually the gallblader size on polaroid images before and after stimulation. The imaging was performed in the left oblique position, whereas with the cranial position of the gallbladder, adipose patients and meteorism, the imaging of the gallbladder is better in this position while the eventual incurvation of the neck would be straightened.

Simultaneously, the measurement in millimeters of the largest vertical and transversal gallbladder diameter, i.e, the length and width of the greatest vertical diameter was performed. In a previous investigation, it has been noted that in the decrease of the size of gallbladder shadow for about a half, the sum of the lenght and width is decreased for about one third. Contraction is medially marked or normal if the sum of the length and width (L + W) after stimulation (B) changes for 1/3 from the sum of the length and width (L + W) before stimulation (A). Figuratively, in the form of formula, the contraction is medium, K = + , if (L + W) B = (L + W) $A - \frac{1}{3}$ (L + W), that is, the sum of the length and width of the gallbladder after stimulation is equal to the sum before stimulation reduced for 1/3 of the sum, which means that contraction is intensified and vice versa.

The gradation of contraction is distributed in 4 degrees: without contraction »O«, mild contraction »–«, medium contraction »+« and marked contraction »++« (Figure 1,2,3,4).

Results

The gallbladder contraction, evaluated visually and on the basis of the measurements of the length and width of the largest diameter has been presented by groups, depending on the type of stimulatory meal.

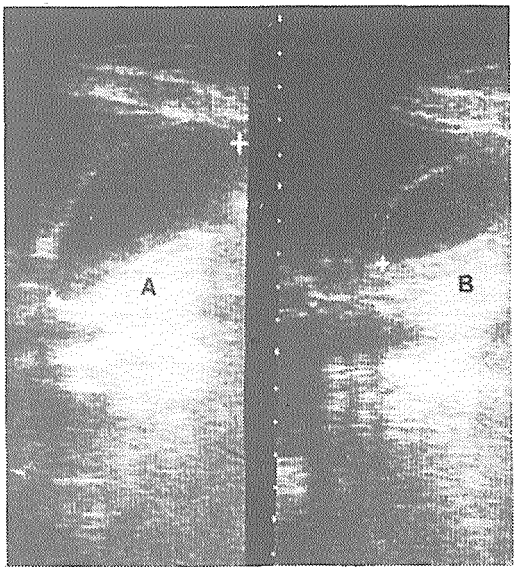

Figure 1. Gallbladder sections: A-before stimulatory meal, B-after stimulatory meal. Changes in size and shape of the section correspond to medium gallbladder contraction (»+«).

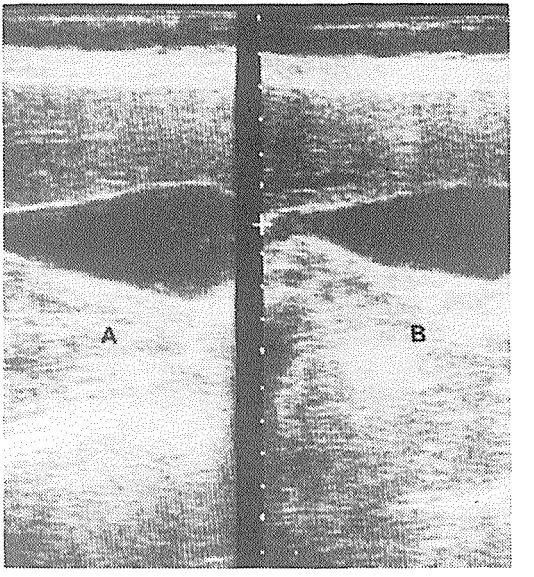

Figure 2. Gallbladder sections. A-before stimulatory meal and B-after stimulatory meal. Gallbladder width is slightly decreased after stimulatory meal, length is almost the same, contractions are low (»–«).

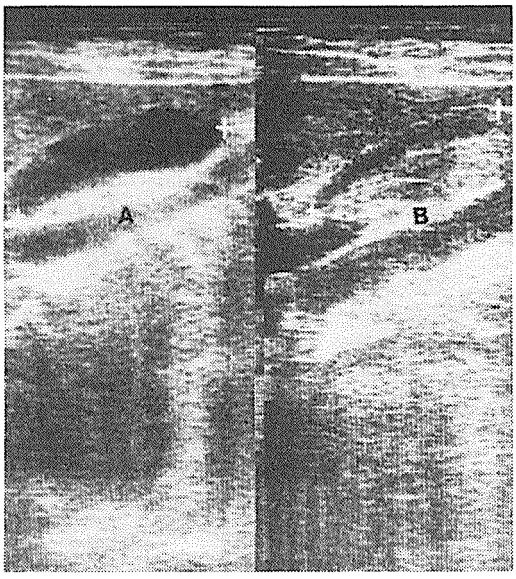

Figure 3. Gallbladder sections: A-before stimulatory meal and B-after stimulatory meal. Very marked gallbladder contractions (»++«), gallbladder length is the same, but the lumen is completely empty and luminal width extremelly decreased.

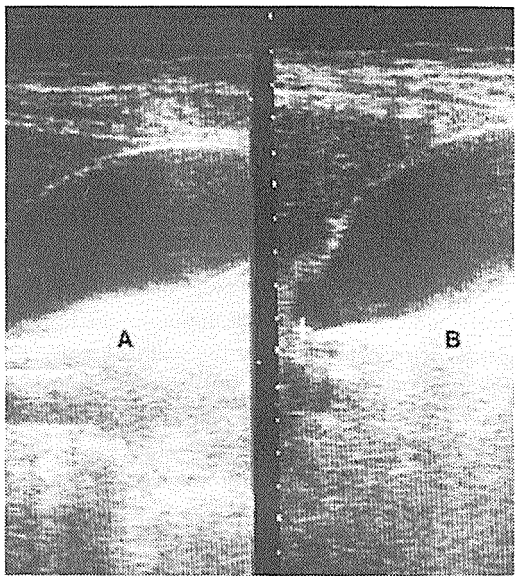

Figure 4. Gallbladder sections: A-before stimulatory meal and B-after stimulatory meal. The shape and measures of gallbladder length and width are unchanged after the stimulatory meal. Contraction unexpressed (»0«).

Table 1. Degree of gallbladder contraction the stimulation by two dried eggs.

Time	Contraction degree				
	0	–	+	++	TOTAL
30 min	32	14	14	18	78
45 min	18	8	16	36	78
60 min	16	6	12	44	78

Table 2. Degree of gallbladder contraction after the stimulation by two egg yolks

Time	Contraction degree				
	0	–	+	++	TOTAL
30 min	18	10	18	32	78
45 min	10	12	22	34	78
60 min	12	8	20	38	78

Table 3. Degree of gallbladder contraction after the stimulation by 25 gr »Eurocreme«

Time	Contraction degree				
	0	–	+	++	TOTAL
30 min	40	17	11	7	75
45 min	25	15	28	7	75
60 min	20	20	17	18	75

Table 4. Degree of Gallbladder Contraction after the Stimulation by 10 Gr. of chocolate

Time	Contraction degree				
	0	–	+	++	TOTAL
30 min	35	12	15	13	75
45 min	19	13	15	28	75
60 min	18	21	13	23	75

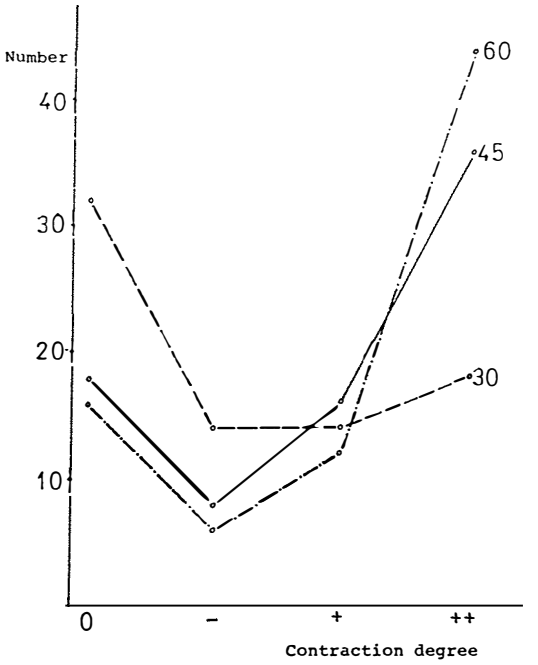

Graph 1. The curves of gallbladder contractions at 30,45 and 60 min after stimulation by two dried eggs.

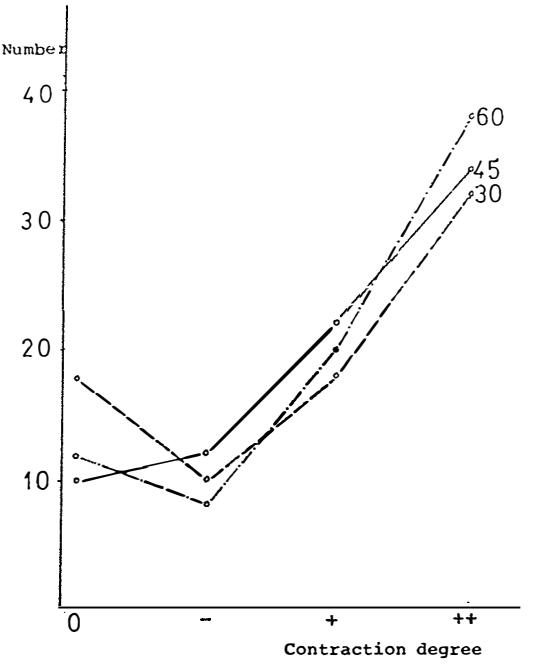

Graph 2. The curves of gallbladder contractions at 30,45 and 60 min after stimulation by two fresh egg yolks.

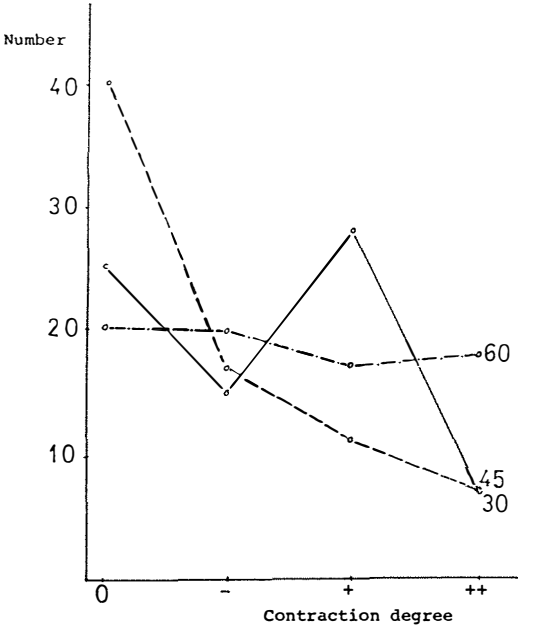

Graph 3. The curves of gallbladder contractions at 30,45 and 60 min after stimulation by 25 gr »Eurocrema«.

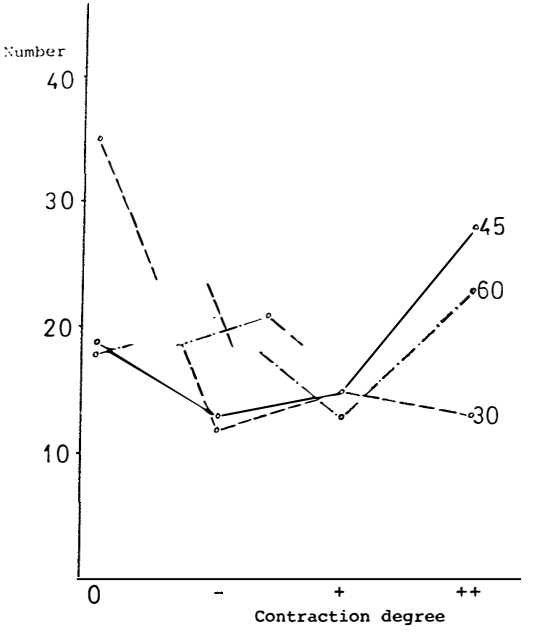

Graph 4. The curves of gallbladder contractions at 30,45 and 60 min after stimulation by 10 gr chocolate.

In the first group of 78 patients, two dried eggs were ingested as a stimulatory meal. The degree of gallbladder contraction and time of the evaluation of contractility is presented in Table 1 and Graph 1. The greatest number of the most intensive contractions 44/78, was obtained after 60 min, but the curve of the contractions intensity with the least oscillations was marked after 45 min.

In the second group of 78 patients, two fresh egg yolks were ingested as a stimulatory meal. The degree of gallbladder contraction relating to the time of 30,45 and 60 min. is presented in Table 2 and Graph 2. The greatest number of the most intensive contractions 38/78 was obtained after 60 min. The most optimal arrangement of the degree of contractions is evidented from the curve after 45 min.

In the third group of 75 patients ingesting 25 gr of »Eurocreme« for stimulation, the low degree of gallbladder contractions was evidented. The greatest number of cases 40/75 without contractions and the least number 7/75 with the highest degree of contractions were evidented after 30 min (Table 3, Graph 3).

In the fourth group of 75 patients 10 gr of chocolate was ingested as a stimulatory meal. The obtained degrees of contractions are presented in Table 4 and Graph 4. Gallbladder contractions were higher than by »Eurocreme« stimulation, but lower than by eggs stimulation.

Discussion

Gallbladder contractions and emptying in peroral cholecystography improve the presentation of gallbladder and visualization of small stones, polyps in hyperplastic cholecystosis, gallbladder deformities, acalculous inflammations, as well as functional and organic disorders of the Oddi's sphincter.[14-16]

Echography has enabled a rapid and simple imaging of the structural pathologic changes in dependently from the possibility of contrast presentation of the gallbladder, which is limited by many other factors. In normal structural findings of the gallbladder a change of contractions and emptying may be caused by the acalculous and unmanifest inflammation or functional changes of the gallbladder and biliary ducts.[5,7,9,11,17,18]

According to Hopmann (1985), the effects of gallbladder contractions after a fatty stimulatory meal were not significantly different relating to the intravenous use of cholecystokynin, which was used by many authors.[5,12,19,20]

Ultrasonographically, for the evaluation of changes in size, some authors measure the volume by method of the sum of cylinders using computer data processing.[10,12,19] The other authors report that the measuring of volume is as successful as by the method of calculating the volume of elypsoide.[11,21] Besides, there are authors who evaluate the gallbladder size, based on the length and width of gallbladder shadow[20] or its cross section.[5]

In our out-patient investigation, there was no possibility of the computerized calculation of volume. Being identical with the roentgenologic image after opacification by contrast material, visual evaluation of the size at echography can be used as a substitute for roentgenologic evaluation of gallbladder contraction. Figure 1 shows a medium gallbladder contraction (»+«) after stimulation. Figure 2 shows a mild (»–«) contraction, Figure 3 very marked (»++«) contraction. Gallbladder in Figure 4 failed to show the signs of contraction (»O«).

Measuring the length and width of the greatest section in millimeters, the evaluation of contraction degree, agreed with the visual evaluation of gallbladder size changes. Measurement can replace imaging in the cases of the lack of films.

The stimulatory meals used: dried eggs, fresh egg yolks, »Eurocreme« and chocolate, were selected because of the availability and possibility to find them in the town and its surroundings.

Conclusion

The changes in gallbladder emptying and contraction intensity are indicative for the diagnosis of the structural and functional pathologic conditions of the gallbladder. Echography enables, a

rapid and simple evaluation of the size changes after stimulatory meal, or measuring the width and length in the image of the cross section. The parameters for evaluation of the contraction intensity are the kind of stimulatory meal and time of evaluation of the degree of contractions after stimulation. On the basis of performed investigation, the best contractions were obtained after the ingestion of two fresh egg yolks, and the most optimal time for evaluation of the degree of contractions is 45 min. after stimulation.

References

1. Boyden EA. Study of behavior of human gallbladder in response to ingestion of food. *Anat Rec* 1926; **33:**201-39.
2. Sussman ML. Emptying of normal gallbladder. *AJR* 1937; **38:**867-71.
3. Ivy AC. Motor dysfunction of biliary tract; analytical and critical consideration. *AJR* 1947; **47:**1-11.
4. Everson GT, Braverman DZ, Johnson ML, Kern F Jr. Acritical evaluation of real-time ultrasonography for the study of gallbladder volume and contraction. *Gastroenterology* 1980; **79:**40-6.
5. Davis GB, Berk RN, Scheible FW, Witztum KF, Gilmore IT, Strong RM, Hofmann AF. Cholecystokinin Cholecystography, Sonography, and Scintigraphy: Detection of Chronis Acalculous Cholecystitis. *AJR* 1982; **139:**1117-21.
6. Marzio L, Di Giammarco AM, Schiavone C, Curccurullo F. Realtime ultrasonography of gallblader emptying in normal subjects. *Ultrasound in med and biology* 1982; **8:**123.
7. Kinugasa T, Fukano S, Sekimoto K. An operative indication of asymptomatic gallstone using realtime ultrasonography. *Ultrasound in Med and Biology* 1982; **8:**96.
8. Ono Y, Tomiyama H, Ochiai Y, Ito T, Shinagawa A, Kawashima Y, Honda T. Observation on gallblader contraction by means of an ultrasound electron scanner. *Ultrasound in Med and Biology* 1982; **8:**145.
9. Bobba VR, Krishnamurthy GT, Kingston E, Turner FE, Brown PH, Langrell K. Gallbladaer Dynamics Induced by a Fatty Meal in Normal Subjects and Patients With Gallstones. *J Nucl Med* 1984; **25:**21-4.
10. Hopman WPM, Kerstens PJSM, Jansen JBMJ, Rosenbusch, Lamers CBHW. Effect of Graded Physiologic Doses of Cholecystokinin on Gallbladder Contraction Measured by Ultrasonography. *Gastroenterology* 1985; **89:**1242-7.
11. Kishk SMA, Darwesh RMA, Dodds WJ, Lawson TL, Stewart ET, Kern KM, Hassanein EH. Sonographic Evaluation of Resting Gallbladder Volume and Postprandial Emptying in with Gallstones. *AJR* 1987; **148:**875-9.
12. Masclee AM, Hopman WPM, Corstens FHM, Rosenbusch G, Jansen JBMJ, Lamers CBHW, Simultaneous Measurement of Gallbladder Emptying with Cholescintigraphy and US during Infusion of Physiologic Doses of Cholecystokinin: A Comparison. *Radiology* 1989; **173:**407-10.
13. Mirić S, Čengić F, Lincender L, Pamučina P, Bajgorić M, Klančević M. et al. Ehografska procjena kontraktilnosti holeciste In: Glas CCCLXIII. Srpska akademija nauka i umjetnosti, Odjeljenje medicinskih nauka. Beograd 1991; **40:**133-9.
14. Berk RN. Oral cholecystography. I. Berk Rn, Ferrucci JT Jr. Leopold GR ed. *Radiology of the gallbladder and bile ducts.* Philadelphia, Saunders. 1983; 83-163.
15. Laufer I, Gledhill L. The value of the fatty meal in oral cholecystography. *Radiology* 1975; **114:**525-7.
16. Harvey IC, Myo T, Low-Beer TS. The value of the fatty meal in oral cholecystography. *Clin Radiol* 1976; **27:**117-21.
17. Weinberger H. Blumhagen JD, Odell JM. Gallbladder Contraction in Biliary Atresia. *AJR* 1987; 149-402.
18. Goldstein F, Grunt R, Margulies M. Cholecystokinin Cholecystography in the Differential Diagnosis of Acalculosis Gallbladder Disease. *Am J Dig Dis* 1974; **19:**835-49.
19. Hopman WPM, Rosenbusch G, Jansen JBM, de Jong AJL, Lamers CBHW. Gallbladder Contraction: Effects of Fatty Meals and Cholecystokinin. *Radiology* 1985; **157:**37-9.
20. Nathan MH, Newman A, Murray DJ. Normal Findings in Oral and Cholecystokinin Cholecystography. *JAMA* 1978; **21:**2271-2.
21. Dods WJ, Gron WJ, Darweesh RMA, Lawson TL, Kishk SMA, Kern KM. Sonographic Measurement of Gallbladder Volume. *AJR* 1985; **145:**1009-1.

Adv Radiol Oncol 1992; 96–8.

The treatment of appendiceal abscess by ultrasonically guided drainage

Drinković I, Brkljačić B, Boko H, Odak D, Vidjak V, Anić P

University Hospital »Dr O. Novosel« Zagreb
Center for Ultrasound

Appendiceal abscess is one of the possible complications of surgically non–treated acute appendicitis. It is presented by palpable, tumourous mass, usually in right lower quadrant, local tenderness, fever and leukocytosis. Therapy of the disease consists in abscess drainage, antibiotics therapy and postponed surgical operation. In the treatment of appendiceal abscess we use ultrasonically guided percutaneous thin catheter drainage which has considerable advantages in comparison with surgical drainage, and its proper performance enhances success of the procedure.

Key words: appendicitis; abscess-therapy; drainage; ultrasonography

Introduction

Acute appendicitis is the most common abdominal surgical emergency. It results from bacterial infection of the vermiform appendix. Contributory factors include intraluminal obstruction by fecaliths, lymphoid hyperplasia, rarely by parasites, or even a carcinoid tumour, or a tumour in the coecum. Obstruction is followed by inflammation which causes edema and ischemia in all layers of appendix and can progress to gangrene and perforation as a result of increased intraluminal pressure. Perforation may occur early in the course of the disease (within 24 to 48 h) and may produce either a localized or general peritonitis which is the result of non–treated peritonitis.[1]

The treatment of appendiceal abscess can be conservative by administering antibiotics, or agressive – surgical or ultrasonically guided drainage.[2,3,4,5] In our department, ultrasonically guided percutaneous thin catether drainage is being performed for the last four years in the treatment of apendiceal abscesses.[6]

Correspondence to: Doc. dr. sci. Ivan Drinković, KB »Dr O. Novosel«, Zajčeva 19, 41000 Zagreb, Croatia.

UDC: 616.346.2-002.3-089.48:534-8

Material and methods

Ultrasonically guided percutaneous appendiceal abscess drainage, using thin catether was performed in 21 patients, in the period of 4 years. All patients were hospitalized on the Department of Surgery, University Hospital »Dr O. Novosel«, Zagreb. Their age was from 29 to 62 years. All abscesses were localized in the region of right lower abdominal quadrant. The smallest abscess was measuring 3 cm in the longest diameter, and the biggest was measuring 15 cm. Ultrasonic images of abscess contents were sonolucent, representing liquid, as seen in Figure 1.

Drainage was performed by using 5 F pigtail catheter. After local anesthesia and skin incision

catheter was positioned by trocar technique and tip of the cateteher was constantly monitored by ultrasound, as seen in Figure 2.

Duration of drainage, employing continuous negative pressure, was up to seven days. Material obtained from abscess is routinely being subjected to culture (antibiogram) analysis. Ultrasonic equipment we used had linear, convex and sector probes of 5 MHz, 6 MHz and 7.5 MHz, respectivelly.

Results

Of 21 patients in whom appendiceal abscess drainage was performed, pus was obtained and successfully evacuated in 16 patients. In 5 patients it was necessary to perform additional isotonic solution lavage through the catheter. Serious complications were not observed. One catheter displacement occured a day after procedure, but reintervention was not necessary. All patients were under antibiotic therapy. Sanation of abscess was accomplished in all patients, and deffinitive surgery was performed in the period of up to 3 months.

Discussion

Acute appendicitis in its natural course has three phases. In up to first 8 hrs after luminal obstruction integrity of appendiceal wall is being gradually lost. Between 2-24 hours of the disease course occurs inflammation, and after that complications in the forms of diffuse peritonitis or appendiceal abscess can take place.

Appendiceal abscess presents itself, following symptoms of acute appenciditis, by palpable tumourous mass, usually in right illeal fosa, local tenderness, fever and leukocytosis. The patients are usually in bad general condition.

While acute appendicitis requires operative treatment, occurence of appendiceal abscess requires drainage, since antibiotics therapy alone is not always sufficient. When appendectomy is deffered under these circumstances, it may be performed a number of weeks after recovery from the acute process.[1]

Treatment of appendical abscess by surgical drainage can be accompanied with some complications[2,3], whereas the ultrasonically guided percutaneous thin catheter drainage has the advantage of only local anesthesia and thin catheter causes less traumatization. Also trocar technique of catheter implacement reduces duration of the whole procedure to the period of only few minutes.[4,5] Ultrasound enables visualisation of the exact localization of abscess and provides information on abscess contents on the basis of echographic structure of abscess internal echos.

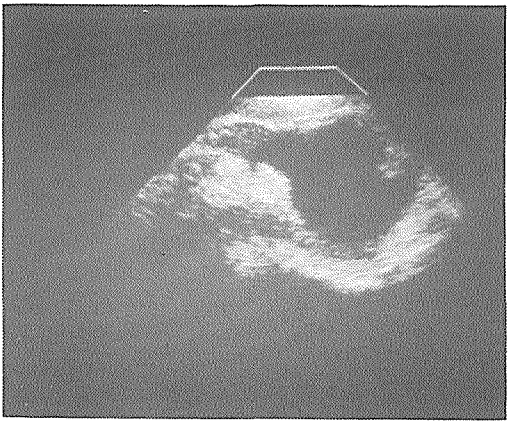

Figure 1. Ultrasonic image of inflammed appendix with thick appendiceal wall and large sonolucent adjacent abscess formation with some internal echoes.

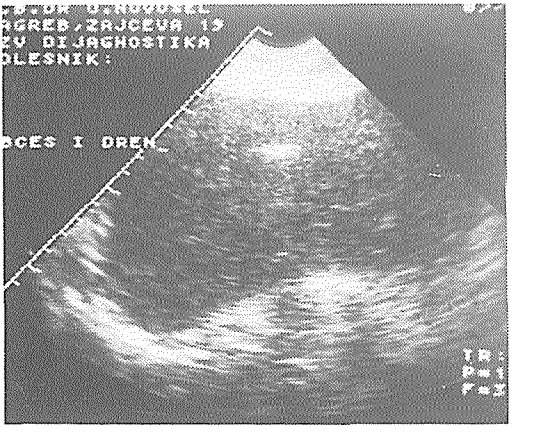

Figure 2. Hyperechoic linear structure representing tip of the catheter which is placed inside the appendiceal abscess. Abscess is sonolucent, with internal echoes.

Once placement of the catheter is performed succesfully, drainage of pus and gass pressure diminishment cause evident improvement of patients general condition, as well as reduction of fever and pain.[2,3,4]

This method is quick, cheap and without complications that might follow surgical drainage. Longer illness duration occuring with only conservative treatment is reduced as well. It is neccessary to emphasize that complete sanation of process cannot be achieved by this method, and appendectomy in the period of up to three months is mandatory, because of the possibility of recurrence and its complications.[1]

We conclude that ultrasonically guided percutaneous thin catether drainage of appendiceal abscess is relatively new and successful method in the treatment of this disease, which enables us to observe progression of abscess and to determine time to perform drainage. Uncertain result of antibiotic therapy and complications that may accompany surgical drainage are therefore being avoided, and patients condition is being improved. The method can be applied in all hospitals that are equipped with adequate ultrasonic equipment.

References

1. Berkow R, ed. *The Merck manual of diagnosis and therapy*. 15th ed. Rahway NJ Merk & Co., 1987, 757-9.
2. Glass C et al. Drainage of intraabdominal abscesses. *Am J Surg* 1984; **147:**315-7.
3. Gary R et al. Percutaneous abscess Drainage. *Gastrointest Radiol* 1985; **10:**79-84.
4. Froelich E et al. Ultrasound guided percutaneous drainage of abdominal abscesses. *Radiol Iugosl* 1990; **24:**393-5.
5. Puylaert J. The appendiceal mas: new perspectives by ultrasound. Proceedings of the 17th international congress of radiology, Paris, 1989.
6. Drinković I et al. New catheter set for US-guided procedures. *Radiol Iugosl* 1990; **24:**409-11.

Adv Radiol Oncol 1992; 99–101.

Ultrasound in diagnostics of muscular injuries

Vidjak V, Drinković I, Brkljačić B, Krmpotić T, Boko H, Odak D

University Hospital »Dr. O. Novosel« Zagreb
Center for Ultrasound

Ultrasonic investigation of 38 patients with muscular injury of thigh, referred to our department was performed. All patients were sportsmen, aged from 21-43 years. Ultrasonic findings were arranged in five categories according to the extent and echostructure of visualized alterations. The most often encountered pattern of echogenicity, in changes observed within 4 days after injury, showed anechoic, inhomogenous intramuscular areas with muscular contours irregularity. The authors conclude that ultrasound can, in wide extent, provide information about type and extent of trauma and about succesfulness of treatment of muscular injuries of thigh.

Key words: muscles-injuries; ultrasonography

Introduction

Ruptures and minor muscle injuries have become more common with expansion of sports, and are of special interest for both sportsmen and phyisicians. Muscular injuries are the consequence of direct hit, muscular hyperextension or puncture. Clinical recognition of ruptures is based on following symptoms: pain in the site of injury, pain on palpation, painful active and passive movements, swelling that may evolve into tumorous formation, as well as functional impairment.[1,2]

Ultrasound provides insight into normal anatomy of extremities, as well as into pathological alterations. It is possible to delineate muscular contours, by visualizing fascia. Longitudinal and transverse sections enable visualization of contours and internal muscular echostructure.[3,4]

Ultrasonic images of traumatical muscular injuries are cathegorized in three levels (according to Burgeois)[3,5]:

I: no changes visible by ultrasound;

II: small rupture areas, measuring less than 2 cm in diameter, with inhomogenous internal echostructure;

III: rupture visible as irregular anechoic zone, measuring more than 2 cm in diameter, with concomitant major muscular injury.

Soft tissues of thigh are very often exposed to traumatic injuries. We present cases of examined patients, referred to our ultrasonic department in the period of three years, on clinical suspicion of thigh muscles injuries.

Correspondence to: Dr. Vinko Vidjak, KB »Dr O. Novosel«, Zavod za radiologiju, Zajčeva 19, Zagreb, Croatia.

UDC: 616.74-001.4-073:534-8

Material and methods

In the period of 3 years, 38 patients with muscular trauma of thigh were examined in our depart-

ment, all male, aged from 21 to 43 years, referred to us by the sport-medicine specialist, after clinical examination. Patients were all active[31] or former [7] sportsmen. Ultrasonic examination was performed by General Electris – RT 4000 machine, having linear 7.5 MHz probe. The examinations were performed by longitudinal and transverse scanning of injured muscles and of the contralateral thigh.

Results

Ultrasonic findings were cathegorized into five types:

1) Seven patients had anamnestic data of injury within 4 days previous to examination, and some clinical indicators (pain on palpation) as well, but it was not possible to visualise ultrasonically any pathological signs in muscular echostructure.

2) Nineteen patients with anamnestic data of injury within 4 days previous to examination had ultrasonic findings indicating certain muscular irregularity with focal anechogenic areas containing no internal echoes (Figure 1). These patients had haematomas, measuring up to 2 cm. In 16 patients, injury of m.vastus lateralis was found, and in 3 patients m.rectus femoris injury was found.

3) In two patients large muscular separation was found, represented ultrasonically by the wider hypoechoic zone with almost no internal echoes, and clear muscular contours delineation (Figure 2); the finding was a result of fresch haematoma caused by muscular rupture and ultrasonically measured dimensions were bigger than 2 cm in diameter (46 mm and 39 mm, respecitvely). In both cases m.rectus femoris was traumatized.

4) In eight patients, who were examined 3-5 weeks following trauma, inhomogenous, predominantly hyperechoic area inside the muscle was found. Delineation was vague (Figure 3). The finding represented organized haematomas. Muscular contours delineation was unclear, and dimensions of haematomas were smaller than 3 cm in

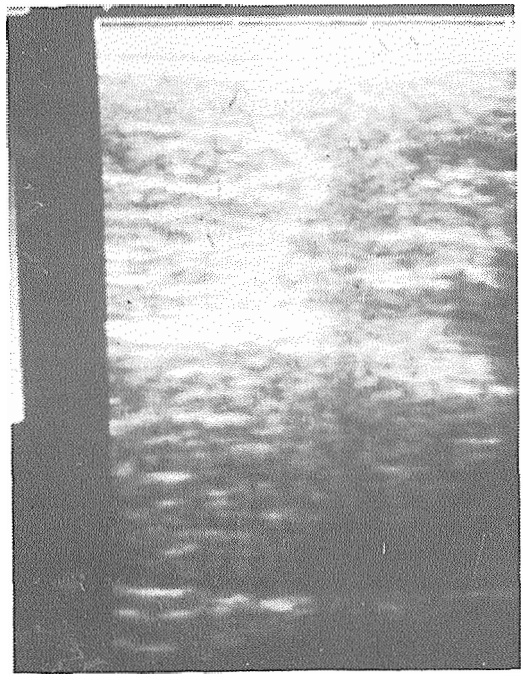

Figure 1. Ultrasonic image showing area of muscular irregularity with small focal anechogenic areas.

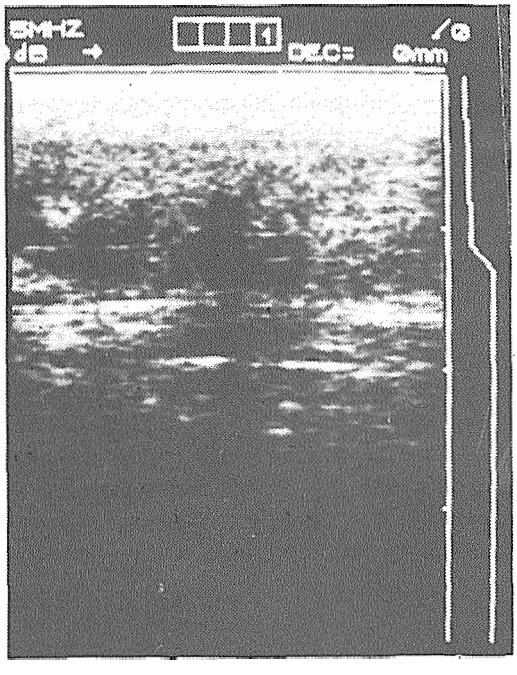

Figure 2. Ultrasonic image of wide hypoechoic zone with no internal echoes, and clear muscular contours delineation.

diameter. Four patients had m.rectus femoris and four m.vastus lat. injury.

5) In two patients, no ultrasonic findings were visualized which could correlate with site of injury occuring 9-12 months prior to examination.

Discussion

Ultrasonic examination proved to be useful method in confirmation of existence or nonexistence of posttraumatic haematomas, as well as for differentiation with other processes that may mimic haematoma (abscess) in some degree.

Using ultrasound it is possible to categorize muscular injuries in three forms, according to Burgeois. We formed simillar classification adding cathegories of injuries examined few weeks after trauma, as well as old trauma with no visible ultrasonic changes, still existing.

Standard radiological methods offer little data about traumatic muscular alterations, while CT provides valuable data but is costly and often inaccessible, not to mention harmfulness of ionizing radiation.

Ultrasound provides possiblity of insight into state and type of muscular injury, the degree of injury and successfulness of treatment. Apart of that, ultrasound is easily accessible, cheap and simple to perform, presenting no harm to the patient.

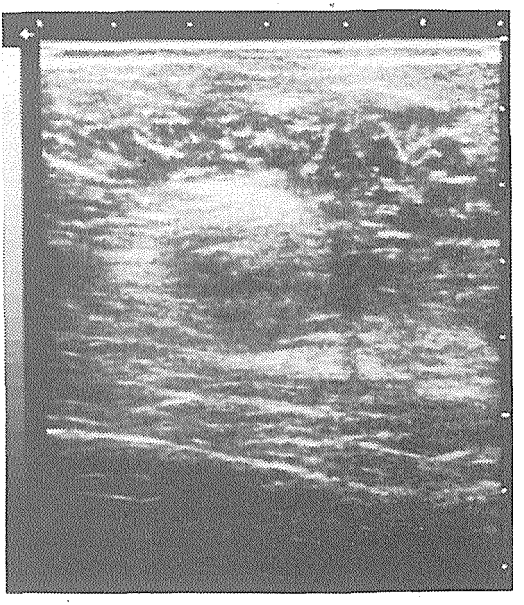

Figure 3. Ultrasonic image of inhomogenous, predominantly hyperechoic area inside the muscle with vague delineation of muscular contours.

References

1. Siwek CW, Rao JP. Ruptures of the extensor mechanism of the knee joint. *J Bone Joint Surg* 1981; **63**:932-7.
2. Robbins SL. *Patologijske osnove bolesti.* Zagreb: Školska knjiga, 1985; 1541-99.
3. Bourgeois JM, Wagner P, Harris A. Ultrasonographic evaluation of muscle injuries in sportsmen. *J Ultrasound Med* 1983; **2**:32.
4. Fornage BD, Touche DH, Segal P, Rifkin MD. Ultrasonography in the evaluation of musculosceletal trauma. *J Ultrasound Med* **1983;** 2:549-54.
5. Matasović T, et. al. *Ultrazvučna dijagnostika sustava za kretanje.* Školska knjiga 1988.

Adv Radiol Oncol 1992; 102–8.

Ultrasound as a diagnostic tool in malignant bone tumours

Babić M and Matovinović D

Special Clinical Orthopaedic Hospital – Lovran

Morbidity of malignant osseous tumours has been present in orthopaedic casuistics with 0,001%. in the available literature we could not find information about the application of this diagnostic method in detecting the intraosseous tumours.
The work connects 10 years of experience that has been made while working with this casuistics. Twenty-five persons were examined with intraosseous malignant formations. Forty healthy persons were »controling group«. Standard linear probes of 3,5 MHz and 5 MHz were used. The examinations were performed in the transversal and longitudinal axis of the bone. The echophenomenal degree was observed, and according to the results obtained, it was possible to speak about the intraosseous tumour existence. Tumour smaller than 1 cm are not diagnosable by this method. According to characteristic echophenomenal findings it was possible to differentiate the findings whether they are benign or malignant, solid or cystic.
It is possible under the ultrasound guidance to perform the puncture of the intraosseous tumour in some cases.

Key words: bone neoplasms; ultrasonography

Introduction

Bone neoplasms account only for 1% of the whole orthopaedic casuistics. Fortunately less than 0,001%[7] are malignant bone tumours (primary and metastatic bone tumours).

Today certain problems still exist in the identification and detection of osseous malignant neoplasms, especially in the early stages. It is of great importance to detect and treat the malignant bony tumours in the stage when the malignant tissue growth has not yet invaded the surrounding soft tissue.

Taking all diagnostic methods at disposal today, with the exception of magnetic resonance imaging, this aim is very difficult to achieve with high probability and accuracy. Therefore we came to the idea that some diagnostic problems could be solved by ultrasound.

Ultrasound as a diagnostic tool becomes inevitable in many fields of orthopeadics. It is preffered in the diagnostics of the congenital dislocation of the hip in children and of certain soft tissue pathological abnormalities of the musculoskeletal system.[1, 2, 4, 5]

The aim of the study

Having in mind the characterictics of the ultrasound we tried to use this method in detecting malignant (expansive) processes inside the bone. According to our knowledge there are no recent reports dealing with the diagnostic possibilities of the ultrasound in revealing the pathological

Correspondence to: dr. Babić M.

UDC: 616.71-006.6-073:534-8

growth inside the bone. Therefore it seemed necessary to apply this diagnostic technology developing at the same time our own approach and method.

Patients and methods

In our ten-year experience we had 16 patients (22 – 60 years old) with malignant bone tumours. In 14, detailed orthopaedic clinical investigation (history, physical examination, imaging studies: plain film roentgenography and tomography, skeletal scintigraphy, angiography and recently CT scan) was made. In two patients the diagnosis of neoplastic growth was confirmed by ultrasound after history and physical examination. These patients were subjected to the echosonographic examination because abnormalities in other organic systems were suspected. With this method we succeded in detecting a metastatic spread in lumbar spine region in 6 patients, as well as 3 metastatic spreads in the pelvic bone area.

In the beginning of our work we examined 40 healthy persons (20 men and 20 women) in order to acquire experience and skills in using this new diagnostic possibility.

In this study we shall not report our experience in applying this diagnostic method in detecting benign tumours of the musculoskeletal system.

According to literature it was not possible to perform an echosonographic examination of the musculoskeletal system. Therefore, after first positive experiences, we had to develop our own technique and methodology of the study.[3, 11]

In this study we used standard linear probes of 3,5 and 5 MHz. It seems that a linear probe of 3,5 MHz, 10 cm in length was preferred in the examination of the musculoskeletal system especially in the process of detection. With this probe it is possible to examine greater areas, and the distinction between normal and abnormal finding becomes more evident. After this first step we proceeded examining using a smaller 3,5 MHz linear probe. In a few patients we used a 5 MHz linear probe with an amplification of the examined structures, which enabled us to make a more distinct differentiation of the examined structures. It is mandatory to examine the normal and abnormal extremity as well as the normal and abnormal spinal area at the same time. The investigation always began in the longitudinal axis in relation to the extremity or spine, in the anteroposterior direction while the patient was lying. The investigation of the extremity was performed with a gentle slipping of the probe along the whole circumference. While examining the spine we gradually moved away to the medial line, to the right and to the left (so called dorsal aproach). After the initial examination was completed the probe was positioned in the sagital axis and afterwards gently moved proximally and distally along the extremity, cranially and caudally along the spine respectively (the so called ventral and dorsal approach).

Results

In the preliminary part of this study we tried to acquire experience in the investigation of the musculoskeletal system among healthy persons as well as among persons with neoplastic growths inside the bone.

After these first experiences a differentiation of skin, subcutis, muscles and periost among healthy persons (controls) as made possible during investigation. The depth of the soft layer depends on the adipous tissue and the muscular mass with the echogenic characteristics of the soft tissue.

When the probe is positioned in the longitudinal axis a line with a distinct hyperechogenic zone comprising 1.3 mm can be seen underneath the soft layer which corresponds to the periost. Underneath this hyperechogenic zone another hyperechogenic homogenous zone can be found corresponding to the cortical and medullary part of the bone (Figure 1, 6, 7). It is seldom possible to find the hyperechogenic zone of the periost on the opposite side again.

Among youngsters, especially children, we almost always succeded in showing the other

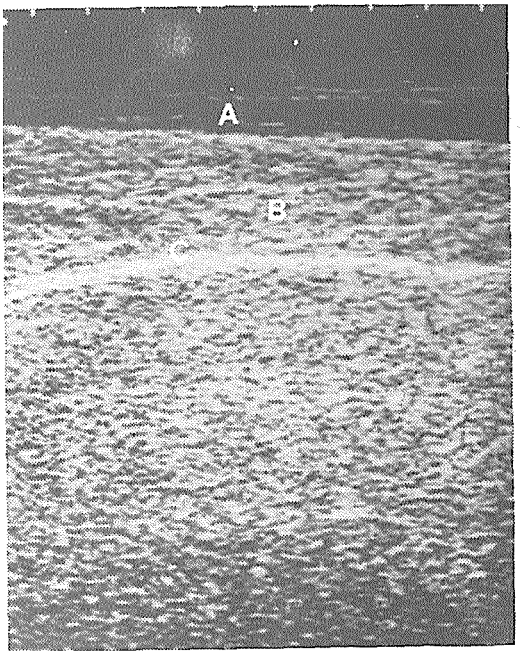

Figure 1. Echosonographic image of a normal bone (5MHz probe longitudinally positioned along the axis of the bone). A – skin and subcutis, B – muscular layer. C – periost and bony structure.

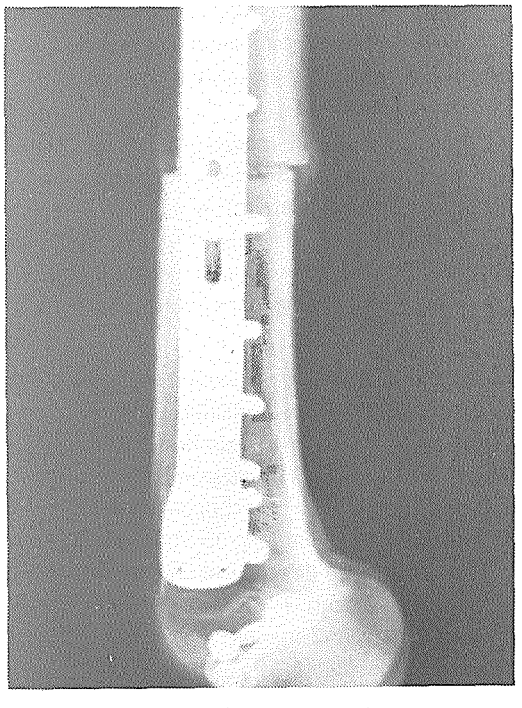

Figure 6. The same patient shown of figures 3., 4., 5., six months after the operation. Homotransplant.

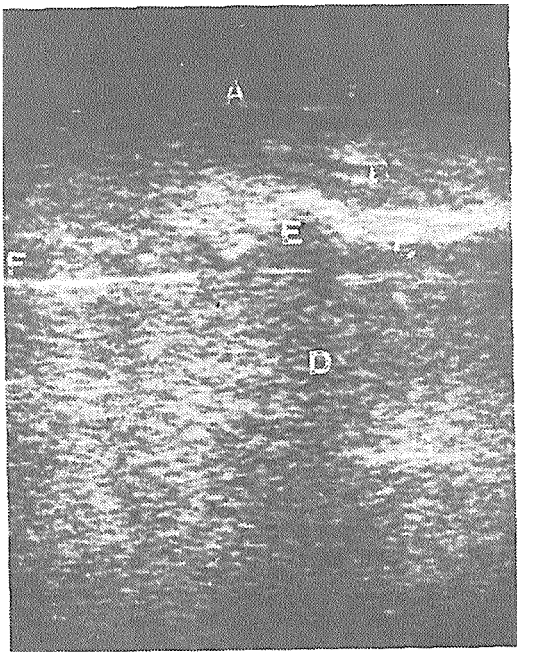

Figure 7. Echosonographic image of the patinet shown of Fig. 6.
A – skin and subcutis, B – muscle, C – periost and the cortical part of the bone, D – the pace of junction of homotransplant and the remaining part of the bone, E – growth of a new bone into the homotransplant, F – alenthesis, E – phenomenon of reveberation

side. Great caution in the evaluation of a picture issued in this way is needed, because of the reveberation phenomenon and the possibility that an artefact issued in this way might be taken as the periost from the opposite side. To avoid any danger of interpreting and evaluating the picture in this way, we must measure the distance from the several analyzed structures in relation to the sufrace, periost – periost to the other side, espectively. Any doubt of the exsistence of the reveberation phenomenon can be releaved or confirmed in this way.

It is necessary to perform the evaluation and analysis of the bony structures while the muscles are maximally relaxed or contracted, ignoring in this way the possibility that fascia is taken for periost, which is sometimes possible.

In the cases when the probe is positioned transversally to the bony axis, a crescent-like

slightly hyperechogenic zone corresponding to the periost can be seen under the soft structures (normoechogenic zone). The ringlike structure of the whole bone can be shown only among children. Under the crescent-like slightly hyperechogenic zone of periost there is a hypoechogenic zone corresponding to the cortical and medullary part of the bone.[3]

Following the ventral approach to the spine it is possible to show a vertebral body projecting itself as a horseshoe-s haped hypoechogenic zone at the bottom of which a triangle-like hyperechogenic zone with an anechogenic center corresponding to the spinal canal can be found. Amplifying the strength of the ultrasound beam a certain degree of echogenicity is reached inside the vertebral body, but in this case it is impossible to analyze structures which could possibly be found inside the body. Spinous and transverse processes and the vertabral arci are examined with more precision and ease following the dorsal approach (with the patients prone), and appear with less echogenicity.[1, 2, 3]

After the necessary experience was acquired with ultrasound examinations of bony structures and the spines of tealthy persons, an investigation of the abnormalities inside the bony system could be performed.

In the beginning of our study, before ultrasound as a diagnostic tool was applied, we applied all other available diagnostic methods (radiography – tomography, biopsy, CT scan) to get a better insight in the possibilities of ultrasound in this area.

During the study we reached the conclusion that a neoplastic mass can be seen more easly when the probe is positioned longitudinally, along the axis of the bone examined. Intraosseally, in the site of the tumours mass, the degree of echogenicity changes, depending on the mass itself.

Using ultrasound as a diagnostic tool we primarily tried to locate the tumour, and to find out whether this mass was localized inside the bone or was also invading surrounding soft tissue (Figure 2).

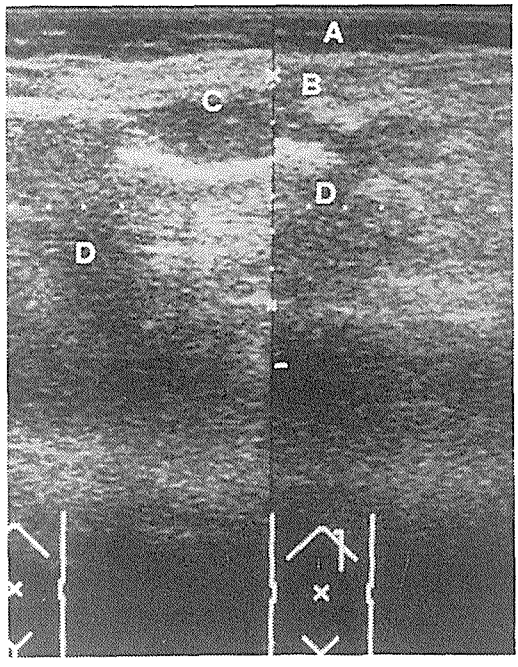

Figure 2. Malignant tumour of the upper and the middle third of the humerus A – skin and subcutis, B – tumour invading soft tissues, C – the pace of the tumour invasion into the soft tissue, D – tumourous mass inside the bone. Tumour 14 cm. Cleary discernible hyper and hypoechogenic zone inside changed structure of the bone, corresponding the tumourous mass.

The character of the finding corresponds to the character of the intraosseal tumour, i.e. whether it is malignant or benign. In the case of a malignant process the echogenity inside the tumours mass has different degrees from anechogenic to hyperechogenic, the borders are not defined and saw-like in respect to healthy bone. A clear border between the bone invaded with the tumour and the healthy bone, can not be found in spite of the fact that this border can be guessed. Inside the tumour itself the hyperechogenic zones correspond to the zones of necrosis and to the zones of calcifications inside the tumour itself. A clear distinction between the tumour itself and the healthy tissue can be made according to the different degrees in echogenicity (Figure 2, 3). A break in the continuity of the periostal hyperechogenic zone points to the inva-

sion of the tumours mass into the surrounding soft tissue (Figure 3). The invasion of the malignant mass into the healthy tissue changes in the same the degree of echogenicity and points to a clear distiction between the healthy and diseased tissue (Figure 3, 4, 5).

In the cases of metastatic spread in the region of the vertebral body, zones of increased echogenicity appear, not clearly limited from their surroundings, while the remaining healthy tissue has an anechogenic projection (Figure 8, 9)

In the past ten years in a total of 16 patients malignant intraosseal neoplasms were revealed using ultrasound as a diagnostic tool. Among 6 patients metastatic spread localized in the lumbar spine and among 3 inside the pelvic bone was found.

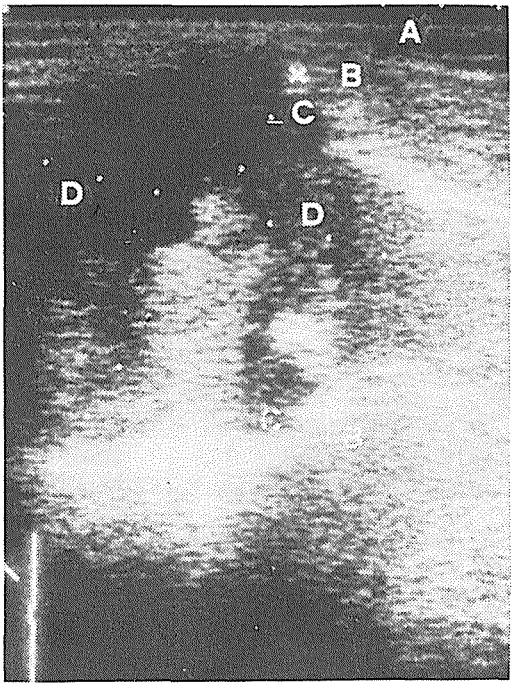

Figure 3. Echosonographic image of femur condyles of a grown-up person. A – skin and subcutis, B – invasion into the soft tissues, C – the pace of invasion of the tumour into the soft tissues, D – tumorous mass, E – periost and the cortical part – healthy tissue.

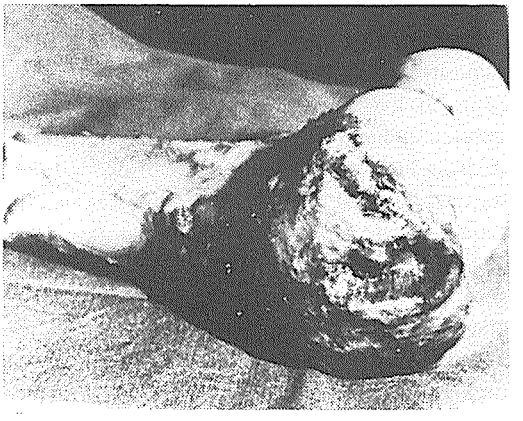

Figure 4. A – pathoanatomical preparation of a tumour gained during the operative treatment. The same tumour is shown by the same technique on Fig. 3

Discussion

The theoretical background for the first diagnostic possibilities for revealing tumours inside the bony system was presented by J M. Heveri 1983. His theoretical work could not find a practical application due to the lack of a suitable ultrasound apparatus.[8]

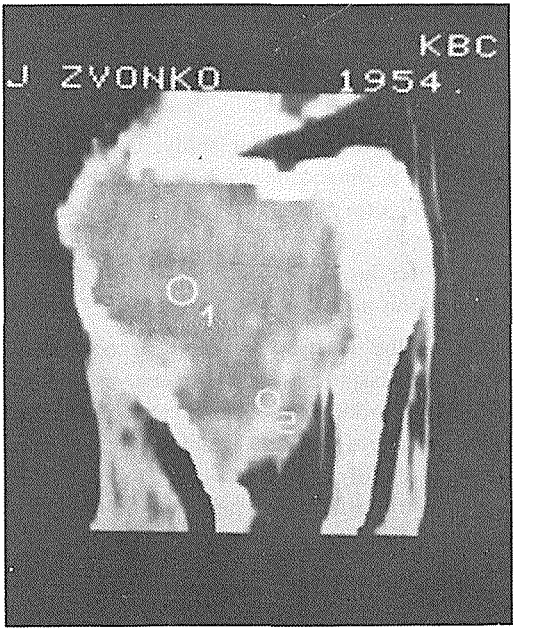

Figure 5. The same tumour Shown by a CT scan

Taking the standpoint that all tissues could be examined by ultrasound under the conditions that the ultrasound wave lenght during penetration through the tissues, acoustic impedence, reflexion of the ultrasound on the borders of certain tissues, the velocity of the ultrasound during the spread through the tissues and specific gravity as well as density of the tissues must be known, we tried to create such relations under which the study of the structures inside the bone with ultrasound an a diagnostic tool would be enabled.[9]

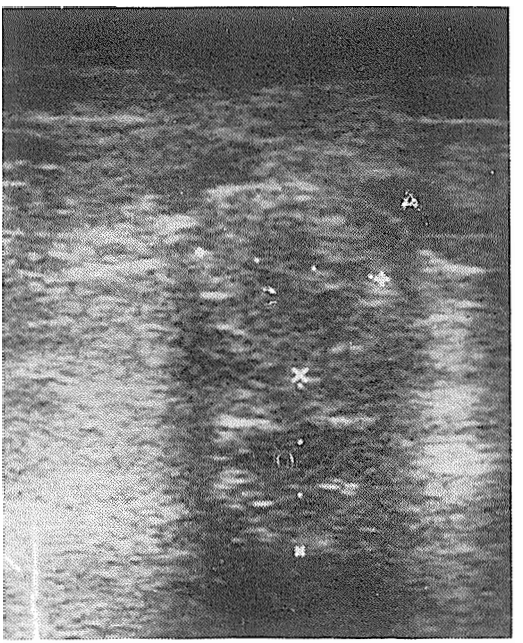

Figure 8. The vertebral haemangioma.
A – body of the vertebra changed by the haemangioma
B – spinal channel

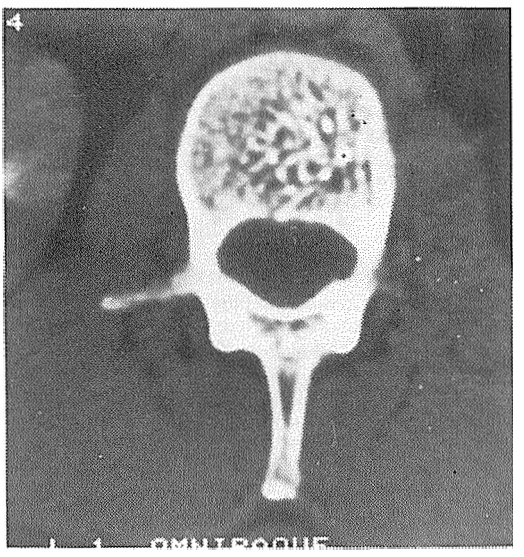

Figure 9. CT scan of the same patient.

To enable the interpretation of achieved results, it was necessary to study the specific physical characteristics of the ultrasound beam when in contact, or during the spread through the bony tisue. While passing through the bony tissue, the ultrasound behaves quite differently than when spreading through soft tissues, homogenous tissues or liquid. On the level of periost, because it is so smooth, there is reflexion of a part of the ultrasound waves, for instance when the ultrasound hits a mirror or any other smooth surface. The second important factor which causes reflexion of a part of the ultrasound waves is the actual difference in acoustic impedence between the muscular mass 1,70 C 10 kg/cm^2) and the bony structures 7,80 C 10 kg/cm^2). Inside the bony system itself the ultrasound beam behaves in a different way than when passing through the muscular or homogenous tissues. This is the result of the special hive-like structure of the bone (bone trabeculae). A part of the ultrasound beam is lost because it is prone to uncontrolled movements through the bone, as well as its reflexions, that is its absorption which is very important. When passing through the bone the ultrasound beam increases, which is a result of the difference in the tissue quality. When compared to the movement of the ultrasound beam through the soft tissue this acceleration is three times greater.[1,10] This must be kept in mind when measuring several distances inside the bone, since the obtained results are not identical to its actual dimension. It can be seen that during the study of the bone by ultrasound several problems emerged that could virtually not be solved. This is why only a small amount of information can be obtained from the study of healthy bone.

In the healthy bone periost and structures directly underneath can be analyzed (Figure 1). Other structures of the healthy bone can usually not be presented with an ultrasound, except on very rare occasions, depending on structure and the mineral composition of the bone itself. According to actual degree of the ultrasound technology pathological mass smaller than 1 cm can not be presented. Only a smaller part of the ultrasound beam is reflected from the healthy bone and this part is accesible for analysis.

Due to the fact that tumorous tissue changes the quality, composition and structure of the bone, the bone becomes more accesible to ultrasound beam. New conditions emerge that allow us to study the primarily diseased bone. Equally, the difference in the echogenicity of the tissues enables us to find the limit between healthy and diseased bone. The early detection of tumours masses which expaned out of the bony system into the soft tissues is based on the same principles. This is of significant help for future treatment and for decisions about the plan of the treatment itself.

Due to interventional ultrasound as a diagnostic tool, it is possible to perform a biopsy and obtain material for pathohistological analysis.

Conclusion

According to known research, diagnostic procedures and follow-up of tumours inside the bony system, some important conclusions have to be made. In view of obtained experience and the evaluation of results, it is obvious that the analysis of tumours greater than 1 cm located intraosseally was possible. It is primarily possible to prove the existence of a mass with osteolytic characteristics. Depending on degree and character of echogenicity a differentiation between tumours (solid – cystic) was made possible. Based on these results it is possible to raise a doubt whether a malignant intraosseal mass is in question.

By using this method we can easily confirm the invasion of the tumour into soft tissues which has a specific impact in planning further treatment.

It is possible to perform a biopsy during the investigation if an interventional probe is available. Material for pathohistological diagnosis is obtained in this way. The method is quite simple if certain guidlines are accepted. It is generally recommended as a screening method.

References

1. Babić M. Mogućnost dijagnostike hernije intervertebralnog diska metodom ultrazvuka. Magistarski rad. Medicinski fakultet Rijeka, 1980;18-28.
2. Babić M. Ultrazvuk u evaluaciji kompresije u lumbosakralnom segmentu. *Liječ Vjesn* 1982; **104:**354-7.
3. Babić M. Matovinović D. Mogućnost primjene ultrazvuka u dijagnostici intraosalnih tumora. *Medicina* 1990;**26:**141-7.
4. Matanović T, Vrdoljak J. Ultrazvučna dijagnostika kuka i natkoljenice. In: Kurjak A. ed *Ultrazvuk u kliničkoj medicini,* Zagreb, Medicinska biblioteka, 1989;779-89.
5. Matanović T. Dijagnostički ultrazvuk u ortopediji. In: Matanović T. ed *Ultrazvučna dijagnostika sustava za kretanje,* Zagreb, Školska knjiga 1989; 23-47.
6. Andrić J, Babić M. Pokušaj dijagnostike migracije totalne endoproteze pomoću ultrazvuka. In: Mikić Z. ur. IX. Kongres ortopeda i traumatologa Jugoslavije - JUOT 1986. Novi Sad 1987;459-63.
7. Richend S, Marcus R.M, Spaiser S.S, Enaeking E.W Surgical treatment for osteosarcoma. *J Bone Joint Surg,* 1988;**70:**1119-24.
8. Hevezi J.M. Physical principles of diagnostic ultrasound. In: Anderson E. ed. *Radiologic and other biophysics methods in tumour diagnosis.* Chichago, 1975; 99-107.
9. Breyer B, Andreić Ž. Fizika ultrazvuka. In: Kurjak A. ed. *Ultrazvuk u kliničkoj medicini,* Zagreb, Medilcinska biblioteka, 1989; 1-3.
10. Breyer B. Fizikalne osebine ultrazvučne dijagnostike, In: Matasović T. ed. *Ultrazvučna dijagnostika sustava za kretanje,* Zagreb, Školska knjiga 1989;9-21.
11. Babić M. Pokušaj dijagnostike intraosalnih tumora ultrazvukom, In: Kurjak A., Sretenović Z. ed III. jugoslavenski kongres o primjeni ultrazvuka u medicini i veterini. Beograd:, Sekcija za ultrazvučnu dijagnostiku Jugoslavije i Srbije, 1989; 193-4.

Chapter III. NUCLEAR MEDICINE

Adv Radiol Oncol 1992; 111–15.

Labelling leucocytes with Tc-99m HMPAO for imaging inflammation

Peters AM

Royal Postgraduate Medical School, London, United Kingdom

Tc-99m HMPAO is an important new development in the imaging of inflammatory diseases and now has an established role in Nuclear Medicine. We are only just beginning to appreciate the appropriate indications of Tc-99m HMPAO and when to use In-111. There is no reason why both agents should not be offered at a diagnostic level. Thus, at least at present, In-111 chloride and HMPAO are about the same price. HMPAO can be kept on the shelf and used at short notice which is the usual requirement for acute sepsis. In-111, on the other hand, will usually be indicated for more chronic processes, which can be imaged more electively, thereby allowing sufficient time for the isotope to be ordered.

Key words: septicemia-diagnosis; leucocytes; technetium

Introduction

In-111 labelled leucocytes have now been in routine use for imaging inflammatory disease for many years. However, since McAfee and Thakur first described the technique of cell labelling with In-111 in 1976, there have been many attempts to label leucocytes with Tc-99m.[1] Indeed, Mc Afee and Thakur (1976) investigated Tc-99m oxine for its cell labelling efficiency but found it too unstable.[1] Shortly afterwards, Schroth et al. described a technique for labelling phagocytic cells with Tc-99m colloids but this never gained a wide clinical acceptance except in Australia.[2, 3] Other efforts, based on Tc-99m pyrophosphate and Tc-99m labelled porphyrins have also failed to gain acceptance.[4, 5]

The advantages offered by a Tc-99m agent over In-111 include better image resolution, greater convenience, lower radiation dose, and it should be cheaper. In 1986, in collaboration with Amersham Interantional plc and RJ Hawker of the Queen Elizabeth Hospital Birmingham, we described the first clinical results with a new Tc-99m agent, HMPAO, which was initially developed for imaging cerebral perfusion but, because of its high lipophilicity, also penetrates blood cells. The labelling of cells is relatively stable because the agent is converted intracellulary from lipophilic to hydrophilic secondary species, which become effectively trapped within the cell.

Labelling

Since Tc-99m HMPAO is, like In-111 oxine and In-111 tropolonate, a lipophilic complex, the

Correspondence to: A. M. Peters, Reader in Nuclear Medicine, Royal Postgraduate Medical School Hammersmith Hospital, Du Cane Road, London, 12 ONN, United Kingdom.

UDC: 616.94:616.155.3:539.163

technique of labelling cells with it is essentially the same as that of labelling with In-111. Thus, the red cells first have to be sedimented leaving a supernatant from which the leucocytes and platelets are then concentrated. The labelling efficiency of Tc-99m HMPAO is satisfactory in a medium containing 20% plasma and this is an advantage from the point of view of ultimate cellular integrity.[6] The agent labels neutrophils with some degree of selectivity, similarly to In-111 oxine and In-111 tropolonate. Although Tc-99m is not as firmly held by the cell as In-111, the stability is adequate for clinical imaging. We initially thought that neutrophils became labelled with Tc-99m with more stability than other cell types but there is some question about this and, indeed, Tc-99m labelled platelets are now being used on a wider scale and are replacing In-111 for imaging thrombus.[7]

Biodistribution

The biokinetics of Tc-99m labelled leucocytes are broadly similar to those of In-111 labelled neutrophils. Thus there is minimal first pass hold-up in the lungs, and although this may appear quite striking on imaging, the cells are rapidly cleared from the lung. The labelled cells enter the splenic pool and display a transit time through it similar to In-111 granulocytes. The liver remains cool while the bone marrow becomes very prominent, more prominent indeed than it does with In-111 granulocytes. The intensity of bone uptake led us to suspect that free Tc-99m HMPAO may be taken up by bone as opposed to bone marrow. However, when we injected supernatant from a medium in which Tc-99m HMPAO labelled cells had been suspended for 30 minutes, we saw urinary activity (and some splenic activity thought to be due to contaminating labelled platelets) but no skeletal activity. Furthermore, comparison of the Tc-99m HMPAO white cell scan with the bone scan in patients with metastatic disease showed that the hot spots on the bone scan were matched by cold areas on the white cell scan, indicating destruction of marrow and abolition of uptake.

Figure 1. Inflammatory bowel disease with involvement of small bowel. Anterior gamma camera image taken 3 hours following injection of Tc-99m HMPAO labelled leucocytes. Abnormal migration to loops of small bowel can be seen in the right iliac fossa (reprinted with permission from Radiology).

The stability of Tc-99m in neutrophils is not high enough for quantitative studies of neutrophil kinetics. *In vitro* studies indicate an elution rate from neutrophils of about 5% per hour. The half time of disappearance from blood of native neutrophils is thought to be about 7 hours.[8] In-111 labelled neutrophils have, in our hands, a half time approaching 7 hours.[9] Whilst our Tc-99m HMPAO labelled neutrophils have a half time of only 4.5 hours it increases to 6.5 hours when a correction is made for isotope elution.[10]

Stability of Tc-99m at the normal sites of labelled neutrophil uptake, i. e. liver, spleen, and bone marrow, is also reduced compared with In-111. Thus, bone marrow activity, which

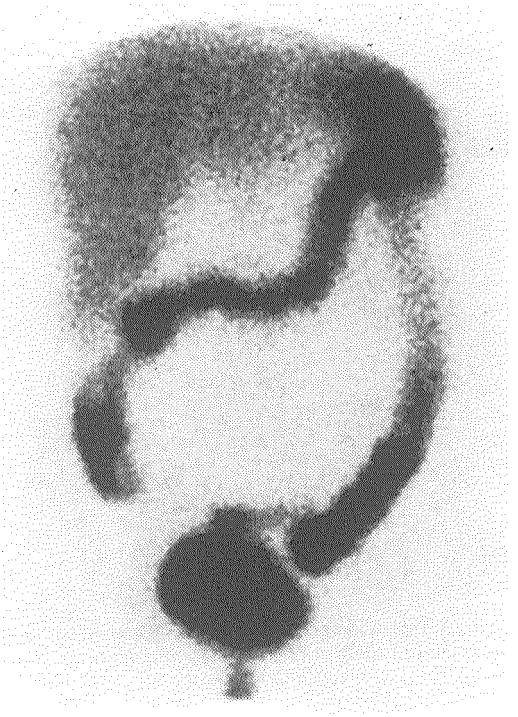

Figure 2. Inflammatory bowel disease with pancolitis. Maked uptake of Tc-99m HMPAO labelled white cells can be seen throughout the colon on this anterior gamma camera image taken 3 hours following injection of labelled cells. Normal uptake is seen in the liver and spleen. Note the urinary activity in the bladder.

rises steeply up to 4 hours after injection of In-111 granulocytes, continues to rise until 24 hours when it reaches a plateau. Tc-99m HMPAO, on the other hand, although showing the same steep rise up to 4 hours, does not show any further increase beyond this time, even though labelled granulocytes continue to circulate. This suggests elution of label from bone marrow reticulo-endothelial cells.

More obvious evidence of elution (though giving no clues to its origin) is seen in the form of urinary activity. The lipophilic nature of Tc-99m HMPAO allows its entry into cells. Once inside the cell, however, the agent undergoes biochemical alteration to secondary species which are hydrophilic and cannot therefore escape from the cells. Although this forms the basis of the relative stability of Tc-99m HMPAO, it also accounts for the appearance of activity in the urine. There is, in addition, significant retention of activity in the renal parenchyma. There is also evidence of biliary excretion of complex and, indeed, the gall bladder is visualised occasionally. Biliary excretion, which may be of a lipohilic complex, is almost certainly the basis for the non specific gut activity that is seen from about 3-4 hours onward. This gut activity is a serious disadvantage of Tc-99m labelled leucocy-

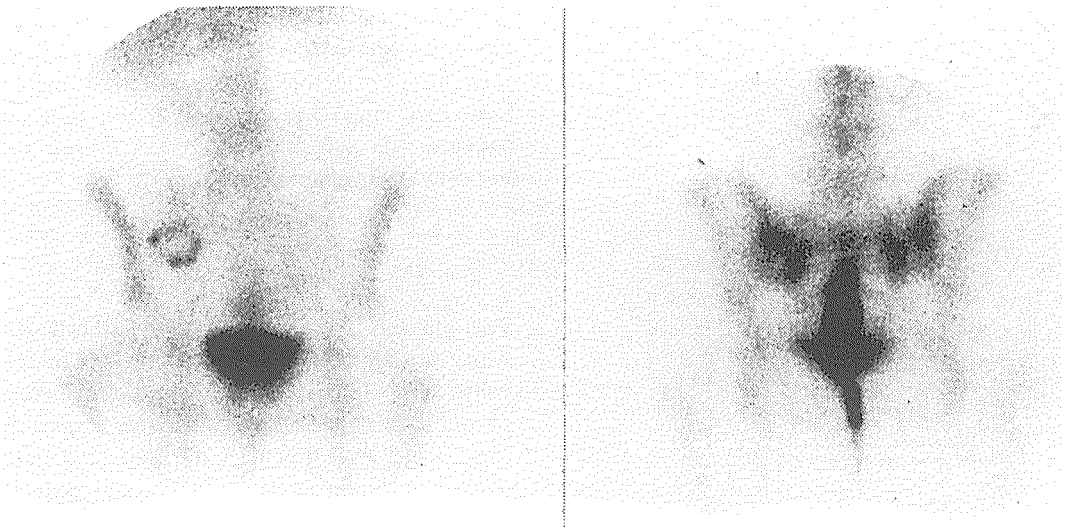

Figure 3. Pre-sacral abscess in a patient with an ileostomy imaged with Tc-99m HMPAO labelled leucocytes. a) Anterior view which demonstrates uptake in the ileostomy; b) Posterior view showing the presacral abscess.

Figure 4. Infection associated with a femoral nail inserted for fractured shaft of femur in a young man. a) plain X-ray; b) accumulation of activity at distal end of femur; c) accumulation of activity at fracture site. Images taken 2 hours after injection of Tc-99m HMPAO labelled leucocytes.

tes and complicates the identification of intra-abdominal sepsis. We frequently see minimal non-specific right iliac fossa activity at about 3 hours and almost always see considerable colonic activity at 24 hours. Non-specific gut activity is not seen, however, before 1,5 hours and it is, therefore, very important to image at this time in patients with inflammatory bowel disease or suspected intra-abdominal sepsis.

Clinical applications

The clinical indications of Tc-99m HMPAO white cells are broadly similar to those of In-111 white cells.[11] Indications which exploit the better resolution offered by Tc-99m include suspected small bowel involvement in inflammatory bowel disease, infection in the cardiovascular system, such as infected values, and osteomyelitis of the small bones. The much greater photon flux of Tc-99m also offers potential in the clinical inve-

stigation of granulocyte migration into acutely infarcted myocardium.[12] Because of the lower radiation dose associated with Tc-99m HMPAO, labelled white cells are widely indicated for use in paediatrics.

Indications for which In-111 probably remains superior to Tc-99m HMPAO are, in general, those in which inflammatory processes are not likely to be acute and in which, therefore, the full duration of the labelled granulocyte residence time in blood and higher stability of In-111 should be exploited. These include musculoskeletal infections, such as infected prosthetic joints, and pyrexia of unknown origin. Because of nonspecific gut activity, abdominal abscess in communication with gut is difficult to diagnose with Tc-99m HMPAO labelled leucocytes. Two groups have recently compared the clinical results of Tc-99m HMPAO and In-111, both finding very similar accuracies.[13, 14] The false positive rate for Tc-99m HMPAO is marginally higher, particularly for abdominal infection, probably because of the non-specific bowel activity. The urinary activity is a theoretical disadvantage of Tc-99m HMPAO labelled leucocytes, especially in suspected urinary sepsis, although, in our experience, has not given any significant practical difficulty. This is because it is readily identifiable as such, especially on the pelvic outlet view.

References

1. McAfee J G, Thakur M L. Survey of radioactive agents for *in vitro* labelling of phagocytic leucocyets. I. Soluble agents,. *J Nucl Med* 1976; **17:**480-487.
2. Schroth H J, Oberhausen E, Berberich R. Cell labelling with colloidal substances in whole blood. *Eur J Nucl Med* 1981; **6:**469-72.
3. Pullman W, Hanna R, Sullivan P, Booth J A, Lomas F, Doe W F. Tc-99m autologous phagocyte scanning: a new imaging technique for inflammatory bowel disease. *Br Med J* 1986; **293:**171-4.
4. Linhart N, Bok B, Gougerot M, Galliard M T, Meignan M. Tc-99m labelled human leucocytes: an in vitro functional study. *Acta Haematol* 1980; **63:**71-80.
5. Zanelli G D, Bjarnason I, Smith T, Crawley J C W, Levi A J, Copeland R I. Tc-99m labelled prophyrin as an imaging agent for occult infections and inflammation *Nucl Med Commun* 1986; **7:**17-24.
6. Saverymuttu S H, Peters A M, Danpure H J, Reavy H J, Osman S, Lavender J P. Lung transit on In-111 labelled granulocytes. Relationship to labelling techniques. *Scand J Haematol* 1983; **30:**151-60.
7. Becker W, Borst K, Krahe T, Borner W. Tc-99m HMPAO labelled human platelets: in vitro and in vivo results. *Eur J Nucl Med* 1989; **15:**296-301.
8. Dancey J T, Deubelbeiss K A, Harker L A, Finch C A. Neutrophil kinetics in man. *J Clin Invest* 1976; **58:**705-15.
9. Saverymuttu S H, Peters A M, Keshavarzian A, Reavy H J, Lavander J P. The kinetics of In-111 distribution following injection of In-111 labelled autologous granulocytes in man. *Br J Haematol* 1985; **61:**675-85.
10. Peters A M, Roddie M E, Danpure H J, Osman S, Zacharopoulos G P, George P, Stuttle A W J, Lavender J P. Tc-99m HMPAO labelled leucocytes: comparison with In-111 tropolonate labelled granulocytes. *Nucl Med Commun* 1988; **9:**449-63.
11. Roddie M E, Peters A M, Danpure H J, Osman S, Henderson B L, Lavender J P, Carroll M J, Neirinckx R D, Kelly J D. Inflammation: imaging with Tc-99m HMPAO labelled leukocytes. *Radiology* 1988; **166:**762-72.
12. Bell D, Jackson M, Millar A M, Nicoll J J, Conell M, Muir A L. The acute inflammatory response to myocardial infarction: imaging with In-111 labeled neutrophils. *Br Heart J* 1987; **57:**23-27.
13. Peters A M, Danpure H J, Osman S, Hawker R J, Henderson B L, Hodgson H J, Kelly J D, Neirinckx R D, Lavender J P. Clinical experience with Tc-99m Hexamethylpropyleneamineoxime for labelling leucocytes and imaging inflammation. *Lancet* 1986; **2:**946-9.
14. Costa D C. Lui D, Ell P J. White cells radiolabelled with In-111 and Tc-99m: a study of relative sensitivty and in vivo viability. *Nucl Med Commun* 1988; **9:**725.31.

Adv Radiol Oncol 1992; 116–22.

COST B2
Cooperation in science and technology: A european programme on the quality assurance of nuclear medicine software

Britton KE

Department of Nuclear Medicine, St. Bartholomew's Hospital, West Smithfield, London

The quality assurance and quality control of Nuclear Medicine software raises the problems and seeks to provide the solutions in what is a microcosm or the problem of testing validating and maintaining the quality of software in Medicine.
The discipline of Nuclear Medicine encompasses the integration of clinical information, image and curve analysis, tomography, the clinical reporting station, knowledge based decision making and the interaction with Hospital Information Systems. In all this complexity of medical management, the COST B2 project provides a philosophy and practice of quality assurance and control of nuclear medicine software that is applicable to general medical software, and develops process and product standards in this field.
The concepts of software phantoms, clinically validated data sets from patients with diseases of the heart, kidney and brain, as quality control test objects, the identification of the need for a software data exchange format – the Interfile approach – the requirements for validation and verification as the core of knowledge based systems, the evaluation of by collaborating test centres and a coordinating centre are the essence of the COST B2 project.

Key words: software, nuclear medicine, quality control.

Introduction

The medical doctor has a simple view of life. He or she wants the equipment to perform the tasks for which it was purchased. This aplies to both the hardware, the embedded software and the applications software. The medical doctor learns very painfully that equipment does not usually perform to its specification and that unreliability and error production are frequent. Since in many situations faulty monitoring or measurement leads to a lack of decision or an incorrect decision, so it may endanger patients' lives. The medical doctor and nursing staff therefore expect to have simple test procedures that clearly identify satisfactory working of clinical equipment or precisely demonstrate the nature and location of the fault.

The essential requirement is that the test procedure is simple: that means simple to apply, reliable, reproducible and rapid. Such test procedures represent attempts at quality control. At present they are often applied after a fault is detected and not on a regular basis to anticipate the development of a fault. The philosophy of a regular monitoring of equipment performance

Correspondence to: Keith E. Britton, Department of Nuclear Medicine, St. Bartholomew's Hospital, West Smithfield, London EC1A 7 BE.

UDC: 616-073.75:539.163:681.3.06

takes the form of preventive maintenance for hardware. The same philosophy is required for the quality assurance of medical software. Quality assurance in medicine is the process of monitoring every step in the production and delivery of a service to a patient so that it is maintained at a level considered acceptable for routine practice. However, safety regulations must not be created which have the effect of prohibiting adequate patient treatment for secondary safety reasons.

The most commonly used Nuclear Medicine system consists of a gamma camera, console and computer system. There are standards (NEMA, etc.) for testing the uniformity, linearity, spatial, temporal and energy resolution and sensitivity of the hardware including its embedded software. Their application daily, weekly or monthly as appropriate are an essential prerequisite to the provision of a nuclear medicine service to hospital inpatients and ambulatory patients. However, there is widespread use of applications software for analysing the image data to provide clinically relevant measurements of function, either provided by the system manufacturers or 'in house' in the nuclear medicine department. This applications software does not undergo any formal quality assurance, although each manufacturer and producer strives for quality in his/her own way. In particular, in house programming, which represents the developing front edge of the subject, has no proper system of quality assurance. Neither is there any system of quality control. At a time when there is an increasing tendency to require the use of only licensed software in the medical context (e. g. F.D. A. of U.S.A.), the development and evaluation of new analyses of physiological measurements of clinical benefit could be inhibited if no system of quality testing is provided.

Quality assurance and quality control of radiopharmaceuticals is also well established. The clearly documented procedures for their preparation in a sterile environment using aseptic techniques attest to their quality assurance. The sampling for pyrogen and bacterial testing, the chromatographic evaluation, the analyses for radionuclide and radiochemical purity are part of the well established quality control.

In contrast, little attention has been paid to the quality assurance of the development, distribution and routine use of nuclear medicine applications software. For example, a survey of left ventricular ejection fraction (LVEF) in the UK hospitals demonstrated a range of lower limits of normals from about 45% to 75%. In short, there is currently no reliable method for checking the accuracy of software packages which purport to produce a quantitative physiological parameter from an image or set of images. In general, the problem applies to manufacturer-supplied software as well as that which is developed in-house. Problems which are encountered using ad hoc, non-standard methods include simple errors ('bugs') as well as design faults. Furthermore, because a software package designed for a specific application can be inappropriately employed for other purposes due, for example, to misunderstanding of its operation, there is also scope for misuse by the end-user.

Quality assurance is required in monitoring any changes that might occur in any stated limits of normal operation due to alterations in protocol, equipment or software in a particular department, but knowledge-based systems, on the other hand, are dependent on absolute and reproducible values independent of the location at which the measurement is made.

The problem of software quality assurance was first addressed in the context of an ad hoc joint task group of the Society of Nuclear Medicine in Europe, SNME, and the European Nuclear Medicine Society, ENMS, through the initiative of E. Vauramo and at the European Nuclear Medicine Congress in Helsinki, 1984. A major problem then is how to test the quality of nuclear medicine software. Based on experience gained with N.J.G. Brown in the early 1970s, when transferring patient renography data on punched paper tape between different departments to check deconvolution analysis programs, Britton proposed at the 1984 congress the term «software phantom» for a clinically validated

patient data set for testing particular software systems. Thus for the quality assurance of programs for the analysis of renal radionuclide studies to detect renovascular disorder, for example, a set of data of typical fully documented patients with hypertension, angiographically confirmed renal artery stenosis, and sustained loss of hypertension following surgery or angioplasty would be established. These data would be given as input to renal analysis software and used to check that a consistent result and interpretation is obtained from use of that particular software. In addition, the quantitative values obtained in different departments from a particular software package could be collated and a consensus of the most probable values to be expected from that software could be obtained.

This approach follows the practice of quality assurance in *in vitro* laboratories. Previously a set of serum samples containing different amounts of Thyroxine were circulated between different radioimmunoassay laboratories for each to determine so that inter-laboratory comparisons could be made, the variance determined and the outliers encouraged to improve their assay. Using a similar approach, well documented patient data sets for the quality assurance of cardiological or cerebral software may be used. For example, data sets from patients with a critical stenosis of the left anterior descending coronary artery with angina of effort to test myocardial perfusion programmes, or with infarction of the prerolandic branch of the middle cerebral artery to evaluate regional cerebral blood flow SPECT programmes would be used as software phantoms for cardiac or cerebral studies.

A potential solution to these problems lies in the development of these *Software Phantoms:* a clinically validated library of patient studies which can be used as a reference data set to test applications software in a system. Initially, the library should include studies derived from patients having a clear diagnosis of the disease which the software is designed to detect. Subsequently, patients with less severe disease can be added to the data base in order to provide a more stringent test of the software. The computer program will usually produce a quantitative index which is compared with a normal range in order to assess the degree of abnormality. The distribution of software phantoms to different centres would therefore enable collation and a consensus of the most probable test result to be obtained. These interlaboratory comparisons would allow the variance in the results to be determined and the outliers would be encouraged to improve their test procedure (e. g. correct faulty software). This methodology could form the basis of a process standard for the quality control of medical software.

To summarise, the key feature of this approach to software quality control is the use of real data from real patients with real diseases. There are three reasons why this is important: the first is authenticity. Simulated data and invented mathematical tests have no validity that can be verified independently. Secondly, real data incorporates the real biological variation that the software will encounter in practice. Thirdly, developments in software can be assessed as beneficial or otherwise if data from patients with a range of clinically confirmed diagnoses are used to test the whole spectrum of performance of the new software.

For a patient data set to be accepted as a software phantom, an international panel of experts is required to agree that it was properly validated and suitable. A second requirement is that there must be an appropriate format for collecting and storing the software phantom and a 'Universal' interface for allowing the software phantom to be entered into a given data analysis system.

To meet these problems, the European software task groulp lead to the establishment of an officially registered project «Quality Assurance in Nuclear Medicine Software» COST B2 within the framework of COST, which is the programme of the European Cooperation in the Field of Scientific and Technical Research.

The Memorandum of Understanding was signed on the 16th September 1988 by four countries, Sweden, West Germany, Austria and Fin-

land and since then fourteen European countries have officially participated the United Kingdom and Yugoslavia signing in 1988, Belgium, Switzerland and The Netherlands, Spain, France, Italy and Hungary as the Szeged Medical University in 1989, Greece in 1990 and Norway in 1991. There are official observers from the European Association of Nuclear Medicine, the International Atomic Energy Agency and the World Health Organisation. Academic units in Poland and Czechoslovakia are seeking to join. The objectives of COST B2 as defined in the first annexe of the Memorandum of understanding are the following:

General objectives

1. To create a European procedure for Quality Assurance in Nuclear Medicine Software.
2. To coordinate and promote national activity at a European level.
3. To stimulate and promote European industry in the field of Nuclear Medicine.

Specific objectives

1. To develop quality assurance procedures and create organbased software phantoms with data bases, standards of data acquisition and other necessary standards.
2. To create procedures for evaluating, testing and accepting software phantoms and software, and
3. To evaluate and coordinate the development of special software like knowledge based systems in Nuclear Medicine.

The Management Committee consisting of two representatives from each country have set up nine Working Groups to meet these objectives.

Working Group 1. Standards for the Exchange of Data in Nuclear Medicine is headed by Frank Deconninck (Belgium) and Andrew Todd-Pokropek (UK) is Secretary. The goal is to define and provide a logical format for data so as to enable the transfer of software phantom data between different participating centres. The final goal is to specify a mechanism of associated formats and protocols for the transfer of images and associated data in general between different systems which require to have access to such data. This interchange of data was formally proposed to be the version 3.2 of the INTERFILE system developed by Professor Trevor Cradduck (London, Ontario). The INTERFILE system is designed to take image data from any manufacturer's computer system and transfer it into a common file from which it can then be translated to any other manufacturer's computer system. In this way the software phantom data sets obtained on one manufacturer's system are valid and viable to be used on another manufacturer's system. The only caveat about this is in the matter of single photon emission tomography which is the province of Working Group 7. To this end, a series of new files have been added to INTERFILE and liaison has been created between the committees of the American Colleges of Radiologists (ACR/NEMA) which had not previously considered Nuclear Medicine but had made proposals suitable for image transfer in general radiology, computer tomography and other aspects of radiological quality control. To improve liaison, Dr. Briandet, representing ACR/NEMA, has attended the working Group 1 workshop and Andrew Todd-Pokropek has attended the Working Group 1 workshop and Andrew Todd-Pokropek has participated in the ACR/NEMA meetings in the USA. The aims are to finalise version 4.0 of the INTERFILE System and propose validation and conformance testing procedures for the translation programmes, probably at three levels of conformance. Finally, pilot conformance testing centres will be set up to complete this work.

Working Groups 2, 3 and 4 are concerned with the quality assurance of organ software. Working Group 2 is on the quality assurance of cardiac software, Chairman Ellinor Busemann-Sokole

(NL), Secretary Michel Bourguignon (F). This Working Group aims to define standard criteria for the selection of software phantoms for the main cardiac studies of interest. Clinical validation criteria have been defined for a selection of normal patients, patients with coronary artery disease including transmural myocardial infarction pattern, myocardial ischaemia pattern, pre and post angioplasty patients and idiopathic cardiomyopathy. Data acquisition and analysis criteria are defined for Thallium 201 SPECT studies and Technetium 99m gated equilibrium blood pool studies. The group is drawing on national work from Finland on SPECT myocardial software phantoms and from the Netherlands, the IAEA gated cardiac blood pool phantoms and from Canada, mathematical software phantoms, from France, the first pass shunt software phantoms, from Germany gated cardiac blood pool software phantoms and from Spain, SPECT myocardial exercise and rest, Thallium and Technetium-99m MIBI studies. Very importantly, this group has coordinated with the European Association of Nuclear Medicine Cardiac Task Group, the European Society of Nuclear Cardiology Task Group and the International Atomic Energy Agency, software cardiac phantoms for developing countries and WHO.

Working Group 3 is on the quality assurance and standardisation of kidney software. The Chairman is Helmar Bergmann (OS) and the Secretary, Phil Cosgriff (UK). This Working Group has defined and published criteria for normal studies, for unilateral renal artery stenosis, and for obstructive nephropathy. They are advanced in the collection of software phantoms for these three studies. These are to be vetted by an international panel of experts before their distribution to selected test centres to test them out in practice.

Working Group 4 is on the quality assurance of brain software. Chairman Dr. Pedro Dominguez-Montero (E), Co-ordinator Dr. Per Åsard (SW), Secretary Dr. K. E. Britton (UK). This Working Group has defined the criteria for acceptance of normal brain SPECT studies and patients with cerebral infarct in the right or left middle cerebral artery territory. The collection of SPECT data with Technetium HMPAO is awaiting the results of Working Group 7 on SPECT to finally confirm the methods of data collection, then software phantoms will be collected. Already Sweden has produced a magnetic resonance based normal brain map, future areas include typical findings of temporal lobe epilepsy and Alzheimer's-type dementia.

Working Group 5 is on knowledge based systems, Chairman Professor D.P. Pretschner (D), Secretary Dr. J.H.C. Reiber (NL). The goals of this working group are the application, development and evaluation of knowledge-based system methodologies such as human experts, tools, shells, models and programming languages for solutions of clinical problems in Nuclear Medicine. They have identified areas in Nuclear Medicine suitable for knowledge based systems, in particular bone, kidney, heart and thyroid. Their aim is the assessment and transfer of artificial intelligence methodology and concepts for Nuclear Medicine, in particular to specify data structures and procedures used in KBS (object orientated model) to specify the human computer interface to specify the terms used in KBS and to specify data and case exchanges. A large number of publications and workshops have been produced by this group.

Working Group 6 is on the bone phantom data base, Chairman Professor D.P. Pretschner (D), Secretary Dr. P. Vassilikos (Gr). The goal of this working group is to evaluate the data structure needed to develop an integrated electronic archive of scintigraphic studies combined with the relevant clinical data in imaging the skeletal system. In this group, the work of Dr. J. Markwardt on quantitative bone imaging and the transmission phantom developed by Dr. A. Skretting (Norway) are important features.

Working Group 7 is on the quality assurance of SPECT. The Chairman is Dr. P.H. Jarritt (UK), Secretary Andrew Todd-Pokropek (UK). The goal of this working group is the provision of expert information regarding the specification of various nuclear medicine systems with respect to single photon emission computed tomography acquisition and analysis. It is involved in the generation and testing of data transfer programmes from INTERFILE to specify systems by members of the working group in relation to cardiac and brain SPECT data and it is concerned with the evaluation of SPECT system reconstruction software through the use of software phantoms. A particular problem concerns the centre of rotation and uniformity and other corrections required for software phantoms obtained from different manufacturers'data. A proposed solution is to define two alternative methods of transfer of such studies via INTERFILE. In the first group, data are supposed to be fully corrected with a flag to indicate this and with some parameters passed on for information. In the second group, key words will be defined to cover basic reconstruction correction methods such as the centre of rotation offset in milllimetres as a function of angle, pointers to the uniformity correction matrix and such-like. In addition, the SPECT working group is evaluating Jaszczak software phantoms, the non-attenuated Jaszczak phantom as an appropriate test object for indicating errors in straight forward reconstruction software and as a test bed for evaluating the INTERFILE format for SPECT data and the attenuated Jaszczak software phantom. This revised phantom using Monte Carlo photon transport methods is in the process of being evaluated.

Working Group 8 is on minimum user requirements for data systems for nuclear medicine. The Chairman is Andrew Todd-Pokropek (UK), Secretary K.E. Britton (UK). This working group has completed a document on user requirements for data systems for nuclear medicine and Andrew Todd-Pokropek is developing a software design ideal computer. This design is thought about in terms of its architecture, its platform and its implementation. The architecture must be as far as possible machine independent so that it can migrate on to different hardware configurations. The software should conform as far as possible to existing and future standards and make use of existing tools to minimise work. The platform for all but real time applications, the UNIX system is proposed and for real time applications the system running under MS-DOS is proposed. The implementation on appropriate hardware requires that it should be capable of at least 10 MIPS in terms of processing. Three hardware platforms are reasonable, INTEL, such as 1860, Motorola such as 86030 and RISC as in SPARC, MIPS and RS 6000. A gamma camera interface is nuclear medicine specific and should therefore be isolated. Finally, the hardware platform including processing display and acquisition modules should not cost more than $US40,000.

Working Group 9 is a computer conference coordinating centre. This coordinating centre is set up to accept the software phantoms from Working Groups 2,3 and 4 once they have been validated and tested, to store them and to then send out appropriate compilations of software phantoms to nuclear medicine departments and to industry so that their software systems can be tested. These quality control objects will be licensed to users, the whole set of data phantoms will be stored on CD ROM and subsets distributed as required. The intention is to update the software phantom package each year and always to hold back a reserve set of software phantoms so that programmes are not designed just for the software phantom. The coordinating centre will collate the information returned and develop statistical methods for evaluating the distribution of results for each organ and each disease system tested by the software phantoms.

In conclusion, it can be seen that the COST B2 Project is ambitious and wide-ranging, that it addresses the problem of quality assurance in

nuclear medicine software not only in a theoretical way but by offering practical solutions. The work of COST B2 is mainly voluntary and the efforts of COST B2 in this field need the support of nuclear medicine societies in every country so that we can continue to improve, monitor and audit the performance of our techniques.

References

1. Bernauer JA. Controlled Vocabulary Framework for Report Generation in Bone-Scintigraphy. In: Millar RA ed. Proc. 14th Symposium on Computer Applications Medical Care 90. Washington: IEEE Computer Society Press, 1990.
2. Bernauer J. Designing a terminology controlled interface for report generation. In: van Bemmel JH et al eds. Proceedings of the software engineering in medical informatics (SEMI-IMIA) Workshop. Amsterdam: Elsevier Scientific Publishing, 1990.
3. Bernauer J, Pretschner DP. Knowledge based report generation for quality assurance in bone scintigraphy. In: Knowledge-based systems to aid medical image analysis. Vol 1. Pretschner DP, Urrutia B, Eds Luxembourg: European Communities – Commission: EUR 12797:164-86. 1990;
4. Busemann-Sokole E. Quality assurance in nuclear medicine imaging: hardware and software aspects. PhD Thesis, University of Amsterdam (December) ISBN 90-9003872-8. 1990.
5. Busemann-Sokole E, Cradduck TD, Erickson JJ. Dynamic cardiac phantoms for use in computer software quality control. In: *Dynamic functional studies in nuclear medicine in developing countries.* Vienna: International Atomic Energy Agency, 1989; 493-8.
6. Busemann-Sokole E., Cradduck TD, Erickson JJ. Experience with gated cardiac software phantoms for quality control of applicatione programmes. *Eur J Nucl Med* 1990; **17:**106-10.
7. Cradduck TD, Bailey DL, Hutton BE, Deconinck F, Busemann-Sokole E, Bergmann H, Noelpp U. A standard protocol for the exchange of nuclear medicine image files. *Nucl Med Commun* 1989; **10:**703-13.
8. Cradduck TD, Busemann Sokole E, Erickson JJ Development of software phantoms for software validation. In: *Dynamic functional studies in nuclear medicine in developing countries.* Vienna: 1989; 483-92. International Atomic Energy Agency.
9. Kotzke K, Pretschner DP. Quality assurance of knowledge-based systems – experience and results from evaluation of the automatic diagnosis of cardiac motility. In: Pretschner DP, Urrutia B Eds. *Knowledge-based systems to aid medical image analysis.* Vol 1. Luxembourg: European Communities Comission, 1990; EUR 12797:96-112.
10. Pretschner DP, Vauramo E. Editorial. New COST project in the field of nuclear medicine software. *Eur J Nucl Med* 1986; **12:**1.
11. Pretschner DP, The current situation, aspects and projects concerning nuclear medicine software in Europe. *Eur J Nucl Med* 1986; **12:**2-4.

Adv Radiol Oncol 1992; 123–34.

New aspects in nuclear cardiology – PET, NMR and SPECT

Henze E, Milčinski M, Lietzenmayer R and Clausen M

Divisions of Nuclear Medicine, Universities of Kiel and Ulm (Germany) and Ljubljana (Slovenia)

Single photon emission computed tomography (SPECT) represents advanced technical possibilities in myocardial perfusion assessment. Thallium 201 and new technetium labeled radiopharmaceuticals enable the detection of resting or stress ischemia, and quantify the extent of perfusion abnormalities. SPECT in radionuclide ventriculography helps to define abnormal contraction pattern in preexcitation syndromes or other severe arrhythmias and accurately evaluates regional wall motion abnormalities.

Nuclear magnetic resonance (NMR) imaging provides a noninvasive assessment of cardiac anatomy and ventricular function, the information similar to that obtained by echocardiography and radionuclide ventriculography. Its unique role, however, can be in the study of biochemistry and blood flow. The real time three-dimensional display of the heart is a realistic prospect. Magnetic resonance spectroscopy (MRS) has its well established role in cardiac research. Possible aid in the diagnostic process and treatment of patients with cardiac disease remains an exciting challenge for future research of this technique.

Positron emission tomography (PET) is a new tomographic technique in nuclear medicine, allowing quantitative in vivo studies of metabolism and blood flow after labeling any organic substrate with short living isotopes e. g. C-11, %-15, N-13 or F-18. Its cost is very high and this limits the use of PET at the moment almost exclusively to cardiologic research. The clinical aspect of vitality of akinetic myocardium can be explained by combining the blood flow tracer N-13 ammonia with the metabolic indicator F-18 deoxyglucose. Myocardial metabolism of isolated substrates – glucose or fatty acids can be analysed as well.

Thus, with these three new imaging modalities – PET, NMR and SPECT – the noninvasive diagnostic work–up of patient with heart disease will be definitely improved, in particular with a new insight into the metabolism and quantification of blood flow and function.

Key words: heart diseases-radionuclide imaging; tomography, emission computed; NMR

Introduction

Positron emission tomography (PET), nuclear magnetic resonance imaging (MRI), nuclear magnetic resonance spectroscopy (MRS), and single–photon emission computed tomography (SPECT) are today the most exciting techniques in nuclear cardiology with most promising properties for future development. These techniques and their impact on cardiological research and clinical practice are described and discussed in this review.

PET is a tomographic scanning technique in nuclear medicine, which enables noninvasive investigation of myocardial blood flow, its metabolism and function. Up to now, there are only few PET centers available worldwide. PET is

Correspondence to: Prof. dr. Eberhard Henze, Director, Abteilung Nuklearmedizin, Arnold–Heller Straße 9, D-2300 Kiel, Germany

UDC: 616.12-073:539.163

based on both the chemistry and physics inherent in positron emitting nuclides which allow ideal labeling of nearly all important biosubstrates with short half-life. Disadvantages of the method are considerably high costs and the necessity of a cyclotron for isotope production and a radiopharmaceutical laboratory for fast synthesis of radiotracers nearby to the PET scanner.

Magnetic resonance imaging (MRI) has two important qualities, in addition to its high spatial resolution, that are likely to dominate future developments in cardiological applications. First, the nuclear magnetic resonance (NMR) phenomenon is extremely sensitive to motion and flow, which makes it potentially an ideal tool for producing images of cardiovascular function in addition to depicting cardiovascular morphology. Second, MRI is considerably more sensitive to paramagnetic substances introduced into the body than e.g. computed tomography (CT) to radiologic contrast agents. This, combined with the fact that MRI is harmless and thus makes it possible to obtain multiple scans at the same level of the body, permits the acquisition of information on the temporal evolution of the distribution of injected contrast agents. For example, high-resolution dynamic scanning of the heart after bolus injection of a contrast agent is possible, providing a combination of morphological and functional images of the cardiovascular system.

Magnetic resonance spectroscopy (MRS) offers a unique possibility to detect important metabolites noninvasively in living tissue. In recent years, an intense research effort has been made into the use of this technique for studying the metabolism of a variety of organs. Most of the cardiac spectroscopy that has been performed so far has involved analysis of high-energy phosphate metabolism *in vitro* and *in vivo*.

Technical advances such as SPECT in radionuclide imaging have important implications for the management of patients with acute myocardial infarction. SPECT with thallium-201 offers greater accuracy than planar imaging in detecting, localizing and sizing myocardial perfusion defects. The use of SPECT with Tl-201 should allow for a more accurate assessment of prognosis after myocardial infarction. A new radiopharmaceutical, Tc-99m methoxyisobutyl isonitrile, provides a number of advantages over Tl-201, including higher quality images, lack of redistribution, and the ability to assess first-pass ventricular function. The use of SPECT with radionuclide ventriculography provides improvements such as reconstruction of planar views oriented according to the long axis of the heart for easier interpretation and more accurate localization of regional wall motion abnormalities.

PET

Positron emission tomography is now for about 15 years a technically realizable nuclear medicine technique providing slice images, which opens due to the physical properties of positrons and the possibility of labeling any substrate a new dimension in terms of an in vivo autoradiographic method for noninvasive cardiological diagnostic studies of cardiac blood flow, metabolism and function.[1,2,3]

One of the main advantages of PET lies in the physical properties of positrons, which – emmitted from the nuclei of appropriate atoms – bounce against electrons of any matter, destroy each other according to the laws of atomic physics and convert into electromagnetic radiation. This radiation consists characteristically of two 511 keV photons moving on the same axis in the opposite way and therefore allow ideal axial tomographic detection for image reconstruction, comparable to an x-ray computed tomography device. Accordingly, in a PET camera there are circular arranged radiation detectors switched in axial coincidence connection, and therefore the external appearance of a PET scanner closely resembles an x-ray scanner.

The second important advantage of PET is determined by the available positron emitting isotopes, such as N-13, O-15, C-11, F-18 or Rb-82. The first three mentioned are isotopes of elements that occur naturally in organic molecules. Thus, radiopharmaceutical synthethis by a

specialized laboratory is possible, and the tracer principle (»make as small a change in the molecule to be traced as possible«) is ideally satisfied. Each interesting organic substrate, e.g. natural and synthetic metabolites, pharmaceuticals etc. can be labeled optimally without changing their biological and chemical properties. In addition, the short half-lives of the radionuclides – C-11: 20 min; N-13: 10 min; O-15: 2 min; F-18: 110 min – permit the acquisition of several studies on the same day with minimum radiation burden to the patient and without background activity from prior injections interfacing with the measurements, allowing repeated studies, e.g. before and after pharmaceutical or invasive intervention, which is of big importance in diagnostic and therapeutic cardiology.

The advantage of short half-life nevertheless implies the main disadvantage, i.e. the necessity of having a cyclotron for continuous isotope production and a powerful radiochemical laboratory for immediate production of radiotracers nearby. Therefore, PET is very expensive with primary costs of about 10 million US$ for a complete PET center and costs of about 1000 US$ per investigation.

Up to now, the worldwide only few functioning PET centers have focussed in cardiologic research on the potential applications of this new technique in animal experiments regarding the noninvasive investigation of problems connected with myocardial ischemia and cardiomyopathies.[3,4,5,6,7] Conclusive results of clinical cardiological PET studies performed mainly in USA are available now for only few years and a relatively limited number of about 30 original papers concerning 200-300 patients.

Table 1 gives a summary of the most important tracers which have been used for monitoring myocardial blood flow, metabolism and adrenoneuronal receptors. These tracers have been used in clinical pilot studies. Because of its possible clinical importance, at present only specific PET techniques have to be discussed, which allow imaging and quantification of marked known changes in heart energy metabolism during hypoxia (stop of fatty acid metabolism and switching over to aerobic and anaerobic glycolysis) simultaneously with blood flow metabolism studies. Ions of Rb-82 and N-13 ammonia proved to be good blood flow tracers analoguously to Tl-201 scintigraphy, whereas F-18 labelled deoxyglucose, F-18 DG, as a tracer of regionally increased glucose utilization, can be regarded as an established positive indicator of regional myocardial ischemia. With the use of this double tracer technique it seems possible to differentiate unequivocally normal myocardium, characterized by normal blood flow and low glucose utilization under fasting conditions, from ischemic but still vital myocardium with decreased blood flow and increased glucose utilization, by this so-called »mismatch«. Additionally, infarcted myocardium (scar tissue) can be identified by F-18 DG and C-11 palmitate as a region of decreased flow and metabolism and quantification of infarct size is possible.[1,2] A typical example of a combined normal, ischemic, and infarcted myocardium is shown in Figure 1.

Nearly all clinically relevant studies deal with the use of PET for specific and at least semiquantitative evaluation and differentiation of normal, ischemic and infarcted myocardial tissue, e.g. after myocardial infarction or for follow-up before and after coronary artery bypass grafting, angioplasty or pharmaceutical intervention.[7,8,9,10,11] Unexpected and partially spectacu-

Table 1. Positron emitting tracers for cardiological PET Studies

Blood flow	
N-13 NH3	
Rb-82	
O-15 H2O	
Metabolism	
C-11 palmitate	metabolism of fatty acids
F-18 deoxyglucose	glucose metabolism
C-11 acetate	O2 consumption in Krebs cycle
C-11 and N-13 amino acids	protein synthesis
Neuronal receptors	
C-11 quinucyclidine	ß-receptor ligand
F-18 metaraminol	adrenergic innervation
Miscellaneous	
O-15 or C-11 CO	blood pool labelling
F-18 misonidazole	demonstration of hypoxia
Rb-81	monitoring the potassium pool

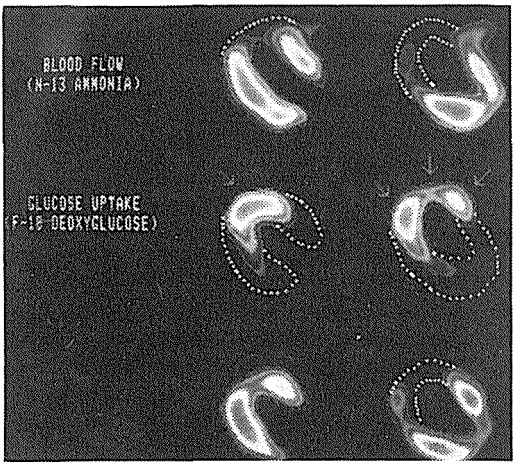

Figure 1. PET tomograms of middle and lower left ventricular myocardium after application of N-13 NH_3 (upper line), F-18 DG fasted (middle line), and F-18 DG postprandial (lower line). There is a perfusion defect of N-13 NH_3 in the apical and inferoapical myocardium. But in the same region anaerobic glycolysis (ischemic but still vital) can be seen (middle line). Only a small area in the inferior center (middle arrow) shows nearly no F-18 DG uptake, corresponding to scar tissue. The lower slices show normal aerobic glycolysis in postprandial normally perfused myocardium.

lar results concerning demonstration of remaining vitality in akinetic myocardial regions, where no Tl-201 uptake could be shown, have been reported. In one study, up to 58 percent of persisting Tl-201 stress/rest perfusion defects interpreted as scar tissue showed metabolic residual activity with F-18 DG.[10] According to these results PET seems to allow prognostic statements concerning the prediction of contraction function of akinetic but still vital myocardial tissue after revascularization. This prediction was true in one study for 85 percent, whereas regions identified as scar tissue by N-13 ammonia/F-18 DG-PET showed functional improvement only in 8 percent.[11]

The clinical value of PET in cardiological routine diagnostics needs a critical estimation due to the small number, the pilot character and in parts contradictory recommendations of studies from the few PET centers [e.g. 2 vs. 3] in combination with the very complex installation and handling of this technique; the importance therefore may be very limited during the next decade. Up to now, there are no studies concerning reproducibility and specificity of regional ischemia assessment by F-18 DG. But such studies would be necessary due to the fact that even normal myocardium postprandially shows massive aerobic glycolysis (see Figure 1) and PET is not able to differentiate aerobic from anaerobic glycolysis. Therefore, all results of the last 15 years of costly PET research show no clear indications for the essential use of PET in cardiology. Under the aspects mentioned above, a more global use of PET in chronic coronary heart disease (CHD) with dysfunction, acute myocardial infarction, cardiomyopathies and heart transplantation is postulated.[2] In addition, an economical concurrence of PET with established techniques such as T1-201 SPECT with comparable sensitivity and specificity of approximately 80 and 90% for both techniques in the recognition of myocardial hypoperfusion caused by CHD seems nearly impossible. Beyond that, Tl-201 combined with late acquisition twelve or more hours after injection is able to identify vital myocardium with high accurarcy.[12,13] But, besides the comparably limited value for cardiological routine diagnostics, the PET method has a unique importance for clinical research due to the nearly unlimited possibilities of non-invasive in vivo investigation.

MRI

The nuclear magnetic resonance (NMR) phenomenon is quantum mechanical in nature, based on the fact that in a system of nuclear spins transitions between low-and high-energy states present in an external magnetic field can be achieved by irradiating the sample with electromagnetic waves.

Magnetic resonance imaging (MRI) is a relatively new technique for imaging the human body that has developed from chemical assay techniques that have been in routine use for many years. Basically, MRI makes use of magnetic fields and radiofrequency waves to generate intensity-modulated images from specific sec-

tions of the body. The intensity of a point within such an image is determined in a complicated fashion by the number of hydrogen nuclei (protons) at the corresponding point in the patient and also the chemical makeup of the tissue at that point. Signal intensity is measured by placing the patient in a strong magnetic field, irradiating the region of interest with radiofrequency waves, and recording the radiation that is reemitted from the patient. Variations in imaging techniques can produce drastic differences in image appearance by emphasizing different aspects of the chemical structure. Thus, not only does MRI produce high quality images of the body anatomy, but it also provides the capability for measuring in vivo body chemistry.

MRI is capable of producing cardiac images with great morphological detail, if image acquisition with ECG triggering is used. To obtain stopped-motion images of the heart, which requires a temporal resolution in the order of 20-40 ms[14] special techniques have to be used in MRI of the heart.[15] Since the main axes of the heart do not coincide with the main axes of the human body, in cardiac MR immaging it is mostly advantageous to acquire sections which are angulated orthogonally to the cardiac axes. As MRI permits slice acquisition in all spatial orientations using electronic angulation, this is achievable without difficult patient positioning.

MRI is able to depict the cardiac walls in different phases of the heart cycle and shows the valves and the chamber lumina. Furthermore, the motion of blood in the chambers can be observed. The pericardium is well visualized and the proximal parts of the coronary arteries can be identified. Normally, the wall thickness has been measured as a function of the cardiac cycle[16] and the results agree with the data obtained by echocardiography.[17] The wall thickness was found to increase normally by roughly 50% from end-diastole to end-systole, therefore the percentage of regional wall thickening can be computed as a function parameter. Using long and short axis views, regional wall motion can be assessed as in cine-ventriculography.[18] However, because MRI is a tomographic method, much more accurate measurements can be obtained. MRI permits also ventricular chamber volumetry to measure quantities such as the end-diastolic, end-systolic, and stroke volumes, as well as the ejection fraction.[19,20] Left and right ventricular stroke volumes can be determined with accuracy in MRI and they are close to unity,[21] as they should be.

Pathologic cardiac morphology and function in MRI has been studied up to now concerning congenital abnormalities, coronary artery disease, cardiomyopathies, valvular disease, other acquired cardiac diseases and pericardial disease.

The large field of view and the good soft tissue contrast help in the evaluation of complex disease, and MRI is a valuable tool in older patients with congenital heart disease.[22,23,24] MRI is particularly useful in the diagnosis of atrial septal defects, which tend to be diagnosed later in life.[25,26,27] Functional information obtainable with MRI includes the exact determination of shunt volumina.[28,29]

Coronary artery disease has been evaluated extensively with MRI, even with the use of contrast agents to enhance ischemic or infarcted myocardial regions. Chronic infarction shows areas of wall thinning and aneurysmatic dilatations.[30] Acute myocardial infarction results in myocardial edema formation, which can be identified due to increase in signal intensity with progressively heavier T2 weighting.[31] The increase in signal intensity is an early sign occurring between 3 and 5 h after the acute event.[32] Correlation between anatomic infarct size and as defined by the region of altered signal intensity is excellent.[33] With the use of contrast agents in animal studies it was possible to differentiate reversible ischemia from irreversible damage.[34] So far, morphological changes in coronaries go undetected, the spatial resolution of the method being insufficient.[35] Limited experience exists in the evaluation of cardiomyopathies other than those due to coronary artery disease.

Valvular disease investigated by special techniques such as gradient echo imaging bear the potential of providing an assessment of the severity of disease and will possibly yield estimations

of valvular orifice surface area like those obtained by echocardiography.

Obviously, MRI is well suited in assessing cardiac and paracardiac masses, because of its superior anatomic delineation of such masses, being often more definitive in the diagnosis than echocardiography.[36] Like echocardiography, MRI is able to detect pericardial disease, such as effusions and pericardial thickening. MRI is more sensitive than echocardiography in identifying localized posterior pericardial effusion.[37]The method appears to be very useful in the evaluation of constrictive pericardial and epicardial disease.[38]

MRS

Magnetic resonance spectroscopy (MRS) describes the property of certain nuclei which, when placed in a magnetic field, respond to the excitation of their spin states by photons of suitable (resonance) frequency. The same nucleus within different chemical environments will be excited at different frequency and give rise to discrete resonances. This so called »chemical shift effect« makes it possible to distinguish between different chemical compounds; e.g. phosphorus-31 MR spectroscopy can differentiate phosphomonoesters, phosphodiesters, inorganic phosphate, AMP, ADP and ATP. The signal amplitude of a particular NMR resonance is proportional to the number of nuclei giving rise to the resonance. Even if absolute quantification is difficult to achieve up to now, semiquantitation is achieved by comparing interesting peaks with peaks arising from internal or external reference material or by calculating peak area ratios. Nuclei that are observable by NMR and clinically useful are H-1, C-13, F-19, Na-23 and P-31. Most work in cardiologic applications to date has involved the P-31 nucleus, which is 100% naturally abundant with a relatively high NMR sensitivity. P-31 spectra allow observation of a selection of high energy phosphates involved in the transduction of energy within the cell. Quantitation of these resonances therefore allows us to study the major biochemical pathways leading to their formation, namely oxidative and anaerobic respiration. Clinically, ischemia and hypoxia are the most important modulators of these processes. Additionally, P-31 MR spectroscopy provides noninvasive measurement of intracellular pH.

The excitement associated with MRS arises from its ability to monitor the metabolism of intact organs noninvasively. Most of the research on cardiac MRS has been directed toward myocardial ischemia. Spectroscopic investigations of ischemia and infarction have ranged from analyses of myocardial tissue samples to image – guided in vivo studies of intact animals and humans. The latter studies have noninvasively shown metabolic alterations due to myocardial ischemia, thus confirming the feasibility of cardiac MRS.

In MRS of the heart much *in vivo* work was carried out using isolated organ perfusion models.[39] Mostly the results of ischaemic insults have been followed in vivo either in open chest models or using depth localization. The diagnosis of ischaemic disease in heart is possible by Pi-31

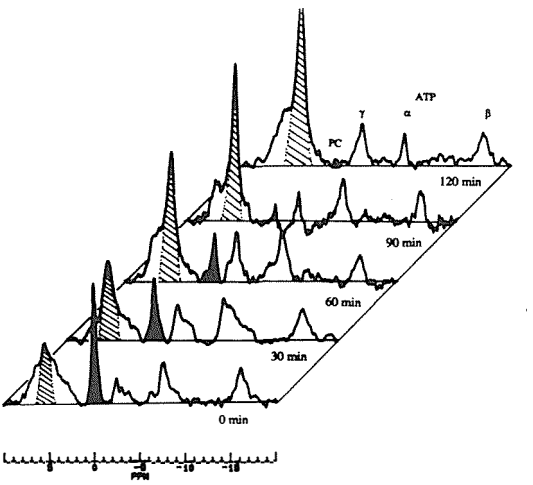

Figure 2. Spectrogram of *in-vitro* heart model after reperfusion with oxigenated blood. Abbreviations: PC = phosphocreatinine, Pi = anorganic phosphate. PC/ ß-ATP is used for quantification of phosphocreatinine pool. The ß/γ-ATP relation gives information about ATP content. Note the gradual disappearance of PC peak and the increasing of Pi as a result of ischemia.

MRS but requires good spatial resolution of the area from where signals are to be obtained.

A special spatial localization technique called DRESS has been applied to human subjects, yielding P-31 MR spectra from the hearts of normal volunteers[40] and from patients with acute myocardial infarction[41] and exercise-induced ischemia.[42] In the last study,[42] the phosphocreatine/ATP ratio decreased during ischemia caused by isometric hand-grip exercise in patients with severe coronary disease. Additional volume-localization techniques, including topical MR[43] and ISIS,[44,45] have been used to monitor phosphate metabolism in human hearts noninvasivelay. P-31 MRS has also been investigated as a means of monitoring cardiac transplant rejection. Studies in humans[46,47] using image-guided volume-localized spectroscopy have shown metabolic changes in hearts that are being rejected, such as reductions in phosphocreatine/ATP or phosphocreatine/inorganic phosphate ratios.

There are no clinical applications of spectroscopy in routine use up to now, but with further improvement in NMR instrumentation and techniques spectroscopy may prove an important technique in the investigation of ischemic disease or assessment of transplant viability.

SPECT

An important new technical advance, which is already widely available, has been the development of single-photon emission computed tomography (SPECT). With this technique, the detector of the gamma camera rotates 180° around the patient for obtaining true tomographic slices; the problem of overlaping of normal and abnormal zones associated with planar imaging is therefore avoided. Thallium-201 (Tl-201) myocardial perfusion imaging is the most common test performed with SPECT. With Tl-201, the initial phase represents the myocardial perfusion at the time of injection, whether at rest or during exercise. The delayed phase provides information about the potassium pool within the myocardium, reflecting the extent of viable myocardium. With planar imaging, inter-and intraobserver variability associated with conventional visual analysis is substantial. This problem is compounded with SPECT, in which a far greater number of images are presented for interpretation – conventionally, a complete set of short-axis and long-axis slices. Thus, quantitative techniques have been developed for analyzing the images objectively. Two widely available approaches to objective analysis have been developed.[48,49,50] Both techninques have been shown to detect and localize myocardial perfusion defects accurately.[49,50,51] Whereas SPECT imaging is comparable to planar imaging in detecting defects in the left anterior descending and right coronary artery, it has almost doubled the detection rate of left circumflex coronary disease over that with planar imaging.[52,53] In addition, SPECT imaging is more accurate than planar imaging for infarct sizing. In dogs excellent correlation between the size of the perfusion defect assessed by SPECT imaging and pathologic infarct size determined by staining with triphenyl tetrazolium chloride has been demonstrated.[54] SPECT imaging appears to be the technique of choice for assessing myocardial perfusion because it provides better detection of circumflex artery disease and permits better sizing of perfusion defects.[55]

Along with advances in technique there have come also advances in radiopharmaceuticals. The most promising agent is technetium – 99m (Tc-99m) methoxyisobutyl isonitrile (Tc-MIBI).[56,57,58] This new agent has undergone extensive preclinical and clinical evaluation, including direct comparison to both Tl-201 and angiography in more than 800 patients. Results of comparisons in various subgroups of patients have recently been reported.[59,60] Tc-MIBI provides several advantages over Tl-201. Thallium, despite its excellent physiologic properties, has suboptimal imaging properties because of its low energy and somewhat long half-life (73 hours). Tc-99m has the ideal energy for gamma camera imaging. Compared with Tl-201, Tc-99m undergoes less scatter and attenuation and results in a brighter flash of the photon within the crystal for

the scintillation camera. These factors result in higher resolution on a count-for-count basis. Tc-99m also has better radiation dosimetry than thallium, so that a 10-fold higher dose can be given, which, when combined with good myocardial uptake, yields higher count rates. The combination of higher resolution per count and higher count rates results in improved image quality of Tc-MIBI studies compared with Tl-201 studies, thereby resulting in greater ease of interpretation and greater certainty of diagnosis. In addition, due to the higher count rates with Tc-MIBI, one can obtain gated tomographic images, which permit assessment of myocardial wall motion as well as perfusion.[61] First-pass ventricular function studies can also be performed, thereby allowing measurements of ejection fraction at the time of injection. Moreover, because the technetium generator is available in virtually every nuclear medicine department, the agent is available for emergency use at any time of the day or night. Data from phase III clinical studies conducted by Du Pont have shown that the first-pass left ventricular ejection fraction measurement with Tc-MIBI correlates well with the standard measurement with other Tc-99m tracers.[62]

In animals, Tc-MIBI has been found to be distributed to the myocardium in proportion to regional myocardial blood flow.[63] The myocardial uptake of Tc-MIBI parallels that of Tl-201 throughout the range of blood flows that might be observed clinically. The slightly lower uptake of Tc-MIBI across the entire flow range indicates that its extraction is lower than that of Tl-201. The most important characteristic of the new agent is that it does not redistribute to any great extent,[64] iln contrast to Tl-201, which redistributes when viable myocardium is present. Therefore, to assess myocardial perfusion with Tl-201, imaging must be performed soon after injection. However, one can wait several hours after injecting Tc-MIBI before commencing imaging, a useful property in assessing thrombolytic therapy. Similar sensitivity and specificity for overall detection of coronary artery disease as well as detection of disease in individual coronary arteries were observed, when comparing the two agents in patients studied with both.[60] But Tc-MIBI shows a trend toward a higher normalcy rate in patients with low likelyhood of having coronary artery disease. With both tracers, the sensitivity for detection of disease in individual coronary arteries was higher with SPECT than with planar imaging.[60] Comparison of the two imaging agents by SPECT for the ability to distinguish between reversible and ireversible defects showed 97% agreement for defect type.[60] It therefore appears that Tc-MIBI will provide improved imaging characteristics and will yield results similar to those obtained with Tl-201. Of note, the acquisition parameters used to date for Tc-MIBI imaging have been those that were optimized for Tl-201 imaging. Preliminary phantom experimental data suggest that further improvement in image quality is likely to occur when these acquisition parameters are specifically tailored to the new agent. This development could lead to improved accuracy in coronary artery disease detection and evaluation when compared with Tl-201.

For example, immediate assessment of arterial patency and myocardial salvage after thrombolytic therapy is an ideal application for Tc-MIBI investigations. A change in the defect size on Tc-MIBI images before and after thrombolytic therapy provides information as to whether the infarct-related artery is open, and it could be demonstrated that a 30% reduction in the size of the defect was strongly predictive of patency of the infarct-related artery.[65,66] The results suggest that Tc-MIBI will provide an objective method for documenting efficacy of thrombolytic therapy and that the approach may provide a mechanism by which this efficacy can be determined immediately. Potentially, this approach could be used to distinguish subgroups of patients who need more thrombolytic therapy or who are candidates for urgent angioplasty.

The SPECT technique can also be applied to radionuclide ventriculography. A fast process has been developed to extract threedimensional scans of Fourier amplitude and phase of the heart by means of gated SPECT. By this techni-

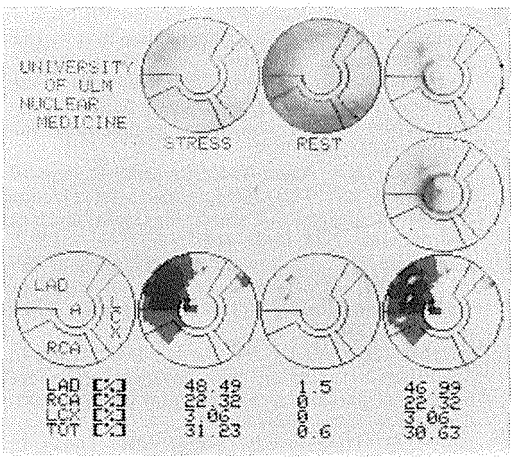

Figure 3. Quantification of myocardial perfusion tomographic study. Representative stress-induced ischaemic changes for anterior region are shown.
Top row: original polar stress, rest and wash-out image.
Bottom row from left to right: standard vessel distributions (LAD, left anterior descending; RCA, right coronary artery; LCX, left circumflex artery; TOT, total myocardial area); stress; rest; difference image, compared with gender related normal data base. Colour coding: white – normal perfusion; grey – significant change; black – highly significant change as compared with perfusion at rest.

que the backprojection of Fourier-data such as the average of the heart period and the sums of the cosinus-and sinus row with the combined advantage of count statistics yield high quality functional slices of the heart by only 15 minute acquisition time.[67] Reducing the data volumes of the functional slices for amplitudes and phases by transforming them in a bull's eye display, it results in superposition-free and position-independent detection of the left ventricular functional state, with an adequate and direct comparison to the Te-201 myocardial SPECT investigation.

For integrated SPECT in radionuclide ventriculography methods have been developed allowing reconstruction of planar views oriented according to the long axis of the heart.[68,69] This technique allows presentation of both ventricles in four views in a similar way as echocardiography, which facilitates the anatomic location of regional wall motion abnormalities and of the areas of first contraction.

Quantitative analysis in myocardial SPECT technique has stimulated tremendous work. However, the impact on routine patient care has grown at a slower pace. The procedure for quantification in myocardial SPECT includes transfer of all data into a standard polar map and comparison with a gender-matched normal data base. The result reveals areas of reduced tracer uptake, color-coded according to the level of significance. A representative display is shown on figure 3. Interpretation of these colored polar maps might appear simple, but in fact requires a substantial amount of knowledge to avoid misinterpretation of the results. This should lead to a restricted use of this quantitative tool: following an initial step of reading the original data in terms of short and long axis slices of the left myocardium, the polar map should only be utilized for verification and for suggestions of additional lesions. This has to be confirmed by a second reading of the slices, and only this last step should define the lesions to be reported. Quantification used in this dialectic approach avoids inclusion of artefacts, and at the same time provides is useful experience for trainees. Furthermore, it allows easy interpretation during clinical conferences and statistical analysis of groups. Quantification in myocardial SPECT can improve patient care if the tool is handled cautiously. However, careful analysis of the original data is essential.[70]

References

1. Henze E. Positron-Emissionstomographie des Herzens. *Z Kardiol* 1987; **76:**255-8.
2. Schelbert HR. Myocardial ischemia and clinical applications of positron emission tomography. *Am J Cardiol* 1989; **64:**46E-53E.
3. Bergmann SR, Fox KAA, Geltman EM, Sobel BE. Positron emission tomography of the heart. *Progr Cardiovasc Dis* 1985; **18:**165-94.
4. Marshall RC, Tillisch JH, Phelps ME, Huang SC, Carson RC, Henze E, Schelbert HR. Identification and differentiation of resting myocardial ischemia and infarction in man with positron computed tomography, F-18-labeled fluorodeoxyglucose and N-13 ammonia. *Circulation* 1983; **67:**766-78.

5. De Landsheere CM, Raets, D, Pierard LA, Berthe, C, Legrand V, Corchelet L, Chapelle JP, Lemaire C, Del Fiore G, Guillaume M, Lamotte D, Kulbertus HE, Rigo P. Thrombolysis in anterior myocardial infarction: effect on regional viability studied with positron emission tomography. *Circulation* 1987; **76(supl IV):**IV-5.
6. Schelbert HR, Henze E, Sochor H, Grossman RG, Huang SC, Barrio JR, Schwaiger M, Phelps ME. Efects of substrate availability on myocardial C-11 palmitate kinetiks by positron emission tomography in normal subjects an patients with ventricular dysfunction. *Am Heart J. 1986;* **111:**1055-64.
7. Hashimoto T, Kambara H, Fudo T, Hayashi M, Tamaki S, Tokunaga S, Tamaki N, Yonekura Y, Konishi J, Kawai C. Non-Q-wave versus Q wave myocardial infarction: regional myocardial metabolism and blood flow assessed by positron emission tomography. *JACC* 1988; **12:**88-93.
8. Nienaber, C, Brunken R, Sherman T, Yeatman L, Gambhir SS, Krivokapich J, Demer L, Child J, Schelbert HR. Recovery of myocardial metabolism by PET precedes improvement of ischemic wall motion after PTCA. *JACC* 1988; **12:**28A.
9. Brunken R, Schwaiger M, Grover-McKay M, Phelps ME, Tillisch J, Schelbert HR. Positron emission tomography detects tissue metabolic activity in myocardial segments with persistent thallium perfusion defects. *JACC* 1987; **10:**557-67.
10. Brunken R, Tillisch J, Schwaiger M, Child JS, Marshall R, Mandelkern M, Phelps ME, Schelbert HR. Regional perfusion, glucose metabolism and wall motion in chronic electrocardiographic Q-wave infarctions. Evidence for persistence of viable tissue in some infarct regions by positron emission tomography. *Circulation* 1986; **73:**951-63
11. Tillisch J, Brunken R, Marshall R, Schwaiger M, Mandelkern M, Phelps M, Schelbert HR. Prediction of cardiac wall motion abnormalities using positron tomography. *N Engl J Med* 1986; **314:**884-8.
12. Dilsizian V, Rocco TP, Freedman NMT, Leon MB, Bonow Ro. Enchanced detection of ischemic but viable myocardium by the reinjection of thallium after stress-redistribution imaging. *N Engl J Med* 1990; **323:**141-6.
13. Berman DS, Kiat H, Maddahi J, Shah PK. Radionuclide imaging of myocardial perfusion and viability in assessment of acute myocardial infarction. *Am J Cardiol* 1989; **64:**9B-16B
14. Green MV, Ostrow HG, Douglas MA et al. High temporal resolution ECG-gated scintigraphic angiocardiography. *J Nucl Med* 1974; **16:**95-8.
15. Crooks LR, Barker B, Chang H et al. Magnetic resonance imaging strategies for heart studies. *Radiology* 1984;**153:** 459-65.
16. Fisher MR, von Schulthess GK, Higgins CB. Multiphasic cardiac magnetic resonance imaging: normal regional left ventricular wall thickening. *AJR* 1985; **145:**27-30.
17. Lieberman AN, Wiss JL, Jujdutt BL et al. Two-dimensional echocardiography and infarct size: relationship of regional wall motion and thickening to the extent of myocardial infarction in the dog. *Circulation* 1981; **63:**739-46.
18. Underwood SR, Rees RSO, Savage PE. Assessment of regional left ventricular function by magnetic resonance. *Br Heart J* 1986; **56:**334-40.
19. Stratemeier DJ, Thompson R, Brady TJ et al. Ejection fraction determination by MR imaging: comparison with left ventricular angiography. *Radiology* 1986; **158:**775-7.
20. Buckwalter KA, Aisen AM, Dilworth LR, Nancini GBJ, Buda AJ (1986) Gated cardiac MRI: ejection fraction determination using the right anterior oblique view. *AJR* 1986; **147:**33-7.
21. Longmore DB, Underwood SR, Hounsfield GN et al (1985) Dimensional accuracy of magnetic resonance in studies of the heart. *Lancet* 1985; **(June 15):**1360-2.
22. Higgins CB, Byrd BF III, Farmer DW, Osaki L, Silverman NH, Cheitlin MD. Magnetic resonance imaging in patients with congenital heart disease. *Circulation* 1984; **70:**851-60.
23. Didier D, Higgins CB, Fisher MR, Osaki L, Silverman NH, Cheitlin MD. Congenital heart disease: gated MR imaging in 72 patients. *Radiology* 1986; **158:**227-35.
24. Guit GL, Bluemm R, Rohmer Jet al. Levotransposition of the aorta: identification of segmental cardiac anatomy using MR imaging. *Radiology* 1986; **161:**673-9.
25. Jacobstein MD, Fletcher BD, Goldstein S, Riemenschneider TA. Evaluation of atrioventricular septal defect by magnetic resonance imaging. *Am J Cardiol* 1985; **55:**1158-63.
26. Dinsmore RE, Wismer GL. Guyer Det al. Magnetic resonance imaging of the interatrial septum and atrial septal defects. *AJR* 1985; **145:**697-703.
27. Diethelm L, Dary R, Lipton MJ, Higgins CB. Atrial-level shunts: sensitivity and specificity of MR in diagnosis. *Radiology* 1987; **162:**181-6.
28. Underwood SR. Functional studies of the cardiovascular system using magnetic resonance imaging. In: Functional studies using NMR. McCready VR, Leach M, Ell PJ, Springer, Berlin 1987.
29. Sechtem U. Pflugfelder P, Cassidy MC, Holt W, Wolfe C, Higgins CB. Ventricular septal defect: visualization of shunt flow and determination of shunt size by cine MR imaging. *AJR* 1987; **149:**689-92.
30. Allgayer B, Rupp N, Bosiljanoff P, Reiser M, Lukas P. Einsatzmöglichkeiten der Kernspintomographie bei Erkrankungen des Herzens. *Fortschr Röntgenstr* 1986; **144:**1-6.
31. Fisher MR, NcNamara MT, Higgins CB. Acute myocardial infarction: MR evaluation in 29 patients. *AJR* 1987; **146:**315-20.
32. Tscholakoff D, Higgins CB, McNamara MT, Derugin N. Early-phase myocardial infarction: evaluation by MR imaging. *Radiology* 1986; **159:**667-72.
33. Rokey R, Verani MS, Bolli R et al. Myocardial infarct size quantification by MR imaging early after coronary artery occlusion in dogs. *Radiology* 1986; **158:**771-4.
34. McNamara MT, Tscholakoff D, Revel D et al. Differentiation of reversible and irreversible myocardial injury by MR imaging with and without gadolinium-DTPA. *Radiology* 1986; **158:**765-9.

35. Paulin S. von Schulthess GK, Fossel E, Krayenbuehl HP. MR imaging of the aortic root and the proximal coronary arteries. *AJR* 1987;**145:**665-70.
36. Go R, O'Donnell JK, Underwood DA et al. Comparison of gated cardiac MRI and 2 D echocardiography of intracardiac neoplasms. *AJR* 1985; **145:**21-5.
37. Sechtem U, Tscholakoff D, Higgins CB. MRI of the abnormal pericardium. *AJR* 1986; **147:**245-52.
38. Soulen RL, Stark DD, Higgins CB. Magnetic resonance imaging of constrictive pericardial disease. *Am J Cardiol* 1985; **55:**480-4.
39. Henze E, Schoser K, Lietzenmayer R et al. Myokard-Stoffwechseluntersuchungen mit der P-31-NMR-Spektroskopie und einem einfachen Herz-Perfusionsmodell von Schlachttieren – ein Ansatz zur Vermeidung von In-vivo-Tierexperimenten. *Z Kardiol* 1989; **78:**553-60.
40. Bottomley PA. Noninvasive study of high-energy phosphate metabolism in human heart by depth-resolved P-31 NMR spectroscopy. *Science* 1985; **229:**769-72.
41. Bottomley PA, Herfkens RJ, Smith LS, Bashore TM. Altered phosphate metabolism in myocardial infarction: P-31 MR spectroscopy. *Radiology* 1987; **165:**703-7.
42. Bottomley PA, Weiss RG, Hardy CJ, Shulman SP. Exercise in patients with coronary artery disease (abstr). In: Book of abstracts, Society of Magnetic Resonance in Medicine. Berkeley, CA: Society of Magnetic Resonance in Medicine. 1989;35.
43. Oberhaensli RD, Galloway GJ, Hilton-Jones D, et al. The study of human organs by phosphorus-31 topical magnetic resonance spectrocopy. *Br J Radiol* 1987; **60:**367-73.
44. Schaefer S, Gober J, Valenza M, et al. Nuclear magnetic resonance imaging-guided phosphorus-31 spectroscopy of the human heart. *J Am Coll Cardiol* 1988; **12:**1449-55.
45. Matson Gb, Twieg DB, Karczmar GS, et al. Application of image-guided surface coil P-31 MR spectroscopy to human liver, heart, and kidney. *Radiology* 1988; **169:**541-7.
46. Herfkens RJ, Charles HC, Negro-Vilar R, Van Trigt P. In vivo phosphorus-31 NMR spectroscopy of human heart transplants (abstr). In: Book of abstracts: Society of Magnetic Resonance in Medicine. Berkeley, CA: Society of Magnetic Resonance in Medicine. 1988:827.
47. Bottomley PA, Weiss RG, Chacko VP, Augustine S, Baumgartner WA. Abnormalities in cardiac high-energy phosphate metabolism in rejecting normal heart transplant patients by P-31 NMR (abstr) In: Book of abstracts: Society of Magnetic Resonance in Medicine. Berkeley, CA: Society of Magnetic Resonance in Medicine 1989;510.
48. Garcia EV, Van Train K, Maddahi J, Prigent F, Friedman J, Areeda J, Waxman A, Berman DS. Quantification of rotational thallium-201 tomography. *J Nucl Med* 1985; **26:**17-26.
49. Maddahi J, Van Train K, Wong C, Prigent F, Gurevitz J, Friedman J, Berman D. Quantitative analysis of T1-201 myocardial single photon emission computerized rotational tomography: development, validation, and prospective application of an optimized computer method (abstr). *JACC* 1986;722A.
50. DePasquale EE, AC, DePuey EG, Garcia EV, Pilcher G, Bredlau C, Roubin G, Gober A, Gruentzig A, D'Amato P. Quantitative rotational thallium-201 tomography for identifying and localizing coronary artery disease. *Circulation* 1988; **77:**316-27.
51. Van Train K, Maddahi J, Berman D. A multicenter trial of the Cedars-Sinai method for quantitative analysis of T1-201 myocardial tomography. *J Nucl Med* 1988; **29:**755 (abstr).
52. Maddahi J, VanTrain KF, Wong, C, Gurewitz J, Prigent F, Youngkin C, Friedman J, Berman D. Comparison of T1-201 single photon emission computerized tomography (SPECT) and planar imaging for evaluation of coronary artery disease. *J. Nucl Med* 1986; **27:**999 (abstr).
53. Fintel DJ, Links JM, Brinker JA, Frank TL, Parker M, Becker L. Improved diagnostic performance of exercise thallium-201 single photon emission computed tomography over planar imaging in the diagnosis of coronary artery disease: a receiver operating characteristic analysis. *JACC* 1989; **13:**600-12.
54. Prigent F, Maddahi J, Garcia EV, Satoh Y, Van Train K, Berman DS. Quantification of myocardial infarct size by thallium-201 single photon emission computerized tomography: experimental validation in the dog. *Circulation* 1986; **74:**852-61.
55. Kiat H, Berman DS, Maddahi J. Comparison of planar and tomographic exercise thallium-201 imaging methods for the evaluation of coronary artery disease *JACC* 1989; **13:**613-6.
56. Willams SJ, Mousa SA. Morgan RA, Carroll TR, Maheu LJ. Pharmacology of Tc-99m isonitrile: agents with favorable characteristics for heart imaging. *J Nucl Med* 1986; **27:**877 (abstr).
57. Mousa SA, Williams SJ, Sands H. Characterization of in vivo chemistry of cations in the heart. *J Nucl Med* 1987; **28:**1351-7.
58. McKusick K, Holman BL, Jones AG, Davison A, Rigo P, Vosberg H, Moretti J. Comparison of three Tc-99m isonitriles for detection of ischemic heart disease in humans. *J Nucl Med* 1986; **27:**878 (abstr).
59. Wackers FJ, Kayden D, Lange RC, Mattera J. Rest-exercise organ distribution of RP-30, a new Tc-99m-labelled myocardial perfusion imaging agent. *JACC* 1987; **9:**27 (abstr).
60. Kiat H, Maddahi J, Roy LT, Van Train K, Friedman J, Resser K, Berman DS. Comparison of technetium 99m methoxy isobutyl isonitrile and thallium-201 for evaluation of coronary artery disease by planar and tomographic methods. *Am Heart J* 1989; **117:**1-11 .
61. McGhie I, Kahn JK, Akers MS, Faber TL, Corbett JR. Tomographic myocardial perfusion imaging with technetium – 99m 2-methoxy isobutyl isonitrile (MIBI) and thallium-201: the sensitivity and reproducibility of semi-quantitative assessments of myocardial perfusion and regional systolic function. *JACC* 1989; **13:**30 (abstr).
62. Baillet G, Mena I, Kuperus J, Robertson J, French W. Simultaneous Tc-99m-MIBI angiography and myocardial perfusion imaging. *J Nucl Med 1989;* **30:**38-44.

63. Okada R, Glover D, Gaffney T, Williams S. Myocardial kinetics of Tc-99m-hexakis-2-methoxy-2-methylpropylisonitrile. Circulation 1988; **77**:491-8.
64. Liu P, Houle S, Mills L, Dawood F. Kinetics of Tc-99m MIBI in clearance in ischemia-reperfusion: comparison with Tl-201. *Circulation* 1987; **76**:IV:IV-216 (abstr).
65. Wackers F, Gibbons R, Kayden D, Pellika P, Behrenbeck T, Verani M, Mahmarian J, Zaret B. Serial planar Tc-99m isonitrile imaging for early noninvasive identification of reperfusion after thrombolysis. *Circulation* 1988; **78**:suppl II:130 (abstr).
66. Gibbons R, Verrani M, Pellika P, Behrenbeck T, Mahmarian J, Chesebro J, Wackers F. Tomographic assessment of myocardial reperfusion during acute myocardial infarction using Tc-99m methoxy isobutyl isonitrile (MIBI). *JACC* 1989; **13**:153 (abstr).
67. Graf G, Clausen M, Henze E, Bitter F, Adam WE, Heidenreich P. Fast process (Flash-SPECT) to extract threedimensional scans of Fourier amplitude and phase of the heart by means of gated single photon emission computed tomography (GASPECT) *NucCompact* 1989; **20**:23-7.
68. Clausen M, Weissmüller P, Weller Ret al. Double-angulated, integral emission-computed-tomography (DA-ISPECT) in radionuclide ventriculography (RNV) with reconstructed planar views oriented according to the long axis of the heart. *Nuc Compact* 1990; **21**:167-70.
69. Clausen M, Henze E, Weller R et al. Tomographic radionuclide ventriculography (RNV) with reconstructed planar views perpendicular to the body axis (ISPECT). *NucCompact* 1990; **21**:95-9.
70. Clausen M, Henze E, Adam WE. Quantitative analysis in nuclear cardiology asisting decision-making during visual lesion detection. *Z Kardiol* 1989; **78** (suppl 7):165-72.

Adv Radiol Oncol 1992; 135--41.

Reflections on immunoscintigraphy and radioimmunotherapy

Roos JC, van Lingen A, Teule GJJ

Dept. of Nuclear Medicine, Free University Hospital, Amsterdam, the Netherlands

Although many reports have been published about the successful diagnostic and therapeutic application of radiolabeled monoclonal antibodies, no antibody is available with the same selectivity and efficacy as ^{131}I for thyroid tissue and thyroid carcinoma, respectively. As a consequence, many problems have to be solved to obtain optimal diagnostic and therapeutic results with radiolabeled antibodies. This review summarizes these problems by discussing factors related to the tumour, antibody, radionuclide, data acquisition and analysis, and dosimetry.

Key words: antibodies, monoclonal; radiotherapy; radionuclide; scintigraphy; therapy;

Introduction

In a recent Newsline in the Journal of Nuclear Medicine[1] it is stated that »the field of specific antibody targeting to tissues is still a very exciting area, and it holds a lot of promise«. In the last decade, statements of this kind are heard very often and are based on the appealing elegancy of this approach and the need for improvement of diagnostic and, especially, therapeutic modalities in cancer patients.

The successful application of radiolabeled monoclonal antibodies is substantiated by many reports.[2-10] The therapeutic successes, however, are relatively scarce and restricted to partial responses in, mainly, melanoma, hepatocellular carcinoma, malignant lymphoma, and chronic lymphocytic leukemia.[11-12] The main reason is that no antibody is available with the same selectivity as, for example iodine for thyroid tissue and, more important, there is no radiolabeled antibody with the same efficacy as ^{131}I against thyroid carcinoma.

The consequence is that many problems need to be solved to obtain optimal diagnostic and therapeutic results. Despite these problems, De Nardo, in the same Newsline[1], urges nuclear medicine practitioners to »get in gear now and start learning because this area is going to be one of the future directions in nuclear medicine«.

This paper lists the problems of the clinical application of a radiolabeled antibody, merely summarizing the fields of immunoscintigraphy, dosimetry, and therapy.

Correspodence to: Jan C. Roos, M.D., Dept. of Nuclear Medicine, Free University Hospital, De Boelelaan 1117, 1081 HV Amsterdam, The Netherlands, Tel: 020-5484811.

UDC: 543.52:615.849

Tumour

Antigen expression

The specificity of the antigen for a certain tumour substantially determines success or failure. The presence of the antigen in the tissue from which the tumour originates or in other normal tissue should be known before a study is initia-

ted. Immunohistochemistry is sometimes necessary before a diagnostic test is performed because the antigen may not be expressed by each tumour of the same type. For example, only about 60% of colo-rectal cancers express the antigen 16.88.[3] Immunohistochemistry further gives information about the antigen distribution. The antigen expression may differ between cells within one localization, between different localizations, and between the primary tumour and its metastases.[13-14] These aspects concerning antigen distribution and heterogeneity should be kept in mind when clinical applications are considered. Fortunately, a heterogeneous distribution does not necessarily preclude a successful diagnosis or therapy.

Antigen accessibility

Immunohistochemistry reveals whether the antigen is present inside or on the surface of the cell. Antibodies will not reach an intracellular antigen unless there is cellular necrosis making the antigen accessible. This necrosis itself may also be an important reason for successful immunoscintigraphy because aspecific retention of antibodies has been observed. This may imply that in a scientific clinical study one has to include an aspecific control antibody before one may conclude that the antibody really specifically locates tumour tissue. A cell-surface bound antigen seems an advantage for immunoscintigraphy.

If tumour cells actively or passively shed the antigen into the circulation, this may substantially reduce the success of immunoscintigraphy or therapy. The administered antibody may form complexes with the circulating antigen and these complexes will be metabolized increasing the background in the liver and decreasing the amount of antibody available for targeting. If it is shed into the surroundings and locoregional lymph nodes, immunoscintigraphy, especially after local administration of the antibody, may show false positive results.

Antigen access further depends on tumour blood flow, vascular permeability, and tumour architecture. Actually, the poor vascularisation of most tumours is an important limiting factor in the clinical application of monoclonal antibodies. For example, successful detection of lymphoma deposits may partly be the consequence of a higher blood flow in comparison to the lower flow in solid tumours.[15] In larger tumours, the antibody may only reach the outer layers of the tumour. Several interventions are possible which may enhance antibody uptake. For example, tumour flow may be increased by pharmacological intervention. Since tumour vessels lack adrenergic regulation, beta-blockers and angiotensin II, will induce vasoconstriction in normal tissue increasing relative blood flow to the nonresponding tumour.[16-17]

An increased tumour blood flow will result in higher target-to-background ratios, which are relevant for the results of immunoscintigraphy. During radioimmunotherapy (RIT) both a higher radiosensitivity, due to improved oxygenation, and increased absorbed doses in tumour or metastases can be achieved. The effective interaction between the radiation energy and the tumour are further related to the emission characteristics of the therapeutic radionuclide (high LET radiation) and to the activity of DNA repair mechanisms.

It remains to be shown whether radioimmunotherapy will become a single agent modality such as ^{131}I treatment of thyroid cancer. Considering the relative low dose rates during radioimmunotherapy, combination with chemotherapy might be considered.

Antibody

In general, the dose (milligrams) of antibodies to be administered consists of foreign body proteins. Toxicity testing, therefore, is mandatory and the production process must be strictly regulated (viral contents). Important factors are the shelf-life of the different components and the final radiopharmaceutical.

Specificity

It is important that the antibody reacts with the tumour-associated antigen and only minorly with other antigens (cross-reactivity). Initially, only polyclonal mixtures were available resulting in high aspecific uptakes. Since Millstein and Kohler,[18] sufficient amounts of one monoclonal antibody may be produced, bringing the »magic bullet« within reach. Binding of the antibody to non-target tissue remains a concerning issue. This aspecific uptake may be decreased by a two-step method (biotin-avidine) or bi-valent antibodies. It has also been suggested to use an excess of cold antibody before administration of the radiolabeled antibody in order to increase the saturation of the aspecific receptor sites.

The immunoreactivity after labeling should be tested and, after validation, these tests may be performed less frequently. The radionuclide may interfere with the variable part of the antibody or may be attached to a non-reactive protein. For this reason, purification after labeling might be necessary.

Structure

Up to now, most studies are performed with murine monoclonal antibodies. The injection of this foreign protein may induce an antibody response which may be allergic (anaphylactoid) in character, anti-idiotypic (against the variable part, Vab, of the antibody), or anti-Fc (constant region of the antibody) directed (complex formation, rapid clearance). This human antimouse antibody (HAMA) response is a serious threat to the successful application of antibodies. Firstly, a HAMA response precludes further diagnostic or therapeutic administrations of the antibody. Secondly, reports are published that HAMA interferes with tests for circulating antigen. For example, if a patient develops HAMA, a serum assay for CEA will give false positive results.

Several approaches may prevent or decrease this interfering HAMA response. The administration of fragments, containing the variable part of the antibody and only a small part of the Fc, is one approach, the concomitant administration of immunoresponse blocking agents another. The most appropriate solution seems the use of antibodies resembling human antibodies as closely as possible. Up to now, only a few complete human antibodies (mostly of the IgM type) are available. Promising results are obtained with an IgM against colon cancer.[3] Chimeric antibodies (human Fc, murine Vab) are more widely availabale.

Dose and route of administration

After the decision which antibody or fragment will be used, the dose to be administered must be discussed. In general, it is unknown which dose of antibody and which specific activity will give optimal targeting. Should an excess of cold antibody be added or given before the administration of the radiolabeled antibody? Some investigators report a positive effect of adding cold antibody on immunoscintigraphy[19] while others[3] could not confirm this. Recently, a nice review about pharmacological aspects of antibodies has been published in the Seminars in Nuclear Medicine.[20]

The route of administration may be intracavitary. This approach may enhance uptake by the local tumour and lessen the uptake by the systemic organs. Subcutaneous administration may visualize the lymphogenic spread, but is inappropriate for therapy because of the local radiation burden to the injection site.

Kinetics

After the administration of the radiolabeled antibody, one should be informed about the metabolism of the compound. Where do the different (radiolabeled) metabolites go to, what are the routes of excretion, is the (free) radionuclide trapped ^{111}In in bone marrow, ^{131}J in the thyroid)? All these factors determine the accumulation and clearance rate constants (k-factors) of each organ and need to be known to deter-

mine the optimal moment for immunoscintigraphy and to calculate the radiation dosimetry.

Fragments, in comparison to intact immunoglobulins will have different kinetics in the human body. The blood and whole body clearance will be faster (less background) and penetration into the tumour also will be faster. The residence time may be substantially shorter (affinity). It is clear that these factors might affect the diagnostic or therapeutic results.

Radionuclide

Historically, the radionuclide used for labeling of the antibodies was ^{131}I. New labeling techniques made it possible to use ^{111}In.

For diagnostic purposes, ^{99m}Tc may be the optimal radionuclide. However, the highest tumour/non-tumour ratios may be obtained only several days after administration[3] and, therefore, other nuclides must be used. In general, the relation between the physical T1/2 and the biological T1/2 of the radiolabeled antibody, with regard to both diagnostic and therapeutic aspects should be given attention. The effective T1/2 is also an important factor in relation to isolation of the patient after the administration of a therapeutic dose.

The selection of the radionuclide will also be influenced by the route of excretion of the metabolites of the radiolabeled antibody. A short coming of ^{111}In may be the minor excretion and high uptake in the liver and bone marrow after metabolization, interfering with the search for metastases in these regions and increasing the radiation dose. Labeling of iodine to antibodies is routine. Dehalogenation, however, easily occurs and blockage of the thyroid is a prerequisite. Developments in immunotechnology (chelators) must bring the right combination of chosen radionuclide and antibody.

Another factor which determines the choice of the radionuclide is the therapeutic approach afterwards. The kinetics of the diagnostic tracer with ^{99m}Tc, ^{111}In, or ^{123}I as a label must resemble the kinetics of the therapeutic tracer (^{186}Rh, ^{90}Y, ^{131}I) as close as possible. From the diagnostic test, one may determine the contribution of each organ to the effective dose equivalent, the dose on the tumour, and the dose limiting organ. The kinetics (immunoscintigram, blood, urine, faeces) will also provide information about the possibilities to increase the therapeutic dose by increasing the excretion of metabolites (diuretics, laxatives) and might indicate whether bone marrow preservation is mandatory.

If therapeutic doses will be administered the radiation hazards for hospital workers need to be considered. How long do patients have to be isolated (facilities), is the patient able to take care of him/herself, what do the nurses think of their risks?

Data management

Equipment

Immunoscintigraphy can be performed with a standard gamma camera, preferably with a large field of view. A double headed camera may prove very efficient for time consuming procedures such as (repeated) whole-body scintigraphy as well as for regional single photon emission computed tomography (SPECT) imaging.

For planar imaging quality control (QC) includes tests for uniformity, resolution, and sensitivity. With SPECT QC is even more important and additional tests have to be performed (center of rotation, motion stability). If a double headed gamma camera is applied the QC mentioned above should be extended by the alignment of both detectors. Finally, with total body scanning the image uniformity with camera position is essential since various mechanisms are in effect with this type of scanning.

Other equipment which can be of use are hand-held probes for localizing sites of high uptake during surgery. These devices should be tested for signal/noise ratio and proper shielding during in vitro experiments (spatial resolution).

One should consider lab-facilities for counting of blood and urine samples. HPLC might facilitate adequate analysis of tracer kinetics.

Also autoradiography of histological specimens may be worthwile in the assessment of the heterogeneity of these samples.

Tissue samples obtained during surgery can be measured in well-counters. The countrate linearity should be addressed since some samples consist of a large volume (cysts) with relatively high amounts of activity resulting in deadtime problems. These larger volumes also result in more self-attenuation (^{125}I) and scatter. Standards with a comparable volume should be used for comparison.

Acquisition

Scintigraphy may be considered for qualitative detection of pathological accumulations (sensitivity/specificity) and for the semi-quantitative assessment of the distribution of the antibody within the human body over time (kinetics, dosimetry). The former may emphasize image resolution more than the latter, which in turn largely depends on sufficient statistics and periodic measurement of the total body. If the optimal moment of targeting is known, high resolution images at that moment would facilitate visual detection of tumour localisation. Otherwise, frequent imaging is mandatory, which often conflicts with patient's comfort. The frequency of measuring blood samples (activity, labeling percentage, immunoreactive fraction) should be adequate for curve analysis.

Finally, a special QC for proper acquisition may be the separate counting of a standard with the radionuclide applied with the gamma camera in the same setting as during the acquisition of the patient's data. The countrate obtained this way should result in a constant camera efficiency (cpm/μCi). In this way it is checked whether image acquisition parameters (window setting, collimator) are selected properly. Total body imaging with such a standard placed near the patient may be a time efficient approach.

Data analysis

For the visual detection of pathology the images obtained may not need additional image processing, and the interpretation of subsequent scintigrams is sufficient. Proper alignment of the images obtained at different moments is essential if blood pool subtraction or dosimetry are considered. Either anatomical landmarks or point-source demarkations are very helpful.

In general, however, image processing is applied to obtain information about the distribution of the antibody activity. Especially when absolute amounts in terms of percentage injected dose per gram have to be derived, specific problems are encountered. These relate to correction for background, attenuation, and scatter. Especially the extra exponential increase of both attenuation and scatter with depth in matter (build-up) interferes with the correct determination of the dosimetric parameters. Corrections for these interfering factors are only possible, if at all, to a certain extent by sophisticated approaches (transmission scintigraphy, geometrical mean, subtraction of a »compton acquisition«).

If dosimetry is considered, MIRD or ICRP schemes may not apply to pathological conditions since the related absorbed dose fractions in tumour tissue are not known and the individual organ measures are derived from a »reference man«. Moreover, the MIRD/ICRP calculation programs assume a homogeneous tracer distribution in an organ or individual cell. To calculate the effective dose equivalent for an individual and the dose to the tumour, these programs have to be adjusted for these variables. However, what is the total volume of bone marrow of an individual, often the dose limiting organ in radioimmunotherapy? Immunoscintigraphy gives some information about the kinetics in bone marrow and the contribution of the surroundings but not the amount of marrow, and certainly not the amount and localization of the important stem cells.

Whole body measurements give some dosimetric information if one assumes homogeneous

distribution of the tracer. Additional information may be obtained from CT and MRI images (overlying tissue thickness and organ depth, distances) and blood and urine analysis.

With SPECT additional problems will be encountered. Filtered backprojection results in recognizable images by virtue of the assumption that the emitted photons originate from a source with a homogeneous distribution of attenuating material. Clearly this is not the case. More advanced methods like the iterative reconstructions could resolve this problem. A priori information e. g. collimation properties, attenuation maps (CT) etc. may be implemented within these reconstructions.

Histological examination after surgery gives information about the amount of tumour, necrosis etc., in scintigraphically detected lesions. This information increases the accuracy of the dosimetric calculations.

Although these calculations may give adequate dosimetric information for most tumours, it is not clear whether the dose should be administered in one or in multiple injections at regular intervals. Moreover, the combination of low dose radiation and chemotherapy may be more successful than each approach separately.

Conclusion

Many factors hamper adequate immunoscintigraphy and dosimetric calculations. Some factors are discussed in dedicated issues of the Seminars of Nuclear Medicine.[11, 12]

Despite the problems encountered in this field of Nuclear Medicine, enough encouraging imaging and even therapeutic successes have been obtained to continue this fascinating work.

Maybe in the near future antibodies will be marketed with a specificity for tumour tissue as iodine for the thyroid. This would make all the limitations which are discussed in this paper less important. The hope for the development of such a »magic bullet« makes one a »believer«.

References

1. Tilyou SM. Targeting disease for diagnosis and treatment. Newsline in: *J Nucl Med* 1990; **12:**15A-20A and 30A.
2. Buist MR, Roos JC, Lingen A van, et al. Immunoscintigraphy with 111In labeled OVTL-3: Improved detection of peritoneal metastases in ovarian cancer patients compared to CT, MRI, and ultrasound. (abstract) *Eur J Nucl Med* 1990; **7:**411.
3. Roos JC, Boven E, Lingen A van, et al. Immunoscintigraphy with 131I labeled human IgM monoclonal antibody 16.88 in colon cancer patients: sensitivity, toxicity, kinetics, and the influence of excess unlabeled antibody. (abstract) *Eur J Nucl Med* 1990: **7:**393.
4. Larson SM, Brown JP, Wright PW, et al. Imaging of melanoma with 131I labeled monoclonal antibodies. *J Nucl Med* 1982; **24:**123-9.
5. Goldenberg DM, Goldenberg H, Sharkey RM, et al. Imaging of colorectal carcinoma with radiolabeled antibodies. *Sem Nucl Med* 1989; **4:**262-81.
6. Miraldi F. Monoclonal antibodies and neuroblastoma. *Sem Nucl Med* 1989; **4:**282-94.
7. Granowska M, Britton KE, Shepherd J. The detection of ovarian cancer using 123I monoclonal antibody. *Radiobiol Radiother* 1984; **25:**153-60.
8. Pateisky N, Philipp K, Sevelda P, et al. Radioimmunoscintigraphy using monoclonal antibodies before second-look surgery in patients suffering from ovarian cancer. *Gynecol Obstet Invest* 1987; **24:**212-6.
9. Thor AD, Edgerton SM. Monoclonal antibodies reactive with human breast or ovarian carcinoma: in vivo applications. *Sem Nucl Med* 1989; **4:**295-308.
10. Chatal JF, Saccavini JC, Fumoleau P, et al. Immunoscintigraphy of colon carcinoma. *J Nucl Med* 1984; **25:**307-14.
11. Monoclonal Antibodies I. Freeman LM, Blaufox MD, eds. *Sem Nucl Med* 1989; vol. 3.
12. Monoclonal Antibodies II. Freeman LM, Blaufox MD, eds. *Sem Nucl Med* 1989, vol. 4.
13. Schlom J, Weeks MO. Potential clinical utility of monoclonal antibodies in the management of human carcinoms. In: Devita VT, Hellman S, Rosenberg SA, eds. Philadelphia, USA: Lippincott, 1985, 170-92.
14. Poste G, Doll J, Brown AE, et al. Comparison of the metastatic properties of B16 melanoma clones isolated from cultured cell lines, subcutaneous tumours, and individual lung metastases. *Cancer Res* 1982; **42:**2770-8.
15. Beaney RP. Some biological aspects of soft tissue tumours as studied by PET. In: Heiss WD, Pawlik G, Herholz K, Wienhard K, eds. *Clinical efficacy of positron emission tomography*. Dordrecht, The Netherlands: Martinus Nijhoff Publ, 1987, 361-70.
16. Bomber P, McCready R, Hammersley P. Propranolol hydrochloride enhancement of tumour perfusion and uptake of Ga67 in a mouse sarcoma. *J Nucl Med* 1986; **27:**243-5.

17. Suzuki M, Hori K, Abe I, et al. A new approach to cancer chemotherapy: selective enhancement of tumour blood flow with angiotensin II. *J Nat Cancer Inst* 1981; **67:**663-9.
18. Kohler G, Milstein C. Continuous culture of fused cells secreting antibodies of predefined specificity. *Nature* 1975; **256:**495-7.
19. Carrasquillo JA, Abrams PG, Schroff RW, et al. Effect of antibody dose on the imaging and biodistribution of 111In 9.2.27 antimelanoma monoclonal antibody. *J Nucl Med* 1988; **29:**39-47.
20. Zuckier LS, Rodriques LD, Scharff MD. Immunologic and pharmacologic concepts of monoclonal antibodies. *Sem Nucl Med* 1989; **4:**166-86.

Adv Radiol Oncol 1992, 142–8.

Interlaboratory comparison study on quality performance of nuclear medicine imaging devices

Karanfilski B

Institute of Pathophysiology and Nuclear Medicine, Medical Faculty, University »Kiril and Metodij«, Skopje, Macedonia

Twenty three laboratories participated in the inter-laboratory comparison study for which transmission thyroid, brain, liver and dynamic heart phantoms were used. The study was organized jointly by WHO and IAEA. A total of 70 imaging devices were tested. Overall results from the phantoms revealed a wide range of targets detected. In general, detectability, as expected increased with target diameter and inversely related to target to background ratio.
These studies permit an assessment of the real situation within laboratories. Information feed back can lead to necessary improvement.

Key words: nuclear medicine-instrumentation; quality control

Introduction

Quality control is an integral part of nuclear medicine operations. One of the means to test the quality of imaging performance in an objective manner is inter-laboratory comparison. Such inter-comparison, also known as external quality control, allows a professional organization to monitor the overall performance of facilities. One way to achive this is by distributing unknown samples or test phantoms among the participating nuclear medicine centres. The test results are subsequently collected and analysed in a comparative way. The report, showing the individual results in comparison with those of the group are returned to the participants enabling them to identify aspects of their own performance.

The WHO and IAEA have coordinated a number of such intercomparative surveys in Europe. The first WHO interlaboratory comparison study on quality performance of nuclear medicine imaging devices was published by Volodin et al.[1] Liver and brain phantoms were used in this study. The second study was also undertaken at an international level to evaluate quality performance of the whole imaging process using thyroid and liver phantom.[2]

An unselected group of nuclear medicine laboratories of Yugoslavia participated in these European inter-laboratory comparison studies between 1985 and 1990. The results of these studies organized jointly by WHO and IAEA are presented here.

Materials and methods

A total of twenty three nuclear medicine institutions (Table 1) took part in the inter-laboratory

Correspondence to: Prof. dr. Borislav Karanfilski, Institute of Patophysiology and Nuclear Medicine, Faculty of Medicine, Vodnjanska 17, 91000 Skopje, Macedonia.

UDC: 621.039.555

comparison studies. To carry out the studies CAP (Colege of American pathologists) thyroid and brain phantom, WHO-IAEA liver phantom and WHO dynamic heart phantom (Danbury), were used.

The thyroid phantom simulated a thyroid gland of normal size and shape. It contained eight targets each of which was in the centre od 2 x 2 cm grid of square. There are four »hot« targets and four »cold« targets, all of which varied in size and target to background ratio (Figure 1). Participants were asked to obtain images of the phantom. Image readers were requested to make observed targets in an outline of the thyroid with superimposed grid and indicate on a separate report form the location and size of targets and whether a target was »hot« or »cold«.

The brain phantom was designed to study the influence of target size on detectability and contained 13 targets with a target to background ratio of 1.7:1 and target size in the range 4-20

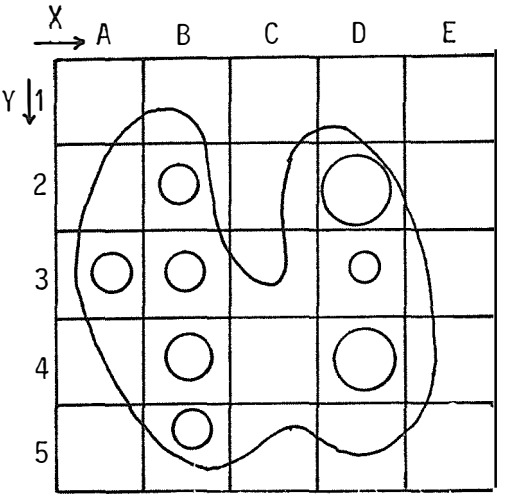

»Cold« targets			»Hot« targets		
Location	Size	Contrast	Location	Size	Contrast
A-3	9 mm	0,9	B-2	9 mm	1,3
B-4	12 mm	0,7	B-3	9 mm	1,1
D-2	16 mm	0,9	B-5	9 mm	1,5
D-4	14 mm	0,8	D-3	7 mm	1,3

Figure 1. Schematic representation of thyroid phantom.

Table 1. Participating laboratories in intercomparison study.

	1985/86 Thyroid phantom	1987/88 Brain phantom	1988/89 Liver phantom	1989/90 Heart phantom
1. Medical center, Zaječar	+	+	+	+
2. Clinical center, Belgrade	+	+	+	+
3. Medical faculty, Novi Sad	+		+	
4. General Hospital, Osijek	+		+	
5. General Hospital, Split	+	+	+	
6. Regional medical center, Banja Luka	+	+	+	
7. Institute of nuclear medicine, Zagreb	+	+	+	+
8. Clinical medical center, Rijeka	+	+	+	+
9. Clinic of nuclear medicine, Ljubljana	+	+		+
10. General hospital, Maribor	+			
11. Medical center, Celje	+			+
12. Medical center, Ankaran	+			
13. Medical center, Šempeter pri Gorici	+			
14. Institute of oncology, Sremska Kamenica				+
15. Regional medical center, Smederevo	+	+	+	
16. Institute od pathophysiology and nuclear medicine, Skopje	+	+	+	+
17. Clinical hospital »M. Stojanović« Zagreb		+	+	
18. Regional medical center, Zadar		+		
19. Institute of nuclear medicine, Sarajevo			+	
20. Clinical medical center, Kragujevac			+	+
21. Institute of nuclear medicine MMA, Belgrade				+
22. Institute of oncology, Belgrade			+	
23. Medical center, Bitola			+	
Total	15	11	15	10

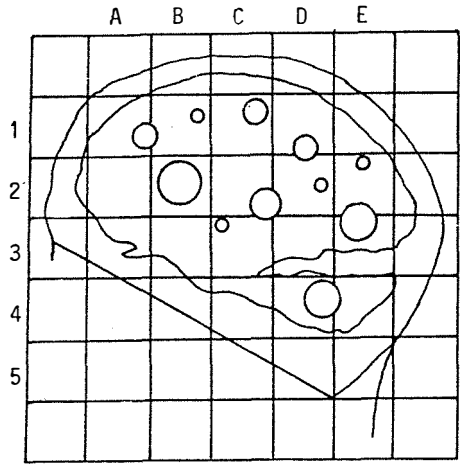

Figure 2. Schematic representation of brain phantom indicating the position of the thirteen targets, with different sizes between 4 and 20 mm (one target each of 20, 16, 14, 11 and 10 mm, and two targets each of 9, 7, 6 and 4 mm). Target to background ratio for all targets is the same (1,7:1).

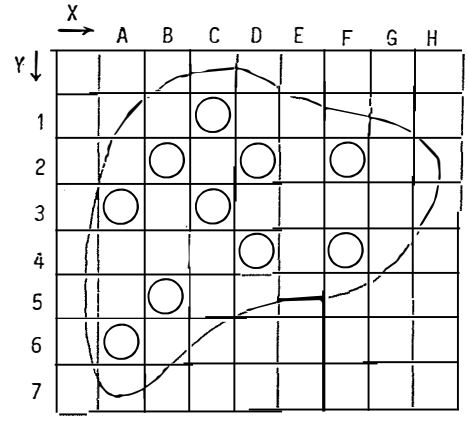

Figure 3. Schematic diagram of the liver phantom indicating the position of the ten targets. The targets had the same diametar, 2 cm, but different target to background ratios between 0,06 and 0,39 for 99mTc. The actual measured values are as follows: A3=0.20, A6=0.39, B2=0.09, B5=0.06, C1=0.26, C3=0.34, D2=0.06, D4=0.23, F2=0.29, F4=0.17.

mm diameter. The area encompassed by the phantom was divided into a grid of squares each measuring 2.5 x 2.5 cm. The phantom comprised 19 such squares and 13 of them contained one target each, or 13 true-positives and 6 squares contained no targets or 6 true-negative (Figure 2).

Figure 3 contains a schematic diagram of the liver phantom indicating the position of ten targets. The targets had the same diameter of 2 cm, but different target to background ratios between 0.06 and 0.39 for 99m Tc. In order to identify these, a 2.5 x 2.5 cm square grid with axes X=A to H and Y=1 to 7 had been superimposed. The liver outline with grid points was only used by image readers to present their individual evaluation. Without prior knowledge of target location they were required to draw in and identify the observed target location. Reported targets were correlated with true targets and assessed in terms of true positives and false positives.

Evaluation of the performance of nuclear cardiology laboratories was done by the use of transmission imaging stimulator named »Danbury Heart« specially designed for this purpose. When properely used, the devices mimic a multigated cardiac study in a 45° left oblique projection. The devices are constructed in such a way that the cyclic movement of two specially shaped metal plates simulates cardiac wall motion and ventricular cavities. The simulated right and left ventricules change in size between end diastole and end systole. The devices are powered by a 60 rpm electric motor which moves the plates in cyclical manner from end diastole to end systole, and back to end diastole at a rate of 60 complete »cardiac cycles« per minute, thus simulating a heart rate of 60 beats per minute. A 1.5 volt battery included in the devices generates a millivolt signal which serves as a R wave trigger. This is accomplished by a small microswitch which is activated only at the end diastole. The simulated R-R interval therefore spans one full cardiac cycle.

The participating laboratories were asked to evaluate »ejection fraction« on the phantom.

Results

The results obtained from each laboratory consisted of an extensive report form requesting information about instrumentation used, imaging protocol adopted, quality control procedures

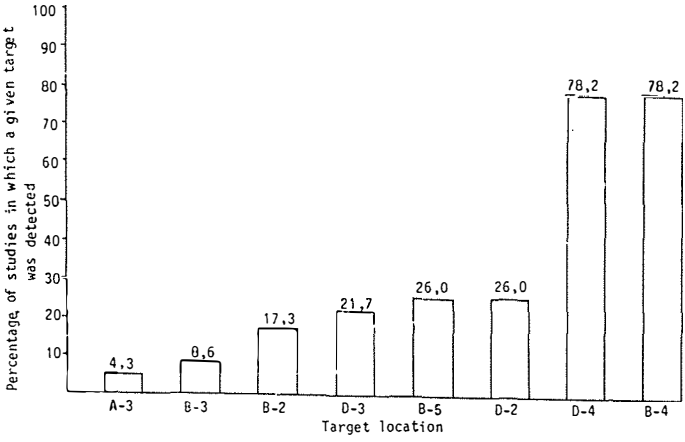

Figure 4. Summary of target detectability in the thyroid phantom.

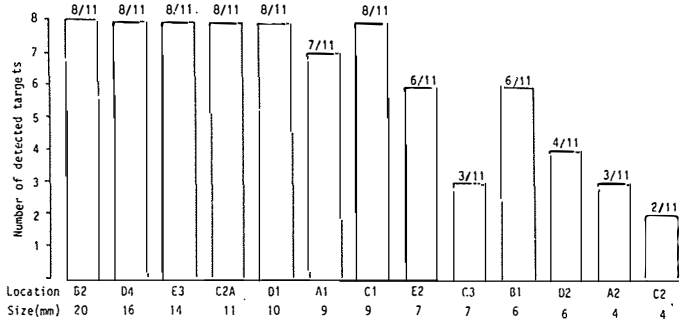

Figure 5. Summary of target detectability in the brain phantom.

routinely performed and observations of the phantom images.

Fifteen laboratories carried out 23 studies with thyroid phantom, where 13 were performed with cameras and 10 with scanners. The scanners were generally older than cameras mostly which were manifactured in the 1970s. Five-inch crystal instruments represented the majority of scanners employed.

Figure 4 depicts the rate of target detection according to target location, size and intrinsic contrast. This shows that the relationship between the three parameters identified with these techniques as determining detectability of targets are such that if two drop below a certain critical level, the target become undetectable regardless of the value of the third parameter.

Eleven laboratories performed 11 studies with brain phantom, by means of gamma cameras. Figure 5 summarizes target detectability results in terms of target diameter for brain phantom. From the histogram in Figure 5 it is clearly demonstrated that detectability, as expected increases with target diameter. In eight of 11 studies targets were correctly identified with diameter between 10 and 20 mm, but detectability significantly decreased for a target diameter 7 mm or smaller.

A total of 15 laboratories participating in the liver study provided results from 18 evaluations,

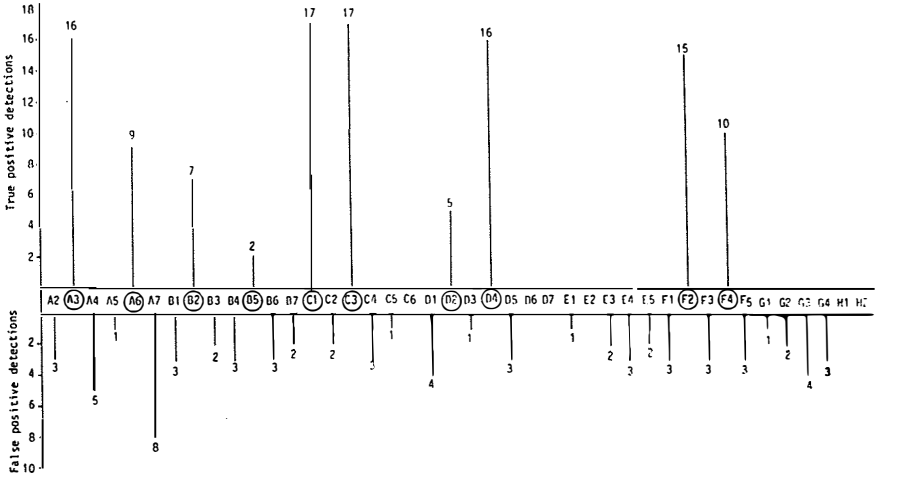

Figure 6. Summary of target detectability in the liver phantom. Total number of true positive and false positive detections. The squares contained targets are marked with circles. Total number of studies 18.

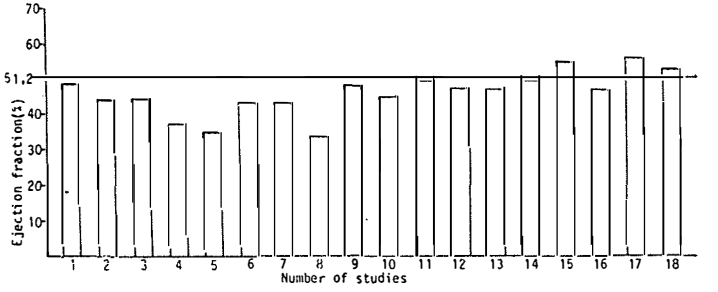

Figure 7. The heart phantom. Results obtained for ejection fraction. Total number of studies 18.

all performed with gamma cameras. Figure 6 depicts the rate of target detection according to target location and intrinsic contrast, presented as true and false positive reports. A decrease in detectability occurred for target to background ratios greater than 0.20:1.

Ten participating laboratories submitted 18 studies performed on cardiac phantom. The mean ejection fraction for the entire group was 45.4 with standard deviation 6.3, coefficient of variation of 13.9% and a range of values from 33 to 55% (Figure 7). The corresponding ejection fraction for our heart phantom according to producer (Medical Designs Inc., Danbury, USA) was 51.2%.

Discussion

The purpose of the intercomparison study on quality performance of nuclear medicine imaging devices is to allow as many as possible interested laboratories to participate within a resonable time period. Participation was voluntary. All laboratories interested were included in the study, without any selection. The study was found to be of great interest to all participants. Effective feed-back between the country coordinator and individual participating laboratories, and presentations of the results received from national nuclear medicine meetings are all an integral part of the organizational mechanism of the

inter-comparison, and play an important role in the improvement of diagnostic possibilities. This inter-laboratory comparison study has provided an opportunity to study the level of total performance in thyroid, brain and liver imaging in most of Yugoslav nuclear medicine institutions. Results of this study do not differ substantially from those obtained with thyroid, brain and liver phantoms un Europe,[1, 2] but there has been relatively low degree of accuracy in target detectability in our studies.

Herrera[3] demonstrated that three of the targets' physical characteristics appeared to play a role in the ability of the participating laboratories to detect the constructed targets. These three parameters were the target diameter, the target-to-background ratio or intrinsic contrast, and the depth of the target within the phantom »body«. Based on these observations, it was concluded that the limit of detectability of low contrast targets using the existing instruments was as follows: minimum size of approximately 10 mm; depth within phantoms less than 7 cm; target to background ratio within 20% of the background radioactivity.

Statistical analysis of the results, including all targets and phantoms used up to 1978, confirmed these findings. Futhermore, the analysis demonstrated that relationship of these factors was such that if two of these parameters were below the critical level, it led to non-visualization of the target regardless of the value of the third one.[4]

When a study of resolution is to be carried out, then the targets must vary in size (brain phantom). If a study of contrast is to be carried out then the lesions must vary in their relative absorbance of the targets to the activity over the background area(liver phantom). In studies of both contrast and resolution, the number of lesions must be included, some varying in absorbance and others in size (thyroid phantom). Whatever parameter is chosen, it is important that some of the targets can be detected by all laboratories and some of the targets by none, so that a complete range of abilities is tested. Since almost every camera or scanner can detect a 2 cm lesion and few can detect a 0.2 cm lession at a distance from the surface of the collimator, the range is fairly obvious. If using the survey to assess the ability to detect contrast changes, the size must be kept constant, as contrast and resolution are not independent variables. In this case the target size must be large enough to be detected by poorly resolving instruments. Then the change in the count density caused by the targets must be varied. Almost no camera system can detect a change of 5 percent but all should certainly detect a change of 50%, or even 25%.

The brain phantom was designed to investigate the relation between target detectability and target size. Figure 5 clearly demonstrates that detectability, as expected, increases with target diameter. With the liver phantom, the variable is target to background ratio and fiugre 6 shows that target detectability is inversely related to target to background ratio.

The number of studies with rectilinear scanner was small with only 10 thyroid studies performed using this type of instrument. Thus, although the number of studies is too small to permit a detailed comparison between camera and scanner, it is of interest to record that for both types of instruments the level at which about 50% of the studies detected a target was similar.

Quality control of nuclear medicine techniques to evaluate left ventricular ejection fraction is hampered by the lack of inexpensive, convenient, commercially avilable phantoms, and the absence of a generally accepted gold standard for the procedures. This reflects the fact that participants of our study were not performing quality control of this procedure in their laboratories. In many instances this technique is implemented on the basis of comparison of results in patients having cardiac cateterization procedures of patients expected to have normal ejection fraction.

The data illustrated in the figure 7 clear reveal considerable variation in the results obtained by participants in this study. This outcome is more striking considering that they were obtained using a simple mechanical device with invariant physical characteristics, uniform background and unhampered by cardiorespiratory movements

and other patient characteristics. In view of this, the data suggest at least equally serious problems in the clinical application of this technique. The causes of the variation demonstrates that, although obviously related to technical procedures, equipment and software employed cannot readily be established by the interlaboratory comparison method. This is a well known limitation of this technique. Also, artificial characteristics of phantom cannot replicate the clinical situation.

References

1. Volodin V, Souchkevitch G, Racoveanu H, Busemann-Sokole E, Deleloye B, Dermentzoglou F, Georgescu G, Herrera N, Jasinski W, Kasatkin Y, Paras P, Mould R, World health organisation interlaboratory comparison study in 12 countries on quality performance of nuclear medicine imaging devices *Eur J Nucl Med* 1985; **10:**193-7.
2. Souchkevitch G, Asikainen M, Bauml A, Bergmann H, Busemann-Sokole E, Carlsson S, Delaloye B, Dermentzoglou F, Herrera N, Jasinski W, Karanfilski B, Mester J, Oppelt A, Perry J, Sketting A, van Herk G, Volodin V, Wegst A, Mould R. The World Health Organization and International Atomic Energy Agency second interlaboratory comparison study in 16 countries on quality performance of nuclear medicine imaging devices. *Eur J Nucl Med* 1988; **3:**495-501.
3. Herrera N. History of the Interlaboratory Comparison Programme. IAEA/WHO Newsletter on Quality Assuarance Programmes in Nuclear Medicine, IAEA, Vienna 1987; **2:**4-6.
4. Herrera N, Hermann GA, Hauser W, Paras P. College of American Pathologists Program Series X Survey Program. In: *Medical Radionuclide Imaging,* 1980, IAEA, Vienna 1981; **2:**177-87.

Chapter IV. CLINICAL ONCOLOGY

Adv Radiol Oncol 1992; 151–66.

Radiosurgery: A review of clinical aspects

Souhami L[1] and Podgoršak EB[2]

[1]Departments of Radiation Oncology and [2]Medical Physics
Montreal General Hospital, McGill University
Montréal, Québec, Canada

Radiosurgery is defined as the delivery, usually in a single session, of a high dose of radiation to a stereotactically localized small intracerebral lesion, while only minimally irradiating adjacent normal brain tissue. The aim of radiosurgery is to destroy or else to affect the function of the targeted volume. Although it was initially developed for the treatment of functional brain disorders, radiosurgery became a major treatment modality for a wide variety of selected malignant or nonmalignant intracranial lesions, including arteriovenous malformations, acoustic neurinomas, meningiomas, and small, solitary metastatic brain disease. Several thousand patients have been treated successfully with radiosurgery to date and the clinical interest in this therapeutic approach is growing rapidly. In this paper an overview of the clinical treatment results on the use of radiosurgery in several intracranial lesions is presented. Proton, charged particles, gamma unit, and linear accelerator-based techniques appear to be equivalent in terms of clinical results. Radiosurgery is an effective and well tolerated procedure for selected patients, it is, however, a complex procedure and should only be performed in institutions with an expert inter-disciplinary team of professionals.

Key words: brain neoplasms–radiotherapy; radiosurgery, stereotactic radiotherapy

Introduction

Stereotactic radiosurgery was developed in Sweden by Leksell more than 30 years ago[1] with the primary intent of treating functional disorders of the brain. Over the years, the technique evolved to become an attractive therapeutic modality for a number of small, selected malignant or non-malignant intracranial lesions. The well proven efficacy of the technique has led to the development of a large number of radiosurgical facilities in major radiotherapy centers. It is estimated that more than 30 gamma units and more than 60 linear accelerator-based radiosurgical facilities are now available worldwide.

The growing interest and enthusiasm for radiosurgery were certainly stimulated by the excellent treatment results reported so far with the various radiosurgical approaches. These results have established radiosurgery as a major treatment modality for selected arterio-venous malformations (AVMs), acoustic neurinomas, meningiomas, pituitary adenomas, and small, solitary metastatic brain tumors.[2-27] To date more than 10 000 patients have been treated by radiosurgery for a wide variety of intracranial lesions. However, in many lesions the number of patients treated is very small and follow-up is inadequate,

Corespondence to: Dr. L. Souhami, Department of Radiation Oncology, Montreal General Hospital, 1650 evenue des Cèdres, Montréal, Québec, CANADA H3G 1A4.

UDC: 616.831-006.6:615.849.5

so that definitive conclusions regarding treatment efficacy cannot be made yet. In this paper, we review the clinical aspects and treatment results on the use of stereotactic radiosurgery in benign and malignant intracranial tumors. The physical aspects of radiosurgery and the various clinically used radiosurgical techniques are discussed in the Chapter VI. Radiophysics.

Clinical considerations in radiosurgery

Radiosurgery is usually performed on an outpatient basis, although some institutions observe patients overnight following the treatment. In our department, a typical patient has the stereotactic frame placed onto the skull under local anesthesia. Frame placement is followed by the required imaging procedures to define the target and by the 3-dimensional treatment planning to define the dose distribution inside and outside the targeted volume. The patient is then set-up on the linear accelerator (linac) and treated with the dynamic rotational technique. Following completion of treatment, the stereotactic frame is immediately removed and the patient is usually discharged on the same day. The entire procedure, from placement to removal of the stereotactic frame, is usually accomplished in 3-4 hours.

Radiosurgery differs from conventional radiotherapy in many important aspects, because in radiosurgery: (i) the need for accurate stereotactic localization of the targeted volume is more pronounced, (ii) the required precision in dose delivery is more stringent, (iii) the volumes treated are generelly smaller, (iv) the dose is usually given in a single session, and (v) the dose fall-off outside the targeted volume has to be very sharp. Table 1 highlights some of the fundamental differences between radiosurgery and conventional radiotherapy.

Table 1. A comparison of parameters of radiosurgery and conventional radiotherapy.

Parameters	Radiosurgery	Conventional radiotherapy
Total dose	20 Gy-50 Gy	50 Gy-70 Gy
N° of treatments	Usually single	Multiple (≈25-35)
Target volume	Small and spherical	Relatively large
Dose fall-off	Extremely important	Important
Patient immobilization	Stereotactic frame	Cast or plastic shells

Table 2. Disorders treated with stereotactic radiosurgery.

Functional disorders	*Benign tumors*
Trigeminal neuralgia	Pituitary adenomas
Parkinson's disease	Acoustic neurinoma
Epilepsy	Meningioma
Psychoneurosis	Craniopharyngioma
Intractable pain	Choroid plexus papilloma
	Fifth nerve neuroma
	Chordoma
	Ganglioneurofibroma
	Hemangioblastoma
Vascular lesions	*Malignant tumors*
Arteriovenous malformations	Astrocytomas
Cavernous angiomas	Pineal tumors
Venous angioma	Metastases
Carotid-cavernous fistula	Lymphoma
Arterial aneurism	Ependymoma
Glomus jugularae	Medulloblastoma
	Oligodendroglioma

In contrast to conventional radiotherapy, in radiosurgery no attempt is made to spare normal cells within the targeted volume by fractionating the total tumor dose. Recently, some centers[18-20] began applying radiosurgical techniques to deliver treatment in multiple fractions to selected intracranial lesions other than AVMs, with the rationale of exploring the well established radiobiological fact that normal tissue generally tolerates fractionated irradiation better than it tolerates single fractions.[21] This could lead to an improved therapeutic ratio. Whether fractionated stereotactic radiotheraphy should be referred to as radiosurgery remains a question of semantics. However, the interest in fractionated schedules using radiosurgical techniques (sometimes referred to as «precision radiotherapy») is rapidly growing and it is likely that an increased number of reports on patients treated with this approach will be available in the near future.

Fractionated stereotactic radiosurgery poses a serious technical problem, since all treatments, not just the first one, must be accomplished with

stereotactic techniques. It would be difficult to submit the staff and the patient through the placement of the stereotactic frame and the target localization procedure for each one of the treatment fractions, therefore reasonable compromises are applied. Fractionation schemes and treatment techniques vary from center to center. Some centers use removable non-invasive stereotactic frames for each treatment.[22] At McGill University the patient is treated with six fractions. The target is localized and the first treatment given with a stereotactic frame. Before the frame is removed after the first treatment, the target center is marked on the patient's skin with tattoos and a head ring or «halo» is affixed onto the patient's skull to help with the immobilization during the subsequent five treatments. The tattoo marks in conjuction with wall and ceiling mounted laser positioning lights are used for proper placement of the target center into the linac isocenter. A patient placed onto the treatment couch with the help of the head ring is shown in Figure 1.

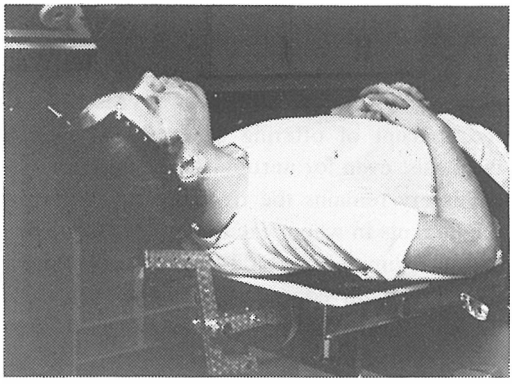

Figure 1. Patient in the treatment position with head ring or »halo« frame in place. The halo frame is used for the fractionated stereotactic radiosurgery and is affixed onto the patient's skull after the first treatment. Laser positioning lights are used for placement of the target center into the linac isocenter.

Since radiosurgery is frequently used to treat histologically benign lesions, sometimes in young patients, it is of utmost importance that the scattered and leakage dose of radiation to sensitive organs be kept low to avoid potential somatic and genetic effects. In both, the gamma unit[23] and linac-based techniques,[24] the surface doses are typically less than 1% of the target dose and the scattered radiation to the thyroid, breast, and gonads amounts to only 0.2%, 0.06%, and 0.02% of the isocenter dose, respectively. The dose to the lens of the eye may be as high as 2.5% of the target dose when the lens is in the path of the beam. The lens dose is thus well below the threshold for cataract formation.

The pathophysiologic mechanisms by which radiosurgery damages AVMs, tumor, and normal brain tissue are not yet entirely clear. Radiation is known to cause injury to small vessels in many different tissues.[25] Several studies support the concept that damage to the microvasculature is the mediator for delayed radiation injury.[26-28] Months or years following radiotherapy, changes such as telangiectasis, asymmetry, and endothelial cell abnormalities are frequently seen in capillaries and sinusoids.[25] Post-radiosurgery endothelial changes have been reported by several authors.[29-31] Small, well demarcated lesions – called »gamma radiolesions« – have been produced by high single doses in patients treated with the gamma unit for functional disorders.[32] In fact, post-mortem studies in 9 patients who had received doses of 180 Gy to 250 Gy revealed necrosis of brain tissues as early as 3 weeks following radiosurgery.[32] Pozza et al.[33] published photomicrographs of biopsy specimens obtained before and 6 months after radiosurgery of low grade brain astrocytoma. These authors were able to demonstrate vascular changes characterized by thickening of vessel walls with occlusion of vessel lumina.

The reported uses of radiosurgery are listed in Table 2, placed into four categories: functional disorders, vascular lesions, benign brain lesions, and malignant brain lesions. Radiosurgery was originally developed to treat functional disorders; the results, however, were inconclusive, so that functional disorders of the brain are now rarely treated by radiosurgery. Among the vascular lesions, AVM is the only disease in which the role of radiosurgery has been well established. There is an increasing interest in the use of

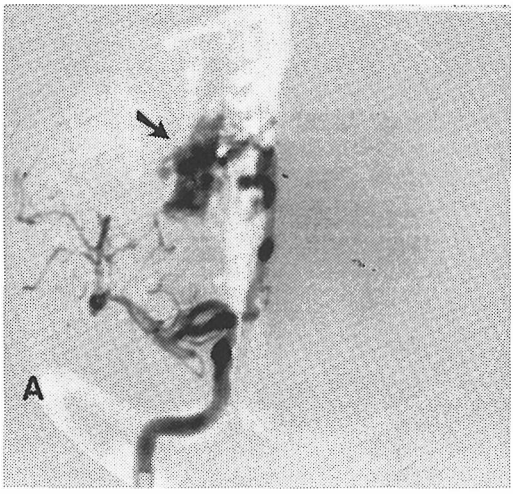

Figure 2. A- An angiogram of a large AVM (arrow) in the right central parietal region before radiosurgery.

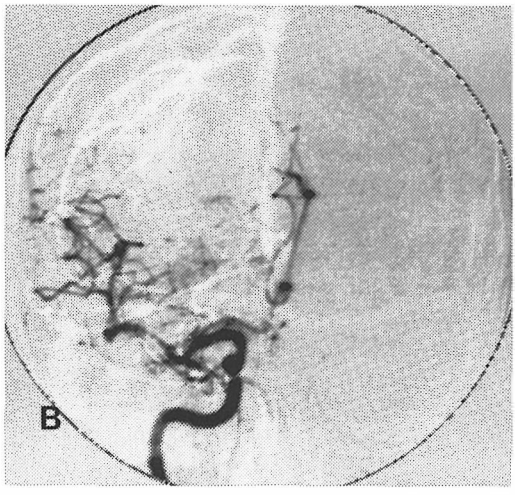

B- Repeat angiography 12 months post-treatment shows complete obliteration of the AVM.

radiosurgery for small, benign or malignant, intracranial tumors, particularly for selected patients with acoustic neurinomas, meningiomas, pituitary adenomas, and isolated metastatic brain disease. For other malignant intracranial diseases, radiosurgery remains to be considered an experimental approach and its therapeutical indication has not been clearly defined yet.

Clinical applications of radiosurgery

Vascular lesions

Arteriovenous malformations (AVMs) are congenital intracranial lesions usually characterized by grossly dilated afferent and efferent vessels, a tangle of pathologic vessels, and rapid circulation time with arteriovenous shunting.[34] Although histologically benign, these intracranial lesions can be the cause of life-threatening hemorrhage and of severe long-term morbidity. The prevalence of AVMs in the general population is estimated to be 0.15%.[35] Spontaneous bleeding is the most common presenting symptom with a mean hemorrhage risk of 2.2% per year.[36] The risk for rebleeding can be as high as 6% in the first year[37] with a mortality rate of 1% per year.[38] In a series of 168 untreated patients with unruptured AVMs followed for a mean period of 8.2 years, Brown et al[36] found a 29% risk of death from AVM rupture with 23% of survivors left with significant long-term morbidity. Thus, the established presence of an AVM should not be regarded as being without potential risks, because the natural history of AVMs supports the concept of offering treatment at time of diagnosis, even for unruptured lesions.

Surgery remains the treatment of choice for the patients in whom excision can be accomplished with limited morbidity. Since the results of treatment with conventionally fractionated radiotherapy were shown to be far from satisfactory[39], radiosurgery became an attractive alternative therapy for lesions in inaccesible regions of the brain or otherwise unsuitable for surgery. The pioneering work in this field is credited to the group at the Karolinska Hospital in Sweden.[40] These investigators have now treated more than 600 patients with AVM and their excellent results using the gamma unit stimulated the development of new radiosurgical techniques based on isocentric linacs.[3-5,41,42] Following radiosurgery, regardless of the radiosurgical technique or apparatus employed, a complete angiographic obliteration of the AVM is expected

to occur in about 35-40% and in 70-80% of the patients at one and two years, respectively. In Figure 2 we show results of treatment in a 56-year old male who underwent linac-based radiosurgery for and AVM in the right central parietal region. The patient was treated with the dynamic radiosurgical technique in our institution and received a dose of 50 Gy in a single session to the periphery of the AVM. Figure 2A shows a pre-treatment angiogram with the AVM clearly displayed, while Figure 2B shows a repeated angiogram one year post-radiosurgery with a complete obliteration of the vascular lesion.

The three factors that play the most important role in the successful complete obliteration of an AVM following radiosurgery are: (i) nidus coverage, (ii) prescribed dose, and (iii) size of the AVM. A partial coverage of the AVM by a dose of less than 20-25 Gy will result in less than optimal obliteration. The entire cluster of pathological vessels corresponding to the nidus must be included in the irradiated target volume. In our institution, the complete obliteration rate at one year post-treatment was 61.5% for those patients in whom the AVM nidus received a minimum dose of 25 Gy. Conversely, when the angiographically evident nidus received less than 25 Gy, not a single patient achieved a complete obliteration.[3] Similar experience has been reported by Steiner[43] in patients treated with a gamma unit and by Levy et al[44] in patients treated with helium ions. As for the size of the AVM, several authors[4,5,45] have found that complete obliteration is less likely to occur in larger AVMs, even when the AVM nidus is properly covered by an adequate dose.

The exact pathophysiological mechanisms of the effect of radiosurgical irradiation in the blood vessels have not been fully defined yet. In patients who underwent proton therapy, histopathological changes included occlusion of blood vessel lumina and a marked thickening of blood vessel walls.[46] Colombo et al.[4] using linac-based radiosurgery have reported similar changes. Other reported changes are an associated vascular thrombosis[2,4] and marked gliosis.[47]

In general, radiosurgery provides an effective and well tolerated treatment for nonsurgical patients with AVMs. However, several issues remain unanswered in the management of these vascular lesions and further studies are necessary. Unsolved problems include the optimal dose/volume relationship, the value of embolization prior to radiosurgery in large AVMs in an attempt to decrease the AVM size and, perhaps, optimize its shape, the normal brain and blood vessel tolerance to radiosurgery, and the potential value of fractionated stereotactic radiosurgery for large AVM lesions. Of fundamental importance is, of course, the proper definition of an angiographic AVM obliteration, which should only be considered complete if the post-treatment angiographic study shows the complete absence of AV shunting, the absence of abnormal vessels in the nidus region, and a normal circulation time. Since protection against hemorrhage is only provided when a complete AVM obliteration is achieved, it is imperative that, before radiosurgery, a detailed assessment of the vascular lesion is performed so as to define the AVM nidus and properly cover it with an adequate dose.

Cavernous angiomas consist of thin-walled sinusoidal vessels of varying sizes with no arteries, veins, or neural tissue within the anomaly.[48] These lesions are angiographically occult vascular malformations and comprise 5 to 13% of central nervous system vascular abnormalities. Cavernous angiomas are increasingly diagnosed with modern imaging techniques, such as CT scan and MRI. Little information is available in the literature on these lesions and their natural history remains obscure. However, Simard et al.[49] reviewed the clinical features of 138 symptomatic, histologically verified cases, and found that at the time of diagnosis, one third of the patients had increased seizure activity, one third had clinical evidence of intracerebral hemorrhage, and one third had mass lesions.

Thus, the role of radiosurgery in the management of angiographically occult vascular malformations has to be defined yet. Levy et al.[8] studied 35 patients treated at the Lawrence Berkeley Laboratory with the stereotactic helium-ion Bragg peak radiosurgery. All patients

were symptomatic and had evidence of hemorrhage prior to treatment. Of 31 patients followed from 12 to 72 months, 24 patients have had normal, stable, or improved neurological status, five have worsened, and two have died. Seven of these 31 patients have experienced recurrent hemorrhage. Kondziolka et al.[50] have reported the preliminary experience of the Pittsburgh group in 24 patients treated with a gamma unit. All patients had sustained two or more hemorrhages. In 19 patients clinical improvement or stabilization was observed, in five patients temporary worsening of the neurological deficits was seen, and in one patient intracerebral bleeding reoccurred. At McGill University, we have treated 10 patients with angiographically occult cavernous angiomas. Radiological reduction in the size of the lesion was seen in two patients only, although symptomatic improvement was observed in six patients. Two of the 10 patients have rebled. The initial results are somewhat disappointing and further clinical experience will be required to properly establish the value of radiosurgery in these occult vascular lesions.

Benign tumors

Acoustic neurinoma, also known as Schwannoma or neurofibroma, is a relatively rare, histologically benign tumor involving the eighth cranial nerve. It is slow-growing, usually unilateral, and most commonly observed after the age of 50. Because of its location, acoustic neurinoma may cause a considerable morbidity, including loss of hearing, disturbed sense of balance, tinnitus, facial pain and weakness, and hydrocephalus.

Surgery has been the standard treatment for medically operable patients with unilateral lesions. Radiotherapy is reserved for patients with residual, recurrent, or inoperable tumors. However, even in experienced hands combined with modern microsurgical techniques, the surgical removal of acoustic neurinomas usually is not accomplished without significant morbidity with the vast majority of the patients developing complete hearing loss in the operated ear and permanent facial weakness.[51] Thus, it is not surprising that radiosurgery with its lower morbidity became an attractive alternative to microsurgery in selected patients.

Norén et al.[10] reported their experience on 110 patients treated with the gamma unit at the Karolinska Hospital between 1969 and 1984. At a mean follow-up time of 4 years, decrease of tumor size or no change was found in 86% of the cases (90% in unilateral tumors and 67% in bilateral). Facial weakness, usually of mild degree, was experienced by 15% of the treated patients but was transitory in all of them. In 64 patients, who were evaluated prior to radiosurgery, preserved hearing was observed in 56% of them at 1 year, 54% at 2 years, and in 28% at 6 years. Based on their experience, the authors recommend a dose of 20 Gy given in a single session to the periphery of the lesion.

Flickinger et al.[11] from the University of Pittsburgh reported on 85 patients treated between 1987 and 1990 with tumor doses ranging between 14 to 50 Gy. At a median follow-up time of 9 months, the tumors decreased in size in 41% of the patients and remained unchanged in 56% of them. In 45 patients (63%), a loss of contrast enhancement in the center of the tumor was detected on follow-up imaging studies, consistent with tumor necrosis. Patients in this series underwent detailed hearing and facial strength pretreatment evaluations. For the patients who had useful hearing prior to radiosurgery, the actuarial rate of useful hearing preservation at 2 years was 46%. New incomplete neuropathies of the trigeminal or facial nerves were observed in 26% and 30% of the patients, respectively. Both the trigeminal and facial nerve functions recovered fully after a median time of 8 to 11 months. Flickinger et al.[11] could not find any relationship between the treatment dose and the risks of decreased hearing, or trigeminal and facial nerve disfunction. However, there appeared to be a relationship between tumor size and complication rate, with no patient with tumor diameter less than 10 mm developing any complication.

Although surgery remains the standard treatment for most of the acoustic neurinoma patients, radiosurgery is emerging as a valid therapeutic option for selected lesions. Hearing preservation remains an important issue and needs to be addressed in future studies. The role of fractionated stereotactic radiosurgery in hearing preservation is presently under evaluation in our center.

Meningiomas are tumors that arise from arachnoidal cells in the meninges. The large majority are histologically benign and surgery is the mainstay of treatment. Radiotherapy has been shown to improve local control in subtotally resected or recurrent disease.[52]

Radiosurgery has been used to treat small unresectable or recurrent lesions. Engenhart et al.[12] from Heidelberg treated 17 patients with intracranial meningiomas with single doses ranging from 10 to 50 Gy. At a median follow-up time of 40 months, 13 patients had no evidence of tumor progression. Late severe side effects were observed in 5 patients, including one patient with a relatively large tumor (73.6 cm^3) who received a maximum target dose of 35 Gy and died 8 months post-treatment from herniation attributable to a radiation-induced tumor necrosis. Based on their experience, the Heidelberg group recommends radiosurgery only for target volumes smaller than 40 cm^3 and limits the prescribed dose to 30 Gy.

Kondziolka et al.[13] have recently reported on the University of Pittsburgh experience with 50 selected patients with meningiomas treated with a gamma unit. Patient selection included tumors at least 5 mm away from the optic chiasm and not larger than 35 mm in diameter. Radiosurgery was the primary treatment in 16 patients only. The other 34 patients received radiosurgery after failing either surgical resection alone or surgery plus conventional radiotherapy. The dose prescribed at the tumor margin ranged from 10 to 25 Gy. Treatments were well tolerated but three patients developed new neurological deficits, which were temporary in all of them. The actuarial 2-year tumor growth control rate was 96%.

Radiosurgery appears to be an effective treatment modality in selected patients with intracranial meningiomas and the results to date are encouraging. Further experience will establish the optimal doses, treatment schedules, and required target volumes for these tumors.

Pituitary adenomas. Tumors in the pituitary region comprise 6 to 10% of all intracranial neoplasms. Conventional radiotherapy is reserved for incompletely resected tumors and will control tumor growth in about 90-95% of the patients. Radiosurgery with proton beams has been used in a large number of patients with endocrine syndromes of pituitary origin, such as acromegaly.[8,14] Cushing's disease,[14,20] Nelson's syndrome[14], and prolactinomas[14] either as primary non-invasive treatment of for residual/recurrent disease following surgery. Since 1954, over 800 patients have received stereotactic helium–ion pituitary radiosurgery at Lawrence Berkeley Laboratory in California with the goal to destroy or inhibit the growth of the pituitary tumor and yet preserve some glandular secreting capacity.[14]Acromegaly patients were treated with doses of 30 to 50 Gy, most often delivered in four fractions over 5 days. Most of the patients experienced a marked clinical and biochemical improvement within the first year. Cushing's disease in 80 patients has also been treated successfully by the same investigators. Doses to the pituitary gland varied from 50 to 150 Gy usually delivered in three or four daily fractions. Serum prolactin levels were reduced in 95% of the patients with prolactin-secreting tumors followed for at least 1 year post helium-ion radiosurgery. Complications have been infrequent and usually restricted to variable degrees of hypopituitarism.

Kjelberg et al.[14] from Boston reported on 22 patients treated with proton beam radiosurgery for acromegaly. Tumor doses varied from 60 to 140 Gy. Fourteen patients were followed for 2 to 36 months with a decrease in the size of hands, feet, or face in nine of them. A marked fall in the levels of human growth hormone was obser-

ved in eight patients. Transient diplopia, headache, and one case of anterior pituitary insufficiency were the complications seen.

The experience with photon radiosurgery in these tumors is more restricted. At the Karolinska Hospital in Stockholm, 61 patients underwent gamma unit radiosurgery for Cushing's disease.[53] Eight of them were children or adolescents. Dose prescription was not standardized and ranged from 70 to 100 Gy. Of 29 adult patients with long-term follow-up (range: 3 to 9 years), 76% achieved a clinical remission. All responding patients remained without evidence of recurrence and no local complications were observed in this population.

Photon or heavy charged particle radiosurgery appears to be an effective and a relatively safe treatment method for pituitary adenomas and may represent a valid therapeutic alternative in selected patients, particularly for those with small recurrent disease following surgery or for those deemed inoperable. Further studies, however, are still needed to clearly define the optimal doses to be used.

Craniopharyngioma originates from the remnants of Rathke's pouch in the region of the pituitary stalk, occuring primarily in children. It can cause symptoms by compressing the optic chiasm or tracts, by depressing pituitary or hypothalamic functions, by increasing the intracranial pressure, or by all of these. Usually craniopharyngioma is managed surgically and conventional external beam irradiation is reserved for incompletely resected lesions or inoperable patients.

The number of patients with craniopharyngioma treated to date with radiosurgery is small. This might be due to the reluctance of the physicians in trying a new treatment modality when the conventionally-used therapy offers satisfactory results. Steiner referred to 36 patients with craniopharyngioma treated by gamma unit radiosuergery but reported no clinical results.[9] Backlund et al.[54] reported on eight patients treated at the Karolinska Hospital. In four patients radiosurgery was the primary treatment and in the other four it was combined with intracystic yttrium-90. In the combined approach, radiosurgery was given to the solid part of the tumor following shrinkage of the cystic component by the radionuclide. Radiosurgical doses varied from 20 Gy to 50 Gy with the periphery of the tumor receiving no more than 10 Gy.[9] At a minimum follow-up time of 10 years, seven patients are alive and well and one patient died from intercurrent disease. Of importance is the fact that no long-term complications were seen, particularly in the optic pathway. Great caution should be exercised in the treatment of tumors near the optic chiasm, because of potential concerns with injury of this structure with radiosurgery. Backlund[55] recommends limiting the dose to the optic nerve to 10 Gy, whereas the group from Pittsrubgh[13] limits its dose to 8 Gy.

At McGill University we have started a program using fractionated stereotactic radiotherapy for craniopharyngiomas and have treated three patients so far. A dose of 36 Gy in six fractions, every other day for 2 weeks, is given to the periphery of the lesion. All patients are doing well and no undue side effects have been observed. Although the preliminary results on craniopharyngiomas are very encouraging, a larger number of patients and further clinical data are needed to determine precisely the role of radiosurgery in the management of this disease.

Malignant tumors

Metastatic brain tumors affect 20% to 30% of the patients with systemic cancer.[56] The recommended treatment for single surgically accessible lesions is surgery followed by whole brain irradiation.[57] Radiosurgery is now being used as an alternative primary treatment modality to the combination of surgery and radiotherapy in patients harboring solitary cerebral metastatic tumors as well as for those patients who have failed previous whole brain irradiation with or without surgery.

Sturm et al.[15] from Heidelberg reported on the use of radiosurgery in 12 previously untreated patients with single brain metastases. The dose varied from 20 Gy to 30 Gy prescribed to the 80% isodose surface, which usually covered the lesion in its entirety. Of seven patients with adequate follow-up, all had marked clinical and radiological improvement. Of interest is the fact that this improvement was observed within a few days from treatment, even though many patients had primary tumors considered »radioresistant» (melanoma, sarcomas, hydronephroma). The Heidelberg group subsequently updated their results on 40 radiosurgically treated patients[58] and reported similar findings. One patient in this series died from an inferior herniation, probably caused by an increase in pre-existing cerebral edema. This patient was treated for a 42 mm lesion and received 25 Gy to the 50% isodose contour.

Loeffler et al.[16] from Boston used radiosurgery in 18 patients with solitary brain lesions who had failed previous conventional external beam irradiation. Single doses between 9 Gy to 25 Gy were delivered to tumors smaller than 27 cm^3. With a median follow-up of 9 months, all tumors have been controlled in the treatment field but two patients failed adjacently to the treated volume. A dramatic and rapid radiographic response was observed in patients with adenocarcinoma but, unlike the results of the Heidelberg group, slight reduction and stabilization occurred in those patients with melanoma, renal cell carcinoma, and sarcoma. Complications were limited and transient.

In Pittsburgh, 24 patients were treated with the gamma unit between May 1988 and March 1990. Primary tumors included melanoma, renal cell carcinoma, and lung cancer. Tumor size was limited to less than 30 mm in diameter. A large majority of the patients received radiosurgery as a «boost» (16 Gy to 20 Gy to tumor margins) to whole brain irradiation (30 Gy to 40 Gy). Only one patient had tumor progression of a radiosurgically treated lesion. The authors have concluded that radiosurgery appears to be as effective as surgery in the control of solitary brain metastases and may eliminate the need for resection and its associated surgical and anaesthetic risks.

At McGill University, Caron et al.[17] studied nine previously irradiated patients who underwent linac-based (dynamic rotation) radiosurgery at time of recurrence. The patients were treated with a single dose of 20 Gy, delivered to spherical target volumes ranging in diameters from 10 mm to 30 mm. Doses were prescribed to the 90% isodose surface, which corresponded to the periphery of the lesion as seen on the imaging studies. Criteria to enter a patient in this program included failure to previous therapy, lesions smaller than 30 mm, and no evidence of disseminated disease. All tumors showed a favorable response, with four patients achieving a complete radiological disappearance of the tumor. Clinical neurological improvement was experienced by the majority of the patients and, similarly to other reports, occurred few days after radiosurgery. No complications attributable to the radiosurgical procedure were seen. Figure 3 illustrates the result of radiosurgary in a patient with metastatic brain disease who received a dose of 20 Gy in a single session. A complete disappearance of the tumor was seen 8 weeks post-treatment.

Stereotactic radiosurgery is assuming an important and exciting role in the palliative management of inoperable and recurrent solitary brain metastases, because of its non-invasive nature, relative safety, the excellent results obtained so far and the additional advantage that treatment is completed in one day instead of several weeks. Whether radiosurgery will effectively replace surgical resection as a therapeutic option in operable patients remains to be determined. Ongoing randomized studies are presently addressing this question.

Low grade astrocytomas. Several centers have reported on the use of radiosurgery in the management of low and high grade astrocytomas.[18,33] However, the numbers of patients treated so far are small and the follow-up is short, making interpretation of results somewhat difficult.

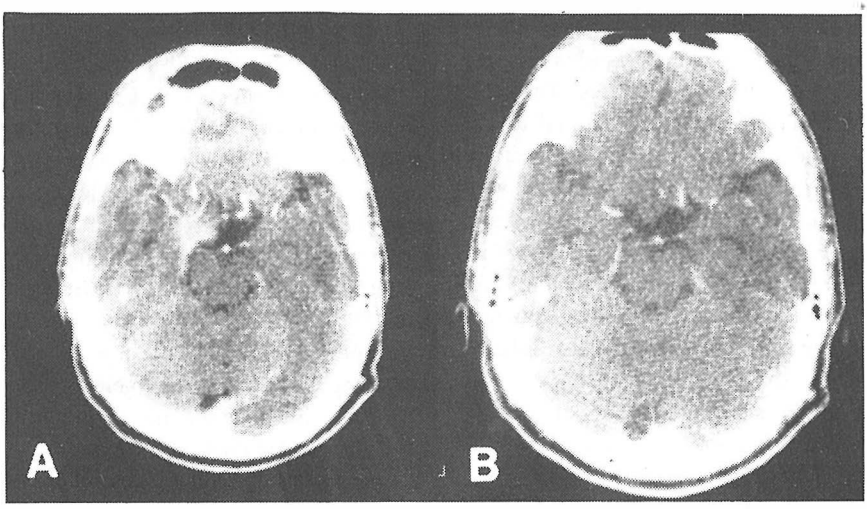

Figure 3. A- CT scan shows a metastatic lesion in the cavernous sinus. The primary lesion was an adenoid cystic carcinoma of the tongue for which the patient had received radical radiotherapy. The base of the skull was included in the irradiation field. The metastatic lesion was treated radiosurgically and a single dose of 20 Gy was given to the 90% isodose surface, which covered the periphery of the tumor. B- A follow-up CT scan 8 weeks after radiosurgery shows complete disappearance of the metastatic lesion.

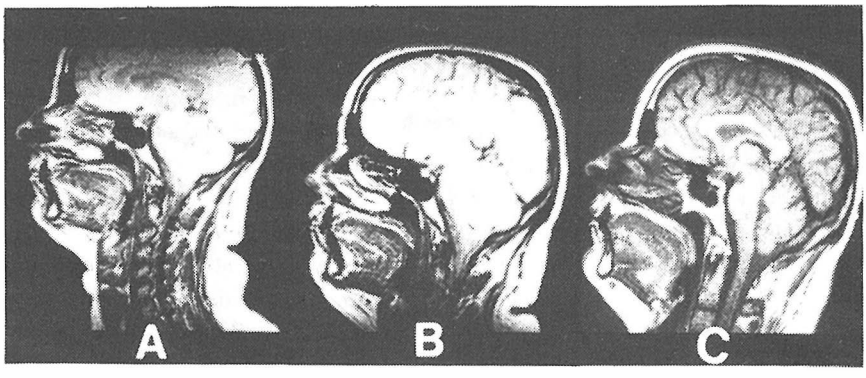

Figure 4. A- Ct scan of a 31-year old female shows a 20 mm tumor in the mid-brain. She presented with multiple cranial nerve involvement, right hemiparesis, and severe right-sided incoordination. A stereotactic biopsy of the lesion revelead a grade II astrocytoma. She underwent fractionated stereotactic radiosurgery and received a dose of 42 Gy to the 90% isodose surface, in six fractions, given on alternate days, with a 20 mm collimator. B- CT scan 3 months post-fractionated radiosurgery shows a partial tumor response. C- CT scan 15 months post-treatment shows complete tumor disappearance. Patient remains disease – and symptom-free 4 years post-therapy.

Pozza et al.[33] from Vicenza treated 14 patients with low grade astrocytomas with doses ranging from 10 Gy to 25 Gy delivered in one or two fractions. Only inoperable tumors with spherical shapes smaller than 30 mm in diameter were entered into the study. Patients' follow-up varied from 11 to 48 months. Of the 14 patients treated, 11 (78.5%) had a marked shrinkage of tumor size, as assessed by post-treatment CT scans. Treatments were well tolerated, although three patients developed a temporary neurologic deterioration. No late toxicity was reported. Of

interest, eight of the patients had increasing edema at 2 to 12 months following treatment and in five of them a contrast enhancing ring appeared on follow-up CT scans. Tumor shrinkage was always preceded by disappearance of the contrast enhanced ring.

At McGill University, we began in 1987[18] a program of fractionated stereotactic radiosurgery for patients with low grade astrocytomas in eloquent areas of the brain. The rationale for such a program was to take advantage of the therapeutic ratio provided by the fractionation, that is, increasing the probability of tumor control without producing clinically significant normal tissue injury. Only small, inoperable, well-circumscribed lesions involving sensitive brain structures in symptomatic patients were considered for fractionated radiosurgery. All patients were fully assessed by the radiosurgical team prior to therapy and underwent complete imaging evaluation. From May 1987 to August 1989, eight patients with tumor diameters varying from 17 to 25 mm entered our program. Tumor dose was 42 Gy prescribed at the periphery of the lesion (90% isodose surface) and given on alternate days during a 2 week period (fraction size = 7 Gy). At a median follow-up of 28 months, seven patients presented a marked clinical neurological improvement, which was usually observed within the first 2 months post-treatment. Radiological tumor disappearance or reduction was observed in five patients (an example is given in Figure 4), with two other patients presenting no changes in the follow-up imaging studies, and another patient showing evidence of tumor recurrence. No acute complications were observed. A late complication, characterized by vasogenic edema around the tumor area, was experienced by one patient 10 months postradiosurgery. She was placed on steroid therapy and gradually improved. A repeat CT scan showed clearing of the edema and a partial tumor response (Figure 5). She is now 40 months post treatment and remains symptom-free. Fractionated sterotactic radiosurgery is a feasible technique and may prove useful for selected patients with intracranial tumors. The preliminary results are encouraging and our study is continuing. Only a larger number of patients with a longer follow-up will allow us to definitovely establish the role of fractionated stereotactic radiosurgery in this group of patients. Other centers have also started evaluating linac-based[19] or proton[20] radiosurgery with several fractions.

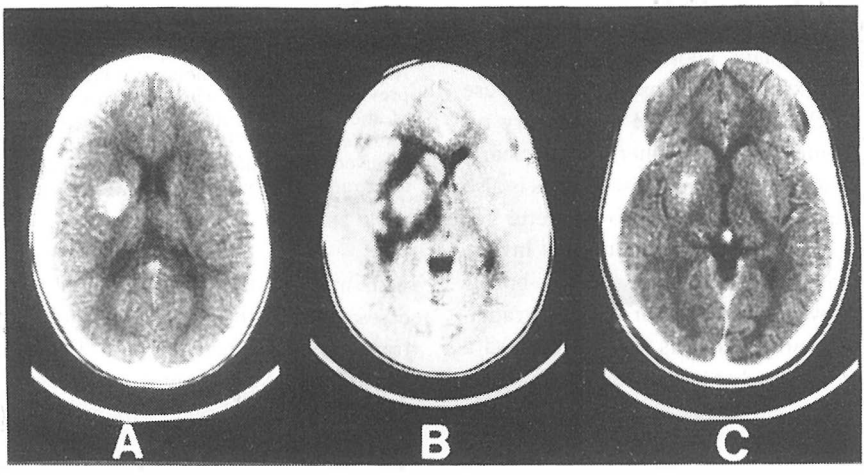

Figure 5. A- CT scan of an 8-year old female shows a 18 mm grade I astrocytoma of the lenticular nucleus. Patient was treated with fractionated stereotactic radiosurgery and received a dose of 37.8 Gy to the 90% isodose surface in six fractions with a 15 mm diameter collimator. B- Ten months after treatment, CT scan shows hypodense area consistent with vasogenic edema. C- At 26 months post-radiosurgery, CT scan shows disappearance of edema and a marked tumor size reduction. The patient has minimal neurological deficit.

High grade astrocytomas. The role of radiosurgery in the management of malignant astrocytomas is not yet clear. However, since recent information suggests that interstitial brain implants improve local control in patients with malignant astrocytomas[60], several centers are now prospectively evaluating the effectiveness of radiosurgery as an adjunct (»boost«) to external beam irradiation in patients with this pathology. The initial results of these studies appear to be similar to those obtained with brachytherapy. At McGill University, we began a prospective phase I/II trial using radiosurgery before accelerated standard external beam irradiation for patients with malignant gliomas in an attempt to improve our previous results of accelerated fractionation.[61] Unlike the other centers, we are using a single session radiosurgery (20 Gy) before the accelerated brain irradiation (60 Gy/4 weeks) with the rationale of trying to overcome accelerated tumor cell repopulation, which is not a specific response but rather results from the killing of tumor cells. Accelerated regrowth of surviving clonogens, triggered by the surgical procedure, would lessen the effect of external beam irradiation leading to a decreased local tumor control.

Until further reports on its efficacy and toxicity are available, stereotactic radiosurgery in patients with malignant gliomas should still be considered an experimental approach and its use restricted to clinical trials. The preliminary results are encouraging but further data is clearly needed. The use of fractionated schedules is also being investigated and may prove useful for deep-seated, well circumscribed tumors involving sensitive brain structures, as a »boost« therapy following standard large-field irradiation, or for recurrent tumors having received a full dose conventional external beam radiotherapy.

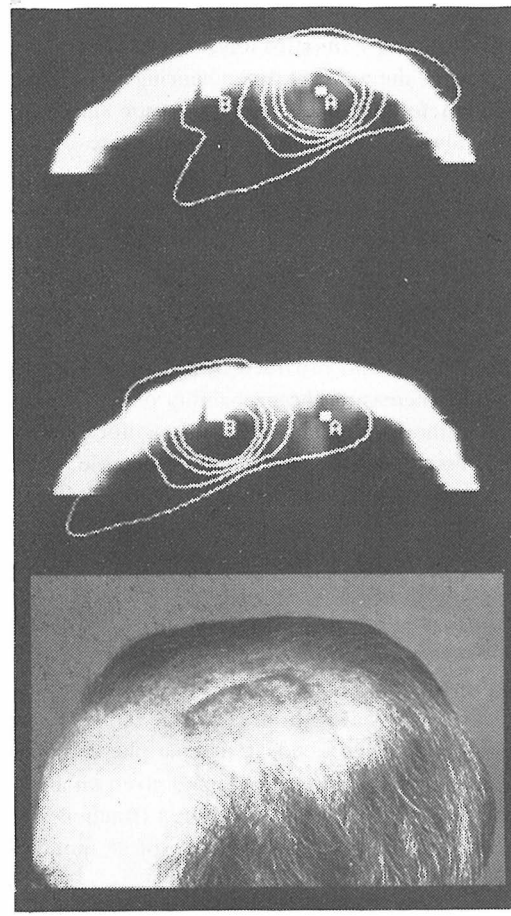

Figure 6. Patient underwent radiosurgical treatment for two dural-based metastatic brain lesions. He had previously received whole brain irradiation. Because of the size of his metastatic tumors, two isocenters (labelled A and B in the figure) were used. He received a dose of 20 Gy to each isocenter. Six weeks after radiosurgery a localized area of alopecia is seen.

Miscellaneous other conditions

Various other, rare intracranial lesions have been treated by stereotactic radiosurgery but thus far the numbers of patients are too small, with most of the centers reporting just a few cases. Tumors that deserve further therapeutical trials include pineal tumors, chordomas of the base of the skull, glomus jugularae, hemangioblastomas, and chondrosarcomas involving the base of the skull.

Clinical complications of radiosurgery

Since radiosurgery is now increasingly used to treat a wide variety of benign and malignant

intracranial lesions, the possible serious acute and late side effects have to be carefully documented and their incidence and consequences properly reported.

Significant *acute side effects* are uncommon. Some degree of discomfort is experienced by most of the patients during frame placement, although usually of mild intensity. For patients undergoing fractionated treatment, skin infection can be observed around the screw insertion sites. Headache, fever, and increased risk of seizure has been reported by Kjellberg et al.[29] as occuring in few patients in the 24 hours following proton radiosurgery. Acute onset of nausea and vomiting has been associated to radiosurgical treatment delivered to the area postrema[62]. Alopecia is uncommon as surface doses are typically less than 1% of the target dose. However, epilation may occur when treatment is delivered to lesions near the inner table of the skull (see example in Figure 6). Trigeminal neuropathy and facial neuropathy developed in 18% and 15%, respectively, of patients treated for acoustic neurinomas with the gamma unit at the Karolinska Hospital[10]. The incidence of such complications was higher in the Pittsburgh series, with trigeminal and facial neuropathies occuring in 37% and 33% of the patients, respectively[11]. The median time of onset of facial and trigeminal neuropathies was similar (≈ 6 months). In both series, these complications were transient and began to improve from one to 17 months after onset.

Late side effects of radiosurgery, characterized by symptomatic, reversible white matter vasogenic edema or radiation necrosis, occur in 2% to 6% of the patients.[3-5,7-9] However, the real incidence of radiological changes following radiosurgery has not been established as a proper prospective analysis, with serial imaging studies, has not been performed. Flickinger et al.[63] reviewed MRI or CT scans in 72 patients with intracranial AVMs treated with a gamma unit and found imaging changes in 31% of patients. These changes caused no symptoms in a majority of the patients (55%) and were usually temporary. In the Flickinger et al.[63] series, treatment volume was the only significant predictive factor for the development of post-radiosurgery imaging changes.

We have recently reviewed our experience with the first 112 patients (116 lesions) treated with the dynamic stereotactic radiosurgical technique at McGill University. Of the treated lesions, 59 were AVM, 13 brain metastases, 11 gliomas, 11 cavernous angiomas, and 22 a variety of other malignant or non-malignant diseases. Treatment was delivered in a single session (median dose = 38.25 Gy) to 86 lesions and was fractionated in the remaining 30 lesions (median dose = 42 Gy). Acute and late complications attributable to radiosurgery developed in 6.3% of the patients. Acute complications were observed in 2 patients and were characterized by transient nausea and homonymous hemianopsia in one patient treated for an AVM, and by transient facial neuropathy in another patient treated for an acoustic neurinoma. Late complications occurred in 5 patients who developed symptomatic white matter edema at 5, 7, 10, 12, and 21 months, respectively, following radiosurgery. Full recovery of the neurologic deficits was seen in 3 patients only. Figure 5 shows serial CT scans in a 8-year old patient with a low grade astrocytoma of the lenticular nucleus who underwent fractionated stereotactic radiosurgery in our center. She received a dose of 37.8 Gy in six fractions with a 15 mm collimator. Symptomatic white matter edema was observed 10 months following treatment. She responded well to tapering doses of oral dexamenthasone.

We could not establish any relationship between complications and prescribed dose, fractionation, collimator diameter, previous irradiation, or anatomical region of the lesion that was treated. However, this finding must be interpreted with caution because of the small number of patients who developed complications.

Although it appears that radiosurgery is a relatively safe procedure and well tolerated by the majority of the patients, it is not without risk. Further clinical experience will be required to establish the real tolerance of various brain

structures to radiosurgery and to define the optimal dose prescription related to volume, previous irradiation, numbers of isocenters, fractionation, and lesion type and location.

Conclusions

Radiosurgery is an exciting modern irradiation modality used in conjunction with stereotaxy in the treatment of certain brain diseases. It already has an established role in the management of inoperable intracranial AVMs. Two years post-treatment complete angiographic obliteration rates of about 70-80% have been reported by several institutions, regardless of the radiosurgical technique or apparatus used. In selected malignant or non-malignant intracranial tumors, such as acoustic neurinomas, meningiomas, pituitary adenomas, and solitary metastatic brain disease, radiosurgery is becoming a major treatment modality. The results of treatment of many other intracranial lesions are much less clear and further clinical experience is warranted.

Although radiosurgery was developed more than 30 years ago and a large number of patients have been treated, several unsolved questions remain to be answered and additional clinical and experimental data are still required, particularly those involving the optimal »safe« dose to be delivered to lesions in sensitive areas of the brain. Presently, interpretation of clinical results is still difficult because of the lack of standardized reporting methods. Radiosurgery usually is tolerated well and appears to be a relatively safe therapeutic approach, but certainly is not without risks. The determination of optimal treatment parameters involves a conjoint effort among neurosurgeons, radiation oncologists, neuroradiologists, and medical physicists and only a multidisciplinary team approach will lead to improved cure rates, while minimizing the potential adverse side effects.

Future directions in radiosurgery will likely include additional studies in fractionated radiosurgical schedules for malignant primary tumors involving sensitive brain structures, in combining radiosurgery with conventional external beam irradiation, radiosensitizers, or chemotherapy for intracranial tumors known to respond poorly to conventional therapies, and in the development of conformal 3-dimensional planning so that non-spherical intracerebral lesions may be treated while sparing the surrounding normal brain tissue.

References

1. Leksell L. The stereotaxis method and radiosurgery of the brain. *Acta Chir Scand* 1951; **102:** 102-316.
2. Souhami L, Olivier A, Podgorsak EB et al. Dynamic stereotactic radiosurgery in arteriovenous malformation. Preliminary treatment results. *Cancer* 1990; **66:** 15-20.
3. Souhami L, Olivier A, Podgorsak EB, et al. Radiosurgery of cerebral arteriovenous malformations with the dynamic stereotactic irradiation. *Int J Radiat Oncol Biol Phys* 1990; **19:** 775-82.
4. Colombo F, Benedetti A, Pozza F, et al. Linear accelerator radiosurgery of cerebralarteriovenous malformations. *Neurosurgery* 1989; **24:** 833-40.
5. Betti O, Munari C, Rosler R. Stereotactic radiosurgery with the linear accelerator: treatment of arteriovenous malformations. *Neurosurgery* 1989; **24:** 311-21.
6. Steiner L. Radiosurgery in cerebral arteriovenous malformations. In: Fein J, Flamm E eds: *Cerebrovascular Surgery*. New York: Spring-Verlag, 1986; 1161-215.
7. Coffey RL, Lunsford LD. Stereotactic radiosurgery using the 201 Cobalt-60 gammaknife. *Neurosurg Clin N Am* 1990; **1:** 933-53.
8. Levy RP, Fabrikant JI, Frankel KA, et al. Charged-particle radiosurgery of the brain. *Neurosurg Clin N Am* 1990; **1:** 955-90.
9. Steiner L. Stereotactic radiosurgery with the cobalt 60 gamma unit in the treatment of intracranial tumors and arteriovenous malformations. In: Schmidek HH, Sweet WSH eds. *Operative Neurosurgical Techniques*. Philadelphia: WB Saunders, 1988; 515-29.
10. Norén G, Arndt J, Hindmarsh T, et al. Stereotactic radiosurgical treatment of acoustic neurinomas. In: Lunsford LD ed. *Modern Stereotactic Neurosurgery*. Boston: Martinus Nijhoff, 1988; 481-9.
11. Flickinger JC, Lunsford LD, Coffey RJ, et al. Radiosurgery of acoustic neurinomas. *Cancer* 1991; **67:** 345-53.
12. Engenhart R, Kimmig BN, Hover KH, et al. Stereotactic single high dose radiation therapy of benign intracranial meningiomas. *Int J Radiat Oncol Biol Phys* 1990; **19:** 1021-6.
13. Kondziolka D, Lunsford LD, Coffey RJ, et al. Stereotactic radiosurgery of meningiomas. *J Neurosurg* 1991; **74:** 552-9.
14. Kjellberg RN, Shintani A, Frantz AG, et al. Proton beam therapy in acromegaly. *N Engl J Med* 1968; **278:** 689-95.

15. Sturm V, Kober B, Hover KH, et al. Stereotactic percutaneous single dose irradiation of brain metastases with a linear accelerator. *Int J Radiat Oncol Biol Phys* 1987; **13:** 279-82.
16. Loeffler JS, Kooy HM, Wen PY, et al. The treatment of recurrent brain metastases with stereotactic radiosurgery. *J Clin Oncol* 1990; **8:** 576-82.
17. Caron J-L, Souhami L, Podgorsak EB. Dynamic stereotactic radiosurgery in the palliative treatment of isolated cerebral metastatic tumors. *J Neuro-Oncol* 1992; **12:**173-9.
18. Souhami L, Olivier A, Podgorsak EB, et al. Fractionated stereotactic radiotherapy for intracranial tumors. *Cancer* 1991; **68:** 2101-8.
19. Schwade JG, Houdek PV, Landy HJ, et al. Small field stereotactic external beam radiation therapy of intracranial lesions: fractionated treatment with a fixed-halo immobilization. *Radiology* 1990; **176:** 563-5.
20. Austin-Seymour M, Munzenrider J, Lingood R, et al. Fractionated proton radiation therapy of cranial and intracranial tumors. *Am J Clin Oncol* 1990; **17:** 349-58.
21. Fowler FJ. What next in fractionated radiotherapy? *Br J Cancer* 1984; **49** (Supp 6): 285 S-300 S.
22. Hariz MI, Henriksson R, Lofroth P-O, Laitinen LV, Saterborg N-E. A non-invasive method for fractionated stereotactic irradiation of brain tumors with linear accelerator. *Radioth Oncol* 1990; **17:** 57-72.
23. Lunsford LD, Flickinger J, Lindner G, Maitz A. Stereotactic radiosurgery of the brain using the first United States 201 Cobalt-60 gamma knife. *Neurosurgery* 1989; **24:** 151-9.
24. Podgorsak EB, Olivier A, Pla M, Lefebvre PY, Hazel J. Dynamic stereotactic radiosurgery. *Int J Radiat Oncol Biol Phys* 1988; **14:** 115-26.
25. Fajardo LJ. *Pathology of Radiation Injury*. Masson Publishing, 1982.
26. Fajardo LJ, Stewart JR. Capillary injury preceding radiation-induced myocardial fibrosis. *Radiology* 1971; **101:** 429-33.
27. Reinhold HS. The influence of radiation on blood vessels and circulation. IV. Structural changes in blood vessels. *Curr Top Radiat Res* 1974; **10:** 58-74.
28. Reinhold HS, Buisman GH. Radiosensitivity of capillary endothelium. *Br J Radiol* 1975; **48:** 727-31.
29. Kjellberg RN, Davis KR, Lyons S, Butler W, Adams RD. Bragg peak proton beam therapy for arteriovenous malformations of the brain. *Clin Neurosurg* 1983; **31:** 248-90.
30. Andersson B, Larsson B, Leksell L, et al. Histopathology of late local radiolesions in the goat brain. *Acta Radiol Ther Phys Biol* 1970; **9:** 385-94.
31. Nilsson A, Wennerstrand L, Leksell D, Backlund EO. Stereotactic gamma irradiation of basilar artery in the cat: preliminary experience. *Acta Radiol Oncol* 1978; **17:** 150-60.
32. Wennerstrand J, Ungerstedt U. Cerebral radiosurgery II: an anatomical study of gamma radiolesions. *Acta Chir Scand* 1970; **136:** 133-7.
33. Pozza F, Colombo F, Chierego G, et al. Low grade astrocytomas: treatment with unconventionally fractionated external beam stereotactic radiation therapy. *Radiology* 1989; **171:** 565-9.
34. Newton TH, Troost BT, Moseley I. Angiography of arteriovenous malformations and fistula. In: Wilson CB, Stein BM eds. *Intracranial Arteriovenous Malformations*. Baltimore: Williams and Wilkins, 1984; 64-104.
35. Luessenhop AJ. Natural history of cerebral arteriovenous malformations. In: Wilson CB, Stein BM eds. *Intracranial Arteriovenous Malformations*. Baltimore: Williams and Wilkins, 1984; 12-23.
36. Brown RD, Wiebers DO, Forbes G, et al. The natural history of unruptured intracranial arteriovenous malformations. *J Neurosurg* 1988; **68:** 352-7.
37. Graj CJ, Perret GE, Torner JC. Bleeding from cerebral arteriovenous malformations as part of their natural history. *J Neurosurg* 1983; **58:** 331-7.
38. Ondra SL, Troupp H, George ED, Schwab K. The natural history of symptomatic arteriovenous malformations of the brain: a 24-year follow-up assessment. *J Neurosurg* 1990; **73:** 387-91.
39. Poulsen MG. Arteriovenous malformations. A summary of 6 cases treated with radiation therapy. *Int J Radiat Oncol Biol Phys* 1987; **13:** 1553-7.
40. Steiner L, Leksell L, Greitz T, Forster DMC, Backlund E-O. Stereotaxic radiosurgery for cerebral arteriovenous malformations. Report of a case. *Acta Chir Scand* 1972; **138:** 459-64.
41. Hartmann GH, Schlegel W, Sturm V, Kober B, Pastyr O. Lorenz WJ. Cerebral radiation surgery using moving field irradiation at a linear accelerator facility. *Int J Radiat Oncol Biol Phys* 1985; **11:** 1185-92.
42. Lutz W, Winston KR, Maleki N. A system for stereotactic radiosurgery with a linear accelerator. *Int J Radiat Oncol Biol Phys* 1988; **14:** 373-81.
43. Steiner L. Treatment of arteriovenous malformations by radiosurgery. In: Wilson CB, Stein BM eds. *Intracranial Arterovenous Malformations*. Baltimore: Williams and Wilkins, 1984; 295-313.
44. Levy RP, Fabrikant JI, Frankel KA, Phillips MH, Lyman JT. Stereotactic heavy-charged particle Bragg peak radiosurgery for the treatment of intracranial arteriovenous malformations in children and adolescence. *Neurosurgery* 1989; **24:** 841-52.
45. Marks MP, Delapaz RL, Fabrikant JI, et al. Intracranial vascular malformations: imaging of charged-particle radiosurgery. *Radiology* 1988; **168:** 447-55.
46. Kjellberg RN, Hanamura T, Davis KR, Lyons SL, Adams RD. Bragg-peak proton-beam therapy for arteriovenous malformations of the brain. *N Engl J Med* 1983; **309:** 269-74.
47. McCormick WF. Pathology of vascular malformations of the brain. In: Schmidek HH, Sweet WH eds. *Operative Neurosurgical Techniques: Indications, Methods, and Results*. Philadelphia: WB Saunders, 1988; 911-5.
48. Stein BM, Mohr JP. Vascular malformations of the brain. *N Engl J Med* 1988; **319:** 368-70.
49. Simard JM, Garcia-Bengochea F, Ballinger WE Jr, Mickle JP, Quisling RG. Cavernous angioma: a review of 126 collected and 12 new clinical cases. *Neurosurgery* 1986; **18:** 162-72.

50. Kondziolka D, Lunsford LD, Coffey RJ, Bissonette DJ, Flickinger JC. Stereotactic radiosurgery of angiographically occult vascular malformations: indications and preliminary experience. *Neurosurgery* 1990; **27:** 892-900.
51. Wiegand DA, Fickel V. Acoustic neuromas: the patient's perspective. Subjective assessment of symptoms, diagnosis, therapy, and outcome in 541 patients. *Laryngoscope* 1989; **99:** 179-87.
52. Taylor B, Marcus R, Friedman W, et al. The meningioma controversy: post-operative radiation therapy. *Int J Radiat Oncol Biol Phys* 1988; **15:** 299-304.
53. Degerblad M, Rahn T, Bergstrand G, Thorén M. Long-term results of stereotactic radiosurgery to the pituitary gland in Cushing's disease. *Acta Endocr* 1986; **112:** 310-4.
54. Backlund E-O, Axelsson B, Bergstrand C-G, et al. Treatment of craniopharyngiomas – the stereotactic approach in ten to twenty-three years' perspective. I. Surgical, radiological and ophtalmological aspects. *Acta Neurochir* 1989; **99:** 11-9.
55. Backlund E-O. Solid craniopharyngiomas treated by stereotactic radiosurgery. In: Szikla G, ed. *Stereotactic Cerebral Irradiation.* Elsevier/North-Holland Biomedical Press, 1979; 271-81.
56. Cairncross JG, Posner JB. The management of brain metastases. In: Walker MD, ed. *Oncology of the Nervous System,* vol 12 of Cancer Treatment and Research. Boston: Martinus Nijhoff, 1983; 341-7.
57. Patchell RA, Tibbs PA, Walsh JW, et al. A randomized trial of surgery in the treatment of single metastases to the brain. *N Engl J Med* 1990; **322:** 494-500.
58. Marin-Grenz M, Kimmig B, Engenhart R, et al. High dose percutaneous stereotactic irradiation of solitary brain metastases using a 15 MeV linear accelerator (Abstract) *Int J Radiat Oncol Biol Phys* 1988; **15** (Supp): 231.
59. Coffey RJ, Flickinger JC, Bissonette, Lunsford LD. Radiosurgery for solitary brain metastases using the Cobalt-60 gamma unit: methods and results in 24 patients. *Int J Radiat Oncol Biol Phys* 1991; **20:** 1287-95.
60. Loeffler JS, Alexander III E, Hochberg FH, et al. Clinical patterns of failure following stereotactic interstitial irradiation for malignant gliomas. *Int J Radiat Oncol Biol Phys* 1990; **19:** 1455-62.
61. Shenouda G, Souhami L, Freeman CR, et al. Accelerated fractionation for high-grade cerebral astrocytomas. Preliminary treatment results. *Cancer* 1991; **67:** 2247-52.
62. Alexander E, Siddon RL, Loeffler JS. The acute onset of nausea and vomiting following stereotactic radiosurgery: correlation with the total dose to area postrema. *Surg Neurol* 1989; **32:** 40-4.
63. Flickinger JC, Lunsford LD, Kondziolka D, et al. An analysis of neurodiagnostic imaging changes after gamma knife radiosurgery. Proceedings of the International Stereotactic Radiosurgery Symposium. Pittsburgh, USA, June 19-21, 1991.

Adv Radiol Oncol 1992; 167–74.

Medulloblastoma, results of treatment at the Institute of Oncology, Ljubljana

Petrič-Grabnar G[1], Župančič N[2], Klun B[3], Umek B[1], Stare J[4], Kopač Š[2], Kragelj B[1], Cindro L[2], Škrbec M[5], Jereb B[1]

[1]The Institute of Oncology, Ljubljana, [2]University Medical Centre, Department of Paediatrics, Ljubljana, [3]University Medical Centre, Department of Neurosurgery, Ljubljana, [4]Institute for Biomedical Informations, Medical Faculty, Ljubljana, [5]University Medical Centre, Department of Rentgenology, Ljubljana

With introduction of irradiation of the whole CNA the survival rates of children have improved significantly. It has also been shown recently that patients with grossly totally excised tumours fare better than patients with more advanced disease and those with residual tumors after surgery and may profit from chemotherapy. We tried to find out whether the effect of proper staging, addition of chemotherapy and improvement of radiation therapy techniques did influence the survival of the patients in our series.
Between 1972 through 1990, 37 patients were postoperatively treated by RT (17 after 1984) 16 had also chemotherapy. At the end of the study 60% of patients were alive, disease free with a mean observation time of 5 years.
The only statistically significant difference in the survival rates was found in relation to the extent of the disease. Patients with grossly totally excised tumours had the best outcome. The survival of those with malignant cells in the CSF was poor as it was also of children less than 2 years old. We could not draw any conclusions about the effect of chemotherapy or improved management on the survival of patients treated more recently.

Key words: medulloblastoma-therapy, survival rate; child

Introduction

Medulloblastomas are the second most common posterior fossa tumours in children, representing about 20% of all childhood intracranial tumours.[1] In Slovenia, about 10 cases of intracranial tumours in children are registered per year, 3-4 of these being medulloblastomas.[2] With the introduction of whole neuroaxis (CNA) irradiation the survival rates of children with medulloblastomas have improved significantly.[3,4] Further, the adequate dose of radiation to the tumour bed (posterior fossa) was established as well as the dose to the CNA.[5,6,7] Recently, however, the question arose, whether the dose of radiation to the CNA in patients with localized and grossly totally excised tumours need to be as high as in others.[8,9,10,11] The role of surgery has been reevaluated recently, after it was found that patients with grossly excised tumours fare better than those with residual tumours after surgery.[4,6] The role of chemotherapy is not quite established; although, complete remissions have been achieved with different agents[12,13,14,15] and it has also

Correspondence to: Berta Jereb, M.D. The Institute of Oncology, Zaloška 2, 61000 Ljubljana, Slovenia.

UDC: 616.831-006.6-053.2-036

been shown that patients with more advanced disease may profit from chemotherapy.[16] One of the major advances in recent years in the management of medulloblastoma is the agreement on the necessity for pre-radiation evaluation of the extent of diesease.[17] It has also been shown that chemotherapy given before radiation results in less neurotoxicity.

We tried to find out the effect of these advances in the management of medulloblastoma on the survival of patients in our series: proper staging, addition of chemotherapy and possible improvement of the radiation techniques.

Material and methods

From 1972 through 1990 37 patients (20 before 1984, 17 after) with medulloblastoma were admitted for postoperative radiation. The youngest was 18 months and the oldest 22 years old. The mean age was 7 years. The diagnosis of medulloblastoma or PNET (2 cases) was confirmed in all patients.

Preoperative evaluation with CT scan was performed at the Institute of Rentgenology, surgery at the Neurosurgical Department and histology at the Institute of Pathology of the Medical Faculty, University of Ljubljana. The surgery consisted of extirpation of the tumour, total in 20 and subtotal in 17 cases. Postoperatively, the protocol called a CT scan, spinal tap for liquor cytology and in cases with malignant cells in the CSF also a myelogram. Such evaluation of the extent of disease was part of the management after 1984, whereas patients admitted earlier had not undergone all these tests. Postoperative CT scan was performed on 22 patients, before 1984 only in 3. The finding on the CT scan was in agreement with the surgical report in 19 patients whereas in 3 patients CT scan showed residual tumour after a »total excision«, – 2 of these also had cells in the CSF.

On the basis of the surgical report and postoperatively performed tests, the patients were classified according to the previously described system (Table 1). A more detailed staging system was not used[18] as the size of tumour was not allways known and because it seemed more important for the prognosis whether the tumour was radically excised or not, in cases of infiltration into vital areas such as the brain stem. Malignant cells were found in the spinal fluid in 5 patients, no cells were found in 16. In 16 patients the CSF was not examined for malignant cells; 13 of these were treated before 1984.

Table 1.

Group I	Grossly totally excised tumour, no local residuum, no spread either within or otuside the CNS
Group II	Grossly not completely excised tumour, (or residual tumour on postop. CT scan), no spread either within or outside the CNS
Group III	All tumours with spread within the CNS, but not outside the CNS
Group IV	All tumours with spread outside the CNS.

Table 2. Patient characteristics

No. of patients	37
Age	1 to 22 yrs (36 pts ≤ 18 yrs)
Mean age	7 yrs
Sex	27 M/10 F
High risk	15 pts
Low risk	22 pts
	17 ≤ 75% resection 7 age ≤ 2 years 5 + CSF

One patient with malignant cells in the CSF had a myelogram. Nineteen patients were alotted to Group I, 10 of these had no CSF cytology; 17 were alotted to Group II, 8 of them had no CSF cytology; 5 had malignant cells in the CSF and were therefore alotted to Group III.

There were no patients with tumour spread outside the CNS. The patients were also divided into a poor-risk and a low-risk group based on a combination of prognostic factors shown in Table 2. The site of the tumour was the posterior fossa in all except one (PNET) patient who had a tumour in the parieto-temporal area.

Sixteen patients had chemotherapy (ChT), one had adjuvant ChT after completion of radiation, 14 had preradiation ChT and one had both.

Adjuvant ChT included CCNU and Vincristine according to the SIOP I[14] protocol. Preradiation ChT was given according to the SIOP II protocol[19] including Methotrexate. Vincristine and Procarbazine was used in 7 patients, 7 were treated with high doses (HD) of Cytoxan, 2 or 3 cycles.

All patients in this series were treated postoperatively with irradiation of the whole CNA, after 1984 irradiation of the cribriform region was added to avoid possible underdosage in this area. Also the process of immobilization in the plaster cast, dose planning and dosimetry (measurement of the accidental dosis to eyes and thyroid gland) were more strictly adhered to.

Patients were treated on the Philips Cobalt-60 unit at 80 cm source-skin distance. During treatment the patient was in prone position in a total body plaster shell. On the simulator several lateral radiograms were obtained to establish the depth of the spinal cord along the whole length of the field.

The first phase of the treatment consisted of a single spade shaped portal from the top of the head down to S_2 level as shown in Figure 1a. This was broken by a set of junctions in 3 cm intervals such as 2,3,4, where necessary. When the treatment began, junctions were cycled daily i.e., day 1:1-2, 2-5, day 2:1-3, 3-5, etc. No separation was left between 1-2 and 2-5 etc. and all beam edges were trimmed with lead blocks to eliminate penumbra beyond the light beam edge to reduce the integral dose. The dose to the eye lenses was measured with thermoluminiscent dosimeters and when this dose approached 500 cGy this portal was discontinued. In the second phase of the course the head was irradiated through two lateral portals extending down to C_2 level. The spinal cord from C_2 to S_2 was then irradiated through a single portal which was again broken, if necessary, by a set of new junctions (2A, 3A, 4A on Figure 1b). Junctions were again cycled, i.e. day 1: C_2-2A, 2A-5, day 2: C_2-3A, 3A-5 etc. In some patients the dose to

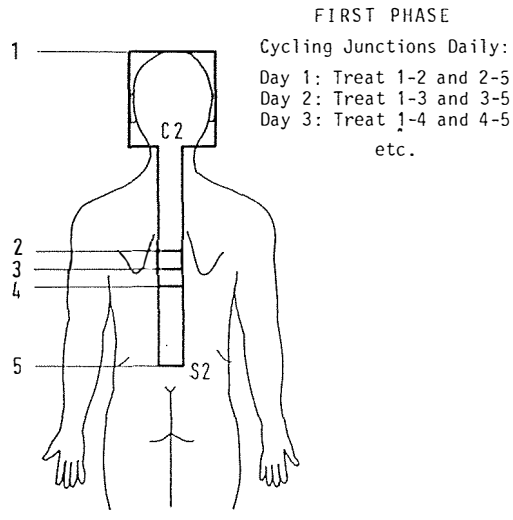

Figure 1a. Outline of fields for the first phase of treatment for medulloblastoma (6).

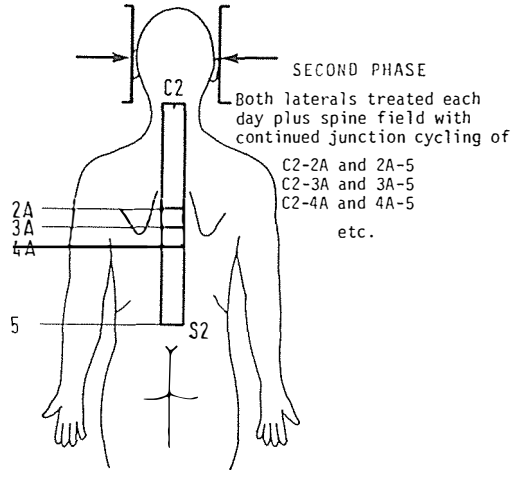

Figure 1b. Outline of fields for the second phase of treatment for medulloblastoma (6).

the eye-lens was again measured with thermoluminiscent dosimeters to estimate the complete dose absorbed in the lens of the patients. All portals were treated each day, five times a week, delivering 150 cGy to the depth of the spinal cord on each section. A total of 3600 cGy was prescribed to the CNA as a rule with exception in 3 very young children. Two of these received

2400 cGy and one of them 1200 cGy in the first course of treatment. As the dose in the first phase of treatment was given to the depth of the spinal cord (3-5 cm), the total dose in the frontal region of the brain received 100 to 450 cGy less.

A boosting dose was given to the posterior fossa through two lateral portals. Ten of the twenty-one patients received an additional dose of 1500 cGy in fractions of 250 cGy, others from 1200 to 2400 cGy in fractions of 200 to 300 cGy given five times weekly. As a result, the patients received about 5000 cGy or more in 40-50 days to the posterior fossa, except for the young ones who had less.

An additional dose was given to the cribriform plate as this region received only about 30% of the target dose due to shielding of the eyes during the second phase of the treatment.[7] A small anterior field was used for electrons 8-12 MeV. Thirteen patients received 4 x 300 cGy or 6 x 250 cGy (5 fractions/week), whereas in other cases the dose applied in this part of treatment varied from 2 x 300 cGy to 10 x 250 cgy (Figure 2).

The follow up ranged between 6 months and 18 years, with a mean of 5 years. The survival was calculated according to the Kaplan-Meyer method from the date of operation until death or date of the last follow up.[20]

The differences in survival of the groups of patients were tested with the log-rank test.

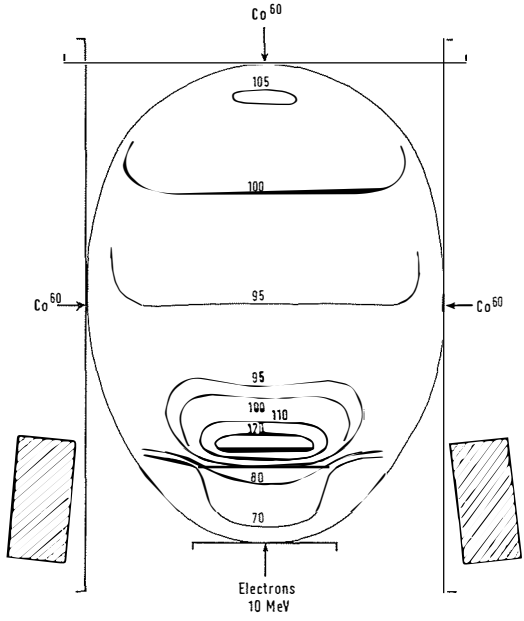

Figure 2. Typical dose distribution through the plane containing the eye shields after completion of the first two phases of treatment and electron boost irradiation (100% = 3600 cGy).

Results

The eye-lens was exposed to irradiation mainly during the first two phases of treatment. After the first phase, the dose to the lens was estimated to be from 380 to 600 cGy, the measured doses beeing in close agreement with the calculated ones. In the second part of the treatment the measured dose to the lens varied markedly between sessions, depending on the position of the eye-shielding block and termoluminiscent dosimeter and ranging from 10% to 60% of the target dose. The dose to the lens during the whole treatment has been estimated in five patients. Four of them received 830 to 1110 cGy with the mean 990 cGy. In patients who received only 2400 cGy to the CNS the dose to the lens was 730 cGy.

At the end of the study, December 1990, 23 of the 37 patients (60%) were alive without signs of tumour for at least 6 months. One patient is at present treated for recurrence.

Eleven out of 17 patients treated before 1984 and 12 out of 20 after 1984 are alive, there is no difference in survival.

There was further no significant difference in the survival according to sex. The older age group did better than the younger, especially under the age of 2 the survival was poor (Figure 3), but statistically not significantly worse.

The only statistical significance was found for the worse prognosis of those patients who had malignant cells in the CSF (Group III), with 2 out of 5 survivors (Figure 4).

Of the 15 patients, classified as Group I, 11 are alive, 4 have died in tumour; consequently

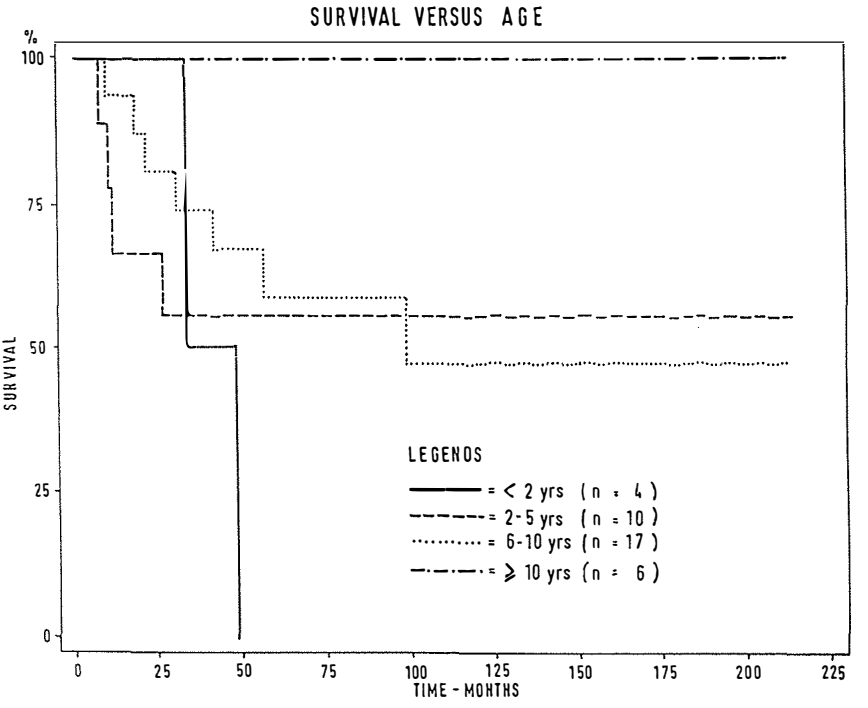

Figure 3.

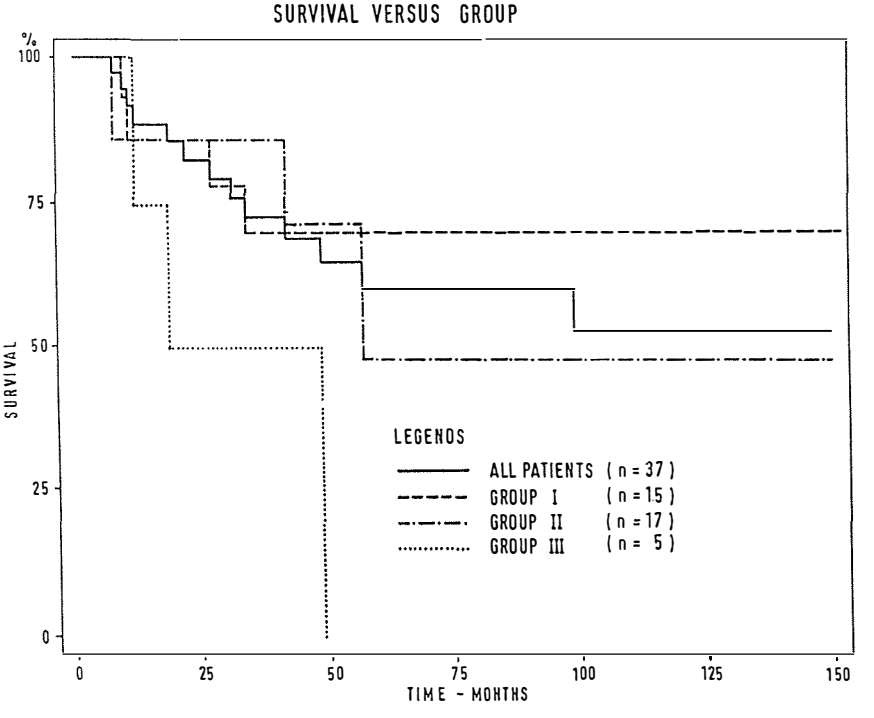

Figure 4.

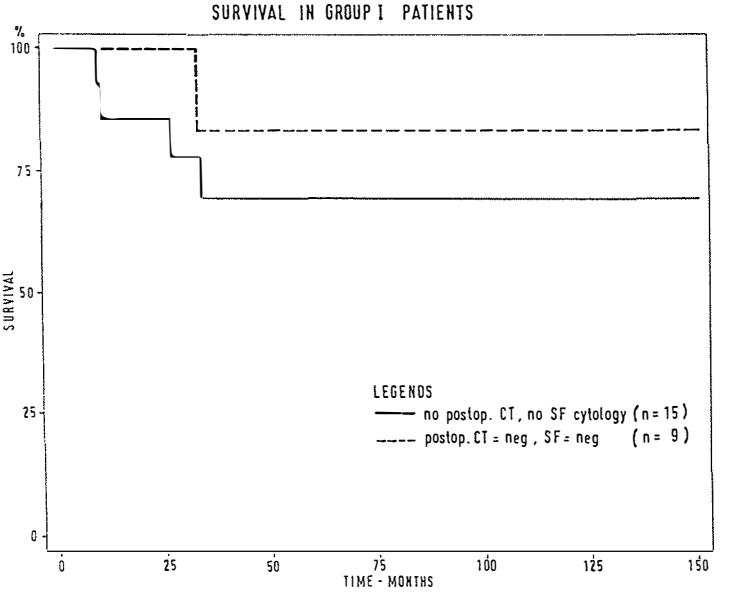

Figure 5.

Table 3. Results in relation to group and chemotherapy protocol

Group	SIOP	HD	Cytoxan	No Cht	TOTAL
ChT	No. of patients: all/alive				
I	–	–		16/11	16/11
II	7/5+	4/2		5/3+	16/10
III	1/1	3/1		1/0	5/2
TOTAL	8/6	7/3	22/14	37/23	

+ – one pt had adjuvant ChT

Table 4. The pattern of recurrences according to prognostic factors

All failures	16 pts
LOW RISK FAILURES	
– supratentorial & CSF	2
– posterior fossa only	1
HIGH RISK FAILURES	
– supratentorial & CSF	3
– CSF only	4^{+}
– supratentorial only	3^{o}
– posterior fossa only	2
– posterior fossa & CSF	1

$+_2$ – recurrences at the junction
o_2 – suprasellar recurrences

of the patients properly classified as Group I, one died in tumour (Figure 5).

Of the 17 patients classified as Group II (8 of them without CSF cytology), 10 are alive. Of the 15 patients who had preradiation ChT, 9 are alive and well. It could not be concluded that ChT had a favourable effect on the survival in this small series, it is, however, interesting to note that the 2 survivors with Group III disease both had preradiation ChT (Table 3).

In sixteen patients the tumour recurred, 2 of these are alive, one still being treated, and one without sign of tumour more than one year after treatment for recurrence.

The pattern of recurrence is shown in Table 4.

Most common was supratentorial recurrence, we could not find, any correlation with a lower dose in the anterior part of the brain.

Ten of the 16 (60%) recurrencies appeared during the first 2 years, 13 (80%) during the first 3 years, another during the 4^{th} year and one recurrence in the posterior fossa more than 7 years after treatment.

Discussion and conclusion

The reports on significant improvement due to treatment could not be confirmed in our study The survival rate in the group treated during the recent period was not better from the survival earlier, despite the improved technique and addition of chemotherapy.

One explanation, of course, is that the 2 groups are not comparable. All small children up to 2 years of age known to have a poor prognosis[5,17] are from the recent group.

The most important factor influencing the outcome is the extent and resectability of the tumour. Patients with completely resected tumours without spread do very well, an observation reported from experience on larger series and confirmed in ours.[4,5,6] In the more advanced – non resectable (Group II) tumours and in those with malignant cells in the CSF our results are poor and chemotherapy did not improve the survival rate, possibly the survival time. It certainly did not contribute to a better survival in those small children treated with a smaller radiation dose and preradiation ChT (HD Endoxan). Both boys less than 2 years at diagnosis had, however, a normal development during treatment and remissions. They were repeatedly in complete clinical remissions after HD Cytoxan and lived more than 3 respectively 4 years from diagnosis. While lower doses of radiation seem to be suficient for cure in some low risk group patients[8], they are insufficient in the high risk group patients comprising children up to 2 years of age who are most in need of less treatment.[9,15,19,22]

The fact that in our series the most common site of recurrence was supratentorial, is unusual, especially the 3 suprasellar recurrences. We have not found any correlation with a possible lower dose in the supratentorial region with the recurrences (less than 3600). As neither daily checking of setups nor consistent checkings with portfilms were possible this finding could allow for suspicion of occasional too generous blocking.

Although the series is small, the observations allow us to conclude the following.

As in other series: children of 2 years or less have poor prognosis, as have the patients with incomplete tumour excision and/or malignant cells in the CSF.[5,17]

Lower doses of radiation to the CNA in combination with HD Cytoxan do not result in cures in young children.

Chemotherapy has not significantly improved the cure rate, but seems to prolong the survival, and possibly postopone recurrence. At present the prognosis in patients with advanced medulloblastoma (more than Group I) is still poor. More effective ChT regimens than those used in our series are needed.

References

1. Schulte FJ. Intracranial tumours in childhood – concepts of treatment and prognosis. *Neuropediatrics* 1984; **15:**3-12.
2. Incidenca raka v Sloveniji 1985. Ljubljana: Onkološki inštitut, Register raka za SR Slovenijo 1989.
3. Dietz R, Graf N. Zur Therapie des Medulloblastoms – Ergebnisse aus den Jahren 1968 bis 1985. *Strahlenther Oncol* 1990; **166:**683-7.
4. Bloom HJG, Glees J, Bell J. The treatment of longterm prognosis of children with intracranial tumours, a study of 610 cases at the Royal Marsden Hospital, 1950-1981. *Int J Radiat Oncol Biol Phys* 1990; **18:**723-45.
5. Hughes EN, Shillito J, Sallen SE, Loeffler JS, Cassady JR, Tarbell NJ. Medulloblastoma at the joint center for radiation therapy between 1968 and 1984. *Cancer* 1988; **61:**1992-8.
6. Jereb B, Reid A, Ahuja RK. Patterns of failure in patients with medulloblastoma. *Cancer* 1982; **50:**2941-7.
7. Jereb B, Krishnaswami S, Reid A, Allen JC. Radiation for medulloblastoma adjusted to prevent recurrence to the cribriform plate region. *Cancer* 1984; **54:**602-4.
8. Halberg FE, Wara WM, Fippin LF et al. Low-dose craniospinal radiation therapy for medulloblastoma. *Int J Radiat Oncol Biol Phys* 1991; **20:**651-4.
9. Kun LE, Constine LS. Medulloblastoma – caution regarding new treatment approaches. *Int J Radiat Oncol Biol Phys* 1991; **20:**897-9.
10. Tomita T, McLone DG. Medulloblastoma in childhood: results of radical resection and low-dose neuraxis radiation therapy. *J Neurosurg* 1986; **64:**238-42.
11. Levin VA, Rodriguez LA, Edwards MSB et al. Treatment of medulloblastoma with procarbazine, hydroxyurea, and reduced radiation doses to whole brain and spine. *J Neurosurg* 1988; **68:**383-7.

12. Allen JC, Helson L, Jereb B. Preradiation chemotherapy for newly diagnosed childhood brain tumours: a modified phase II trial. *Cancer* 1983; **52**:21-6.
13. Kovnar EH, Kellie AJ, Horowitz ME and al. Preirradiation ciscplatin and etoposide in the treatment of high-risk medulloblastoma and other malignant embryonal tumours of the central nervous system: a phase II study. *J Clin Oncol* 1990; **8**:330-6.
14. Lefkowitz IB, Packer RJ, Siegel KR, Sutton LN, Schut L, Evans AE. Results of treatment of children with recurrent medulloblastoma / primitive neuroectodermal tumours with lomustine, cisplatin, and vincristine. *Cancer* 1990; **65**:412-7.
15. Loeffler JS, Kretschmar CS, Sallan SE et al. Pre-radiation chemotherapy for infants and poor prognosis children with medulloblastoma. *Int J Radiat Oncol Biol Phys* 1988; **15**:177-81.
16. Tait DM, Thornton-Jones H, Bloom HJG, Lemerle J, Morris-Jones P. Adjuvant chemotherapy for medulloblastoma: the first multicentre control trial of the International society of Paediatric oncology (SIOPI). *Eur J Cancer* 1990; **26**:464-9.
17. Deutsch M. Mudulloblastoma: staging and treatment outcome. *Int J Radiat Oncol Biol Phys* 1988; **14**:1103-7.
18. Harisiadis L, Chang CH. Medulloblastoma in children: a correlation of staging and results of treatment. *Int J Radiat Oncol Biol Phys* 1977; **2**:833-41.
19. Neidhardt MK, Bamberg M, Riehm H. Medulloblastoma: strategies for therapy. *Monogr Paediat* 1986; **18**:296-315.
20. Kaplan EL, Meier P. Non-Parametric estimation for incomplete observation. *J Am Statis Assoc* 1958; **53**:457-81.
21. Mulhern RK, Horowitz ME, Kovnar EH et al. Neurodevelopmental status of infants and young children treated for brain tumours with preirradiation chemotherapy. *J Clin Oncol* 1989; **7**:1660-6.
22. Shalet SM, Beardwell CG, Morris-Jones PH et al. Pituitary function after treatment of intracranial tumours in children. *Lancet* 1975; **2**:104-7.

Adv Radiol Oncol 1992; 175–80.

Intrapleural application of human leukocyte interferon (IFN-α) in breast cancer patients with pleural carcinosis

Jereb B[1], Štabuc B[1], Us-Krašovec M[1], Cerar O[1], Stare J[2]

[1]The Institute of Oncology, Ljubljana, [2]The Institute for Biomedical Informatics Medical Faculty, Ljubljana

Ten patients with breast cancer and pleural carcinosis, receiving IFN-α intrapleurally in addition to conventional treatment, were compared with 20 control patients who had no IFN-α. The effect of IFN-α. was evaluated with cellular morphology of the pleural fluid and with the patients'survival. After application of IFN-α intrapleurally reactive cells appeared and malignant cells disappeared eventually. The mean survival time after onset of pleural carcinosis was 15 months in the experimental group and 9 months in the control group. Three patients out of the 10 in the experimental group are alive, 2 of them (both had inflammatory cancer) are NED off treatment more than 1 respectively 2 years. One patient of the 20 in the control group is alive with disease. There were no complications. IFN-α looks promising as supplementary treatment in these patients.

Key words: breast cancer, pleural carcinosis, IFN-α

Introduction

In a previously reported series of 7 patients with breast cancer and ipsilateral pleural carcinosis it was observed that a crude product of IFN-α was locally highly effective.[1] Malignant cells disappeared from the pleural fluid, but aplications of IFN-α were painful and also produced pleural adhesions. The effect on survival could not be evaluated. We therefore continued the investigation with a more purified product, and tried also to find out whether local applications of IFN-α do affect the survival of patients with breast cancer.

Correspondence to: Berta Jereb, M.D., The Institute of Oncology, Zaloška 2, 61000 Ljubljana, Slovenia.

UDC: 618.19-006.6-085:616.25-006.6-085

Material and methods

Ten women with breast cancer of both the experimental (10 pts) and the control group had pleural effusion diagnosed during 1985 through 1989. All had had the diagnosis of pleural carcinosis proven by cytology.

In both groups the treatment was decided upon by the caring physician, regardless of whether the patient was to receive IFN-α or not. The patients of the experimental group were chosen at random. The systemic treatment for breast carcinoma either primary or for recurrences was rather uniform through the years under investigation.

The age of the patients was between 37-70, and the mean for the experimental group was 49, and 57 for the control group.

The *control group* consisted of 20 patients, with ipsilateral effusion in 18 and bilateral in 2.

Eleven patients had locally advanced (T_3 and T_4) and 9 had operable (T_1T_2) breast cancer at diagnosis. The primary treatment was radical mastectomy in 15 (with adjuvant chemotherapy in 7 and hormonal treatment in 2,6 had radiation therapy, 5 of which also had chemotherapy).

Pleural carcinosis was found at diagnosis in 5 patients, 16 had bone and soft tissue metastases, 10 had lung and 4 had liver metastases at onset of pleural carcinosis.

All patients had systemic treatment and 9 had also 1 or 2 instillation of Bleomycin (30-60 mg) into the pleural cavity.

The clinical data of the *experimental group* are presented in Table 1. Four patients had locally advanced inflammatory cancer with pleural carcinosis at diagnosis, 4 had diffuse pulmonary carcinosis at onset of bilateral pleural effusion and 2 had (inflammatory) cancer »on cuirrasse« – carcinomatous lymphangitis of the chest wall.

In Table 2 and 3 the clinical data and treatment of the 2 groups are compared.

They were also comparable as to the over-all survival from diagnosis with a median survival of 60 months for the control group and 75 months for the experimental group.

IFN-α was applied with a thin needle after the fluid was removed from the pleural cavity or 20 cm^3 aspirated for cytologic examination, 20 x 10^6 IU was injected in 20 ml distilled water.

Only the patients No 1 and No 2 were treated with daily instillations through a chest tube and continuous fluid drainage. The remaining 8 patients had IFN-α application adjusted to their clinical status, and concommitant treatment in order to minimize the time of hospitalization. They received HLI-α at weekly intervals until the pleural fluid disappeared (4 patients) or until progress of the disease ocurred either with pleural effusion or in other organs (4 patients).

The effect of treatment was evaluated at each instillation by cytologic examination as regard to aspects: degeneration of malignant cells and appearance of reactive cells in the pleural fluid.

The survival was calculated according to the Kaplan Meyer statistical method from the day of diagnosis (biopsy) and to the date of last follow up and also from the day of onset or diagnosis of pleural carcinosis (cytology) until death or last follow up.

Results

Two patients were not evaluable as to effect of IFN-α on the cytomorphology of the pleural fluid, because the number of cells in the pleural fluid was to scarce.

Malignant cells disappeared in the remaining patients of the experimental group except in patients No 5 in whom they were still present at the 5th application, and in patients No 3 who had progressive liver metastases and had only 2 applications of IFN-α.

After application of IFN-α, lymphocytes (even immature forms) histiocytes, granulocytes and monocytes apeared in the pleural fluid. The time of appearance as well as the quantity of this cells varied from patient to patient. Among the 5 patients with appearance of the reactive cells were those in whom malignant cells eventually completely disappeared. The number of nonmalignant cells also diminished during treatment and in all patients at the end of treatment only few solitary cells were seen. Figure 1-4.

The 2 patients who are alive NED had both abundant appearance of reactive cells in the pleural fluid during IFN-α treatment.

The survival after the onset of pleural carcinosis (Figure 1) was only slightly but not significantly ($p < 0.10$) better in the experimental as compared to the control group; the 25 percentile survival time in the experimental group was 23 and it was 16 months in the control group. It might be worth mentioning that 2 patients out of the 3 who are alive after treatment with IFN-α are NED and off treatment. In the control group the patient who is alive has active disease.

There were no complications of treatment with IFN-α except for occasional fever (3 patients).

Table 1. Clinical data on 10 patients of the experimental group

Nr.	Age	Diagnosis		1st treat-ment	Date of 1st rec. and previous treatment	Onset of pleural carcinosis		No. of application	Concomitant treatment	Survival		Date + cause of death
		date of	stage at			date/site	other sites of extens.	IFN-α		from diagn.	from treatment IFN-α	
1	37	02/84	$T_{4d}N_{1b}M_0$	10/85 RM+CMF+ RT+H	07/85	11/85 ipsil	chest–wall	10 x (dayly)	Epidoxarubicin +Vincristine	40 mos	22 mos	10/87 at home (cancer)
2	46	06/76	$T_{4d}N_2M_0$	RT+CMF	11/79 CMF, H+A+Vincristine M+Vinblastine	12/85 bil	lung carcinosis	10 x (dayly)	M+Vinblastine + RT	11yrs	22 mos	10/87 metastasis (lung, liver)
3	50	03/86	$T_{4d}N_{1b}M_0$	CMF+RM+ +RT+H	09/87 M+A	10/88 ipsil	chest–wall lung, liver	2 x (weekly)	–	31 mos	1 mos	11/87 metastasis (liver, skeleton, lung, chest–wall
4	69	01/88	$T_{4d}N_2M_1$			01/88 ipsil	chest–wall lymph nodes	10 x (weekly)	RT+CMF	2 yrs	2 yrs	NED
5	50	07/87	$T_2N_1M_0$	RM+RT	09/88 CMF (2 cycl.)	11/88 ipsil	chest–wall	6 x (weekly)	Cyclophospha-mide+A+ +5-FU	23 mos	9 mos	06/89 at home (cancer)
6	43	05/66	$T_3N_2M_0$	RT+RM+RT	09/84 H+RT+CMF, H+A+M	11/88 bil	lung carcin., skeleton, liver	3 x (weekly)	H	24 yrs	5 mos	04/89 at home (cancer)
7	46	10/88	$T_{4d}N_3M_1$	RM+CMF (2 cycl.) progress		12/88 bil	lung carcin., chest–wall	5 x (weekly)	M+A	14 mos	3 mos	03/90 at HOME (cancer)
8	56	10/84	$T_2N_1M_0$	RM+CMF		12/88 ipsil	chest–wall (inflammat.) lymph nodes, skeleton	3 x (monthly)	M+A	6 yrs	2 yrs	AWD (skin+chest–wall)
9	39	06/86	$T_2N_{1b}M_0$	RM+CMF+H		02/89 bil	lung carci-nosis	7 x (monthly)	Cyclophospha-mide+Epidoxa-rubicin+5–FU	4 yrs	1 yrs	NED
10	50	01/83	$T_2N_0M_0$	RM	03/85 H+RT+CMF, M+A	03/89 bil	skeleton, lung carci-nosis	5 x (weekly)	THIO–ATEPA+ Vinblastine	72 mos	2 mos	06/89 at home (cancer)

LEGENDS: RM = radical mastectomy, RT = radiation therapy, NED = no evidence of disease, AWD = alive with disease, ipsil = ipsilateral, bil = bilateral, CMF = cyclophosphamide, methotrexatem 5-fluorouracil 5-FU = 5-fluorouracil, H = hormones, A = Adriamycin, M = Mitomycin

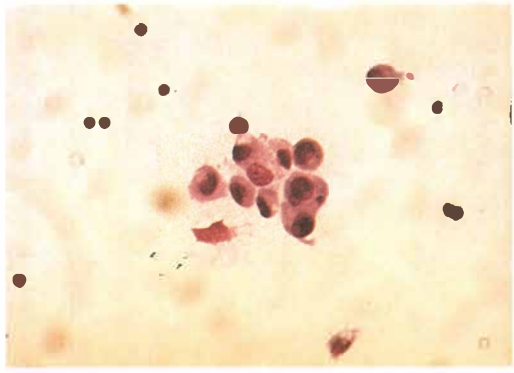

Figure 1. Patient No. 4. Pleural effusion. Group of malignant cells, few lymphocytes and erythrocytes. Giemsa, original magnification 25 x 4.

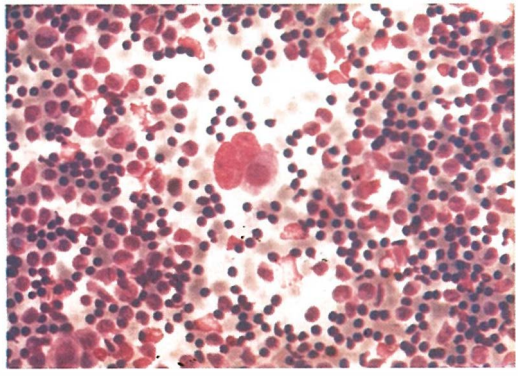

Figure 2. Same patient. Pleural effusion after 1st application of IFN-α Scattered enlarged malignant cells, increased number of leucocytes and histiocytes. Giemsa, original magnification 25 x 4.

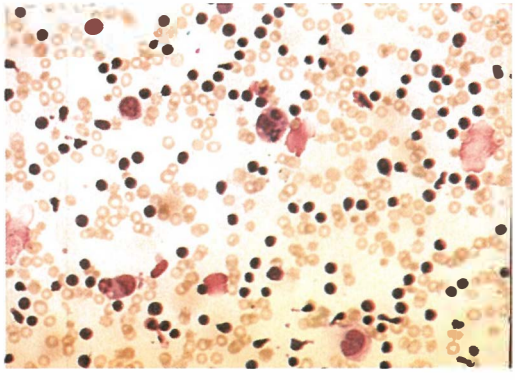

Figure 3. Same patient. Pleural effusion after 3rd application of IFN-α Lymphocytes and few degenerated (malignant?) cells. Giemsa, original magnifiction 25 x 4.

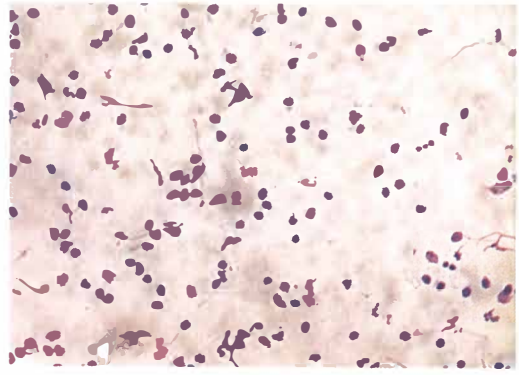

Figure 4. Same patient. Pleural effusion 3 months after treatment. Lymphocytes few granulocytes and cell debris. Giemsa, original magnification 25 x 4.

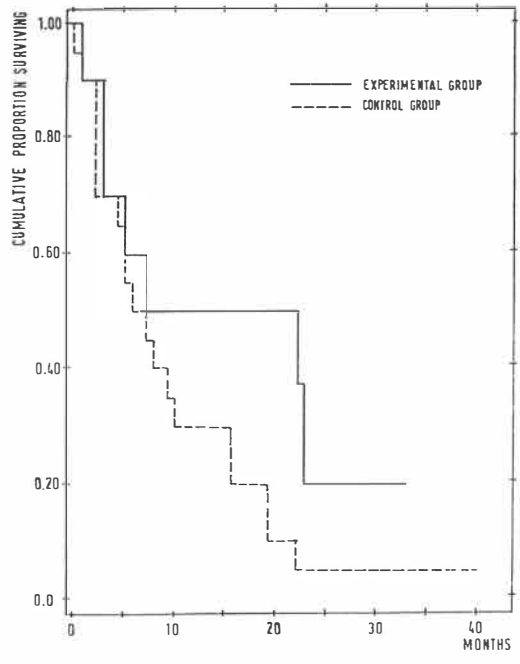

Figure 5. Survival from the diagnosis of pleural carcinosis.

Discussion

How much IFN-α given intrapleurallyl, is responsible for the changes in cytology of the pleural fluid is difficult to establish. There might

Table 2. Clinical data at onset of pleural carcinosis for experimental (10 patients) and control group (20 patients)

CLINICAL DATA	GROUP			
	experimental		control	
	nr.	of pts	nr.	of pts
Inflammatory cancer at diagnosis		4		5
pleural carcinosis at 1st treatment	2		2	
pleural carcinosis at recurrence	2		3	
Pleural carcinosis at recurrence		8		15
1st	4		6	
2nd	4		9	
Ipsilateral pleural carcinosis and involvement of chest wall		5		10
Bilateral pleural carcinosis and lung carcinosis		5		10
Involvement of other organs		4		13
liver	2		4	
bone	4		10	
lymph nodes	2		7	

Table 3. Systemic treatment for pleural carcinosis for experimental (10 patients) and control group (20 patients)

CHEMOTHERAPY	GROUP			
	experimental		control	
	nr.	of pts	nr.	of pts
Mitomycin & Adriablastin		3	8	(5)
Methotrexate & 5-Fluorouracil		2	5	(1)
Mitomycin & Vinblastine		1	–	
Epidoxarubicin & Cytoxan & 5-Fluorouracil		1	–	
Epidoxarubicin & Vincristine		1	–	
THIO-TEPA & Vinblastine		1	–	
CCNU-Nitrosurea & Dacarbazin & 5-Fluorouracil		1	2	
Hormones		1	2	(2)
None		1	3	(3)

( ) = also Bleomycin locally

be other reasons for changes in the appearance of cell, f.i. concomitant chemotherapy. On the whole, however, it can be said that during treatment with IFN-α malignant cells degenerated and finally disappeared, while at the same time reactive cells were observed. Allthough this effect might vary in degree, it is rather uniformely observed in a previous and in this group of patients. In this series, however, the impression was, that the appearance of reactive cells was less expressed in the more recently treated group of patients. This could be a consequence of more purified interferon as well as of concomitant chemotherapy.

It is generally agreed upon that pleural carcinosis is associated with poor prognosis and has to be treated with aggressive chemotherapy even in the absence of other evidence of metastasis is.[2-5] The kind of additional local treatment might, however, still be a matter of different choices. There are few randomized studies, and a clear superiority of one modality or agent has not been established. Bleomycin seems to be one of the most effective agents but its severe toxicity was reported.[6,7]

As addition to systemic therapy in patients who already have been, in the majority of cases, treated previously with chemotherapy and therefore at risk for toxicity, an approach with a less toxic agent would be more advisable. IFN-α as it was used in this series is a harmless and effective tool for palliative treatment of pleural carcinosis in breast cancer.

The series is too small to allow conclusions as to its effect on the survival; encouraging are the 2 patients without evidence of active disease. In women with inflammatory cancer at diagnosis and pleural effusion IFN-α should be tried.

References

1. Jereb B, Us-Krašovec M, Červek J, Šooš E. Intrapleural application of human leukocyte interferon (HLI) in breast cancer patients with ipsilateral pleural carcinomatosis. *J Interferon Res* 1987; **7**:357-63.
2. Raju RN, Kardinal CG. Pleural effusion in breast carcinoma: analysis of 122 cases. *Cancer* 1981; **48**:2524-7.
3. Izbicki R, Weyhing BT III, Baker I, Caoili EM, Vaitkevicius VK. Pleural effusion in cancer patients: a prospective randomized study of drainage with the addition of radioactive phosphorous to the pleural space vs. pleural drainage alone. *Cancer* 1975; **36**:1511-8.
4. Fentiman IS, Rubens RD, Hayward JL. Control of pleural effusions in patients with breast cancer. *Cancer* 1983; **52**:737-9.

5. Rosso R, Rimoldi R, Salvati F et al. Intrapleural natural beta interferon in the treatment of malignant pleural effusions. *Oncology* 1988; **45:**253-6.
6. Ostrowski MJ, Halsall GM. Intracavitary bleomycin in the management of malilgnant effusions: a multicenter study. *Cancer Treat Rep* 1982; **66:**1903-7.
7. Ostrowski MJ, Priestman TJ, Houston RF, Martin WMC. A randomized trial of intracavitary bleomycin and corynebacterium parvum in the control of malignant pleural effusions. *Radiother Oncol* 1989; **14:**19-26.

Adv Radiol Oncol 1992; 181–95.

Soft tissue sarcomas in childhood
Experience of the Austrian cooperative rhabdomyosarcoma study (A–RMS 82)
A final report

Ladenstein R, Grümayer ER, Hawliczek R, Krepler R, Fink FM, Haas H, Mutz I, Ploier R, Stöllinger O, Thun-Hohenstein L, Tulzer W, Urban C and Gadner H

From the Austrian Rhabdomyosarcoma Study Group. Cooperating centers: St. Anna Children's Hospital, Vienna (R.L., E.R.G., H.G.); Clinic of Radiation Therapy and Radiobiology, University Vienna (R.H.), Institut for Pathology, University Vienna (R.K.), Departments of Pediatrics: University of Innsbruck (F.M.F.), Kardinal Schwarzenberg'sches Krankenhaus, Schwarzach im Pongau (H.H.), Landeskrankehaus Leoben (I.M.), Landeskrankenhaus Steyr (R.P.), Krankenhaus der Barmherzigen Schwestern Linz (O.S.), University of Vienna (L.TH.), Landeskrankenhaus Linz (W.T.), University of Graz (C.U.);

Fifty–two children with soft tissue sarcomas were treated according to the Austrian Study A–RMS 82. First surgery included non–mutilating primary tumor removal or biopsy only. Stratification to treatment arms was based on site of primary tumor, stage of disease and response to initial multi–agent chemotherapy. Treatment duration was 36 weeks for clinical groups I to IIA and 56 weeks for clinical groups IIB, III and IV, respectively. Median age at diagnosis was 5.5 years, the median observation time 65 months. The overall complete response rate was 82.5%. The probability for overall survival was 71%, for event free survival (pEFS) 63% at 65 months. Protocol patients had a pEFS of 86% in clinical groups I to IIA and of 64% in clinical group III. Rapid tumor response to initial chemotherapy was a positive prognostic indicator. Extremity sites had an excellent 74% pEFS rate. Preservation of involved urogenital tract organs was achieved in all patients with this primary site. Early shifting of nonresponders to enhanced, six drug chemotherapy resulted in additional complete remissions. However, prognosis of patients with retroperitoneal sites and metastatic disease was poor.

Key words: rhabdomyosarcoma; child

Introduction

Soft tissue sarcomas (STS) represent about 10% of all malignant solid tumors in children[1] with rhabdomyosarcoma (RMS) as the most frequent. Treatment of RMS with surgery of radiotherapy alone or even a combination of both had been disappointing illustrated by an overall survival (SU) of 10%.[2] The addition of single[3,4] and later of multidrug chemotherapy to local treatment improved overall SU in a range from 28% to 37%.[5,6] Consequently, multimodality aproaches to treatment developed. They included surgical resection of primary tumors, radiotherapy to the tumor bed if microscopic disease remained and chemotherapy, reflecting the advancement through a variety of drug schedules. In this way considerable further improvement of survival

Correspondence to: Helmut Gadner, MD, (senior investigator)
St. Anna Children's Hospital, Kinderspitalgasse 6, A–1090 Vienna, Austria. Phone: 0043/222/40170/250

UDC: 616.74-006.364.04-053.2

rates within the range of 45% to 54% was achieved.[7-11] Various prognostic factors like primary site, stage of disease, histology and tumor response to chemotherapy were identified.[12-16] Compared to RMS less data are available about chemosensitivity and optimal treatment approaches for other STS in childhood.[17-21]

We report on 52 patients treated according to the cooperative Austrian Rhabdomyosarcoma Study A–RMS 82, which was designed in close collaboration with the German Soft Tissue Sarcoma Study Group.

The objectives of the study were: 1. Enrolling of all children with soft tissue sarcomas to a common treatment concept. 2. Avoidance of primary mutilating surgery, in particular in children with involvement of the urogenital tract. 3. Treatment intensification for extremity tumors. 4. Introduction of a six–drug salvage therapy in the early treatment phase in case of non–response to initial chemotherapy and for clinical group IV.

Patient and methods

A total of 52 patients were registered from January 1982 till September 1987 and received treatment in 9 pediatric centers in Austria. There were 29 male and 23 female patients with an average age of 5.5 years at diagnosis (range: 2 weeks to 18 years). Full evaluability required review of histopathology, chemotherapy, surgery and radiotherapy data.

Eligibility requirements have been fullfilled by 39 protocol patients (P pts). Thirteen patients were excluded from detailed survival analysis because of different pretreatment or violations of guiding principles, but have been followed as study patients (S pts).

Histology

Fourty patients (77%) presented with RMS. The distribution of histologies in the other 12 patients (23%) was as given: 2 primitive neuroectodermal tumors (PNET), 2 synovial sarcomas (SyS), 2 angiosarcomas, 2 spindle–cell sarcomas, 1 extrasceletal Ewing's sarcoma (EES), 1 hemangiopericytoma, 1 fibrosarcoma and 1 rhabdoid tumor. Within the RMS group 24 patients displayed the embryonal, 10 patients the alveolar and 2 patients the pleomorphic subtype. Four patients presented with undifferentiated RMS. Seven out of 15 patients with extremity sites exhibited the alveolar subtype.

Primary tumor sites and clinical groups

Details on the primary tumor sites and clinical groups of the 52 patients are shown in Table 1. treatment and course of disease are given in Table 2. The percentage of patients within clinical groups I to IV was 17%, 15%, 56%, and 12%, respectively. The most common site was the extremity (29%), followed by UG (17%). An equal number of patients was found for tumors of the orbit, other head and neck locations (orbit excluded) and retroperitoneal sites (UG and paratesticular sites excluded), each accounting for 11%. The remaining patients had tumors arising from paratesticular sites (8 %) and paraspinal sites (4%).

Diagnosis

Clinical evaluation. Initial stage of disease was assessed by a complete physical examination, x–ray, ultrasound and CT of primary tumor site to evaluate initial extent and size of tumor; complete blood count, complete serochemical

Table 1. Primary sites and clinical groups

Primary Sites	Number of Patients	Clinical Groups after First Surgery			
		I	II(A/B)	III	IV
Head & Neck	6	1		4	1
Orbit	6		1(1/0)	4	1
Thorax	4	1	2(2/0)		1
Paraspinal Sites	2		1(1/0)	1	
Urogenital Tract	9	1	1(1/0)	7	
Paratesticular	4	2			2
Retroperitoneal	6			4	2
Extremity	15	4	3(3/0)	7	1
Total	52	9	8	29	6

screening, bone marrow aspirate from the iliac crest, CT of the chest, abdominal ultrasonography and 99 Tc–total body scintigraphy, i.v. urography and lumbar puncture when indicated. All patients were grouped according to the modified Intergroup Rhabdomyosarcoma Study clasification[10] based on the extent of disease and type of primary surgery performed (Table 3).

Table 3. Clinical grouping.

GROUPS	CLASSIFICATION
I:	Localised disease, completely resected, regional lymphnodes negative.
IIA:	Grossly resected tumor with microscopic residual disease, regional lymph nodes negative.
IIB:	Grossly resected tumor (completely resected or microscopic residual disease), regional lymph nodes involved but resected.
III:	Incomplete resection or biopsy with gross residual disease with or without lymph node involvement.
IV:	Metastatic desease present at onset.

Definition of response

Response evaluation was based on local CT and/or ultrasonography. Second look surgery provided analysis of histological response. Complete response (CR) was defined as non evidence of disease. Partial response (PR) criteria were reduction to one third of the maximum tumor diameter after the first chemotherapy cycle and at least 50% reduction after the second course including dissappearance of all metastatic lesions, eventually. Non–response (NR) included persistence as well as progression of disease.

Study design (Figure 1)

Assignment to therapy arms. Patients were classified first to clinical groups I–IV according to the result of first surgery (biopsy only or resection) or due to metastatic disease. Second, all patients with localised extremity or urogenital (UG) tract tumors were assigned to the more intense treatment of clinical group III irrespective of initial post surgical grouping to reduce the

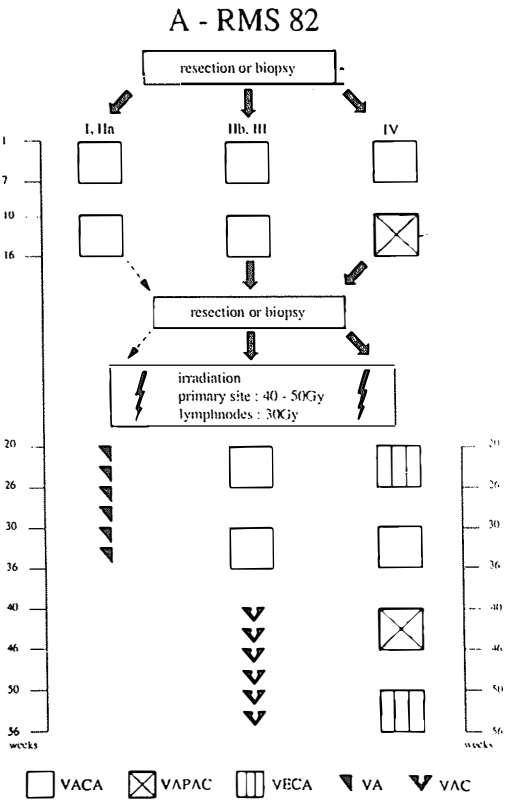

Figure 1 Schematic presentation of the Austrian Rhabdomyosarcoma Study 82. Treatment plan. VACA: vincristine (VCR), doxorubicin (ADR), cyclophosphamide (CYC), dactinomycin (AMD); VAPAC: VCR, ADR, cisplatin (CDDP), AMD, CYC; VECA: VCR, etoposid (VP16), CYC, AMD; VA: VCR, AMD; VAC: VCR, AMD, CYC;

known high risk of relapse in the former and to increase the chance of preserving UG organs in the latter. Patients with parameningeal tumor sites received intrathecal therapy in addition[22]. In case of tumor non–response to initial chemotherapy a third classification step was employed. These patients were shifted to the enhanced treatment arm as used for clinical group IV.

Systemic therapy. The initial chemotherapy for all patients was one VACA cycle (Figure 2) including vincristine (VCR), doxorubicin (ADR), cyclophosphamide (CYC) and dactinomycin (AMD). In clinical groups I–III a second VACA

Table 2. Patients characteristics at diagnosis, treatment strategy, response and outcome

Pts No. P/S	Sex	Age at Dx	Primary Site	Histology	Primary Tumor Size	Clinical Group / Treatment Arm	Response at Weeks 9 and 16	B / R Stage after S.L.S.	Irradiation Gy (local+ly.no. /+ met./+ lungs)	Clin. Status at CT end / Follow Up / Site of REL or OCD (mo after Dx)
14P	m	14.11yr	H & N	alveolar	> 10 cm	III / III	PR / CR	n.d	5O + 3O	CR / DOD / L.F.(23)
17S	f	15.9yr	H & N	pleomorph	> 10 cm	III / IV NR	NR / PR	B/IIA	7O (earlier)	CR / DOD / met.(29)
24P	m	0.5yr	H & N	undiff.	3 - 5 cm	III / III	CR / CR	B/I	n.d.	CR / NED
37P	m	11yr	H & N	embryonal	3 - 5 cm	III / III	PR / NR			PD / DOD
47P	f	13.11yr	H & N	embryonal	5 - 10 cm	IV / IV	PR / CR	R/I	4O /+25 /+15	CR / NED
48P	m	2.11yr	H & N	angio	< 3 cm	I / I				
8P	m	5.3yr	orbit	embryonal	3 - 5 cm	III / III	PR / CR	n.d.	4O	CR / NED
20S	m	2 weeks	orbit	rhabdoid	< 3 cm	II / IV NR	NR / PR	scar	5O	CR / NED
29P	m	8.1yr	orbit	embryonal	< 3 cm	III / III	CR / CR	B/IIA	5O	CR / NED
32S	m	12.9yr	orbit	hemangio	< 3 cm	III/IVNR	NR / PR	R/I	5O	CR / NED
40P	f	1.7yr	orbit	embryonal	< 3 cm	IV/IV	PR / PR	n.d.	5O /+4O	CR / OCD (MCCL(8))
52S	f	5yr	orbit	embryonal	< 3 cm	III/IVNR	NR / NR	R/IIA	5O	PD / DOD
2P	f	18yr	thorax	PNET	5 - 10 cm	I/I	CR / CR	n.d.	n.d.	CR / NED
25S	f	1.9yr	thorax	alveolar	5 - 10 cm	IV/IV	PR / CR	n.d.	50 + 3O /+5O	CR / NED
30P	f	0.4yr	thorax	undiff.	> 10 cm	II/III	CR / CR	n.d.	n.d.	CR / NED
39S	m	0.8yr	thorax	embryonal	3 - 5 cm	II/II	CR / CR	n.d.	n.d.	CR / NED
21P	f	11.10yr	paraspinal	undiff.	< 3 cm	II/II	CR / CR	n.d.	4O	CR / DOD / L.F.(10)
23P	f	1.4yr	paraspinal	EES	5 - 10 cm	III/III	CR / CR	n.d.	4O	CR / NED
5S	m	17yr	retroperit	angio	> 10 cm	III/III	PR / PR	n.d.	experimental	CR / LTFU
7P	f	17.4yr	retroperit	embryonal	> 10 cm	IV/IV	NR			PD / DOD
15P	m	12.7yr	retroperit	alveolar	> 10 cm	III/III	CR / CR	B/I	4O + 3O	CR / NED
33P	m	2yr	retroperit	embryonal	5 - 10 cm	III/III	PR / CR	B/I	4O + 3O	OCD (ARF(12))
44P	f	11.1yr	retroperit	undiff.	> 10 cm	III/III	PR / NR			PD / DOD
50S	m	4.7yr	retroperit	embryonal	> 10 cm	IV/IV	PR / PR	R/IIA	4O	PD / DOD

Table 2. Patients characteristics at diagnosis, treatment strategy, response and outcome

Pts No. P/S	Sex	Age at Dx	Primary Site	Histology	Primary Tumor Size	Clinical Group / Treatment Arm	Response at Weeks 9 and 16	B / R Stage after S.L.S.	Irradiation Gy (local + ly.no. /+ met./+ lungs)	Clin. Status at CT end / Follow Up / Site of REL or OCD (mo after Dx)
6P	m	5.6yr	urogenital	embryona	15 - 10 cm	III/III	PR / PR	B/I	5O + 3O	CR / NED
9P	m	0.9yr	urogenital	embryonal	> 10 cm	III/IVNR	NR / PR	R/IIA	5O + 3O	CR / NED
11P	m	2.3yr	urogenital	embryonal	< 3 cm	III/III	CR / CR	B/I	5O + 3O	CR / NED
13P	f	1.5yr	urogenital	embryonal	5 - 10 cm	III/IVNR	NR / CR	B/I	5O + 3O(earlier)	CR / NED
27P	f	4.6yr	urogenital	embryonal	> 10 cm	II/III	CR / CR	B/I	n.d.	CR / NED
36P	m	15.1yr	urogenital	embryonal	> 10 cm	III/III	PR / NR			PD / DOD
45P	m	1.2yr	urogenital	embryonal	5 - 10 cm	III/IVNR	NR / PR			PD / DOD
46P	m	1.5yr	urogenital	embryonal	> 10 cm	III/III	PR / PR	R/IIA	5O + 3O	CR / LTFU
34P	f	1.9yr	perianal	embryonal	< 3 cm	I/I	CR / CR	n.d.	n.d.	CR / NED
1P	m	3.4yr	paratest.	embryonal	3 - 5 cm	I/I	CR / CR	n.d.	n.d.	CR / NED
19P	m	14.7yr	paratest.	embryonal	3 - 5 cm	I/I	CR / CR	n.d.	n.d.	CR / NED
35S	m	16.4yr	paratest.	embryonal	3 - 5 cm	III/III	PR / PR	R/I	4O + 3O	CR / NED
43S	m	6.6yr	paratest.	spindle-c.	< 3 cm	III/III	CR / CR	B/I	n.d.	CR / NED
3P	f	15yr	extremity	PNET	3 - 5 cm	II/III	CR / CR	n.d.	4O + 3O	CR / NED
4P	f	2.8yr	extremity	alveolar	5 - 10 cm	III/III	PR / PR	R/I	4O + 3O	CR / NED
10P	m	2.7yr	extremity	embryonal	> 10 cm	III/IVNR	NR / PR	R/I	4O + 3O	CR / NED
12P	f	5.2yr	extremity	alveolar	5 - 10 cm	III / III	PR / CR	n.d.	5O + 3O	CR / DOD / met.(42)
16P	m	7.6yr	extremity	alveolar	3 - 5 cm	I / III	CR / CR	n.d.	4O + 3O	CR / NED
18S	f	2.7yr	extremity	spindle-c	5 - 10 cm	III / III	PR			/ DOD
22P	m	0.3yr	extremity	fibro	3 - 5 cm	III / III	PR / CR	R/I	4O + 3O	CR / NED
26P	f	7.2yr	extremity	alveolar	5 - 10 cm	III / III	PR / CR	B/I	5O + 3O	CR / NED
28P	m	14yr	extremity	embryonal	< 3 cm	I / III	CR / CR	B/I	4O + 3O	CR / NED
31P	f	9.11yr	extremity	SyS	< 3 cm	III / IV NR	NR / PR	n.d.	5O + 3O	CR / NED / met.(1O)
38P	m	16yr	extremity	SyS	3 - 5 cm	I / III	CR / CR	n.d.	5O + 3O	CR / DOD / met.(28)
41S	f	8.6yr	extremity	alveolar	5 - 10 cm	IV / IV NR	PR / NR			PD / DOD
42P	m	2yr	extremity	alveolar	5 - 10 cm	II / IV NR	NR / CR	earlier	5O + 3O	CR / NED
49S	f	13.11yr	extremity	alveolar	> 10 cm	II / III	CR / CR	n.d.	4O + 3O	L.F.(7) / NED
51P	f	1yr	extremity	pleomorph	3 - 5 cm	I / III	CR / CR	B/I	40 + 3O	CR / NED

Pts No: patients number, P/S: protocol or study patient, DX: diagnosis, S.L.S.: second look surgery, B/R: biopsy or resection, ly. no.: lymph nodes, met: metastases, mo: months, m: male, f: female, yr: years, H&N: head and neck, undiff.: undifferentiated RMS, angio: angiosarcoma, rhabdoid: rhabdoid tumor, hemangio: hemangiopericytoma, Pnet: peripheral neuroectodermal tumor, EES: extra-osseous Ewing's sarcoma, spindle-c: spindle-cell sarcoma, fibro: fibrosarcoma, SYS: synovial sarcoma, CR: complete response, PR: partial response, NR: non-response, NED: no evidence of disease, L.F.: local failure, PD: progressing disease, DOD: dead of disease, OCD: other cause of death, LTFU: lost to follow up, ARF: acute renal failure, MCCL: megacaryocytic leukemia

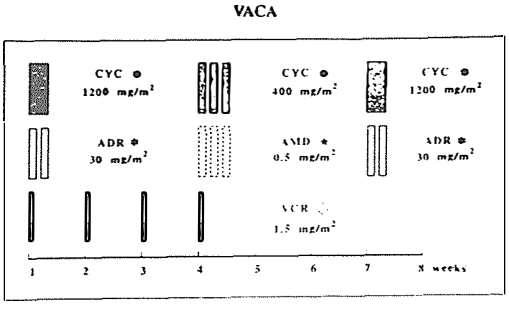

Figure 2. VACA Treatment schedule. VACA: vincristine (VCR), doxorubicin (ADR), dyclophosphamide (CYC), dactinomycin (AMD).

cycle was applied. Clinical group IV and patients with non–response to the first VACA cycle received as second cycle VAPAC, a modification of VACA, in which CYC was replaced by cisplatin (CDDP, 120mg/sqm, day 3) at weeks 1 and 7.

Further chemotherapy for clinical groups I and IIA consisted of six pulses of VA (VCR–1.5mg/sqm and AMD: 1.5mg/sqm) in a three week interval. Clinical groups IIB and III received two more VACA cycles and 6 further VAC pulses (VCR: 1.5mg/sqm, AMD: 1.5mg/sqm and CYC: 20mg/kilogramm). In clinical group IV ADR was replaced by etoposide (VP16: 150mg/sqm, days 1-3) at weeks 1 and 7 in the third cycle called VECA. The first three cycles were then repeated in this group once more. Thus treatment duration was 36 weeks for clinical groups I and IIA and 56 weeks for clinical groups IIB, III and IV, respectively.

Patients with parameningeal tumors received additional intrathecal chemotherapy eight times during the first 16 weeks. The age adapted dosage was for infants, children of 1-2 years, 2-3 years and for those older than 3 years for methotrexate: 6mg/ 8mg/ 10mg/ 12mg, for cytosin–arabinosid: 20mg/ 26mg/ 34mg/ 40mg and for hydrocortisone: 4mg/ 6mg/ 8mg/ 10mg, respectively.

Local Treatment. The issue of initial surgery was non–mutilating tumor removal or assessment of histology by biopsy only. Second look surgery was demanded for patients with residual disease at week 16 and had the purpose of radical resection. Patients in clinically complete remission at week 16 were desired to have biopsies of the primary tumor region to assess their histological remission.

Radiotherapy was timed after second look surgery for local tumor control as well as distant tumor sites, using super–voltage equipment with wide margins. Patients in clinical groups I and IIA received non radiation therapy except for tumors of extremity and urogenital sites or in case of proven microscopic residual disease for clinical group IIA at second look surgery. In all other patients local irradiation with 40 Gy (fraction size 1.8 Gy, 5-6 times per week) was applied within 5 to 6 weeks. If residual disease remained at second look surgery, a boost to 50 Gy was given. The first, non–involved lymph node level was irradiated with a dose of 30 Gy in all patients. In cases of primary lymph node involvement irradiation with 40 to 50 Gy was given, depending on histological response. The next negative lymph node level was irradiated to 30 Gy in these cases. Metastates were irradiation up to 40 to 50 Gy, depending on local organ tolerance as dose limiting factor. In parameningeal sites the base of the scull was included into the radiation field for the high risk of tumor extension to the meninges and brain. In patients with documented involvment of the base of the skull the neurocranium was irradiated to 30 Gy in addition. In case positive liquor cytology the neuroaxis was also irradiated to 30 Gy.

Statistical methods

Probability estimates of overall survival (SU) and event–free survival (EFS) were obtained by the Kaplan–Meier method.[23] For the latter, the events of interest were failure to achieve complete reponse, relapse, or death from any cause. The starting point for survival time was the date of primary treatment; statistical analysis was performed on February 15, 1990 at a median

Table 4. Response analysis in clinical group II & IV patients

Clin. Group	Response Week 7 No of Pts	Treatm. Arm	Response Week 16 No of Pts	No of Pts/ S.L.S.(B/R) (Histol. Result)	No of Pts/ Follow Up No of pts
III	CR/6	III	CR/6	4 B (4 I)/1 n.d. 1 B (IIA)	6 NED
PR/15	III	CR/6	2 B (I)	1 NED/1 OCD 1 R (I) 3 n.d.	1 NED 1 NED/2 DOD
			PR/5	1 B (I)/1 n.d. 2 R (1 I, 1 IIA)	1 NED/1 LTFU 2 NED/1 LTFU
			NR/4		4 DOD
NR/8	IV NR	CR/1	1 B (I)	1 NED	
			PR/6	3 R (2 I, 1 IIA) 1 R (IIA) 2 n.d.	3 NED 1 DOD 1 NED/1 DOD
			NR/1	1 R (IIA)	1 DOD
IV	PR/5	IV	CR/2	1 R (I)/1 n.d.	2 NED
			PR/2	1 R (IIA)/1 n.d.	1 DOD, 1OCD
			NR/1	1 n.d.	1 DOD
	NR/1	IV			1 DOD

No of Pts: number of patients, S.L.S.: second look surgery, DOD: dead of disease, OCD: other cause of death, LTFU: l B/R: biopsy or resection, CR: complete response, PR: partial ost to follow up
response, NR: non-response, NED: no evidence of disease,

follow up of 65 months, range 32 to 97 months. Differences between survival patterns were evaluated by the log–rank test.

Results

Primary tumor sites

Orbit

Six patients had tumors of the orbit. Embryonal RMS was found in 4 patients, a hemangiopericytoma and a rhabdoid tumor in two further ones. One girl (no. 52) with embryonal RMS neither responded to the intensified treatment arm and irradiation nor surgery was effective in terms of tumor control. She died with progressing disease and brain involvement. One girl (no. 40) developed megakaryocytic leukemia 1 month after termination of treatment. Four patients are in remission with preserved eyes and were all treated according to protocol criteria.

Head and neck

Six patients presented with the head and neck as primary site, two of them with parameningeal locations (patients no.37 and 17). Three patients with undifferentiated sarcoma, angiosarcoma and embryonal RMS, respectively, fared well. The boy (no.37) with embryonal RMS of the epipharynx developed lung metastases before local treatment was iniated after a very good local response to the first two VACA cycles. The girl (no.17) with pleomorphic RMS of the nasal cavity responded to the NR treatment arm, but suffered a distant relapse 29 months after diagnosis. A boy (no.14) with alveolar RMS of the right cervical side sustained a local relapse 23 months after diagnosis.

Urogenital tract

Embryonal RMS was found in all 8 patients with the urogenital tract as primary site. An adolescent (no.36) with embryonal RMS of the bladder/prostate achieved PR with initial chemotherapy, but died with cerebral metastases, which were not observed on the initial cranial cat scan. Another patient with involvement of the bladder (no.45) developed again progressing disease after a PR to the enhanced treatment arm. Five patients, 3 with the bladder and 2 with the prostate as primary tumor site, are long term survivors. One patient with the bladder as primary site was lost to follow up. None of them required radical surgery at week 16. Urinary bladder dysfunction was not observed in these patients. One girl (no.34) had a primary perianal tumor resembling embryonal RMS.

Paratesticular sites

Four patients were found with this primary site, 3 tumors were classified as embryonal RMS and 1 as spindle–cell sarcoma. All of them are in continuous complete remission.

Thorax

Three patients presented with tumors of the chest wall classified as PNET, alveolar RMS and undifferentiated sarcoma, respectively. An infant (no.30) was the only patient with an intra–thoracal tumor involving the mediastinum. In this case radiation therapy was omitted due to the risk of heart disease. All these patients are alive with no evidence of disease.

Retroperitoneal sites

Patients with retroperitoneal tumors faired poorly. Five children presented with hughe tumors of more than 10 cm in diameter, one with a tumor of 5-10 cm. The histologies in this group were 3 embryonal RMS, 1 alveolar RMS, 1 undifferentiated sarcoma and 1 angiosarcoma. The boy (no. 5) with angiosarcoma had involvement of muscles of the gluteal and iliac region. He suffered of associated symptoms like loss of stool, dysuria and palsy of one leg. He achieved PR after initial chemotherapy. Tumor related symptoms had improved. He was selected for experimental radiation with heavy particles (negative pions) in Villingen, Switzerland, because surgery for residual disease would have caused paraplegia. At the end of treatment he had a normal walking function, but his bladder function remained impaired. There was no evidence of disease at treatment termination, but he was then lost to follow up. Three patients died with progressing disease, another one (no.33) in CR with treatment related acute renal failure at the end of therapy.

Extremities

Extremities were the most common primary site and were observed in 15 children. Pathohistology revealed 10 RMS (7 alveolar, 2 embryonal, 1 pleomorph), 2 SyS, 1 PNET, 1 fibrosarcoma and 1 spindle–cell sarcoma. Eleven patients are alive with no evidence of disease. A girl (no.49) with trisomy 21 experienced the only early local relapse 7 months after diagnosis while still on therapy. This relapse appeared at the margin of the radiation field and higlights the importance of safety clearance of tumor margins. Patient no.31 had synovial sarcoma of the right hand. She suffered distant relapses. The latter two patients responded to relapse chemotherapy and are alive in complete remissions. A girl (no.18) with spindle–cell sarcoma of the right forearm achieved PR after 16 weeks. Further treatment was omitted by her parents and she died with lung metastases after palliative amputation. A girl with alveolar RMS of the forearm (no.12) suffered a late distant relapse 42 months after diagnosis. Another girl (no.41) with alveolar RMS of the thigh developed progressing disease after intermediate PR to enhanced chemotherapy.

Others

Two patients had tumors originating from paraspinal sites. One of them (no.21) experienced a local relapse 10 months after diagnosis and died.

Response to treatment

Forty–three patients (pts) achieved complete remission at various points of time during the treatment course. Thus the overall complete response rate was 82.5%. The response behaviour of clinical groups during the first 16 weeks is demonstrated in detail on Tables 2 & 4. A total of 35 children (67.3%) responded to treatment well. After initial surgery and the first VACA cycle 15 children in clinical groups I and II were in CR and 6 children in clinical group III. Eight further patients achieved CR (clinical groups III: 6 pts and IV: 2 pts) after the second VACA cycle. Second look surgery obtained CR in 3 patients in clinical group III. Finally, radiation therapy attributed to CR in 3 children in clinical groups III (2 pts) and IV (1 pt).

Eight patients (15.4%) with initial poor or no–response achieved CR after shifting to enhanced chemotherapy. Three patients received additional local treatment before week 16. Two of them (no.31,42) had early second look surgeries for tumor progression, the other one (no.13)

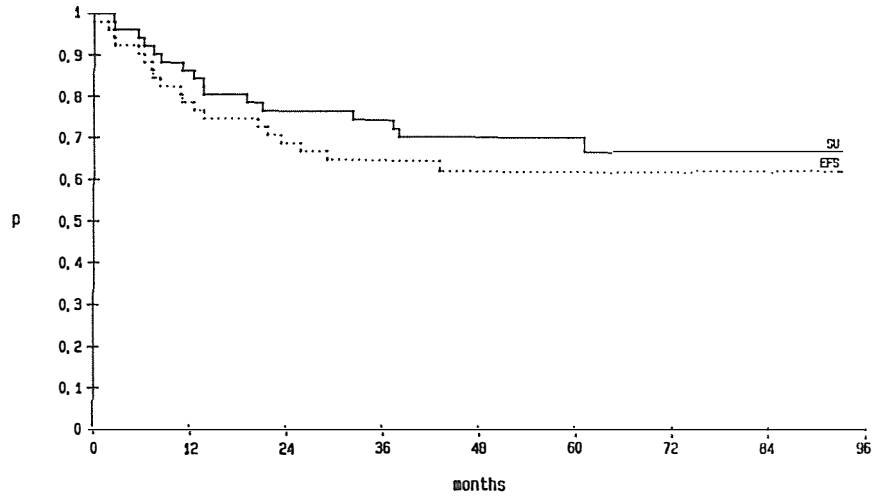

Figure 3. Probability (p) of overall and event-free survival for all 52 children with soft tissue sarcomas in the A-RMS 82 Study.

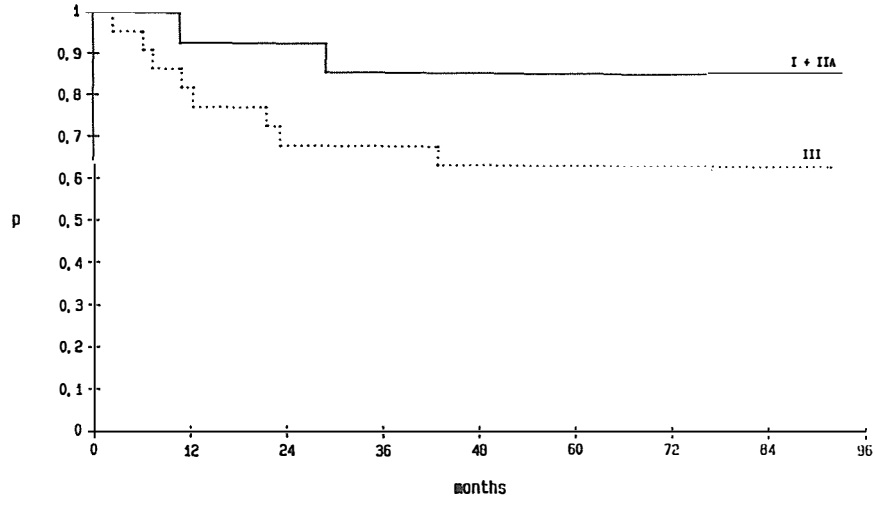

Figure 4. Probability (p) of event-free survival for 14 protocol patients in clinical groups I and IIA compared to 22 protocol patients in clinical group III, all treatments combined.

early irradiation. Out of the latter patient group, 2 children of clinical groups II an III (no.13, no.43) were in CR by week 16. Second look surgery at week 16 assisted to obtain CR in 2 patients belonging to clinical group III. Radiation therapy resulted in CR in further 3 patients of clinical groups II (pt no.20) and III (pts no.9, no.31). One patient (no.17) was in CR at termination of chemotherapy.

Seven patients (13.5%) of clinical groups III (5 pts) and IV (2 pts) achieved only partial remissions. Four of them died during initial treatment, the other three after week 16. Two

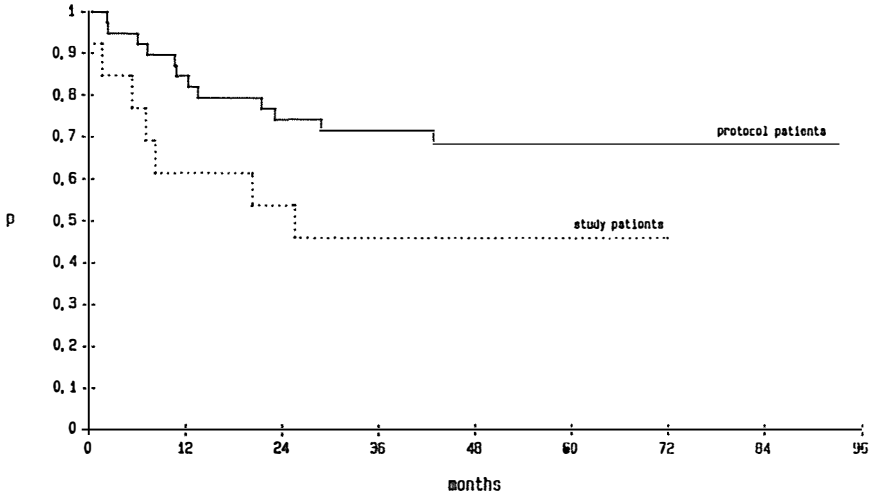

Figure 5. Probability (p) of event-free survival for the 39 protocol patients and 13 study patients in the A-RMS 82 Study.

patients (3.8%) were non-responders to chemotherapy and died with disease progression.

Relapses occured in 8 patients (15.4%) with initially localised disease, four experienced local failure and four developed distant metastases. Five of them died, but 3 achieved CR again by salvage treatment (relapse regimen included: ifosfamide 3g/m^2, days 1-2; CDDP 20mg/m^2, days 1-5; VP-16 150 mg/m^2, days 3-5;)

Fifteen (28.8%) patients died. Two deaths were treatment related (acute renal failure, septicemia), one child died due to a second malignancy (megakaryocytic leukemia), 5 patients died in relapse and 7 patients due to pregressive disease.

Survival analysis

Statistical evaluation of all patients demonstrated a probability (p) for overall SU and EFS of 71% and 63%, respectively, at 65 months (Figure 3). The estimation of EFS in clinical groups I to IIA was 86%, in clinical groups III 64%, respectively, with no statistical difference (Figure 4). The pEFS of protocol and study patients differed slightly ($P < 0.1$; Figure 5). The pEFS of RMS versus all other STS was 71% and 62% at 65 months, demonstrating no statistical difference (Figure 6). The 65-months EFS estimation for extremity sites was 74%. There was no significant statistical difference in comparison to other primary sites (orbit and paratesticular sites: pEFS 80%, UG tract organs: pEFS 71%, all other primary sites: pEFS 60%; Figure 7). The pEFS estimation for alveolar RMS was 83% and for embryonal RMS 67% at 65 months revealing no statistical difference. Response evaluation at week 7 estimated 89% for EFS in CR pts (n=18), 50% in PR pts (n=14) and 57% in NR pts (n=7) at 65 months. The pEFS of PR and NR patients demonstrated in comparison to CR patients p-values of < 0.05 and < 0.1, respectively. Statistical evaluation of the response at week 16 showed the following pEFS at 65 months: 80% for CR pts (n=27), 62% for PR pts (n=8) and 0% for NR pts (n=3). There was no statistical difference for PR in comparison to CR, but for NR a p-value < 0.01 occurred.

Discussion

Soft tissue sarcomas remain a challenge concerning the optimal treatment approach. The pre-

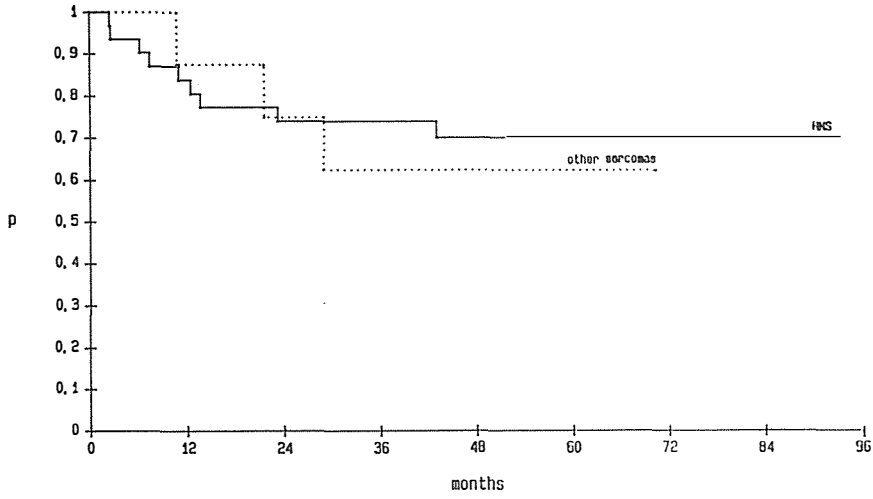

Figure 6. Probability (p) of event-free survival for protocol patients in the A-RMS 82 Study by major histological groups (31 rhabdomyosarcoma, 8 other soft tissue sarcomas)

sented national A–RMS 82 study was the first standardized, risk adapted treatment concept for STS in childhood in Austria and achieved an overall SU and EFS estimate of 71% and 63% at 65 months.

The favourable results of the A–RMS 82 study may be attributed to the following factors. Surgery had distinct purposes in the treatment plan aiming either at nonmutilating primary tumor removal, resection of residual disease or after assessment of remission. Thus it assisted to determine risk–adapted radiation dose, namely 40 Gy for stage III or 50 GY, if residual disease remained at S.L.surgery. This is in accordance with Etcubanas et al.[24], who concluded that delayed surgery permits the use of lowerdose radiotherapy. The inclusion of the first lymph node level neighbouring the primary tumor site for non–detected, microscopic tumor involvement, or the next non–involved lymph node level was part of the A–RMS 82 radiation concept, being supported by the following reports. A review by Lawrence et al[25] showed a 10% incidence of identifiable lymphatic tumor spread for 1415 IRS I and II patients without distant metastases and a 14% incidence for RMS patients. The proportion of patients in the latter group was the highest for prostate (41%), paratesticular sites (26%), GU sites overall (24%) and finally extremity lesions (12%). Heyn et al reported a 35% incidence of nodal involvement in patients with alveolar RMS of the extremities when 60% had their regional nodes biopsied[26]. Ghavimi et al even observed a 40% incidence when surgical–histological information was obtained in 80% of the patients.[27] The report of Lawrence[25] demonstrated a lower survival expectancy in patients with disease extension to lymph nodes. Their 3–year SU estimate was 54% versus 78% for patients without lymphatic metastatic disease. Furthermore, patients of clinical groups I and II with tumors involving the extremity or the UG sites received intensified treatment in our study and thus experienced improvement of SU expectancy. Finally, high risk patients (non–responders and stage IV patients) were shifted to enhanced chemotherapy which resulted in additional complete remissions. Similar potential effect of CDDP and VP 16 were also observed by Crist et al.[27] and Carli et al.[28] Study patients, whose sequence of therapy elements varied or who suffered a treatment delay, did not fare as well as protocol patients, demonstrated by an pEFS of 46% versus 69%. Variations

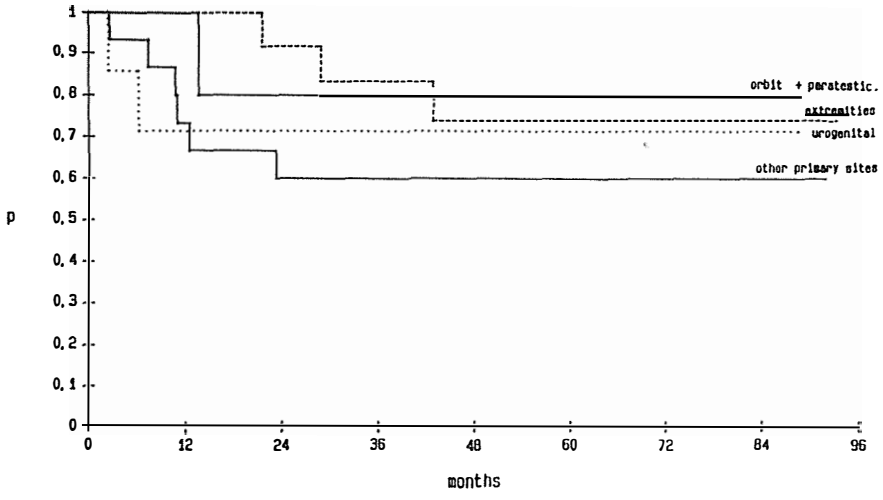

Figure 7. Probability (p) of event-free survival for protocol patients in the A-RMS 82 Study by primary site groups (5 orbit and paratesticular sites, 12 extremity sites, 7 urogenital tract primaries, 15 other primary sites).

and delay of treatments were correlated with poorer tolerance for treatment in some cases, but nevertheless stress the importance of a consequent treatment according to the given guidelines whenever possible.

A pEFS of 71% for RMS and 62% pEFS for all other STS showed an overall satisfactory response of the rare soft tissue sarcomas. Various types of STS, apart from RMS, were also analyzed by the German CWS–81 study which demonstrated relapse free survival (RFS) rates of 66% in SyS, 48% in EES and 38% in undifferentiated sarcomas, respectively.[21] Both results highlighted the chemosensitivity of STS and the positive impact of multimodality treatment approaches for these rare childhood sarcomas.

In the A-RMS 82 study prognosis related to the various primary sites was comparable to results reported. Only in patients with extremity sites we observed a more favourable results. Primary tumors of the orbit[29] and the paratesticular sites[30] were emphasized for their extremely good prognosis with survival data in the range from 80% to 94%. A pEFS of 80% was achieved for these sites in our study. Parameningeal sites were observed to carry a high risk of spread to the CNS and thus revealed inferior RFS rates of 45% versus 75% in other head and neck areas, exluding the orbit.[31] Our two patients with this primary site were lost despite intense treatment along with intrathecal therapy in addition. An EFS of 74% was recently reported for patients with GU tract primaries[10], including the bladder, prostate, the paratesticular sites and the female reproductive organs. Excluding the paratesticular site from analysis a relapse–free survival of 67% was demonstrated by Treuner et al.[11] Our study showed a pEFS of 71% for UG sites (paratesticular sites excluded). Since only about 20% of bladder RMS arise from the dome where primary partial resection is possible, this site remains a challenge for organ preserving treatment. The majority of tumors developed from the bladder base, the trigonal area, the bladder neck and often infiltrate the prostatic urethra as also observed in our study. Therefore, differentiation between primary bladder or prostate RMS was often difficult.[32] Our study along with others[10,11,33] demonstrated that anterior pelvic exenteration and urinary diversion can be avoided with the current multimodality treament. All our patients retained their bladder and do well without therapy sequelae and functional deficit. In general, retroperitoneal sites have an

inferior prognosis due to significantly larger tumors at diagnosis exceeding more than 10 cm in diameter, often in combination with disseminated disease. They are often unresectable and difficult to irradiate because of the limited tolerance of adjacent tissues. Ransom et al reported 28% DFS fot this primary site[34], whereas Crist et al demonstrated an improved prognosis of 42% RFS at 3 years in the IRS studies I&II.[35] In our study, four out of six patients died, three with disease progression and one because of acute renal failure. The poor outocome for patients with primary metastatic disease (2 pts out of 6 pts alive) and of those who relapsed (3 pts out of 8 pts alive) was similar in our study as in previously reported series.[10,11,36,37]

Ten cases were classified as alveolar RMS and occurred particularly in patients with the extremity as primary tumor site (7 pts). Alveolar histology did not appear as a poor risk factor in our study. The pEFS for RMS of the alveolar subtype was 83% versus 67% for embryonal RMS and 62% for other sarcomas. This is in contrast to literature, where the alveolar subtype is considered a poor prognostic indicator[14,15,38], with disease free survival (DFS) estimates in a range from 23% to 43%.[11,16] Ghavimi et al. reported an estimated 5-year survival rate of 44% for RMS of the extremity.[26] In the IRS studies an improvement of DFS up to 73% was achieved after the introduction of treatment intensification with radiation to 45 Gy for group II, but no irradiation for group I.[26] Should one irradiate group I patients with alveolar extremity sites or not? This issue still remains controversial. The German CWS-81 study group concluded that stage I and II patients do need irradiation for local tumor control. They observed improvement of RFS from 0% (7pts) to 61% (11pts) after the introduction of intensified local treatment.[11] In the A-RMS 82 study the 5-year pEFS was 72% for all STS extremity tumors. Amputation was not performed in any of the RMS patients. The favourable result of alveolar RMS in our hands should be explained by the intensified treatment regimen used for extremity sites. The remaining three patients with alveolar RMS also received a similar intensive therapy since they were part of clinical groups III and IV. We conclude that the risk of alveolar histology can be modifed by more agressive chemotherapy and that radiation is necessary to assure local control.

Owing to diseases, which made radical, nonmutilating resection impossible as well as due to location or extent of the tumors, most of our children were assigned to clinical group III. Analysis of chemotherapy reponse of the clinical groups III and IV revealed a superior survival of patients achieving CR till week 7 compared with CR patients at week 16. Partial responders may still be treated successfully by effective local means. However, patients with NR to the first line chemotherapy required intensification with additional cytostatic agents, such as CDDP and VP-16. Our study demonstrated a 89% probability for CR patients at week 7 and 80% for the CR group of patients at week 16. NR patients at week 7 still had an estimated 57% EFS at week 7 versus 0% for those still non-responding at week 16, which highlights the efficacy of the enchanced treatment arm and the positive prognostic impact of early complete response.

Conclusion

From these results, we conclude that STS in childhood can be successfully treated by integration of rational, delayed surgical resection in combination to enhance the prospect for local tumor control and long term survival in children with primary unresectable, localised disease without severe functional or cosmetic sequelae. In accordance, the German CWS-81 study[15,39] demonstrated, based on multivariate analysis of 129 available patients, that the response per unit of time was an important prognostic factor.

Acknowledgments

The authors are indebted to Mag. Irmgard GATTERER-MENZ for statistical analysis and Chri-

stine BÖHM for assistance in collection of clinical data. They also thank O.A. HAAS, MD, for reviewing the manuscript.

References

1. Heyn RM. The role of chemotherapy in the management of soft tissue sarcomas. *Cancer* 1975; **35**:921-4.
2. Pratt CB, Hustu HO, Flemming ID, Pinkel D. Coordinated treatment of childhood rhabdomyosarcoma with surgery, radiotherapy, and combination chemotherapy. *Cancer Res* 1972; **32**:606-10.
3. Pinkel D, Pickren J. Rhabdomyosarcoma in children. *JAMA* 1961; **1975**:293-8.
4. Ortega JA, Rivard GE, Isaac H, Hittle RE, Hays DM, Pike MC, Karon MR: The influence of chemotherapy on the prognosis of rhabdomyosarcoma. *Med Pediatr Oncol* 1975; **1**:227-34.
5. Sutow WW, Sullivan MP, Ried HL, Tailor HG, Griffith KM. Prognosis in childhood rhabdomyosarcoma. *Cancer* 1970; **25**:1384-90.
6. Grosfeld JL, Weber TR, Weetman RM, Beahner RL. Rhabdomyosarcoma in childhood: Analysis of survival in 98 cases. *J Pediatr Surg* 1983; **18**:141-6.
7. Heyn R, Holland R, Joo R, Johnson D, Newtown W Jr, Tefft M, Breslow N, Hammond D. Treatment of rhabdomyosarcoma in children with surgery, radiotherapy and chemotherapy. *Med Pediatr Oncol* 1977; **3**:21-32.
8. Kingston JE, McElwain TJ, Malpas JS. Childhood rhabdomyosarcoma: Experience of the children's solid tumor group *Br J Cancer* 1983; **48**:195-207.
9. Flamant F, Hill C. The improvement in survival associated with combined chemotherapy in childhood rhabdomyosarcoma. A historical comparison of 345 patients in the same center. *Cancer* 1984; **53**:2417.21.
10. Maurer HM, Beltangady M, Gehan EA, Crist W, Hammond D, Hays DM, Heyn R, Lawrence W, Newton W, Ortega J, Ragab AH, Raney RB, Ruyman FB, Soule E, Tefft M, Webber B, Wharam M, Vietti T. The Intergroup Rhabdomyosarcoma Study-I. A final report. *Cancer* 1988; **61**:209-20.
11. Treuner J, Kaatsch P, Anger Y, Seipp A, Spaar HJ, Gerein V, Suder J, Niethammer D. Treatment results in rhabdomyosarcomas in children: Cooperative soft tissue sarcoma study (CWS-81) of the german society of pediatric oncology. *Klin Pädiatr* 1986; **198**:208-17.
12. Neifeld JP, Maurer HM, Godwin D, Berg JW, Salzberg AM: Prognostic variables in pediatric rhabdomyosarcoma before and after multimodality therapy. *J Pediatr Surg* 1979; **14**:699-703.
13. Gehan EA, Glover FN, Maurer HM. Prognostic factors with rhabdomyosarcoma. *Natl Cancer Inst Monogr* 1981; **56**:83-92.
14. Hays DM, Newton W, Soule EH, Foulkes MA, Raney RB, Tefft M, Ragab A, Maurer HM: Mortality among children with rhabdomyosarcoma of the alveolar histologic subtype. *J Pediatr Surg* 1983;**18**:412-7.
15. Suder J, Stienen U, Kaatsch P, Harms D, Schmidt D, Sppar HJ, Treuner J. Univariate and multivariate analysis of prognostic factors in childhood rhabdomyosarcoma: A preliminary report from the german soft tissue sarcoma study (CWS-81). *Klin Pädiatr* 1986; **198**:218-23.
16. Rodary C, Rey A, Olive D, Flamant F, Quintana E, Brunat-Mentigny M, Otten J, Youte P. Prognostic factors in 281 children with nonmetastatic rhabdomyosarcoma at diagnos. *Met Pediatr Oncol* 1988; **16**:71-7.
17. Soule EH, Newton W, Moon TE, Tefft M. Extrasceletal Ewing's sarcoma. A preliminary review of 26 cases encountered in the Intergroup Rhabdomyosarcoma Study. *Cancer* 1978; **42**:259-64.
18. Marina NM, Etcubanas E, Parham DM, Browman LC, Green A. Peripheral primitive neuroectodermal tumor (peripheral neuro-epithelioma) in children. A review of the St. Jude experience and controversies in diagnosis and managemant. *Cancer* 1989; **64**:1952-60.
19. Ortega JA, Finkelstein JZ, Isaak H, Hittle R, Hastings N. Chemotherapy of malignant hemangiopericytoma of childhood. *Cancer* 1971; **27**:730-5.
20. Atkinson JB, Mahour GH, Issak H, Ortega J. Hemangioperictoma in infancy and children. *Am J Surg 1984;* **148**:372-4.
21. Treuner J, Suder J, Gerein V, Beck J, Winkler K, Weinel F, Gnekov A, Niethammer D: Results of the treatment of non-rhabdomyosarcomatous soft tissue neoplasms within the scope of the CWS-81 study. *Klin Pädiatr* 1987; **199(3)**:209-17.
22. Raney RB, Tefft M, Newtown W, Ragab AH, Lawrence W, Gehan EA, Maurer HM. Improved prognosis with intensived treatment of children with cranial soft tissue sarcomas arising in nonorbital parameningeal sites. A report from the intergroup rhabdomyo-sarcoma study. *Cancer* 1987; **59**:147-55.
23. Peto R, Pike MC, Armitage P: Design and analysis of randomized clinical trials requiring prolonged observation of each patient. *Br J Cancer* 1977; **35**:1-39.
24. Etcubanas E, Rao B, Kun L, Horowitz ME, Parham DM, Hustu O, Green A. The impact of delayed surgery on radiotherapy dose and local control of rhabdomyosarcoma. *Arch Surg* 1987; **122**:1415-4.
25. Lawrence W, Hays D, Heyn R, Tefft M, Crist W, Beltangady M, Newton W Jr, Wharam M. Lymphatic metastases with childhood rhabdomyosarcoma. A report from the intergroup rhabdomyosarcoma study. *Cancer* 1987; **60**:910-5.
26. Heyn R, Beltangady M, Hays D, Lawrence W, Newton W, Crist W, Tefft M, Maurer HM: Results of intensive therapy in children with localised alveolar extremity rhabdomyosarcoma: A report from the intergroup rhabdomyosarcoma study. *J Clin Oncol* 1989; **7**:200-7.
27. Crist WM, Raney RB, Ragab A, Heyn R, Wharam M, Webber B, Johnston J, Beltangady M. Inten-

sive chemotherapy including cisplatin with or without etoposid for children with soft-tissue sarcomas. *Med Pediatr Oncol* 1987; **15**:51-7.
28. Carli M, Perilongo G, Cordero di Montezemolo L, De Barnardi B, Ceci A, Paolucci G, Pianca C, Calculli G, Di Tullio MT, Grotto P, Tamaro P, Pastore G. Phase II trial of cisplatin and etoposid in children with advanced soft tissue sarcoma: A report from the italian cooperative rhabdomyosarcoma study group. *Cancer Treat Report* 1987; **71(5)**:525-7.
29. Wharam M, Beltangandy M, Hays D, Heyn R, Ragab A, Soule E, Tefft M, Maurer H. Localised orbital rhabdomyosarcoma. An interim report of the intergroup rhabdomyosarcoma study comittee. *Ophthalmology* 1987; **94(3)**:251-4.
30. Raney RB, Tefft M, Lawrence W, Ragab AH, Soule E, Beltangady M, Gehan EA. Paratesticular sarcoma in childhood and adolescence! A report from the intergroup rhabdomyosarcoma studies I and II, 1973-1983. *Cancer* 1987; **60**:2337-43.
31. Sutow WW, Lindberg RD, Gehan EA, Ragab AH, Raney RB, Ruyman F, Soule EH: Three-year relapse-free survival rates in childhood rhabdomyosarcoma of the head and neck. Report from the Intergroup Rhabdomyosarcoma Study. *Cancer* 1982;**49**:2217-21.
32. Burger RA, Riedmiller H, Gutjahr P, Hohenfeller R. Extent of surgery in rhabdomyosarcoma of urogenital structures. *Eur Urol* 1989; **16(2)**:114-22.
33. Ortega JA. A therapeutic approach to childhood pelvic rhabdomyosarcoma without pelvic exenteration. *J Pediatr* 1979; **94**:205-9.
34. Ransom L, Pratt CB, Hustu O. Retroperitoneal rhabdomyosarcoma in children. *Cancer* 1980; **45**:845-9.
35. Christ WM, Raney RB, Tefft M, Heyn R, Hays MD, Newton W, Beltangady M, Maurer HM. Soft tissue sarcomas arising in the retroperitoneal space in children. A report from the intergroup rhabdomyosarcoma study (IRS I) comittee. *Cancer* 1985; **56**:2125-32.
36. Okamura J, Sutow WW, Moon E. Prognosis in children with metastatic rhabdomyosarcoma. *Med Pediatr Oncol* 1977; **3**:243-51.
37. Raney RB, Crist WM, Maurer HM, Foulkes MA. Prognosis of children with soft tissue sarcomas who relapse after achieving a complete response. A report from the intergroup rhabdomyosarcoma study I. *Cancer* 1983; **52**:44-50.
38. Newton WA Jr, Soule EH, Hamoudi AB, Reiman HM, Shimada H, Beltangady M, Maurer H. Histopathology of childhood sarcomas, intergroup rhabdomyosarcoma studies I and II: Clinicopathological correlation. *J Clin Oncol* 1988; **6(1)**:67-75.
37. Treuner J, Suder J, Keim M, Kaatsch P, Niethammer D. The predictive value of initial cytostatic response in primary unresectable rhabdomyosarcoma in children. *Acta Oncol* 1989; **28(1)**:67-72.

Adv Radiol Oncol 1992; 196–201.

Our experience in treating children with osteogenic sarcoma

Benedik–Dolničar M

University Medical Centre Ljubljana
University Department of Pediatrics

Results of 10 patients with high grade osteogenic sarcoma are reported. 8 were primary osteogenic sarcomas, and 2 were secondary osteogenic sarcomas. Immediately after fine needle aspiration biopsy or open biopsy the patients were treated with chemotherapy using Rosen's T 10 protocol or modified T 10 protocol. Three children were treated with resection. 3 children died of disease, one because of toxic side effects of chemotherapy. Five children are in primary remission 44-46 months from diagnosis, one is in secondary remission 10 months from right pneumoectomy for large pulmonary metastases.

Key words: osteosarcoma-therapy; child

Introduction

Osteogenic sarcoma (OS) is the most common primary bone tumour of children and adolescents; it comprises 4,7% of all malignancies up to 15 years of age[1, 2] and is mostly diagnosed during the second decade.[1-4]

Over 80% of OS occur in the methapysis of distal femur, proximal tibia or proximal humerus,[5] while it occurs in the axial skeleton only in 10% of patients. It is most often found in fast growing bone.[6] It is a fast growing tumour with an average doubling time of 34 days, destroys the bony cortex and invades the adjacent soft tissues early.[4] The metastases are almost exclusively hematogenous, with 80% of the patients having micrometastasis at diagnosis, mostly in the lungs.[6] Gross metastatic disease in the lung or bone is present at diagnosis in 10-20% of all patients with OS.[4] Early lymphangitic spread is rare, due to the lack of a bony lymphatic system.[6] The etiology of OS is unclear; bone growth promoting factors may play a role, as may genetic ones.[4] The tumour was found in 16 siblings and its incidence in patients with hereditary type of retinoblastoma is 500 times the average, whether or not they have received radiation therapy.[4]

The survival of patients, treated with surgery only, until about 1970, was less than 20%.[6-9] With the introduction of adjuvant chemotherapy, notably high dose methotrexate (HDM) and citrovorum factor rescue, Adriamycin (ADR), Cisplatin (CDDP), Ifosfamide, the survival rate rose to 60–80% in patients without macroscopic metastasis.[4, 6, 10]

Osteogenic sarcoma is radioresistant and requires radical surgery and if possible with salvage of the affected limb.[5] Today, a limb salvage procedure is possible in 80% of the cases.[6] The tumour must be totally removed with a surrounding margin of normal tissue, and sufficient

Correspondence to: dr. Majda Benedik Dolinčar, Univerzitetni klinični center, Univerzitetna pediatrična klinika, Vrazov trg 1, 61104 Ljubljana, Slovenia.

UDC: 616.71-006.34.04-08-053.2

normal tissue must remain to allow as much preservation of limb function as possible.[3]

Neo–adjuvant chemotherapy i.e. pre–operative chemotherapy has been introduced for several reasons. Its effect on micro–metastasis is immediate during the preparatory phase of limb salvage surgery that usually takes one month. Also, chemoherapy may cause tumour regression and thus increase the proportion of limb salvage procedures. Preoperative chemotherapy also provides the opportunity for evaluating the efficacy of this treatment in vivo by evaluation of tumour necrosis. In the case of a poor response the preoperative chemotherapy may be changed accordingly. Finally preoperative chemotherapy may reduce the danger of tumour spread during surgery.

In neoadjuvant chemotherapy of OS the real dose intensity delivered is a determinant of treatment outcome and therefore every effort should be made to avoid reductions of doses and delays of cycles of chemotherapy in these patients.[11]

Osteogenic sarcoma is the most common secondary malignancy, most often arising after radiation therapy.[12] These lesions were seen after a median latent period of 10,5 years.[12] The risk period for the development of OS began two years after the diagnosis of the initial tumour and ended with the date of death, or the date of diagnosis of OS whichever occurred first.[13] Antracyclines significantly shortened the interval by approximately 3 years.[12] The primary diagnosis also significantly affected the interval, with leukemia/lymphomas having the shortest interval and retinoblastoma the longest.[12] The lesions that develop in unirradiated tissues, occur in the usual sites for OS whereas those that develop in radiation – treated tissues generally occur in less common sites.[12] However, one study of patients with OS treated only by radical surgery has shown a 50% incidence of secondary tumours.[14]

Patients and methods

10 children with OS were treated from 1986 to 1989. They were 10-15, 5 years of age (mean age was 12,3), 4 were girls, 6 were boys. In 2 of these OS appeared as a secondary tumour. It was located in the femur[4] (3 primary, 1 secondary), humerus 1, iliac bone 1, mandible 1 (secondary). Only in one girl were distant metastases present at the time of diagnosis.

In the patient with a secondary mandibular tumour, this tumour appeared 8 years after the initial treatment for acute lymphatic leukemia at the margin of the treatment field for prophylactic radiation of the CNS. The other secondary tumour appeared in the femur of a boy, 6 years after combined treatment of a Ewing sarcoma in the same location.

All children were examined by roentgenograms of the afflicted area, technetium 99 bone scan, computerized tomography and the majority also by arteriography. PA and lateral views used in roentgenographic search for pulmonary metastasis.

The clinical diagnosis of OS has been confirmed by fine needle aspiration biopsy (FNAB) in 7 cases, by open surgical biopsy in 3. All were of a highly malignant variety: osteoblastic in 7, with fibroblastic component in one, chondroblastic component in one and teleangiectatic variety (by FNAB) in one.

All patients were treated primarily by chemotherapy. Seven received 4 x HDM 8 – 12 g/m^2 pre-operatively according to Rosen's protocol T 10[7,16,17] (Table 1); patient No. 2 also received preoperatively Bleomycin, Cyclophosphamide, Actinomycin D (BCD); patient No.4 in addition to that also received ADR and CDDP. Patients No. 9 received a combination of HDM intravenously and CDDP intra–arterially (IA) 3 times (Table 1).

6 patients had amputations, 3 had limb salvage resections.

5 patients with less than 90% tumour necrosis received post operative chemotherapy according to protocol T 10 A, i.e. without HDM.[7, 16, 17] The four remaining patients received individual postoperative chemotherapy treatments. All four received ADR. Patient No.8, who had 100% tumour necrosis, received also BCD with only two treatments of HDM because of a Mtx

Table 1. Patient characteristics

Pat. No.	Age (yr)	Sex	Date of Diagnosis	Location and Biopsy Method	Primary Secondary	Preoperative Chemotherapy	Surgery	Pathologic Subtype	% Tumour Necrosis	Adjuvant Chemotherapy	Duration of Therapy (mo.)	Current Status
1	10.5	M	JAN., 1986	Pr. Tibia FNAB	OS/—	4 x HDM	Amputation	Osteoblastic	60%	T1OA (ADR, CDDP, BCD),	11	66 mo NED
2	13.5	F	JAN., 1986	Ramus of Mandible FNAB	ALL/OS	7 x HDM 1 x BCD	Resection	Osteoblastic, Infiltrated Margin	50%-90%	T10A (ADR, CDDP, BCD)	11	66 mo NED
3	11	M	OCT., 1986	pr. Tibia FNAB	OS/—	4 x HDM BCD, ADR CDDP	Resection	Osteoblastic, Chondroblastic component	50%-90%	2 x HDM, IFOSFAMIDE CDDP, ADR	8	56 mo NED
4	12.5	M	NOV., 1986	distal Femur FNAB	OS/—	4 x HDM	Amputation	Osteoblastic, Infiltrated Margin	50%-90%	CDDP, ADR	16	21 mo DOD
5	12	M	MARCH, 1987	Iliac open biopsy	OS/—	4 x HDM	Resection	Osteoblastic, Chondroblastic component	›90%	T10B, (HDM, BCD, ADR)	9	52 mo NED
6	14.5	F	NOV., 1987	distal Femur FNAB	OS/—	4 x HDM	Amputation	Osteoblastic	70%	T10A (ADR, CDDP, BCD)	10	44 mo NED
7	15.5	M	AUG., 1987	pr. Femur open biopsy	EWING/OS	4 x HDM	Hemipel-vectomy	Osteoblastic high fibroblast-ic component	40%	T10A (ADR, CDDP, BCD)	10	26 mo RPM 36 mo OP now 10 mo NED
8	12	M	AUG., 1987	pr. Tibia open biopsy	OS/—	4 x HDM	Amputation	Osteoblastic	100%	2 x HDM, BCD, ADR	8	19 mo DOD
9	10	M	MARCH, 1988	distal Femur FNAB	OS/—	3 x HDM 3 x 1A CDDP	None	* Telangiect-tatic, FNAB	0%	NONE	2	2 mo died xx Rea chemo.
10	12	F	JAN., 1989	pr. Humerus FNAB	OS/—	4 x HDM	Amputation	Osteoblastic	10%	T10A (ADR, CDDP, BCD)	9	9 mo DOD

pr: proximal; FNAB: fine nedle aspiration biopsy; OS: osteogenic sarcoma; ALL: acute lymphatic leukemia; HMD: high-dose methotrexate with leucovorin rescue; BCD: Bleomycin, Cyclophosphamide, Dactinomycin; ADR: Adriamycin; CDDP: cisplatin; IA: intraarterial; NED: no evidence of disease; DOD: died of disease; RPM: right pulmo metastasis; OP: operation-right pneumoectomy; Rea: reaction

shortage. Patient No.5, who had 90% tumour necrosis, received chemotherapy according to protocol T 10 B with HDM and BCD. Patient No.4 who had 50 – 90% tumour necrosis received also CDDP and radiotherapy for metastases discovered at diagnosis (Table 1). Patient No.3, who also had 50 – 90% tumour necrosis, received Ifosfamide, CDDP and only 2 treatments of HDM due to a low tumour necrosis (Table 1).

In 8 patients the whole course of treatment lasted 8 – 11 months. One patient with metastases at diagnosis was treated for 16 months and one patient who had lethal toxic reaction to chemotherapy expired two months after diagnosis during of preoperative treatment.

Results

The survival rate has been computed from the date of the diagnosis to the date of the last follow up or patient death. The follow–up period was concluded June 1991. Six patients are alive 44 to 66 months after diagnosis; 4 had primary tumours and 2 secondary OS. One of the latter two had multiple right pulmonary metastases 3 years after diagnosis of secondary osteosarcoma and is now disease free 10 months after pneumoectomy.

The tumour necrosis was 10% in one patient, 40% in one, between 50% and 90% in 6, 90% in one and 100% in one (Table 1).

Three patients have died of metastatic OS, two of them with pulmonary metastasis 21 and 19 months respectively after diagnosis. The third had pulmonary and bone metastases 11 months after diagnosis. The fourth patient died preoperatively because of toxic effects of chemotherapy.

Discussion

Long–term survival is a realistic prognosis for about 60–80% of patients with OS due to effective adjuvant chemotherapy.[3-7, 9-12, 18] The quality of life is also improved in these patients since a limb-salvage operation with adequate margins carries the same risk for local recurrence (less than 5%) as the transmedullar amputation.[6]

Limb salvage surgery is ussually contraindicated in cases of neurovascular structure invasion, pathological fracture, infected biopsy site, significant tumour invasion of soft tissues, and skeletal immaturity.[6] Arteriography, which correlates remarkably well with the degree of tumour necrosis, is essential in choosing the type of surgery.[6, 20] It is not yet clear whether intra–arterial or intra–venous CDDP is more efficacious. Recent studies however, have demonstrated that CDDP is highly effective when administered by the IA ruote, rendering many patients suitable candidates for safe surgical limb-salvage procedure.[22] IA CDDP does not prolong disease free survival and does not reduce the occurrence of metastasis.[6]

Good team–work in a center with accumulated experiences is essential for effective treatment. It is also important for the patient to have the biopsy properly done in this center, since a poorly chosen biopsy site can preclude later limb–salvage surgery.[6]

FNAB has shown to be adequate for diagnosis in our institution. Open surgical biopsy is only necessary when FNAB has not yielded sufficient material. Both have to be performed at the site which will later be removed.

Three of our patients have died of metastatic disease 11-21 months from diagnosis. This corresponds to other studies showing that about 90% of relapses occur within two years of diagnosis;[4, 10] first relapses after five years are unusual.[4] Patient No.4 had at diagnosis bilateral pulmonary metastases, metastasis in thoracic vertebral body 11 and an unusually large primary tumour in the distal femur. Furthermore, her surgery was delayed for 5 months due to parental indecision. Other centers also have poor survival rates of patients with metastasis at diagnosis.[4] For patient No.8 one would expect a favorable outcome, based on tumour necrosis of 100%, which usually correlates very well with survival.[6, 8, 21] We can only surmise that he died because he only recei-

ved HDM twice, owing to a shortage of methotrexate. Patients No.10 was resistant to HDM; her disease progressed during pre–operative chemotherapy and the tumour necrosis at surgery was only 10%. Poor response to preoperative chemotherapy identifies patients at a high risk of early relapse.[7] Good responders to pre–operative chemotherapy have a much better prognosis (81% at 5 years) than poor responders (45%).[18] The patient No.7 had right pulmonary metastasis 3 years after diagnosis of secondary OS and is now disease free 10 months after right pneumonectomy. About one third of the patients with pulmonary metastasis are curable with metasectomy but there is no evidence of a beneficial effect of postoperative chemotherapy.[6]

A combination of complete (wide) surgical resection or amputation and aggressive chemotherapy offers the best chance of long term survival.[23] From our study it seems that secondary osteogenic sarcoma does not have a poorer prognosis that primary osteogenic sarcoma.

Acknowledgements

The author wishes to thank the orthopedic surgeon Dr Boštjan Baebler, the oncologic surgeon Dr Janez Novak, the pediataricians Dr Nasta Mihevc, Dr Jožica Anžič and many other doctors of several specialities who collaborated in the diagnosis or treatment of these patients. The author also wishes to thank Dr Berta Jereb for her advice and support and Nada Pušnik for preparing the manuscript.

References

1. Altman AJ, Schwartz AD. The Cancer Problem in Pediatrics: Epidemiologic Aspects. *Major Probl Clin Pediatr* 1983;**18:**1-21.
2. Barjaktarević Ž, Kezić J, Mitrović M, Višacki R, Aleksandrović S, Subotić Z, Atanacković M, Olujić D, Brzaković P, Oprić M. Treatment of Children with Osteosarcoma. *Acta Orthop Jugosl* 1988;**19:**52-8.
3. Gillespy T, Mnfrini M, Ruggieri P, Spanier S, Petterson H, Springfield D. Staging of Intraosseous Extent of Osteosarcoma: Correlation of Preoperative CT and MR, Imaging with Pathologic microslides. *Radiology* 1988;**167:**765-67.
4. Goorin AM, Abelson HT, Frei E. Osterosarcoma: Fifteen Years Later. *N Engl J Med* 1985;**313:**1637-43.
5. Jürgens H. Bone Tumours, Diagnostic Methods and Treatment Possibilities. European School of Oncology, Postgraduate Course on Pediatric Oncology, June 1990, Višegrad, Hungary.
6. Meyer WH, Malawer MM. Osteosarcoma. *Pediatr Clin North AM* 1991;**38:**317-48.
7. Winkler K, Beron G, Kotz R, Salzer–Kuntschik M, Besk J, Beck W, Brandeis W, Ebell W, Erttmann R, Göbel U, Havers W, Henze G, Hinderfeld L, Hocker P, Jobke A, Jürgens H, Kapisch H, Preusser P, Prindull G, Ramach W, Ritter J, Sekera J, Treuner J, Wüst G, Landbeck G. Neoadjuvant Chemotherapy for Osteogenic Sarcoma: Results of a Cooperative German/Austria Study. *J Clin Oncol* 1984;**2:**617-24.
8. Bacci G, Picci P, Ruggieri P, Mercuri M, Avella M, Capanna R, Brach del Prever A, Mancini A, Gherlinzoni F, Padovani G, Leonessa C, Biagini R, Ferraro A, Ferruzzi A, Cazzola A, Mnfrini M, Campanacci M. Primary Chemotherapy and Delayed Surgery Neoadjuvant Chemotherapy for Osteosarcoma of the Extremities. *Cancer* 1990;**65:**2539-53.
9. Elomaa J, Siimes MA, Blomqvist C, Karaharju E, Ryöppy S, Laasonen E, Halmstrom T. Ten Years' Experience in Patients with Osteogenic Sarcoma in Finland. *Eur J Surg Oncol* 1990;**16:**147-52.
10. Hudson M, Jaffe MR, Ayala A, Raymond AK, Carrasco H, Wallace S, Murray J, Robertson R. Pediatric Osteosarcoma: Therapeutic Strategies, Results, and Prognostic Factors Derived From a 10–year Experience. *J Clin Oncol* 1990;**8:**1988-97.
11. Bacci G. Picci P, Avella M, Dallari D, Ferrari S, Prasad R, Di Sciascio M, Malaguti C, Caldora P. The Importance of Dose–intensity in Neoadjuvant Chemotherapy of Osteosarcoma: Retrospective Analysis of High–dose Methotrexate, Cisplatinum and Adriamycin used Preoperatively. *J Chemother* 1990;**2:**127-35.
12. Newton WA, Meadows AT, Shimada H, Bunin GR, Vauter GF. Bone Sarcomas as Second Malignant Neoplasms Following Childhood Cancer. *Cancer* 1991;**67:**193-201.
13. Tucker MA D'Angio GJ, Boice JD, Strong LC, Li FP, Stovall M, Stone BJ, Green DM, Lambardi F, Newton W, Hoower RN, Fraumeni JF. Bone Sarcomas Linked to Radiotherapy and Chemotherapy in Children. *N Engl J Med* 1987;**317:**588-93.
14. Beattie EJ, Harvey JC, Marcove R, Martini N. Results of Multiple Pulmonary Resections for Metastatic Osteogenic Sarcoma After Two Decades. *J Surg Oncol* 1991; **46:**154-55.
15. Rosen G, Caparros B, Huvos AG, Kosloff C, Nirenberg A, Cacavio A, Marcove RC, Lane JM, Mehta B, Urban C. Preoperative Chemotherapy for Osteogenic Sarcoma: Selection of Postoperative Chemotherapy Based on the Response of the Primary Tumour to Preoperative Chemotherapy. *Cancer* 1982;**49:**1221-30.
16. Rosen 6, Huvos AG, Marcove R, Nirenberg A. Telangiectatic Osteogenic Sarcoma. *Clin Orthop* 1986;**207:**164-73.

17. Brunat–Mntigni M, Biron P, Kohler R, Blondet R, Berard J, Chauvod P, Bouffet E, Carret JP, Jonas P, Patricot LM. Developments in the Treatment of Osteosarcoma since 1979. Report of the Statistics at the Centre Leon–Berard. *Bull Cancer* 1990;**77:**933-40.
18. Kashdan BJ, Sullivan KL, Lackman RD, Shapiro MJ, Bonn J, Weiss AJ, Gardiner GA. Extremity Osteosarcoma: Intraarterial Chemotherapy and Limb–sparing Resection with 2-year Follow–up. *Radiology* 1990;**177:**95-99.
19. Bilbao JI, Martin Algarra S, Martinez de Negri J, Lecumberri F, Longo J, Sierrasesumaga L, Canadell J. Osteosarcoma: Correlation between Radiological and Histological Changes after Intra–arterial Chemotherapy *Eur J Radiol* 1990;**1:**98-103.
20. Delepie N, Delepine G, Trifaud A, Voisin MC, Mazabraud A, Jasmin C. Evaluation of the optimal length of neo–adjuvant chemotherapy in osteogenic sarcoma. *Neoadjuvant Chemother* 1986;**137:**581-86.
21. Epelman S, Estrada J, Jaffe N, Bianci A. Pediatric Osteosarcoma. Successful Retreatment of Relapsed Primary Tumour and Soft Tissue Recurrence With Intraarterial Cis-Diamni nedichloroplatin–II. *Cancer* 1990;**66:**801-5.
22. Kozakewich, Perez Atayde AR, Goorin AM, Wilkinson RH, Gebhardt MC, Vawter FG. Osteosarcoma in Young Children. *Cancer* 1991;**67:**638-42.

Adv Radiol Oncol 1992; 202–7.

Recent strategies in the treatment of malignant germ cell tumour

Clemm Ch

Dept. of Internal Medicine III, Klinikum Großhadern, University of Munich, FRG

Since cisplatin was introduced into chemotherapy in 1979, there has been a radical improvement in the treatment of malignant testicular tumour. Cure rates of over 80% are now possible. For seminoma, the treatment strategy has changed from radiotherapy to chemotherapy in advanced stages of disease with long term remission of 90%. The introduction of carboplatin more recently will possibly bring about further good results. HCG–positive seminoma has no worse prognosis than others. In the case of non–seminoma, tumour markers play an important role in prognosis. Early detection as well as the earliest possible beginning of consequent therapy that is stage conform is of primary importance in achieving long term remission for our patients. Beware of «wait–and–see» strategies. In stage I we carry out RLA, in stage IIA and IIB good results have been achieved with adjuvant chemotherapy, in future possible neoadjuvant. Stages IIC-IV require intensive therapy strategies using standard therapies but with questionable bleomycin reduction. Very advanced stage of disease demands therapy intensification, treatment with high dose protocols plus cytokines and in some cases autologous bone marrow transplantation, which can only be carried out in a few specialized centers.

Key words: testicular neoplasms–therapy; dysgerminoma

Introduction

The therapy of malignant testicular tumours has changed radically during the past few years. While in 1960 only 5% of all patients reached long term remission, more than 60% of patients even in metastasized stages of disease have been curable since 1980. The incidence is slightly rising, at the moment 7 of 100.000 male inhabitants are afflicted per year. In addition to improvements in therapy, diagnosis has also been highly improved during the last years. Histological examination has been made more accurate by using immune peroxidase technique. The analysis of the tumour markers AFP (alphafoetoprotein) and hCG (human chorionic gonadotropine) in the serum has led to a more differentiated diagnosis as has the use of radiological techniques such as cat–scans and more recently nuclear magnetic resonance.

In spite of all efforts, and even with improved polychemotherapy as a result of the introduction of cisplatin in 1979, more than 200 patients die yearly in the FRG.[1] This shows quite clearly that theoretical improvement of therapy as described in studies has not yet been fully put into practice. It is thus highly desirable that patients with this curable tumour are diagnosed as early as possible and then treated consistently. In order to do so, the most complete possible survey of these patients as well as consistent treatment within a

Correspondence to: Doc. dr. Christoph Clemm, Ludwig–Maximilians–Universität München Klinikum Großhadern, Postfach 701260, 8000 München, Deutschland.

UDC: 616.681-006.884-08

network of controlled studies is necessary. With this as a prerequisite, the complete remission rates are at about 80% at the moment and still tend increase.[2] It has also proved favorable if these patients are treated at a tumour center, and therapy is coordinated or monitored from there. This goes as well for the follow–up treatment. While previously the treatment of seminoma consisted of radiotherapy, teratoma and combination tumours had always been treated surgically and chemotherapeutically. In recent years, the treatment strategy of seminoma has changed, as has the use of chemotherapy in the case of non–seminoma patients. Both tumour entities shall now be discussed.

Seminoma

In earlier years, seminoma patients received radiation even in advanced stages of disease. Nowadays, due in part to the success of chemotherapy in the treatment of non–seminomas, chemotherapy has been implemented for the treatment of seminomas. Since the relapse rates for advanced stage of disease with lymph node metastases larger than 5cm as well as organ metastases increase to approximately 30%, a primary radiation therapy should not be indicated here.[3] The results achieved here with polychemotherapy reach 90% in these stages. Small lymph nodes (less than 5 cm) can be treated successfully with radiotherapy alone, here long term results also range at about 95%. In addition to the combination therapy with cisplatin, etoposide and bleomycin, ifosfamide is effectively used as a bleomycin substitute. Our results here with 45 patients are very good, showing a complete remission rate of 91% (Table 1). Stable remission rates of 68%–100% can be reached with other combination therapies as well. One must pay attention to the toxicity of the therapy, since patients with seminomatous tumour are as a rule 10 years older than patients with non–seminoma. Combination therapies show increased bone marrow toxicity and require strict surveillance and possibly dose reduction. Therapy must be carried out with continous hyperhydration to prevent a cisplatin–induced nephrotoxicity.

In recent times we have seen the results of monotherapy treatment, at first with cisplatin and more recently with carboplatin. Here long term NED was observed in almost 90% of the patients. But the rate of complete remissions in a carboplatin monotherapy seems to be somewhat lower (Table 2). In Great Britain and Ger-

Table 1. Chemotherapy results in literature (Polychemotherapy) – seminoma.

Author	Year	Patients	Therapy	CR	Remission duration
Einhorn	1980	19	PVB + A	63%	17 + months
Vugrin	1981	9	PC –	89%	19,5 + months
Samuels	1983	32	P + C	94%	24 + months
Peckham	1983	7	BEP	100%	no data
Schmoll	1984	15	PVB ∓ I	80%	no data
Wettlaufer	1984	12	VinPC	92%	24 + months
Stanton	1985	28	PVBCD	85%	32 + months
Schuette	1985	28	PVB ⓘ A/I	89%	28 + months
Friedman	1985	20	PVB or PE	90%	24 + months
Pizzocaro	1986	31	PVBor PEB ∓ A	84%	34 + months
Fossa	1987	54	PVB/PEB	91%	36 + months
Loehrer	1987	60	PVB ∓ A/PEB	68%	no data
Einhorn	1989	111	multiple	84%	no data
Clemm	1991	45	VIP/EIP	91%	45 + months

P = Cisplatin, V = Vinblastine, B = Bleomycin, A = Adriamycin, C = Cyclophospahmide, E = Etoposide, I = Ifosfamide, V = Vincristine, D = Dactinomycine, Carboplatin, CR = complete remission, PR = partial remission

Table 2. Monotherapy results.

Author	Year	Patients	Therapy	CR	Remission duration
Oliver	1984	14	P	71%	15 + months
Horwich	1989	34	Carboplatin	42% 55% PR	26 + months
Harstrick	1990	41	Carboplatin	71% 17% PR	22 + months

many more than 40 patients have been studied and showed a good response to this therapy regimen, whereby it is not necessary to hospitalize the patients or carry out the therapy with continuous hyperhydration, but patients are treated ambulatory. Our present experiences are not yet long term and have not been verified for a longer period of time, thus there might be a higher rate of relapse.[4] In order to compare this very well tolerated and potentially very effective therapy with better known combination therapies as far as effectiveness and tolerability are concerned, a study is being carried out presently in the FRG. Here a monotherapy using carboplatin is being compared with a combination therapy consisting of etoposide, ifosfamide and cisplatin. This study is meant to disclose information about primary risk factors, the tolerability and effectiveness of therapy as well as the relapse rate and information about possible indications for secondary surgery in the case of residual tumour.[5] In patients with pure seminoma one finds vital tumour remains in much fewer cases which is one of the reasons why a number of authors recommend; omission of surgical intervention, or operating only if lymph nodes are larger than 3 cm. In addition to organ metastases e.g. in the bone, as well as visceral metastases in the lung or liver, possible risk factors can also be tumour entities that show hCG producing seminoma cells or synciotrophoblastic cells. These are also seen in pure seminoma, but an hCG level higher than 1.000 U/1 should give rise to the suspicion that one might be dealing with a chorion carcinoma and thus these patients should not be treated as pure seminoma patients.[6]

Non–seminoma

An important difference between non–seminoma and pure seminoma can be established by histological analysis of the tumour markers hCG and AFP as seen in the histological section. Determining these two markers as well as lactate dehydrogenase is a must in serum. While hCG and LDH increase can be seen in pure seminoma as well, AFP is always consistent with the diagnosis is of non-seminomatous tumour. These patients may not be treated as pure seminoma patients but must be consistently and intensively treated in the same way as teratoma or combination tumour patients (Table 3). In Munich we have achieved good results with a stage conform therapy. In stage I the tumour is only in the testis, stage II shows lymph nodes below the diaphragm, IIA with lymph nodes up to 2 cm, IIB lymph nodes 2-5 cm, IIC lymph nodes 5-10 cm, and IID lymph nodes exceeding 10 cm in diameter. Stage III implies lymph nodes above the diaphragm and stage IV organ metastases.

Depending on the tumour stage we consistenly operate in the case of non–seminoma, if the histology shows no evidence of chorion carcinoma and hCG levels are not extremely elevated (over 1.000 U/1) and indicate a rapidly proliferating trophoblastic tumour. Following an inguinal semicastration, these patients are treated primarily with chemotherapy, which is also documented in other studies.[7] Yet other authors observe good results in stage I with «wait and see» strategy, i.e. forfeiting additional surgical or chemotherapeutic measures after inguinal semicastration. Peckham et al. have reached very good long – term results with 137 patients, but a

Table 3. Treatment strategy for malignant germ cell tumour
High inguinal semicastration.

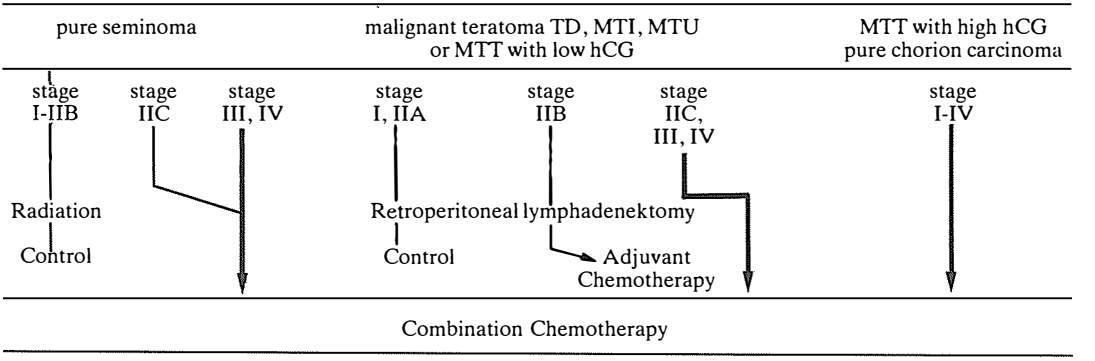

Table 4. Definition for »Bulky« tumour.

1. Metastases size:	Lymph nodes ≥ 10 cm diameter (abdominal/mediastinal) Lungfiliae ≥ 5 cm diameter
2. Metastases number:	more than 10 lungfiliae
3. Metastases location:	CNS/Liver/Bone several organs simultaneously
4. Tumormarker:	hCG higher than 10.000 U/l AFP higher than 1.000 ng/ml LDH higher than 500 U/l
5. Primary extragonadal germ cell tumours	

relapse rate of 30% must be taken into account. If the relapse is discovered early, long – term results and chances of survival are good with 96%. These results have been confirmed in several studies.[8]

We do not treat in accordance with these studies because we prefer primary surgery due to possible lack of compliance on the part of the patients as well as the difficulties of discovering a relapse in time. The possible advantage of maintaining ejaculation by doing without surgery is weakend by the relapse rate of 30%. We have thus decided to carry out a modified retroperitoneal lymphadenectomy even if there is a negative cat–scan of the abdomen in stage I. This modified surgery has the advantage that in contrast to earlier operating techniques where there was a loss of ejaculation in over 80% of the patients (or retrograde ejaculation), we now have only 15 to 40% patients suffering from loss of ejaculation. The relapse rate has not risen decisively because of the modified surgery and dispensing with contralateral resection.[9] If lymph node metastases are found during the operation, a radical resection is carried out depending on the size of the nodes. If histologically the lymph nodes are smaller than 2 cm, the patient will only be controlled after RLA. If, on the other hand, the lymph nodes exceed 2 cm in diameter, we administer adjuvant chemotherapy. This is also done when there are several small lymph nodes or negative tumour markers indicating a possible relapse that might be discovered too late.

The indication for adjuvant chemotherapy is not considered as strictly in other tumour centers. Thus Williams et al. have published data where in relinquishing adjuvant therapy, patients who relapsed (up to 50% of the patients) they still achieved good cure rates by administering chemotherapy to treat the relapse.[10] We consider this mode of treatment as too risky to be carried out outside a tumour center, even though it has been tried out in studies. Patients with liver metastases of extended lymph node metastases are often discovered late, leading to poor prognosis. Many studies propagate a reduction of adjuvant chemotherapy cycles from 4 to 2 cycles. We have not carried out these studies, but advocate a median adjuvant therapy of 3 cycles.

The experience and results with our patients with this therapy are very good. In 65 patients only one showed new tumour and the relapse was successfully treated with renewed intensive chemotherapy. This patients is now tumour – free since more than 4 years.

On the other hand, patients who had only been operated on primarily and did not receive chemotherapy until they relapsed, had a clearly worse prognosis and in many case also CNS metastases. This important restriction when transposing study results and bringing them into general practice must be mentioned, since the results could be influenced negatively hereby.

A new method of reducing the side effects of surgery consists in the so–called neoadjuvant chemotherapy proceedings; this is implemented if lymph node metastases of 2–5 cm are already evident in the cat–scan. If they exceed 5 cm, chemotherapy should be carried out by all means (Table 4) prior to surgery. Some authors recommend prior chemotherapy even if lymph nodes are smaller than 5 cm but exceeding 2 cm, because adjuvant chemotherapy would have been carried out after surgery anyhow. This neoadjuvant procedure is also carried out outside the studies and has the advantage that if the lymph nodes disappear completely, in 80% of the cases it is possible to do without lymphadenectomy. We do not share this view because of the unreliability of cat–scan checks , and are awaiting the results of a study that is presently being carried out in Germany.

Further attempts at minimalizing therapy in low tumour stages consist in doing without the fourth cycle of chemotherapy, which Einhorn has shown as being feasible in a randomized study. Other studies that leave out bleomycin show a clear risk, which is the reason why we could not decide to leave out bleomycin per se. New data about a combination of cisplatin /etoposide as opposed to carboplatin/etoposide show equal effects and results for both regimens, but a higher relapse rate for carboplatin, which is why we do not recommend this treatment strategy outside of studies.

Highly advanced tumour stages

While in low tumour stages a minimization of therapy is documented, whereby therapy success must be maintained, all efforts concentrate on a maximization of therapy and improvement of results in the case of advanced tumour stages. Some studies with double dose cisplatin showed very little improvement in results, combination therapy with cyclophosphamide and ifosfamide brought some improvement, but this was not reliably proven in statistics.

Patients with very advanced stage of disease should not be treated with the conventional regimen (PEB) in individual cases, but with more intensive therapy. A German study is presently testing the dosis escalation of cisplatin, etoposide and ifosfamide with the addition of a granulocyte–macrophage–stimulating factor. Results also seem very positive with autologous bone marrow transplantation, but toxicity is strong and the long – term improvement controversial.[11] Efforts must be concentrated on early diagnosis and consistent therapy in low tumour stages, in order not to risk any chances for a complete remission. It is important to note that the primary extragonadal tumour, which makes up 5% of all advanced germ cell tumours, is connected to the absence of a palpable testis tumour. This accounts for the fact that these patients are often diagnosed in a later stage and the disease is already well advanced. It is useful in this context to remember that as far as young men between 20 and 30 years of age are concerned, germ cell tumours are (besides lymphoma) the most frequent tumours. In 2/3 of these patients the AFP and hCG levels can already be elevated. A major surgical diagnosis should give way to a small mediastinoscopy and quick and consistent treatment, in order to give these patients a good chance of reaching complete remission and long term survival.[12]

References

1. Clemm Ch, Sauer H, Hartenstein R. Behandlung nicht-seminomatöser Hodentumoren im Stadium I-IIB. *Dtsch Med Wchschr* 1989; **114**:1276-82.

2. Einhorn LH. Treatment of advanced disseminated germ cell tumours. *Annals of Oncology* 1991; **2:**167f.
3. Clemm Ch. Hartenstein, R. Willich et al. Vinblastine-ifosfamidecisplatin treatment of bulky seminoma. *Cancer* 1986; **58:**2203-7.
4. Horwich A, Dearnaley D P, Duchesne G M. et al. Simple Nontoxic Treatment of Advanced Metastatic Seminoma with Carboplatin. *J Clin Oncol* 1989; **7:**1150-6.
5. Clemm Ch. Phase III-Studie: Cisplatinkombinationstherapie vs. Carboplatinmonotherapie bei metastasierten Seminom. *Urologe (A)* 1991; **30:**75f.
6. Mann K. Tumormarker beim Hodenkarzinom. In: *Urogenitaltumoren,* Hrsg. Ch. Clemm, W. Zuckschwerdt Verlag, München (1991) 3-18.
7. Pont J, Höltl W, Kosak D et al.: Risk-adapted Treatment Choice in Stage I Nonseminomatous Germ Cell Cancer by Regarding Vascular Invasion in the Primary Tumour: A Prospective Trial. *J Clin Oncol* 1991: **8:**16-20.
8. Stephenson R A. Surveillance for Clinical Stage I Nonseminomatous Testis Carcinoma: Rationale and Results. *Urol Int* 1991; **46:**290-3.
9. Weißbach, Bussar-Maatz. *Operative Maßnahmen beim Hodentumour.* Onkologisches Forum 3 (1988) 19-28.
10. Williams, S D, Stablein D M, Einhorn L H et al.: Immediate Adjuvant Chemotherapy Versus Observation with Treatment at Relapse in Pathological Stage II Testicular Cancer. *N Engl J Med* 1987; **317:**1433-8.
11. Nichols C R, Tricot G, Williams S D et al.: Dose-Intensive Chemotherapy in Refractory Germ Cell Cancer – A Phase I/II Trial of High-Dose Carboplatin and Etoposide with Autologous Bone Marrow Transplantation. *J Clin Oncol* 1989; **7:**932-9.
12. Clemm Ch, Mair W, Voigt G et al.: Chemotherapy in extragonadal germ cell tumours. *J Cancer Res and Clin Oncol* 1990; **116:** suppl 589.

Adv Radiol Oncol 1992; 208–13.

Thyroid status following irradiation for laryngeal cancer

Dimitrovska A[1], Karanfilski B[2], Georgieva B[2], Velkov K[1], Jovanovski D[1], Nikolova L[1]

[1]*Institute of Radiotherapy and Oncology and* [2]*Institute of Pathophysiology and Nuclear Medicine, Skopje*

The effect of Co-60 irradiation on the thyroid gland was studied in 174 patients, 75 previously operated. While clinically manifest hypothyroidism showed 5 (3%) cases, a significant proportion of patients were noted to have vague, nonspecific symptoms (7%) or latent hypothyroidism (25%). Low radioiodine 24 hour uptake was measured in 16%, low thyroxine and triiodthyronine in 7% and 15% respectively, elevated serum thyroid-stimulating hormone (TSH) in 31%. The thyrothropin releasing hormone test revealed augmented TSH response in a further 14 patients. 33% of patients had elevated titers of thyroid antibodies. 42% showed J-131 scan abnormalities. The data suggest that standard doses of external irradiation induce thyroid functional and morphological changes which signals the need for further evaluation of the gland in patients successfully treated for head and neck cancer.

Key words: laryngeal neoplasms – radiotherapy; thyroid function tests

Introduction

Thyroid dysfunction following irradiation of the neck region has been found in a rather high percentage of lymphoma patients.[1,2,3,4,5,6] In patients with head and neck tumors who receive higher doses of irradiation the incidence of the thyroid damage varies from 0-100% which depends on the duration of the follow-up and the sensitivity of the tests employed.[1,5,7,8,9,10,11,12,13] In 1961, Félix[8] first reported a case with myxedema appearing 6 years after radiotherapy (RT) for laryngeal cancer. In 1965, Markson and Flatman[12] described 5 cases with hypothyroidism 4-36 months after RT for different neoplasms in the neck region. In one of the first systematic examination of the thyroid, Čočina and associates[7] found normal J-131 uptake in 50 patients soon following doses of 60 Gy to the neck. Koulumies and associates[11] also did not find thyroid dysfunction in 118 patients with laryngeal cancer in the first year after RT judged by normal RAI uptake, but 17 of 34 patients had displayed low PBI after more measurements. Greig[10] determined normal RAI uptake and PBI in 20 patients following doses of 37-65 Gy. Latter studies, however, using more sophisticated tests currently available refer considerably higher percentage of thyroid dysfunction due to irradiation.[1,9,13,14,15,16]

This paper is a continuation of the investigation of the thyroid gland after radical RT for laryngeal cancer started 1980. The findings obtained for 146 patients tested once have previously been described.[17] Since 1982 a half of the obser-

Corespondence to: Doc. dr Aneta Dimitrovska, Institute of Radiotherapy and Oncology, Vodnjanska 17, 91000 Skopje, Macedonia.

UDC: 616.22-006.6:615.849.06:616.441

ved patients have been followed for thyroid abnormalities including 30 new cases. The results after more than one examination of the patients will be presented.

Material and methods

174 patients followed for laryngeal cancer were evaluated for thyroid abnormalities. They had received 60-70 Gy in 6-7 weeks Co-60 irradiation 2 months to 18 years prior to the examination of the gland. The patients were grouped and analysed according to the time interval between irradiation and the tests performed. The first group consisted of patients examined 2 and 6 months after completion of treatment, seen on the first and the third follow-up, the second after 1 year, the next after 2,3,4,5 and more than 5 years after RT. None of the patients had any known disorders of the thyroid before treatment. In 99 (57%) patients some of the thyroid tests were repeated 2-5 times with the interval from the first to the next examination of minimum 1 year. 75 (43%) were treated with surgery and RT and 99 (57%) received RT alone.

To assess the thyroid status after clinical examination the patients were subjected to the following tests: 24-hour radioactive iodine (RAI) uptake, serum total thyroxine (T_4) using a modification of the competitive protein-binding method of Murphy,[18] triiodthyronine (T_3) and thyroid stimulating hormone (TSH) measured by radioimmunoassay,[19,20] serum TSH response to the thyrotropin-releasing hormone (TRH test,[21,22] the determination of thyroid antibodies by the modified method of Boyden[23] and J-131 scans obtained 24 hours after oral administration of 50 mCi radioiodine by means of a commercial scanner Nuclear Chicago.

Results

Clinically manifested hypothyroidism was recognized and later proven by laboratory tests in 5 (3%) of 174 patients. Three of them have had surgery prior RT and 2 have received irradiation as the sole therapy. The following symptoms were recorded: fatigue, sensitivity to cold, constipation, muscle aches, weakness. Despite the poor appetite 3 of the patients gained in weight and complained of requiring more sleep. The puls was slow and the skin dry and rough. One patient (woman) had a swelling of the eye-lids and hands and the other only of the eye-lids. Electrocardiogram showed bradicardia in 3 of 5 examined. In all of them replacement hormone therapy with T_4 was prescribed. Substitution (tab. Novothyral and later Vobenol) was successful in 4 cases. Besides clinical improvment the serum TSH and T_4 normalized their values. The fifth patient developed lung metastases 6 month after commencement the substitution, the therapy was discontinued and he died a year later. Others are under the control of an endocrinologist and are doing well.

Table 1. Subnormal T_4 in different intervals after radiotherapy

	Operated	Non-operated	Both	
< 1 year	0/12	0/25	0/37	–
1 year	1/12	1/25	2/37	5%
2 year	0/14	0/12	0/26	–
3 year	0/10	2/10	2/20	10%
4 year	0/5	0/7	0/12	–
5 year	1/2	2/8	3/10	30%
> 5 year	4/20	1/12	5/32	16%
Total	6/75 (8%)	6/99 (6%)	12/174	(7%)

However, laboratory tests revealed pathological findings in a great proportion of asymptomatic patients. Reduced RAI uptake was recorded in 16% (18% operated and 14% non-operated) of the patients. 12 (7%) patients has subnormal T_4 (Table 1). The mean value was 42 ± 11,96 nmol/1, 40 ± 13,53 nmol/1 in the group with surgery and 44 ± 12,05 nmol/1 in the group without surgery. There was no difference between the two groups in regard to the incidence of the subnormal T_4 (8% vs, 6%). First cases with low T_4 appeared one year after RT. The longer the follow-up the greater was the number of the hypothyroid patients. Table 2 shows the

other laboratory findings in patients with subnormal T_4. The first 5 are clinically and biochemically hypothyroid. Nine (75%) of 12 patients had a raised TSH level, 5 had low T_3, 9 showed pathological scan.

The serum T_3 level varied in a great number of patients from one to another measurement. After 1-5 tests 15% showed increased and 25% reduced level of T_3.

The TSH was determined in 158 patients and 49 (31%) had elevated level (Table 3). It was noted the tendency of the TSH to raise with the time of follow-up. As seen from the table 16% and 18% of the examined patients displayed elevated TSH concentration within the first year after RT. After the second year of irradiation elevated TSH ranges from 32%-55%. Some of the patients tested in the first year after RT showed transitory elevation of TSH. Of 49 patients having elevated TSH level 9 and 22 exhibited subnormal T_4 and T_3 respectively. Five of these had both reduced level of T_4 and T_3. Forty (25%) cases were recorded with elevated TSH and normal T_4.

The findings of thyroid scans are seen in Table 4. In 73 (42%) of 174 patients one or more abnormalities were noted, most commonly a reduced size of the gland. The number of the pathological scans was higher in the group with surgery (52%).

Thyroid antibodies were determined in 83 patients who had displayed subnormal T_4 and T_3 and/or elevated TSH. Positive antibody titers were found in 27 (32,5%) cases, more often antimicrosomal (in 25 or 30% of the patients) than antithyroglobulin (in 6 or 7% of the patients) antibodies. All, exept one showed low titers.

The TRH test confirmed hypothyroidism in 14 of 17 cases suspected as hypothyroid on the basis of the previously documented borderline values of T_4 and TSH.

The results of all tests carried out in 174 patients are summarized on the Table 5.

Discussion

Early and late histopathological changes in the irradiated thyroid had been widely studied.[10,24,25,26,27,28] While follicular epithelial cells and follicles tolerate high doses of irradiation, small blood vessels can be damaged with moderate doses which results with their degeneration, necrosis, thrombosis and obliteration as well as an early interstitial fibrosis.[26,27] At doses of 60-70 Gy fine vascular damage and impairment of circulation cause secondary parenchymal atrophy and a decrease of the functional activity of the gland. Minimum time required for late

Table 2. Laboratory findings in patients with low T_4

Patient/ Treatm.	T_4	T_3	TSH	RAI uptake	Thyr. MG	Antib. TG	SCAN	Interval from irrad.
1/oper.	25	0,98	70	12%	1:80	Ø	small size	1 year
2/nonop.	48	0,9	18	31%	Ø	Ø	cold nod.	1 year
3/nonop.	20	1,4	13,5	13%	Ø	Ø	small size	5 year
4/oper.	20	2,4	70	22%	Ø	Ø	small size	9 year
5/oper.	39	1,3	40	23%	Ø	1:40	normal	11 year
6/nonop.	44	1,6	8,4	15%	–	–	small size	3 year
7/nonop.	46	1,8	5	34%	Ø	Ø	small size	5 year
8/oper.	49	1,4	40	25%	1:20	Ø	one lobe	10 year
9/ oper.	52	2,2	0,5	23%	–	–	normal	5 year
10/nonop.	51	2,3	35	18%	Ø	Ø	one lobe	10 year
11/oper.	46	2,1	60	23%	Ø	Ø	small size	7 year
12/nonop.	53	1,3	3,7	33%	Ø	Ø	normal	3 year

Normal values: T_4-54-160 nmol/1, T_3-1,5-3,4 nmol/1,
TSH– 0-5 nU/ml, RAI uptake 20% -50%

Table 3. Elevated TSH in different inteervals after radiotherapy

	Operated	Non-operated	Both	
< 1 year	1/10	4/20	5/30	16%
1 year	2/9	3/19	5/28	18%
2 year	5/13	3/12	8/25	32%
3 year	3/10	6/10	9/20	45%
4 year	2/6	3/8	5/14	36%
5 year	1/1	4/8	5/9	55%
> 5 year	8/20	4/12	12/32	37%
Total	22/69 (32%)	27/89 (30%)	49/158	(31%)

Table 4. Scan abnormalities in different periods after radiotherapy

	Operated	Non-operated	Both	
< 1 year	2/12	3/25	5/37	13%
1 year	8/12	13/25	21/37	57%
2 year	6/14	3/12	9/26	35%
3 year	8/10	7/10	15/20	75%
4 year	0/5	2/7	2/12	17%
5 year	1/2	2/8	3/10	30%
> 5 year	14/20	4/12	18/32	56%
Total	39/75 (52%)	34/99 (34%)	73/174	(42%)

Table 5. End results after 1-5 thyroid tests following irradiation

Test	Patients	Normal Findings	Pathological Findings	
Clinical exam.	174	169 (97%)	5 (3%)	Hypothyroid
RAI uptake	168	136 (81%)	27 (16%)	Low
			5 (3%)	high
T_4	174	159 (91,3‰)	12 (7%)	Subnormal
			3 (1,7%)	high
T_3	161	96 (60%)	41 (25%)	Subnormal
			24 (15%)	high
TSH	158	109 (69%)	49 (31%)	Elevated
Thyr. antibodies	83	56 (67,5%)	27 (32,5%)	
Scan	174	101 (58%)	73 (42%)	

effects of irradiation to be manifested is 6 months or more. In our material first hypothyroid patients and most of scan abnormalities appeared after the first year of RT. Some of the pathological tests done 2 or 6 months following irradiation have tendency to be transitory, particularly TSH and T_3.

Obtained results in this study confirm reports which indicate that a high percentage of patients who had received RT in the neck region have abnormal thyroid tests.[1,2,3,5,9,13,16] Clinically evident hypothyroidism showed 5 (3%) patients, slightly less than in the series of Einhorn and Wikholm.[9] They detected 3 (7,3%) hypothyroid patients and in the rest 38 out of 41 patients reduced thyroid response 24 hour after TSH administration. The mean follow-up had been 18 years. They have pointed out the state of the reduced thyroid reserve after high doses of irradiation if the period of follow-up is sufficiently long. 7% of the examined patients had low T_4 and 25% had low T_3, most of them having low RAI uptake and elevated TSH. The data are similar with those reported by Fuks[1], Murken[15] and Brase.[29] Elevated TSH had 49 (31%) cases. 40 (25%) of the patients having raised TSH but normal T_4 were defined as being in latent hypothyroidism. In these cases a reduction in thyroid activity has been compensated for by an increasing output of TSH to maintain an euthyroid state.[30,31] Our findings are identical with those of Fuks[1] who also found 25% (13 of 52) patients with elevated TSH and normal T_4.

There was no correlation between the presence of antibodies and the onset of manifest of latent hypothyroidism. Elevated TSH was observed in 11 (41%) of 27 patients with antibodies and in 49 (31%) of the whole group, while reduced level of T_4 was found in 3 (11%) in the group with antibodies and in 12 (7%) in the whole group of 174 patients. The difference is not statistically significant. An autoimmune pro-

cess does not appear to be a major factor in the development of hypothyroidism.

Scan abnormalities appeared in 42% of 174 patients. In the literature available only Nelson[4] reports the thyroid scans findings in lymphoma patients using Tc-99m. She detected pathological scan in 17 of 45 (38%) cases, the data that are similar with ours.

There was no difference in obtained results between patients treated with or without surgery exept for 2 cases having hemythyroidectomy with total laryngectomy and one patient with hemityroid who were hypothyroid. In this respect our findings correspond with others.[14,15,16,32]

The presence of some abnormality in more than one half of the examined group signals the need for close evaluation of the thyroid in patients successfully treated for head and neck tumors. Periodically measurement of TSH as a sensitive index of subtle impairment of the gland seems to be the most appropriate test for evaluation of the thyroid damage due to external irradiation.

References

1. Fuks T, Glatstein E, Marsa GW, Bagshaw MA, Kaplan HS. Long term effects of external radiation on the pituitary and thyroid glands. *Cancer* 1976; **37**:1152-61.
2. Glatstein E, McHardy-Young S, Brast, Eltringhalm JR, Kriss JP. Alterations in serum thyrotropin (TSH) and thyroid function following radiotherapy in patients with malignant lymphoma. *J Clin Endocrinol Metab* 19071; **32**:833-41.
3. Kim YH, Fayos JV, Sisson JG. Thyroid function following neck irradiation for malignant lymphoma. *Radiology* 1980; **134**:205-8.
4. Nelson DF, Reddy KV, O'Mara R.E., Rubin P. Thyroid abnormalities following neck irradiation for Hodgkin's disease. *Cancer* 1978; **42**:2553-62.
5. Schimpff SC, Diggs CH, Wiswell JG, Salvatore PC, Wiernik PH. Radiation related thyroid dysfunction: implications for the treatment of Hodgkin's disease. *Ann Intern Med* 1980; **92**:91-8.
6. Tamura K, Shimaoka K, Friedman M. Thyroid abnormalities associated with treatment of malignant lymphoma. *Cancer* 1981; **47**:2704.
7. Čočina KN, Švarcberg EM. Issledovanie funkcii štitovidnoi železi pri pomošti radioaktivnogo joda pri lučevoi lečenii raka gortani. *Med Radiol* 1960; **8**:14-8.
8. Félix H, Durpé N, Drapé M, Court L. Incidence à long terme d'une radiothérapie pour cancer du larynx sur l'apparition d'un myxoedeme. *Lyon Méd* 1961; **93**:1043-50.
9. Einhorn J, Wikholm G. Hypothyroidism after external irradiation to the thyroid region. *Radiology* 1967; **88**:326-8.
10. Greig WR, Boyle JA, Buchanam WW, Fulton S. Clinical and radiobiological observations on lattent effects of X irradiation on the thyroid gland. *J Clin Endocr* 1965; **25**:1009-14.
11. Koulumies M, Voutilainen A, Koulumies R, Effect of X ray irradiation of laryngeal cancer on the function of the thyroid gland. *Ann Int Med Fenn* 1964; **53**:89-96.
12. Markson JL, Flatman GE. Myxoedema after deep X ray therapy to the neck. *Br Med J* 1965; **1**:1228-30.
13. Samaan NA, Vieto R, Schultz PN, Maor M, Meoz RT, Sampiere VA, Cangir A, Ried HL, Jesse RH. Hypothalamic, pituitary and thyroid dysfunction after radiotherapy to the head and neck. *Int J Radiat Oncol Biol Phys.* 1982; **8**:1857-67.
14. Lavelle RJ. Thyroid function after radiotherapy and total laryngectomy in the treatment of carcinoma of the larynx. *Ann Otol Rhinol Laryngol* 1971; **80**:593-8.
15. Murken RE, Duvall AJ. Hypothyroidism following combined therapy in carcinoma of the laryngopharynx. *Laryngoscope* 1972; **82**:1306-14.
16. Shafer RB, Nuttal FQ, Pollak K, Kuisk H. Thyroid function after radiation and surgery for head and neck cancer. *Arch Intern Med* 1975; **135**:843-64.
17. Dimitrovska A, Georgievska B, Jovanovski D, Velkov K. Thyroid function after irradiation and surgery for laryngeal cancer. *Radiol Iugosl* 1982; **16**:331-5.
18. Aleksić Ž. Šestakov Đ. Comparative measuring of thyroxine by radioimmunologic method (RIA) and competitive method. *Radiol Iugosl* 1978;**2**:450-1.
19. Šestakov Đ, Ivanovski R. Radioimmunoassay of triiodthyronin using thermo-denaturated serum and separation on charcoal. *Radiol Iugosl.* 1978; **2**:451-2.
20. Šestakov Đ, Ivanovski R. Radioimmunoassy of TSH – experience with labeling, storage and determination with calbiochem kit. *Radiol Iugosl* 1978;**2**:453-4.
21. Oliver C, Chartet JL, Codaccioni J, Vague J. Radioimmunoassay of thyrotropin-releasing hormone (TRH) in human plasma. *J Clin Endocrinol Metab* 1974; **39**:406-9.
22. Ormstron BJ, Garry R, Cryer RJ, Besser GM, Hall R, Thyrotropin-releasing hormone as a thyroid function test. *Lancet* 1971;**2**:10-4.
23. Boyden SV. The absorption of proteins on erytrocytes treated with tannic acid subsequent haemagglutination by antiprotein sera *J Exp Med* 1951;**93**:107.
24. Aubin PM, Kinsley RM, Andrews GA. External irradiation of the thyroid gland in dogs. Effects of large doses of roentgen rays upon histologic struc-

ture and J-131 metabolism. *Am J Roengenol Radium Ther Nucl Med* 1957; **78:**864-75.
25. Lindsay S, Dailey ME, Jones MD. Histologic effects of various types of ionizing radiation on normal and hyperplastic human thyroid glands. *J Clin Endocrinol* 1954; **14:**1179-218.
26. Michaelson SM, Quinlan W, Casarett GW, Mason WB. Radiation induced thyroid dysfunction in the dog. *Rad Res* 1967; **30:**38-47.
27. Rubin, Casarett GW. The endocrine glands. In: *Clinical radiation pathology*, vol 2, Philadelphia, W.B. Saunders 1968; 721-67.
28. Shively JN, Epling GP, Early changes in the fine structure of the midlethally irradiated thyroid dogs. *Rad Res* 1969; **37:**71-82.
29. Brase AR, Sippel R. Zur hypothyreosehäufigkeit nach perkutaner telekobaltbestrahlung des larynxkarzinoms. *Strahlentherapie* 1973; **145:**147-54.
30. Bigos ST, Ridgway EC, Kourides JA, Maloof F. Spectrum of pituitary alterations with mild and severe thyroid impairment. *J Clin Endocrinol Metab* 1978; **46:**317-25.
31. Ingbar S.H. *Thyroid today. An endocrine update.* Medcom Inc. Learning Systems, 1973; 58-65.

Adv Radiol Oncol 1992; 214–20.

Tumor markers in clinical oncology

Novaković S and Serša G

Institute of Oncology, Department of Tumor Biology and Biotherapy, Ljubljana

Quick and accurate diagnosis is a prerequisite in planning of treatment in oncology. Differences between normal and tumor cells are used as a lead in the development of tumor markers. This quickly developing field of tumor markers has started in the 60's with alphafetoprotein and carcinoembryonic antigen. The second hallmark in development was the production of monoclonal antibodies and therefore more specific markers, tumor associated antigens. These markers have many characteristics of an ideal tumor marker, but they are still insufficiently specific for screening. The main advantage is in their ability to follow up tumor growth either by treatment response evaluation or early detection of recurrences. Apart from diagnostics, tumor markers are used also in tumor treatment, as targets of monoclonal antibodies conjugated with cytotoxic agents. Tumor markers have found broad application in oncology, as target therapy, which will further expand with development of new more specific markers and contribute to early detection and treatment of cancer.

Key words: neoplasms-diagnosis; tumor markers, biological

Introduction

In the normal process of differentiation precursor cells loose the ability to proliferate. However, in the tissues dying cells are replaced by proliferating precursor cells which in the process of differentiation obtain specific morphology and function. Malignant cells also develop from precursor cells by malignant transformation under the influence of biological, chemical or physical agents. They proliferate with impaired regulatory mechanisms, and develop specific properties reflected in the content and activity of DNA, changes in cell surface antigens, as well as in altered enzyme metabolism of the cells.

Correspondence to: Srđan Novaković, M. Sc. Institute of Oncology, Department of Tumor Biology and Biotherapy. Zaloška 2, 61000 Ljubljana, Slovenia.

UDC: 616-006.6-07-097

The target of carcinogens is predominantly cellular DNA, which results in morphological, physiological and functional changes of the cells. This concept is supported by the following findings:[1,2]

a) Incidence of some rare tumors is proportional to hereditary factors,

b) Higher incidence of cancer in the individuals with deficient ability of DNA lesion repair,

c) Specific types of cancers have higher incidence of well defined chromosomal changes in cancer cells,

d) Existence of a number of oncogens which can by activation transform normal cells into cancer cells.

Despite the known differences between normal and malignant cells, there is still no laboratory test which could be used for diagnosis of all malignancies, based on the genetic, histochemical or immunological distinction between normal and transformed cells. Therefore, markers for

specific malignancies are being developed in association with other known diagnostic procedures. One of such specific, rapidly developing fields are tumor markers.

Substances which are produced in malignant cells or under the influence of malignant cells and are detectable in the body fluids and/or in tissues are tumor markers.[1] These can be biochemically new substances or normal components of the organism, but in ectopic production. Biotechnology of monoclonal antibodies (MoAb) has enabled the development of new tests for the determination of specific antigenic determinants of different malignancies either on cells or in body fluids. Although these markers tend to be specific, they are not always associated with malignancy; sometimes they are produced in high concentrations in benign or other pathophysiological changes in the organism. Even when they are associated with malignant transformation their serum concentrations do not always reflect tumor burden in the organism.

As an example, alphafetoprotein (AFP) is an oncofetal antigen, which is normally produced during embryional growth in hepatic cells, yolk sac cells and mucosal cells of gastrointestinal tract. Therefore, high serum concentrations of AFP are detectable during the embryonal life, and after birth its concentration is rapidly decreasing. High serum concentrations are detectable also in patients with hepatocellular carcinomas, but in some instances also in nonmalignant diseases such as hepatitis and liver cirrhosis. Because tumor markers can be associated with embryogenesis, benign diseases or other patho-physiological changes in the organism, they cannot be regarded as specific for cancer screening.

An ideal tumor marker, useful also for screening, should have the following properties:[3,4] It should be:

- produced only by tumor cells,
- organ and tumor specific,
- detectable in all patients with the same tumor type,
- detectable at initial stages of tumor growth and
- in serum concentrations that follow tumor volume.

Tumor marker applications

Tumor markers are used in clinical oncology for several purposes[5,6,7] (Table 1), but predominantly in the follow up of tumor growth, response to therapy, recurrence of the disease, and as an additional test to confirm diagnosis.

Some tumor markers are more useful for the confirmation of the primary disease whereas others are used for early detection of recurrences or follow up of treatment response. Simultaneous determination of several tumor markers increases the reliability of findings. Combination of specific and complementary tumor markers is recommended. For example, in nonseminous testicular tumors, choriogonadotropin (HCG) and AFP have 90% specificity and 60% sensitivity; by combining both markers, the sensitivity can be increased to 95%.[8]

Table 1. Application of tumor markers in oncology.

I) Diagnosis and follow up
1) determination of tumor markers in body fluids
a) screening,
b) diagnostic tool in suspicious cases,
c) determination of extent of the disease,
d) follow up of the treatment,
e) early detection of recurrence;
2) immunoscintigrapy and lymphoscintigraphy
3) immunopathology
a) diagnostic dilemma: malignant/benign,
b) differential diagnosis of tumor type,
c) tumor subclassification;
II) Therapeutic applications
1) direct cytototoxicity of MoAb
a) complement binding on specific MoAb,
b) binding of cytotoxic cells specific MoAb,
2) drug conjugation of MoAb,
3) toxin conjugation of MoAb,
4) radionuclide conjugation of MoAb,
5) inhibition of receptors for growth factors.

Prognostic value of tumor markers

Malignant process should be monitored by tumor markers before, during and after therapy. Careful follow up gives an insight into the aggressiveness of the disease and therefore has a prognostic value.

Wang et al. have determined carcinoembryonic antigen (CEA) in women with breast cancer before and after mastectomy, and found that recurrence rate was higher in group of patients with high CEA serum levels after surgery.[9] Also Myers et al. found that high CEA serum levels after mastectomy in women with primary breast cancer indicated bad prognosis, i.e. high probability of reccurrence and shorter remission interval.[10, 11]

Taken together, abnormal serum concentrations of tumor markers are regarded as a bad prognostic factor for progression of the disease.[12-20]

Classification of tumor markers

The existing tumor markers can be classified into:

- oncofetal proteins,
- hormons or carcinoplacental antigens,
- enzymes,
- tumor associated antigens,
- miscellaneous markers.

Oncofetal proteins

Oncofetal proteins are antigens synthesised in the fetus during embryonal growth. In adults their production is reduced or stopped; ectopic production is associated with a derepression of the corresponding DNA, as in neoplastic cell transformation.

Carcinoembryonic antigen (CEA) is a representative member of oncofetal proteins, first described by Gold and Freedman.[21] It is a glycoprotein of 200 KD, isolated from extracts of colon adenocarcinoma. In embryonal growth during the second and sixth month it is produced in epithelial cells of gastrointestinal tract, liver and pancreas.[8] First, CEA was considered as an ideal tumor marker for colorectal carcinomas, but it was soon recognised that it could be synthesised also in some normal tissues and thus associated with non-malignant or benign diseases.[8,22,23,24] Elevated levels of serum CEA are associated with: heavy smoking, bronchitis, gastritis, duodenal ulcer, liver damage, pancreatitis and polyps of colon and rectum. In malignant diseases elevated serum CEA concentrations are associated with adenocarcinoma of the colon and rectum, carcinoma of the pancreas, lung, breast, stomach, thyroid, ovary and endometrium.

Serum CEA concentrations in cancer patients are dependent on several factors: tumor mass, vascularization of the tumor, necrotic processes and differentiation of the tumor cells. Less differentiated tumors produce smaller amounts of CEA.

Nevertheless, CEA is an important marker for follow up of colorectal carcinoma with respect to treatment response and early detection of relapse. In mammary, ovarian, pancreatic, lung and liver carcinomas it is associated with progression of the disease, especially with dissemination.[8,22,24,25,26]

Alphafetoprotein (AFP) is also an oncofetal antigen discovered by Abelev in 1963 in serum of hepatocellular carcinoma bearing mice. It is a glycoprotein of 70 KD produced in yolk sac, gastrointestinal epitelium and liver during embryonal growth.[8,27]

Elevated serum concentrations are associated with acute virus hepatatis, liver cirrhosis, obstructive icterus, as well as in malignant diseases as pancreatic, lung and stomach cancer. It is useful in follow up of hepatocellular cancer (specificity 80%) and nonseminomatous testicular tumors (specificity 60%). Besides its high specificity it correlates well with tumor burden in patients with hepatocellular carcinoma.

Hormons or carcinoplacental antigens

Hormons or carcinoplacental antigens are proteins produced in placenta during pregnancy,

and associated with some malignancies.[8] Representative antigen is *choriogonadotropin* (HCG) glycoprotein of 45 KD.[28] Elevated HCG serum concentrations, detectable in patients with choriocarcinomas and nonseminomatous testicular tumors and useful in prognosis of complete remission and in response to therapy.[28] In combination with AFP the prognostic value of HCG for nonseminous testicular carcinomas is increased. If serum concentrations of both markers is within normal range, complete remission is expected in 90%, if only one of the markers is within normal range complete remission is expected in 37% of cases.

Enzymes

Ectopic production of some enzymes is associated with a malignant disease. *Prostatic acid phosphatase* is an enzyme which is produced in normal tissue of the prostate. Elevated levels of this marker are associated with prostatic cancer especially in advanced stages of the disease.[29]

Alkaline phospatase is produced in normal tissues of the liver, bones and placenta. Elevated serum concentrations in patients with malignant diseases indicate metastatic spread in the liver and or in the bones.[30,31]

Neuron specific enolase (NSE) is a glycolytic enzyme consisting of three, immunologically distinct subunits: alpha, beta and gamma. Gamma subunit is detectable in high concentrations in neurons and in neuroendocrine cells.[32,33,34] High serum concentrations of NSE are associated with neuroblastoma tumors, small cell lung carcinoma and medullary thyroid carcinoma.

Tumor associated antigens

Tumor associated antigens are markers which have been determined on specific malignant cells with monoclonal antibodies. Therefore they are numerous and highly specific for different malignancies. Although their concentrations are significantly elevated in the serum of cancer patients, they can be detected also in non malignant diseases.

Cancer-associated antigen 15-3 (CA 15-3) is specific for mammary carcinoma, but is useful also in the follow up of ovarian carcinoma.[35]

Mucin-like carcinoma-associated antigen (MCA) is a new tumor marker for mammary carcinomas discovered by Stähli et al.[36,37,38] Specificity of MCA which is predominantly secreted from mucinous mammary carcinomas, is 83% and sensitivity 70%.[38] In normal adults MCA is synthesised in normal mammary epithelium as well as in the kidneys, endometrium, urethra, and prostatic epithelium.[38] It is interesting that MCA is not produced in germinal cells of the ovaries and testes.

MCA serum concentrations in healthy women seldom (5%) exceed cut-off limit 17 U/ml.[39] Urine MCA concentrations are ten times higher in healthy males, with cut-off limit 180 U/ml.[40] Similar molecule to MCA of 450 KD was discovered also in human milk.[38]

Average serum concentration in healthy adult women is below 10 U/ml, while in patients with mammary carcinoma the values are significantly elevated and can reach 5000 U/ml.[39,41] At evaluation of the results the possibility of pregnancy should be taken into account since MCA serum concentrations are elevated in 57.2% of cases, especially in the third trimester.[42]

Ovarian cystadenocarcinoma antigen (OCAA) was described by Bhattacharya and Barlow.[43,44] It is specific for ovarian cancer and to a lesser extent with cervical, breast and colon cancer.

Cancer-associated antigen 125 (CA 125) is a tumor associated antigen, which is synthesised in more than 80% of nonmucous epithelial ovarian carcinomas. It is a glicoprotein with molecular weight of 200 KD.[45-49] During embryonal growth CA 125 is detectable in coelomic epithelium, Müller's ducts, serous pleural epithelium, peritoneum and pericard.[50] In healthy population it is present in milk, cervical mucosa and lung tissue.[51,52,53]

CA 125 is not produced by healthy ovarian epithelium either during embryonal growth or in adults, but it is present in epithelial ovarian

carcinomas and other malignant and benign gynecological tumors (endometrial carcinoma, cervical carcilnoma, lung carcinoma, and prostatic carcinoma).[50,54,55,56,57] Besides in some neoplastic and benign tumors, elevated CA 125 serum concentrations are detectable in women with an inflammatory process in the pelvis caused by N. gonorrhea, C. trachomatis and H. simplex Type 2.[58]

CA 125 is detectable also in ascites, but determination of this marker in ascites is not useful for follow up of patients with ovarian carcinoma.[59,60,61,62] Therefore, serum concentrations proved more suitable for this purpose. An increase in tumor mass is accompanied by elevated serum concentrations of CA 125, but the relationship is not linear.[46,59,63,64,65,66,67] Nevertheless, low serum concentrations indicate early stages of epithelial ovarian carcinoma, small tumor mass, and better response to therapy.[15-19] High CA 125 concentrations indicate a progressive disease, poor prognosis and worse response to therapy. CA 125 concentrations correlate also with differentiation of tumor cells; well differentiated cells produce higher concentration of CA 125.[18,24] Sex and age do not influence serum concentrations.[46]

Carbohydrate antigen 19-9 (CA 19-9) is a tumor associated antigen specific for carcinomas of the pancreas and liver. Elevated levels of this marker are detectable also in colon carcinomas, rectum, ovarian carcinoma and carcinoma of the stomach.[68,69,70,71]

Miscellaneous tumor markers

Miscellaneous tumor markers represent a heterogeneous group comprising markers as *poliamins, nucleosides, tissue polipeptide antigen* (TPA), *isoferritin and others.*

Conclusions

Tumor markers enable the physician to quickly and efficiently follow a malignant disease, in association with other diagnostic methods. Their usefulness is in evaluation of treatment response and early detection of recurrences.

Methods used for the determination of serum tumor markers are uninvasive and therefore suitable also for patients in bad psycho-physical condition or in patients in whom more invasive methods are contraindicated.

Because of a big variability in serum concentrations of tumor markers in patients with certain malignant diseases, it is recommended to determine them before and after therapy, as well as at periodical check-ups. When this is not possible, single values significantly exceeding the cut-off limit can be indicative of the presence of malignancy. In this respect, it has to be taken into consideration that some non-malignant diseases can induce overproduction of tumor markers.

An ideal tumor marker still does not exist, since presently known markers are insufficiently specific, but in the future, with the development of new more specific monoclonal antibodies, further advances in this field may be expected.

References

1. Hill RP, Tannock IF. Introduction: cancer as a cellular disease. In: Tannock IF, Hill RP eds. *The basic science of oncology*. New York: Pergamon Press, 1987:1-4.
2. Philips RA. The genetic basis of cancer. In: Tannock IF, Hill RP eds. *The basic science of oncology*. New York: Pergamon Press, 1987:24-51.
3. Klee GG, Go VLW. Carcinoembryonic antigen and its role in clinical practice. In: Ghosh BC, Ghosh L eds. *Tumor markers and tumor-associated antigens*. New York: McGraw-Hill, 1987:22-43.
4. Kudlacek St. Tumormaker. *Wien Med Wochenschr* 1988; **138:**228-42.
5. Ghosh BC, Rob CG. Tumor markers. In: Ghosh BC, Ghosh L eds. *Tumor markers and tumor-associated antigens*. New York: McGraw-Hill, 1987:1-10.
6. Thor A, Ohuchi N, Szpak CA, Johnston WW, Schlom J. Monoclonal antibodies and immunopathology: aplications to human carcinomas. In: Ghosh BC, Ghosh L eds. *Tumor markers and tumor-associated antigens*. New York: McGraw-Hill, 1987:238-68.
7. Pruet CW, Ghosh BC. Antigens and markers in head and neck cancer. In: Ghosh BC, Ghosh L eds. *Tumor markers and tumor-associated antigens*. New York: McGraw-Hill, 1987:313-7.

8. Malkin A. Tumor markers. In: Tannock IF, Hill RP eds. *The basic science of oncology*. New York: Pergamon Press, 1987:192-203.
9. Wang DY, Bulbrook RD, Hayward JL et al. Relationship between plasma carcinoembryonic antigen and prognosis in women with breast cancer. *Eur J Cancer* 1975; **11**:615-8.
10. Myers RE, Sutherland DJ, Meakin JW et al. Carcinoembryonic antigen in breast cancer. *Cancer* 1987; **42**:1520-6.
11. Myers RE, Sutherland DJ, Meakin JW et al. Prognostic value of postoperative blood levels of carcinoembryonic antigen (CEA) in breast cancer, In: Lehmann FG eds. *Carcino-Embryonic Proteins*. North-Holand, 1979:133-8.
12. Torosian MH. The clinical usefulness and limitations of tumor markers. *Surg Gynecol Obstet* 1988; **166**:567-79.
13. Podczaski E, Whitney C, Manetta A et al. Use of CA 125 to monitor patients with ovarian epithelial carcinomas. *Gynecol Oncol* 1989; **33**:193-7.
14. Bruzzone M, Onetto M, Campora E et al. CA 125 monitoring in the management of ovarian cancer. *Anticancer Res* 1990; **10**:1353-60.
15. Einhorn N, Bast RC Jr, Knapp RC, Tjernberg B, Zurawski VR Jr. Preoperative evaluation of serum CA 125 levels in patients with primary epithelial ovarian cancer. *Obstet Gynecol* 1986; **67**:414-6.
16. Kivinen S, Kuoppala T, Leppilampi M, Vuori J, Kauppila A. Tumor-associated antigen Ca 125 before and during the treatment of ovarian carcinoma: *Obstet Gynecol 1986;* **67**:468-77.
17. Niloff JM, Knapp RC, Lavin PT et al. The CA 125 assay,as a predictor of clinical recurrence in epithelial ovarian cancer. *Am J Obstet Gynecol* 1986; **155**:56-60.
18. Vergote IB, Bormer OP, Abeler VM. Evaluation of serum CA 125 levels in the monitoring of ovarian cancer. *Am J Obstet Gynecol* 1987; **157**:88-92.
19. Alvarez RD, To A, Boots LR et al. CA 125 as a serum marker for poor prognosis in ovarian malignancies. *Gynecol Oncol* 1987; **26**:284-9.
20. Serša G, Rudolf Z, Plesničar S. Prognostic value of slope angle calculation in patients with colorectal cancer. *Radiol Iugosl* 1983; **17**:193-6.
21. Gold P, Freedman SO. Demonstration of tumor-specific antigens in human colonic carcinomata by immunological tolerance and absorption techniques. *J Exp Med* 1965; **121**:439-62.
22. Lamerz R, Leonhardt A,l Ehrhart H, Lieven van H. Serial carcinoembryonic antigen (CEA) determinations in the management of metastatic breast cancer. *Oncodevelop Biol Med* 1980; **1**:123-35.
23. Beard DB, Haskell CM. Carcinoembryonic antigen in breast cancer. *Am J Med* 1986; **80**:241-5.
24. Daunter B. Tumor markers in gynecologic oncology. *Gynecol Oncol* 1990; **39**:1-15.
25. Plesničar S, Rudolf Z, Berčič I. Klinična vrednost določanja karcinoembrioničnega antigena (CEA) v serumu bolnikov z gastrointestinalnimi malignomi. *Zdrav Vestn* 1977: **46**:677-80.
26. Torosian MH. The clinical usefulness and limitations of tumor markers. *Surg Gynecol Obstet* 1988; **166**:567-79.
27. Sell S. Alphafetoprotein: the epitome of cancer markers. In: Cimino F, Birkmayer GD, Klavins JV,m Pimentel E, Salvatore F eds. *Human tumor markers*. Berlin: Walter de Gruyter, 1987:301-13.
28. Nagell van Jr, Pavlik EJ, Gay EC. Tumor markers in gynecologic cancer. In: Nagell van JR, Barker HRK eds. *Modern concept of gyneocologic oncology*. Boston: John Wright PGS Inc, 1982:624-9.
29. Bruce AW, Mahan DC, Sulivan LD, Goldenberg L. The significance of prostatic acid phosphatase in adenocarcinoma of the prostate. *J Urol* 1981; **125**:357-62.
30. Yam LT, Winkler CF, Janckila AJ, Li CY, Lam WKW. Prostatic cancer presenting as metastatic adenocarcinoma of undetermined origin: Immunodiagnosis by prostatic acid phosphatase. *Cancer* 1983; **51**:283-7.
31. Schacht MJ, Garnet JE, Grayhack JT. Biochemical markers in prostatic cancer. *Urol Clin North Am* 1984; **11**:253-9.
32. Zeltzer PM, Parma AM, Dalton A et al. Raised neuronspecific enolase in serum of children with metastatic neuroblastoma. *Lancet* 1983; **2**:361-3.
33. Essher T, Steinholtz L, Bergh J, Nou E, Nilsson K, Pahlman S. Neurone specific enolase: a useful diagnostic serum marker for small cell carcinoma of the lung. *Thorax* 1985: **40**:85-90.
34. Berhiot G, Marechal F, Cattan A and Deltour G. Serum levels of CA-50, CA-19-9, CA-125, neuron specific enolase and carcinoembryonic antigen in lung cancer and benign diseases of the lung. *Biomed Pharmacother* 1989; **43**:613-20.
35. Pons-Anicet DMF, Krebs BP, Mera R, Namer M. Value of CA 15.3 in the follow up of breast cancer patients. *Br J Cancer* 1987; **55**:567-9.
36. Stähli C, Takacs B, Miggiano V, Staehelin T, Carmann H. Monoclonal antibodies against antigens on breast cancer cells. *Experientia* 1985; **41**:1377-81.
37. Stähli C, Caravatti M, Aeschbacher M, Kocyba C, Takacs B, Carmann H. Mucin-like carcinoma-associated antigen defined by three monoclonal antibodies against different epitopes. *Cancer Res* 1988; **48**:6799-802.
38. Zenklusen HR. Stähli C, Gudat F, Overbeck VJ, Rolilnk J, Heitz PU. The immunohistochemical reactivity of a new antiepithelial monoclonal antibody (MAb b-12) against breast carcinoma and other normal and neoplastic human tissues. *Virch Arch A. (Pathol Anat).* 1988; **413**:3-10.
39. Novaković S, Krošl G, Plesničar S. Prognostic value of a mucin-like carcinoma-associated antigen (MCA) in patients with breast carcinoma. *Tumor Diagn Ther* 1989; **10**:136-41.
40. Novaković S, Marolt F, Serša G. The use of MCA and CEA in prostatic cancer follow up. *Radiol Iugosl* 1990; **24**:417-21.
41. Eskelinen M, Tikanoja S, Collan Y. A new tumor marker MCA in breast cancer diagnosis. *Anticancer Res* 1988; **8**:665-8.
42. Novaković S, Serša G, Krošl G, Plesničar S. CEA, MCA and CA 125 tumor markers in pregnant women. *Radiol Iugosl* 1990; **24**:79-84.
43. Bhattacharya M, Barlow JJ. Immunologic studies of human serous cystadenocarcinoma of the ovary: demonstration of tumor associated antigens. *Cancer* 1973; **31**:588-95.

44. Bhattacharya M, Barlow JJ. An immunologic comparison between serous cystadenocarcinoma of the ovary and other human gynecologic tumors. *Am J Obstet Gynecol* 1973; **117**:849-53.
45. Bast RC Jr, Feeney M, Lazarus H, Nadler LM, Colvin RB, Knapp RC. Reactivity of a monoclonal antibody with human ovarian carcinoma. *J Clin Invest* 1981; **68**:1331-7.
46. Bast RC Jr, Klug TL, St. John E et al. A radioimmunoassay using a monoclonal antibody to monitor the course of epithelial ovarian cancer. *New Engl J Med* 1983; **309**:883-7.
47. Klug TL, Bast RC Jr, Niloff JM, Knapp RC, Zurawski VR Jr. Monoclonal antibody immunoradiometric assay for an antigenic determinant (CA 125) associated with human epithelial ovarian carcinomas. *Cancer Res* 1984; **44**:1048-53.
48. Davis HM, Zurawski VR Jr. Bast RC Jr, Klug TL. Characterization of the CA 125 antigen associated with human epithelial ovarian carcinomas. *Cancer Res* 1986; **46**:6143-8.
49. Olt J, Berchuck A, Bast RC. Gynecologic tumor markers. *Semin Surg Oncol* 1990; **6**:305-13.
50. Altaras MM, Goldberg GL, Levin W, Darge L, Bloch B, Smith JA. The value od cancer antigen-125 as a tumor marker in malignant germ cell tumors of the ovary. *Gynecol Oncol* 1986; **25**:150-9.
51. Hanisch FG, Uhlenbruck G, Dienst C, Stottrop M, Hippaunf E. Ca 125 and CA 19-9: two cancer associated sialylsaccharide antigens on a mucus glycoprotein from human milk. *Eur J Biochem* 1985; **149**:323-30.
52. Bruijn de HWA, Beeck Calkoen-Carpay van T, Jager S, Duk JM, Aalders JG, Fleuren GJ. The tumor marker CA 125 is a common constituent of normal cervical mucus. *Am J Obstet Gynecol* 1986; **154**:1088-91.
53. Nouven EJ, Pollet DE, Eerdekens HW, Hendrix PG, Briers TW, Broe de ME. Immunohistochemical localisation of placental alkaline phosphatase, carcynoembryonic antigen and cancer antigen CA-125 in normal and neoplastic human lung. *Cancer Res* 1986; **46**:866-76.
54. Niloff JM, Knapp RC, Schaetzl E, Reynolds C, Bast RC Jr. CA 125 antigen levels in obstetric and gynecologic patients. *Obstet Gynecol* 1984; **64**:703-7.
55. O'Brien TJ, Hardin JW, Bannon GA, Norris JS, Quirk JG Jr. CA 125 antigen in human amniotic fluid and fetal membranes. *Am J Obstet Gynecol* 1986; **155**:50-5.
56. Matsuoka Y, Nakashima T, Endo K et al. Recognition of ovarian cancer antigen CA 125 by murine monoclonal antibody produced by immunization of lung cancer cells. *Cancer Res* 1987; **47**:6335-40.
57. Sakamoto K, Haga Y, Yoshimura R, Egami H, Yokohama Y, Akagi M. Comparative effectiveness of the tumour diagnostics, CA 19-9, CA 125 and carcinoembryonic antigen in patients with diseases of the digestive system. *Gut* 1987; **28**:323-9.
58. Halila H, Stenman UH, Seppala M. Ovarian cancer antigen CA 125 levels in pelvic inflammatory disease and pregnancy. *Cancer* 1986; **57**:1327-9.
59. Meier W, Stieber P, Fateh-Moghadam A, Eiermann W, Hepp H. CA-125 in gynecological malignancies. *Eur J Cancer Clin Oncol* 1987; **23**:713-7.
60. Touitou Y, Bogdan A. Tumor markers in non-malignant diseases. *Eur J Cancer Clin Oncol* 1988; **24**:1083-91.
61. Bergmann JF, Beaugrand M, Labadie H, Bidart JM, Bohuon C. CA 125 (ovarian tumour-associated antigen) in ascitic liver diseases. *Clin Chim Acta* 1986; **155**:163-6.
62. Bergmann JF, Bidart JM, George M, Beaugrand M, Levy VG, Bohuon C. Elevation of CA 125 in patients with benign and malignant ascites. *Cancer* 1987; **59**:213-7.
63. Peters WA, Bagley CM, Smith MR. CA-125: use as a tumor marker with mixed mesodermal tumors of the female genital tract. *Cancer* 1986; **58**:2625-7.
64. Zurawski VR Jr, Orjaseter H, Andersen A, Jellum E. Elevated serum CA 125 levels prior to diagnosis of ovarian neoplasia: relevance for early detection of ovarian cancer. *Int J Cancer* 1988; **42**:677-80.
65. Cruickshank DJ, Fullerton WT, Klopper A. The clinical significance of pre-operative serum CA 125 in ovarian cancer. *Br J Obstet Gynecol* 1987; **94**:692-5.
66. Gadducci A, Ferdeghini M, Ceccarini T et al. A comparative evaluation of the ability of serum CA 125, CA 19-9, CA 15-3, CA 50, CA 72-4 and TATI assays in reflecting the course of disease in patients with ovarian carcinoma. *Eur J Gynecol Oncol* 1990; **11**:127-33.
67. Zurawski VR, Sjovall K, Schoenfeld DA et al. Prospective evaluation of serum CA 125 levels in a normal population, phase I: The specificities of single and serial determinations in testing for ovarian cancer. *Gynecol Oncol* 1990; **36**:299-305.
68. Motoyama T, Watanabe H, Takeuchi S, Watanabe T, Gotoh S, and Okazaki E. Cancer antigen 125, carcinoembryonic antigen, and carbohydrate determinant 19-9 in ovarian tumors. *Cancer* 1990; **66**:2628-35.
69. Safi F, Beger GH, Bittner R, Buchler M, and Krautzbergerm, W. CA 19-9 and pancreatic adenocarcinoma. *Cancer* 1986; **57**:779-83.
70. Steinberg W. The clinical utility of the CA 19-9 tumor-associated antigen. *Am J Gastroenterol* 1990; **85**:350-5.
71. Safi F, Roscher R, Beger HG. The clinical relevance of the tumor marker CA 19-9 in the diagnosing and monitoring of pancreatic carcinoma. *Bull Cancer* 1990; **77**:83-91.

Adv Radiol Oncol 1992; 221–6.

The predictive significance of CA 15-3 for the first relapse in early breast cancer patients

Nešković-Konstantinović Z[1], Vuletić L[1], Tasić S[2], Ogrizović N[1], Šušnjar S[1]

[1]Institute of Oncology and Radiology: Breast Cancer Dept. and [2]Laboratory of Nuclear Medicine, Belgrade

Serum levels of CA 15-3 were determined in 91 operable breast cancer (BC) patients during adjuvant chemo – and/or hormonal treatment, as well as after termination of chemotherapy, mostly in three–month intervals. During the follow–up period of 1.5 to 4.5+ years 43 patients relapsed. With the cut-off value of 33 U/ml, elevated CA 15-3 levels were found in 25/43 patients at the time of relapse, whereas in 23/43 patients the increase in tumour marker value preceded clinical signs of relaps for 2-30 months. The sensitivity of CA 15-3 for the presence of metastatic lesions was 0.58, and for the prediction of relapse 0.53. The specificity for metastatic disease was 0.73, with the positive predictive value of 0.65, and negative predictive value of 0.66. Our results suggest that the cut-off value should be set at a higher level when this marker is used for predicting the first relapse in disease-free BC patients. The relationship between increased marker values and the site of the first metastasis is considered.

Key words: breast neoplasms; antigens, tumour-associated, carbohydrate

Introduction

CA 15-3 is one of the breast cancer-associated antigens[1] with a considerable clinical value in the follow-up of metastatic breast cancer patients.[2] Its value in the early search for new metastatic lesions has recently been demonstrated.[3]

Possible use of systemic treatment in non-metastatic patients with increased CA 15-3 is still questionable[4], whereas there is no doubt about the usefulness of this tumour marker in screening plans for metastatic disease appearance.

The aim of this work was to analyse the clinical relevance of tumour-associated antigen CA 15-3 in the prediction of metastatic spread of breast cancer.

Correspondence to: Nešković-Konstantinović Z. MD. Institute of Oncology and Radiology, Pasterova 14, Belgrade, Yugoslavia.

UDC: 618.19-006.6-097

Patients and methods.

CA 15-3 was measured using the ELISA method kits of International CIS. The value of 33 U/ml was taken as cut-off level of 15-3. This tumour marker was determined in the serum of operable breast cancer patients a month after radical surgical treatment, prior to the beginning of adjuvant treatment. Thereafter, measurements were done in three-month intervals till the relapse, or till the last follow-up examination. Tumor marker values were analysed in 91 breast cancer patients, aged 30-70 years (median 52), premeno- (34) or posmenopausal (57), during follow-up period of 1.5 to 4.5+ years (median 3 years). All patients except three were treated by some kind of adjuvant treatment, according to the histological tumour grade, nodal status, steroid receptor status and menstrual status: 56 pts. received ajuvant CMF chemotherapy, 21 were treated by

adjuvant hormonal treatments (castration by irradiation or Tamoxifen), and 11 by chemo-hormonal ajuvant therapy. All patients belonged to the »high-risk« group, i. e. they were either node-negative with grade III primary tumours or they were node positive.

The patients were examined on diagnosis and followed-up by standard methods - clinical, radiographic, scintigraphic and laboratory examinations, ultrasonic and computed tomography if necessary etc. So far, the first relapse was diagnosed in 43/91 patients (47%). All CA 15-3 values, determined within 1 month prior to the relapse occurrence were thought to be the relapse-values, and those determined from one to more months earlier were considered as pre-relapse values. Most of the patients had the first relapse in bones (24 pts), or in soft tissue (10 pts). The sensitivity, specificity and the prognostic value of CA 15-3 were determined according to the methods described elsewhere[5], Mann-Whitney test was used for testing marker levels.

Results and comments

During a follow-up period of 1.5-4.5+ years increased CA 15-3 values were found in the time of relapse in 23/43 patients, ranging from 37 to 2135 U/ml (median 149). The increased CA 15-3 values preceded the relapse occurrence in 23/43 patients, ranging from 34-1255 U/ml, (median value 80 U/ml). They were found from 2-30 months prior to relapse. It has to be noted that the patients with increased marker values in the time of relapse and before the relapse occurrence were not strictly the same patients: in 7 patients the increased marker values were found only in relapse, but not before it, whereas in 4 patients the increased marker values preceded the relapse, being normal at the time of its occurrence. This later group of patients had increased CA 15-3 again very soon after the first relapse, or at the time of the next relapse of the disease, but this is beyond the scope of this paper.

Figure 1 represents marker values in some of the patients with relapse. Some of them had a sudden increase in marker levels only at the time of relapse, or just before it (Figure 1-C). The other group (Figure 1-A), had increased values of CA 15-3 initially, decreasing during adjuvant treatment, and then increasing again before, or simultaneously with relapse occurrence. In some patients who relapsed very early, within the first 12 months after surgical treatment, the increased values were detected continuously from the beginning to the relapse (Figure 1-B), being the highest of all serum marker values measured in this group of 91 pts. Since it is assumed that tumour marker levels reflect the tumour burden, our results seem to support some recently published opinions.[3]

Firstly, they point out that besides the qualitative CA 15-3 values, the quantitative ones may be even more important, predicting the first relapse, and possibly the aggressiveness of the disease as well. This is supported by the fact that pts. represented in Figure 1.B had not only a very short disease-free interval, but also a very fast progressive recurrent disease. Nevertheless, their response to systemic treatment was variable: two of them were almost unresponsive till the end of the disease, while other two patients responded well. In any case, it seems necessary to collect more information about that. Secondly, the decrease in tumour marker values during adjuvant treatment in patients whose tumours produce CA 15-3, seems to be another important result (Figure 1-A). It is uncommon that this tumour marker is produced in an increased concentration by small operable breast tumours.[6, 7] There are also very deficient data about the half-life of this tumour marker.[8] Because of that, the question remains open as to whether the increased tumour marker values during the first months after surgery could be due to tumour production, or rather to the presence of subclinical metastatic disease. If the latter possibility could be confirmed, that would probably be the very first demonstration of a biochemical marker reflecting directly the effectiveness of adjuvant treatment.

CA 15-3 values in some pts. with «false» tumour marker increase (Figure 2) were occasionally (A), or continuously registered (B), being in one case only higher than 57 U/ml. One

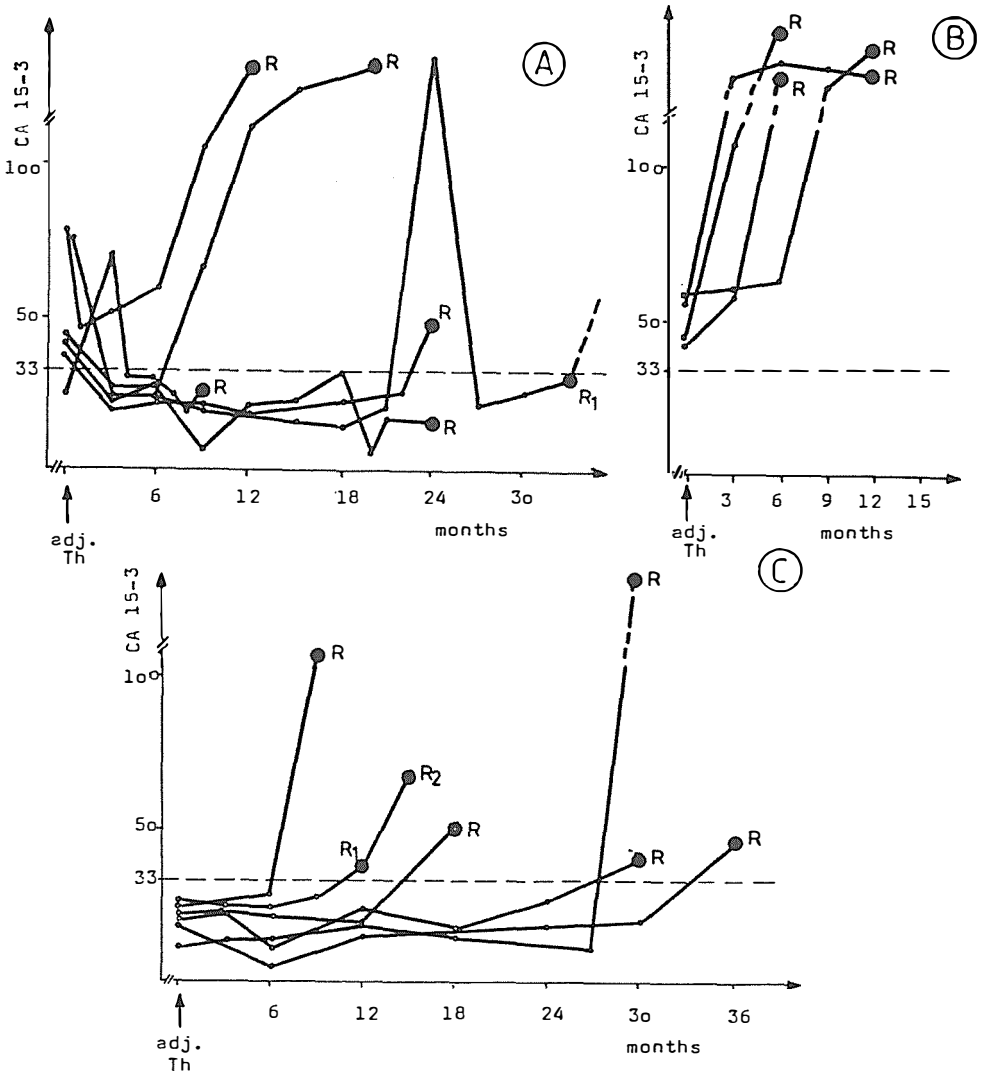

Figure 1. CA 15-3 in patients with relapse.
A – Patients with initially increased CA 15-3 and subsequent relapse (R)
B – Patients with continuously increased marker after surgery till early relapse (R)
C – Increased CA 15-3 in relapse only (R)

patient (Figure 2.C) with increased CA 15-3 values, which were measured during a remission of 30+ months, developed histologically confirmed ovarian carcinoma. This group of patients with false CA 15-3 increase was followed from 1.5 to 4 years (median follow-up 3 years). As it is well known, the expected relapse rate in such a high-risk patient group is more than 50%[9], and is expected to be highest in the first 3-3.5 years after surgery. The reported follow-up period, and relapse rate have not been reached yet in our group of patients. It means that only truly «false» negative, and truly positive results are final. At the same time, the observed false positive results in disease-free patients still need to be confirmed (Table 1). These values are presumably preliminary, and the future results could possibly influence the final specificity,

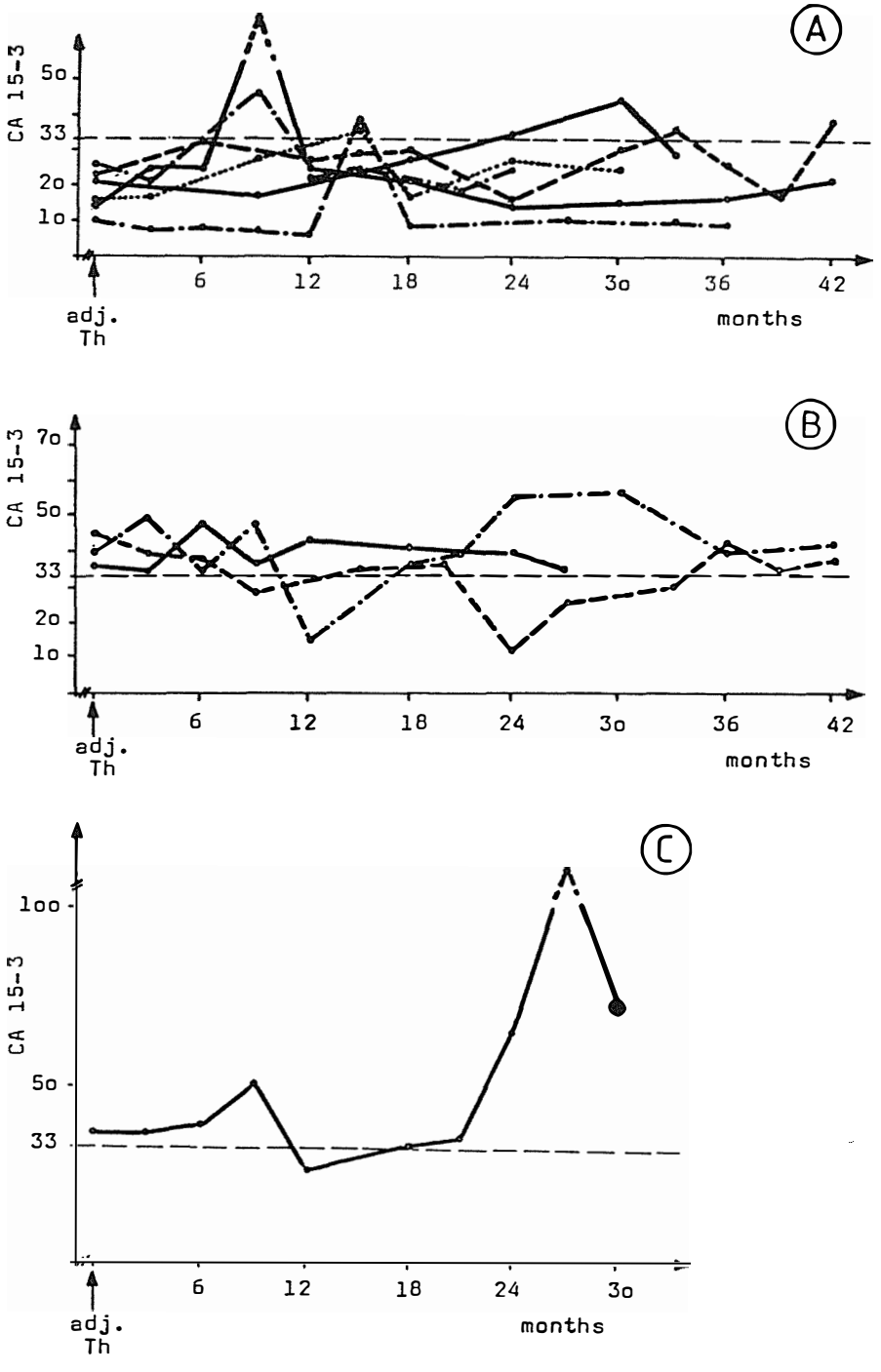

Figure 2. CA 15-3 in patients still in remission:
A – Patients with occasional moderately increased CA 15-3.
B – Patients with continuously increased CA 15-3.
C – One patient who developed ovarian carcinoma without a relapse of BC

Table 1. CA 15-3 at the time of relapse and prior to the first relapse.

	CA 15-3		
	Increased	Normal	Total
No of relapsed pts.	25	18	43
No of pts. in remission	13	35	48
Total	38	53	91
No of pts. with later remission	13	35	48

Sensitivity for the presence of metastatic disease =0.58
Specificity for the present metastatic disease =0.73
PPV for metastatic disease =0.65
NPV for metastatic disease =0.66
Sensitivity for the prediction of metastatic disease =0.53

sensitivity and prognostic value of this tumour marker. Sensitivity, defined as the proportion of patients with increased marker value in relapse (true increase) was 0.58. Specificity, the proportion of patients without relapse who had true negative marker values, was 0.73. The positive predictive value (PPV), representing the probability that a pt. had the relapse if marker was increased, was 0.65, and the negative predictive value (NPV), representing the probability that a patient did not have the disease if marker value was normal, showed the value of 0.66.

Clinical relevance of CA 15-3 in the prediction of the first relapse is possibly greater than the importance of this tumour marker in diagnosis of already manifested metastatic disease. There is no doubt about the usefulness of this tumour marker in screening for subclinical metastatic disease. Nevertheless, the possible use of systemic treatment in disease-free patients with increased CA 15-3 is still questionable. The reason is not only the chance of a false increase in tumour marker, which actually exists, but also the impossibility of predicting the localization of the first relapse, which could influence the choice of systematic or local treatment. On the other hand, the arbitrary choice of cut-off values is influenced by the tumour marker concentration in normal healthy persons. The crucial question here is the difference between truly disease-free breast cancer patients and subclinically metastatic patients. Therefore, we analysed the quantitative values of CA 15-3 in disease-free patients and in relapsed patients at the time of relapse and before it, using in the first and latter case the maximal registered value (Figure 3). There was no statistically significant difference between the quantitative marker levels at the time of relapse, and the maximal CA 15-3 levels preceding the relapse occurrence. However, both of these two marker values were significantly higher than the maximal tumour marker values in non-relapsed patients. The same result was obtained when only the marker levels were tested, representing patients whose tumours seemed to produce this tumour marker at any time. We also noted that in 95% of disease-free patients the maximal values never

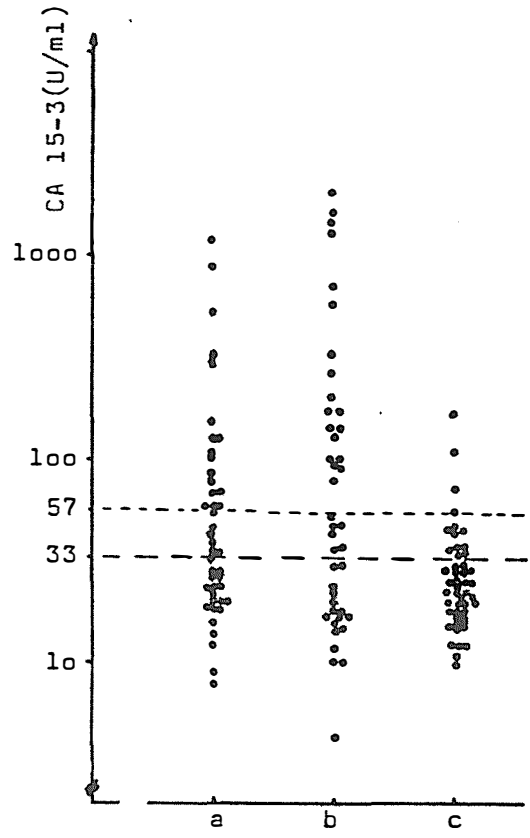

Figure 3. Quantitative CA 15-3 values in patients with relapse (a – prior to relapse – maximal values, b – at the time of relapse) and c – in disease-free patients – maximal values. Logarithmic scale is used.

exceeded 57 U/ml. Using this as a cut-off value, the obtained sensitivity was 0.44, specificity 0.93, positive predictive value 0.86, and negative predictive value 0.65. The obtained sensitivity in relapse prediction was even lower (0.39), but predictive values were nearly the same (0.85 and 0.63, respectively). Further follow-up of this particular group of patients is necessary to confirm these results, and to propose the rise of the upper cut-off limits to 57 U/ml. In any case, quantitative marker values in addition to qualitative data, seem to be significant for relapse prediction.

Concerning the pattern of the first relapse, it seems that an early increase of CA 15-3 is more frequent in BC patients who would develop bone metastases: in 16/24 patients the CA 15-3 preceded the bone relapse. The increased marker values preceded the soft tissue relapse in 1/10 pts., pleuro-pulmonal in 1/4 pts., liver metastases in 2/3 pts., and the multiple site of relapse in 2/2 pts. So, the increased CA 15-3 values in disease-free patients suggested the need for a more careful search for metastatic disease, particularly in the bones.

In conclusion, CA 15-3 has been confirmed as a sensitive tumour marker both for diagnosis of metastatic disease and for predicting the first relapse.

References

1. Hayes DF, Sekine H, Ohno T, et al. Use of murine monoclonal antibody for detection of circulating plasma DF3 antigen levels in breast cancer. *J Clin Invest* 1985; **75:**1671-8.
2. Martoni A, Ercolini L, Bellanova B, et al. CA 15-3 and CEA plasma level monitoring in patients with breast cancer. *Int J Biol Markers* 1988; **3:**154-8.
3. Tondini C, Hayes DF, Kufe DW. Circulating tumour markers in breast cancer. *Hematology/Oncology Clinics of North America* 1989;**3:**653-74.
4. Kallioniemi OP, Oksa H, Aaran RK, at al. Serum CA 15-3 assay in the diagnosis and follow-up of breast cancer. *Br J Cancer* 1988; **58:**213-5.
5. Malkin A. Tumour Markers. In: Tannock JF & Hill RP ed. *The Basic Science of Oncology,* Pergamon Press 1987; 192-204.
6. Safi F, Kohler I, Röttinger E et al. Comparison of CA 15-3 and CEA in diagnosis and monitoring of breast cancer. *Int J Biol Markers* 1989; **4:**207-14.
7. van Dalen A. Pre-operative tumour marker levels in patients with breast cancer and their prognosis. *Tumor Biol* 1990; **11:**189-95.
8. Kiang DT, Greenberg LJ, Kennedy BJ. Tumor marker kinetics in the monitoring of breast cancer. *Cancer* 1990; **65:**193-9.
9. McGuire WL, and Clark GM. Prognosis in Breast Cancer. In: Senn HJ, Goldhirsch A, Gelber RD and Osterwalder B, eds. *Adjuvant therapy of primary breast cancer.* Springer-Verlag Berlin Heidelberg 1989; 170-4.

Chapter V. EXPERIMENTAL ONCOLOGY

Adv Radiol Oncol 1992; 229–35.

Prostaglandins in malignant tumors: Role in tumor growth and therapy

Milas L

University of Texas M.D. Anderson Cancer Center, Department of Experimental Radiotherapy, 1515 Holcombe Boulevard, Houston,

Using a number of murine tumors we have demonstrated that prostaglandins (PGs) are important in regulating tumor growth and response to radiotherapy. Tumors may or may not produce PGs; those that produce them will respond to the inhibiton of PGs by slowing their growth rate. Inhibition of PGs was achieved by treatment of tumor hosts with indomethacin, an inhibitor of PG-synthase. The antitumor activity of indomethacin was found to be mediated mainly through inhibition of tumor neoangiogenesis. Indomethacin also potentiates tumor response to ionizing radiation, but by eliciting or augmenting the antitumor immune reactions. In contrast, indomethacin either does not affect normal tissue radioresponse or it protects some normal tissues against radiation injury. Thus, indomethacin can greatly improve the therapeutic ratio of radiotherapy, which can be further improved by combining indomethacin with other radiosensitizers or radioprotectors that have different mechanisms of action from those of indomethacin. These studies are important for understanding the role of PGs in the growth regulation of malignant tumors and their response to therapy, and may have potential implications to clinical radiotherapy.

Key words: neoplasms-therapy; prostaglandins

Introduction

Eicosanoids are metabolites of unsaturated fatty acids, principally of arachidonic acid, that play a regulatory role in many biological processes. Virtually all mammalian cells produce eicosanoids, which are further classified into two major groups: prostaglandins (PGs) and leucotrienes. These are produced via the cyclooxygenase and lypooxygenase pathways, respectively. However, advances in eicosanoid research have come mostly from studies on PGs. The biological activities of PGs are many and include immunomodulation, vasoregulation (constriction or dilatation), platelet aggregation, cell growth and differentiation, and tumor development and growth.[1] With regard to the latter, PGs regulate both the initiation and promotion steps of carcinogenesis, rate of tumor growth and tumor dissemination.[1]

The discovery that PGs play a role in tissue response to ionizing radiation represents a recent development in research on eicosanoids.[2,3] The reported findings have, however, been conflicting because both the addition of PGs,[2,3] as well as their inhibition,[4,5] have been found to protect a number of normal tissues from radiation damage. Our own research has been aimed at increasing the therapeutic efficacy of radiotherapy through modulation of PGs production, prima-

Corespondence to: Luka Milas, M.D., Ph.D., Professor and Chairman, Department of Experimental Radiotherapy – 66, M.D. Anderson Cancer Center, 1515 Holcombe Boulevard, Houston, Texas 77030 USA.

UDC: 616-006.6-08:615.277.3.015.43

rily of that in tumors. Our initial hypothesis was that inhibition of PGs in tumors would increase tumor radioresponse presuming that PGs act radioprotectively. We have already reported a number of observations made in rodent tumors and normal tissues on the role of PGs inhibition in tumor radiotherapy.[6-11] This report is a brief account of our major findings.

PGS synthesis by tumors and their inhibition

It has been well documented that malignant tumors in man[1,12] and in experimental animals[1,13] produce PGs. The production varies both quantitatively and qualitatively among tumors of different histological types as well as among individual tumors with the same histology. An illustration of this wide variability in PG and other eicosanoid production is shown in Table 1, which contains our own analysis of eicosanoids produced by five different murine tumors.[6] Of five tumors analyzed, only three produced PGs. However, even among the three PG-producing tumors there was a marked difference in the type and amount of individual PGs produced. Similarly, there were significant differences in production of leukotrienes. Most PG production was by tumor cells. However, it is likely that host cells that infiltrate these tumors, such as macrophages and lymphocytes, also participated in PG production. Macrophages are known to be good producers of the PG classes PGE2 and TXB2.[14] Also, endothelial cells of tumor blood vessels could participate in PG production, and especially in the production of PGI2.[15] Because different types of PGs exhibit different biological actions, the action of PGs in regulation of tumor behaviors will depend on the type and quantity of a given PG produced by the tumor. For example, while tumors that produce high quantities of TXB2 are expected to be prone to the clogging of their blood vessels, tumors that are high producers of PGI2 should have good blood flow. This is because TXB2 stimulates and PGI2 inhibits platelet aggregation, and through this process regulate blood coagulation.

That PGs participate significantly in the overall regulation of tumor growth and its spread has been shown in many ways. Inhibition of PGs is a prominent method that has frequently been used.[11] Inhibition of PGs is readily achieved using indomethacin or other nonsteroidal anti-inflammatory agents that block the cyclooxygenase pathway in arachidonic acid metabolism. This inhibition is frequently associated with a retardation in tumor growth, which indirectly implies that PGs are stimulators of tumor growth. The antitumor action of indomethacin is

Table 1. Eicosanoid metabolites of mouse tumors[a].

	Mouse tumors				
Eicosanoid	FSA	NFSA	SA–NH	MCA–K	HCA–I
$6KPGF_{1\alpha}$	102.8[b]	135.1	3.7	ND[c]	10.3
TXB_2	46.2	31.9	ND	ND	28.6
$PGF_{2\alpha}$	ND	11.3	ND	ND	24.3
PGE_2	336.1	36.6	ND	ND	14.5
PGD_2	ND	ND	ND	ND	6.2
LTB_4	ND	28.9	10.7	64.0	ND
HHT	83.5	35.4	2.8	14.7	45.7
di–HETEs	ND	ND	12.1	65.6	ND
15–HETE	ND	19.3	ND	ND	ND
5– or 12–HETE	146.7	30.5	26.6	86.9	115.7
Total metabolites	715.3	329.0	55.9	231.2	245.0

[a]Tumors were generated by 5 x 10^5 tumor cells injected into the muscles of the right thighs. Tumors were assayed for eicosanoid metabolites when approximately 9 mm in diameter.
[b]Values in ng/gm are given as the mean of two samples. Each sample was obtained from a pool of 4 to 6 tumors.
[c]ND, not detectable!
Reprinted from Furuta et al.,[6] with permission.

variable, with only a fraction of the tumors tested showing a good response. Most frequently, only a retardation in tumor growth rate is seen after indomethacin treatment. Complete and long lasting tumor regressions have been extremely rare.

The mechanisms which mediate the antitumor effects of indomethacin are still a matter of considerable controversy. The effect has most commonly been attributed to the ability of indomethacin to elicit or potentiate antitumor immune mechanisms through the inhibition of production of immunosuppressive PGs, notably PGE2.[1,16,17] Our own studies[8] question the involvement of the immunological reactions and point to other, probably more important, mechanisms. We have observed that the antitumor activity of indomethacin is independent of both tumor immunogenicity and host immunocompetence.[6,8] Tumors in mice that are generally immunocompetent or lacking T-lymphocytes respond to indomethacin as well as tumors in normal mice.[8] Importantly, however, the effect of indomethacin depended entirely on PGs production. Only tumors that produce PGs respond to indomethacin.[6] This discovery has a valuable clinical implication in that it may be possible to predict which tumors will respond to this therapy by assaying the PG profile of individual patients prior to therapy.

Indomethacin has no direct cytostatic or cytotoxic effect for tumor cells[6], but it slows tumor cells proliferation[6] by indirect means. A possibility that we recently investigated was that indomethacin inhibits tumor vascularization, and thus reduces the blood supply to tumor cells. Tumor cells would then become deficient in oxygen and other nutrients, which would slow their proliferation. This hypothesis is based on the evidence that PGs stimulate tumor angiogenesis.[18] Using an intradermal assay that we recently developed for studying tumor angiogenesis in mice[19], we demonstrated that indomethacin reduced the formation of new vessels at the site of tumor cell injection, which preceded the slowing of tumor growth[8] (Figure 1). Based on this evidence, we conclude that inhibition of tumor neovascularization is a major mechanism by which indomethacin exerts its antitumor action.

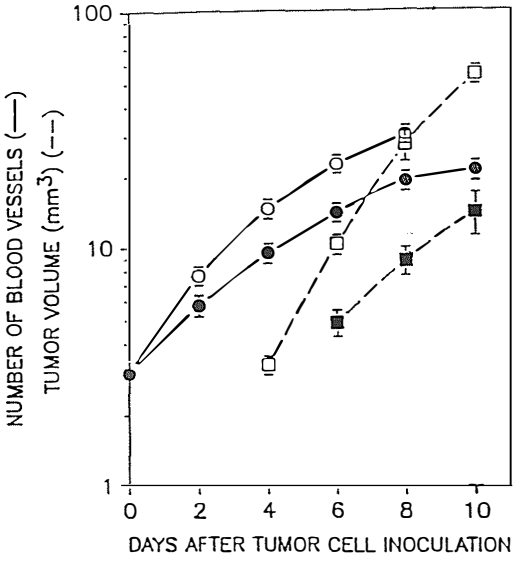

Figure 1. Effect of indomethacin on tumor angiogenesis. The mice were given intradermal inoculation of 10^6 NFSA cells, and the number of vessels at the injection site was determined on the indicated days thereafter in indomethacin-treated (closed circle) and control (open circle) mice. Tumor volume in indomethacin-treated (closed square) and indomethacin-untreated (open square) mice was also plotted. Vertical bars are S.E. of the mean values. Treatment with indomethacin, 35μg/ml in drinking water, was started 1 day after tumor cell inoculation and was continued daily for 9 days. Reprinted from Milas et al.,[8] with permission.

Indomethacin-induced potentiation of tumor radioresponse

The hypothesis was that if PGs act as radioprotectors, a reduced level of PGs in tumors should make the tumors more responsive to radiation. Indeed, we observed that inhibition of PGs in tumors by using indomethacin was accompanied by an augmentation of the radioresponse of PG-producing tumors[7,8,10] as assayed either by the tumor growth delay or the TCD50 assay (radiation dose yielding 50% local tumor control). The degree of indomethacin-induced augmentation of tumor radioresponse ranged from a factor of 1.3 to > 2, and depended on many factors including tumor type, choice of fractionation in radiation treatment schedule, timing of indomethacin administration in relation to tumor irradiation, and the endpoint of tumor response.

The augmentation was greater with fractionated than with single dose irradiation.[8] Figure 2 illustrates the indomethacin–induced potentiation of radioresponse of a murine sarcoma.

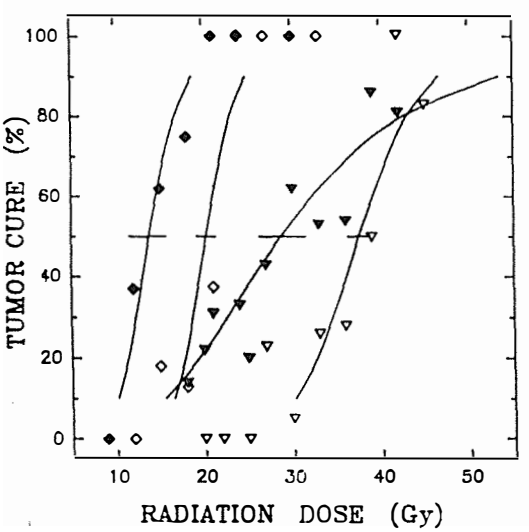

Figure 2. Radiation dose response curves for local tumor control of 8-mm FSA tumors growing in the legs of mice treated with radiation alone (▽) or with radiation plus INDO (▼), MISO (◇), or both INDO and MISO (◆). Error bars, TCD_{50}, 95% confidence limits. Treatment with INDO, 35 μg/ml in drinking water, was started when FSA tumors were 6 mm and continued for 10 days. MISO (1 mg/g) was given i.p. 30 min before local tumor irradiation. Points, data presented here are from 2-6 separate experiments. Reprinted from Milas et al.,[10] with permission.

Our studies on the mechanisms by which indomethacin potentiated tumor radioresponse failed to support the initial hypothesis that the potentiation was the result of lowering the level of PGs.[8] This was established by showing that indomethacin augmented tumor radioresponse when given after irradiation was completed, indicating that in order to potentiate tumor radioresponse, the hypothetical radioprotective PGs need not be removed or reduced at the time of radiation exposure. This finding is also inconsistent with a second mechanism which we advanced earlier[7], namely that indomethacin potentiates tumor radioresponse by arresting tumor cells in the G2/M and G1 cell cycle phases which are more sensitive to radiation than cells in the S-phase.

However, the radiopotentiating effect of indomethacin was greatly reduced or abolished in mice immunosuppressed by whole body irradiation or in nude mice that selectively lack T-lymphocytes.[8] This implies that the potentiation of tumor radioresponse was mainly, if not exclusively, mediated through the antitumor immune mechanisms elicited or augmented by indomethacin. As discussed above, this is in contrast to the nonimmunological mechanism of antitumor activity found to be operative when indomethacin is applied alone. The existence of two different mechanisms of the indomethacin action which appear to operate under different experimental conditions is difficult to explain on the basis of currently available data. A plausible explanation may be that, in combination with radiotherapy, the antitumor immune reaction induced by indomethacin, even if it is weak, may be effective in eliminating those few viable tumor cells that survived radiation. Such a process is, however, unlikely to be effective in slowing the growth of established tumors that contain large numbers of tumor cells, as exemplified by tumors treated with indomethacin alone. It is logical then that in this case the antiangiogenic mechanism of indomethacin would predominate.

Modification of normal tissue radioresponse by indomethacin

To render a therapeutic advantage, indomethacin must be more effective in augmenting tumor radioresponse than that of normal tissues within the radiation field. For this purpose we have investigated the effect of indomethacin on the radioresponse of the following tissues and organs: hematopoietic tissue, lung, esophagus, jejunum, colon, hair follicles and tissues responsible for radiation-induced leg contractures.[7,9-11] In contrast to its potentiating effect on tumor radioresponse, indomethacin did not alter radioresponse of most of the listed tissues and actually protected two of them: hematopoietic tissue and the lung. Protection of hematopoietic tissue was

demonstrated by the increase of hematopoietic spleen colonies (Figure 3) and by the reduction of mouse lethality.[9] Protection, which in the spleen colony assay was by a factor of 1.3 (Figure 3), was achieved only when indomethacin was given before irradiation. Indomethacin did not alter the radiosensitivity of hematopoietic stem cells; rather, it exerted its radioprotective action indirectly by stimulating the proliferation of hematopoietic cells. The mechanism(s) of indomethacin induced lung radioprotection remains unknown at present. This information, together with that on tumor radioresponse, clearly shows that indomethacin can significantly increase the therapeutic ratio of tumor radiotherapy.

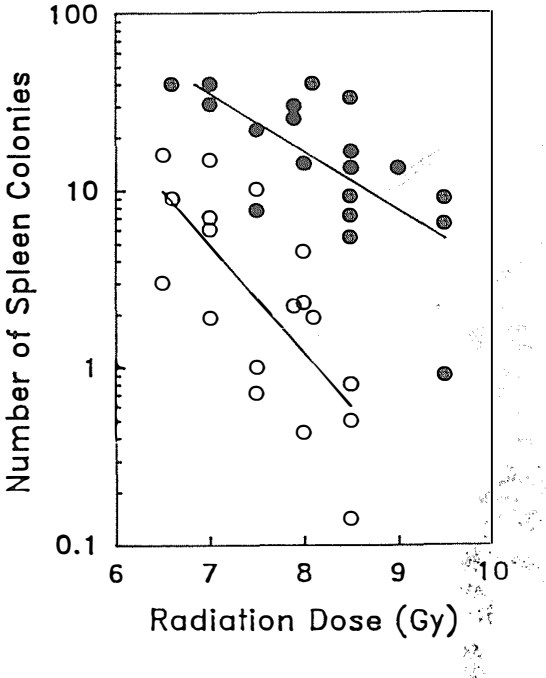

Figure 3. Effect of indomethacin on endogenous spleen colony survival after total body irradiation (TBI). Vehicle or indomethacin was given for 6 days before TBI. Mice were sacrificed 8 or 9 days after TBI, spleens were removed and fixed in Bouin's solution, and the number of colonies were counted. A higher number of spleen colonies was observed in the indomethacin-treated mice (closed circle) than in the control mice (open circle). The protection factor at level of 10 spleen colonies was 1.3. The data are from six separate experiments; each symbol is a mean value of number of spleen colonies obtained within individual experiments. The lines were fitted by least-squares regression analysis. Reprinted from Nishiguchi et al.,[9] with permission.

Combination of indomethacin with true radiosensitizers and radioprotectors

Our observations that indomethacin augments tumor radioresponse through immunological reactions and protects some normal tissues by stimulating cell proliferation suggested the possibility of combining indomethacin with agents that affect tumor or normal tissue radioresponse through mechanisms different from those of indomethacin. Hypothetically, this combination should further increase the therapeutic ratio of radiotherapy. Figure 2 shows that combining indomethacin with misonidazole, a prototype of those agents that specifically sensitize hypoxic cells to radiation, increased tumor radioresponse significantly more than indomethacin or misonidazole alone. Likewise, combining indomethacin with WR-2721, a true radioprotector, was significantly more radioprotective for hematopoietic tissue than were the individual drugs alone.[9] More detailed information about these combinations is given in our recent reports.[9-11] This is a new line of our research that is currently under extensive investigation.

Conclusions

Malignant tumors may or may not be good producers of PGs. PGs regulate the growth of malignant tumors mainly through stimulation of tumor neovascularization. Inhibition of neovascularization by indomethacin restrains tumor cell proliferation and consequently retards tumor growth. The antitumor activity of indomethacin is independent of tumor immunogenicity and of the ability of the tumor host to mount antitumor immunological response.

Indomethacin treatment results in inhibition of PG production by tumors, and in a significant potentiation of tumor radioresponse. Only PG-producing tumors exhibit this potentiation. The

extent of potentiation varies between 1.3 and > 2.0 and depends on a number of factors and experimental conditions. The radiopotentiating effect of indomethacin is greatly dependent on tumor host immunocompetence, and was reduced or abolished by preventing the host to mount immunological reaction to the tumor. Therefore, whereas the antitumor activity of indomethacin alone is mediated primarily through inhibition of tumor angiogenesis, the radiopotentiating effect of indomethacin is mainly an immunological phenomenon.

In contrast to its effect on tumor radioresponse, indomethacin does not influence the radioresponse of some normal tissues and it protects some, notably hematopoietic tissue and lung. The protection of hematopoietic tissue was mediated indirectly via stimulation of stem-cell proliferation.

Therefore, while indomethacin renders a significant increase in tumor radioresponse, it either does not affect or reduces the response of normal tissues, thus providing a significant increase in the therapeutic gain of radiotherapy. This gain can be improved even further by combining indomethacin with either hypoxic cel radiosensitizers, such as misonidazole, or true radioprotective agents, such as WR-2721, which modulate tumor or normal tissue radioresponse by mechanisms different from that of indomethacin. It should be noted here that there already exists some evidence that the inhibition of PGs by nonsteroidal anti-inflammatory agents can improve the therapeutic efficacy of clinical radiotherapy.[20,21]

References

1. Honn VK, Bockman RS, and Marnett LJ. Prostaglandins and cancer: A review of tumor initiation through tumor metastasis. *Prostaglandins* 1981; **21:**833-64.
2. Hanson WR, Ainsworth EJ. 16-16 Dimenthyl prostaglandin E_2 induces radioprotection in murine intestinal and hematopoietic stem cells. *Radiat Res* 1985; **103:**196-203.
3. Walden TL Jr, Patchen M, and Snyder SL. 16-16 Dimethyl prostaglandin E_2 increases survival in mice following irradiation. *Radiat Res* 1987; **109:**440-9.
4. Northway MG, Libshitz HI, Osborne BM, Feldman MS, Mamel JJ, West HH, and Szwarc IA. A radiation esophagitis in the opossum: radioprotection with indomethacin. *Gastroenterology* 1980; **78:**833-7.
5. Suzuki JB, Emmering TE, Kishiby JS, Schonfeld S, Sowle J, Tatum RC, and Van Dyke T. Protection of irradiated parotid by prostaglandin syntesis inhibitors. *J Am Dental Assoc* 1986; **112:**179-81.
6. Furuta Y, Hall ER, Sanduja S, Barkley HT Jr, and Milas L. Prostaglandin production by murine tumors as a predictor for therapeutic response to indomethacin. *Cancer Res* 1988; **48:**3002-7.
7. Furuta Y, Hunter N, Barkley HT Jr, Hall E, and Milas L. Increase in radioresponse of murine tumors by treatment with indomethacin. *Cancer Res* 1988; **48:**3008-13.
8. Milas L, Furuta Y, Hunter N, Nishiguchi I, and Runkel S. Dependence of indomethacin-induced potentiation of murine tumor radioresponse on tumor host immunocompetence. *Cancer Res* 1990; **50:**4473-7.
9. Nishiguchi I, Furuta Y, Hunter N, Murray D, and Milas L. Radioprotection of hematopoietic tissues in mice by indomethacin. *Radiat Res* 1990; **122:**18-92.
10. Milas L, Ito H, Nakayama T, and Hunter N. Improvement in therapeutic ratio of radiotherapy for a murine sarcoma by indomethacin plus misonidazole. *Cancer Res* 1991; **51:**3639-42.
11. Milas, Nishiguchi I, Hunter N, Murray D, Fleck R, Ito H, and Travis E. Radiation protection against early and late effects of ionizing irradiation by the prostaglandin inhibitor indomethacin. In: *Advances in Space Research* 1992; **12:**265-71.
12. Rolland PH, Martin PM, Jacquemir J, Rolland AM, and Toga M. Prostaglandin in human breast cancer: Evidence suggesting that an elevated prostaglandin production is a marker of high metastatic potential for neoplastic cells. *J Natl Cancer Inst* 1980; **64:**1061-70.
13. Fitzpatrik FA, Stringfellow DA. Prostaglandin D_2 formation by malignant melonoma cells correlates inversely with cellular metastatic potential. *Proc Natl Acad Sci* USA 1979; **76:**1765-9.
14. Goldyne ME, Stobo JD. Immunoregulatory role of prostaglandins and related lipids. CRC *Critical Reviews in Immunology* 1981; **2:**189-223.
15. Vermylen J, Chamone DAF, and Verstraete M. Stimulation of prostacycline release from vessel wall by Bay g 6575, an antithrombotic compound. *Lancet* 1979; **1:**518-20.
16. Plescia OJ, Smith AH, and Grinwich K. Subversion of immune system gy tumor cells and role of prostaglandins. *Proc Natl Acad Sci USA* 1975; **72:**1848-51.
17. Fulton AM. Interactions of natural effector cells and prostaglandins in the control of metastasis. *J Natl Cancer Inst* 1987;**78:**735-41.
18. Ziche M, Jones S, and Gullino PM. Role of prostaglandin E_1 and copper in angiogenesis. *J Natl Cancer Inst* 1982; **69:**475-81.
19. Runkel S, Hunter N, and Milas L. An intradermal assay for quantitation and kinetics studies of tumor angiogenesis in mice. *Radiat Res* 1991 ;**126:**237-43.

20. Weppelmann B Monkemeier D. The influence of prostaglandin antagonists on radiation therapy of carcinoma of the cervix. *Gynecol Oncol* 1984; **17:**196-9.

21. Pillsbury HC, Webster WP, and Rosenman J. Prostaglandin inhibitor and radiotherapy in advanced head and neck cancers. *Arch Otolaryngol Head Neck Surg* 1986; **112:**552-3.

Adv Radiol Oncol 1992; 236–40.

Problems in tumour cell repopulation during irradiation treatment of squamous cell carcinoma of head and neck

Budihna M and Škrk J

The Institute of Oncology, Ljubljana

The repopultion rate of clonogenic cells is discussed in the light of our patients with head and neck squamous cell carcinoma and reports in the literature. Saunders' data of survival of patients with head and neck carcinoma treated by continuous hyperfractionated accelerated radiotherapy (CHART) and conventional irradiation treatment were used to estimate when in the course of the treatment the clonogenic cells accelerate their division rate. By means of Overgaard's dose response curves for laryngeal carcinoma the TCD_{50} for CHART and conventional treatment was estimated. The difference of TCD_{50} and overall treatment time between CHART and conventional treatment was used for calculation when the repopulation begins. Assuming that the maximum repopulation rate expressed in Gy is 0.6 Gy per day as obtained by Withers it was calculated that the repopulation begins toward the end of the second week of irradiation treatment in advanced tumours and probably sooner in early tumours.

Key words: head and neck carcinoma; head and neck neoplasms-radiotherapy; clonogenic cells, repopulation;

Introduction

The cure of carcinoma is achieved when all clonogenic tumour cells are killed in the course of the irradiation treatment.[1] Usually clonogenic cells represent a small proportion of tumour cells, i.e. aproximately 1% of the tumour population.[2] Their properties cannot be determined by microscope or flow cytometry. According to the simplest radiobiological theory, the curative radiation dose depends only on the radiosensitivity of the clonogenic tumour cells and on their number. If the number of tumour clonogens which are not killed by irradiation increases in the course of treatment a higher radiation dose is needed for cure. Thus, the speed of repopulation of clonogenic cells is extremely important.

The only available method to measure it during a certain period of treatment is based on the determination of dose difference in two radiation treatment schedules of different duration, normalized to the same tumour dose per fraction, both giving the same tumour response.

The aim of this paper is to discuss the repopulation of clonogenic cells in the tumour. There are three questions to be answered in this respect: how fast is the repopulation of the clonogenic cells? Does the speed of the repopulation change during the irradiation treatment and when does the change occur?

Correspondence to: Budihna Marijan M. D., Ph. D; Institute of Oncology, Zaloška 2, 61000 Ljubljana,, Slovenia.

UDC: 616-006.6-08:615.849:611.92/.93

Material, methods and results

How fast is the repopulation of the clonogenic cells?

The division rate of clonogenic cells in favorable living conditions is best correlated with the potential doubling time (T_{pot}). T_{pot} can be measured quickly by monoclonal antibodies to BUdR or IUdR on denaturated DNA in which the thymidine analog Iodo- or Bromo-deoxyuridine is incorporated into DNA[3]. The length of T_{pot} was less than 6 days in half of the head and neck carcinomas as measured by McNally[4]. As defined by Steel[2] T_{pot} is a combined information resulting from cell cycle time and growth fraction (the latter being very much in correlation with the clonogenic fraction), and it represents the doubling of the cell population if there was no cell loss. A cell loss factor of 90 or 95% would mean that the tumour volume doubling time is 10 or 20 times greater than T_{pot}[5]. This, in fact, can be seen in untreated squamous cell carcinoma of the head and neck which doubles its volume in aproximately 2 to 3 months. Assuming that the growth fraction and cell-loss factor change little over a small number of volume doubling times, the preirradiation volume doubling time is also approximately the doubling time of tumour clonogens.[7]

Does the speed of the repopulation rate change during the irradiation treatment?

In 1980 Budihna et al.[8] calculated, on the basis of the difference between the total tumour dose in the split-course and conventional irradiation treatment of the laryngeal carcinoma and the duration of the split-course interval, that the doubling time of clonogenic cells in the rest interval is 3.5 ± 0.5 days; 0.4 Gy were needed to kill the daily regrowth of the clonogenic cells. It was assumed that cells grow exponentially. This was regarded as an acceleration of the pretreatment tumour growth and accounted for by better living conditions of the clonogenic tumour cells surviving the first part of the split-course irradiation treatment. This, in fact, was also the first observation of the kind on human data reported in the literature.

From the data of Galante[9] published in 1982 it can be seen that the median value for the doubling time of the postoperative recurrences of head and neck carcinomas was 7.8 days, assuming the exponential growth of tumour.

Maciejewski in 1983[10] noted that the total tumour dose needed for the 50% control of laryngeal carcinoma (TCD_{50}) had to be increased for 8 Gy if the overall time of irradiation treatment was prolonged for 16 days. He assumed that 2 Gy are necessary to compensate for one doubling of clonogenic cells. Based on that, he calculated that the doubling time of clonogenic cells during irradiation treatment did not exceed 4 days.

Budihna et al. in 1986[11] found on the basis of the difference between the total tumour doses of conventional and split-course irradiation treatment and the duration of split-course rest interval that the doubling time of the clonogenic cells of nasopharyngeal carcinoma in the rest-interval of split-course irradiation treatment is 3.5 – 4.5 days. Here again the exponential tumour growth was assumed; 0.4 Gy were needed to kill the daily regrowth of clonogenic cells.

Overgaard in 1988[12] demonstrated by means of dose-response curves for conventional and split-course irradiation the need for an increase in the total dose of approximately 12 Gy in the split-course irradiation regimen to obtain an equal effect in both treatment regimens. He hypothesized that if 6 Gy were necessary to reduce the clonogenic cell population with a factor 10, 12 Gy meant a hundredfold increase of clonogenic cells in three weeks of the rest interval. From the above data he calculated that the clonogens of laryngeal carcinoma, in the rest interval of the split-course treatment doubled their number in 3-4 days.

Withers in 1988[6] noted that TCD_{50} normalized to 2 Gy, had to be increased for 0.6 Gy per each day of treatment prolongation. Assuming that 2.4 Gy in a 2 Gy fraction regimen were required to compensate for each doubling in clonogen number, he calculated that the doubling time of

the clonogenic cells during the irradiation was 2.4 Gy : 0.6 Gy/day = 4 days.

Thus, from the presented studies, it can be seen that the repopulation rate of the clonogenic cells of squamous cell carcinoma changes very much in the course of irradiation: it accelerates up to 10-20 times of its pretreatment value. The doubling time of clonogenic cells during the course of irradiation and in the split course rest-interval is, therefore, close to the T_{pot}. This means that the cell loss factor of the tumour falls during the irradiation treatment to zero.[5]

When does the acceleration of the repopulation begin?

Withers[6] suggested that there is a lag period of about 4±1 week after the beginning of treatment during which there is on average little change in TCD_{50} (i.e.: before a burst of rapid repopulation of head and neck squamous cell carcinoma begins).

Saunders et al.[13], analysed the survival of 2 groups of patients with head and neck carcinoma irradiated conventionally in the duration of 6–7 weeks or with continuous hyperfractionated accelerated radiotherapy (CHART) in the duration of 12 days. Two-year survival of patients treated by CHART was almost 2 times better than that of those treated conventionally. Because of that he suggested that the accelerated repopulation of clonogenic cells might occur within a short while of the initiation of irradiation therapy. However, she did not give an explanation why it is so. Yet, Trott[14] in the same Saunders' data could only see that the tumour control rates as achieved by CHART were at least as good as those achieved elsewhere with conventional treatment by giving 70 Gy in 7 weeks in head and neck cancer.

Since it was not quite apparent from Sounders' data when the rapid repopulation began we tried to estimate what could be the TCD_{50} from his data and present it in relation to the overall treatment time as Withers did[6] in order to see when the burst of repoulation started.

Our approach using Saunders'[13] data.

In conventional treatment of Saunders' study[13], 60 to 70 Gy, mostly 2 Gy per fraction, were applied 5 times weekly. In CHART 3 x 1.4 to 1.5 Gy per day in 12 consecutive days were given, the total tumour dose being 50.4– 54 Gy. But in fact almost always the tumour dose was 1.5 Gy per fraction.[15] Patients in both groups were matched by tumour stage.

The two year survival of patients, obtained by CHART scheme was 63% for all patients, 63% for T-3 and T-4 tumours taken together and 57% for T-4 tumours alone as estimated from the graphs. The survival of patients treated by conventional irradiation was as follows: all patients survived 45%, whereas those with T-3 and T-4 tumours in 33%, and the patients with T-4 tumours alone survived in 23%.

Our working hypothesis was that the tumor dose per fraction in CHART was 1.5 Gy, and total tumor dose 54 Gy. In the conventional treatment the tumor dose was 2 Gy per fraction, and the total tumor dose 65 Gy. The equivalent total tumor dose in CHART scheme ($D_{2\ Gy}$) if the tumor dose per fraction were 2 Gy would be 53 Gy as calculated by formula:

$$D_{2\,Gy} = D_{1.5\,Gy} \times (\alpha/\beta + 1.5) : (\alpha/\beta + 2)$$

where $D_{1.5}$ Gy is the total tumour dose in CHART, and α/β was taken as 25 Gy (as Withers et al. did in their paper 1988).

For further analysis it is necessary to determine TCD_{50} for both irradiation schemes under discussion. But it is impossible to derive TCD_{50} from Saunders' data[13] because we cannot construct a dose response curve. To get an approximate estimation of what could be TCD_{50} we borrowed the dose response curve for laryngeal carcinoma from Overgaard et al.[12] Drawing this curves (which are taken parallel because the groups of patients are matched) through survival values of patients as obtained by Saunders we estimated TCD_{50} for each treatment group of patients whose survival is being compared (Figure 1). The TCD_{50} values obtained in this way are shown in the Table 1.

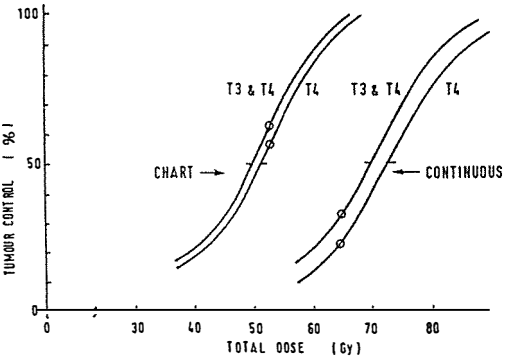

Figure 1. The estimation of TCD_{50} for Saunders,[13] survival data (oper circles) for T-3 & T-4 and T-4 stages treated by CHART and conventional irradiation by means of Overgaard's dose response curves.[12]

Table 1. TCD_{50} for patients of different stages (T) treated by CHART normalized to 2 Gy daily dose, and conventional treatment.

Irradiation scheme	T–3 & T–4	T–4
$CHART_{2\,Gy}$	50.0 Gy	51.5 Gy
$Conventional_{2\,Gy}$	70.0 Gy	73.0 Gy

Assuming that 50 Gy the $CHART_{2\,Gy}$ were applied in about 11 days and 70 Gy of conventional treatment in 47 days we would get a dose increase 0.56 Gy/day due to repopulation effect (20.0 Gy divided by 36 days) in the group of T–3 & T-4 tumours. Similarly, for T–4 tumours we calculate that the daily increase of dose is 21.5 Gy divided by 37.5 (assuming that 73.0 Gy would be delivered in 49 days and 51.5 Gy of $CHART_{2\,Gy}$ in 11.5 days) which amounts to 0.57 Gy/day.

Dividing the difference between the total tumour dose applied by $CHART_{2\,Gy}$ and the total tumour dose applied by conventional irradiation treatment by 0.6 Gy/day (as obtained by Withers) the duration of accelerated repopulation in conventional treatment is obtained. Subtracting this value from the overall treatment time of the Saunders' conventional irradiation it can be estimated when the accelerated repopulation begins: it appears, that the tumour repopulates with full speed already on the 13-th or 14-th day after the beginning of irradiation treatment.

Discussion

These figures for daily repopulation dose are obtained assuming that the slope of dose response curve is such as reported by Overgaard for laryngeal carcinoma[12] and that the total tumour dose of CHART was 54.0 Gy, whereas that of the conventional treatment was 65.0 Gy.

If the slope of the curve was less steep, the difference between TCD_{50} for CHART and conventional irradiation treatment would be more pronounced which would mean a full speed repopulation, already on about the 14-th day of treatment. If, on the other hand, the slope of the dose response curves was steeper, the differences between TCD_{50} for CHART and conventional treatment would be smaller. Assuming that the maximum speed of repopulation in tumor is 0.6 Gy/day as calculated by Whithers[6], the start of the repopulation would begin to accelerate somewhere in the middle of the third week. But steeper dose response curves are probably less likely to occur because a considerable heterogeneity in the human tumours exists already within one stage.

If the average total tumour dose in conventional irradiation approached 70 Gy, the values of repopulation of clonogens in the tumour would still be about 0.6 Gy/day; again, this would indicate that the repopulation begins toward the end of the second week of irradiation treatment.

The quick repopulation of clonogenic cells is probably caused by better living conditions of cells surviving the irradiation and a consequent drop in cell loss. In clinical practice we often see smaller tumours in the head and neck area shrinking and disappearing earlier in the course of irradiation than the bulkier ones. It would be logically to expect that in small tumours the events which lead to the burst of repopulation take place sooner than in bulky tumours. This would in turn mean that short-course irradiation treatment would be relatively less advantageous in early than in advanced tumours. This, in fact

becomes apparent in the Saunders' study:[13] the statistical significance in survival difference in favour of CHART was the largest in T–4 tumours ($p = 0.007$), less pronounced if T–3 and T–4 tumours were taken together ($p = 0.018$) and was nonsignificant when T–2, T–3 and T–4 tumours were compared together ($p = 0.097$). This supports the belief that in early tumours the repopulation is accelerated well before the end of the CHART scheme.

Conclusions

The repopulation rate of clonogenic cells increases during the course of radiotherapy. Using Saunders' data we calculated that the clonogenic cells begin to accelerate their division rate at the end of the second week of the treatment in T–3 and T–4 tumours and probably earlier in T–1 and T–2 tumours.

References

1. Trott K-R, Kummermehr I. What is known about tumour proliferation rates to choose between accelerated fractionation or hyperfractionation? *Radiother Oncol* 1985; **3**:1-9.
2. Steel GG. Cell proliferation kinetics in tumours. In: Steel GG, Adams GE, Horwich A eds. *The biological basis of radiotherapy*. e. ed. Amsterdam-New York-Oxford: Elsevier, 1989; 77-88.
3. Nias AHW. *An introduction to radiobiology*. Chichester: John Wiley & Sons, 1990; 29-45.
4. McNally NJ. Can cell kinetic parameters predict the response of tumours to radiotherapy? *Int J Radiat Biol* 1989; **56**:777-86.
5. Fowler JF. Fractionation and therapeutic gain. In: Steel GG, Adams GE, Horwich A. *The biological basis of radiotherapy*. 2. ed. Amsterdam-New York-Oxford: Elsevier, 1989; 181-207.
6. Withers HR, Taylor JMG, Maciejewski B. The hazard of accelerated tumour clonogen repopulation during radiotherapy. *Acta Oncol 1989;* **27**:131-46.
7. Withers HR, Thames HD. Dose fractionation and volume effects in normal tissues and tumours. *Am J Clin Oncol* 1989; **11**:313-29.
8. Budihna M, Škrk J, Šmid L, Furlan L: Tumor cell repopulation in the rest interval of split-course radiation treatment. *Strahlentherapie Onkol* 1980; **156**:402-8.
9. Galante E, Gallus G, Chiesa F, Bono A, Bettoni I, Molinari R. Growth rate of head and neck tumours. *Eur J Cancer Clin Oncol* 1982; **18**:707-12.
10. Maciejewski B, Preuss-Bayer G, Trott K-R. The influence of the numer of fractions and of overal treatment time on local control and late complication rate in squamous cell carcinoma of the larynx. *Int J Radiat Oncol Biol* Phys 1983; **9**:321-8.
11. Budihna M, Šmid L. Deljeno (split-course) obsevanje karcinoma epifarinksa. *Radiol Iugosl* **20**:4, 391-398, 1986.
12. Overgaard J, Hjelm-Hansen M, Johansen LV, Andersen AP. Comparison of conventional and split-course radiotherapy as primary treatment in carcinoma of the larynx. *Acta Oncol* 1988; **27**:147-52.
13. Saunders MI, Dische S, Hong A et al. Continuous hyperfractionated accelerated radiotherapy in locally advanced carcinoma of the head and neck region. *Int J Radiat Oncol Biol Phys* 1989; **17**:1287-93.
14. Trott K-R. Cell repopulation and overall treatment time. *Int J Radiat Oncol Biol Rhys* 1990; **19**:1071-75.
15. Saunders MI. (personal communications) 1991.

Adv Radiol Oncol 1992; 241–8.

Dipyridamole enhances the cytotoxicity of drugs and radiation in HeLa and V79 cells *in vitro*

Ban J, Sorić J, Bistrović M, Dujmović I, Miletić Z

Central Institute for Tumors and Allied Diseases, Zagreb
Laboratory for Experimental Cancerology and Department of Radiotherapy

Dipyridamole (DP) was utilized as the nucleoside transport inhibitor in combination with anti-cancer drugs which directly damaged DNA. It was also used in combination with radiation. Cytotoxic action of DP alone on HeLa cells was concentration and time dependent. DP, on incubation for 10 days, killed human tumor HeLa cells with an IC_{50}= 15 μM measured by clonogenic assay. In combination with doxorubicin or epirubicin, DP significantly enhanced their killing action on HeLa cells. Synergistic cell kill was also obtained with bleomycin or BCNU, producing a 2.2 or 2.6-fold reduction in 10% inhibitory concentration at a DP concentration of 15 μM, respectively. Combination of mustargen or dacarbazine plus DP gave only an additive cytotoxic effect. DP intensively influenced the killing action of radiation. Using isobologram method, it was demostrated that the interaction was truly synergistic. This combination was also slightly synergistic in normal V79 cells. These cells are less sensitive to both DP and irradiation than tumor cells. DP killed V79 cells with IC_{50}= 23 μM after 5 days of incubation. DP together with particular anticancer drugs on V79 cells was tested for comparison. The magnitude of cytotoxic effects on normal cells was examined.

Key words: HeLa cells-drug effects; V79 cells-drug effects; dipyridamole, radiation

Introduction

Dypyridamole (DP) is used in this study on the basis of *in vitro* and *in vivo* studies which indicate that DP enhances the cytotoxic effect of some antitumor drugs by inhibiting the uptake of nucleosides into cancer cells.

DP i.e. 2,6-bis-diethanolamino-4,8-dipiperidinopyrimido-(5,4d)-pyrimidine, or persantin is a pyrimidopyrimidine derivative that is a licensed drug in the US Pharmacopoeia and is among the 50 most commonly prescribed drugs.[1]

DP is clinically used as a vasodilatator and an antithrombotic agent. The mechanism of its antiplatelet activity is attributed to the inhibition of phosphodiesterase and thus to an increase of cAMP in platelets.[1,2] It is effective inhibitor of purine and pyrimidine nucleoside incorporation into macromolecules.[3,4]

It was demonstrated earlier that the salvage pathway of DNA synthesis is important for

Abbreviations: DP, dipyridamole; DX, doxorubicin; EPI, epidoxorubicin; BCNU, carmustine; DTIC, Dacarbazine; MS, Mustargen; BLEO, Bleomycin; PBS, phosphate buffered saline; FCS, fetal bovine serum; MEM, minimal essential medium; cAMP, cyclic adenosine monophosphate; Do, mean lethal dose equal to the concentration required to reduce survival by 63% on the exponential part of the survival curve; Dq, quasithreshold dose equal to the intercept with the abscissa of the exponential part of the survival curve; IC_{50}= 50% inhibitory concentration.

Correspondence to: Ban J Ph.D., Central Institute for Tumors and Allied Diseases, Ilica 197, 41000 Zagreb Croatia.

UDC: 615.277.3.015.44

proliferation of tumor cells. Weber and coworkers also showed that in tissue culture the transition from quiescence to a proliferative state, the earliest parameters rise were the incorporation of nucleosides.[5] Purine and pyrimidine nucleosides protect tumor cells from inhibitors of the *de novo* pathway of DNA synthesis.[2] Therefore, it has been suggested to block the salvage pathway for DNA synthesis.

One strategy to block nucleoside salvage is based on the inhibition of nucleoside uptake by DP. It was proposed and demonstrated that DP would block nucleoside salvage and thereby enhance acivicin cytotoxicity.[3,4]DP also has been used both *in vitro* and *in vivo* to enhance the cytotoxic activity of a number of anticancer agents including acivicin,[6,7,8,9,10] cytarabine[11] N-phosphonacetyl-L-aspartate,[12,13] methotrexate,[14,15,16] 5-fluorouracil[17,18] vincristine,[2] vinblastine[19] and doxorubicin.[19,20]

Therefore it was of interest to test whether DP and various anti-cancer drugs might be effective agents in combination chemotherapy. We also examined the action of DP and radiation on cell survival. For this purpose the stability, reversibility and the lethal effect of DP, as the function of drug concentration and incubation time, on normal V79 cells was investigated first and then the combination of two agents was tested. In combination chemotherapy we compared the magnitude of obtained effects on normal and tumor cell populations.

Materials and methods

Cell lines

Employed cultures were human cervical carcinoma cells, a subline of HeLa line purchased from Flow Laboratories (Scotland) designated 'HeLa-FA3' and Chinese hamster lung cells (V79). Both cell lines were grown in monolayer cultures in plastic 60-mm disposable Petri dishes in MEM (both: Flow Laboratories Irvine, Scotland) with 10% FCS. For HeLa cells 1% of non essential amino acids were added. Cells were incubated in 5% CO_2:95% air. To keep cells in logarithmic growth, both HeLa and V79 were subcultured twice or three times a week.

Cell growth

Cell multiplication was determined by counting the cells by Coulter Counter (England).

Dose-response survival experiments

Experiments were performed with proliferating cultures. For this reason 2 x 10^5 cells were seeded and incubated for 24 h. Five hundred of these cells were seeded and incubated for the next 20 h. The cells were then exposed to a single agent or to simulataneous treatment of two different agents. V79 or HeLa cells were incubated for 5 or 10 days, respectively. Medium was removed and the cells were stained with a saturated solution of crystal violet in 0.85% sodium chloride.[21] Colonies containing more than 50 cells were counted and results were expressed as percentage of colonies grown in untreated samples. The plating efficiency of untreated cells was 69% for V79 and 47% for HeLa culture. Mean values and standard errors were calculated for each surviving fraction. T-test was used for determining the significant difference.

In experiments with radiation the appropriate number of cells was incubated in order to gain the same number of colonies in irradiated, treated and control dishes. The cell suspension was diluted to yield about 100 colonies per dish.[22] After plating dishes were incubated as described above and irradiated. Immediately after irradiation DP was added and incubated for colonies. The average cell multiplicity (ACM) was approximately 4 or 3 for V79 or HeLa cells, respectively.

Drugs and irradiation

Doxorubicin i.e. 14-hydroxy – daunorubicin, also named adriamycin (NSC-123127), and epirubicin, also named 4'-epidoxorubicin (IMI 28) supplied as hydrochloride were obtained from Farmitalia Carlo Erba, Milan, Italy; deticene or dacarbazine from Laboratoire Roger Bellon, Neuilly/Sei-

ne, France; bleomycin (lyophilisiertes bleomycinsulfat) from H. Mack Chem. Pharm. Fabrik Bayern, Germany; mustargen (mechlorethamine HC1) from MSG, Div. of Merck and CO. Inc., West Point PA., USA and dipyridamole from Belupo 1, Ludbreg, Croatia; BCNU or carmustine i.e. 1,3-BI(2-chloroethyl)-1-nitro-sourea was obtained from Laboratoires Bristol, Paris, France.

Drugs were stored at 4°C, dissolved in sterile PBS just before use, and immediately added to the cell cultures. The irradiation was performed by a Co-60 radiotherapy unit (CGR) at a dose rate 3 Gy/m.

Results and discussion

Effect of DP on cell growth

DP was tested in V79 cell culture for its inhibitory activity, i.e. V79 growth inhibition (Figure 1). Cells were treated with different concentrations of DP for increasing time of incubation. Concentrations for 50% growth inhibition were 55,30 or 15 μM for incubation intervals of 24, 48

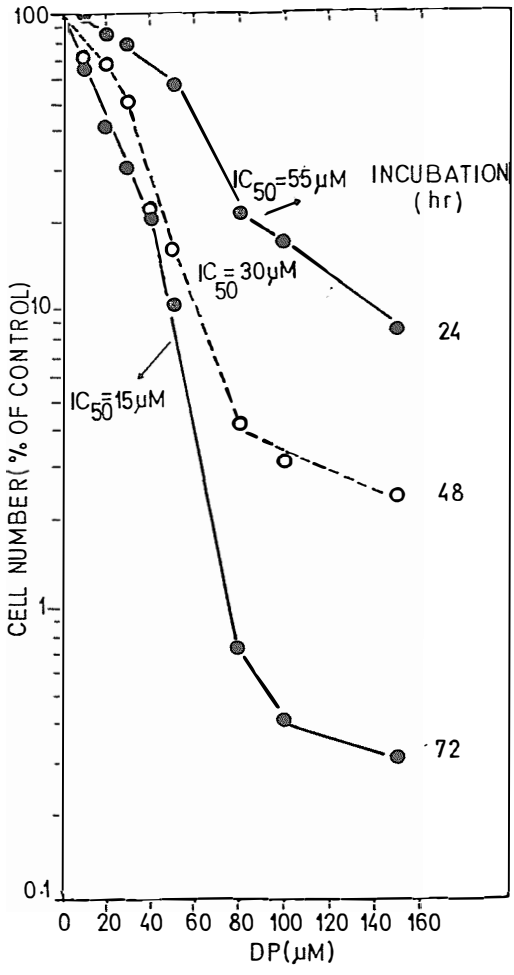

Figure 1. Effect of DP on the growth of chinese hamster V79 cells. The cells ($1x10^5$/Petri dish) were plated and allowed to grow in the presence of increasing concentrations of DP. Cells were incubated for different periods of time, samples were trypsinized and cell number was determined. Results were expressed as % of cell number of untreated culture. Points are mean values for triplicate assay.

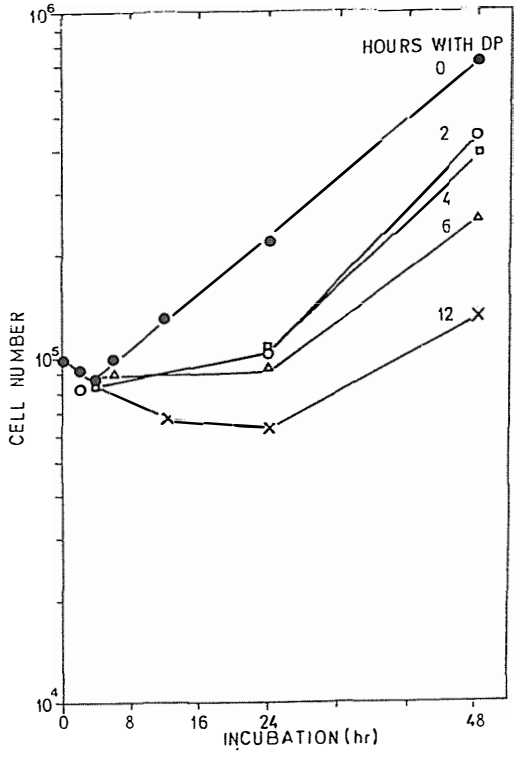

Figure 2. The test for reversibility of DP effect on cell growth of chinese hamster V79 cells. 100 μM DP was added to cell cultures ($1x10^5$ cells/Petri dish) for 2 (○); 4 (□); 6 (△) and 12 (X) hr, followed by washing of cells and incubation with drug–free medium. At indicated intervals the cell number was determined. Untreated control (●). Points are mean values for triplicate assays.

or 72 hr, respectively. The degree of the cell growth inhibition was concentration and time-dependent.

We also examined the reversibility of effects caused by DP. For this purpose V79 cells were incubated with 100 μM of DP for 2, 4, 6 and 12 hr as indicated in Figure 2. After treatment DP was washed out and cells were grown in medium up to 48 hr. Cells were counted after varying time intervals. Proliferating V79 cells grew in culture with a doubling time of about 15 hr. Exposure of cells to DP resulted in a dose dependent decline of cell proliferation. Cells treated with DP for 2 and 4 hr were not dividing for the first 24 hr but after that the cell division became of the same rate as in untreated control. The presence of DP for 6 or 12 hr inhibited the cell growth for the next 12 hr but further incubation without the drug increased the doubling time to approximately 18 or 24 hr, respectively. We concluded that the action of DP on cell growth was reversible.

Action of DP on cell survival

In order to examine the killing action of DP on normal and tumor cell lines we tested the cytotoxicity of the drug on cell survival. Thus, the proliferating V79 cells were exposed to increasing concentrations of DP for 5 days to form colonies. The survival of treated cells was evaluated by colony counts. The survival curve was of the threshold-exponential type with IC_{50}= 23 μM (Figure 3). Minimum effective dose was 1μM, D_o=8 and D_q=20 μM. For comparison human tumor HeLa cells were also treated with different concentrations of DP for 10 days. The threshold-exponential type of dose-response survival curve with IC_{50}=15 μM, D_o=3 μM and D_q=15 μM is shown in Figure 3. The curves show that HeLa cells were 1.5-fold more sensitive as compared to the killing action of DP on normal V79 cells.

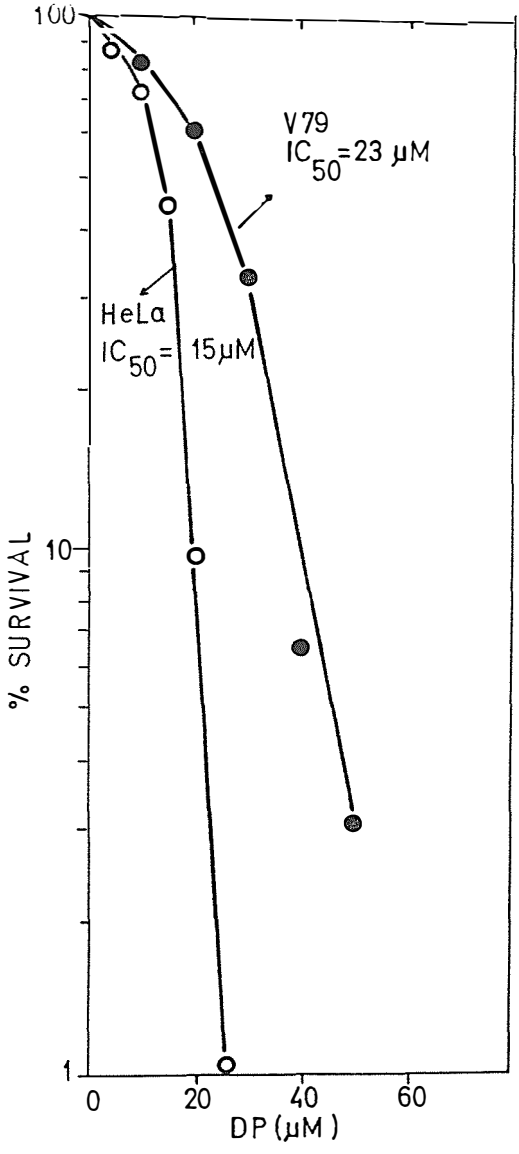

Figure 3. Survival curves of proliferating chinese hamster V79 (•) and human cervix carcinoma HeLa cells (○) exposed to increasing concentrations of DP. Cells were seeded (500/Petri dish) and supplemented with the drug for 5 (V79) or 10 (HeLa) days. Colonies were counted and the counts expressed as % of colonies of untreated cells. Each point is the average of triplicate samples of 3 experiments.

Stability of DP in different solutions

It was relevant to examine the stability of DP under experimental conditions because of the duration of some experiments. For this reason the drug was tested for the stability of its activity in different solutions. The drug (20 and 50 μM) was dissolved and preincubated at 37°C in complete medium containing FCS and in PBS (in the absence of FCS) for various periods of time; it was then added to proliferating V79 cells

and after 5 days of incubation the percent survival was measured by colony counts. Surviving fractions of cells treated more than 4 hr with preincubated DP in both solutions were about 60% higher than those of cells treated immediately (Table 1). There were no differences between the survivals of cells treated with DP preincubated in complete medium or in buffer solution. DP lost some of its killing activity with the duration preincubation time. The above results do not allow to conclude that drug has been bound to serum proteins in medium. Our *in vitro* data do not contradict the data obtained *in vivo*. D binds to the specific human serum protein, α_1-acid glycoprotein[23], which can significantly influence the inhibition of adenosine uptake *in vivo*.[8,9,10,23]

Influence of DP on the cytotoxicity of various anticancer drugs

In order to test the hypothesis that DP enhances the cytotoxicity of drugs which directly damage DNA, proliferating HeLa cells were exposed to specific drug combination. Cells were treated with incresing concentrations of tested antitumor agents alone or in combination with DP added in its IC_{50} value (15μM). Cells were then incubated for 10 days to form colonies. To test the influence of intercalating agents, cells were exposed to various concentrations of DX or EPI. Results are shown in Figure 4. Threshold exponential type of dose-response survival curves were obtained with DX or EPI, with D_o= 0.014 or 0.009 μM and D_q=0.01 or 0.022 μM, respectively. DP significantly enhanced the killing ability of both anthracyclines. Observed dose response curves also are of a threshold exponential type with D_o=0.018 or 0.007 μM and D_q=0.004 or 0.006 μM for DX or EPI plus DP, respectively. The predicted dose-response curves are identically shaped as those of DX or EPI but shifted downwards for the amount corresponding to the DP toxicity. This shift indicates the multiplication only. The translated dose–response curve represents the level of expected survival if no mutual potentiation of drugs occurred. The predicted survivals and possible synergism were

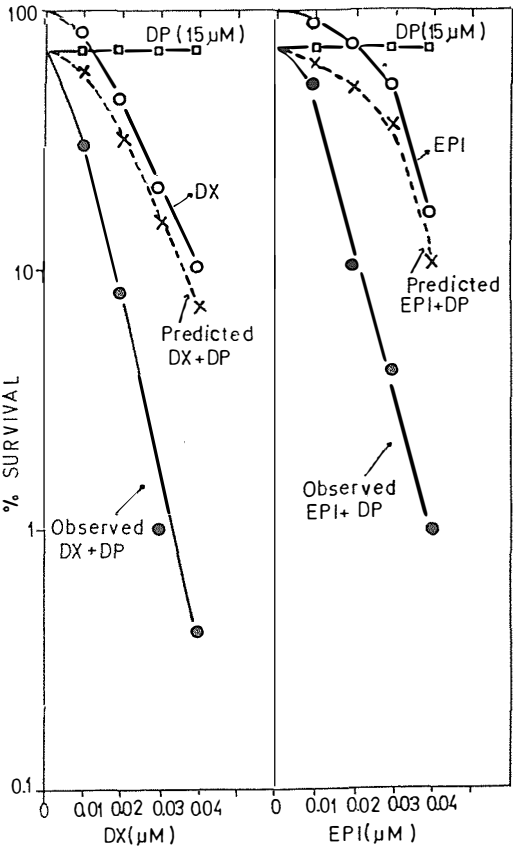

Figure 4. Survival curves of proliferating human tumor HeLa cells exposed to increasing concentrations of DX or EPI and a fixed dose of DP (15 μM), used separately or in combination. Cells were treated for 10 days, colonies were counted and results calculated as in Figure 3. Each point is the average of triplicate samples. The result is from a representative experiment. Predicted survivals = (mean % of drug survival) x (mean % of DP survival)/100. Observed survivals are all significantly lower than predicted ($p < 0.001$).

calculated according to Webb.[24] Mean survival values by corresponding doses of the single agents were used for calculating predicted survival. All experimentally obtained survivals were significantly lower.

Similar dose-response survival curves of normal V79 cells exposed to various concentrations of DP alone or with added DX or EPI were obtained. The isoboles were constructed[22, 25], and those for 10% survivals showed a concave up shape i.e. DP enhanced the sensitivity of

tumor and normal cells toward DX or EPI (Figure 5).

DP also enhanced the sensitivity of tumor or normal cells to BLEO producing a 2.2 or 2.5-fold reduction in 10% inhibitory concentrations, respectively. This combination could be of interest for *in vivo* experiments because HeLa cells were more sensitive to DP and nearly 250 times more sensitive to BLEO than normal cells (Table 2).

HeLa cells were also treated with some other antitumor drugs as indicated in Table 2. DP enhanced the sensitivity of HeLa cells to BCNU producing a 2.6-fold reduction in 10% inhibitory concentration. Synergistic cell kill was observed only when higher concentrations of BCNU were combined with DP, indicating that this combination was concentration dependent.

This interaction could be of interest for *in vivo* treatment. Namely, highly synergistic interaction could be expected in the peritoneal cavity, but much lesser interaction in the plasma where drug concentrations are much lower.[23] V79 cells were more sensitive to BCNU and 3.0-fold reduction in IC_{10} value was obtained (Table 2). This fact has to be taken into account for *in vivo* experiments.

Mustargen or DTIC applied in combination with DP gave only summation in HeLa cells but synergistic interaction was observed in normal cell population (Table 2). These data suggest that above combinations could not be recommended for clinical use since normal cells were killed at a relatively higher rate.

The effect of DP on radiation damage

DP affects the killing ability of radiation. HeLa cells were first irradiated with increasing doses of radiation and immediately after-wards treated with various concentrations of DP for 10 days. The results of interaction (10% survivals) are shown in Figure 6. A concave-up isobole was obtained indicating a slight synergism. For the comparison, V79 were also treated with the combination of DP and radiation. The result was similar: a slight synergism. Data not presented here also showed that DP combined with higher

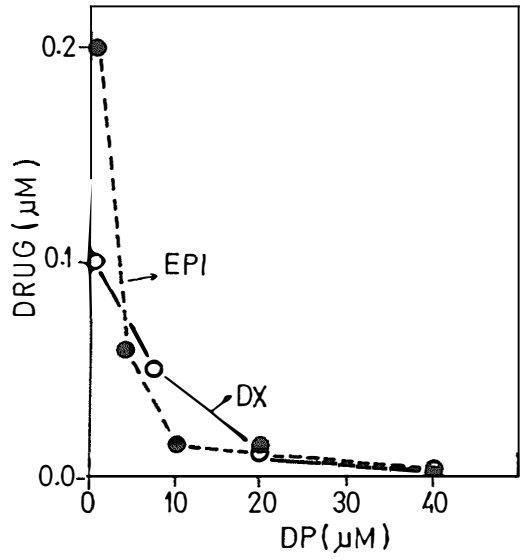

Figure 5. Combined cytotoxic effect of EPI or DX plus DP on V79 cells. Isoboles are based on the data taken from the dose–response survival curves. Cells were treated with drugs for 5 days to form colonies. Isoboles for cell survivals of 10% are shown. Each point is the average of triplicate samples.

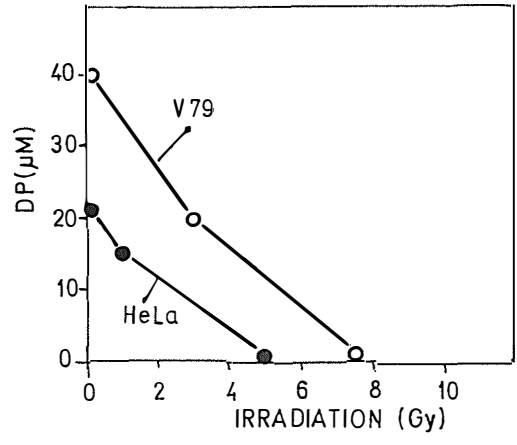

Figure 6. Combined cytotoxic effect of DP plus radiation on HeLa and V79 cells. Cells were irradiated and DP was added immediately. Cells were incubated to form colonies with the drug for 5 or 10 days for V79 or HeLa cells, respectively. Isoboles are based on the data taken from the dose–response survival curves. Isoboles for cell survivals of 10% are presented. Each point is the average of triplicate samples.

doses of radiation gave only summation. Therefore the combination of DP plus radiation could be recommended for tumor cell treatment. Ho-

Table 1. Stability of biologic activity of DP in different solutions.

Preincubation of DP in solutions at 37°C (hr)	DP (μM)	% survival[x] MEM+FCS	% survival[x] PBS[+]
0	20	50	50
	50	0.0	0.0
4	20	50	44
	50	0.2	0.0
6	20	80	79
	50	8.4	8.3
48	20	83.5	82
	50	7.5	7.5

[x] Proliferating V79 cells were exposed to DP for 5 days.

[+] All values are not significantly lower than those for DP preincubated in complete medium ($p < 0.05$). Mean values of triplicate determinations are given.

Table 2. Effect of DP on the survival of cultured cells treated with different cytostatics.

	IC_{10} values (μM)			
	HeLa		V79	
Drug	DP(–)	DP(15μM)	DP(–)	DP(20μM)
BLEO	0.074	0.034[x]	18.0	7.0
BCNU	90.0	35.0[x]	30.0	10.0[x]
MS	0.9	0.07	0.1	0.04[x]
DTIC	110.0	100.0	65.0	28.0[x]

IC_{10} = 10% inhibitory concentration. Concentrations were from the dose–response survival curves. Cell survivals (% control) were determined after single or combined drug treatment. (Procedure as in Fig. 3).
DP = dipyridamole added or not.
[x] Concentration of cell survival which is significantly lower than predicted ($p < 0.01$). Predicted survivals were calculated as in Fig. 3. Mean values of triplicate determinations are given.

wever these *in vitro* data suggest that using lower doses of both agents a selective chemotherapy could be developed.

A hypothetical explantation of synergism between DP and anticancer agents

There were two reasons for this investigation. One was to examine the suggested block of the salvage pathway for DNA synthesis. DP blocks the utilization of exogenous nucleosides by the cells and has a long history of safe clinical use. Another reason was that so far DP was mainly used in combination with inhibitors affecting *de novo* pathways of DNA synthesis. The activity of *de novo* and salvage enzymes in pyrimidine metabolism were as earlier recognized elevated in tumor tissue.[6,7]

Recently it was noted that DP enhanced the sensitivity of cancer cells to the drugs which belong to other classes of drugs.[2,19,20,23] Our earlier results with radiation and EPI showed synergistic cytotoxicity in V79 cell culture.[22] For these reasons we tested DP together with drugs classified as alkylating agents, bleomycin, anthracycline antibiotics and also radiation.

Some tested agents, e.g. radiation, DX, EPI, BCNU and BLEO in combination with DP gave synergistic kill of tumor cells. The mechanism of these combinations could be explained by a complementary inhibition of DNA synthesis at two different levels. Salvage pathways of DNA synthesis were blocked by the presence of DP. Radiation alone damages directly DNA nucleosides causing free radicals. Intercalating agents, DX or EPI, bind nonocoalently to DNA and also are inhibitors of DNA polymerase, thus preventing deoxyribonucleotide incorporation into DNA. BLEO or BCNU are template active drugs which alter DNA replication or RNA transcription by causing DNA breaks or reacting covalently with DNA, respectively.[26] Combined with DP, DNA synthesis could be complementary inhibited.

Investigation of DP in normal and tumor cells showed that DP was a useful antitumor agent. It killed HeLa cells in a concentration and time-dependent manner. For this drug a long-term treatment in combination chemotherapy could be recommended. The highest synergistic interaction was achieved with DX or EPI. These combinations exhibited also relatively high cytotoxic effects in V79 normal cell population. This

fact has to be taken in consideration for *in vivo* experiments. Examinations with BLEO and BCNU in combination with DP showed synergistic kill of HeLa cells. The benefit of these combinations was discussed earlier. The association of DP with radiation could be recommended because tumor cells are very sensitive to both DP as well as to radiation. Synergistic interaction is more expressive in tumor cells. The variety of effects obtained by various combinations of drugs indicates a possibility for the development of a more selective chemotherapy based on *in vitro* models.

Acknowledgements

The authors would like to thank Ms. Marija Taiber and Mrs. Brigita Golik–Galina for exellent technical assistance, Mrs. Bosiljka Šikić for drawing the figures and Mrs. Marjana Sajnica for typing the manuscript.

References

1. Fizgerald GA. Drug therapy – dipyridamole. *N Engl J Med* 1987; **316**:1247-57.
2. Hirose M, Takeda E, Ninomiya T, Kuroda Y, Miyao M. Synergistic inhibitory effects of dipyridamole and vincristine on the growth of human leukaemia and lymphoma cell lines. *Br J Cancer* 1987; **56**:413-7.
3. Weber G, Lui MS, Natsumeda Y, Faderan MA. Salvage capacity of hepatoma 3924A and action of dipyridamole. *Advan Enzyme Regul* 1983; **21**:53-69.
4. Zhen YS, Lui MS, Weber G. Effects of acivicin and dipyridamole on hepatoma 3924A cells. *Cancer Res* 1983; **43**:1616-19.
5. Weber G, Olah E, Denton JE, Lui MS, Takeda E, Tzeng Y, Ban J. Dynamics of modulation of biochemical programs in cancer cells. *Advan Enzyme Regul* 1981; **19**:87:102.
6. Weber G. Biochemical strategy of cancer cells and the design of chemotherapy: G.H.A. Clowes Memorial Lecture. *Cancer Res* 1983; **43**:3466-92.
7. Zhen YS, Reardon MA, Weber G. Amphotericin B renders stationary phase hepatoma cells sensitive to dipyridamole. *Biochem Biophys Res Comm* 1986; **140**:434:39.
8. Fischer PH, Willson JKV, Risueno C, Tutsch K, Bruggink J, Ranhosky A, Trump DL. Biochemical assessment of the effects of acivicin and dipyridamole given as a continuous 72-hour intravenous infusion. *Cancer Res* 1988; **48**:5591-6.
9. Willson JKV, Fischer PH, Tutsch K, Alberti D, Simon K, Hamilton RD, Bruggink J, Oeller JM, Tormey DC, Earhart RH, Ranhosky A, Trump DL. Phase I clinical trial of a combination of dipyridamole and acivicin based upon inhibition of nucleoside salvage. *Cancer Res* 1988; **48**:5585-90.
10. Fischer PH, Pomukcu R, Bitner G, Willson JKV. Enhancement of the sensitivity of human colon cancer cells to growth inhibition by acivicin achieved through inhibition of nucleic acid precursor salvage by dipyridamole. *Cancer Res* 1984; **44**:3355-59.
11. King ME, Naporn A, Young B, Howell SB. Modulation of cytarabine uptake and toxicity by dipyridamole. *Cancer Treat Rep* 1984; **68**:361-6.
12. Chan TCK, Young B, King ME, Taetle R, Howell SB. Modulation of the activity of N–(phosphonacetyl)–L–aspartate by dipyridamole. *Cancer Treat Rep* 1985; **69**:425-30.
13. Chan TCK, Howell SB. Mechanism of synergy between N–phosphona cetyl–L–aspartate and dipyridamole in a human ovarian carcinoma cell line. *Cancer Res* 1985; **45**:3598-604.
14. Nelson JA, Drake S. Potentiation of methotrexate toxicity by dipyridamole. *Cancer Res* 1984; **44**:2493-96.
15. Van Mouwerik TJ, Pangallo CA, Willson JKV, Fischer PH. Augmentation of methotrexate cytotoxicity in human colon cancer cells achieved through inhibition of thymidine salvage by dipyridamole. *Biochem Pharmacol* 1987; **36**:809-14.
16. Cabral S, Leis S, Bauer L, Nembrot M, Mordoh J. Dipyridamole inhibits reversion by thymidine of methotrexate effect and increases drug uptake in sarcoma 180 cells. *Proc Natl Acad Sci USA* 1984; **81**:3200-3.
17. Grem JL, Fischer PH. Augmentation of 5–fluorouracil cytotoxicity in human colon cancer cells by dipyridamole. *Cancer Res* 1985; **45**:2967-72.
18. Remick SC, Grem JL, Fischer PH, Willson JKV, Tutsch K, Alberti D, Simon K, Trump DLA. Phase I trial of concurrent continuous infusion of 5–fluorouracil and dipyridamole. *Proc Am Assoc Cancer Res* 1987; **28**:227-31.
19. Howell SB, Hom D, Sanga R, Vick JS, Abramson IS. Comparison of the synergistic potentiation of etoposide, doxorubicin, and vinblastine cytotoxicity by dipyridamole. *Cancer Res* 1989; **49**:4147-53.
20. Kusumoto H, Maehara Y, Anai H, Kusumoto T, Sugimachi K. Potentiation of adriamycin cytotoxicity by dipyridamole against HeLa cells in vitro and sarcoma 180 cells in vivo. *Cancer Res* 1988; **48**:1208-12.
21. Ban J, Olah E, Weber G. Action of lycurim and pyrazofurin on hepatoma 3924A cells in culture. *Cancer Treat Rep* 1982; **66**:343-9.
22. Ban J, Bistrović M, Maričić Ž, Kolarić K. Combined treatment of 4'–epi–doxorubicin and radiation on hamster lung cells. *Tumori* 1986; **72**:339-44.
23. Howell SB, Hom DK, Sanga R, Vick JS, Chan TCK. Dipyridamole enhancement of etoposide sensitivity. *Cancer Res* 1989; **49**:4147-53.
24. Webb JL. Enzyme and metabolic inhibitors. New York, NY, Academic Press, Inc. 1963; **1**:487-512.
25. Berenbaum MC. Criteria for analysing interactions between biologically active agents. In: *Advances in Cancer Research*, Klein G, Weinhouse S. (eds) New York, Academic Press 1981; **35**:269-336.
26. Pratt WB, Ruddon RW. *The anticancer drugs*. New York, Oxford: Oxford Univ Press, 1979.

Adv Radiol Oncol 1992; 249-60.

Stress, tumor metastasis and antitumor chemotherapy in mice

Giraldi T, Perissin L, Rapozzi V and Zorzet S

Institute of Biology, Faculty of Medicine, University of Udine, I-33100 Udine, Italy.
Institute of Pharmacology, Faculty of Pharmacy, University of Trieste, I-34100 Trieste, Italy.

A simplified and common conceptual framework employed for analyzing the effectiveness of antitumor chemotherapy considers exclusively the cytotoxic action of the drugs on tumor cells. In reality, a complex network of reciprocal interactions occur between the tumor, antitumor resistance factors of the host and the antitumor drugs employed. Moreover, the immune and natural resistance factors of the host may be subjected to modulation by the central nervous system via neuro-vegetative and –endocrine circuits. In this connection a relatively scarce attention appears to be paid in the available literature on the specific relevance of these aspects on the treatment of tumor metastasis, and particularly on the possible influence of neuroimmunomodulation by stress on the outcome of chemotherapy. The available literature will be reviewed, and original findings presented. The results illustrated indicate that the application of experimental stressors to mice bearing Lewis lung carcinoma specifically influences tumor metastasis: the nature of the underlying neuroimmuno-modulatory mechanisms is preliminarily identified and described. The observation that the antitumor action of cyclophosphamide and the antimetastatic action of razoxane are reduced by the appliction of the experimental stressor, spatial disorientation, appear original and of considerable interest. The experimental and clinical implications of these data are finally discussed.

Key words: neoplasm metastasis; antineoplastic agents; stress

Introduction

The possibility to treat human cancers with antitumor drugs is a relatively recent accomplishment of medical scientific research, which dates back to the time of the Second World War.[1] Since the first successful use of nitrogen mustard to treat malignant lymphoma, a group of about 40 cytotoxic antitumor drugs with different chemical structure, mechanism of action and spectrum of activity has been shown to possess definite effectiveness against human malignancies. These drugs are currently included into combined clinical modalities of cancer treatment, eventually associated with surgery and/or radiotherapy, and significantly contribute to the overall success of present cancer therapy.[2, 3]

The development of new antitumor drugs, of new derivatives, and the study of their mechanism of action, has been traditionally made within a purely mechanistic conceptual frame. A binary system was considered, consisting of the tumor on one side and the drug on the other. Antitumor drugs effective in producing «cures» (i. e. indefinitely prolonging the survival time of the host) were considered to have a therapeutic index high enough to reach *in vivo* concentra-

Abbreviations used: BRL 51308: 4-carbethoxy-5-(3,3-dimethy1-1triazeno)-2-methyl-imidazole
DGA: N-diazoacetyl-glycin-amide
DTIC: 5-(3,3-dimetyhyl-1-triazeno)-imidazole-4-carboxamide

Correspondence to: Giraldi T.

UDC: 616-006.6-033.2-056.13:615.277.3

tions sufficient to kill all the tumor cells, thus sterilizing the host. A more sophisticated view implies that a «cure» is obtained when the treatment with an antitumor drug is capable to reduce the number of tumor cells below a threshold, under which the immune system of the host can totally eradicate the remaining clonogenic tumor cells.[4]

In reality, a ternary system composed of the tumor, the immune system of the host, and of the antitumor drug is involved, and should be jointly considered.[5] Indeed, a complex system of interactions exists between the tumor and the immune system of the host. Antitumor drugs, almost without exception, cause immunodepression as a side effect[6], and this may lead to an unfavorably reduced resistance of the host to tumor progression. On the other hand, antitumor drugs may cause in some instances, independently from direct cytotoxicity, chemical xenogenization of tumor cells, thus augmenting the control of tumor growth exerted by the immune system of the host.[7] It thus appears that the overall therapeutic action of each antitumor drug depends on the balance between cytoreductive effects, immunosuppressive potency and the eventual occurrence of chemical xenogenization. Moreover, the more common and serious problem encountered during clinical cancer treatment is the occurrence of metastasis, and tumor metastatic deposits appear to respond either to immune effectors of the host or to treatment with antitumor drugs in a way which may show significant differences from the primary tumor.[8]

This conceptual frame is based on the assumption that immunological functions are stable in time, and are identical in different (inbred) individuals. A considerable amount of evidence has been recently made available, showing that psycho–social factors may be elaborated by the central nervous system, leading to modulation of the function of immune effectors via the mediation of neurovegetative and neuroendocrine mechanisms.[9] No study about the possibility that neuroimmunomodulation might affect the overall effectiveness of antitumor chemotherapy *in vivo* appears to have been published to the best knowledge of the authors.

The aim of this work is therefore to provide a brief overview of the most relevant literature available, and to illustrate the experimental work in progress in the laboratory of the authors, on the effects of stress on the growth and metastasis of solid malignant tumor(s) in syngeneic mice, and on their response to chemotherapy with antitumor drugs.

Antimetastatic action and immunodepressive side effects of antitumor drugs

Cytotoxic antitumor drugs in many instances act differently on primary tumor as compared with metastatic tumor nodules, and drugs acting specifically on tumor metastasis have been identified.[10] The differential effects on the primary tumor in relation to metastasis have been studied in some detail for dimethyl–triazenes and for N–diazoacetyl derivatives of aminoacids. A selective inhibition of spontaneous *in vivo* dissemination of transplantable solid malignant tumors and leukemias, which is unrelated with the cytotoxic action directed against tumor cells, has been shown for N-diazoacetyl-glycin-amide (DGA)[11,12] and triazenes.[13] For triazenes, the antimetastatic action was shown for the clinically used derivative DTIC and for its imidazole analog BRL 51308.[14] Among a series of benzenoid dimethyl-triazene derivatives examined in a quantitative structure–activity relationship study, DM-COOK was found to posses an optimized, potent and highly selective antimetastatic action[15]. For DTIC and DM-COOK, the mechanism of the antimetastatic action was shown not to consist in the cytotoxicity for tumor cells, but, for metastasis of solid tumors, rather in the inhibition of the presence of circulating tumor cells in the blood stream.[13]

Typical results obtained in a representative experiment with DGA and DM-COOK in mice bearing Lewis lung carcinoma are illustrated in Table 1. Both drugs appear devoid of significant effects on primary tumor growth, and at the

same time significantly depress to a similar extent the formation of spontaneous lung metastases; a similar proportion of animals is found free of macroscopically detectable lung tumor colonies on sacrifice (differences between treatments are not statistically significant).

On the contrary, a remarkable difference in the effects of DGA and DM-COOK is found when the drugs are used as pre-operative adjuvants combined with surgical removal of the primary tumor. The administration of DM-COOK for 8 days preceding surgery results in about 50% of long-term survivors (cures), whereas the survival time of mice treated with DGA is the same as that of drug untreated controls. Both drugs were administered according to the same schedule, using dosages which were equitoxic, maximum tolerated doses, equieffective and optimal on spontaneous metastases without surgery.[16] It appears that these drugs markedly inhibit the formation of metastases, but widely differ in their capacity to prolong survival when used as adjuvants in combination with surgery.

A possible interpretation of this finding might consist in the different action of the drugs on the relationships between the tumor and the immune system of the host. When the animals cured by the preoperative treatment with DM-COOK followed by surgery are re-implanted with the same tumor, the number and weight of either spontaneous or artificial lung metastases is significantly reduced, as compared with controls which underwent drug treatment and surgery bot no previous tumor implantation.[16] This result suggests that an immune response of the host was elicited by the treatment, which possibly contributed to the direct action of DM-COOK and surgery on the tumor. In this connection, the lack of effects of DGA might be attributed to its immunodepressive action. Indeed, when tested for prolongation of allogeneic skin graft rejection in mice at dosages effective on metastases, DGA shows an immunosuppressive activity comparable with that of azathioprine and slightly smaller than that of methotrexate[17], whereas DM-COOK is devoid of significant effects on the same test (Table 2).

It thus appears that the action of the antimetastatic drug DM-COOK requires the cooperation of effective immune responses of the host. This view is supported by the finding that the antimetastatic action of the stable prostacyclin analog Iloprost is suppressed in mice pretreated with cyclophosphamide.[18] Moreover, the antimetasta-

Table 1. Antimetastatic effects of DGA and DM-COOK in mice bearing Lewis lung carcinoma.

Drug	Dose mg/Kg/day	Primary tumor volume (%T/C)[a]	Effects on metastasis (%T/C)[a]		
			number	weight	animals free
DM–COOK	50	65.3±12.9	31.5±5.1*	1.1.±0.9*	4/10
DGA	300	88.3±18.0	16.2±4.8*	11.4±5.2*	3/10

[a] – %T/C is the percent ratio of the average of each treated group to controls
* – significantly different from drug untreated controls, $p<0.05$, Student–Newman–Keuls test[69]
The animals were treated daily on days 1-14 from tumor inoculation with optimal, maximum tolerated doses of the drugs. Primary tumor growth and lung metastasis were measured on day 14 and 21, respectively.[12]

Table 2. Allogeneic skin graft rejection in mice treated with DM–COOK or DGA.

Drug	Dose mg/Kg/day	Allograft rejection time (%T/C)[a]	Ref.
DM–COOK	60	118.1±11.0	(17)
DGA	250	153.1±20.3*	(70)

a – %T/C is the percent ratio of the average of each treated group to controls.
* – significantly different form drug untreated controls, Wilcoxon two–sample test, $p<0.05$[71].
Drugs were administered i.p. at the dosage indicated daily on days 1–6 (DM–COOK) or 1–4 (DGA) from grafting.

tic effects of the anticoagulant drug warfarin have been shown to require an intact function of host's NK immune efectors.[19]

Stress and metastasis

The notion that psycho-social factors can be related with tumor incidence and progression has been repeatedly put forward for clinical cancer[20, 21], and a considerable amount of experimental evidence supports this view. The application of stressor paradigms to laboratory animals resulted in the modification of the growth of spontaneous and transplanted tumors, and several available reviews deal in detail with the results obtained.[22-25] It has to be noted that rather conflicting evidence was obtained from these investigations and tumor progression was found to be either enhanced, or decreased or left unaffected in some instances.[26,27] It has been proposed that these discrepancies may be explained, at least partially, by the different naure of the stressors examined, by the timing of their application in relation to the phase of tumor growth, and by the acute or chronic administration of the stressors themselves.[28] Moreover, the different investigations performed used widely different tumor-host systems, including spontaneous tumors and tumors induced by carcinogens (viral, chemical and physical ones), or transplanted neoplasms; some of the tumors were solid, and sometimes ascitic or leukemic lines were used.[28] A majority of tumor-host systems were allogeneic, and only a limited number of reports specifically studied the effects of stress on tumor metastases, in spite of its crucial clinical relevance. The interest of the potential effects of psychological stress on tumor metastases is further indicated by unequivocal data, showing that the physical stress resulting from diagnostic and therapeutic procedures, such as radiotherapy[29-32], chemotherapy[33-35], anesthesia[36] and surgery[32, 36-38] increases metastasis formation in laboratory animals bearing malignant tumors.

In the perspective outlined above and in the preceding paragraph, the effects of the application of controlled paradigms of psychological stress to mice bearing a syngeneic solid malignant tumor which spontaneously metastasizes to the lungs, Lewis lung carcinoma, have been examined. Housing in a low stress (protected) environment in comparison with a conventional animal room, and the anxiety caused by the periodic application of spatial disorientation to the animals kept in the protected environment have been examined as originally devised by Riley et al.[24] The other stressors employed include maternal deprivation[39], physical restraint[40] and behavioral despair.[41] The effects of the application of these stressors have been examined differentially on the growth of the primary s.c. tumor, and on the formation of spontaneous metastases.

In order to gain information on the neuro-endocrine mechanisms underlying the effects of psychological stress on tumor metastasis, direct hormonal assays were performed, and pharmacological inhibitors of nervous and endocrine functions were used in tumor-bearing mice subjected to spatial disorientation. The hormones assayed were corticosterone in plasma, and the urinary excretion of melatonin. For elucidating the role played by this hormone, different light-dark cycles effective in controlling pineal function, were also used. The pharmacological agents tested *in vivo* include mitotane as an adrenal gland suppressor, naltrexone as an antagonist of β-endorfin, bromocryptine as a prolactin inhibitor, and the adrenolytic agents reserpine and guanethidine. The results obtained are illustrated below.

Effects of animal housing, spatial disorientation and other stressors

Representative results obtained in examining the effects of housing in conditions and spatial disorientation on primary tumor growth and spontaneous lung metastasis formation in mice bearing Lewis lung carcinoma are presented in Table 3, which is prepared with minor modifications from citation[42]; the replication of the experiment on numerous further occasions provided substantially identical results. When the tumor is implanted in mice adapted before tumor implantation, and afterwards further maintained in a protected environment, the weight of sponta-

neous pulmonary metastases is significantly reduced in comparison with mice kept in conventional housing throughout the duration of experiment. The application of spatial disorientation to animals continuously kept in the protected housing before and after tumor implantation, significantly increases the number and weight of pulmonary metastases. No statistically significant difference results for the values obtained with mice continuously kept in conventional housing, as compared with mice placed in the protected environment after tumor implantation, and eventually subjected to spatial disorientation. The handling for daily intraperitoneal administration of physiological saline in mice constantly kept in the protected environment significantly increases the weight and number of lung metastases to a value not significantly different from that observed after application of spatial disorientation. The effects of handling for daily intraperitoneal administration of saline are not additive with those caused by the application of spatial disorientation to animals kept in the protected environment, and are not significant in other experimental groups, including animals constantly kept in the conventional housing. A statistically significant increase in primary tumor growth is observed with the group of animals continuously kept in the protected environment and subjected to spatial disorientation, as compared with other experimental groups; this increase remains evident also when handling is combined with spatial disorientation.[42]

The effects of other stressors have been examined applying the paradigms used to animals maintained in a partially protected environment. Maternal deprivation, consisting of early weaning at 14 days, is devoid of significant effects in male mice; in female mice early maternal separation causes a significant decrease in lung metastases weight. Limited physical restraint, obtained by placing individual animals in relatively large plastic tubes (length 10 cm, diameter 5 cm), is devoid of significant effects when compared with non–restrained controls, whereas a more severe restraint (tubes of 10 cm length diameter 2.8 cm) significantly increases the weight and number of lung metastases. On the other hand, behavioral despair induced by tail suspension significantly increases primary tumor growth, and decreases the number and weight of pulmonary metastases in the same animals.[43]

These findings show that usually disregarded housing factors and experimental procedures, such as handling for parenteral drug administration, can significantly affect tumor growth and metastases. They also are in agreement with previous findings concerning primary tumors, showing that different stressor paradigms can either increase or decrease, depending on the nature and timing of stressor application, tumor metastases besides primary tumor.[28]

Table 3. Effects of housing conditions, spatial disorientation and handling for parenteral saline administration on primary tumor growth and spontaneous lung metastasis formation in mice bearing Lewis lung carcinoma.

SD (days)	Housing before tumor inoculation	Housing after tumor inoculation	Intraperitoneal saline administration	Tumor weight (g)	Metastasis		
					number	weight	(mg)
–	Conventional	Conventional	–	1.6±0.2▼°	44.2±5.8*◆	220.2±	61.6*
–	Conventional	Conventional	+	1.9±0.2▼°	47.3±7.6*◆	205.3±	30.1*
–	Protected	Protected	–	2.0±0.3#	32.6±6.7#	70.7±	25.6#
–	Protected	Protected	+	2.0±0.4▼	57.8±9.0*	278.0±	76.7*
0–6	Protected	Protected	–	4.0±1.7*■	80.5±7.0*▲	281.2±	80.8*
0–6	Protected	Protected	+	3.7±1.2*●	59.0±8.8*	223.0±	44.8*

Spatial disorientation (SD) was applied to mice in the protected housing for 7 (0-6) days from tumor inoculation. Each value is the mean (±SE) obtained in groups of 5 mice. When indicated, the animals received 0.1 ml of isotonic NaCl solution (9 g/l) i.p. on days 1–21.
t-test for grouped data[72] $p<0.05$; * – significantly different from#; ▼ – significantly different from ■; ● – significantly different from°; ◆ – significantly different from ▲.

Plasmatic corticosterone and effects of mitotane

The application of spatial disorientation to animals kept in protected environment causes a significant increase in the plasmatic level of corticosterone, which accompanies the significant increase in metastasis weight and number. When the animals are treated with mitotane, the drug does not modify the base level of corticosterone, but totally abolishes the increase caused by spatial disorientation. In spite of this inhibitory effects on corticosterone level, the increase in lung metastasis formation caused by spatial disorientation remains evident in mice treated with mitotane.[44]

These findings indicate that althought the pituitary-adrenal axis is activated by spatial disorientation, plasmatic glucocorticoids do not participate in the metastasis enhancing effects of this stressor.

Effects of the treatment with pharmacological inhibitors of neuro-vegetative and endocrine functions

When mice implanted with Lewis lung carcinoma are treated with the drug tested, no significant alteration of primary tumor growth is observed, and naltrexone is also devoid of effects on metastasis. On the contrary, a significant reduction in the number and weight of lung metastases is caused by bromocryptine and guanethidine, and a remarkably pronounced inhibition is caused by reserpine.[45]

These results suggest a negligible participation of neuropeptides, a limited participation of prolactin, and a significant involvement of adrenergic responses is controlling natural antitumor responses of the host, directed against lung metastases. This finding is further supported by additional data, showing that the pretreatment of the animals with immunosuppressive dosages of cyclophosphamide abolishes the reduction caused by reserpine in the metastatic increase caused by spatial disorientation, whereas the effects of reserpine are not modified by the pretreatment with macrophagic poison carrageenan. These results provide a direct evidence that the effects of this drug and of this stressor are mediated by the immune system of the host (unpublished results).

Urinary melatonin excretion in relation to tumor growth and metastases

Pineal gland function and secretion of melatonin have been shown to be involved in several patho–physiological processes, including neuroimmunomodulation[46], stress responses[47] and tumor metastasis.[48-50] The participation of pineal gland functions in the modulation of metastasis by spatial disorientation have therefore been examined either by means of non-invasive measurement of urinary melatonin excretion, or by the use of cycles and intensities of illumination capable to influence pineal function.

When different cycles of illumination with an intensity of 2,100 lux are used (light/dark 12/12 or 24/0 hr), the effects of the application of spatial disorientation consist of a significant reduction in the weight of lung metastasis, which is accompanied by a non significant influence on primary tumor growth and metastasis number. This reduction is more pronounced for constant lighting, in contrast to the results presented in Table 3, which were obtained with a light-dark cycle of 12/12 h and an intensity of 5 lux. The nocturnal urinary excretion of melatonin is consistently higher than that determined during light hours, with the light cycles examined. Nocturnal melatonin levels are markedly and significantly increased by the application of spatial disorientation when the animals are kept under constant illumination (Table 4, prepared with modification from ref. 51). These results further indicate that and additional housing factor, i.e. cycle and intensity of illumination, can significantly influence tumor metastases. They also support the view that stressors can modify in different ways tumor dissemination, and indicate an interesting association between pineal gland function and tumor metastases. The latter result is in agreement with an enhancement of metastasis observed in mice subjected to surgical pinealectomy.[52]

Stress and effects of antitumor drugs

In the perspective outlined above, the magnitude of the effects of antitumor drugs has been determined as a function of the application of spatial disorientation in mice bearing Lewis lung carcinoma. The first drug which has been examined is ICRF 159, an antitumor agent which, besides having a certain cytotoxic action for tumor cells,[53] specifically and markedly reduces metastasis formation.[54] Limited effects were observed on primary tumor growth, which were not significantly modified by spatial disorientation. On the contrary, the number and weight of metastases are markedly reduced by the treatment with ICRF 159; 2 mice out of 5 do not have metastases at necroscopy. Upon application of spatial disorientation for 7 days following tumor implantation and initiation of treatment, the reduction in metastasis number and weight is limited to non significant levels, and all of the animals present metastases (Table 5). A similar and more striking result is obtained when spatial disorientation is applied to mice treated with cyclophosphamide. The treatment with this drug is curative in 10/10 animals kept in the protected environment; the application of spatial disorientation to these animals reduces the cure rate to 0/10, with a significant reduction of primary tumor and metastasis number and weight as compared with drug untreated controls (Tale 5).[45]

These results indicate that spatial disorientation, in addition to causing an increase in metastasis in mice kept in protected environment, also reduces the magnitude of the effects of an antimetastatic and of a cytotoxic antitumor drug. These results can be interpreted considering that spatial disorientation reduces, via neuroimmunomodulation, natural factors of host resistance to tumor progression, which participate to, and

Table 4. Effects of different light cycles and stress on urinary excretion of melatonin and tumor spread in mice bearing Lewis lung carcinoma.

SD	Light/ dark cycles	Urinary melatonin excretion (pg) light	dark	Tumor weight (G)	Metastasis number	weight (mg)
–	12/12	6.4±2.4	68.9±17.0◆	3.6±0.3	36.9±4.4	167.4±26.4
+	12/12	6.0±2.1	92.0±21.0◆	3.2±0.4	26.4±2.9	107.4± 9.8◠
–	24/0	6.6±1.5ξ	46.8±15.3*,◆	3.1±0.3	44.8±5.7	219.1±37.7■
+	24/0	6.8±2.1ξ	152.0±20.0*,▼	2.8±0.3	29.1±5.2	95.1±22.4◠

Spatial disorientation (SD) was applied to mice from tumor inoculation until sacrifice on day 21. Melatonin was determined by a radioimmunoassay (RIA-2AB Nuclear Medica, Italy) on day 15 (ξ: 8 a.m.–8 p.m.; *: 8 p.m.–8 a.m.). Student-Newmann-Keuls test $p<0.05$[69], ◆ – significantly different from ▼; ◠ – significantly different from ■.

Table 5. Primary tumor growth and spontaneous lung metastasis formation in mice bearing Lewis lung carcinoma kept in protected housing, subjected to spatial disorientation, treated with ICRF 159 or cyclophosphamide.

SD (Days)	Treatment	Primary tumor weight	Metastasis number	weight	free	Ref.
–	–	1.1±0.6	63±18	67±22	0/5	
–	ICRF 159	0.9±0.2	18± 7	19±15	2/5	(60)
(0–6)	ICRF 159	2.1±0.5	52±15	53±18	0/5	
–	–	2.1±0.5	41± 6[a]	127±19[b]	0/10	
–	CYCLO	–	–	–	10/10	(45)
(0–21)	CYCLO	1.1±0.3	13± 2[a]	26± 4[b]	0/10	

Means with the same letter are significantly different, t-test for grouped data ($p<0.05$)[72].
Spatial disorientation (SD) was applied as indicated starting from tumor inoculation. Groups of 5 or 10 mice were used for ICRF 159 or cyclophosphamide (CYCLO), respectively. Drugs employed were administered per os admixed to powdered food daily on days 1–21 for ICRF 159 (25 mg/Kg/day) and 1–6 for cyclophosphamide (240 mg/Kg/day) from tumor inoculation.

crucially determine, the effectiveness of (at least) the antitumor drugs (tested).

Conclusions

A relatively large number of reports exists in the literature, showing that stress can influence the incidence and progression of tumors in laboratory animals.[22-25,27,28,55] The data available indicate that the physical stress produced by therapeutic procedures increases tumor metastasis in experimental animaltumor systems. Psychological stressors, including isolation or overcrowding during animal housing, have also been shown to influence the incidence and growth of tumors in laboratory rodents.[22,24,25] The results obtained with psychological stressors are rather conflicting, and appear to depend on the experimental conditions chosen, i.e. the animal-tumor system used, the acute or chronic application of the stressor, as well as its nature.[28] Moreover, the majority of the animal-tumor systems employed in these studies were allogeneic, and metastasis was rarely examined[28] in spite of the clinical relevance of this phenomenon. An absolute distinction between physical and psychological stressors appears to be difficult. For instance, a certain degree of subjective cognitive and emotional reactions are presumably always present during coping with physical stressors. The main stressor paradigms presently examined have been housing conditions, handling the animals for intraperitoneal drug administration and the periodic application of spatial disorientation. These stressors appear mainly to be of psychological nature, and spatial disorientation in particular was suggested to be an emotional stressor (anxiety)[24], since the centrifugal acceleration caused in the cages by rotation is smaller than 0.15 g. Using these conditions, with a light-dark cycle of 12-12 hr and an intensity of 5 lux in the cages, and Lewis lung carcinoma implanted into syngeneic BD2F1 mice as the animal-tumor system, the results reported show that tumor metastasis is reduced independently from primary tumor growth by housing the animals in a low stress environment. The application of spatial disorientation, and handling the animals for the intraperitoneal administration of physiological saline, increases the number and weight of metastases and primary tumor growth in animals kept in the low stress housing. This increase is not additive when spatial disorientation and handling are combined, and it is not observed when the mice are not adapted before, and kept after, tumor implantation in the low stress housing. The tumor responses presently caused by housing conditions, handling and spatial disorientation are of a similar magnitude. Their observed non-additive action might depend on the fact that each of them is the maximal degree of control that the host exerts in response to the stressors applied. This interpretation is consistent with the data obtained in several other studies, which show that in certain circumstances the effect of one stressor can be non-additive with, modified by, and even reverted by the combined application of further stressors, depending on their nature and timing of application.[26,27] This view is further supported by the (unreported) results obtained in the combination of surgery with spatial disorientation which indicate that the effects of spatial disorientation are reverted by surgery, leading to a reduction of tumor metastasis.

When ICRF 159 or cyclophosphamide is administered to mice in the protected environment, the effectiveness of the drugs is reduced upon application of spatial disorientation. The drug treatment performed for the experiments reported in this work was applied orally, admixing the drug with powdered food, in order to eliminate the significant influence caused by the handling of the animals for parenteral administrations, illustrated above. It is noteworthy that spatial disorientation abolishes the curative action of cyclophosphamide in animals receiving the drug in a dosage and schedule which strongly depresses T-cell-dependent and NK-mediated immune responses.[4,56]

The results presented are consistent with the view that the central nervous system modulates natural antitumor responses of the host via neuro-vegetative and endocrine mechanisms[9]; coping with stressors may lead to a reduction in these responses.[57,58] During the present investi-

gation an examination has been consequently performed in order to determine the significance of some of the mediating mechanisms among a number of ones which have been suggested in general to mediate the effects of stress on tumor progression.[57-59] The evidence presented allows to rule out a significant influence of corticosteroene in the experimental conditions used. This conclusion is further supported by the reported observation that the antimetastatic action of ICRF159 is not modified when the treatment with this drug is combined with mitotane.[60] β-endorphin similarly appears to have a marginal role, as indicated by the ineffectiveness of the *in vivo* treatment of tumor bearing mice with naltrexone, at dosages capable to antagonize in *vivo* the analgesic effects of morphine in mice.[61] The significant effects of the treatment with bromocryptine on metastasis, at dosages effective to maintain the plasmatic prolactin levels similar to those of hypophysiectomized mice[62], suggest a substantial influence of prolactin. Finally, the adrenergic system appears to play a significant role in the modulation of tumor metastasis by spatial disorientation, as indicated by the remarcable inhibition caused by reserpine and guanethidine. The effectiveness of both drugs indicates that central and peripheral adrenergic mechanisms are involved; for reserpine, sedation can be excluded as the cause of the reported effects, since the treatment with barbiturates at sedative dosages is ineffective (unreported results). Moreover, the ineffectiveness of reserpine in mice immunosuppressed with cyclophosphamide indeed indicates that neuroimmunomodulation of host's antitumor responses is actually operative.

Numerous biological functions have been found to implicate the pineal gland and melatonin.[63] As far as neoplasms are concerned, pineal function and melatonin secretion have been related to the control of tumor growth[64], immune functions[65] and stress responses[66] in general, and to the process of tumor metastasis in particular.[48-50] The results presented indeed indicate that pineal function is involved in tumor metastasis and its modulation by stress. In fact, different intensities of illumination with constant light-dark cycles, and different light-dark cycles with the same intensity of illumination, significantly influence metastasis formation. This finding is in agreement with the already reported effects of different light cycles, which were limited to primary tumor only[26] and to the use of modification in light cycles considered as an experimental stressor.[67] Urinary excretion of melatonin is increased by stress in mice under intense illumination, and this increase is associated with a reduction in metastasis formation. The complexity of the central neurochemical mechanisms governing pineal function and melatonin increase, and the ambiguity of its peripheral targets and actions[68], makes it difficult to further interpret at this stage of research the results illustrated.

In conclusion, the experimental results presented indicate that psychological stressors can influence tumor metastasis in mice bearing a syngeneic solid malignant tumor, in a way which is independent from the effects on primary tumor; the mediation of multiple neuroendocrine mechanisms has been preliminarily identified. The finding that the effectiveness of antitumor chemotherapy is significantly reduced by a psychological stressor appears noteworthy. Moreover, the presented results support the possibility previously indicated by Riley that pharmacological agents can be used in order to inhibit host's responses to applied stressors.[26] Further research is needed, and is partially in progress, aiming to additionally identify and characterize the neuroendocrine and immunological mediators of the responses to the stressors presently used; the actual data seem, however, of interest for their experimental and clinical implications.

Acknowledgements

This work has been supported by Italian National Research Council, Special Project 'Oncology' contract n° 88.00691.44, and by grants from the Ministry of Education (MPI 40 and 60%). The outstanding technical assistance of Mr. G. Fonzari is recognized, and the generosity of Fondazione C. & D. Callerio in providing the protected animal rooms is gratefully appreciated.

References

1. Calabresi P, Welch AD. Chemotherapy of neoplastic disease. *A Rev Med* 1962;**13:**147-202.
2. Frei E. III. Curative cancer chemotherapy. *Cancer Res* 1985;**45:**6523-37.
3. Frei E. III. Curative cancer chemotherapy. *Cancer Res* 1987;**47:**3907-8.
4. Hilgard P, Phol J, Steckar J, Voegeli R. Oxaphosphorines as biological response modifiers – experimental and clinical perspectives. *Cancer Treat Rev* 1985;**12:**155-62.
5. Giraldi T, Sava G, Perissin L, Zorzet S. Role of host responses in the drug treatment of metastasis. In: Prodi G, Liotta LA, Lollini PL, Garbisa S, Gorini S, Hellmann K eds. *CAncer metastasis, biological and biochemical mechanisms and clinical aspects.* New York–London: Plenum Press, 1987;351-60.
6. Cadman E. Toxicity of chemotherapeutic agents. In: Becker FF ed. Cancer Vol. 5. New York–London: Plenum Press, 1977;59-111.
7. Puccetti P, Romani L, Taramelli E, Bonmassar E, Fioretti MC. Drug mediated changes of tumor cell immunogenicity and antigenicity. *Int J Tiss React* 1982;**IV:**189-99.
8. Heppner GH, Miller BE. Tumor heterogeneity: biological implications and therapeutic consequences. *Cancer Metastasis Rev* 1983;**2:**5-23.
9. Riley V, Fitzmaurice MA, Spackman H. Immunocompetence and neoplasia: role of anxiety stress. In: Lewy SM ed. Biological mediators of behavior and disease: neoplasia. New York: Elsevier Biomedical, 1982;175-218.
10. Giraldi T, Sava G. Selective antimetastatic drug (Review). *Anticancer Res* 1981;**1:**163-74.
11. Giraldi T, Guarino AM, Nisi C, Baldini L. Selective antimetastatic effects of N-diazoacetylglycyne derivatives in mice. *Eur J Cancer* 1979:**15:**603-7.
12. Giraldi T, Sava G., Nisi C. Mechanisms of the antimetastatic action of N-diazoacetylglycinamide in mice bearing Lewis lung carcinoma. *Eur J Cancer* 1980;**16:**87-92.
13. Giraldi T, Perissin L, Zorzet S, Rapozzi V. Antimetastatic action of triazenes derivatives. In: Giraldi T, Connors TA, Cartei G eds. Triazenes: chemical, biological, and clinical aspects. New York: 1990;45-62.
14. Giraldi T, Houghton PJ, Taylor DM, Nisi C. Antimetastatic action of some triazene derivatives against the Lewis lung carcinoma. *Cancer Treat Rep* 1978;**62:**721-5.
15. Lassiani L., Nisi C, Giraldi T, Sava G, Cuman R. Selective antimetastatic trazenes: a quantitative approach. *Quant Struct–Act Relat* 1984;**3:**59-62.
16. Giraldi T, Sava G, Cherubino R, Lassiani L, Bottiroli, Mazzini G. In: Davis W, Maltoni C, Tannemberger St eds. Metastasis: mitostatic drugs. Berlin: Akademie–Verlag, 1983;55-62.
17. Hršak I. Ruđer Bošković Institute, Zagreb, Yugoslavia; personal communication to T. Giraldi.
18. Giraldi T, Rapozzi V, Perissin L, Zorzet S. Antimetastatic action in mice of PGI_2 analog Iloprost. In: Honn KV, Marnett LJ, Nigam S, Walden TL. Jr eds. Eicosanoids and Bioactive Lipids in Cancer & Radiation Injury. Boston–London: Kluwer Academic Publishers, 1991;415-418.
19. Gorelik E. Augmentation of the antimetastatic effect of anticoagulant drugs by immunostimulation in mice. *Cancer Res* 1987;**47:**809-15.
20. Rosch PJ. Stress and cancer. In: Cooper CL ed. *Psychosocial stress and cancer.* Chichester: John Wiley & Sons Ltd, 1984;3-20.
21. Greer SG, Watson M. Mental adjustment to cancer: its measurement and prognostic importance. *Cancer Surveys* 1987;**6:**439-53.
22. Steplewski Z, Robinson Goldman P, Vogel WH. Effects of housing stress on the formation and development of tumors in rats. *Cancer Lett* 1987;**34:**257-61.
23. Vogel W.H. Stress – the neglected variable in experimental pharmacology and toxicology. *Trends Pharmacol* Sci 1987;**8:**35-7.
24. Riley V, Fitzmaurice MA, Spackman DH. Animals models in biobehavioral research: effects of anxiety stress on immunocompetence and neoplasia. In: Weiss SM, Herd JA, Fox BH, eds. Perspectives on behavioral medicine. New York: Academic Press, 1981;371-400.
25. Labarba RC. Experiential and environmental factors in cancer. *Psychosom Med* 1970;**32:**258-76.
26. Riley V. Cancer and stress: overview and critique. *Cancer Detect Prev* 1979;**2:**163-95.
27. Sklar LS, Anisman H. Stress and cancer. *Psychol Bull* 1981;**89:**369-406.
28. Justice A. Review of the effects of stress on cancer in laboratory animals: importance of time of stress application and type of tumor. *Psychol Bull* 1985;**98:**108-38.
29. Van den Brenk HAS, Kelly H. Stimulation of growth of metastases by local X-irradiation in kidney and liver. *Br J Cancer* 1973;**28:**349-53.
30. Withers HR, Milas L. Influence of preirradiation of lung on development of artificial pulmonary metastases of fibrosarcoma in mice. *Cancer Res* 1973;**33:**1931-6.
31. Furuse T, Kasuga T. Effects of irradiation with fast neutrons or X-rays on the incidence of metastasis of transplanted B16 melanoma in mice. *Gann* 1982;**73:**35-41.
32. Peters LJ. A study of the influence of various diagnostic and therapeutic procedures applied to a murine squamous carcinoma on its metastatic behaviour. *Br J Cancer* 1975;**32:**355-65.
33. De Ruiter J, Cramer SJ, Smink T, van Putten LM. The facilitation of tumor growth in the lung by cyclophosphamide in artificial and spontaneous metastases model. *Eur J Cancer Clin Oncol* 1979;**15:**1139-49.
34. Orr FW, Adamson IJR, Young L. Promotion of pulmonary metastasis in mice by bleomycin-induced endothelial ijury. *Cancer Res* 1986;**46:**891-7.
35. Ormerod EJ, Everett CA, Hart IR. Enhanced experimental metastatic capacity of a human tumor line following treatment with 5-azacytidine. *Cancer Res* 1986;**46:**884-90.
36. Lundy J, Lowett EJ, Hamilton S, Conran P. Halothane, surgery, immunosuppression and artificial pulmonary metastases. *Cancer* 1978;**41:**827-30.
37. Agostino D, Agostino N. Role of operative trauma: explosive metastases of similar size following amputation of the primary leg tumor. *Tumori* 1979;**65:**527-38.

38. Pollock RE, Babacock GF, Ronsdahl MM, Mishioka K. Surgical stress-mediated suppression of murine natural killer cell cytotoxicity. *Cancer Res* 1984;**44:**3888-91.

39. LaBarba RC, White JL, Lazar J, Klein M. Early maternal separation and the response to Ehrlich carcinoma in Balb/C mice. *Develop Psychol* 1970;**3:**78-80.

40. Gotoh T, Ganhon L, Yoshikura H. Effects of physical restraint on leukemogenesis by Friend virus. *Gann* 1986;**77:**985-91.

41. Porsolt RD, Chermat R, Lenegre A, Avril I, Janvier S, Steru L. Use of the automated tail suspension test for the primary screening of psychotropic agents. *Arch Int Pharmacodyn* 1987;**288:**11-30.

42. Giraldi T, Perissin L, Zorzet S, Piccini P, Rapozzi V. Effects of stress on tumor growth and metastasis in mice bearing Lewis lung carcinoma. *Eur J Cancer Clin Oncol* 1989;**25:**1583-8.

43. Giraldi T, Perissin L, Rapozzi V, Zorzet S. Stress tumor metastasis and effectiveness of antitumor chemotherapy. In: Proceedings of Symposium on Psychoneuroimmunology, Hannover September 14-16 1989, in press.

44. Perissin L, Zorzet S, Piccini P, Rapozzi V, Giraldi T. Corticosterone does not mediate the effects of stress on tumor metastasis. *Pharm Res* 1989,**21:**461-2.

45. Giraldi T, Perissin L, Piccini P, Rapozzi V, Zorzet S. Stress, tumor progression and success of chemotherapy in mice. In: Hadden JW, Masek K, Nisticò G eds. *Interaction among CNS, neuroendocrine and immune system.* Rome–Milan: Pythagora Press, 1989;429-38.

46. Maestroni GJM, Pierpaoli W. Pharmacological central of hormonally modulated immune response. In: Ader R ed. *Psychoneuroimmunology.* New York: Academic Press, 1981;405-25.

47. Maestroni GJM, Conti A, Pierpaoli W. Role of the pineal gland in immunity. III Melatonin antagonizes the immunosuppressive effect of acute stress via an opiatergic mechanism. *Immunology* 1988;**63:**465-9.

48. Barone RM, Das Gupta TK. Role of pinealactomy in Walker 256 carcinoma in rats. *J Surg Oncol* 1970;**2:**313-22.

49. Lapin V. Influence of simultaneous thymectomy and pinealectomy on the growth and formation of metastases of the Yoshida sarcoma in rats. *Exp Path* 1974;**9:**108-12.

50. Lapin V. The pineal and neoplasia. *Lancet* 1975;**1:**341.

51. Perissin L, Zorzet S, Rapozzi V, Giraldi T. Effects of different light cycles and stress on urinary excretion of melatonin and tumor spread in mice bearing Lewis lung carcinoma. *Pharm Res 1989;21:*131-2.

52. Das Gupta TK, Terz J. Influence of pineal gland on the growth and spread of melatonina in the hamster. *Cancer Res* 1967;**27:**1306-11.

53. Herman EH, Witiak DT, Hellmann K, Waravdekar VS. Biological properties of ICRF-159 and related bis (dioxopiperazine) compounds. *Adv Pharmacol Chemother* 1982;**19:**249-90.

54. Giraldi T, Sava G, Cuman R, Nisi C, Lassiani L. Selectivity of the antimetastatic and cytotoxic effects of 1-p-(3,3-dimethyl-1-triazeno) benzoic acid potassium salt, (±) –1, 2-di (3, 5-dioxopiperazin-1-yl) propane, and cyclophosphamide in mice bearing Lewis lung carcinoma. *Cancer Res* 1981;**41:**2524-8.

55. Burchfield SR. The stress response: a new perspective. *Psychosom Med* 1979;**41:**661-72.

56. Mantovani A, Polentarutti N, Alessandri G, Vecchi A, Giuliani F, Spreafico F. Activation of K cells in mice with transplanted tumors differing in immunogenicity and metastasizing capacity. *Br J Cancer* 1977;**36:**453-60.

57. Borisenko M, Borisenko JZ. Stress, behavior and immunity: animal models and mediating mechanisms. *Gen Hosp Psychiatry* 1982;**4:**59-67.

58. Borisenko M, Kandil O. Stress-induced decline in natural killer cell activity, cytotoxic cell function and interleukin-2 production. Relationship with tumor growth in C3H/HeJ mice. In: Bennett CB ed. *Neuroimmunomodulation.* Bethesda: Published by the International Working Group on Neuroimmunomodulation, 1985; 262-5.

59. Borisenko JZ. Higher cortical function and neoplasia: psychoneuroimmunology. In: Lewy SM ed. *Biological mediators of behavior and disease: neoplasia.* New York: Elsevier Biomedical, 1982; 29-53.

60. Giraldi T, Perissin L, Sava G, Zorzet S, Nicpali S, Rodani MG. Is effectiveness of cancer chemotherapy influenced by stress? In: Lobo A, Tres A eds. *Psychosomatica y cancer.* Madrid: Graficas Solana, 1988; 73-9.

61. Zagon IS, McLaughlin PJ. Modulation of murine neuroblastoma in nude mice by opioid antagonists. *JNCI* 1987;**78:**141-7.

62. Rao MR, Bartke A, Parkening TA, Collins TJ. Effect of treatment with different doses of bromocryptine on plasma profiles of prolactin, gonadotrophins and testosterone in mature male rats and mice. *Int J Androl* 1984;**7:**258-68.

63. Axelrod J. The pineal gland: a neurochemical transducer. *Science* 1974;**184:**1341-48.

64. Lissoni P, Barni S, Tancini G, Crispino S, Paolorossi F, Lucini V, Mariani M, Cattaneo G, Esposti D, Esposti G, Fraschini F. Chemical study of melatonin in untreatable advanced cancer patients. *Tumori* 1987;**73:**475-80.

65. Jankovic BD, Isakovic K, Petrovic S. Effect of pinealectomy on immune reactions in the rat. *Immunology* 1970;**18:**1-6.

66. Pierpaoli W, Maestroni GJM. Melatonin: a principal neuroimmunoregolatory and anti-stress hormone: its anti-aging effects. *Immunol Lett* 1987;**16:**355-62.

67. Kort WJ, Zondervan PE, Hulsman LOM, Westbroek DL. Light-dark-shift stress with special reference to spontaneous tumor incidence in female BN rats. *JNCI* 1986;**76:**439-46.

68. Brown GM, Niles LP. Studies on melatonin and other pineal factors. In: Besser GM, Martini L eds. *Clinical Neuroendocrinology*. Vol. II New York: Academic Press, 1982;205-53.
69. Sokal RR, Rohlf FJ. Single classification analysis of variance. In: Biometry. San Francisco: Freeman WH, 1969.
70. Brambilla G, Parodi S, Cavanna M, Baldini L. The immunodepressive activity of N-diazoacetylglycine amide in some transplantation systems. *Transplantation* 1970;**10:**100-5.
71. Laurence DR, Bacharach AL eds. Evaluation of drug activities: pharmacometrics. New York: Academic Press, 1964.
72. Tallarida RJ, Murray RB eds. Manual of Pharmacologic calculation with computer programs. New York: Springer–Verlag, 1987.

Adv Radiol Oncol 1992; 261-7.

Combining photodynamic therapy with immunotherapy: Will it work?

Krošl G and Korbelik M

Cancer Imaging, British Columbia Cancer Research Centre, Vancouver, B.C., Canada V5Z 1L3

The principal objective of this article is to present evidence of multiple ways in which the host immune system participates in the events occurring with photodynamic therapy (PDT) of a solid tumour. It is shown that tumour associated macrophages (TAM) can be a major factor in selective tumour localization of photosensitizers, which is important for effectiveness of PDT. It is illustrated how photosensitizer content in TAM (and consequently in the tumour as a whole) can be increased or decreased using specific agents. This offers potential for increasing photosensitizer tumour levels by TAM targeted immunotherapy, which would improve the selectiveness of the photosensitizers tumour localization. The events following the induction of phototoxic damage in tumour by PDT are analyzed, and it is shown that multiple processes that were reported to occur following or even during the light treatment represent, in fact, a typical inflammatory reaction. It is concluded that so called secondary or indirect killing effect by PDT, i.e. tumour necrosis induction by destruction of its vasculature, is based on a strong local acute inflammatory reaction. It is proposed that potentiation of tumour destruction can be achieved by combining PDT with TAM targeted immunotherapy. This is based on a concept that an optimal type of immunotherapy will sustain and direct PDT-induced immune reaction towards more efficient tumour eradiaction. Examples are given of successful application of combined PDT and immunotherapy on animal tumour models.

Key words: neoplasms–therapy, phototherapy; immunotherapy

Introduction

Photodynamic therapy (PDT) is a major new modality for treatment of malignant disease. In PDT, a phototoxic drug (photosensitizer) is first administered to the patient, and time is allowed (24-72 hours) for the drug to remain selectively localized in the malignant tissue. The tumour is then illuminated with a specific wavelength of drug-activating light.[1, 2] Phase III clinical trials for the treatment of endobronchial lung cancer, esophageal cancer and superficial bladder cancer are currently in progress.[3] Previous Phase II trials showed that PDT is extremely effective in eradicating in situ and microinvasive carcinomas of lung and esophagus.[4, 5, 6, 7] Likewise, PDT was found to be very reliable in preventing recurrence of superficial bladder cancer.[3, 8] It is also effective in the palliative treatment of obstructive bronchial and esophageal cancers, and in the treatment of metastatic breast carcinoma, certain brain tumours, head and neck tumours, colorectal cancer, skin and gynecological tumours.[3, 4, 5] Of special interest is the possible

Correspondence to: dr. Mladen Korbelik

UDC: 616-006.6-08:615.831:615.37

application of PDT for peritoneal seeding of ovarian tumours.[9] It is also believed that PDT has a great potential to be used after surgical tumour removal.

The only photosensitizer used currently in clinics is Photofrin or very similar drug preparations manufactured in several countries. Photofrin is an empirically developed preparation, which is a very complex mixture of porphyrins in monomeric and oligomeric form and their self-aggregates.[10] Much research in the field of PDT is devoted to development of new, more clinically effective photosensitizing drugs.[1, 11, 12]

Cytotoxicity of photosensitizers, responsible for direct tumour cell destruction in PDT, results from their light-induced excitation. Energy from excited triplet state of the photosensitizer is transferred to molecular oxygen, which is excited to its extremely reactive singlet state.[13, 14] The primary target of singlet oxygen on cellular level are probably outer membranes and membranes of cellular organelles.[15] Active species from Photofrin preparation, being hydrophobic, localize primarily in membrane structures.[15, 16]

The process of tumour destruction by PDT is still under investigation. The existence of two distinct mechanisms has been recognized in this respect: i) direct killing of tumour cells by phototoxic action, and ii) indirect killing of tumour cells through necrosis induced by destruction of tumour vasculature.[4, 11] Another important element contributing to successful tumour eradication was proposed to be PDT-induced immune reaction.[17, 18]

Tumour localization of photosensitizers: Role of tumour associated macrophages

Selective localization of a photosensitizer in a tumour as compared to surrounding normal tissues is a prerequisite for successful PDT. A number of phototoxic drugs with very divergent chemical structures have been found to possess tumour localizing property.[1, 12] This property does not necessarily imply selective accumulation of the drug in tumour parenchymal cells. Studies with Photofrin and its less purified version hematoporphyrin derivative (HPD) have found most of the photosensitizer within the tumour to be localized in areas within and around blood vessels, or in certain elements and cells of non-vascular stroma, notably macrophages and mast cells.[19, 23] The examination of the uptake of Photofrin by macrophages under a variety of conditions *in vitro* and *in vivo* has shown that these cells have a capacity for photosensitizer accumulation that is superior to that of tumour cells.[22, 24] Several lines of evidence suggest that this property of macrophages is based on their ability to internalize large quantities of photosensitizer by phagocytosis of drug aggregates. For instance, the disaggregation of Photofrin by its interaction with serum markedly reduces the uptake of the photosensitizer by macrophages.[24] A strong inhibitory effect of this uptake by cytochalasin B, a classical inhibitor of phagocytosis, was also observed.[24]

Using a technique based on fluorescence activated cell sorting,[22] we have examined the distribution of Photofrin between tumour cells and tumour associated macrophages (TAM). The measurements in two mouse tumour models, SCCVII squamous cell carcinoma and Lewis lung adenocarcinoma, have shown consistently higher Photofrin levels in TAM than in malignant tumour cells,[21, 25] These tumours contain up to 40% of TAM in their total cell populations, which means that more photosensitizer in total can be contained in the TAM population than in the malignant cell population. It should be emphasized that many animal and human tumours are characterized by high TAM contents.[26, 27, 28.]

Phagocytic activity of macrophages can be altered by different agents. We have shown that such effects can either increase or decrease the amount of photosensitizer accumulated in TAM.[29] Administration of cytochalasin B to mice bearing Lewis lung carcinoma concomitantly with Photofrin resulted in reduced photosensitizer levels in TAM (in comparison to the levels seen when only Photofrin was administered), with photosensitizer levels in tumour cells remaining unchanged.[29] Similar effect was obser-

ved after administration to the mice of cyclooxygenase inhibitor indomethacin 24 hours prior to Photofrin. The opposite effect, an increase in photosensitizer level in TAM, was observed with dodecylglycerol (DDG). This drug was established as a potent macrophage activator.[30] Another macrophage activator, SPG (known also as Sonifilan or Sizofiran) was shown to increase the total tumour Photofrin levels in Lewis lung and SCCVII carcinomas.[18]

These results indicate that it is possible to increase photosensitizer tumour levels by TAM targeted immunotherapy. A number of agents (including cytokines interferon gamma, interleukin 1-beta, granulocytemacrophage growth factor, tumour necrosis factor) have been reported to activate TAM *in vivo,* and some also to enhance macrophage infiltration into the tumour.[31] Such drugs have the potential to increase selectiveness of tumour localization of Photofrin and other photosensitizers that accumulate in macrophages, by stimulating the phagocytic uptake of these drugs by TAM.[18, 29]

Photosensitizer-antibody conjugates for selective tumour delivery

It was reported that photosensitizers can be conjugated to monoclonal or polyclonal antibodies which recognize specific antigen on tumour cells.[32, 33, 34] This was done with the objective to achieve improved photosensitizer localization in solid tumours. Photosensitizer antibody-conjugates may also have potential for use in bone marrow purging before autologous tranplantation.[33]

It was suggested that by targeting the photosensitizer to tumour tissue with antibodies, photosensitizer levels in circulation would be reduced and skin toxicity may be decreased.[33] Since antibodies in the conjugate are responsible for targeting to the tumour, photosensitizers with no intrinsic tumour localizing property can be used with this technique.[32] However, it was noted that, at least in some conjugates, binding of the photosensitizer to the antibody may reduce its phototoxic potential.

The phototoxicity to ovarian carcinoma cell line *in vitro* of photosensitizer chlorin e_6 conjugated to monoclonal antibody was shown to be increased when the cells were pretreated with interferon gamma (IFN-γ).[32] This result illustrates the capability of lymphokines to increase the expression of tumour associated antigens (TAA) and MHC antigens on tumour cells and thereby to improve the tumour selectivity of the conjugates. Similar results with INF-γ were reported for Mab-drug conjugates *in vitro* and *in vivo*.[35]

The induction of immune reaction by PDT

The earliest changes in PDT treated tumour or normal tissue can be observed histologically in the vasculature, and they already occur during the course of light illumination. These events include accumulation of polymorphonuclear leucocytes (neutrophils and eosinophils), platelet aggregation, vasoconstriction (followed by vasodilatation), vascular stasis, hemorrhage and edema.[36, 37] The shutdown of blood vessels and destruction of tumour neovasculature results in rapidly evolving hypoxia and necrosis of tumour tissue.[38]

Within seconds after the initiation of the light treatment, phototoxic damage induced in outer membranes of endothelial cells is recognized as «foreign» antigen and bound by a recognition component of the immune system. This can be concluded from the detection of proteins of the complement system in the endothelium of tumour vasculature, which demonstrates activation of the complement cascade.[39] The complement derived anaphylatoxins (e.g. C5a) are potent leukocyte chemoattractants and promoters of neutrophil adherence to endothelial cells. Indeed, polymorphonuclear leukocytes were observed to accumulate very early in blood vasculature of PDT treated tissue.[37, 38] The next phase that follows very quickly is migration of polymorphs into the surrounding tissue (a process known as diapedesis) and their phagocytosis of damaged tumour cells. Concomitantly, these cells produce platelet-activating factors (PAFs)

that trigger the coagulation cascade, causing rapidly evolving platelet aggregation. Blood clotting within the tumour vasculature is observed early after the initiation of PDT treatment.[37] In addition, activated neutrophils release a number of enzymes from their cytoplasmic granules, including phospholipases that degrade membrane phospholipids to arachidonic acid. Arachidonic acid is metabolized into a variety of products, including leukotriens, prostaglandins, tromboxanes, and prostacyclins; all of these are potent mediators of the inflammatory process. Some of these factors are also released by platelets during the clotting process.[40]

Immunoglobulins with attached photodamaged structures recognized as antigens bind to Fc receptors on the membranes of mast cells and monocytes/macrophages. This event induces a release of contents of cytoplasmic granules from mast cells (e.g. histamine), as well as synthesis and secretion of biologically active metabolites of arachidonic acid.[41, 42] Mast cell products increase vascular permeability by contracting endothelial cells, and induce serotonin production. Phagocytosis of immune complexes by macrophages results in release of cytokines, such as interleukin 1 and tumour necrosis factor alpha (TNF-α), or presentation of processed antigen to T lymphocytes, which then produce lymphokines such as interleukin 2 and interferons. These and other cytokines trigger further activation and amplification of the immune system in order to contain toxic products and destroy damaged cells.

All these processes discussed above are, in fact, a typical acute inflammatory reaction. Its visual symptoms (e.g. edema and redness around the treated tumour) are regularly observed after the PDT treatment.[37] During the inflammatory process there is a massive infiltration of the cells of host immune system (polymorphs, macrophages, lymphocytes) into the PDT treated tumour.[17, 43] The immune reaction is, therefore, directly involved in the eradication of PDT treated tumour. The so called »indirect killing effect« by PDT, denoting tumour necrosis induction by destruction of its vasculature[4, 11, 44] is actually a strong local acute inflammatory process.

The PDT induced immune response in humans was demonstrated by Nseyo and coworkers.[45] They have shown that cytokines interleukin 1β and TNF-α are released into the urine of patients treated with PDT for bladder cancer. There were also reports of increased numbers of interstitial lymphocytes, plasma cells, and histiocytes present in post PDT bladder biopsy specimens.[46]

The hemorrhagic necrosis seen histologically in tumours treated with PDT is very similar to necrosis induced by systemic application of TNF.[47] Since high levels of TNF can be released by activated macrophages, a study was initiated which showed that peritoneal exudate macrophages are activated to produce TNF when exposed to Photofrin based PDT. [48] It was observed in this study that TNF yield was light dose dependent; however, there was a suppression of the TNF release after high energy doses. In another study, it was reported that prostaglandin E is released from peritoneal macrophages after exposure to Photofrin and light treatment *in vitro*.[49] It was also shown that mouse peritoneal macrophages are activated by exposure to very low concentration of HPD followed by red light treatment.[50]

Some of the soluble cytokines released in high levels after PDT, notably prostaglandins and interleukin-1, are known to mediate suppression of immune response. Indeed, PDT-induced immunosuppression was demonstrated with a murine model.[51, 52, 53] The suppressive effects are systemic (depressed contact hypersensitivity response at distal irradiated sites), and are adoptively transferred by macrophages.[53] Continuous low dose indomethacin treatment was shown to prevent the suppressive effect,[52] which indicates an important role of cyclooxygenase pathway in this process. Toxic effects of PDT, with symptoms very similar to TNF-induced cahexia were also described.[54] Indomethacin (used in clinics for treatment of inflammation) was also shown to strongly inhibit tumour destruction by PDT,[40] which supports the notion that »indirect killing effect« by PDT is based on the inflammatory process.

PDT and immunotherapy

Since PDT treatment invokes a profound local immune reaction, an investigation into a possibility of amplification of this immune response by immunotherapy seems merited. Positive results were already reported in the literature. Myers and co-workers have observed enhancement of tumour response to PDT when host's immune system was boosted by a killed vaccine *Corynebacterium parvum*.[55] In another study, Bellnier combined TNF-α administration with PDT, and obtained better tumour eradication than with PDT alone.[53] The cytokine TNF-α is not only selectively toxic to tumour cells, but is also known as a potent immune defense modifier.[57]

As discussed above, macrophages are one of major protagonists in generation of immune response to PDT treatment. This prompted us to propose that TAM targeted immunotherapy can potentiate the effect od PDT.[18] We hypothesized that, in addition to increasing the selectiveness of photosensitizer tumour localization, PDT in combination with immunotherapy can produce a synergistic effect on TAM activation, rendering these cells higher potency for destruction of tumour cells. It is well established that macrophages have uniquely powerful capacities for tumour destruction. However, tumours that have in their growth broken the barrier of immunosurveillance, subvert macrophages to serve as a supportive factor in tumour progression.[27] Since other levels of immune reactivity are interlinked with macrophage activity, an enhancement of TAM antitumour action will further amplify the overall immune response.

We have started to investigate the potential of combined PDT and TAM targeted immunotherapy by examining the effects of immunoactivator SPG. This high molecular weight β-glucan is well established anti-tumour agent.[58-61] It can activate macrophages directly, and also stimulate recruitment of these cells from bone marrow.[60] Our results have shown that SPG therapy (7 daily doses, 15 mg/kg, i.m.), administered before Photofrin based PDT doubles the cure rate of C3H mice bearing SCCVII tumour, when compared to PDT treatment only.[18]

These encouraging results suggest that there is a potential benefit in introducing specific immunotherapy as an adjuvant to clinical PDT. Before this is realized, pre-clinical research on ways to sustain and direct The PDT-induced immune reaction towards more efficient tumour destruction should be pursued further.

Acknowledgment

This work was supported by operating and scholarship grants awarded by British Columbia Health Research Foundation.

References

1. Dougherty T J. Photosensitizers: Therapy and detection of malignant tumours. *Photochem Photobiol* 1987;**45:**879-889.
2. Dougherty T J. Photodynamic therapy. In: Withers HR, Peters LJ eds. *Medical radiology innovations in radiation oncology* Springer – Verlag, Berlin & Heidelberg, 1988;178-88.
3. Marcus S L. Current status of photodynamic therapy for human cancer. *SPIE* 1991;**1426:**301-10.
4. Dougherty T J.: Photodynamic therapy: Status and potential. *Oncology* (Roswell Park) 1989;**3:**67-73.
5. Dougherty T J. Photodynamic therapy for the treatment of cancer: Current status and advances. In: Kessel D. ed. *Photodynamic therapy of neoplastic disease* Vol. I, CRC Press, Boca Raton FL, 1990;1-19.
6. Edell E S, Cortese D A. Bronchoscopic phototherapy with hematoporphyrin derivative for treatment of localized bronchogenic carcinoma: a 5 year experience. *Mayo Clin Proc* 1987;**62:**8-17.
7. Konaka C, Kato H, Hayata Y. Lung cancer treatment by photodynamic therapy alone: survival for more than five years. *Laser Med Sci* 1987;**2:**17-20.
8. Marcus S L. Photodynamic therapy of human cancer: Clinical status, potential and needs. In: Gomer C J. ed. *Future directions and applications in photodynamic therapy* SPIE Press, Bellingham WA, 1990;5-56.
9. Sindelar M F, DeLaney R F, Tochner Z, Thomas G F, Dachoewski L J, Smith P D, Friauf M S, Cole J M, Glatstein E. Technique of photodynamic therapy for disseminated intraperitoneal malignant neoplasms. *Arch Surg* 1991;**126:**318-24.
10. Dougherty T J. Studies on the structure of porphyrins contained in Photofrin II. *Photochem Photobiol* 1987; **46:**569-73.
11. Henderson B W. Photodynamic therapy – coming of age. *Photodermatol* 1989; **6:**200-11.

12. Kreimer-Birnbaum M. Modified porphyrins, chlorins, phathalocyanies, and purpurins: second generation photosensitizers for photodynamic therapy. *Semin Hematol* 1989;**26:**157-73.
13. Parker J G. Optical detection of the photodynamic production of singlet oxygen *in vivo*. *Lasers Surg Med* 1986;**6:**258.
14. Weishaupt K R, Gomer C J, Dougherty T J. Identification of singlet oxygen as the cytotoxic agent in photodynamic inactivation of a murine tumour. *Cancer Res* 1976;**36:**2326-9.
15. Girotti A W. Mechanisms of photosensitization. *Photochem Photobiol* 1983;**38:**745-51.
16. Dubelman TMAR. Porphyrin – photosensitized modification of subcellular structures. In: Jori G, Perria C. eds. *Photodynamic therapy of tumours and other diseases.* Edizioni Liberaria Progetto, Padua (Italy), 1985;93-9.
17. Henderson B W. *Photodynamic therapy – current status and mechanism of tissue destruction.* Symposium: Clinical Photodynamic Therapy and Fluorescence Localization of Tumours, Amsterdam, September 6, 1991.
18. Korbelik M, Krosl G, Chaplin D J. Can PDT be potentiated by immunotherapy? *SPIE press* (in the press).
19. Bugelski P J, Porter G W, Dougherty T J. Autoradiographic distribution of hematoporphyrin derivative in normal and tumour tissue of the mouse. *Cancer Res* 1981;**41:**4606-12.
20. Evensen J, Moan J, Hindar A, Sommer S. Tissue distribution of ^{3}H– hematoporphyrin derivative and its main components, ^{67}Ga and ^{131}I– albumin in mice bearing Lewis lung carcinoma. In: Dorion D R and Gomer C J. eds. *Porphyrin localization and treatment of tumours,* A. R. Liss, New York 1984;541-62.
21. Korbelik M, Krosl G, Lam S, Chaplin D J, Palcic B. Microlocalization fo Photofrin in neoplastic lesions, *SPIE* 1991; **1426:**172-9.
22. Korbelik M, Krosl G, Olive P L, Chaplin D J. Distribution of Photofrin between tumour cells and tumour associated macrophages. *Br J Cancer* 1991;**64:**508-12.
23. Malsky M, Waner M, Sanders M, Kerr W. Microscopic localization of hematoporphyrin derivate in an experimental tumour. Bienn. Mtg. of the Internatl. Photodynamic Association, Buffalo NY, July 17-21, 1990.
24. Korbelik M, Krosl G, Chaplin D J. Photofrin uptake by murine macrophages. *Cancer Res* 1991;**51:**2251-5.
25. Korbelik M. Photofrin and other photosensitizers for use in photodynamic therapy of cancer (a review). *Period Biol* 1991 (in the press).
26. Eccles S A, Alexander P. Macrophage content of tumours in relation to metastatic spread and host immune reaction. *Nature* 1974;**250:**667-9.
27. Milas L, Wike J, Hunter N, Volpe J, Basic I. Macrophage content of murine sarcomas and carcinomas: association with tumour growth parameters and radiocurability. *Cancer Res* 1987;**47:**1069-75.
28. Svennvig J L, Svaar H. Content and distribution of macrophages and lymphocytes in solid malignant human tumours. *Int J Cancer* 1979;**24:**754-8.
29. Korbelik M, Krosl G, Chaplin D J. The effect of immunomodulators on Photofrin levels in solid tumours. *Photochem, Photobiol* 53 (Suppl.): 1991. 102s.
30. Yamamoto N, St. Clarie D A, Homma S, Ngwenya B Z. Activation of mouse macrophages by alkylglicerols, inflammation products of cancerous tissues. *Cancer Res* 1988;**48:**6044-9.
31. Fidler I J. Macrophage and metastasis – a biological approach to cancer therapy. Presidential address. *Cancer Res* 1985;**45:**4714-26.
32. Hasan T, Chen N, Anderson T, Deak M R, Linden K, Granstein R, Zurawski V R. Flotte T. Immunologic targeting of cancer cells. *SPIE* 1989;**1065:**80-86A.
33. Mew D, Lum V, Wat C K, Towers G H N, Sun C C H, Walter R J, Wright W, Berns M W, Levy J G. Ability of specific monoclonal antibodies and conventional antisera conjugated to hematoporphyrin to label and kill selected cell lines subsequent to light activation. *Cancer Res* 1985;**45:**4380-6.
34. Oseroff A R, Ara G, Ohuoha D, Aprille J, Bommer J C, Yarmush M L, Foley J, Cincotta L. Strategies for selective cancer photochemotherapy: antibody–targeted and selective carcinoma cell photolysis. *Photochem Photobiol* 1987;**46:**83-96.
35. Matsui M, Nakanishi T, Noguchi T, Ferrone S. Synergistic in vitro and in vivo anti-tumour effect of Daunomycin-anti-96-kDa melanoma associated antigen monoclonal antibody CL 207 conjugate and recombinant IFN-γ. *Immunol* 1988;**141:**1410-7.
36. Henderson B W, Bellnier D A. Tissue localization of photosensitizers and the mechanism of photodynamic tissue destruction. *Ciba Found Symp* 1989;**146:**112-30.
37. Zhou C. Mechanisms of tumour necrosis induced by photodynamic therapy. *J Photochem Photobiol B Biol* 1989;**3:**299-318.
38. Gomer C J, Rucker N, Ferrario A, Wong S. Properties and applications of photodynamic therapy. *Radiat Res* 1989;**120:**1-18.
39. Liaw L H L, Nelson J S, Steubing R S, Lim G P, Berns M W. Complement activation during tumour photodynamic therapy. *Int. Conf. on Photodynamic Therapy and Laser Medicine*, Beijing, Oct. 15-17, 1991.
40. Fingar V H, Wieman T J, Weber Doak K. Role of thromboxane and prostacyclin release on photodynamic therapy-induced tumour destruction. *Cancer Res* 1990;**50:**2599-603.
41. Kerdel F A, Soter N A, Lim H W. *In vivo* mediator release and degranulation of mast cells in hematoporphyrin derivative-induced phototoxicity in mice. *J Invest Dermatol* 1987;**88:**277-80.
42. Lim H W, Gigli I, Wasserman S I. Differential effects of protoporphyrin and uroporphyrin on murine mast cells. *J Invest Dermatol* 1987;**88:**281-6.
43. Korbelik M, Krosl G, Chaplin D J. Host cell infiltration into PDT-treated tumour. *SPIE Press* (in the press).
44. Henderson B W, Waldow S M, Mang T S, Potter W R, Malone P B, Dougherty T J. Tumour destruction and kinetics of tumour cell death in

two experimetal mouse tumours following photodynamic therapy. *Cancer Res* 1985;**45:**572-576.
45. Nseyo U O, Whalen R K, Duncan M R, Berman B, Lundahl S L. Urinary cytokines following photodynamic therapy for bladder cancer. *Urology* 1990;**36:**167-71.
46. Shumaker B P, Hetzel F W. Clinical laser photodynamic therapy in the treatment of bladder carcinoma. *Photochem Photobiol* 1987;**46:**899-901.
47. Asher A, Mule J J, Reichert C M. Studies on the anti-tumour efficacy of systemically administered recombinant tumour necrosis factor against several murine tumours *in vivo*. *J Immunol* 1987;**138:**963-74.
48. Evans S, Wilbert M, Perry R, Fraker D, Norton J, Pass H I. Effect of photodynamic therapy on tumour necrosis factor production by murine macrophages. *J Natl Cancer Inst* 1990;**82:**34-9.
49. Henderson B W, Donovan J M. Release of Prostaglandin E_2 from cells by photodynamic treatment *in vitro*. *Cancer Res* 1989;**49:**6896-900.
50. Yamamoto N, Homma S, Sery T W, Donoso L A, Hoober J K. Photodynamic immunopotentiation: *in vitro* activation of macrophages by treatment of mouse peritoneal cells with hematoporphyrin derivative and light. *Eur J Cancer* 1991;**27:**467-71.
51. Elmets C A, Bowen K D. Immunological suppression in mice treated with hematoporphyrin derivative photoradiation. *Cancer Res* 1986;**46:**1608-11.
52. Lynch D H, Haddad S, Jolles C J, King V J, Ott M J, Robertson B, Straight R C. Immunologic effects of peritoneal photodynamic treatment. *SPIE* 1989;**1065:**55-65.
53. Lynch D H, Haddad S, King V J, Ot M J, Straight R C, Jolles C J. Systemic immunosuppression induced by photodynamic therapy (PDT) is adoptively transferred by macrophages. *Photochem Photobiol* 1989;**49:**453-8.
54. Ferrario A, Gomer C J. Systemic toxicity in mice induced by localized porphyrin photodynamic therapy. *Cancer Res* 1990;**50:**539-43.
55. Myers R C, Lau B H S, Kunihira D Y, Torrey R R, Wooley J L, Tosk J. Modulation of hematoporphyrin derivative-sensitized phototherapy with Corynebacterium parvum in murine transitional cell carcinoma. *Urology* 1989;**33:**230-5.
56. Bellnier D A. Potentiation of photodynamic therapy in mice with recomibant tumour necrosis factor alpha. *J Photochem Photobiol B Biol* 1991;**8:**203-10.
57. Semenzato G. Tumour necrosis factor: a cytokine with multiple biological activities. *Br J Cancer* 1990;**61:**345-61.
58. Inomata T. Ogawa Y, Terashima M, Nishioka A, Oshida S, Meada T, Seguchi H. An experimental study on the effects of radiation therapy and a long term administration of Sonifilan (SPG) on MM46 tumour inoculated into C3H/He mice. Analysis with immunohistochemical method. *Rad Syst Res* 5(Suppl): 1988;229-32.
59. Okamura K, Suzuki M, Chihara T and 19 others: Clinical evaluation of Schizophyllan combined with radiation in patients with cervical cancer. A randomized controlled study. *Cancer* 1986;**58:**865-872.
60. Sugawara I, Lee K C, Wong M. Schizophyllan (SPG)–treated macrophages and anti-tumour activities against syngenic and allogenic tumour cells. 1. Characteristics of SPG-treated macrophages. *Cancer Immunol Immunother* 1984;**16:**137-44.
61. Tsuchiya Y, Igarashi M, Inoue M, Kumagai K. Cytokine-related immunomodulating activities of an anti-tumour glucan sizofiran (SPG). *J Pharmacobio-Dyn* 1989;**12:**616-25.

Adv Radiol Oncol 1992; 268–74.

Role of DNA flow cytometry and cytomorphology in the search of effective chemotherapy for chemoresistant tumours (Renal cell carcinoma)

Auersperg M[1], Us–Krašovec M[1], Stanovnik M[1], Čufer T[1], Bešić N[1] and Goehde W[2]

[1]*The Institute of Oncology, Ljubljana*
[2]*Institute of Radiology, Muenster*

The clinical applicability of flow cytophotometric dual parameter DNA and protein measurements together with cytomorphological studies for monitoring and planning chemotherapy is illustrated by a case of metastatic renal cell carcinoma. After vinblastine and interferon treatment in standard doses had proved ineffective, a complete response of a metastatic lymph node was obtained by individual timing of low–dose vinblastine and adriamycin infusions based on the results of DNA and protein flow cytophotometric studies.

Key words: carcinoma, renal cell-drug therapy; flow cytometry; vinblastine, adriamycin

Introduction

By measuring DNA in tumours, data on DNA ploidy and proliferative characteristics of tumours can be obtained. Cells in G_1 and resting phase of the cell cycle (G_0/G_1) contain a constant amount od DNA and form a peak; during synthesis of DNA (S–phase) the amount of DNA increases and reaches double amount in G_2 and M phases, forming a peak in the DNA distribution at twice the DNA content of G_1 peak. DNA values of S phase cells have intermediate values between G_1 and G_2 peaks.[1, 2]

As many cytostatic agents are phase–specific, i.e. act predominantly in one phase of the cell cycle, the knowledge on the distribution of tumour cells throughout the cell cycle would be of paramount importance for rational planning of chemotherapy (CHT). Malignant tumours can have a diploid amount of DNA, i.e. the same as normal human cells, but often the amount of DNA differs from diploid – such tumours are called aneuploid. The DNA index is a ratio of the DNA content of the tumour cells in G_o/G_1 to the diploid G_o/G_1 peak of normal cells. By measuring the DNA index, different levels of aneuploidy can be quantified. The distribution of tumour cells in different phases of the cell cycle yield information on how fast the tumour is growing. The S phase fraction is a ratio of S phase cells to the total number of cells. Both, the DNA index and S phase fraction are important prognostic factors correlating with survival and disease-free interval.[2] DNA flow cytometry (FC) is widely used for the determination of prognosis in a variety of human solid tumours.[2,3,4,5,6,7] Aneuploid tumours mostly carry a worse prognosis than diploid.[2]

In contrast to many publications dealing with DNA as a tumour marker or prognostic factor,

Correspondence to: prof. M. Auersperg. Institute of Oncology, Zaloška 2, 61000 Ljubljana, Slovenia.

UCD: 616.61-006.6-091.83

there are only few reports on the use of FC DNA measurements for the evaluation of solid tumour treatment.[11,12,13,14] There have been, to our knowledge, no reports on the use of FC DNA measurements combined with cytomorphological studies for testing the efficacy of antitumour agents in human solid tumours with the aim to use these data for rational chemotherapy planning.

In a previous study we explored the feasibility of single cell DNA measurements and cytomorphological studies for planning of treatment in a variety of human solid tumours *in vivo*.[8,9,10] In the present on-going study on the use of FC DNA measurements for individualisation of chemotherapy we have enrolled 63 patients with chemoresistant tumours who failed standard treatment.[15] The detailed results will be reported elsewhere. The results of these methods in a case of chemoresistant metastatic renal cell carcinoma will be presented to illustrate the clinical application of FC DNA measurements and cytomorphological studies for planning chemotherapy.

Renal cell carcinoma responds poorly to CHT. The response rate to single agents or combined CHT are mostly under 20%.[17,18,19] A combination of interferon (IFN) and vinblastine (VLB) improved the response rate according to some reports[20] but this issue is still controversial.[17]

Material and methods

A 68-year old male patient with metastatic renal cell carcinoma entered the study on individualised CHT in September 1989. The patient underwent three surgical interventions for liposarcoma in the left gluteal region from 1985-87. In December 1988 a tumour was discovered in his left kidney by ultrasound (US). Fine needle aspiration biopsy (FNAB) of the tumour showed a renal cell carcinoma. A left nephrectomy and removal of regional lymph nodes was performed. On histology there was moderately differentiated renal cell carcinoma with metastatic involvement of the lymph nodes in renal hilus and of the paraaortic lymph nodes. Because of lymph node involvement postoperative irradiation was delivered to the region of the left kidney and involved lymph nodes (180 cGy per day, TD 4500 cGy, linear accelerator) concomitantly, immunotherapy with IFN 6 x 10^6/day x 8 in 3-week intervals was applied after surgery. Five months after nephrectomy during immunotherapy the tumour relapsed in the supraclavicular lymph nodes and was treated with concomitant chemoimmunotherapy (VLB 7 mg in bolus and IFN 6 x 6^6/day x 8 in 3-week intervals) and irradiation (200 cGy/day; TD 3000 cGy). This treatment resulted in stabilisation of the disease for 3 months. In August 1989 the tumour escaped: progression of supraclavicular metastasis, appearance of new metastases in the mediastinal lymph nodes and in a paraaortic lymph node were diagnosed. As the mediastinal tumour caused respiratory distress this tumour site was treated by irradiation in combination with low doses of adriamycin (Adria 40 mg and 20 mg) whereas the supraclavicular metastasis was used for testing the efficacy of adriamycin. For evaluating the effect of Adria, FNAB of supraclavicular metastasis were performed before and at uneven intervals after Adria 40 mg and Adria 20 mg.

The FNAB specimens were Giemsa stained for morphological studies. FNAB samples were taken for FC DNA and protein measurements as well. Specimens were fixed in 75% ethanol and stored at –20°C until measuring. Fixed specimens were centrifuged at 1500 rpm for 5 min. One ml of 0.5% Pepsin (Serva 31855, Heidelberg) in HCl (1 mol/L) were added to one drop of pellet and shaken gently for 5 minutes. Eight ml of a mixture of fluorochromes DAPI (Serva No. 18860) and SR 101 (Serva No. 3598–Heidelberg) were added. After 2 hrs of staining the specimen was filtered through a nylon mesh (50 microns).

The measurements of DNA and proteins were carried out on a PAS II (Partec Muenster) cytophotometer. For the excitation of both fluorochromes a mercury high pressure lamp HBO-100 (Osram, Muenchen) and UG1 excitation filter (Schott, Meinz) were used. For the fluorescence of DAPI a GG 455 barrier filter and for SR-100 fluorescence a RG 590 barrier filter were

used. Up to 50.000 cells were measured in samples. The CV of samples before chemotherapy were below 5%.

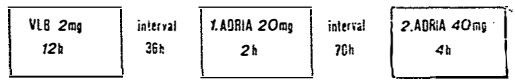

Figure 1. Chemotherapeutic schedule for a metastatic renal cell carcinoma planned individually on the basis of FC dual parameter analysis of DNA and protein and cytomorphological studies.

Results

Clinical results

Treatment with the combination of irradiation (3000 cGy) and Adria (40 mg and 20 mg in 14–day interval) resulted in a stabilisation of mediastinal tumour and a minor response in supraclavicular tumour with the relief of clinical symptoms. Because of poor condition of the patient who had repeated urinary and respiratory infections, poor nutritional status, elevated creatinine and urea, CHT could be repeated only 5 weeks later. At this time the patient had peritoneal carcinosis with ascites, minor progression of supraclavicular metastasis and new metastases in the axillary lymph nodes measuring 5 and 3 cm respectively. FNAB of supraclavicular and axillary lymph nodes were performed and the efficacy of the infusion of 2 mg of VLB over 12 hrs was tested by FNAB 12 and 36 hrs after the termination of infusion. On the basis of FC dual parameter analysis of DNA and proteins and cytomorphological studies of specimens after a previous Adria application, and testing the efficacy of VLB by the same methods, a combination of infusions of VLB and Adria was planned with individual intervals according to FCM measurements (Figure 1). Eight days after this CHT a painful enlargement of supraclavicular metastasis occurred. FNAB demonstrated a complete necrosis of tumour cells in the supraclavicular metastasis and more than 50% of damaged cells in the axillary lymph node. Clinically, supraclavicular and one of the axillary metastases regressed completely, whereas the other axillary metastases showed a partial response. The disease in the abdomen was stabilised. After 5 weeks the disease progressed in the lungs and abdomen whereas the response in the axilla and supraclavicular region still persisted. A second cycle of individualised CHT was started with VLB in December 1989, but the patient refused further treatment, was discharged from the hospital and died in February 1990 with progressive disease in the abdomen and lungs. An autopsy was not performed.

Cytomorphological and flow–cytophotometrical results

Cytomorphological examination of FNAB smears after Adria 40 mg showed no major changes up to 90 hrs after Adria application. Only at 90 hrs after Adria enlargement of tumour cell nuclei and degenerative changes in tumour cells became apparent. In the specimen taken 12 days after Adria 40 mg the changes of tumour cells were more expressed than in samples 90 hrs after Adria. A second dose of Adria 20 mg was applied 14 days after the 1st dose of Adria 40 mg. Cytomorphology showed enlargement of cells and degenerative changes on a part of tumour cell population. These changes appeared as early as 24 hrs after Adria 20 mg. Morphological changes appeared earlier and were more expressed than after the first application of Adria, despite the lower 2nd dose of Adria.

Cytomorphological examination of FNAB samples showed that Adria was effective in this particular tumour. After VLB 2 mg in a 12–hour infusion morphological changes in tumour cells were detected already 12 hrs after the termination of infusion and were more expressed in specimen taken 36 hrs after VLB. Dissociation of tumour cells, nuclear enlargement, multinucleated cells, micronuclei and mitoses were demonstrated (Figure 3). Samples taken 72 hrs after CHT with VLB and Adria in combination showed degenerative changes in nuclei, enlarge-

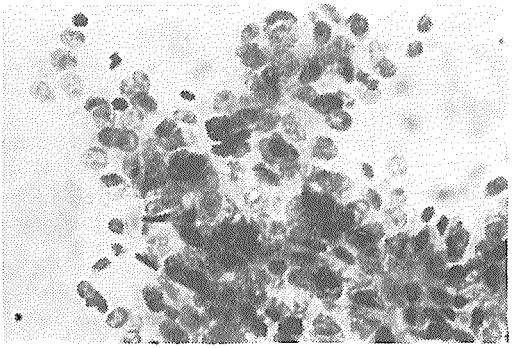

Figure 2. FNAB cell sample of a metastatic renal cell carcinoma – supraclavicular lymph node metastasis before CHT. Giemsa, orig. magn. 200x.

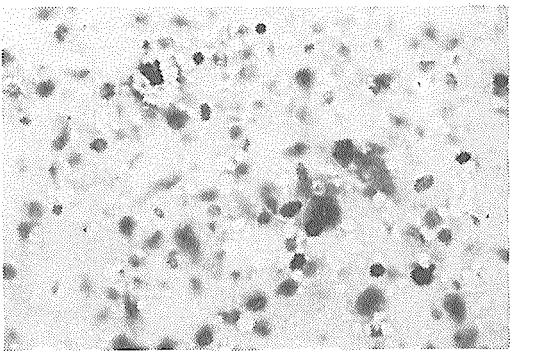

Figure 5. FNAB of the same tumour 8 days after CHT. Giemsa, orig. magn 200x. Complete disintegration of tumour cells; macrophages are present.

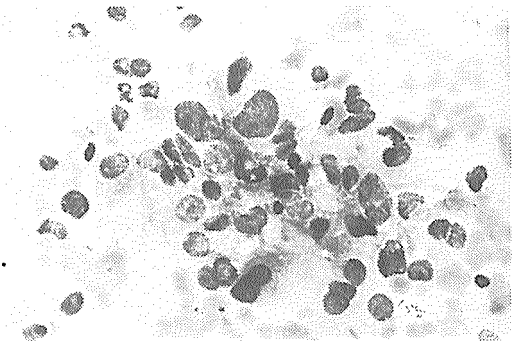

Figure 3. FNAB of the same tumour site 12 hrs after the termination of VLB infusion (2 mg over 12 hrs). Giemsa, orig. magn. 200x. Enlarged nuclei can be seen.

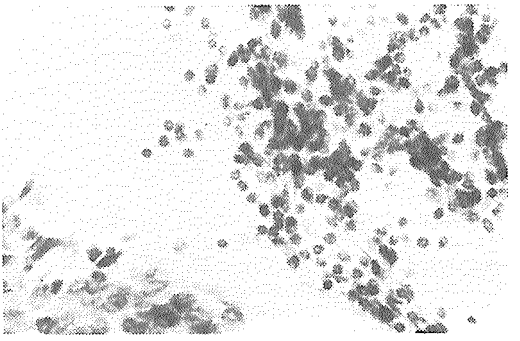

Figure 4. FNAB of the same tumour 69 hrs after the 1 st Adria in individually planned CHT schedule (according to Fig. 1). Giemsa, orig. magn. 200x. Groups of morphologically undamaged tumour cells as well as groups of damaged pyknotic cells are present.

ment or pyknosis, many cells were in mitoses. Eight days after chemotherapy a complete necrosis of the tumour was demonstrated by cytology (Figure 5). The sequence of morphological changes in FNAB samples before and after CHT are demonstrated in Figure 2-5.

Flow-cytophotometric measurement of DNA and protein

FC measurement before CHT showed a hypodiploid tumour (Figure 6A); 12 hrs after VLB a slight increase in protein content reflecting increasing cell volume was seen. As a result of cell disintegration debris appears in the histograms.

A slight increase in the S cell compartment is also demonstrated (Figure 6B). At 36 hrs after VLB the amount of debris and S cells increased (Figure 6C). The DNA and protein distribution pattern remain unchanged 69 hrs after the 1 st Adria in the CHT schedule (Figure 6D) whereas 72 hrs after the completion of CHT with VLB and Adria 1 + Adria 2 the amount of protein was increased as well as the S phase compartment and debris (Figure 6E). Eight days after CHT only debris was demonstrated in the histogram (Figure 6F).

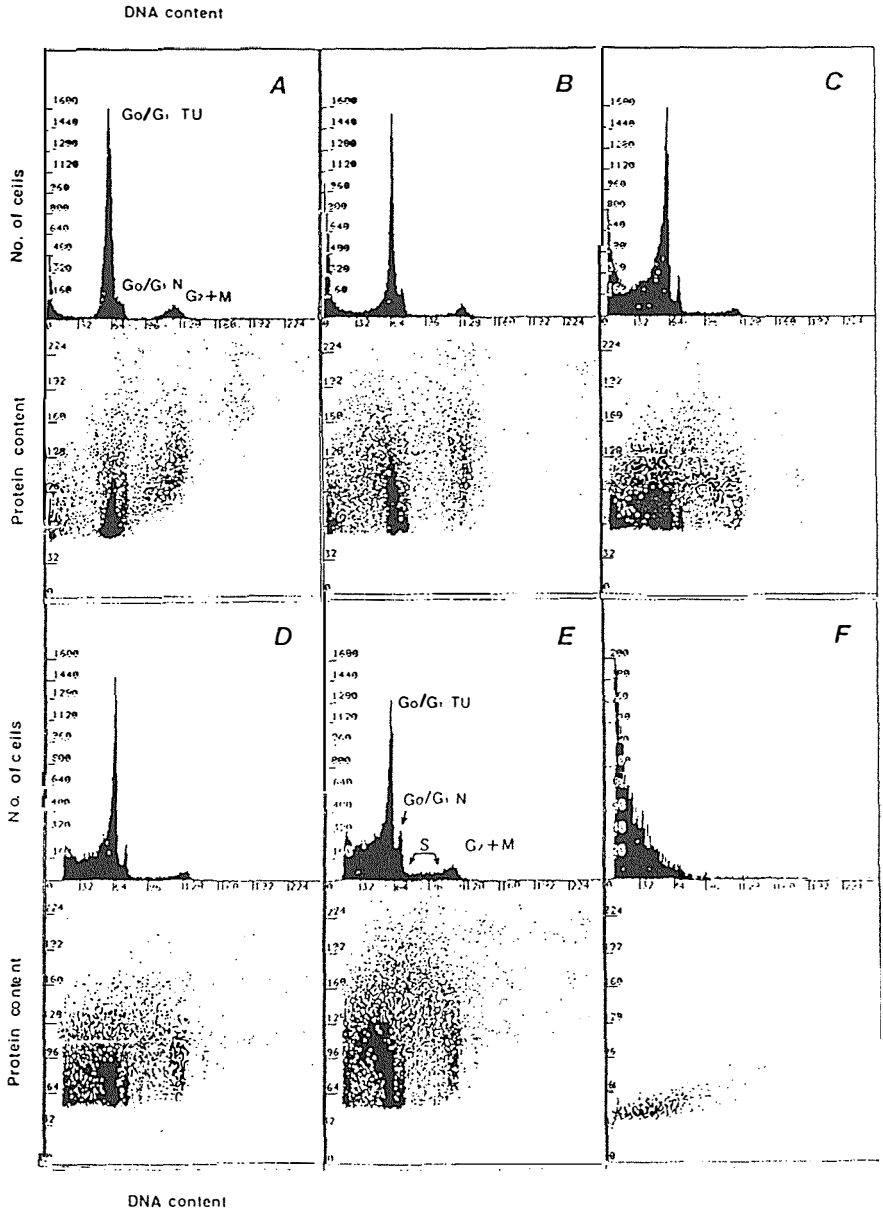

Figure 6A-F. DNA and protein dual parameter FC measurement of renal cell carcinoma metastasis in the supraclavicular lymph node. DNA measurements are shown in the upper part of Figs. A-F. Underneath a scattergram representation of DNA vs. protein analysis is illustrated. DNA is displayed on the horizontal and protein on the vertical axis. G_o/G_1 peak of the tumour cells is marked with Tu, the corresponding peak of normal cells with N (Fig. 6A), the S phase compartment is marked with arrows (Fig. 6E): A) DNA and protein distribution before CHT showing a hypodiploid tumour with a rather high protein content. The 1st peak represents G_o/G_1 of the tumour, the 2nd peak G_o/G_1 of normal cells, the 3 rd peak $G_2 + M$ of the tumour cells. B) The same tumour site 12 hrs after VLB infusion 2 mg/12 hrs – a slight increase in protein content, S phase compartment and debris. C) 36 hrs after VLB – a large amount of debris (left to the 1st peak – increase in S phase compartment. D) 69 hrs after VLB and 1. Adria. The DNA and protein distribution unchanged as compared to C; E) 72 hrs after completed CHT – increase in S phase compartment and protein content. F) 8 days after CHT only debris is demonstrated.

Discussion

For planning effective CHT the knowledge of cell kinetic changes of tumours evoked by single chemotherapeutic drugs or their combinations would be very important. There have been extensive studies on the effect of CHT drugs performed on experimental tumours as well as in human tumour cell lines *in vitro* and in animals.[21, 22, 23, 24, 25, 26] In contrast, there is little knowledge on cell cycle perturbation as a result of treatment in human solid tumours *in vivo*. Dyson[11] used FC DNA measurements for studying the radioresponsiveness of cervical carcinoma and found that aneuploid tumours were more radiosensitive than diploid tumours. Fietkau studied cell kinetic changes in head and neck tumours during irradiation and found an increase in S and G_2 + M compartment after 10 and 20 Gy.[12] Recently, Hemmer used *in vitro* Bromodeoxyuridine (BUdR) labelling method and FC DNA measurements in surgical biopsies of 6 patients treated with intraarterial cisplatinum and epirubicin for oral carcinomas for the evaluation of the response to CHT.[13, 14] In effective CHT elimination of aneuploid tumour clones was demonstrated by DNA measurements and an interruption of cell cycle progression by a lack of BUdR incorporation into cellular DNA.[13, 14] Lack of reports on monitoring treatment could be attributed to the ethical problems in taking repeated surgical biopsies of tumours for FC DNA measurements. Modern development of techniques in FC enabled reliable and reproducible measurements of DNA on FNAB obtained samples. FNAB is much less traumatic than surgical biopsy and causes minimal discomfort to the patient. The danger of sampling different tumour populations by FNAB can be minimised by regular comparison of DNA measurements and cytomorphological pictures of the samples. In our previous studies we successfully used single-cell DNA measurements of FNAB samples for monitoring and planning CHT in various solid tumours.[8, 9, 10] The gain of such a study for the benefit of a particular patient to our opinion greatly outweighs the minimal discomfort of FNAB. According to our experience DNA measurements combined with cytomorphological studies of FNAB samples have great individual predictability for the outcome of treatment in a particular patient. As FC DNA measurements are much faster than single-cell measurements the monitoring of CHT will be applicable to a greater number of patients. Since 1988 we studied the effect od CHT in 63 patients with various solid tumours. This study suggests that a block of cells in S phase or elimination of aneuploid cells predicts a good effect of CHT.[15] More data have to be collected before any final conclusions can be drawn.

Renal cell carcinomas are particularly CHT resistant. This was proved in patients[17, 18, 19] as well as by *in vitro* experiments.[28] The patient presented in this report had an aggressive tumour which progressed during immunotherapy with IFN as well as during chemo–immunotherapy with VLB and IFN. Nevertheless, a complete regression of the supraclavicular metastasis and a partial regression of axillary lymph node metastasis was achieved with a combination of infusions of VLB and Adria which were planned according to DNA measurements and cytomorphological findings. Approximately three times lower doses of VLB and two times lower dosis of Adria than applied in standard schedules were used in this patient in individually planned CHT (according to Figure 1). We assume that the dramatic response in the supraclavicular metastasis was obtained because of the appropriate timing of VLB and Adria infusions. Adria is particularly effective for cells in S, G_2 + M phases. Therefore, two doses of Adria during the time of increased number of cells in S phase compartment (detected by FC DNA measurement) resulted in a complete necrosis of the tumour. Despite very efficient chemotherapeutic schedule, this particular patient did not gain much of CHT. Because of his poor general condition, nutritional status, repeated urinary and pulmonary infections the interval between individually planned CHT was too long (7 instead of 2–3 weeks). During that interval a repopulation in the tumour must have occurred which resulted in the ultimate treatment failure.

More experience is needed in the interpretation of FC DNA and protein measurements during CHT. Our preliminary experience indicates that a combination of DNA measurements and cytomorphological studies can represent an important tool in individually tailored treatment strategies adapted to the individual cytokinetic characteristics of a particular tumour.

References

1. Gray JW, Dolbeare F, Pallavicini MG, Beisker W, Waldman F. Cell cycle analysis using flow cytometry. *Int J Radiat Biol* 1986;**49:**237-55.
2. Williams NN, Daly JM. Flow cytometry and prognostic implications in patients with solid tumours. *Surg Gynec Obstet* 1990;**171:**257-66.
3. Beerman H, Kluin PM, Hermans J, van de Velde VCJ, Cornelisse CJ. Prognostic significance of DNA ploidy in a series of 690 primary breast cancer patients. *Int J Cancer 1985;***45:**34-9.
4. Ferno M, Baldetorp B, Akerman M. Flow cytometric DNA ploidy analysis of soft tissue sarcomas. A comparative study of preoperative fine needle aspirates and postoperative fresh tissue and archival material. *Anal Quant Cytol Histol* 1990;**12:**251-8.
5. Alvegard TA, Berg NO, Baldetorp B et al. Cellular DNA content and prognosis of high–grade soft–tissue sarcoma. The Scandinavian sarcoma group experience. *J Clin Oncol* 1990;**8:**538-47.
6. Grignon DJ, Ayala AG, El-Naggar A et al. Renal cell carcinoma: a clinicopathologic and DNA flow cytometric analysis of 103 cases. *Cancer* 1989;**64:**2133-40.
7. Ljungberg B, Stenling R, Ross G. DNA content and prognosis in renal cell carcinoma: a comparison between primary tumours and metastases. *Cancer* 1986;**57:**2346-50.
8. Auersperg M, Porenta O, Us-Krašovec M, Oblak M, Furlan L. *Cytophotometric DNA studies in human head and neck tumours after cis–platinum infusion.* 13th International congress of chemotherapy, Vienna 1983. Proceedings:280/10.
9. Auersperg M, Zorc R, Us-Krašovec M et al. DNA measurements used for planning of multimodal treatment in sarcomas. 14th international cancer congress, Budapest 1989. Abstracts 2:637.
10. Auersperg M, Zorc R, Us-Krašovec M, Pogačnik A, Petrič G. Porenta–Vraspir O. Chemotherapy for Huerthle cell carcinoma based on sequential DNA measurements. *Radiol Iugosl* 1988;**22:**269-75.
11. Dyson JED, Joslin CAF, Rothwell RI, Quirke P, Khoury GG, Bird CC. Flow cytofluorometric evidence for the differential radioresponsiveness of aneuploid and diploid cervix tumours. *Radiother Oncol* 1987;**8:**263-72.
12. Fietkau R, Langer E, Iro H et al. Impulszytophotometrische Messungen vor und wahrend der Strahlentherapie bei Kopf–Hals–Tumoren. *Strahlenther Oncol* 1989;**165:**34-42.
13. Hemmer J. Rapid in vitro bromodeoxyuridine labeling method for monitoring of therapy response in solid human tumours. *Cytometry* 1990;**11:**603-9.
14. Hemmer J. Cellular proliferation of oral carcinomas during chemotherapy assessed by DNA flow cytometry and bromodeoxyuridine labeling. *Tumourdiagn Ther* 1991;**12:**16-20.
15. Auersperg M, Us-Krašovec M. Goehde W et al. DNA and protein flow cytometry in human solid tumours used for planning chemotherapy. 13th European congress of pathology, Ljubljana 1991. Abstracts. *Pathol Res Pract* 1991;**187:**651.
16. Auersperg M, Us-Krašovec M, Pogačnik A, Pohar Ž, Goehde W, Jaffe N. DNA flow cytometry and cytomorphology for evaluation of chemotherapy. 15th International cancer congress Hamburg 1990. Poster Abstracts. *J Cancer Res Clin Oncol* 1990;116.**478:** Supl.
17. Figlin RA, deKernion JB, Maldazys J, Sarna G. Treatment of renal cell carcinoma with alpha (human leucocyte) interferon and vinblastine in combination: a phase I–II trial. *Cancer Treat Rep* 1985;**69:**263-7.
18. Dexeus FH, Logothetis CJ, Sella A, Finn L. Interferon alternating with chemotherapy for patients with metastatic renal cell carcinoma. *Am J Clin Oncol* 1989;**12:**350-4.
19. Kish JA, Ensley JF, Al-Sarraf M. Phase II evaluation of 4'deoxydoxorubicin in advanced renal cell carcinoma. *Am J Clin Oncol* 1990;**13:**17-8.
20. Bergerat JP, Ford J, Herbrecht R et al. Recombinant alphainterferon plus vinblastine in metastatic renal-cell cancer: analysis of response and survival in 58 evaluable patients. *Prog Clin Biol Res* 1988;**348:**137-50.
21. Lanks KW, Lehman JM. DNA synthesis by L929 cells following doxorubicin exposure. *Cancer Res* 1990;**50:**4776-8.
22. Frankfurt OS, Seckinger D, Sugarbaker EV. Flow cytometric analysis of DNA damage and repair in the cells resistant to alkylating agents. *Cancer Res* 1990;**50:**4453-7.
23. Severin E, Hagenhoff B. Die Synchronisation von Tumorzellen mit 5–Fluorouracil plus Uracil und mit vinblastin und die Bestrahlung synchronisierter Kulturen. *Strahlenther Onkol* 1988;**164:**165-72.
24. Baral E, Auer G. In vitro effect of doxorubicin on nonproliferating and proliferating epihtelial cells. *Int J Radiat Oncol Biol Phys* 1990;**19:**963-5.
25. Wagner W. DNA index – parameter for the prediction of prognosis and primary radioresistance. *J Cancer Res Clin Oncol* 1990;**116:**315-7.
26. Jackel M, Kopf–Maier P. Influence of cisplatin on cell–cycle progression in xenografted human head and neck carcinomas. *Cancer Chemother Pharmacol* 1991;**27:**464-71.
27. Gohji K, Maeda S, Sugiyama T, Tshigami J, Kamidono S. Enhanced inhibition of anticancer drugs by recomibant gammainterferon for human renal cell carcinoma in vitro. *J Urol* 1987;**137:**539-43.
28. Bazeed MA, Scharfe T, Recht E, Schmidt J, Jacobi GH, Thuroff JW. In vitro chemosensitivity testing of renal cell cancer. Short–term culture technique. *Urology* 1988;**31:**240-4.

Adv Radiol Oncol 1992; 275–9.

Flow–cytometric DNA ploidy and clinicopathologic variables in primary breast carcinoma

Us-Krašovec M[1], Bračko M[1], Čufer T[1], Goehde W[2], Košmelj K[3], Lamovec J[1], Pogačnik A[1]

[1]The Institute of Oncology, Ljubljana, [2]Institute of Radiobiology, University Muenster, Germany, [3]Biotechnical Faculty, University Ljubljana

DNA ploidy was investigated by flow cytometry in 108 primary invasive breast carcinomas. Aneuploidy was found in 74% of the tumours. Whereas DNA ploidy was not associated with age, menopausal status, clinical T stage, lymph-node involvement or ER status, significant correlation was found between DNA ploidy and PR status (P=0.03), tumour size (P=0.03), histologic type (P=0.003) and histologic grade (P=0.000001).

Key words: breast neoplasm-pathology; flow cytometry; ploidy

Introduction

The prognosis of breast cancer patients is determined by clinical TNM staging, histologic subtyping and histologic malignancy grading. The axillary lymph-node status is considered the single most important prognostic factor. In spite of these prognostic indicators, the clinical course of breast cancer remains variable and unpredictable. Approximately 30% of patients having negative axillary lymph nodes, i.e. good prognosis, will develop metastases and will not survive 10 years.[1]

Current knowledge regarding the biology and epidemiology of breast cancer indicates that the disease is not a homogeneous entity. Besides, both clinical staging and histologic grading systems are subjective and have low inter– and intra–observer reproducibility.[2, 3] Therefore, additional and more objective prognostic criteria are required for identification of patients who are at higher risk for tumour recurrence, especially among lymph-node negative patients.

Flow cytometry (FCM) and cell image analysis (IA), two quantitative analytical methods developed in the past decades, enable a rapid and objective measurement and quantification of cells and cellular constituents.[4, 5] Investigators, having two new instruments and following the conceptual idea that the main characteristic of malignant tissue is abnormal genome, have focused their interest on deoxyribonucleic acid (DNA) content of malignant tumours. DNA is one of the cell constituents which has been currently most extensively studied by FCM and IA as a potential prognostic parameter.

During recent years a substantial number of papers reporting results of DNA analysis of breast cancer have been published. Both retrospective and prospective studies have provided rather conflicting data regarding the value of

This work was supported by the Slovenian Research Council under contract URP No. 16/B

Correspondence to: prof. dr. Marija Us-Krašovec. The Institute of Oncology, Zaloška 2, Ljubljana, Slovenia.

UDC: 616.19-006.6-091.83

DNA analysis for determining the prognosis of women with invasive breast cancer.[6]

Material and methods

The present study was based on 108 cases of breast cancer selected at random from patients who underwent mastectomy or lumpectomy with axillary node dissection at the Institute of Oncology, Ljubljana, in 1989 or 1990. Cases of noninvasive or minimally invasive carcinoma were excluded from the study, as were patients with recurrent tumors and those who were given preoperative radiotherapy or chemotherapy. The information on age, menopausal status, clinical TNM stage, tumour size, nodal status, estrogen receptor (ER) and progesteron receptor (PR) status were retrieved from the patients' records. The original histologic tumor material was reviewed independently by two of the authors. Classification and grading was performed according to a modification of the Bloom and Richardson grading system.[7]

For FCM analysis, tissue slices of approximately 50 mm^3 were taken from fresh unfixed surgical specimens and stored at –20° C. Before the measurement, the tissue was thawed, minced with scalpel and treated in 2 ml of 0.5% pepsin solution (Serva, Heidelberg) at pH 1.8 with light agitation at room temperature for 5 to 10 minutes. The cell suspension was filtered through a 50 nm nylon mesh and stained with a combination of 4,6–diamidino–2–phenylindole (DAPI, Serva, Heidelberg) and sulforhodamine (SR 101, Serva, Heidelberg). DNA content was measured on a PAS II flow cytometer (Partec, Muenster) equipped with a 100 W high pressure mercury lamp, and analysed using a Partec software package. On average more than 10 000 cells were measured from each tumor cell suspension. The mean coefficient of variation was 4.37 ± 1.66 (range, 2.28–9.53).

Tumours showing only one G_{01} peak were classified as diploid and those with one or more additional G_{01} peaks as aneuploid (Figure 1). In the latter, the leftmost peak was considered to represent the nonneoplastic diploid population. Tumour ploidy was expressed by DNA index (DI) representing the ratio between the modal channel number of the tumour G_{01} peak and the diploid G_{01} peak. A diploid tumor has thus, by definition, a DI of 1.0.

Statistical evaluation was based on the analysis of contingency tables using Chi-square test.

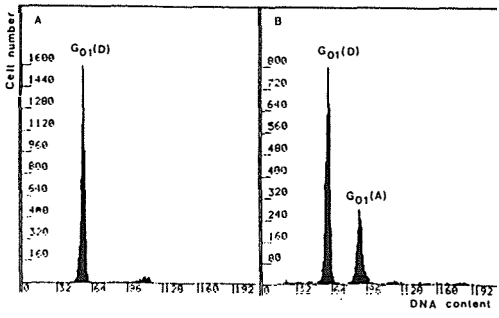

Figure 1. DNA histograms of (A) a diploid tumour (DI = 1) and (B) an aneuploid tumour (DI = 1.44).

Results

Clinico-pathologic variables

The mean age of patients included in this study was 54.4 years, 62 (57%) of them were older than 50 years. Sixty (56%) patients were postmenopausal.

Clinical estimation of tumour size was as follows: T_1 in 10 patients, T_2 in 65 patients, T_3 in 23 and T_4 in 10 patients. Steroid receptor analysis revealed positive ER in 54 (50%) patients and positive PR in 47 (44%) patients.

On gross pathologic examination, only one tumour was less than 10 mm in size, 22 measured 10-19 mm, 77 measured 20-49 mm and 8 measured more than 50 mm.

Eighty-five (79%) tumours were ordinary invasive ductal carcinomas, 12 (11%) lobular, 5 papillary, one mucinous, one medullary and 4 unclassified carcinomas. Ductal carcinomas were graded on a three-grade scale. There were 10 grade I (well differentiated) tumours, 34 grade II (moderately differentiated) tumours and 41 grade III (poorly differentiated) tumours.

On average, 18 axillary lymph nodes (range, 5-39) were examined in each case. Microscopic examination revealed metastases in 59 patients (55%); 30 of them had 1-3 metastatic nodes and 29 more than three.

DNA values

Eighty (74%) of 108 examined breast carcinomas were aneuploid. DI of aneuploid tumours ranged from 1.09 to 3.72 (Figure 2). No significant differences in percentage of aneuploid tumours were found between patients younger or older

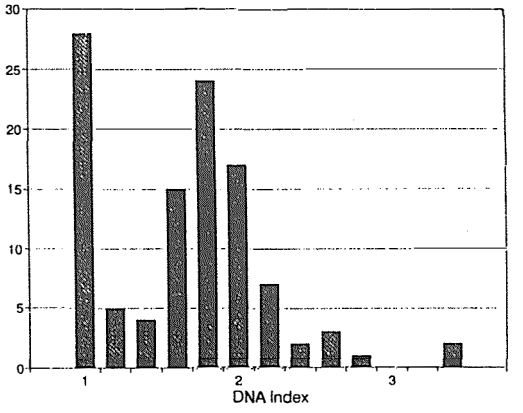

Figure 2. Frequency distribution of DI values in 108 breast cancer samples.

than 50 years nor between premenopausal and postmenopausal patients.

Aneuploid DNA values were observed in 60% of stage T_1 tumours, 74% of stage T_2, 83% of stage T_3, and 70% of stage T_4 tumours.

Seventy-eight percent of ER negative and 70% of ER positive tumours were aneuploid. Aneuploidy was found in 82% of PR negative and 65% of PR positive tumours.

The proportion of aneuploid tumours was higher in larger tumours: 55% in tumours 10-19 mm, 79% tumours 20-49 mm and 88% tumours more than 50 mm of size.

Eighty percent of ductal carcinomas were aneuploid. DNA aneuploidy was found in all 5 papillary carcinomas, in single medullary and in 2 out of 4 unclassified carcinomas. Of 12 lobular carcinomas only 4 (33%) were aneuploid.

In the group of ductal carcinomas, 20% of grade I tumors, 79% of grade II and 95% of grade III tumours were aneuploid.

Sixty-nine percent of lymph-node negative patients had aneuploid tumours, compared to 73% of patients with 1-3 positive lymph nodes and 83% of patients with more than 3 positive lymph nodes.

Discussion

In the present series 74% of the tumours were aneuploid. This finding is in agreement with the results obtained in some other studies. In most of them a minor fraction of malignant tumours had diplod DNA content. The lowest proportion of aneuploid tumours (41%) has been reported in a series of 155 lymph-node negative patients.[8] In the majority of studies the percentage of aneuploid tumours was higher, ranging from 52 to 92%.[9,10,11,12,13,14,15,16,17,18]

At present, the question why all malignant tumours are not aneuploid and why there are such differences in DNA prifiles remains unanswered. The differences in FCM methodology and examined specimens, different criteria for identification of diploid peak and selection of patients for the study are some of the reasons which may account for different DNA distribution pattern in breast cancer obtained so far.

Aneuploidy has been reported initially as highly specific for malignant tissue. However, aneuploid pattern has also been demonstrated in non-invasive breast cancer as well as in mild and atypical ductal hyperplasia. There were no significant differences between DI values of benign lesions and well differentiated non invasive adenocarcinoma.[19, 20, 21] Thus, it seems that aneuploidy, especially of minor degree, cannot be used alone as an independent criterion of malignancy in breast tumors.

In accordance with most previous studies we have also not found any significant correlation between DNA ploidy and age, menopausal status and clinical tumour stage (Table 1).[8,12,13,15,16,17,22]

Table 1. DNA ploidy, clinical variables and steroid receptors.

	No.	Diploid No. (%)	Aneuploid No. (%)
Age < 50	46	12 (26)	34 (74)
> 50	62	16 (26)	46 (74)
		P = NS	
Premeno-pausal	47	12 (26)	35 (74)
Postmeno-pausal	60	16 (27)	44 (73)
		P = NS	
Clinical tumour stage			
T_1	10	4 (40)	6 (60)
T_2	65	17 (26)	48 (74)
T_3	23	4 (17)	19 (83)
T_4	10	3 (30)	7 (70)
		P = NS	
ER			
negative (–)	54	12 (22)	42 (78)
positive (+)	54	16 (30)	38 (70)
		P = NS	
PR			
negative (–)	61	11 (18)	50 (82)
positive (+)	47	17 (36)	30 (64)
			P = 0.03

Table 2. DNA ploidy and pathologic variables.

	No.	Diploid No. (%)	Aneuploid No. (%)
Tumour size			
0 – 9 mm	1	1	0
10 – 19 mm	22	10 (45)	12 (55)
20 – 49 mm	77	16 (21)	61 (79)
> 50 mm	8	1 (12)	7 (88)
		P = 0.03	
Tumour type			
Ductal Ca.	85	17 (20)	68 (80)
Lobular ca.	12	8 (67)	4 (33)
Papillary ca.	5	0	5 (100)
Mucinous ca.	1	1	0
Medullary ca.	1	0	1
Unclassified ca.	4	2	2
		P = 0.003	
Tumour grade (ductal ca.)			
I	10	8 (80)	2 (20)
II	34	7 (21)	27 (79)
III	41	2 (5)	39 (95)
			P = 0,000001
Lymph node status			
Negative	49	15 (31)	34 (69)
1-3 positive	30	8 (27)	22 (73)
3 positive	29	5 (17)	24 (83)
			P = NS

There are controversial data concerning steroid receptor status correlated to the ploidy.[10, 15, 23, 24] In our study group we have found a significant association between ploidy and progesterone receptors (P = 0.03) but not estrogen receptors.

Correlation between DNA ploidy and pathologic variables is presented in Table 2.

Axillary lymph-node status, which is considered the most important prognostic factor in breast cancer, did not correlate significantly with ploidy: 69% of lymph node negative tumours had aneuploid values as compared to 73% of tumours with 1-3 and 83% of tumours with more than three positive lymph nodes. In the majority of FCM studies presence or absence of lymph-node metastases was also not found to be related to ploidy.[13,22,23,25]

Three pathologic parameters, i. e. tumour size, tumour type and tumour grade were found to correlate with tumour DNA content.

In several studies which have analysed the prognostic relevance of established pathologic parameters, tumour size has been found to contribute most important information about early recurrence.[26] In our study group a significant increase of aneuploidy incidence was found in larger tumours (P = 0.03): 79% of tumours measuring 20 to 49 mm and 88% of tumours measuring more than 50 mm were aneuploid, as opposed to 52% of tumours measuring less than 20mm. In a majority of FCM studies, however, this association has not been observed.[12,13,17,27]

Statistically important differences in DNA values were found among different tumour types (P = 0.003): 80% of ductal carcinomas were aneuploid, whereas only 4 (33%) out of 12 lobular carcinomas had abnormal DNA values. A low proportion of aneuploid lobular carcinoma has also been reported in other studies (14,28). In contrast to other series where only about 30% of papillary carcinoma had aneuploid values[6], in our group all five tumours of this type were aneuploid.

Tumour grade, one of the important prognostic parameters, and DNA ploidy correlated

significantly. An aneuploid pattern was found in 79% of grade II tumours and in 95% of grade III tumours, whereas only 20% of grade I tumours were aneuploid (P = 0.000001). Good correlation between ploidy and histologic grading according to Bloom and Richardson method has been observed by the majority of investigators.[6]

There is still a lack of agreement about correlation between ploidy level and established prognostic variables. Some data indicate that DNA profile alone or in combination with proliferative activity may have independent prognostic significance. Further prospective and cooperative studies are needed to evaluate the prognostic value of DNA ploidy and to confirm whether DNA ploidy and cell cycle analysis can provide additional prognostic information to the established prognostic parameters in invasive breast cancer.

References

1. deVita VT. Breast cancer therapy: experiencing all our options. *New Engl J Med* 1989; **320:**527-9-
2. Stenkvist B, Westman-Naeser S et al. Analysis of reproducibility of subjective grading systems for breast carcinoma. *J Clin Pathol* 1979; **32:**979-85.
3. Delides GS, Garas G, Georgouli G et al. Interlaboratory variations in the grading of breast cancer. *Arch Pathol Lab Med* 1982; **106:**126-8.
4. Shapiro HM. Multistation multiparameter flow cytometry: a critical review and rationale. *Cytometry* 1983; **3:**227-43.
5. Wied GL, Bartels PH, Bibbo M, Dytch HE. Image analysis in quantitative cytopathology and histopathology. *Hum Pathol* 1989; **20:**549-71..
6. Frierson HF Jr. Ploidy analysis and S-phase fraction determination by flow cytometry of invasive adenocarcinomas of the breast. *Am J Surg Pathol* 1991; **15:**358-67.
7. Elston CW. Grading of invasive carcinoma of the breast. In: Page DL, Anderson TJ eds. *Diagnostic histopathology of the breast.* Edinburgh: Churchill Livingstone, 1987: 300-311.
8. Lewis WE. Prognostic significance of flow cytometric DNA analysis of node-negative breast cancer patients. *Cancer 1990;* **65:**2315-20.
9. McDivit RW, Stone KR, Craig RB, Meyer JS. A comparison of human breast cancer cell kinetics measured by flow cytometry and thymidine labeling. *Lab Invest* 1985; **52:**287-91.
10. Bichel P, Poulsen S, Andersen J. Estrogen receptor content and ploidy of human mammary carcinoma. *Cancer* 1982; **50:**1771-4.
11. Kute TE, Muss HB, Hopkins M, Marshall R, Case D, Kammire L. Relationship of flow cytometry results to clinical and steroid receptor status in human breast cancer. *Breast Cancer Res Treat* 1985; **6:**113-21.
12. Dressler LG, Seamer LC, Owens MA, Clark GM, McGuire WL. DNA flow cytometry and prognostic factors in 1331 frozen breast cancer specimens. *Cancer* 1988; **61:**420-7.
13. Dowle CS, Owainati A, Robins A et al. Prognostic significance of the DNA content of human breast cancer. *Br J Surg* 1987; **74:**133-6.
14. Feichter GE, Mueller A, Kaufmann M et al. Correlation of DNA flow cytometric results and other prognostic factors in primary breast cancer. *Int J Cancer* 1988; **41:**823-8.
15. Hedley DW, Rugg CA, Ng ABP, Taylor IW. Influence of cellular DNA content on disease-free survival of stage II breast cancer patients. *Cancer Res* 1984; **44:**5398-8.
16. Beerman H, Kluin PM, Hermans J, van de Velde CJH, Cornelisse CJ. Prognostic significance of DNA-ploidy in a series of 690 primary breast cancer patients. *Int J Cancer* 1990; **45:**34-9.
17. Taylor IW, Musgrove EA, Friedlander ML, Foo MS, Hedley DW. The influence of age on the DNA ploidy levels of breast tumours. *Eur J Cancer Clin Oncol* 1983; **19:**632-8.
18. Olszewski W, Darzynkiewicz Z, Rosen PP, Schwartz MK, Melamed MR. Flow cytometry of breast carcinoma: I. relation of DNA ploidy level to histology and estrogen receptor. *Cancer* 1981; **48:**980-4.
19. Norris HJ, Bahr GF, Mikel VU. A comparative morphometric and cytomorphometric study of intraductal hyperplasia and intraductal carcinoma of the breast. *Analyt Quant Cytol Histol* 1988; **10:**1-9.
20. Teplitz RL, Butler BB, Tesluk H et al. Quantitative DNA patterns in human preneoplastic breast lesions. *Analyt Quant Cytol Histol* 1990; **12:**98-102.
21. Erhardt K, Auer GU. Mammary carcinoma comparison of nuclear DNA content from in situ and infiltrative component. *Analyt Quant Cystol Histol* 1987; **9:**263-7-
22. Ewers S-B, Langstrom E, Baldetorp B, Killander D. Flowcytometric DNA analysis in primary breast carcinomas and clinicopathological correlations. *Cytometry* 1984; **5:**408-19.
23. Muss HB, Kute TE, Case LD et al. The relation of flow cytometry to clinical and biologic characteristics in women with node negative primary breast cancer. *Cancer* 1989; **64:**1894-900.
24. Meckenstock G, Bojar H, Hort W. Differentiated DNA analysis in relation to steroid receptor status, grading, and staging in human breast cancer. *Anticancer Res* 1987; **7:**749-54.
25. O'Reilly SM, Camplejohn RS, Barnes DM et al. DNA index, S-phase fraction, histological grade and prognosis in breast cancer. *Br J Cancer* 1990; **61:**671-4.
26. Wallgren A. *Prognostic factors in operable mammary carcinoma.* Doctor thesis. Stockholm 1976.
27. Baildam AD, Zaloudik J, Howell A et al. DNA analysis by flow cytometry, response to endocrine treatment and prognosis in advanced carcinoma of the breast. *Br J Cancer* 1987; **55:**553-9.
28. Horsfall DJ, Tilley WD, Orell SR, Marshall VR, Cant ELK. Relationship between ploidy and steroid hormone receptors in primary invasive breast cancer. *Br J Cancer* 1986; **53:**23-8.

Adv Radiol Oncol 1992; 280–3.

Correlation of DNA-ploidy and estrogene and progesterone receptor content in primary breast cancer

Čufer T[1], Bračko M[1], Goehde W[2], Lamovec J[1], Košmelj K[3], Pogačnik A[1], Us-Krašovec M[1]

1 – The Institute of Oncology, Zaloška 2, Ljubljana, Slovenia
2 – Institut für Radiobiologie, Universität Muenster, Germany
3 – Biotechnical Faculty, University of Ljubljana, Slovenia

Our study was aimed to establish possible correlation between hormone receptor status and DNA-ploidy in 108 patients with invasive breast cancer. Approximately 74% of tumours were found to be aneuploid. A statistically significant correlation was found between DNA ploidy and PR-status ($p = 0.03$). There were 82% of aneuploid tumours found among PR-negative and 64% among PR-positive tumours. A higher percentage of aneuploidy was established in ER-negative group in comparison with ER-positive group (78% vs. 70%), though the difference was not statistically significant. After the stratification of patients into node-negative and node-positive groups, no statistically significant correlation could be established between DNA-ploidy and ER or PR status respectively.

Key words: breast neoplasms; flow cytometry; receptors, estrogen; receptors, progesterone; ploidy

Introduction

The course of disease in patients with primary breast carcinoma depends on several clinicopathological factors known to be of prognostic significance, such as tumor size, axillary lymph node involvement, histological type and pathological grade of tumour.[1] These are known as classical prognostic indicators. Recently, it has been attempted to find possible new prognostic factors which would help to identify more aggressive breast cancer tumour types, i. e. DNA-ploidy, S-phase fraction, oncogene amplification, proliferation antigen (e. g. Ki67) and others.[1] The latter proved of decisive importance particularly in patients lacking the classical prognostic factors, for example in patients with negative axillary lymph nodes, and those in whom neoadjuvant CHT represents a primary treatment. In order to determine the value of these new prognostic factors it is essential to establish whether, and to what extent, they correlate with the classical ones.

Thus, the prognostic value of hormonal receptors has been based on the fact that the patients with positive estrogen (ER) and progesterone (PR) receptors had a better disease-free survival as well as overall survival in comparison with hormonal-receptor-negative patients. There have been many studies on the correlation between hormonal receptor status and DNA-ploidy reported in the existing literature. The information, however, is controversial, since in contrast to the authors who have not found any such correlation,[2, 3, 4, 5] there are many others[6, 7, 8, 9, 10,11,12,13,14] who claim that such a relation exists:

Correspondence to: dr. Tanja Čufer, The Institute of Oncology, Zaloška 2, 61000 Ljubljana, Slovenia.

UDC: 616.19-006.6-074

this has been confirmed particularly in the studies done on large series of patients.[6,7,8]

Therefore, it was our intention to study the correlation between hormonal receptor status and DNA-ploidy on a group of 108 primary breast cancer patients treated at the Institute of Oncology in Ljubljana.

Material and methods

So far, 108 patients with primary breast cancer have been included in our study. All tumours were histologically confirmed as invasive carcinomas. For flow-cytometric analysis and hormonal receptor assay, tissue segments were taken from fresh unfixed surgical specimens and stored at –20°C. DNA values of tumour cells were measured on a PAS II (Partec, Muenster), a high-pressure-mercury-lamp based flow cytometer. DNA values were expressed by DNA index which represents the ratio between modal channel number of aneuploid G_0 peak and diploid G_0 peak. Tumours with DNA index 1.00 were classified as diploid.

For ER and PR assay a Dextran-coated charcoal technique was used. ER values >10 fm/mg protein and PR values >20 fm/mg protein were considered positive.

Statistical analysis has been based on contingency tables. Pearson's chi-square statistics has been calculated to determine the correlation between DNA-ploidy and other variables of interest.

Results

Our analysis for DNA ploidy and hormone receptor status included 108 invasive breast cancers. Among these, 80 (74%) showed measurable aneuploidy (Table 1). The same samples were analysed for hormonal receptor status which is presented in Table 2. The rate of DNA-aneuploid tumours was slightly higher in ER-negative than in ER-positive tumours (78 vs 70%), but the difference was not statistically significant (Table 3). In contrast, a statistically significant correlation (p = 0,03) was found between DNA-ploidy and the absence of progesterone receptors i. e. aneuploidy was found in 82% of PR-negative and in 64% of PR-positive tumours (Table 4). For the combined receptor status the absence of one or both receptors was found to be significantly associated with the presence of DNA-aneuploidy (Table 5) After the stratification of patients according to axillary lymph-node involvement, no significant correlation between DNA-ploidy and estrogene and progesterone receptor content respectively was found either for negative or positive patients (Table 6), despite the fact that especially in node positive groups the percentage of DNA-aneuploidy is much higher in PR negative than in PR positive group of patients.

Table 1. Ploidy analysis in primary breast cancer.

No. of cases	DNA-diploid No. (%)	DNA-aneuploid No. (%)
108	28 (26)	80 (74)

Table 2. Frequency of ER and PR combinations in primary breast cancer.

Receptor Status	No. of cases	(%)
ER+ PR+	31	29
ER+ PR–	23	21
ER– PR+	16	15
ER– PR–	38	35

Table 3. DNA–ploidy in relation to the content of estrogen receptors.

Estrogen receptor	No. of cases	DNA-aneuploid No. (%)
ER negative	54	42 78
ER positive	54	38 70 p=0,37

Table 4. DNA–ploidy in relation to the content of progesterone receptors.

Progesterone receptor	No. of cases	DNA-aneuploid No. (%)
PR negative	61	50 (82)
PR positive	47	30 (64) p=0,03

Table 5. DNA–ploidy in relation to the combined receptor status.

Hormone Receptor Status	No. of cases	DNA-aneuploid No. (%)
ER+ PR+	31	18 (58)
ER+ PR–	39	32 (82)
ER– PR+		
ER– PR–	38	30 (78) p=0,052

Table 6. DNA–ploidy in relation to the hormone receptors by lymph node status.

Node negative pts		
Hormone Receptor Status	No. of cases	DNA-aneuploidy No. (%)
ER negative	21	15 (71)
ER positive	28	19 (67) p=0,78
PR negative	23	18 (78)
PR positive	26	16 (61) p=0,20
Node positive pts		
Hormone Receptor Status	No. of cases	DNA-aneuploid No. (%)
ER negative	33	27 (81)
ER positive	26	19 (73) p=0,42
PR negative	38	32 (84)
PR positive	21	14 (66) p=0,11

Discussion

In our group of 108 breast cancer patients, DNA aneuploidy was found in 74% of tumours. These results are in agreement with those reported by other authors according to which DNA aneuploidy has been established in 50-92% of tumours (10). As to the correlation between DNA-ploidy and hormone receptor status, the results of different authors are controversial. In a majority of studies performed so far, possible correlation between DNA-ploidy and hormonal receptors could not be confirmed, whereas in one third of these reports a statistically significant correlation was found between DNA-ploidy and ER, and in one fourth between DNA-ploidy and PR.[15] It should be pointed out, however, that positive correlation results were established in studies with the highest number of included patients.[6, 7, 8] A review of so-far published reports also indicates that the correlation between ER and DNA-ploidy was invariably associated with PR and DNA-ploidy correlation.[6, 7, 8, 9, 10, 12, 13, 14] In this respect our results differ from those reported by other authors. Namely, in our study, a significant correlation was found only for PR and DNA-ploidy, though the percentage of aneuploid tumours found among ER-negative tumors was somewhat higher. The only author who established a statistically more significant correlation between PR and DNA-ploidy ($p = 0.0006$) than between ER and DNA-ploidy ($p = 0.04$) was Kallionemi.[13] It is possible that the difference between our and his results could be attributed to the fact that his series of patients was approximately three times larger than ours.

Comparing the DNA-ploidy and combined receptor status, we found a statistically significant correlation between the presence of both receptors and DNA-ploidy. Nearly equal values of aneuploidy were found in patients with both receptors negative as well as in those with only one negative receptor.

Considering the known fact that ER status is prognostically more relevant in node-negative patients and PR status in node-positive ones[1], our patients were distributed into node-positive and node-negative groups. After this stratification, no statistically significant correlation could be established between DNA-ploidy and ER or PR status respectively. It should be pointed out, however, that the rate of aneuploidy was generally higher in the receptor-negative groups. The difference in the percentage of aneuploid tumours between PR negative and PR positive patients was particularly great (18%) in the node-positive group, i. e. in the group where PR status has proved to be prognostically most relevant. We believe that the reliability of our results could be significantly improved by increasing the number of patients included in the subgroups.

The suggested inclusion of a larger number of patients would also help to solve the problem whether a statistically significant correlation exists only between PR status and DNA-ploidy or also between ER status and DNA-ploidy.

References

1. McGuire WL. Prognostic factors for recurrence and survival in human breast cancer. *Breast Cancer Res Treat* 1987; **10**:5-9.
2. Abondowitz HM, Ow KT, Hardy D, Keightley DD, Sarfaty GA, Nash AR, Relationship between flow cytometric parameters, steroid receptors, and menopausal status in breast cancers. *Oncology* 1987; **44**:24-9.
3. Dowle CS, Owainati A, Robins A, Burns K, Ellis IO, Elston CW, Blamey RW. Prognostic significance of the DNA content of human breast cancer. *Br J Surg* 1987; **74**:133-6.
4. McDivitt RW, Stone KR, Craig RB, Palmer JO, Mayer JS, Bauer WC. A proposed classification of breast cancer based on kinetic information. Derived from a comparision of risk factors in 168 primary operable breast cancers. *Cancer* 1986; **57**:269-76.
5. Muss HB, Kute TE, Case LD, et al. The relation of flow cytometry to clinical and biologic characteristics in women with node negative primary breast cancer. *Cancer* 1989; **64**:1894-900.
6. Cornelisse CJ, van de Velde CJH, Caspers RJC, Moolenaar AJ, Hermans J. DNA ploidy and survival in breast cancer patients. *Cytometry* 1987; **8**:225-34.
7. Hedley DW, Rugg CA, Gelber RD. Association of DNA index and S-phase phraction with prognosis of nodes positive early breast cancer. *Cancer Res* 1987; **47**:4729-35.
8. Dressler LG, Seamer LC, Owens MA, Clark GM, McGuire WL. DNA flow cytometry and prognostic factors in 1331 frozen breast cancer specimens. *Cancer* 1988;**61**:420-7.
9. Moran RE, Black MM, Alpert L, Straus MJ. Correlation of cell – cycle kinetics, hormone receptors, histopathology, and nodal status in human breast cancer. *Cancer* 1984; **54**:1586-90.
10. Feichter GE, Mueller A, Kaufmann M, et al. Correlation of DNA flow cytometric results and other prognostic factors in primary breast cancer. *Int J Cancer* 1988; **41**:823-8.
11. Stal O, Wingren S, Carstensen J et al. Prognostic value of DNA ploidy and S–phase fraction in relation estrogen receptor content and clinicopathological variables in primary breast cancer. *Eur J Cancer Clin Oncol* 1989; **25**:301-9.
12. Horsfall DJ, Tilley WD, Orell SR, Marshall VR, McCant EL. Relationship between ploidy and steroid hormone receptors in primary invasive breast cancer. *Br J Cancer* 1986; **53**:23-8.
13. Kallionemi O, Blanco G, Alavaikko M et al. Improving the prognostic value of DNA flow cytometry in breast cancer by combining DNA index and S–phase fraction. *Cancer* 1988; **62**:2183-90.
14. Kute TE, Muss HB, Hopkins M, Marshall R, Case D, Kammire L. Relationship of flow cytometry results to clinical and steroid receptor status in human breast cancer. *Breast Cancer Res Treat* 1985; **6**:113-21.
15. Frierson HF. Ploidy analysis and S–phase fraction determination by flow cytometry of invasive adenocarcinomas of the breast. *Am J Surg Pathol* 1991; **15**:358-67.

Adv Radiol Oncol 1992; 284–98.

Potentials of hyperthermia in clinical use

Lešničar H and Budihna M

The Institute of Oncology, Ljubljana

More than 10.000 articles have been published around the world in recent 10 years constantly showing the possible benefit of hyperthermia in the treatment of cancer. Despite of all this accumulated knowledge on this subject there is still a lot of problems in introducing hyperthermia as an conventional treatment modality. The biological rationales that strongly support the clinical use of hyperthermia are: direct cytotoxicity of heat and its radiosensitizing effect. However, difficulties with determination of thermal dose and construction of really safe and low cost equipment currently inhibit the definite promotion of thermotherapy.
Nevertheless, a number of encouraging clinical results suggest that hyperthermia in the future has to be considered as a topic of general interest.

Key words: neoplasms-therapy; hyperthermia, induced

Introduction

Hyperthermia can be defined as an increase in temperature beyond that normally found in the body. For the therapeutic intent elevated temperature may be limited to local or regional area, or it may involve the entire body. Therefore, the terms local, regional and systemic hyperthermia treatment are used in clinical practice. With regard to the way of access to the body area of interest we distinguish between percutaneous or external, intraluminal, intracavitary, perfusional and interstitial type of thermal therapy.[1]

Althoug cauterization for local tumor destruction in old Egiption medicine,[2] as well as systemic hyperthermia in ancient India[3] has been widely used even millenniums B.C., the first documented reports on the therapeutic effect of elevated body temperature dated from very end of the 19-th century.[4] Already at that time the importance of distinction between the two approaches (local and systemic) to the cancer therapy using hyperthermia was recognized. For whole body treatment the proposed temperature rarely exceeded 40°C, in order to be well tolerated by the organism. On the other hand, local hyperthermia required considerably higher temperatures, usually beginning with 42°C.[1] With later investigations it was presumed that two different mechanisms play role in the tumoricidal effect of heat. Whereas the host's defence mechanism, most likely through the immune system, should be responsible for the effect of whole body hyperthermia on cancer cells,[5] in local application the heat itself, with a number of various damaging effects on cell constituents directly induces lethal cell injury.[2]

Despite of this early reports on the usefulness of hyperthermia in clinical practice, the lack of reports with similar results confirmed by other

Correspondence to: Hotimir Lešničar M.D., The Institute of Oncology, Zaloška 2, 61105 Ljubljana, Slovenia.

UDC: 616-006.6-073:615.832

therapists has driven the whole hyperthermia business into the past.[6] Many decades had to pass before the renewed interest for thermotherapy was born. In early 70's much of the pioneer work on studying the effects of ionizing radiation on cell reproductive capacity was done. In some of these studies it was found that heating combined with radiation increased the cell-killing effect of radiation applied alone.[7-10] Based on these observations numerous clinical trials were carried out mostly on comparable superficial malignant lesions treated by either radiotherapy alone or in combination with hyperthermia. There is a strong evidence that adjuvant thermotherapy considerably increases the probability of a good tumor control.[11-23]

The rationales for clinical use of hyperthermia

In last decade, the greatest effort of radiotherapists has been focused on the problem how to augment the limited effect of radiotherapy on *hypoxic fraction* of tumor cells. The marked radioresistancy of this specific segment of tumor burden, with no doubt, is highly responsable for the local treatment failure. Hyperoxygenation, accelerated charged particles with high LET, electron affinic drugs and cytotoxic drugs, as well as many unorthodox fractionation regims have been tested to overcome the problem of hipoxia.[24] Many of them have failed to prove its suitability for daily exploitation either on basis of high cost or major toxicity to normal tissue. Although the first documented clinical results on hyperthermia used as an adjuvant to radiotherapy, appearing in the initial stage of clinical usage of X-rays,[25] indicated a significant improvement of the irradiation effect, many decades had to pass for hyperthermia to be recognized as one of the modern experimental clinical techniques. Soon after the first few experimental data on heat-induced cellular toxicity had been published,[26,27] the need for fundamental knowlege of the heat impact on normal and malignant cells stimulated a large number of laboratory investigations.[28] Although radiation effect on different types of cells may be related also to an intrinsic radiosensitivity,[29] there is no systematic difference in radiation sensitivity between the cells of normal and neoplastic origin.[30,31] Therapeutic gain in radiotherapy, therefore, bases mainly in cell proliferation kinetic differences between tumor and surrounding normal tissue.[32]

But, do we know what is the explanation for the benefit of using hyperthermia treatment?

Contrary to rather optimistic statement that »selective heat sensitivity of cancer cells« really exists,[2,33] stay an evident bilief, based on more relevant observations, that no general therapeutic gain can be expected from higher inherent thermosensibility of malignant cell.[34] Measurements of the intrinsic thermosensitivity obtained on human tumors in vitro showed marked differences even among histologically identical tumor specimens.[35] Hence, the explanation for obvious difference between the hyperthermic response in vitro and in vivo most likely bases in changes of microenvironmental conditions occurring in heated tumor tissue.[36] There is an augmentation of normal tissue blood flow, while heated, reflecting in important cooling effect, which prevents appearance of thermal damage. Although, this physiological effect occurs also in the first few minutes of heating of the neoplastic tissue, the lack of vascularity inside the tumor makes the maintaining of increased blood flow through the heated volume impossible. If heating is prolonged or the temperature over 43°C are used, it results in selective rising of the intratumoral temperature.[37] Therefore, tumors act as relative heat reservoir. Moreover, this impact of elevated temperature on tumor tissue blood flow also induces drops in tumor tissue pH and/or pO_2 levels, thus amplifying the direct cell killing effect of hyperthermia.[38,39]

At least two different mechanisms are involved in biological interaction between heat and irradiation:

1) direct heat-induced cytotoxicity
2) hyperthermic radiosensitisation

Ad 1) Cultured cells exposed to temperatures above 41°C response with similar shapes of survival curves as those treated with ionizing

radiation.[40] Despite this similarity there are some marked differences in mechanisms through which lethal injury develops:[41-50]

Irradiation

- cell death occurs after mitosis
- cells in proliferation are radiosensitive
- S-phase of cell-cycle is the most radioresistant
- hypoxic cells are radioresistant
- sufficient nutrition is needed
- DNA damage is for major importance

Hyperthermia

- cell death is of interphase type
- non-proliferating cells are thermosensitive
- S-phase of cell cycle is the most thermosensitive
- hypoxic and oxic cells have equal thermosensitivity
- glucose deprivation and low pH enhances thermosensitivity
- cell death occurs due to a number of biochemical events damaging membrane structures, protein synthesis, aminoacids and ions transportation, enzyme functions, combined with inhibition of respiration, increase of anaerobic glycolysis and impaired lysosomal activity

Ad 2) Hyperthermia administered even in lower (non-lethal) heat doses can increase the response to radiation treatment. Some of the possible mechanisms involved in influence of hyperthermia are listed below:

- decreased repair of sublethal damage
- increased lethal damage
- sensitisation of cells in the radioresistant phases of the cell cycle
- sensitisation of hypoxic cells
- inhibition of repair of potential lethal damage

When radiotherapy is combined with cytotoxic doses of heat (above 42.5°C) then it results even in greatest cell-killing effect, but unfortunately also in more expressed normal tissue damage.[51-53]

There are many evidences that hyperthermia potentiates the cytotoxic effect of chemotherapeutic agents as well. The possible mechanisms of action in this association of treatment modalities are:

- an increase in intracellular concentration of the drug due to modification of membrane permeability induced with hyperthermia
- inhibition of repair of chemically induced lesion
- change in biochemical environment of the cells

However, the great number of cytotoxic drugs with different modes of action, leading to controversial experimental data, are still demanding additional systematic investigations.[54-56]

Several groups of investigators reported also of the possible benefit of simultaneous use of hyperthermia, hypoxic cell sensitizers and radiotherapy.[57-59] The rationale for such a combination should be in findings that the proportion of tumor hypoxic cells (but not their absolute number) significantly increases few hours after heating,[60,61] due to vascular occlusion.

Clinical hyperthermia

The all above listed amount of preclinical data offers new aspects of a possible role of clinical hyperthermia but still there are some unsolved questions to be answered:

Is one hyperthermia treatment enough?

If not, how many treatments are advisable?

What is the best time-interval between radiotherapy and hyperthermia?

Is there any problem in sequencing these two modalities?

What is the definition of thermal dose?

We already mentioned that there are two possible patterns for gaining profit from combination of radiotherapy and hyperthermia treatment. If we want to benefit only out of the cytotoxic effect of each treatment modality, probably one »good« hyperthermia treatment should be enough. In this connection the greatest problem is to reach optimum uniformity of temperature distribution inside the tumor volume. Interstitial methods, which provide minimum fluctuation of temperature, are thus the therapeutic approach of choise.[62,63] More problems arise when external methods of heating are

imployed. Marked differences in vascular capacity of various tumor parts (good vascularity of the tumor perifery vs. undersupplied necrotic central portions) result in noticeable variation of tumor temperatures. It is impossible to obtain homogeneous heat distribution with present heating techniques. Using percutaneous hyperthermia devices temperatures measured in different parts of tumor may vary considerably, that means in the extent of several degrees.[37,64-66] It would be easy to solve this problem either with prolongation of the treatment time, or with repeating thermal treatments. Unfortunately, there is a process known as *thermotolerance* omitting such a strategy. The shortest definition for thermotolerance is: temporary resistance to heat injurie induced by a previous heating. In other words, cells surviving one heat shock tend to be transiently resistant to a second heat shock. In large series of investigations it was found that special genes are activated under temperature (or other stress) manipulations, leading to production of high molecular density proteins, which most likely influence the development of thermotolerance. These, so called, »heat shock proteins« are also present in normal cells, but it seems that they acquire a specific function under stress conditions.[67] Whether this protection of heated cells is due to increased repair mechanism or to the prevention of induction of the heat damage is yet not known.[68,69] For the time present it is obvious that promotion of heat shock proteins is not the only mechanism providing heat protection of cells, but also changes in membrane structures very likely play an important role.[70] The magnitude and the kinetics of thermotolerance development differs due to the size of the priming heat treatment.[71] However, heat resistance gradually decayes and completely disappears at a 120-hr interval after previous hyperthermia treatment.[72-74]

The phenomenon of thermotolerance has a great impact on clinical use of hyperthermia. First, at the present time we are still unable to heat tumors uniformely. If different parts of tumor are heated to a different temperature, they will express unequal heat sensitivities due to the variations in the developed thermal resistance. Second, heat treatment should be given in large fractions with intervals long enough to allow thermotolerance to develop and decay. Third, the role of thermotolerance in combined hyperthermia and radiation treatment is even more complex.[71]

Studying the effect of time interval between hyperthermia and irradiation investigators came to the conclusion that simultaneous applying of both methods provides maximum cell-killing effect *in vitro*.[33,40] Unfortunately the therapeutic gain, which expresses advantage of tumor cell-killing effect over unwanted reactions of normal tissue, was with simultaneous treatment even negative. If heat had been administrated 1hr or more after irradiation better therapeutic gain on experimental animal was assured.[75,76] In clinical trials big effort has been dedicated to the problem of the determination of an optimal treatment schedule form combined hyperthermia and irradiation. However, regardless to the total number of hyperthermia fractions, different intervals between radiotherapy and hyperthermia and various fraction sizes of radiotherapy used, most of these studies revealed an obvious improvement of response rates compared to those obtained with radiotherapy alone. In Table 1 results of several clinical trials are listed with a special regard to the differences in treatment response to radiotherapy alone vs combined radiotherapy and hyperthermia treatment.[77]

Despite this superior efficacy of combined treatment over use of radiation alone, there are several important parameters which need to be considered when assesing the role of hyperthermia. All these variables are inter-related and may have a considerable influence on the final outcome of treatment.[23] Many authors had demonstrated that *tumor volume* is an adverse predictor of tumor control. Much better complete response rate were obtained with tumors less than 3 cm in the greatest diameter.[11,15,20,23,78-82] This is, however, in contrast with the fact that bulky tumors have insufficient vascularity with predictably easier chances for heating. It looks like that presently available

Table 1. Results of clinical trials comparing the effect of radiotherapy alone (RT) vs. combined radiotherapy and hyperthermia (RT + HT).

Reference	Lesions	Total number of tumors	% CR* (RT)	% CR (RT + HT)
Arcangeli (11)	neck nodes melanoma metastases	81	42	79
		38	53	76
Kim (15)	melanoma metastases	99	42	65
Lindholm (16)	superficial tumors	85	25	46
	breast tumors	34	25	57
Valdagni (23)	neck nodes	46	36.8	83.3
(78)	neck nodes	35	35	68
Perez (20)	breast tumors (diameter 1–3 cm	2	33	80
	> 3 cm)	63	42	65

* Percent of tumors with complete response after therapy

technology, unable of heating at greater depths, omit this advantage. This problem is much more noticeable in deep-seated tumors,[83-85] although it may play an important role also in the treatment of the superficial lesions.[86] Different histologic subtypes, on the other hand, do not greately affect the response rates.[87-88]

The administered *total radiation dose,* however, is remarkably important. In brief, higher the total dose, better the outcome of the combined treatment.[89-90] Dose per fraction and number of fractions do not seem to have such an important impact on the therapy outcome, except for malignant melanoma.[78,91] Some experimental data suggest that only very high dose-rates (> 300 cGy/min) as well as extremely low dose-rates (< 0.5 cGy/min) potentiate heat radiosensitization, and practically no benefit is to be expected from using conventional radiotherapeutic dose-rates.[92] At this place it is important to stress that practically all studies with hyperthermia mainly included reccurences of previously irradiated tumor lesions. Thereafter reirradiation mostly consisted of lower total tumor doses.

Yet, the radiotherapy variables in the combined treatment are still much easier to determine in comparison to thermal variables. It is so because in hyperthermia currently no functional equivalent to the absorbed energy per unit mass (as Gray in radiotherapy) existed.[23] Many attempts had been made to quantitate the *thermal dose.* Mainly the concept of thermal dose bases on biological isoeffect relationship between treatment time an temperature, frequently expressed as »equivalent heating time at 43°C«.[93] From numerous experimental studies done on various cell cultures and different types of tissue it was found that this relationship is not a simple linear product of the two observed parameters. There is a transition point which normaly occurs between 42°C and 43°C. For the production of the same degree of thermal injury each step of 1°C above this point results in reduction of the heating time by factor 2. In other words if 1 hour of heating at 43°C is needed for acquireing a certain thermal damage, only 30 min at 44°C enables the development of the same effect. On the other hand, if temperature below this point is used 6 x longer heating time is required for each decrease of 1°C. In Table 2 approximate

Table 2. Aproximate values of treatment time for various clinically relevant treatment temperatures.

Temperature in °C	41	42	43*	44	45
Treatment time in minutes	2160	360	60	30	15

* Transition point

values of treatment time for various treatment temperatures are listed according to the data published by Field and Morris.[94]

Since the biological rationals for thermal events occurring at the breaking point (between 42°C and 43°C) are not fully understood, it seems that the development of thermotolerance during heat treatment with lower temperatures is somehow responsible for the big difference in treatment time needed for same treatment results as obtained with temperatures above transition point.[95] Further research is needed for real safe application of thermal isoeffect dose concept in clinical practice,[96,97] although for the moment time/temperature formula provides a resonable method for comparing clinical hyperthermia treatments.[98]

From several clinical trials it can be concluded that the possibility of obtaining a high local tumor control rate especially corelates with *minimum tumor temperatures.* If these temperatures were still in the cytotoxic range much better treatment results were acquired.[23,99] That is the reason why good multiple point intratumoral thermometry is an essential demand in clinical hyperthermia.

The fractionation in hyperthermia is a constant subject of discussion. Slow rate of decaying of thermotolerance dictates at least 72 hours of interval between two hyperthermia sessions, thus permitting one or at most two treatments weekly. Greater problem is a total number of fractions. Retrospective analyses failed to show an improvement of local control when multifraction courses of hyperthermia were used in clinical trials.[45,91] Moreover, in recently published randomized prospective study, including matched paired lesions in the same patient, there were no demonstrable difference found in two arms comparing six vs. two hyperthermia treatments.[100] The other problem which needed to be solved is *sequencing of hyperthermia and radiotherapy.* From the results of thermobiological investigations (seé above) one can conclude that simultaneous treatment with both modalities guarantees the best treatment results. However, presently available technique does not allow a real simultaneous therapy. We must not overlook the fact that hyperthermia should have an opposite effect regarding radiosensitivity of normal and tumor tissue. Mild hyperthermia may cause an increased blood flow through the normal tissue resulting in improved oxigenation and therefore an enhanced sensitivity to the subsiquent radiotherapy. On the other hand higher temperatures in tumour tissue may result in vascular stasis with subsequent tumor hypoxia and decreased radiation sensitivity.[45] That is why several studies were done to confirm which of two treatment strategies (radiation before or radiation after hyperthermia) gives better therapeutic gain.[17,45,91] From these studies a treatment plan can be derived prefering radiotherapy folowed by hyperthermia with a possibility of normal tissue (skin) cooling.

Although there are some reports in literature which proved a role of hyperthermia as a palliative method in combination with moderate radiotherapy[101-103], or even used alone[104] in treatment of previously irradiated tumor lesions, the results of recent RTOG study suggest a real benefit from combination of hyperthermia with definitive radiation as a primary therapy[21].

Finaly if we want to summerize an answer to few questions presented previously in our text, we have to determine that at the present time we have no general propositions regarding the combination of hyperthermia and radiation treatment. In the majority of lately designed clinical trials the most often proposed protocol consists of few large heat treatments (minimum tumor temperature > 42.5°C, treatment duration time approximately 45 min.) given once or twice weekly after radiotherapy. Expected results should be better if normal full dose radiotherapy is used[46].

It is important to accent that previous data dealing the combination of hyperthermia and irradiation reffered only to the local appliance of both treatment. The problems regarding *whole body hyperthermia* are far more complex. Although tumour regression after deliberate induction of erisipelas causing elevated body temperature, reported by Coley in 1893, was recognized

as one of the first published articles of hyperthermia effect on cancer patient, the problem of severe side effect gave the priority to the development of the local type of treatment[105]. Lately a variety of methodologies has been innovated which permit somehow safer delivering of elevated temperature to the entire body. Whole body hyperthermia can be induced by energy input via the surface of the patient, such as by using paraffin wax[106,107], hot air and radiofrequency[108] or water perfused blankets and suits[109,110]. Another method is warming the patient by heating the blood circulating in an extracorporeal circuit[111]. The greatest problem in systemic use is maintaining constant body temperature which should not exceed 41.8-42°C, otherwise causing deleterious and even fatal side effects. With that purpose numerous rectal, oesophageal, nasopharyngeal, intramuscular, temperature probes has to be placed for temperature monitoring[112]. Although not all[113], most of currently used whole body hyperthermia systems has to be given under general anaesthesia, that is why also an introduction of the bladder catheter is needed. Inspite of all precautions the probability of getting various cardio-pulmonary, liver and neurologic complications, whether they are transient or not, is rather high[114,115]. Because temperatures used in whole body hyperthermia have to be tolerated by some critical tissues, they are rather low. Therefore considerable prolongation of the treatment time (approximately 2 hours) is necessary to obtain some cytotoxic effect[112]. If even lower temperatures were used (39.5 – 40° C), at least in animal experiments, increased natural killer (NK) cells activity was observed, suggesting that antitumoral effect of whole body hyperthermia with mild temperatures is mediated through the immune system[116]. An immediate pain relief after the whole body hyperthermia, which was most oftenly one of the leading treatment issues, was associated with marked

Table 3. Types of non–invasive (percutaneous) hyperthermia techniques

	Radiofrequency			Microwave	Ultrasound
	(electric)	inductive coupling (magnetic)	capacitive coupling		
References	122 – 124	125,126	127,128	129,130	131,132
Frequency range		8 – 100 MHz		433,915 and and 2450 MHz	0,3 – 3 MHz
Applicator positioning	1. Two electrodes positioned oppositely 2. Bolus is required	1. Pancake coil positioned ca 3cm above the skin 2. Bolus not requi red	1. Large electrodes (diameter 20-25 cm) Concentric, coaxial -or helical coils and annular phased array	1. Direct contact applicators with or without bolus	1. Direct contact or use of water immersion
Advantages	1. Ability to heat large volumes at depth	1. Penetration of 3 – 4 cm in tumour or muscle tissue 2. Size and shape of applicators may be changed	1. Treatment of larger volumes at greater depth (ca 6cm)	1. Pennetration better for frequencies lower than 1000MHz 2. Possible treatment of larger areas by using more than one applicator	1.Better penetration than microwaves 2. With multi transducers system tissue depth of 7–10 cm could be obtained
Disadvantages	1. Production of cold and hot spots due to tissue inhomogeneitis 2. Excessive heating of superficial and fatty tissue		1. Excessive heating of superficial tissue	1. Poor penetration for small applicators 2. Poor penetration in tissue at high frequencies 3. Stray microwave radiation	1. Large reflections between soft tissue and gas or bone

rise in plasma endorphin levels[117]. As hyperthermia is nonmyelosuppressive, its use in multimodality treatment of systemic cancer, potentiating the effect of radiotherapy, chemotherapy or immunotherapy is attractive. However, clinical trials using whole body hyperthermia are to be planned only in selected institutions with appropriate technical equipment and well trained personnel[118,119].

Heating techniques and thermometry

Heating technique system capable of delivering reproducible treatment presents a major challenge for physicists and engineers dealing with clinical hyperthermia. The problem is far from being solved. A detailed information on this subject is beyond the scope of present paper and one can get it elsewhere in the literature[120,121]. Regardless to the problem of whole body hyperthermia, in general, clinical hyperthermia techniques can be classified into two groups: non-invasive or percutaneous and invasive or interstitial. In both of them radiofrequency and microwave applicators are mostly used. In some centers ultrasound applicators has been constructed for percutaneous deep tissue heating. In Table 3 characteristics of non-invasive heating techniques are listed according to some published datas.

The currently used methods for interstitial hyperthermia can be devided on those using electromagnetic waves (implantable microwave antennas and applicators using localised current fields) and so called »hot sources« (ferromagnetic seed technique and circulating hot water technique). In Table 4 some of the characteristics of invasive techniques are listed together with available literature.

Table 4. Types of invasive (interstitial) hyperthermia techniques.

	Electromagnetic		Hot sources	
	radiofrequency (localised current fields)	microwave (coaxial cables)	ferromagnetic seeds	circulating hot water
References	133 – 137	133,134,138–141	133,134,142–144	145–148
Operating frequencies	0.2 – 1 MHz	0 – 5 – 1 GHz	/	/
Optimum spacing of applicators/needles	1 cm	1.5 cm	1 cm	1 cm
Advantages	1. Less prominent thermometry artefacts when using low frequency currents	1. Antennas could be flexible	1. Together with I-125 seeds ferromagnetic seeds are usable for permanent implants 2. Heating of deep-seated tumors is possible 3. Reapeted heatings are possible 4. Seeds can be placed within movable catheters	1. Hot water should be considered as a constant temperature source 2. The fall-off the temperature along the tube is minumum 3. Maximum temperature in tissue cannot exceed water temperature 4. Thermometry is easy to perform 5. Cooling of normal tissue is possible
Disadvantages	1. Electrodes are rigid 2. Spacing of electrodes needs to be more dense than in the case of microwaves 3. There is a need for adjusted voltage between pairs of electrodes 4. Temperature homogeneity is not easy to achieve 5. Insulation of normal tissue is immanent	1. Temperature distribution on the longitudinal axis is non-uniform individual designed antennas 3. Thermometry in microwave fields is problematic	1. The real constant temperature seeds are still under investigation 2. Adjustment of seeds impossible (for permanent implants) 3. Pretreatment planning is of major importance 4. Equipement is high-cost and is not portable	1. Good geometry and parallelism are of major importance 2. Rigid metalic tubes offer better thermal conduction

Table 5. Comparison of percutaneous and interstitial hyperthermia techniques

	Percutaneous	Interestitial
Advantages	1. Application of heat is easy to perform – no need for total anesthesia 2. It is possible to repeat treatments (the optimum number is still under investigation) 3. It is possible to treat larger volumes 4. Use in combination with convetional percutaneous radiotherapy	1. Almost perfect localisation of treatment volume 2. Temperature distribution is more homogene 3. It is possible to shield normal tissue 4. Temperature monitoring is easier to perform 5.Same implant is used for brachytherapy 6. One (or two) »good« hyperthermia treatment is probably enough
Disadvantages	1. There is a marked inhomogeneity of temperature distribution when larger volumes are heated 2. It is hard to avoid heat damage of the surrounding normal tissue 3. Temperature monitoring is more complex 4. High cost of technical equipment	1. Insertion of implants needs special training – total anesthesia is needed 2. A good geometry of implants is of major importance 3. Lesser possibility for repeated treatments (except for permanent implants with ferromagnetic seeds)

The amount of power deposit per unit mass of tissue can be calculated for electromagnetic waves using techniques. The distribution of so-called specific absorbtion rate (SAR, W/kg) can be measured and used for comparison of different treatment methods. However, even in situation where the SAR in the tissue is quite uniform, the temperature variations are quite marked. Here it has to be emphasized that resulting temperature distribution associated with any heating technique depends not only on SAR but also on geometry, specific heat conductivity of tissues and blood flow rate.[149,150] From the medical point of view the only data which realy counts is the therapeutic level of temperature measured inside the heated volume.

The above mentioned recognition thus means that only *good thermometry* provides effective hyperthermia treatment. Unfortunately, the lack of non-invasive methods for temperature monitoring inside the treatment volume presents, at the moment, one of the greatest unsolved problems relating the clinical use of hyperthermia. Invasive thermometry is based on conventional thermistors and thermocouples. In general, a good accuracy (0.1–0.2°C) and optimum spacial resolution (5–10mm) are required for an useful thermometry.[121] Invasive thermometry could be achieved with multisensor probes installed inside the treatment volume or moved stepwise through a catheter. For that purpose invasive thermometers should have the smallest diameter possible to minimise trauma to the patient. Due to various factors effecting temperature distribution the temperature measurement are to be as dense as possible. This is the only way to avoid the possible underheated areas inside the tumor volume on one hand, and overheated surrounding normal tissue on the other. Special care has to be taken in positioning of thermocouples inside the electromagnetic fields in order to minimise the measurement errors.[151-154] Lately, various noninvasive methods of temperature measurement i.e. ultrasound technique, X-ray tomography and magnetic resonant imaging attracted much attention.[155,156] Perhaps the use of microwave radiometers for noninvasive temperature sensing in superficial treatments is the most promising one.[157]

Closing remarks

A great number of published articles refering the clinical use of hyperthermia are showing a constant rise of interest on this subject. Local application (either percutaneous or invasive) is for the moment the most widely used method of hyperthermia cancer treatment. Because it offers variety of possibilities for the combination with radiotherapy is the development of thermotherapy almost strictly associated with tasks at

radiation therapy departments. Although there are some advantages in the use of invasive hyperthermia treatment over the percutaneous therapy, particularly in the term of more uniform heating pattern, both methods can be used quite safely. Table 5 shows the advantages and disadvantages of the two local hyperthermia systems. Also some recently developed systems, i.e. intracavitary[158,159] or perfusional[160] offer new treatment possibilities.

Hyperthermia therapy has two different parts which need to be investigated hand in hand: technical and clinical. In the technical field a lot has to be done to develop safe and low cost equipment with computerised machinery and practical thermometry. On the other side, a number of well designed and carefully performed clinical trials are needed to investigate all benefits that thermotherapy offers. Nevertheless, it looks like, that hyperthermia already possess a definite place in cancer treatment. With the acception of the clinical hyperthermia as an important contribute to a modern anticancer therapy, no longer it will be the dommain only of a few scientific centers but it will become widely used also throughout less prominent oncology departments.

References

1. Hornback NB. Historical aspects of hyperthermia in cancer therapy. *Radiol Clin N Amer* 1989; **27:**481-8.
2. Streffer C. Biological basis of thermotherapy. In: Gautherie M ed.: *Biological Basis of Oncologic Thermotherapy*. Berlin: Springer, 1990: 1-71.
3. Singh BB. Hyperthermia: an ancient science in India. *Int J Hyperthermia* 1991; **7:**1-6.
4. Meyer JL. Hyperthermia as an anticancer modality – a historical perspective. *Front Radiat Ther Oncol* 1984; **18:**1-12.
5. Pettigrew RT, Ludgate CM, Gee AP. Whole-body hyperthermia combined with chemotherapy in the treatment of advanced human cancer. In: Streffer C ed. *Cancer Therapy by Hyperthermia and Radiation*. Baltimore: Urban and Schwarzenberg, 1978: 337-9.
6. Manning MR. Hyperthermia: renewed interest in an old treatment of cancer. *Arizona Med* 1977; **34:**19-20.
7. Dewey WC, Hopwood LE, Sapareto SA, Gerweck LE. Cellular responses to combinations of hyperthermia and radiation. *Radiology* 1977; **123:**463-74.
8. Field SB. The response of normal tissues to hyperthermia alone or in combination with X-rays. In: Streffer C ed. *Cancer Therapy by Hyperthermia and Radiation*. Baltimor: Urban and Schwarzenberg, 1987: 37-48.
9. Overgard J. Effect of hyperthermia on malignant cells in vivo. A review and hypothesis. *Cancer* 1977; **37:**2637-48.
10. Westra A, Dewey WC. Heat shock during the cell cycle of Chinese hamster cells in vitro. *Int J Radiat Biol 1971;* **19:**467-77.
11. Arcangeli G, Benassi M, Cividalli A, Lovisolo GA, Mauro F. Radiotherapy and hyperthermia. Analysis of clinical results and identifications of prognostic variables. *Cancer* 1987; **60:**950-56.
12. Dunlop PRC, Hand JW, Dickinson RJ, Field SB. An assesment of local hyperthermia in clinical practice. *Int J Hyperthermia* 1986; **2:**39-50.
13. Kim JH, Hahn EW, Tokita N, Nisce LZ. Local tumor hyperthermia in combination with radiation therapy. 1. Malignant cutaneous lesions. *Cancer* 1977; **40:**161-9.
14. Kim JH, Hahn EW. Clinical and biologic studies of local hyperthermia. *Cancer Res* 1979; **39:**2258-61.
15. Kim JH, Hahn EW, Ahmed SA. Combination hyperthermia and radiation therapy for malignant melanoma. *Cancer* 1982; **50:**478-82.
16. Lindholm CE, Kjellen E, Nilsson P, Hertzman S. Microwave–induced hyperthermia and radiotherapy in human superficial tumours. Clinical results with a comparative study of combined treatment versus radiotherapy alone. *Int J Hyperthermia* 1987; **3:**393-411.
17. Overgaard J. Fractionated radiation and hyperthermia. Experimental and clinical studies. *Cancer* 1981; **48:**1116-23.
18. Overgaard J, Overgaard M. Hyperthermia as an adjuvant to radioterapy in the treatment of malignant melanoma. *Int J Hyperthermia* 1987; **3:**483-501.
19. Overgaard J. The current and potential role of hyperthermia and radiotherapy. *Int J Radiat Oncol Biol Phys* 1989; **16:**535-49.
20. Perez CA, Kuske RR, Emami 8, Fineberg B. Irradiation alone or combined with hyperthermia in the treatment of recurrent carcinoma of the breast in the chest wall. A nonrandomized comparison. *Int J Hyperthermia* 1986; **2:**179-87.
21. Scott R, Gillespie B, Perez CA et al. Hyperthermia in combination with definitive radiation: results of a phase I/II RIOG study. Int J Radiat Oncol Biol Phys 1988; **15:**711-16.
22. Shidnia H, Hornback NB, Shupe R, Shen RN, Yune M. Correlation between hyperthermia and large dose per fraction in treatment of malignant melanoma (Abstract). In: Proceedings of International Clinical Hyperthermia Society Annual Meeting, Lund, June 14-17, 1987; **26.**
23. Valdagni R, Amichetti M, Pani G. Radical radiation alone versus radical radiation plus microvawe hyperthermia for N3 (NTM-UICC) neck nodes: a prospective randomized clinical trial. *Int J Radiat Oncol Biol Phys* 1988; **15:**13-24.
24. Nias AHW. Experimental therapy. In: Nias AHW ed. *Clinical Radiobiology*. Edinburgh: Churchill Livingstone 1988; 226-252.

25. Muller C. Therapeutische Erfahrungen an 100 mit Kombination von Roentgenstrahlen und Hochfrequenz, resp. Diathermie behandelten boesartigen Neubildungen. *Münch Med Wochenschr 1912;* **28:**1546-9.
26. Dewey WC. Inactivation of mammalian cells by combined hyperthermia and raddiation. *Front Radiat Ther Oncol* 1984; **18:**29-40.
27. Freeman ML, Raaphorst GP, Dewey WC. The relationship of heat killing and thermal radiosensitation to the duration of heating at 42°C. *Radiat Res* 1979; **78:**172-5.
28. Moylan JM, Alexander GA, Leeper DB, Waterman FM, Nerlinger RE. Hyperthermia. Scientific basis and clinical application. In: Mansfield CM ed. *Therapeutic Radiology.* Amsterdam: Elsevier, 1989; 531.
29. Fertil B, Malaise EP. Inherent cellular radiosensitivity as a basic concept for human tumor radiotherapy. *Int J Radiation Oncology Biol Phys* 1981; **1:**621-9.
30. Hall EJ. Radiation biology. *Cancer* 1985; **55:**2051-7.
31. Tubiana M. Cellular effects of ionizing radiation. Cell survival curves. In: Tubiana M, Dutreix J, Wambersie A. eds. *Introduction to Radiobiology.* London: Taylor & Francis, 1990: 111.
32. Denekamp J.: Cell proliferation to cancer therapy. Paper presented at Progress in Radio-Oncology IV, Vienna, September, 1988.
33. Field SB, Bleehen NM. Hyperthermia in the treatment of cancer. *Cancer Treat Rev* 1979; **6:**63-94.
34. Raaphorst GP, Spiro IJ, Azzam EI, Sargent M. Normal cells and malignant cells transfected with the HRas oncogene have the same heat sensitivity in culture. *Int J Hyperthermia* 1987; **3:**209-16.
35. Hinkelbein W, Bruggmoser G, Wurdinger A, Fiebig HH. Intrinsic thermosensitivity of various human tumors. *Rec Res Cancer Res* 1988; **109:**198-202.
36. Overgaard J. The effect of local hyperthermia alone, and in combination with radiation, on solid tumors. In: Streffer C ed. *Cancer Therapy by Hyperthermia and Radiation.* Baltimore: Urban&Schwarzenberg, 1978: 39-61.
37. Emami B, Song CW. Physiological mechanisms in hyperthermia; A review. *Int J Radiat Oncol Biol Phys* 1984; **10:**289-95.
38. Storm FK, Harrison WH, Elliott RS, Morton DL. Normal tissue and solid tumor effect of hyperthermia in animal models and clinical trials. *Cancer Res* 1979; **39:**2245-51.
39. Mueller-Klieser W, Manz R, Otte J, Vaupel P. Effect of localised hyperthermia on tumor blood flow and oxygenation In: Ring EFJ and Phillips B ed. *Recent Advances in Medical Thermology.* New York: Plenum Press, 1984: 669-76.
40. Stone HB, Dewey WC. Biological basis and clinical potential of local-regional hyperthermia. In: Phillips TR and Wara W eds. *Radiation Oncology.* New York: Raven Press, 1987: 1-41.
41. Dickson JA, Suzangar M. A predictive in vitro assay for the sensitivity of human solid tumours to hyperthermia (42°C) and its value in patient management. *Clin Oncol* 1976; **2:**141-55.
42. Gerweck LE. Effect of microenvironmental factors on the response of cells to single and fractionated heat treatments. *Natl Cancer Inst Monogr* 1982; **61:**19-26.
43. Gerweck LE. Hyperthermia in cancer therapy: The biological basis and unresolved questions. *Cancer Res* 1985; **45:**3408-14.
44. Kim JH. Combined hyperthermia and radiation therapy in cancer treatment: Current status. *Cancer Invest* 1984; **2:**69-80.
45. Oleson JR, Calderwood SK, Coughlin CI et al. Biological and clinical aspects of hyperthermia in cancer therapy. *Am J Clin Oncol* 1988; **11:**368-380.
46. Overgaard J, Nielsen OS, Lindegaard JC. Biological basis for rational design of clinical treatment with combined hyperthermia and radiation. In: Field S.B, Franconi C eds. *Physics and Technology of Hyperthermia, Dordrecht: Martinus Nijhoff, 1987: 54-79.*
47. *Spiro IJ, Denman DL, Dewey WC. Effect of hyperthermia on isolated DNA polymerase-beta. Radiat Res* 1983; **95:**68-77.
48. Streffer C. Metabolic changes during and after hyperthermia. *Int J Hyperthermia* 1985; **1:**305-19.
49. Tamulevitius P, Schmidt K, Streffer C. The effect of X irradiation, hyperthermia, and combined modality treatment on poly(ADPR) synthetase activity in human melanoma cells *Radiat Res* 1984; **100:**65-77.
50. Yi P.N, Fenn JO, Dykes BH, Jarrett JH. Mobilization of amino acids in tumor cells by hyperthermia. *Cell Biol Int Rep* 1983; **7:**797-806.
51. Ben-Hur E, Elkind MM, Riklis E. The combined effects of hyperthermia and radiation in cultured mammalian cells. In: Streffer C ed. *Cancer Therapy by Hyperthermia and Radiation.* Baltimore: Urban&Schwarzenberg, 1978: 29-36.
52. Field SB. Hyperthermia and radiotherapy. *Strahlentherapie 1984;* **160:**715-20.
53. McGhie JB, Wold E, Pettersen EO, Moan J. Combined electron radiation and hyperthermia. Repair of DNA strand breaks in NHIK 3025 cells irradiated and incubated at 37, 42.5 or 45°C. *Radiat Res* 1983; **96:**31-40.
54. Bleehen NM. *Hyperthermia with drugs: Current status Strahlentherapie* 1984; **160:**721-4.
55. Krishnamurti S, Shanta V, Vasanthan A, Balakrishnan IS, Jayaraman R. Radiation, Peoplemycin and hyperthermia in the therapy of locally advanced squamous cell carcinoma of the buccal mucosa. *Clin Oncol* 1990; **2:**10-13.
56. Pilepich MV, Jones KG, Emami BN, Perez CA, Fields JN, Myerson RJ. Interaction of Bleomycin and hyperthermia – results of clinical pilot study. *Int J Radiat Oncol Biol Phys* 1989; **16:**211-3.
57. Bleehen NM, Walton MI, Workman P. Interactions of hyperthermia with hypoxic cell sensitisers. *Rec Res Cancer Res* 1988; **109:**136-48.
58. Goldfeder A, Brown DM, Berger A. Enhancement of radioresponse of a mouse mammary carcinoma to combined treatments with hyperthermia and radiosensitiser misonidazole. *Cancer Res* 1979; **39:**2966-70.
59. Haveman J, Wondergem J. Thermal enhancement of the cell killing effect of x-irradiation in mammalian cells in vitro and in transplantable mouse

tumor: Influence of pH, thermotolerance, hypoxia and misonidazole. *Rec Res Cancer Res* 1988; **109:**149-60.
60. Song CW, Rhee JG, Levitt SH. Effect of hyperthermia on hypoxic cell fraction in tumor. *Int J Radiat Oncol Biol Phys* 1982; **8:**851-6.
61. Wondergem J, Haveman J, van der Schueren E, van der Hoeven H, Breur K. Effect of hyperthermia and misonidazole on the radiosensitivity of a transplantable murine tumor: influence of factors modifying the fraction of hypoxic cells:*Int J Radiat Oncol Biol Phys* 1982; **8:**1323-31.
62. Cosset JM, Dutreix J, Dufour J et al. Combined interstitial hyperthermia and brachytherapy: institute Gustave Roussy technique and preliminary results. *Int J Radiat Oncol Biol Phys* 1984; **10:**307-12.
63. Joseph CD, Astrahan M, Lipsett J, Archambeau J, Forell B. Interstitial hyperthermia and interstitial iridium-192 implantation: a technique and preliminary results. *Int J Radiat Oncol Biol Phys* 1981; **7:**827-33.
64. Arcangeli Gior, Arcangeli Gian, Guerra A et al. Tumour response to heat and radiation: Prognostic variables in the treatment of neck node metastases from head and neck cancer. *Int J Hyperthermia* 1985; **1:**207-17.
65. Song CW. Effect of local hyperthermia on blood flow and microenvironment: A review. *Cancer Res (Suppl.) 1984;* **44:**4721s-30s.
66. Meyer JL. The clinical efficacy of localized hyperthermia. *Cancer Res (Suppl.)* 1984; **44:**4745s-51s.
č67. Hatayama T, Kano E, Taniguchi Y et al. Role of heat shock proteins in the induction of thermotolerance in Chinese hamster V79 cells by heat and chemical agents. *Int J Hyperthermia* 1991; **7:**61-74.
68. Hahn GM. The heat shock response: Events before, during, and after gene activation. In: Gautherie M ed. *Biological Basis of Oncologic Thermotherapy*. Berlin: Springer, 1990: 135-66.
69. Anderson LR, Herman TS, van Kersen I, Hahn GM. Thermotolerance and heat shock protein induction by slow rates of heating. *Int J Radiat Oncol Biol Phys* 1988; **15:**717-25.
70. Anderson LR, Tao TW, Betten DA, Hahn GM. Heat shock protein levels are not elevated in heat resistant B16 melanoma cells. Radiat Res 1986; **105:**240-6.
71. Overgaard J, Nielsen OS. The importance of thermotolerance for the clinical treatment with hyperthermia. *Radiother Oncol* 1983; **1:**167-78.
72. Kamura I, Nielsen OS, Overgaard J, Andersen AH. Development of thermotolerance during fractionated hyperthermia in a solid tumor in vivo. *Cancer Res* 1982; **42:**1744-8.
73. Nielsen OS, Overgaard J. Studies of fractionated hyperthermia in L1A2 tumor cells in vitro: response to multiple equal heat fractions. *Int J Hyperthermia* 1985; **1:**193-203.
74. Nielsen OS, Overgaard J. Influence of time and temperature on the kinetics of thermotolerance in L1A2 cells in vitro. *Cancer Res* 1982; **42:**4190-6.
75. Hill SA, Fowler JF. Combined effect of heat and X-rays on two types of mouse tumor. In: Streffer C ed. *Cancer Therapy by Hyperthermia and Radiation.* Baltimore: Urban & Schwarzenberg, 1978: 251-2.
76. Stewart FA, Denekamp J. Combined X-rays and heating: Is there a therapeutic gain? In: Streffer C ed. *Cancer Therapy by Hyperthermia and Radiation.* Baltimore: Urban & Schwarzenberg, 1978: 249-50.
77. Oleson JR. Hyperthermia. In: De Vita VI, Hellman S Rosenberg SA eds. *Cancer-Principles and Practice of Oncology*. Philadelphia: Lippincott, 1989: 2426-35.
78. Valdagni R, Kapp DS, Valdagni C. N3 (INM-UICC) metastatic neck nodes managed by combined radiation therapy and hyperthermia: clinical results and analysis of treatment parameters. *Int J Hyperthermia* 1986; *2:*189-200.
79. Fazekas JI, Nerlinger RE. Localized hyperthermia adjuvant to irradiation in superficial reccurent carcinomas: a preliminary report on 46 patients. *Int J Radiat Oncol Biol Phys* 1981; **7:**1457-63.
80. Perez CA, Nussbaum G, Emami B, VonGerichten D. Clinical results of irradiation combined with local hyperthermia. *Cancer* 1983; **52:**1597-603.
81. Valdagni R, Liu FF, Kapp D. Important prognostic factors influencing outcome of combined radiation and hyperthermia Int J Radiat Oncol Biol Phys 1988; **15:**959-72.
82. Van der Zee J, van Putten WLJ, van den Berg AP. Retrospective analysis of the response of tumors in patients treated with a combination of radiotherapy and hyperthermia. *Int J Hyperthermia* 1986; *2:337-49.*
23. Emami B, Myerson RJ, Scott C, Gibbs F, Lee C, Perez CA. Phase IIII study, combination of radiotherapy and hyperthermia in patients with deep-seated malignant tumors: report of a pilot study by the radiation therapy oncology group. Int J Radiat Oncol Biol Phys 1991; **20:**73-9.
84. Hornback NB, Shupe RE, Shidnia H, Marshall CU, Hauer T. Advanced stage IIIB of the cervix treatment by hyperthermia and radiation. *Gynecol Oncol* 1986; **23:**160-7.
85. Petrovich Z, Langholz B, Gibbs FA et al. Regional hyperthermia for advanced tumors: a clinical study of 353 patients. *Int J Radiat Oncol Biol Phys* 1989; **16:**601-7.
86. Scott R, Johnson RJR, Kowal H, Krishnamsetty RM, Story K, Clay L. Hyperthermia in combination with radiotherapy: a review of five years experience in the treatment of superficial tumors. *Int J Radiat Oncol Biol Phys* 1983; **9:**1327-33.
87. Perez CA, Kopecky W, Rao DV, Baglan R, Mann J. Local mycrowave hyperthermia and irradiation in cancer therapy: preliminary observations and directions for future clinical trials. *Int J Radiat Oncol Biol Phys* 1981; **7:**765-72.
88. Urbon J, Murthy AK, Taylor SG, Hendrickson FR, Lanzl LH. Retrospective analysis of hyperthermia for use in the palliative treatment of cancer: a multy-modality evaluation. *Int J Radiat Oncol Biol Phys* 1990; **18:**155-63.
89. Luk KH, Francis ME, Perez CA, Johnson RJ. Combined radiation and hyperthermia: comparison of two treatment schedules based on data from a registry esthablished by the radiation therapy oncology group (RTOG). *Int J Radiat Oncol Biol Phys* 1984; **10:**801-9.

90. Van der Zee J, Treurniet-Donker AD, The SK. Low dose reirradiation in combination with hyperthermia: a palliative treatment for patient with breast cancer reccuring in previously irradiated areas. *Int J Radiat Oncol Biol Phys* 1988; **15:**1407-13.
91. Arcangeli G, Cividalli A, Nervi C, Creton G. Tumor control and therapeutic gain with different schedules of combined radiotherapy and local external hyperthermia in human cancer. *Int J Radiat Oncol Biol Phys* 1983; **9:**1125-34.
92. Gerner EW, Oval JH, Manning MR, Sim DA, Bowden GI, Hevezi JM. Dose-rate dependence of heat radiosensitization. *Int J Radiat Oncol Biol Phys* 1983; **9:**1401-4.
93. Overgaard J. Some problems related to the clinical use of thermal isoeffect doses. *Int J Hyperthermia* 1987; **3:**329-36.
94. Field SB, Morris CC. The relationship between heating time and temperature: its relevance to clinical hyperthermia. *Radiother Oncol* 1983; **1:**179-186.
95. Sapareto SA. Thermal isoeffect dose: adressing the problem of thermotolerance. *Int J Hyperthermia* 1987; **3:**297-305.
96. Dewhirst MW, Winger JM, Edelstein-Keshet L et al. Clinical application of thermal isoeffect dose. *Int J Hyperthermia 1987;* **3:**307-18.
97. Sapozink MD. The application of thermal dose in clinical trials. *Int J Hyperthermia* 1987; **3:**157-64.
98. Field SB. Studies relevant to a means of quantifying the effects of hyerthermia. *Int J Hyperthermia* 1987; **3:**291-96.
99. Gonzales D, van Dijk JDP, Blank LECM. Chest wall recurrences of breast cancer: Results of combined treatment with radiation and hyperthermia. *Radiother Oncol* 1988; **12:**95-103.
100. Kapp DS, Petersen IA, Cox RS et al. Two or six hyperthermia treatments as an adjunct to radiation therapy yield similar tumor responses: Results of a randomized trial. *Int J Radiat Oncol Biol Phys* 1990; **19:**1481-95.
101. Luk KH, Purser PR, Castro JR, Meyler TS, Phillips TL. Clinical experiences with local microwave hyperthermia. *Int J Radiat Oncol Biol Phys* 1981; **7:**615-619.
102. Sapozink MD, Gibbs FA, Gates KS, Stewart JR. Regional hyperthermia in the treatment of clinically advanced deep seated malignancy: Results of a pilot study employing an annular array applicator. *Int J Radiat Oncol Biol Phys 1984;* **10:**775-86.
103. Barnett TA, Kapp DS, Goffinet DR. Adenoid cystic carcinoma of the salivary glands. Management of reccurent advanced, or persistent disease with hyperthermia and radiation therapy. *Cancer* 1990; **65:**2648-56.
194. Gabriele P, Orecchia R, Ragona R, Tseroni V, Sannazzari G, L. Hyperthermia alone in the treatment of reccurences of malignant tumors. *Cancer* 1990; **66:**2191-5.
105. Robins IH, Hugander A, Cohen JD. Whole body hyperthermia in the treatment of neoplastic disease. *Radiol Clin N Amer* 1989; **27:**603-10.
106. Pettigrew RT, Galt OM, Ludgate CM, Horn DB, Smith AN. Circulatory and biochemical effect of whole body hyperthermia. *Br J Surg* 1974; **61:**727-30.
107. Levin W, Blair RM. Clinical experience with combined whole body hyperthermia and radiation. In: Streffer C ed. *Cancer Therapy by Hyperthermia and Radiation.* Munchen: Urban and Schwarzenberg, 1978: 322-25.
108. Pomp H. Clinical application of hyperthermia in gynecological malignant tumors. In: Streffer C ed. *Cancer Therapy by Hyperthermia and Radiation.* Munchen: Urban and Schwarzenberg, 1978: 326-7.
109. Larkin JM, Edwards WS, Smith DE, Clark PJ. Systemic thermotherapy: description of a method and physiologic tolerance in clinical subjects. *Cancer* 1977; **40:**3155-59.
110. Barologie B, Corry Pm, Yip E et al. Total body hyperthermia with and without chemotherapy for advanced human neoplasms *Cancer Res* 1979; **39:**1485-93.
111. Parks LC, Minaberry D, Smith DP, Neely WA. Treatment of far–advanced broncohogenic carcinoma by extracorporeally induced systemic hyperthermia. *J Thorac Cardiovasc Surg* 1979; **78:**883-92.
112. Van der Zee J, van Rhoon GC, Wike–Hooley JL, Faithfull NS, Reinhold HS. Whole–body hyperthermia in cancer therapy: a report of a phase I–II study. *Eur J Cancer Clin Oncol* 1983; **19:**1189-200.
113. Robins HI, Dennis WH, Neville AJ et al. A nontoxic system for 41, 80C whole body hyperthermia: Results of a phase I study using a radiant heat device. *Cancer Res* 1985; **45:**3937-44.
114. Herman TS, Zukoski CS, Anderson RM. Review of the current status of whole body hyperthermia administred by water circulation technique. *Natl Cancer Inst Monogr* 1982; **61:**365-9.
115. Levin W, Blair RM. Pettigrew technique of inducing whole–body hyperthermia. *Natl Cancer Inst Monogr* 1982;**61:**377-9.
116. Shen RN, Hornback NB, Lu L, Shidnia H. Effect of hyperthermia on NK cell activity in tumor–bearing mice and in advanced cancer patients (abstract). In Proceedings of International Clinical Hyperthermia Society Annual Meeting, Lund, June 14-7 1987:48.
117. Robins HI, Kalin N, Shelton SE et al. Neuroendocrine changes in patients undergoing whole body hyperthermia. *Int J Hyperthermia* 1987; **3:**99-103.
118. Bull JMC. A review of systemic hyperthermia. *Front Radiat Ther Oncol* 1984; **18:**171-6.
119. Robins HI, Longo WL, Steeves RA et al. A pilot study of whole body hyperthermia and local irradiation for advanced non–small cell lung confined to the torax. *Int J Radiat Oncol Biol Phys* 1988; **15:**427-31.
120. Hand JW, Gail ter Haar. Heating techniques in hyperthermia Introduction and assessment of techniques. *Br J Radiol* 1981; **54:**443-66.
121. Hand JW. Heat delviery and thermometry in clinical hyperthermia. *Rec Cancer Res* 1987; **104:**1-23.

122. Brezovich IA, Lilly MB, Durant JR, Richards DB. A practical system for clinical radiofrequency hypertermia. *Int J Radiat Oncol Biol Phys* 1981; **7:**423-30.
123. Doss JD. Calculation in electric fields in conductive media. *Med Phys* 1982; **9:**566-73.
124. Wiley JD, Webster JG. Analysis and control of the current distribution under circular dispersive electrodes. *IEEE Trans Biomed Eng* 1982; **29:**381-5.
125. Bach Andersen J, Baun A, Harmark K, Heinzl L, Rosmark P, Overgaard J. A hyperthermia system using a new inductive applicator. *IEEE Trans Biomed Eng* 1984; BME-**31:**21-7.
126. Guy AW, Lehmann JF, Stonebridge JB. Therapeutic application of electromagnetic power. *Proc IEEE* 1974; **62:55-75.**
127. Oleson JR. Hyperthermia by magnetic induction: I. Physical characteristics of the technique. *Int J Radiat Oncol Biol Phys* 1982; **8:**1747-56.
128. Storm FK, Harrison WH, Elliott RS, Silberman AW, Morton DL. Thermal distribution of magnetic loop induction hyperthermia in phantoms and animals: effect of the living state and velocity of heating. *Int J Radiat Oncol Biol Phys* 1982; **8:**865-71.
129. Vaguine VA, Tanabe E, Giebeler RH, McEven AH, Halin GM. Microwave direct-contact applicator system for hyperthermia therapy research. *Natl Cancer Inst Monogr* 1982; **61:461-4.**
130. Hand JW, Hind AJ, Cheetam JL. Multi-element microwave applicators for localised hyperthermia. *Strahlentherapie* 1985; **161:**535.
131. Fessenden P, Snderson TL, Marmor JB, Pounds B, Sagerman R, Strohbehn JW. Experience with a deep heating ultrasound system. *Rad Res* 1982; **91:**415.
132. Fessenden P. Ultrasound methods for inducing hyperthermia. *Front Radiat Ther Oncol* 1984; **18:**62-9.
133. Coughlin CT, Strohbehn JW, Interstitial thermoradiotherapy. *Radiol Clin N Amer* 1989; **27:**577-88.
134. Mechling JA, Strohbehn JW. A theoretical comparison of the temperature distributions produced by three interstitial hyperthermia systems. *Int J Radiat Oncol Biol Phys* 1986; **12:**2137-49.
135. Cosset JM, Dutreix J, Haie C, Gerbaulet A, Janoray P, Dewer JA. Interstitial thermoradiotherapy: a technical and clinical study of 29 implantations performed at the Institut Gustave-Roussy. *Int J Hyperthermia* 1985; **1:**3-13.
136. Strohbehn JW. Temperature distributions from interstitial RF electrode hyperthermia system: Theroretical predictions. *Int J Radiat Oncol Biol Phys* 1983; **9:**1655-67.
137. Emami B, Perez C, Leybovich L, Straube W, Vongerichten D. Interstitial thermoradiotherapy in treatment of malignant tumours *Int J Hyperthermia* 1987; **3:**107-11.
138. Strohbehn JW, Bowers ED, Walsh JE, Douple EB. An invasion microwave antenna for locally-induced hyperthermia for cancer therapy. *J Microw Power* 1979; **14:**339-50.
139. Taylor LS. Implantable radiators for cancer therapy by microwave hyperthermia. *Proc IEEE* 1980; **68:**142-9.
140. Trembly BS. The effect of driving frequency and antenna lenght on power deposition within an microwave antenna array used for hyperthermia. *IEEE Trans Biomed Eng BME* 1985; **32:**152-7.
141. Coughlin CT, Douple EB, Stronhbehn JW, Eaton WL, Trembly BS, Wong TZ. Interstitial hyperthermia in combination with brachytherapy. *Radolopgy* 1983; **148:**285-8.
142. Brezovich IA, Atkinson WJ. Temperature distributions in tumor models heated by self-regulating nickel-copper alloy thermoseeds. *Med Phys* 1984; **11:**145-52.
143. Brezovich IA, Meredith RF. Practical aspects of ferromagnetic thermoseed hyperthermia. *Radiol Clin N Amer 1989;* **27:**589-602.
144. Meredith RF, Brezovich IA, Weppelmann B et al. Ferromagnetic thermoseeds: suitable for an afterloading interstitial implant. *Int J Radiat Oncol Biol Phys* 1989; **17:**134-46.
145. Schreier K, Budihna M, Lesnicar H et al. Preliminary studies of interstitial hyperthermia using hot water. *Int J Hyperthermia* 1990; **6:**431-44.
146. Handl-Zeller L, karcher KH, Schreier K, Handl O. Optimierung interstitieller Hyperthermie-Systeme. *Strahlentherapie* 1986; **163:**460-3.
147. Lesnicar H, Budihna M, Handl-Zeller L, Schreier K. Interstitial water hyperthermia: temperature distribution data obtained in animal experiments compared to human application measurements. *Radiol Iugosl* 1989; **23:**295-7.
148. Budihna M, Lesnicar H, Handl-Zeller L, Schreier K. Animal experiments with interstitial hot water hyperthermia. In: Handl-Zeller L ed. *Interstitial hyperthermia.* Wien, New York: Springer (in press).
149. Jones KM, Mechling JA, Trembly BS, Strohbehn JW. SAR distribution for 915 MHz interstitial microwave antennas used in hyperthermia for cancer therapy. *IEEE Trans Biomed Eng* 1988; **35:**851-7.
150. Strohbehn JW, Douple EB. Hyperthermia and cancer therapy: A review of biochemical engineering contributions and challenges. *IEEE Trans Biomed Eng* 1984; BME-**31:**779-87.
151. Dickinson RJ. Thermal conduction errors of manganin-constantan thermocouple arrays. *Phys Med Biol* 1985; **30:**445-53.
152. Samulski TJ, Lyons BE, Britt RH. Temperature measurements in high thermal gradients: II analysis of conduction effect. *Int J Radiat Oncol Biol Phys* 1985; **11:**963-71.
153. Vaguine VA, Christensen DA, Lindley JH, Watson TE. Multiple sensor optical thermometry system for application in clinical hyperthermia. *IEEE Trans Biomed ENG* 1984; BME-**31:**168-72.
154. Waterman FM. The response of thermometer probes inserted into catheters. *Med Phys* 1985; **12:**368-72.
155. Nasoni RL, Bowen T, Dewhirst MW, Roth H. In vivo temperature dependence of the speed of sound in mammalian tissue and its possible use in hyperthermia. *Natl Cancer Inst Monogr* 1982; **61:**501-4.
156. Fallone BG, Moran PR, Podgorsak EB. Non-invasive thermometry with a clinical X-ray CT scanner. *Med Phys* 1982; **9:**715-21.

157. Ludeke KM, Kohler J. Microwave radiometric system for biomedical tissue temperature and emissivity measurements. *J Microwave Power* 1983; **18:**277-83
158. Liu RL, Zhang EY, Gross EJ, Cetas TC. Heating pattern of helical microwave intracavitary oesophageal applicator. *Int J Hyperthermia* 1989; **7:**577-86.
159. Astrahan MA, Sapozink MD, Cohen D, Luxton G, Kampp TD, Boyd S. Microwave applicator for transurethral hyperthermia of benign prostatic hyperplasia. *Int J Hyperthermia* 1989; **5:**283-96.
160. Fujimoto S, Shrestha RD, Kokobun M et al. Clinical trial with surgery and intraperitoneal hypertheric perfusion for peritoneal recurrence of gastrointestinal cancer. *Cancer* 1989;**64:**154-60.

Chapter VI. RADIOPHYSICS

Adv Radiol Oncol 1992; 301–10.

Radiosurgery: A review of physical aspects

Podgoršak EB[1] and Souhami L[2]

[1]Departments of Medical Physics and [2]Radiation Oncology, Montreal General Hospital, McGill University, Montréal, Canada

Radiosurgery, in conjunction with stereotaxy, is a focal irradiation technique used in treatment of small intracranial structures or lesions. Its main goal is to deliver with a high degree of spatial accuracy a large radiation dose to the targeted volume within the brain, concurrently with as small as possible a dose to the rest of the brain tissue. The radiation sources and beams currently used in radiosurgery are cobalt beams from gamma units, heavy charged particles from cyclotrons, and high energy x-rays from linear accelerators. The relative ease with which isocentric linear accelerators can be modified for radiosurgery, combined with their wide availability in major medical centers, in recent years has resulted in great interest in radiosurgery and a rapid proliferation of medical centers offering this treatment modality. In this paper the historical background and physical aspects of radiosurgery are discussed in general. Various contemporary radiosurgical techniques using protons, gamma rays or x rays are briefly discussed. It is shown that linear accelerator-based radiosurgery can be considered an inexpensive alternative to the traditional and expensive methods of radiosurgery with the gamma unit or proton beams. The techniques for target localization and treatment planning for radiosurgery are also addressed.

Key words: radiosurgery, stereotaxy, linear accelerator, brain irradiation, small field radiotherapy

Introduction

Of the recent new techniques in radiotherapy, it is the introduction of radiosurgery that has created the most interest and excitement. In standard radiotherapy a total dose of several thousand cGy is given to a relatively large target volume in daily fractions of about 200 cGy each. Radiosurgery, on the other hand, is a focal brain irradiation technique which delivers in a single session a high dose of ionizing radiation (few 1000 cGy) to small (few cm^3), preselected and stereotactically localized intracranial structures or lesions. A stereotactic frame is an integral component of all radiosurgical techniques and is used for accurate target localization, treatment setup, and patient immobilization during the treatment. The requirements for the accuracy in target localization and for the subsequent spatial and numerical precision of dose delivery to the target are considerably more stringent in radiosurgery than in radiotherapy, because in radiosurgery very small volumes in the immediate vicinity of vital structures within the brain are treated with a high radiation dose in a single session.

Radiosurgery was in clinical use since the early 1950s and is thus by no means a new treatment

Correspondence to: Dr. Ervin B. Podgoršak, Department of Medical Physics, Montreal General Hospital, McGill University, 1650 avenue des Cèdres, Montréal, Québec, Canada H3G 1A4.

UDC: 616.831-006.6:615.849

modality. It is, however, new to radiotherapy departments, because until recently it was practiced with highly sophisticated and expensive equipment (proton cyclotron and gamma unit) only in a few specialized neurosurgical centers around the world. These centers have obtained excellent results in the treatment of functional disorders and inoperable vascular malformations. The treatments, however, were very expensive and therefore not widely available. The introduction of new imaging modalities, combined with the development of radiosurgical techniques based on isocentric linear accelerators (linacs) has recently introduced these techniques to radiotherapy departments and thus made them more practical, less expensive, and potentially available in most major medical centers.

Four groups of intracranial diseases are currently treated with radiosurgery: vascular malformations, functional disorders, well circumscribed benign or malignant primary tumours, and solitary metastatic tumours. The treatment of the first group is now considered routine and follows fairly standard protocols. The treatment of the latter three groups, on the other hand, is still experimental and the treatment protocols are only now being developed. The radiations that are currently used in radiosurgery are gamma rays from gamma units, protons or heavier ions, such as helium, carbon, and neon, from cyclotrons or synchrocyclotrons, megavoltage x rays from linacs, or neutrons from neutron generators.

Historical background

The term *»radiosurgery«* and the technique itself were introduced in 1951 by Leksell[1], a Swedish neurosurgeon. Leksell initially used 200 kVp x rays approaching the stereotactically determined intracranial target from several directions to concentrate the dose in the target and spare the surrounding vital brain structures as much as possible. However, it soon became apparent that x rays in the orthovoltage range (100 – 350 kVp), even when used in a large number of beams focused onto the target, are not penetrating enough to produce dose distributions with a uniform dose inside the targeted volume and a sharp dose falloff outside the target. Therefore, radiosurgery based on orthovoltage x rays was discontinued in the late 1950s. The idea of focal irradiation, however, was carried over to other more penetrating radiation beams, first in the late 1950s to protons from cyclotrons, then in the late 1960s to focused cobalt-60 gamma ray beams from gamma units and more recently to megavoltage x rays from linacs.

The high costs of cyclotrons and gamma units combined with difficulties in stereotactic target localization have ensured that for a long time radiosurgery was available in only a few specialized neurosurgical centers around the world. However, the excellent clinical results that these centers obtained with radiosurgery and improvements in target localization through advances in new imaging modalities, such as computerized tomography (CT), digital subtraction angiography (DSA), and magnetic resonance imaging (MRI), introduced in 1970s, have stimulated a search for new, preferably less expensive, yet as effective, radiosurgical techniques.

Linacs were first proposed as radiation sources for radiosurgery by Larsson and co-workers[2] in 1974 and by the mid-1980s several radiosurgical techniques based on isocentric linacs in the 4-20 MV range were developed. The earliest reports on clinical linac-based radiosurgery were published in 1984 by Betti and Derechinsky[3] and in 1985 by Colombo and colleagues[4] and Hartmann and co-workers.[5] In 1986 linac-based radiosurgery was started in North America in Boston and Montréal. Radiosurgery achieved such a growth in subsequent years that by 1991 some 80 centers in the United States were offering or seriously considering to offer this treatment modality.

In the late 1980s there were also advances in radiosurgery with particle beams, most notably with heavier charged particles, such as helium, carbon, or neon from synchrocyclotrons.[6] A radiosurgical technique with neutrons from an isocentrically mounted cyclotron has also been reported recently.[7]

Radiosurgical techniques

Stereotactic frames

All current radiosurgical techniques rely on stereotactic frames for target localization, treatment setup, and patient immobilization during the dose delivery. The stereotactic frame is a rigid device in the form of a hollow cube or cylinder, which is fastened with pins to the patient's head. With modern imaging modalities, Cartesian or cylindrical coordinates of any arbitrary point within the cranium can be determined with respect to the origin of the stereotactic frame. Subsequently, assuming that the frame remains rigidly attached to the cranium, the same points may be accessed either invasively (stereotactic biopsy or surgery) or non-invasively with radiation beams (radiosurgery). A stereotactic frame* attached to patient's skull in preparation for radiosurgery is shown in Figure 1. The coordinates of the target center are marked on the target localization plates which are attached to the stereotactic frame.

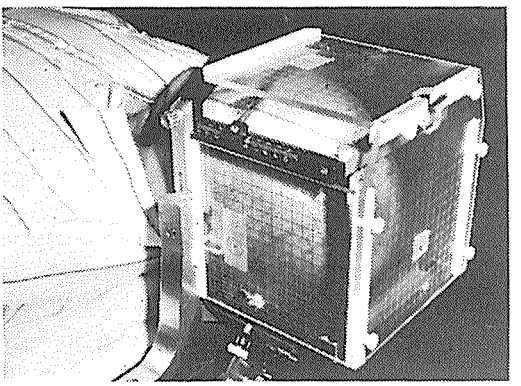

Figure 1. A stereotactic frame (Olivier, Bertrand, Tipal stereotactic frame, Tipal Instruments, Ltée, Montréal, Canada) attached to patient's skull in preparation for radiosurgery. Coordinates of target center are marked on the target localization plates which are attached to the stereotactic frame.

The intracranial targets are stereotactically localized with one or more of three modern imaging modalities: CT, MRI, and DSA. The target localization with the first two modalities is based on a set of transverse scans and special fiducial makers on the stereotactic frame, while that with the DSA is based on two orthogonal images: anteroposterior and lateral. Several manufacturers world-wide now offer stereotactic frames that are compatible with modern imaging equipment and can be adapted for radiosurgery. Compatibility with CT implies that the frame is made of low-atomic-number materials, such as plastics or aluminum, to minimize the interference of the frame with the diagnostic CT x ray beam. An MRI-compatible frame is made of non-ferous materials and designed in such a way that closed-current loops within the frame structure are avoided during the MR imaging.

Radiosurgery with heavy charged particles

The cyclotron-produced proton beam radiosurgery originated in the late 1950s with the work of Larsson and Leksell in Uppsala, Sweden[8]. Soon thereafter, it was introduced in Berkeley, California by Lawrence and colleagues[9] and later in Boston by Kjellberg and associates.[10] The technique is based on advantageous Bragg peak dose distributions, which result from the Coulomb interactions (collisional losses) of proton or heavier ion beams with the atoms and nuclei of brain tissues. The dose distribution curve for a heavy charged particle beam penetrating a medium shows that the energy loss at the surface is relatively small. At larger depths in the medium, however, the rate of energy loss increases slowly as the particle velocity decreases. Near the end of the range, where the particle has little energy left and is traveling slowly, the rate of energy loss suddenly increases (Bragg peak) and then falls to zero as the particle comes to rest at a depth referred to as the particle range in the medium. The particle range and the position of the Bragg peak are proportional to the initial energy of the charged particle and inversely proportional to the atomic number of

* Olivier, Bertrand, Tipal stereotactic frame, Tipal Instruments, Ltée, Montréal, Canada

the attenuating medium as well as the mass and charge of the particle.

The relative magnitude of the Bragg peak dose, which is about 3 times as large as the surface dose, may be used in charged particle radiosurgery to concentrate the dose in the targeted volume. The differential between the dose inside and the dose outside the target is further increased by approaching the target with several beams (typically 6 to 12) from different directions in order to concentrate the dose in the target and spread the dose outside the target over as large a volume as possible.

In principle, the Bragg peak radiosurgical technique seems simple. In practice, however, it has several problems in addition to being expensive. First, the Bragg peak in the beam direction is too narrow (typically 5 mm) to encompass most intracranial targets with a single beam. This can be overcome by superimposing beams of various energies or by attenuating the beams with bolus materials to broaden the Bragg peak. In this case the target will be covered from a single beam direction but the differential between the net target dose and the net surface dose will largely be lost. Some of this differential is recovered by using multiple beams pointing toward the target, as discussed above. The second problem is that, as the beam aproaches the target from various directions, the exact distance between the target center and the surface of the cranium has to be determined with stereotactic procedures in order to place the Bragg peak into the target center for each individual beam. This makes radiosurgery with the charged particle Bragg peaks complicated and labor intensive.

It is interesting to note that in Moscow, Russia a proton beam radiosurgical technique was developed which uses protons of sufficiently high energies for the Bragg peak to occur beyond the beam exit point at the opposite side of the cranium (i.e., outside the patient) for all beam directions. The target is then in the beam crossfire from all directions, however, all the dose-differential advantages of the Bragg peak are lost. The Moscow technique is considerably simpler than the Bragg peak technique used in Sweden and the United States, but it gives a shallower dose falloff outside the target than the charged particle technique based on Bragg peaks.

Radiosurgery with the gamma unit

Concurrenly with using proton beams for radiosurgery, Leksell was also developing a dedicated radiosurgical unit based on cobalt-60 gamma ray beams. A prototype of this unit was used clinically by 1968 and contained 179 cobalt sources, spread uniformly over a spherical segment of 60^{o} x 160^{o}[11]. Each source produced a circular beam, which was aimed toward the focus within the unit. This unit subsequently evolved into the commercially available gamma unit*, currently incorporating 201 cobalt-60 sources and sometimes referred to as the gamma knife*. The sources have a nominal activity of 1 TBq (30 Ci) and a half-life of 5.3 years. The 201 circular beams are all collimated with a primary collimator and directed toward the focus of the unit with a relatively short source-focus distance of 39.5 cm.

The final collimation is achieved by one of the special helmets which contain 201 tungsten collimators precisely positioned such that they align with the primary collimators when the treatment couch reaches the treatment position. The helmets produce circular beams with diameters in the range form 8 mm to 18 mm, which implies that the targeted volumes to be treated are spherical with diameters from 8 to about 18 mm. The patient is positioned stereotactically with respect to the helmet in such a way that the center of the targeted volume coincides with the focal spot of the unit when the shutter of the unit is opened and the patient is brought into the treatment position. A photograph of a typical patient setup on a gamma unit is shown in Figure 2, whereas the points of beam entry on the patient's head for the gamma unit are shown in Figure 3*a*.

* Electa Instruments, AB, Stockholm, Sweden

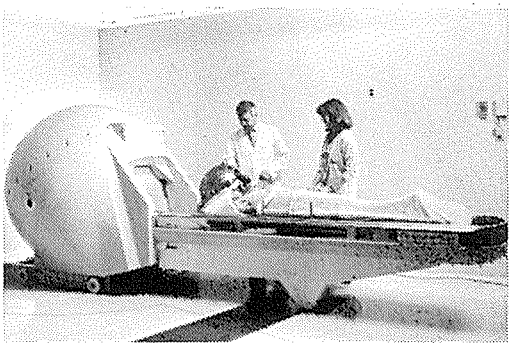

Figure 2. Patient prepared for treatment on a gamma unit (photo: courtesy of Electa instrument AB, Stockholm, Sweden).

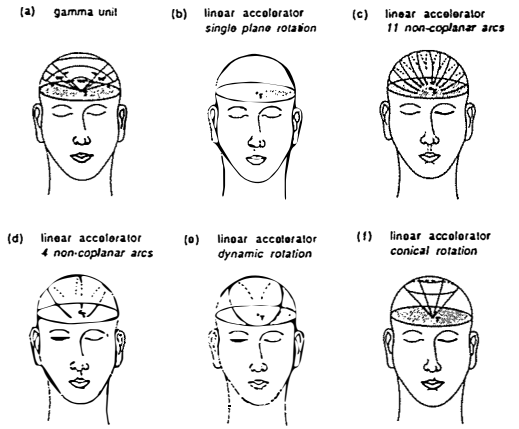

Figure 3. Points of beam entry into the patient's skull for various radiosurgical techniques.

The gamma unit represents a very practical and elegant solution to radiosurgery. Its main drawbacks, however, are its considerable cost and a dedicated operation, which limits its use only to treatment of small brain lesions. These drawbacks ensure that gamma units will never become widely available, since the capital and operating costs (source changes) are prohibitive for most medical centers even in the industrialized world. Nonetheless, there are close to a dozen gamma units currently in clinical operation around the world and several thousand patients have been treated successfully with the unit to date. Because the unit is commercially available and has been proven clinically, it can be applied as a standard against which any new technique for radiosurgery can be measured.

Linac-based radiosurgery

Linacs used for radiosurgery are isocentrically mounted and normally used for routine cancer therapy. The modifications and additions needed to adapt modern isocentric linacs to radiosurgery are relatively simple and inexpensive, and typically consist of a set of additional collimators to define the small, circular radiation beams with diameters from 5 mm to 35 mm; a remotely controlled motorized couch or treatment chair rotation; brackets or a floor stand for mounting the stereotactic frame; interlocked readouts for angular and height positions of the couch; and special brakes to immobilize the longitudinal and lateral couch motions during the treatment.

Figure 4 shows two typical patient setups for linac-based radiosurgery. In both setups the patients are supine on the treatment couch, however, in part (a) the stereotactic frame is attached to a floor stand which in turn is bolted to the pedestal of the treatment couch, while in part (b), the stereotactic frame is fastened directly to the treatment couch. The latter couch mounting is safer, as any inadvertent couch motion does not pose a safety hazard to the patient. Moreover, the patient setup with the direct couch mounting is easier and the gantry rotation below the patient is unimpeded. The two setups in Figure 4 also show two different commericially available stereotactic frames and two different collimators used to produce the small diameter circular radiation fields.

The requirements on mechanical stability of linacs are even more stringent in radiosurgery than in routine radiotherapy. All current clinical linac-based radiosurgical techniques involve rotations of the gantry and the treatment couch or chair. Therefore, the isocenter of the linac, which is the point of intersection between the horizontal gantry rotation axis and the vertical rotation axis of the couch or chair, should be

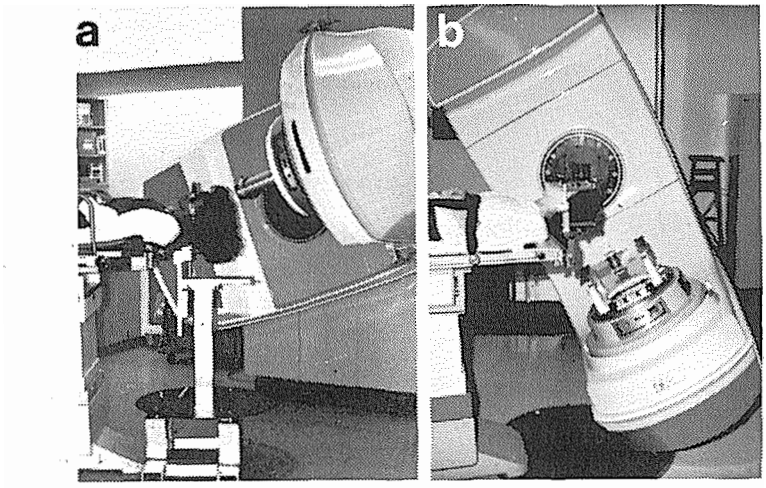

Figure 4. Two typical patient setups for linac-based radiosurgery: (a) the technique used by the Joint Center for Radiation Therapy in Boston, USA: patient on treatment couch, stereotactic frame attached to a floor stand (photo: courtesy of Dr. J.S. Loeffler). (b) The McGill technique used in Montréal, Canada: patient on treatment couch, the stereotactic frame fastened directly to the couch. Two different stereotactic frame models and two designs for the special collimators that define the circular x-ray fields also can be seen.

within ±1 mm for any arbitrary gantry and couch or chair position. Specifications for standard radiotherapy usually state an isocenter accuracy within ± 2 mm, yet, despite the complexities in equipment design and the considerable weight of the gantry and the couch, manufacturers of modern linacs can, with some effort, meet the ±1 mm specification. Unlike linacs, no parts of the gamma unit move during the treatment, thus its theoretical isocenter accuracy is within a fraction of a milimeter and is limited only by the machining precision of the collimator helmets. Although the isocenter accuracy achievable with linacs is inferior to that of the gamma unit, it is of the same order of magnitude as the target localization accuracy possible with modern imaging techniques (also within ±1 mm), and therefore can be considered acceptable.

The linac-based radiosurgical techniques are characterized by the particular approach they take toward fulfilling the goal of delivering the prescribed dose to the target with a sharp dose fall-off outside the target volume. The techniques rely on specific combinations of the linac gantry and treatment counch/chair rotations, and currently fall into four categories: *single plane rotation, multiple non-coplanar converging arcs, dynamic rotation, and conical rotation.* The convention used here for rotations of the gantry (angle ϕ) and couch or chair (angle θ) of linacs is shown in Figure 5.

Developed by Houdek and co-workers at the University of Miami[12], the *single plane rotation* is the simplest radiosurgical technique. It is similar to rotational techniques used in standard radiotherapy, except that in radiosurgery the radiation field is very small, the dose is given in a single session, and a stereotactic frame is used for treatment setup and patient immobilization during the treatment. The patient is placed supine on a stationary couch ($\phi = 0^\circ$), and the gantry rotates from $\theta = 0^\circ$ to $\theta = 360^\circ$ during the treatment. In the direction perpendicular to the plane of rotation, the dose falloff outside the targeted volume is very steep, but in the plane of rotation (transverse plane), it is very shallow as a result of the dose superposition outside the target of an infinite number of parallel-opposed beams. The shallow dose falloff in the transverse plane produces dose distributions which compare unfavorably with those obtained for the gamma

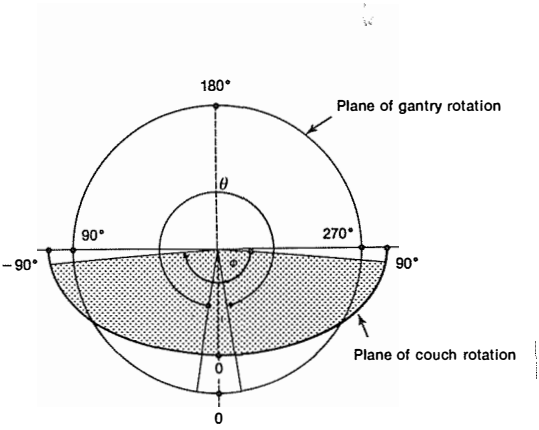

Figure 5. Schematic representation of the gantry (angle θ) and couch (angle ϕ) rotational motions for linac--based radiosurgical procedures.

unit. This then precludes the use of single plane rotation in contemporary radiosurgery. The beam entry trace for a full single plane rotation is in a transverse plane and coincides with the beam exit trace, as shown in Figure 3*b*.

To improve the dose falloff outside the targeted volume, Betti and Derechinsky[3], Colombo and colleagues[4], and Hartmann and colleagues[5], devised the *multiple noncoplanar converging arcs* technique on isocentric linacs. A series of arcs, each with a different stationary position of the treatment chair[3] or couch[4,5], is used to spread the dose outside the targeted volume over as large a volume as possible. The angles of arcs are usually smaller than 180° to avoid parallel-opposed beams in the plane of the arc. Hartmann's group in Heidelberg has used up to 11 arcs, each either from 20° to 160° or from 200° to 340°, depending on the treatment couch position. The beam entry traces on the patient's head for the Heidelberg technique are shown in Figure 3*c*. Lutz and coworkers at the Joint Center for Radiotherapy in Boston have shown that reasonable dose fall'offs can be obtained with only 4 arcs[13]. The stereotactic frame is attached to a floor stand, as shown in Figure 4*a*, and one 260° arc is given in the transverse plane (couch angle $\phi = 0°$) from $\theta = 50°$ to $\theta = 310°$, and 100° arcs are given with couch angles ϕ of 90°, 45°, and -45°. The beam entry traces on the patient's head for this technique are shown in Figure 3*d*. Currently, in Boston four to nine noncoplanar arcs are used in clinical radiosurgery, depending on the size, type, and location of the target treated.

The *dynamic radiosurgery* method was developed by Podgorsak and colleagues at McGill University in Montréal.[14,15] A 10 MV isocentric linac is used, with the patient in the supine position on the treatment couch. The stereotactic frame is attached directly to the couch, as shown in Figure 4*b*. The main feature of the dynamic rotation is the continuous and simultaneous rotation of the gantry and couch during the treatment. The gantry rotates 300° from θ=30° to $\phi = 330°$ and the couch 150° from $\phi = 75°$ to our error $\phi = -75°$. Thus, each degree of couch rotation corresponds to two degrees of gantry rotation. The beam entry trace on the patient's skull has a peculiar pattern (see Figure 3*e*) but always lies in the upper hemisphere, causing all beam exit points to lie in the lower hemisphere. Thus, even though all beams intersect in the targeted volume and the gantry travels almost a full circle (300°), there never is a parallel-opposed beam situation which would degrade the steepness of the dose falloff outside the target.

Recently, McGinley and associates from Emory University in Atlanta[16] originated a linac-based radiosurgical technique in which the patient rotates on a special treatment chair from ϕ=0° to ϕ=360°, while the gantry is stationary at a given angle θ between 90° and 180°. The stereotactic frame is attached to a pedestal, which in turn is mounted to the base plate of the patient support assembly. Up to three gantry positions (θ=100°, 120°, and 145°) are used for a typical treatment, resulting in coaxial circles for beam entry traces in the upper hemisphere and a conical irradiation pattern, as illustrated for two gantry positions in Figure 3*f*.

Computerized treatment planning for radiosurgery

In radiosurgery, as discussed above, the goal of minimizing the dose to tissues surrounding the

targeted volume for a given target dose is achieved by aiming the radiation beam toward the target from a large number of noncoplanar directions. The calculation of radiosurgical dose distributions is therefore a 3-dimensional problem that cannot be handled with 2-dimensional techniques used in standard radiotherapy treatment-planning computers. Radiosurgical treatment planning is based on stereotactic 3-dimensional data obtained from CT, MRI, or DSA in conjunction with stereotactic frames. Target localization within the stereotactic frame coordinates is an important component of the dose calculation algorithm. In addition, information about the patient's anatomical contours, which is obtained from a series of CT or MR images, also plays an important role in the calculation of the dose distribution, providing the appropriate depth in tissue for each point-of-interest on the dose calculation matrix, thus enabling an accurate calculation of dose for each individual radiation beam. The patient's anatomic information, obtained with CT, MRI or DSA, usually is displayed on orthogonal planes through the target. In radiosurgery, it is imperative that the calculated dose distribution be directly superimposed onto the clinical CT, MR or DSA images, so that doses are known not only within the targeted volume but also to sensitive brain structures outside the target.

Until recently, the few centers that offered radiosurgery also developed their own 3-dimensional radiosurgical treatment planning systems. The recent rapid proliferation of linac-based radiosurgery, however, provided the incentive for development of commercial radiosurgical treatment planning systems and currently several such systems are available, offering various degrees of sophistication. It is essential that each medical center introducing clinical radiosurgery has access to a reliable 3-dimensional target localization and treatment planning system.

In Figure 6, we show a few typical examples of radiosurgical treatment plans. The dose distributions were calculated with the McGill treatment planning system and algorithm developed by Pike et al.[17] for four linac-based radiosurgical

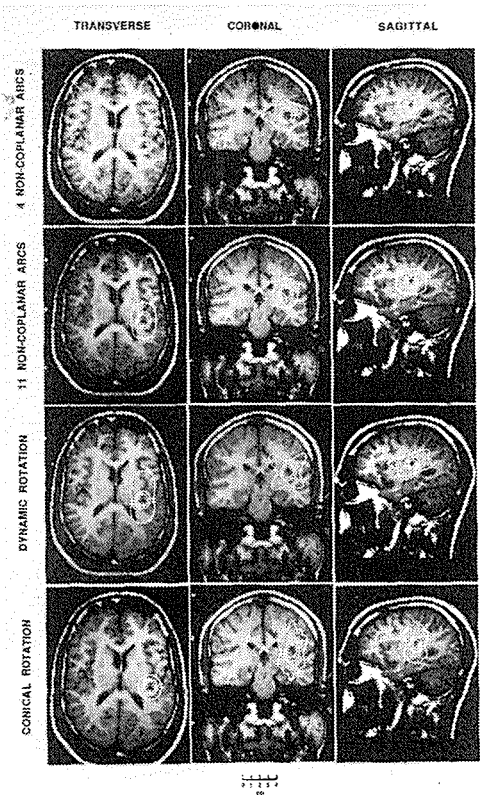

Figure 6. Isodose distributions calculated with the McGill treatment planning system[17] for various linac-based radiosurgical techniques. The calculated dose distributions are normalized to 100% at the isocenter and directly superimposed onto the transverse, coronal, and sagittal MRI slices of a typical patient. The radiation beam energy and diameter were 10 MV and 1.5 cm, respectively. The 90% isodose surface covers the spherical target volume with a diameter of 1.5 cm, the other isodose surfaces displayed are 50% and 10%.

techniques in clinical use: Boston 4 noncoplanar arcs, Heidelberg 11 noncoplanar arcs, McGill dynamic rotation, and Emory conical rotation. The beam energy and diameter were 10 MV and 1.5 cm, respectively, the lesion, located in the left deep parietal region, was spherical with a diameter of 1.5 cm. The dose distribution is normalized to 100% at the isocenter, the isodose surfaces dispayed are 90%, 50% and 10%, directly super-imposed on the patient's transverse, coronal and sagittal MR slices through the target center.

Several features of the dose distributions of Figure 6 are immediately apparent: (i) the dose falloff estimated from the distance between the 90% and 10% isodose surfaces is reasonably sharp for all techniques, however, the falloff depends on the direction of measurement, (ii) the 90% isodose surface is spherical and covers the targeted volume, (iii) the 50% isodose surface, similarly to the 90% isodose surface, is essentially isotropic, irrespective of the treatment technique, (iv) for all techniques the dose falloff from the 90% to the 50% isodose surface is very sharp, on the order of a few mm, (v) from the 90% at the edge of the targeted volume down to the 50% isodose surface, the four radiosurgical techniques give essentially the same isodose distributions in spite of the considerable differences in methods they employ for dose delivery, and (vi) the 10% isodose surfaces are anisotropic and their shapes reflect the particular dose delivery technique used.

Each radiosurgical technique may be characterized by the sharpest and shallowest dose falloffs outside the targeted volume, with all other falloffs situated between the two extremes. The closer the two are to each other, the more isotropic is the dose distribution and the better satisfied is the radiosurgical requirement for a sharp dose falloff outside the target. From Figure 6 one may conclude that the Heidelberg technique gives the most isotropic dose distribution, i.e., the sharpest dose falloff outside the target. It turns out, however, that from 90% down to 20%, all clinically used linac-based techniques exhibit very similar dose falloff characteristics and that only in the dose region below the 20% surface the dose falloffs for techniques with a larger number of arcs are sharper. However, the 20% isodose surface is usually in the range of normal brain tissue tolerance dose and a sharp dose falloff in this region is no longer of vital importance. The dose falloff characteristics are therefore not a determining factor in the choice of a particular linac-based technique for clinical use. Other factors, such as simplicity of operation, availability of technical help, availability of an appropriate target localization and treatment planning system, and the ingenuity of staff, decide on which technique to introduce clinically.

A comparison of dose falloffs for linac-based techniques to those obtained recently for the gamma unit[18], shows that from the dose falloff point-of-view, radiosurgery with noncoplanar arcs, dynamic rotation, or conical rotation is comparable to radiosurgery with the gamma unit. A detailed comparison among various photon beam radiosurgical techniques and a study of the adequacy of linacs for radiosurgery have been published recently.[19,20]

Conclusions

During the past five years, radiosurgery has developed from a relatively obscure neurosurgical technique, for three decades practiced in only a few specialized medical centers around the world, into a sophisticated radiotherapeutic technique that most major medical centers use or plan to use in the near future. The recent rapid proliferation of radiosurgery was timulated by the following: (i) excellent treatment results, both short term and long term, were obtained during the past three decades by the pioneers in the field, (ii) new imaging modalities that greatly facilitated the target localization were introduced in the 1970s (computerized tomography) and 1980s (magnetic resonance imaging and digital subtraction angiography), (iii) radiosurgical techniques were developed on linear accelerators making radiosurgery much less expensive and therefore more widely available in comparison with the traditional techniques based on gamma units or protons from cyclotrons, and (iv) radiosurgical target localization programs based on stereotactic frames and 3-dimensional treatment planning systems became commercially available.

The basic requirement for radiosurgery, which in essence is the delivery of prescribed dose to the targeted volume with a high degree of spatial and numerical accuracy combined with a sharp dose falloff outside the targeted volume, can be adequately met by isocentric linear accelerators.

It should be remembered, however, that technical and clinical requirements for radiosurgery are far more stringent than those applied to standard radiotherapy. No matter what equipment it employs, radiosurgery is a complex treatment modality for which a successful clinical outcome requires a collaborative team effort by several hospital–based professionals, including neurosurgeons, radiation oncologists, neuroradiologists and medical physicists.

The clinical aspects of radiosurgery are discussed in the Chapter IV Clinical oncology.

References

1. Leksell, L. The stereotaxis method and radiosurgery of the brain. *Acta Clin Scan* 1951; **102:**316-9.
2. Larsson B, Liden K, Sarby B. Irradiation of small structures through intact skull. *Acta Radiol* TPB 1974; **13:**513-34.
3. Betti OO, Derechinsky VE. Hyperselective encephalic irradiation with linear accelerator. *Acta Neurochirurgica* 1984; Supl. **33:**385-90.
4. Colombo F, Benedetti A, Pozzo F, Avanzo RC, Marchetti C, Chierego G, Zanardo A. External stereotactic irradiation by linear accelerator. *Neurosurgery* 1985; **16:**154-60.
5. Hartmann GH, Schlegel W, Sturm V, Kober B, Pastyr O, Lorenz WJ. Cerebral radiation surgery using moving field irradiation at a linear accelerator facility. *Int J Radiat Oncol Biol Phys* 1985; **11:**1185-92.
6. Lyman JT, Kanstein L, Yeater F, Fabricant JI, Frankel KA. A helium-ion beam for stereotactic radiosurgery of CNS disorders. *Med Phys* 1986; **13:**695-99.
7. Griffin BR, Warcola SH, Mayberg MR. Stereotactic neutron radiosurgery for arteriovenous malformations of the brain. *Medical Dosimetry* 1988; **13:**179-82.
8. Larsson B, Leksell L, Rexed B, Sourander P, Mair W, Anderson B. The high energy proton beam as a neurosurgical tool. *Nature* 1958; **182:**1222-3.
9. Lawrence JH, Tobias CA, Born JL, Wang C, Linfoot JA. Heavy particle irradiation in neoplastic and neurologic disease. *J Neurosurg* 1962; **19:**717-22.
10. Kjellberg RN, Shintani A, Frantz AG, Kliman B. Proton beam therapy in acromegaly. *N Eng J Med* 1968; **278:**689-95.
11. Leksell L. Cerebral radiosurgery I. Gamma thalamotomy in two cases of intractable pain. *Acta Clin Scand* 1968; **134:**585-95.
12. Houdek PV, Fayos JV, Van Buren JM, Ginsberg MS. Stereotaxis radiotherapy technique for small intracranial lesions. *Med Phys* 1985; **12:**469-72.
13. Lutz W, Winston KR, Maleki N. A system for stereotactic radiosurgery. *Appl Neurophysiol Int J Radiat Oncol Biol Phys* 1988; **14:**373-81.
14. Podgorsak EB, Olivier A, Pla M, Hazel J, deLotbinière A, Pike BG. Physical aspects of dynamic stereotactic radiosurgery. *Appl Neurophysiol* 1987; **50:**263-8.
15. Podgorsak EB, Olivier A, Pla M, Lefebvre PY, Hazel J. Dynamic stereotactic radiosurgery. *Int J Radiat Oncol Biol Phys* 1988; **14:**115-25.
16. McGinley PH, Butker EK, Crocker IR. A patient rotator for stereotactic radiosurgery. *Phys Med Biol* 1990; **35:**649-57.
17. Pike BG, Podgorsak EB, Peters TM, Pla C. Dose distributions in dynamic stereotactic radiosurgery. *Med Phys* 1987; **14:**780-9.
18. Walton L, Bomford CK, Ramsden D. The Sheffield sterotactic radiosurgery unit: physical characteristics and principles of operation. *Br J Radiol* 1987; **60:**897-906.
19. Podgorsak EB, Pike GB, Olivier A, Pla M, Souhami L. Radiosurgery with high energy photon beams: a comparison among techniques. *Int J Radiat Oncol Biol Phys* 1989; **16:**857-65.
20. Podgorsak EB, Pike GB, Pla M, Olivier A, Souhami L. Radiosurgery with photon beams: physical aspects and adequacy of linear accelerators. *Radiother Oncol* 1990; **17:**349-58.

Adv Radiol Oncol 1992; 311–22.

A survey of radiation biophysics for the radiotherapist

Bistrović M

Central Institute for Tumours, Zagreb

The present paper is a short introduction into the contemporary radiobiology from the point of interest of a radiotherapist. The basic concepts of cellular radiobiology were represented on the experimental model of cells cultivated in dishes under specific conditions. The linearquadratic model of cell survival and the concept of the repair of sublethal damage (Elkind repair) were explained by the theory of dual radiation action. Assuming that there is no essential difference between cells in a tissue and those in a dish, the difference between early and late responding tissues was derived from the shape of the survival curve. Since the total dose in a radiotherapy treatment is delivered either in fractions or continuously in the due course of time, particular attention was paid to the repair and proliferation phenomena playing an important role regarding the final effect on cells.

Key words: radiotherapy; biophysics

Introduction

The LQ-model of cell survival, although not revolutionary from the point of view of standard fractionation schedules, allows the the rapist to understand better which alterations can be expected in tumour and normal tissue reactions after the schedule has been modified.

Namely, the new model compares the effects of radiation on various types of tissue characterized by specific parameters. Therefore the new concept requires a better knowledge of radiobiology.

This paper aims to enlighten the approach to the radiobiological background involved in various types of fractionation schedules.

Correspondence to: Prof. dr. Matija Bistrović, Central Institute for Tumours, Ilica 197, 41000 Zagreb, Croatia.

UDC: 615.849:539.1

Normal tissue, tumours and the response to radiation

The radiatherapist must distinguish two types of normal tissue. One, H-type[10], consists of hierarchically organized cells growing from stem cells. Stem cells divide and after a few generations of differentiation they mature for the role they will play within the organism. The original stem cells have a long doubling time because their role is to save the genetic material for any later need for renewal of the functional tissue. However, the transit cells which participate in the maturation sequence have a short doubling time. So they will rapidly renew the functional strain of cells which are usually short living. The entire cell system is balanced by a feed-back mechanism causing the enhancement of stem cells' division if the rate of mature cell production is too low.

H-type tissues are bone marrow (haematopoietic system), epidermis, gastrointestinal mucosa and other mucosae.

The other type of tissue, flexible or F-type, consists of highly differentiated functional cells with very long doubling time or not dividing at all i.e. resting in G_o phase. The damaged tissue will substitute the lost number of cells very slowly and with difficulty. If there is any cell division, it will preserve the degree of differentiation of the mother cells. F-type cells are those of the lung, brain, liver, kidney, urether, spinal cord etc.

The irradiated cells do not necessarily die and can repair radiation damage i.e. save their reproductive ability. The severely damaged cells will die after the first division or will lose an entire posterity after a few divisions. Therefore, every tissue has a characteristic latency period after which the cell damage will become visible on tissue.

In H-type tissue the transit cells rapidly divide and the degradation of functionality will take place after the entire maturation sequence is finished. After the latency period repopulation, an accelerated division in stem cells will start, in order to compensate the loss of functional cells. In the bone marrow and in the gastrointestinal mucosa the latency takes 1-2 days, and in the epidermis and other mucosae 14-21 days. Since these latencies are relatively short, H-type tissues are also known as early responding tissue. On the other hand, in F-type tissues the latency period is very long because of a large number of cells resting in G_o phase. In this way functional damage can appear after many months and even years. These are late responding tissues.

Tumour cells have a relatively short dividing cycle and die soon after irradiation. Therefore, they may be considered to be early responding tissue. In so far as tumour tissue is not functional at all, the question of differentiation is pointless.

Radiotherapists who irradiated head and neck tumours using the split course techniques[3] observed that an additional dose was required to obtain a cure rate equivalent to that achieved with conventional fractionation. This showed that tumour cells divided during the therapy. Thus, if we whish to kill the tumour we have to kill the most rapidly growing cells and our fractionation schedule must overtake the growth rate. The effective doubling time of that cell line is usually called potential doubling time and denoted by T_{pot} or T_p; it can be determined either by a careful analysis of results of radiotherapy or by specific measurements on tumour samples in laboratory[12]. Recently, efforts have been made to introduce the routine measurement of T_p into the clinical practice.

The linear-quadratic model of survival curve

Most of our knowledge about the irradiation of human cells originates from the experiments with mammalian cells in culture. Various cell lines of animal and human origin are cultivated for years in an adequate liquid medium in Petri dishes. They can be separated in single cells, implanted in new dishes where they will attach to the bottom. In convenient circumstances (37°C and humidified atmosphere with 5% CO_2 in a thermostat and adequate growth medium) they will grow exponentially. This means that the number of cells will be reduplicated after the doubling time T_r. The factor of cell multiplication is given by

$$F = e^{0.693*T/Tr)} \qquad [1]$$

where e = 2.713.

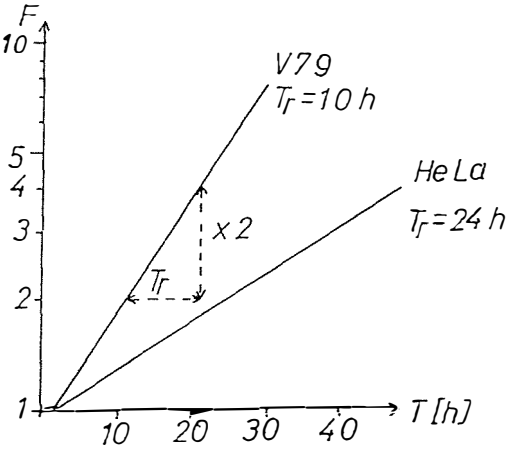

Figure 1. Cell number growth. After a short delay the number of cells increases exponentially.

In a semilog coordinate system (T, F) the exponential growth is represented as a climbing straight line (Fig. 1).

In this representation equal shifts along the ordinate mean multiplication by a factor > 1. Thus, if T increases by T_r, the ordinate F will always increase by an equal shift meaning multiplication by two. Typical mammalian cells are HeLa cells and V79 cells with respective doubling times of 24h and 10h.

Experiments are usually carried through by irradiating the cells immediately after they have been attached to the dish bottom. After the experiment, samples are incubated in a thermostat for 5-10 days. During that period of time the surviving cells will form visible colonies which will be counted in irradiated samples as well as in untreated ones. The surviving fraction of cells S < = 1 will be represented by the ratio of cell count in the treated and those in the untreated dishes. If we represent the values of S as they depend on the dose d given to the sample in a (d, S) coordinate system, the result may look like the sigmoidal curve shown in Figure 2a. So far many arguments have been submitted for the representation of that curve by the function

$$S = e^{-(\alpha d + \beta d^2)} \qquad [2]$$

where α and β are the parameters characterizing the specific cell line. The exponent is linear and quadratic in d and hence the name : LQ-model.

Since radiobiology requires a representation of surviving fractions down to the order of magnitude 0.0001, a more appropriate system for the representation are semilog coordinates as shown in Figure 2b. In the semilog system the equal shifts down the ordinate always represent a constant diminishing factor < 1. Thus, the factor 0.1 is represented by a repeated equal shift down the ordinate generating the sequence of survivals: 0.1, 0.01, 0.001 etc. In such a system the survival curve is given as a segment of certain parabola. Due to this system of representation, any part of the curve below a certain level of survival S may be considered to be a quite independent survival curve in a new coordinate system (d_1, S_1) which is generated by a translation of the original one along the survival curve. The increase of its initial slope in the new coordinate system indicates that the preirradiation sensitized the cells against the additional amounts of radiation.

A graphical interpretation of parameters α and β is shown in Figure 3. The parameter α is responsible for the initial slope and parameter β for the rate of increase of the slope. If β = 0 then (2) becomes purely exponential

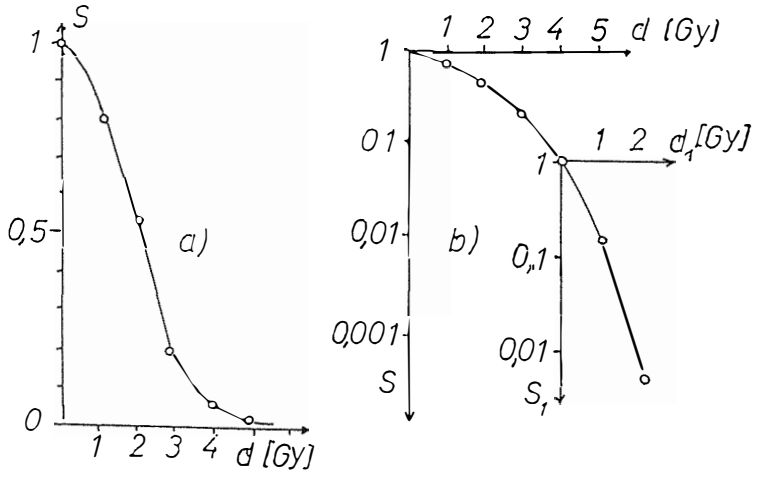

Figure 2. The survival curve in a) a linear and b) a semilog system of coordinates.

$$S = e^{-\alpha d},$$

and in the semilog system this is a straight line (Figure 4a). It is typical of neutrons and other heavy particles, the so-called densely ionizing radiation. On the other hand, if $\beta = 0$ then (Figure 4b):

$$S = e^{-\beta d2}.$$

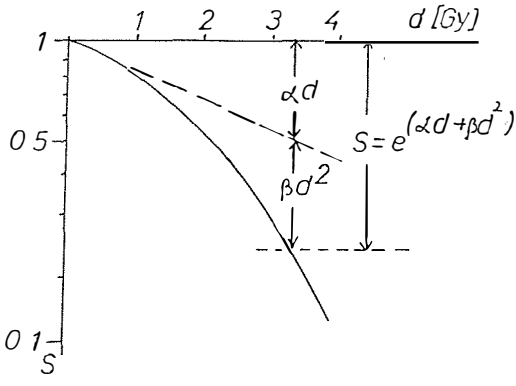

Figure 3. Interpretation of the role of parameters α and β.

This curve is represented by a semiparabola with no initial slope. It is only of theoretical interest because all known cells and radiations exhibit initial slopes, e.g. those for sparsely ionizing radiation (X-rays, γ -rays and electrons) are similar to the curve shown in Figure 3.

The LQ-model of cell survival results from the theory of dual radiation action (4,9), which presumes that ionizing radiation may produce one and two step final damage to the cell. It is practical, although not quite correct, to imagine the damage as an irreparable two strand break on the DNA chain – let us call it a lesion. On the other hand, the one-strand break, the sublesion, will be considered as reparable since the opposite chain is saved as a matrix for reconstruction of the complementary chain. According to the LQ-model, there are two types of lesion production: a simultaneous break of both DNA-strands when the ionization particle passes, known as one-event lesion or damage (Figure 5a) and two-event lesion or damage (Figure 5b). Namely, the ionizing particle first produces a sublesion. It is clear that at any instant during the radiation there is a lot of not yet repaired sublesions. If in the next few

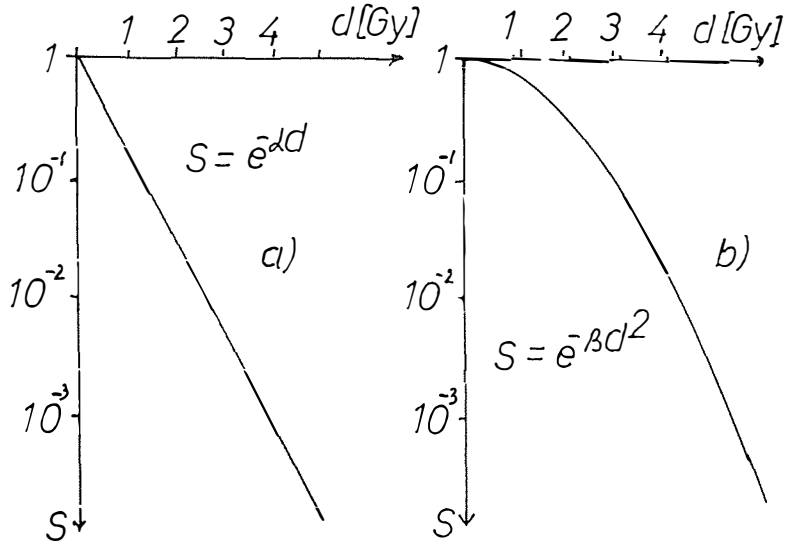

Figure 4. Parameters α and β are responsible for a) the exponential and b) the parabolic shape of the survival curve respectively.

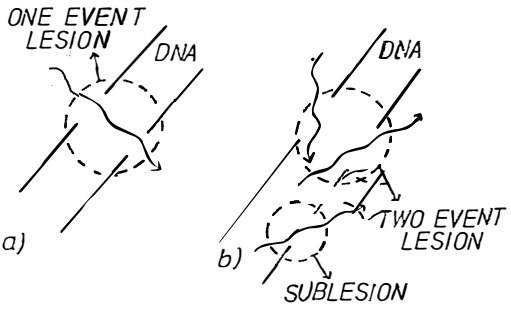

Figure 5. Ionizing particles may cause a) α-lesions and b) β-lesions from two sublesions.

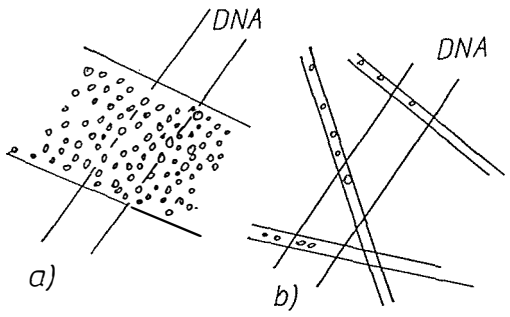

Figure 6. The difference between a) densely ionizing radiation and b) sparsely ionizing radiation.

hours no other sublesion occurs on the other chain and in the vicinity of the opposite site, the sublesion will repair. We can define the sublesion half-lilfe parameter $T_{1/2}$ as the repair time of 50% of sublesions – after irradiation has been interrupted. For most cell lines $T_{1/2}$ is within the range of 0.5 – 2 h. On the other hand, if we keep irradiating, it is highly probable that a certain number of sublesions will be complemented by a sublesion on the opposite site and thus promoted into two-event lesions.

In fact, the sizes of parameters α or β are closely related to the amount of production of the one-event or two-event lesions. Let us first consider a heavy particle (neutron, proton of α-particle). The ionization events are densely and widely spread around its track (Figure 6a) and will give no chance to sublesions. Thus, one-event lesions will dominate within the total amount of damage. Since all one-event lesions are lethal, the surviving cells are left untouched and must behave as though they have not been preirradiated at all. Thus, the survival curve must be exponential i.e. a straight line, because this is the unique shape which remains identical in all coordinate systems translated along it. Obviously, the size of parameter α is somehow the measure of the contribution of one-event lesions. On the contrary, if the track of ionization events is less dense (Figure 6b) a certain amount of sublesions, proportional to the given dose, will also be present. Therefore, if we continue to irradiate immediately, the rate of production of two-event lesions will be enhanced proportionally to the actually delivered dose. This selfenhancing character of two-event damage is reflected as a shoulder on the survival i.e. the increase of its steepness with the received dose. However, parameter β is responsible for the parabolic component and also for the production of two-event damage. Conversely, the shouldered shape of the curve reflects the presence of sublesions and two-event lesions. This also means that the surviving cells containing only sublesions will completely recover from the damage after a few hours and will behave as though they have never received any radiation.

The ability of normal tissue to repair after radiation is of great importance for radiotherapy and therefore sparsely ionizing radiation is the most suitable for everyday clinical practice. The repair phenomenon can be studied experimentally in the following way. First, we preirradiate all samples with e.g. d=4 Gy. Thus we reach the point matched with a circle in Figure 7. If we deliver an additional amount of radiation immediately, we shall follow the dotted extension of the survival curve. On the contrary, if we leave the cells 2-3 h to repair the sublesions, the survivals after additional doses will follow the curves with repaired shoulder. After 6 h the shoulder will be completely repaired and 2d = 8 Gy given in two portions with a 6h-pause, will result with a higher S than after 2d given in a single portion.

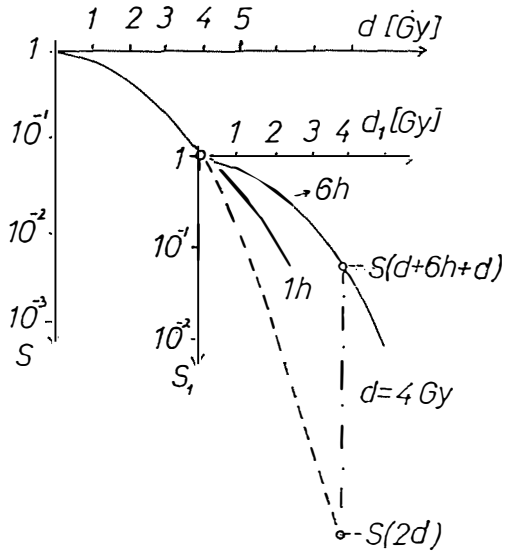

Figure 7. Elkind repair of the repair of sublethal damage.

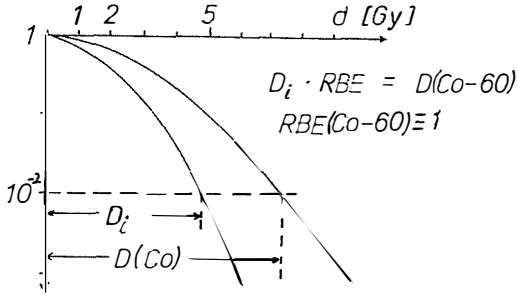

Figure 8. Definition of RBE with respect to Co-60 radiation as reference quality.

The ratio

$$F = S\ (d+6h+d)/S(2d) \qquad [3]$$

is the repair ratio and depends on d and the extent of sublesions repaired during the pause. The presence of the shoulder on the survival curve and the ability of cells to repair it are known as the ability to accumulte sublethal damage (SLD) and the sublethal damage repair (SLDR). They are typical of sparsely ionizing radiation (X-rays, γ-rays and electrons). Certainly, neutrons and other densely ionizing particles exhibit no SLDR since the survival curve is purely exponential i.e. with no shoulder. The SLDR is also known as Elkind repair after its discoverer, but also as fastr epair. This term is to be distinguished from the slow repair meaning repopulation of the tissue. Regarding the duration of SLDR, we can deliver the dose in two modes. One is the acute mode when the dose is delivered within a very short interval $T<<t_{1/2}$ and cells have no time for SLDR during the radiation. Another is the protracted mode where $t>=t_{1/2}$. In the latter case the effect of radiation will be somewhat weakened due to partial SLDR.

As said, all sparsely ionizing radiations exhibit a shouldered survival curve, but its shape and values of α and β change. For instance, 20 kV X-rays exhibit a steeper survival curve than Co γ-rays do. This is explained by an increase in the efficiency of production of both types of damage. However experiments show[2] that at equal survival S the repair ratios F (formula [3]) do not differ. This means that the amount of one event-damage versus two-event damage is the same at the same S. Thus, X-rays, γ-rays and electrons would cause an effect fully equivalent to that of a certain referent quality, provided the doses are corrected by a certain correction factor for obtaining the same survival. The correction factor is the well known radiobiological efficiency, RBE. If Co γ-rays are chosen for the referent quality with RBE=1, then

$$D_1 * RBE_1 = D_2 * RBE_2 = D\ (\text{Co}\ \gamma\text{-rays}), \qquad [4]$$

where subscripts indicate different radiation qualities (Figure 8). Aproximate values of RBE's are given in table 1. In the further text we shall consider various modes of radiation always referring to the reference quality i.e. to Co γ-rays.

Table 1. RBE for various qualities of radiation.

Radiation quality	RBE
Co-60 γ-rays	1
5-40 MeV electrons	1
3-42 MV X-rays	1
200 kV X-rays	1.10
70 kV X-rays	1.20
20 kV X-rays	1.40

Due to the equality of the damage, results of our considerations will be always translatable to any other quality by dividing all doses by the appropriate RBE.

Extrapolted response dose with complete SLDR

The most important radiobiological task of radiotherapy is to divide radiation into small acutely given fractions in order to kill the tumour at a relatively low cost to the surrounding functional tissue. In other words, the question is how to compare various regimes of fractionation regarding both the therapeutical effect and the tolerance of normal tissue of both types.

Earlier approaches to this problem were based more on clinical experience than on assumed *in vitro* systems as confident models for the actual *in vivo* situation. However, in the early eighties the LQ-model was recognized[1,7] as essential for explaining the early and late effects in radiotherapy. A basically new assumption is that the true measure of radiation damage is the surviving fraction of stem cells. Thus the logic of the cells within a tissue is analogous to the logic of the cells cultivated within the dish. This means that the same LQ-type of survival curve will remain valid and the same effect will mean the same level of S. Thus, the difference between the tissues (early-, late-responding and tumour) must be reflected in tissue parameters α and β. For the sake of simplicity, however, the effect will be represented by the nagative natural logarithm instead by S. This step is necessary in order to obtain an additive quantity increasing with the actual effect. Thus, after a single fraction d, the efect is represented by

$$ef = -\ln S = \alpha d + \beta d^2 = d^*(\alpha + \beta d). \qquad [5]$$

If there is a sufficiently long time interval between fractions, and 24 h is more than sufficient, cells will completely repair SLD. If we neglect the proliferation of cells, ef will be a purely additive quantity. Namely, if N equal fractions are given (Figure 9), the total effect EF will be

$$EF = N^*d^*(\alpha + \beta d). \qquad [6]$$

Now the extrapolated response dose, ERD, the quantity which is the measure of the overall radiation effect, is defined as

$$ERD = EF/\alpha = D^*(1 + \frac{d}{\alpha/\beta}) = D^*RE, \qquad [7]$$

where D=Nd is the total dose. It is useful to note that ERD differs only by the factor α from the logarithm of the total survival S i.e. ERD directly reflects the level of the final cell survival. The factor

$$RE = 1 + \frac{d}{\alpha/\beta} > 1$$

is called relative efficiency, RE, and is similar to the RBE concept. It expresses the efficiency of the total dose D: D must be multilplied by RE in order to obtain the total effect ERD. RE is essentially dependent on the size of the single fraction d and on the size of parameter α/β which has various values for various types of tissue: its value is 8 – 20 Gy for tumours and early responding tissues, and 2-4 Gy for late responding tissues (see e.g. 11).

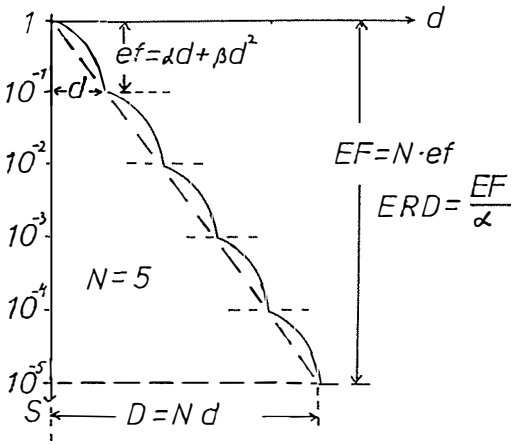

Figure 9. Definition of ERD – extrapolated response dose.

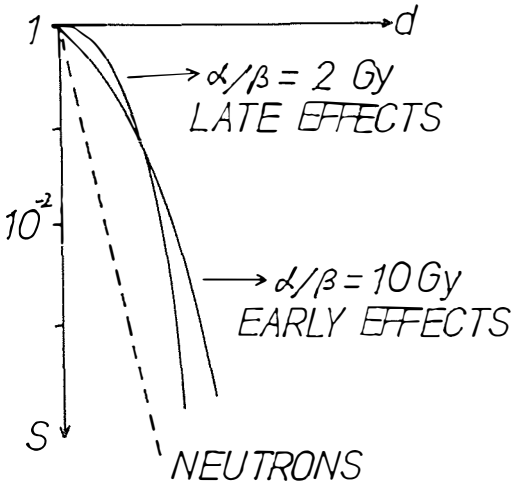

Figure 10. Difference between the survival curves of the late responding tissue ($\alpha/\beta = 2$Gy) and early responding tissue ($\alpha/\beta = 10$Gy) cells. The dotted straight line represents the survival curve for neutrons.

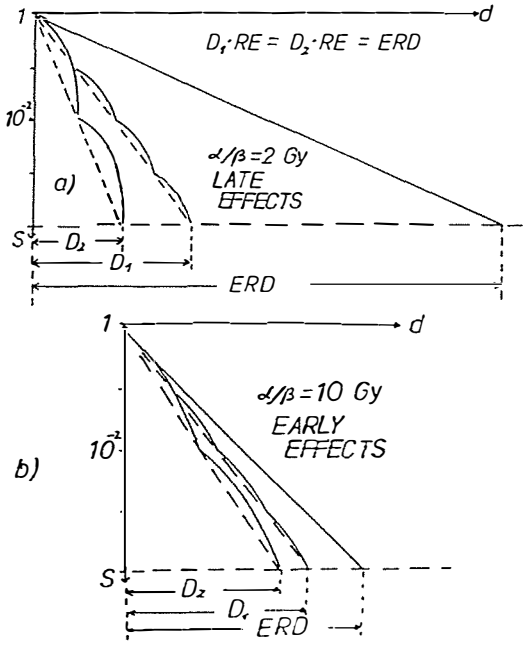

Figure 11. The relationship between RE and ERD for a) late and b) early respondig cells.

Two survival curves, one with a smaller α and with $\alpha/\beta = 2$ Gy respresentative of the late responding tissue and another one with a larger α and $\alpha/\beta = 10$ Gy as representative of the early responding tissue are compared in Figure 10. Graphically, a smaller α of the late responding tissue means a smaller initial slope of the survival curve and expresses the fact that a small single dose d may kill more cells in a tumour (or early responding tissue) than it does in a late responding tissue. On the other hand, at large single dose d the killing effect may turn in favour of late responding tissue owing to the manifoldly larger β and the production of a two-event damage.

This fact is graphically reflected as a very pronounced shoulder. The matter of fact is, however, that we never compare the effects in different types of tissues and particularly not by comparing the cell survival even in typologically identical tissues. Effects are rather compared by macroscopic manifestations like erythema, indurations or a complete withdrawal of the tumour. This fact is reflected as division by α in the definition of ERD (formula [7] and declaring the ratio α/β for the fundamental radiobiological parameter of a tissue. Thus ERD is an adequate measure of the damage only if applied to the same type of tissue.

Generally, we may ask at which single dose the contribution of one-event damages becomes equal to the contribution of two-event damage. Figure 3 shows that the corresponding dose d must meet the requirement $\alpha d = \beta d^2$ and hence $d = \alpha/\beta$. Thus parameter α/β has a specific meaning and that is the threshold dose such that at $d = \alpha/\beta$ the contribution of one-event damage dominates over the two-event damage, whereas at $d > \alpha/\beta$ the selfenhancing two-event damage becomes dominant. Thus if we change the size of a single dose from d = 2 Gy to d = 6 Gy the one-event damage will remain prevalently responsible for the tumour killing and no drastic change to killing efficiency could be expected: namely RE changes from 1.2 to 1.6. On the other hand the contribution of two-event damage to late responding tissue has triplicated: namely RE increases from 2 to 8.

If two regimes give the same effect i.e. the same level of survival, then ERD's will be the

same: $ERD_1 = ERD_2 \equiv ERD$, where indices refer to the regimes. Using (7) and (8)

$$D_1 * RE_1 = D_2 * RE_2 = ERD. \qquad [9]$$

Thus, if we calculate the $ERD = D_1 . RE_1$ using the first regime, we can calculate the total dose D_2 for another isoeffective regime provided the size of the new fraction d_2:

$$D_2 = \frac{ERD}{RE_2}, \quad \text{where} \quad RE_2 = 1 + \frac{d_2}{\alpha/\beta}$$

Equations [4] and [9] show the similarity of dimensionless quantities RE and RBE. The product $D * RE = ERD$ is the isoeffective dose given by the referent fractionation regime with $RE = 1$. This becomes true at $d = 0$. Thus the referent regime will be represented by the one where the dose is given quite slowly in order to allow a complete SLDR but with no proliferation. Obviously, both requirements cannot be met simultaneously and thus ERD remains only a thereotical extrapolation. In Fig. 11a and 11b ERD is explained as the isoeffective dose obtained by drawing a tangent to the initial part of the survival curve. This tangent indeed represents a superposition of many small initial sections of the curve. Graphical representation also shows why the change of the fractionation schedule causes drastic changes in the late responding tissue and quite small changes on the tumor kill effects.

Generally speaking, there are two conditions for the validity of the model. A sufficiently long pause between fractions to allow a complete SLDR, and no proliferation of cells. Under these circumstances the ERD model is quite independent of time and the only possible change is the altered size of the single fraction d. Of course, proliferation cannot be stopped and therefore, without corrections, the model must not be used unless the overall duration of therapy is unchanged. Later on, the model will be expanded by corrections for the proliferation and SLDR.

Under the condition of completed SLDR i.e. a minimum 6h time interval between the fractions, ERD is additive. Also, if a regime consists of several subregimes giving partial ERD_1, ERD_2, etc. and the pause between them is longer than 6h then ERD for the total regime is

$$ERD = ERD_1 + ERD_2 + \ldots \text{etc.} \qquad [10]$$

Example 1: After 15f (fractions) x 2Gy, the conventional plan of 30f x 2Gy must be accelerated by 3Gy daily fractions. Calculate a) the total dose for obtaining the same effect on the tumour ($\alpha/\beta = 10$Gy) and b) the change of ERD regarding the late effects ($\alpha/\beta = 2$Gy).

Solution: a) For the tumour: ERD(30fx2Gy) = DxRE = 60x(1+2/10) = 72Gy. Using formulae [8] and [10] ERD_1(15fx2Gy) = 36Gy and $ERD_2 = ERD - ERD_1 = 36$Gy. Since $RE_2 = 1+3/10 = 1.3$, the corresponding $D_2 = ERD_2/RE_2 = 36/1.3 = 28$Gy. Thus the total dose is D = 58 Gy.

b) For the late effects: ERD(30fx20Gy) = DxRE = 60x(1+2/2) = 60x2 = 120 gy. For the combined regime $ERD = ERD_1 + ERD_2$ and ERD = 30x2 +28x(1+3/2) = 60+70 = 130Gy. The risk of late effects has slightly increased.

Extrapolated response dose with incomplete SLDR and with proliferation

When the time interval between fractions becomes equal to or less than $t_{1/2}$ or if the radiation is delivered by protracted mode, there is not enough time for the complete SLDR. At such accelerated fractionation many more cells might not recover from the sublesions before the next fraction. Therefore, the increased amount of total damage schould be accounted for. The basic equation ERD=DxRE remains valid, but RE must be calculated as (Dale 1986):

$$RE = 1 + \frac{d}{\alpha/\beta} * \frac{1}{N} * \frac{N(1-k^2) - 2k(1-k^N)}{(1-k)^2}, \qquad [11]$$

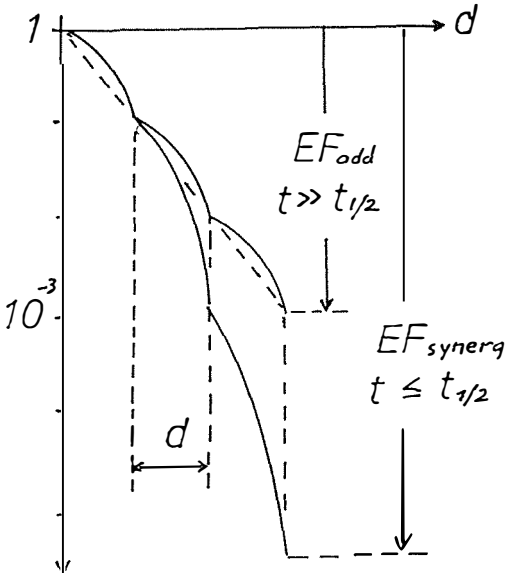

Figure 12. Fractionation with time inteervals $t = < t_{1/2}$ causes a synergistic i.e. more than an additive effect.

where $k = e^{-\mu t}$ and t is the time interval between fractions, while μ is a constant typical of various tissues[5,6]. This formula seems to be complicated, but it is quite easily overcome by a short computer programme.

Under conditions of incomplete SLDR it is important to keep in mind that ERD is no longer additive and the earlier expressions are no longer valid. The expression [11] will give a larger value for RE (Figure 12) since the next fraction always interferes synergistically with previous, not yet repaired sublesions. On the other hand, if several subregimes are separated by a pause sufficient for complete SLDR, formula [10] is still valid.

Example 2:

Instead of with one daily fraction, the tumour is irradiated twice a day: 2fx2Gy, with a 4h time interval between fractions, every two days, until 60Gy is obtained. Compare the late effect with the one of conventional schedule ($\alpha/\beta = 2$Gy, $\mu = 0.46\ h^{-1}$).

Solution:

Two close fractions are not additive and the ERD_{2f} will be first calculated using [11]; one obtains $k = e^{-0.46*4} = 0.16$ and using [11]: $RE_{2f} = 2.16$ and $ERD_{2f} = 4* 2.16 = 8.32$Gy; since the alternative interval is 44h i.e. sufficiently long for complete SLDR, so that fifteen 2f-subregimes may be considered additive, one obtains ERD = 15 * 8.32 = 130Gy; the result of previous example was ERD = 120Gy for late response at complete SLDR so that a slightly increased risk of late effect due to an incomplete SLDR may be expected.

Under protracted radiation we shall consider radiation given continuously at a constant dose

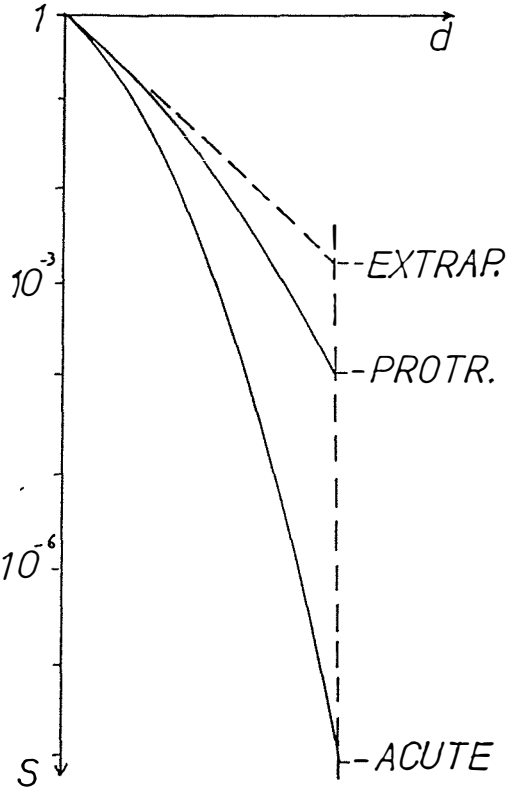

Figure 13. Accute radiation does not allow SLDR, however there is a partial SLDR during the protracted radiation. As SLDR becomes more complete, the survival curve for protracted radiation assimptotically aproaches to the extrapolated tangenta.

rate during a certain time interval. Protracted radiation can be imagined as though consisting of very small fractions as well of very short time intervals between fractions. It is supposed that the amount of one-event damage will not depend on dose rate. On the contrary, during the production of two-event lesions there are two antagonistic processes which depend on the dose rate. The first is the production of sublesions, SLD, and the other is their repair, SLDR. Namely, with the growing dose rate, the effect of SLDR becomes negligible and the final effect progressively becomes similar to that of a single dose fraction. On the other hand, if the dose is delivered at a progressively decreasing dose rate, the SLDR becomes complete and the total dose approaches the value of ERD (Figure 13). For protracted radiation RE can be calculated from the expression (Dale 1985):

$$RE = 1 + \frac{2R}{\alpha/\beta} * \frac{1}{\mu} * \left(1 - \frac{1}{\mu T} * (1 - e^{-\mu T})\right), \quad [12]$$

where R is the dose rate in $Gy*h^{-1}$ units and T the overall duration in hours. This formula can also be easily implemented as a computer programme. It is simplified for T > 100h:

$$RE = 1 + \frac{2R}{\alpha/\beta} * \frac{1}{\mu}.$$

Example 3:

Determine the RD for D = 60 Gy, given by protracted mode during the time intereval T = 168h i.e. with dose rate R = 60/168 = 0.36 Gy h^{-1}. Find the formula for the exposure expressed as the function of dose rate, requiring a constant late effect ERD (α/β = 4Gy, μ = 0.46 h^{-1}).

Solution:

From formula [13] one obtains RE = 1.391 and ERD = 60*1.391 = 83.5Gy. Using the same formula and equation ERD = RE*D = RE*R*T, one obtains T = ERD/(RE*R), namely T = 83.5/(R*(1+1.08696)). Using this formula for the dose rates 0.5, 0.6, 0.7, 0.8, 0.9 and 1.0 Gy h^{-1}, one obtains exposures of 108, 84, 68, 56, 47 and 40 h, respectively. These exposures are almost identical to those widely used in the interstitial radiotherapy.[8] The value of parameter α/β = 4Gy allows to conclude that the late effect tolerance and not the effect on tumour has been taken as criterion of these clinical exposures.

Earlier clinical experience has shown that the radiation effect decreases with the prolongation of radiotherapy and can be compensated by increasing the total dose delivered to tumour. This is obviously due to »repair phenomena« occurring within the cell and tissue. One of repair mechanisms is fast repair, SLDR, and takes place during a few hours between the fractions. On the other hand, during the course of radiotherapy one observes a repair on the time scale of weeks and this is the slow repair i.e. repopulatilon of cells in the tumour. The repopulation i.e. proliferation is characterized by the parameter T_p defined as the doubling time of the fastest clonogenic fraction in the tumour. The

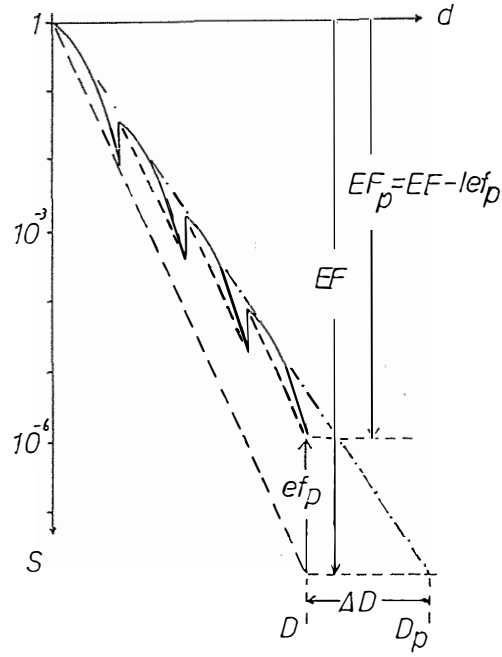

Figure 14. The proliferation of tumor cells requires a correction. A supplementary dose $D = D_p - D$ is necessary to compensate it.

knowledge of T_p allows to modify the concept of ERD in the following way: since the number of cells multiplies by the factor F given in equation [1], the corresponding proliferative effect will be given by

$$ef_p = -\ln F = -(\ln 2)*T/T_p.$$

Using [6] and taking into account that ef_p is a negative quantity, the entire corrected effect will be:

$$EF_p = N*ef - I\ ef_p\ I,$$

where II denotes the absolute value. Dividing by α one obtains the corrected ERD_p:

$$ERD_p = EF_p/\alpha = ERD - (0.693/\alpha) * (T/T_p). \quad [14]$$

Thus the expression for ERD can now be corrected for the proliferation of tumour cells, provided parameters α and T_p are known. The above equation shows that the total ERD is diminished by a term proportional to the total duration of therapy (Figure 14). Therefore, the proliferation has for the consequence the necessity for additional dose in order to compensate the slow repair effect.

Example 4:

According to Budihna et al. (1985) the 'split course' radiotherapy of glottis and supraglottis – total dose $D_1 = 60$y during $T_1 = 40$ days was supplemented up to $D_2 = 75$Gy due to the prolongation up to $T_2 = 70$ days together with a 3.5 week pause and unchanged daily fractionation d = 2Gy. Determine T_p of the clonogenic cell fraction ($\alpha = 0.3\ Gy^{-1}$, $\alpha/\beta = 10$Gy).

Solution

Using [14] one obtains for the conventional regime:

$$Erd_{p1} = D_1 * RE - (0.693/\alpha) * (T_1/T_p);$$

and for the 'split course' regime one obtains:

$$ERD_{p2} = D_2 * RE - (0.693/\alpha) * (T_2/T_p):$$

since $ERD_{p1} = ERD_{p2}$, after subtraction of equations and using notation $\Delta D = D_2 - D_1$ and $\Delta T = T_2 - T_1$ one obtains:

$T_p = 0.693/(\alpha * RE * (\Delta D/\Delta T))$; since $\Delta D/\Delta T = (75-60)/70-40) = 0.5$ Gy/day and RE = 1.2, T_p is $T_p = 0.693/(0.3 * 1.2 * 0.5) = 3.85$ days.

References

1. Barendsen GW. Dose fractionation, dose rate and isoeffect relationships for normal tissue response. *Int J Radiat Oncol Biol Phys* 1982;**8:**1981-97.
2. Bistrović M, Bišćan M, Viculin T. RBE of 20 kV and 70 kV X-rays determined for survival of V79 cells. *Radiother Oncol* 1988; **7:**175-80.
3. Budihna M, Škrk J, Šmid L, Furlan L. Tumour cell repopulation in the rest interval of split-course radiation treatment. *Strahlentherapie* 1980; **136:**402-8.
4. Chadwick KH, Leenhouts HP. A molecular theory of cell survival. *Phis Med Biol* 1973; **18:**78-87.
5. Dale RG. The application of the linear-quadratic dose-effect equation to fractionated and protracted radiotherapy. *Brit J Radiol* 1985; **58:**515-28.
6. Dale RG. The application of the linear-quadratic model to fractionated radiotherapy when there is incomplete normal tissue recovery between fractions and possible implications for treatments involving multiple fractions per day. *Brit J Radiol* 1986; **7:**175-80.
7. Fowler JF. Total doses in fractionated radiotherapy – implications of new radiobiological data. *Int J Radiat Biol* 1984;**46:**103-20.
8. Habič M. Personal communication, 1990.
9. Kellerer AM, HH Rossi. The theory of dual radiation action. *Current topics in radiation research quarterly* 1972; **8:**85-158.
10. Nias AHW. *Clinical radiobiology*. Churchill Livingstone, Edinburgh 1988.
11. Thames HD, Bentzen SM, Turesson I, Overgaard M, Van den Bogaert W. Time-dose factors in radiotherapy: a review of human data. *Radiother Oncol* 1990; **19:**219-35.
12. Trott KR, Kummermehr J. What is known about tumour proliferation rates to chose between accelerated fractionation or hyperfractionation? *Radiother Oncol* 1985; **3:**1-9.

Adv Radiol Oncol 1992; 323–9.

A practical method of TBI *in vivo* dosimetry based on real scatter contributions

Vrtar M

Institute of Oncology and Radiotherapy, KBC Rebro, Zagreb

The use of in-vivo dosimetry in anterior-posterior (AP) ^{60}Co total body irradiation (TBI) makes possible to determine the absorbed dose in the patient's mid plane point by means of entrance and exit dose readings for the direction of certain beam ray. The arithmetic mean of this two readings for each location must be corrected by a factor which depends on geometrical and physical conditions of the applied TBI. Here, the local tissue air ratio method (local TAR) was used. The theoretical method, which included different sizes of TBI phantoms in length, widths and lung inhomogeneity dimensions, was established. The practical tables of correcting factors for a number of important locations in TBI in-vivo dosimetry, based on real scatter contributions (i. e. including the influence of the local field for dose determination points), were presented. The correlation to the literature data was also discussed.

Key words: whole body irradiation; radiotherapy dosage

Introduction

The continuation and enlargement of the method of local dosimetric functions, as earlier introduced in TBI in-vivo dosimetry,[1] must lead to such possibilities of application which would cover the whole practical range of real irradiation procedures. Experimental and theoretical approach were performed on the assumption that an effective field in TBI phantom in the surroundings of location, where the absorbed dose has to be determined, can be defined by the range of scattering contributions. Aside from the primary dose, scattering reflects the shape, characteristic dimensions and mass arrangement in the nearest neighborhood of single location. The importance and validity of these assumptions was confirmed in the investigation on an anatomic phantom,[2] so that the use of standard central axis data,[3] even taking into account the finite phantom dimensions,[4, 5] can not be recommended in TBI. It can be best seen from the behavior of local TAR. Further, during in-vivo TBI, as in ^{60}Co gamma AP - PA irradiation at extended distance of 4 m, the absorbed dose in the mid-plane point of some location is not a simple arithmetic mean of entrance and exit readings (measured with semiconductor or thermoluminescent dosimeters) for places in certain beam ray direction. It must be corrected with a factor which depends on geometrical and physical conditions of the considered TBI method. Therefore, each location at AP/2 depth has its own factor as a consequence of all the irradiation conditions. Also, the effects of the »finite« local phantom AP widths would be

Correspondence to: Dr. Mladen Vrtar, Institute of Oncology and Radiotherapy, KBC Rebro, Kišpatičeva 12, 41000 Zagreb, Croatia.

UDC: 615.849.5

included in this model as well as contours and dimensions of the whole phantom which is situated in a large field.

Material and methods

The results of measurements of local TAR in an anatomic-cubical phantom, which was constructed to represent the patient lying on his side (as in parallel opposite AP-PA irradiation technique), indicated a close agreement with the theoretical model based on TBI adapted sector integration method, i. e. better than 2% for all depths of AP/z on average. But, the model was restricted to a 70 kg-weight water phantom, 150 cm in length and with carefully selected dimensions of local AP widths, which was further used as a reference. In order to cover the applicability of the presented method to various real situations, a generalization to variable phantom dimensions has been imposed to it. Therefore, the characteristics of 11 proportional phantom dimensions, including the referential one, were theoretically investigated. The lengths of phantoms were (in cm) from 100 to 200 with step 10.

The associated factors of proportionality (referred to 150) were applied to the height too, so that from the source eye view, the phantoms were similar in a geometrical sense. The appropriate widths corresponded to the considered locations, so that the factors of proportionality in this dimension were defined from the following AP widths (cm): head (H), 11, 12,... 21; Neck (N), 7, 8,... 17; Shoulder (S), 5, 6... 15; Lung (Lg), 12, 14,... 32; Mediastinum (M), 12, 14,... 32; Abdomen (A), 10, 12,... 30; Thigh (T), 10, 12,... 30; Leg (L), 7, 8, 9, 11,... 21, 22, 23; Knee (K), 6, 8,... 14, 15, 16,18,... 24; Foot, 5, 6,... 15. The reference AP values of the respective locations were H(16), N(12), S(10), Lg(22), M(22), A(20), T(20), L(15), K(15), F(10), and their corresponding coordinate system), H(65,4), N(50,2), S(40,21), Lg(30,8), M(30,1), A(0,0), T(-10,10), L(-30,3), K(-42,-2,5), S(-70,-7.5). So for example, the phantom No. 4 in the case of lung had the following factors of proportionality 0.867, 0.867, 0.818. In order to find the reduction factor for dose, because of the finite local phantom width, the determination of an effective field had to be performed for a number of cases, i. e. 10 x 11 = 110 different phantom dimensions. Here again, as in the reference case,[1] the earlier results for the reduction of TAR[1] were used, but care was taken in the interpolation procedures of various phantom widths. The explicite presentation of the values of reduction factor in all locations L and depths d, i. e. $(RF)^L_d$ was omitted here for the sake of brevity.

Homogeneous phantom

In order to determine the absorbed dose, the arithmetic mean of two readings during the TBI in-vivo dosimetry, entrance (input) reading R_{in} and exit (output) reading R_{out}, as measured in the direction of beam ray passing a considered location, must be corrected by the factor F_{TBI}, because dose decrease is not linear. Is depends on the geometrical and physical conditions of the applied TBI. Therefore, the absorbed dose in patient's mid plane point can be found from

$$D_{mid} = F_{TBI}\ (R_{in} + R_{out})/2 \qquad (1)$$

where

$$F_{TBI} = \frac{2\,TAR_{TBI}(AP/2)}{TAR_{TBI}(AP)\,G^2 + TAR_{TBI}(dm)\,H^2} \qquad (2)$$

$TAR_{TBI}(AP/2)$, $TAR_{TBI}(AP)$ and $TAR_{TBI}(dm)$ are local TAR values for depths of AP/2, AP and dm = 0.5 cm (maximum ionisation for ^{60}Co gamma), respectively, while G and H contain TBI geometry

$$G = \left(\frac{SMD}{SMD - AP/2 - r_d}\right)^2,$$

$$H = \left(\frac{SMD}{SMD + AP/2 + r_d}\right)^2 \qquad (3)$$

Here, SMD is the source mid plane distance (in our case 420 cm), and r_d is the radius of detector which is fixed on skin (for ex. semiconductor

DPD-5 Therados). Local TAR values can be found by means of the mentioned adapted sector integration method[1] and contain all relevant phantom data for the location of interest.

Lung inhomogeneity

The development of the dose calculation methods for inhomogeneous phantoms was specially stimulated by the introduction of computed tomography (CT) in clinical practice. There is a general intention towards such algorithms which will use the CT density values and the associated inhomogeneity contours in the body, thus reflecting the real situation as closely as possible. The presented method, though referring to cubic-anatomical TBI water phantom with lower density regions representing the lungs, can be applied to the real irradiation conditions. The TBI situation is specific because the whole lungs are inside the irradiation field. Therefore, the contribution of scattered photons to the absorbed dose, TAR and further to the correcction factor (CF) in lungs will be a direct consequence of the surroundings of the considered point for dose determination. As stated in the earlier investigations[1], the concept of local TAR with the associated effective field, and the effect of the loss of scatter because of the finite phantom width, significantly influence the CF values and reflect the size and position of phantom. Also, in the region of lower density, the primary photons experience less interactions than in unit density media. Therefore, the fluence of primary photons in the lungs is stronger. On the other hand, due to decreased amount of interactions, less scattered photons will be generated. This effect has to be taken into account in considering the reduction factor RF for TAR in lung inhomogeneity (as introduced previously), because of the finite local phantom width. Further we concentrate on correcting the RF values for AP/2 depth i.e. in the lung mid plane where the TBI dosimetry is recommended, and to apply the mentioned algorithm to the cases where the dimensions of TBI phantom, lung wall thickness and lung size can be changed.

The reduction factor for each location has been introduced to correct the absorbed dose value (further TAR) for incomplete scatter contributions, i.e. for the lack of backward scattering due to the »finite« phantom width. This principle was used in the case of lungs as well as in other parts of TBI phantom with unit density. But, strictly speaking, in the lung's region the total amount of scattering centers, which would contribute to the dose in the measuring point, is reduced. So, replacing the lung's volume V^{Lg} of the whole unit density TBI phantom V, by a lower density medium containing n^{Lg} electrons per volume, instead of n as in water, the total amount of scattering centers must be decreased. Also, the point in the mid plane at AP/2 depth separates the volume of lung in two parts: the first contributes the dose from the forward scattering to this point, the second part, signed by V^{Lg}_{backw} is responsible for backward scattering. In symmetrical case the two columes have the same value, but in an asymmetrical position of the lungs (e.g. when the front chest wall thickness is larger than the back wall one – female case), a correction has to be introduced. As $(RF)^{Lg}$ depends on the loss of backward scattering, we can separate the total scattering dose in TBI phantom in »forward« and »backward« part, in order to point out that the latter includes the changed scattering conditions. Also another correction, in the form of quotient of scattered dose in lung volume only and corresponding scattered dose in water (TBI phantom volume being excluded), has to be added. We named it as the reduced phantom »lung to water« correction. Now the total absorbed dose D_d^{Lg} at d = AP/2 depth can be expressed as

$$D_d^{Lg} = (RF_0)_d^{Lg}\left[D_d^{Lg,prim} + D_d^{Lg,scatt} a\left(b^{forw} + \right.\right. \\ \left.\left. + b^{backw} c\right)\right] \qquad (4)$$

where $(RF_0)_d^{Lg}$ is the previously defined reduction factor[1] without taking into account the change in scatter due to lower densitiy. $D_d^{Lg,prim}$ for monoenergic ^{60}Co gamma can be presented in an exponential form, containing lung density μ/ϱ= 0.05283 cm/g, μ=0.0641 cm/g for water[6] and wall

thickness (Fig. 3.[1]). $D_d^{Lg,scatt}$ means the total uncorrected scattering contribution in the point of dose determination in TBI mid plane in the lungs, performed by the use of adapted sector integration method, as described in an earlier investigation[1], while a, b^{forw} b^{backw} and c correct the reduction factor in the case of the lungs.

$$a = [n^{Lg} V^{Lg}] / [n V] + [V - V^{Lg}] / V \qquad (5)$$

reduces the total number of scatterers involved in TBI dose, where $n^{Lg} = \varrho^{Lg} Z_{eff}^{Lg} N_A / M_{eff}^{Lg}$ and $n = \varrho Z_{eff} N_A / M_{eff}$ are the corresponding numbers of electrons per volume, for the lung and water. N_A is Avogadro's number, $\varrho^{Lg} = 0.30$ (in the presented case, but it can take any other value of lung's density), $\varrho = 1.00$, $Z_{eff}^{Lg} = 7.488$ and $Z_{eff} = 7.420$ are the effective atomic numbers of lung and water as calculated by Mayneord relation[7] and use of ICRU data of composition by weight[6], while M_{eff}^{Lg} and M_{eff} are the effective atomic weights with values 14.1719 and 18.0158.

$$b^{forw} = [\sigma]_0^{90} / [\sigma]_0^{180}, \; b^{backw} = [\sigma]_{90}^{180} / [\sigma]_0^{180} \qquad (6)$$

show the percentage of all scattering in forward i.e. backward directions for ^{60}Co gamma irradiation, where σ values are the integrated Klein-Nishina collision differential cross sections within the range of defined limits. It follows that the total number of photons that are scattered in an angle 0^0 to 90^0 versus that scattered between 0^0 and 180^0 gives $b^{forw} = 0.74414$. A similar calculation gives $b^{backw} = 0.25586$. This is in the case of full scattering conditions. On the contrary, we do not have an infinite phantom, but just definite AP widths. The reduction in dose due to these reasons for unit density phantom was incorporated in $RF_\bullet$, as defined before. But there is an additional correction because of the presence of lungs, so that c factor in eq. (4), is

$$c = [n^{Lg} D_{red.phan}^{Lg,scatt} / n D_{red.phan}^{scatt}] \; [V_{backw}^{Lg} / V_{backw}^{Lg,sym}] \qquad (7)$$

In the second bracket there is the quotient of lung volume beyond the lung mid plane, contributing the backward scattering. V_{backw}^{Lg} is the actual volume arising from the »movement« of the whole lung volume in referrence to mid plane, induced by a different chest wall thickness, while $V_{backw}^{Lg,sym}$ is the volume such as it would be in the case of symmetrical position of the lung. n^{Lg} and n in the first bracket are the corresponding numbers of scattering centers per volume, in the lungs and water (see also before), while $D_{red.phan}^{Lg,scatt}$ and $D_{red.phan}^{scatt}$ represent the scattered doses to mid plane point from the lung volume only (we call it reduced phantom, i.e. with TBI phantom excluded) in the cases of lung and water densities respectively.

In order to include these effects in lung correction factor for d = AP/2 depth, we have to enlarge the part of denominator defining CF, i.e. eq.5 in the earlier work[1], so that scattering contribution should be replaced as follows

$$(RF_o)_{AP/2}^{Lg} \quad f(2)\,\triangle SAR(r,d_2)\,\frac{\triangle\theta}{2\pi} \longrightarrow \longrightarrow \quad (RF_o)_{AP/2}^{Lg} \; a\,(b^{forw} + b^{backw}\,c)\; f(2)\,\triangle SAR(r,d_2)\,\frac{\triangle\theta}{2\pi} \qquad (8)$$

Here again, f denotes the in-air dose distribution of the primary ^{60}Co beam, △SAR is the Scatter Air Ratio and integration should be performed over the variable point 2 in the plane of dose determination, as defined in geometry for absorbed dose determination (Fig. 3, earlier work[1]).

Now, using the known expression for TAR_{TBI} (AP/2) in water and the definition of CF(AP/2) (eq.2 and 4, earlier work[1]), we can find the TBI lung dose factor F_{TBI}^{Lg} which multiplies the input skin reading R_{in}^{Lg}, and determine the mid plane lung dose

$$D_{mid}^{Lg} = F_{TBI}^{Lg} \; R_{in}^{Lg} \qquad (9)$$

where

$$F_{TBI}^{Lg} = CF(AP/2) \; \frac{TAR_{TBI}(AP/2)F}{TAR_{TBI}(dm)} \left[\frac{SMD - AP/2 - r_d}{SMD} \right]^2 \qquad (10)$$

The TBI lung dose factor comprises all the information about the size of phantom and lung inhomogeneities, such as contour at the depth of AP/2, density and chest wall thickness; further it depends on local TAR values which reflect the real scattering situation in the surroundings of dose determination point.

Results

The corrective factors F_{TBI} (for all locations except the lung) and F^{Lg}_{TBI} (for the case of lung), as functions of AP widths, were introduced in TBI in-vivo dosimetry to take into account that the dose decrease is not linear. The calculation was performed by use of special software set up for this purpose (including local TAR, CF, F_{TBI} and F^{Lg}_{TBI}) with the possibility of proportional change in phantom dimensions. It is evident from the results in Table 1 that the factor varies with AP width in certain limits which are the characteritics of locations. It is also clear that the values depend on the energy applied in TBI, so the presented results refer to ^{60}Co gamma irradiation but the principle can be used in any other case. The calculated values refer to 11 different dimensions of phantom AP width of the certain location, the other missing values can be found by interpolation. Correction factor for the case of lungs for proportional phantom dimensions (including proportional lung sizes and thorax wall thicknesses of 2.2, 2.6, 2.9, 3.2, 3.7, 4.0, 4.4, 4.7, 5.1, 5.5, 5.8 cm, referring to the corresponding lung AP widths respectively) can be found in the last column of the Table 1. In Figure 1, F^{Lg}_{TBI} as the function of AP and chest wall thickness t, was systematically investigated, while the dependence on side of the equivalent square s of lung area (as seen from the direction of input irradiation) in different phantoms was presented in Table 2. Here, the wall thickness was constant (t=4 cm) and the lung widths were proportional to AP widths of the corresponding phantoms (as before). All calculations were performed with lung density 0.30 g/cm^9, but the mentioned software can be used for any other density and phantom dimension.

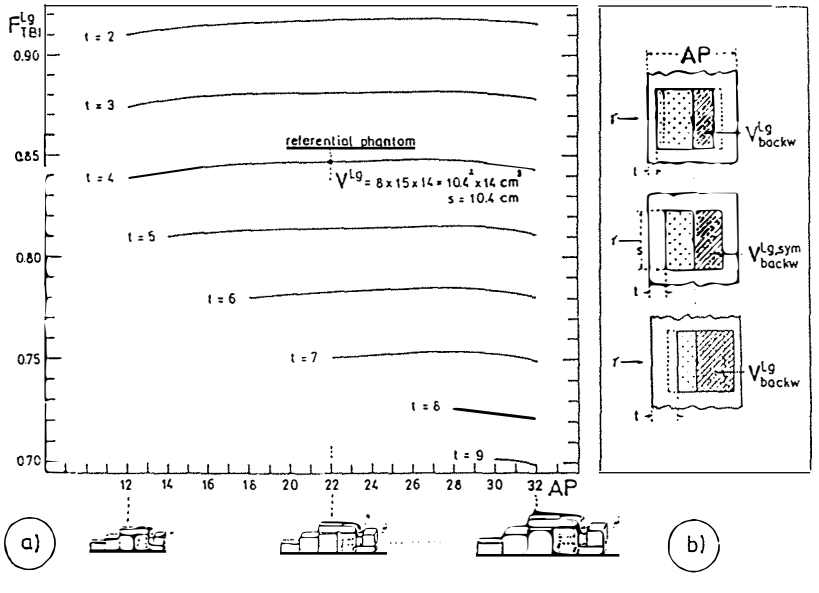

Figure 1. a) Lung dose correction factor F^{Lg} as function of AP width and chest wall thickness t in proportional sized phantoms in ^{60}Co TBI b) The principle od different backward scattering contributing to the mid plane point, because of the change in lung volume beyond mid plane caused by various thicknesses t.

Discussion

The values of the correction factor F_{TBI} are strictly dependent on the applied location and AP width of the phantom. All values are within 1.0586 and 0.9305 limits. There is a report, concerning this theme, by Dutreix and Bridier[8], about the measured values of the correction factors in the case of 5.6 MeV x-ray beam for thicknesses between 12 and 26 cm, where the factor varied from 1.04 to 0.98. But the cited method was restricted to simple cubic phantom and central axis geometry, i.e. without consideration of the local fields. Further, in the case of lungs, because of a different approach which takes into account the chest wall thickness, F_{TBI}^{Lg} has another meaning. But, in the calculation chain, the lung correction factor for mid plane point CF(AP/2) must be found preliminary. Taking into consideration the presented method, the value for AP = 22 cm phantom width was found to be 1.235. As a comparison the value by Marinello[9], using the modified equivalent TAR method in a phantom of simpler shape (but the same AP), was 1.24. On the other hand, in AP = 28 cm case by Mauceri and Kase[10], as measured in 30x30x28 cm^3 heterogeneous phantom with 13 cm of lung material after 5 cm of solid water thickness (chest wall) and field size 10x10 cm^2, the reported value was CF(14) = 1.25 (for 9 cm depth in lung material). If we apply the earlier presented theoretical method to this model, considering the lung dimensions approximated by a 10 cm sided equivalent square in »reduced« phantom approach with all other conditions being the same, the calculated value was 1.276, i.e. differing only for 2%. It means that the method is applicable also to different phantom shapes and not to TBI conditions only.

Table 1. Correction factor for calculation of the mid plane dose in ^{60}Co TBI ($F_{TBI}^{H \cdots F}$ according to eq. 2, F_{TBI}^{Lg} according to eq. 10 and $\varrho^{Lg} = 0.30$ g/cm^3)

AP (cm)	Head (H)	Neck (N)	Shoul. (S)	Media. (M)	Abdom. (A)	Thigh (T)	Leg (L)	Knee (K)	Foot (F)	Lung (Lg)
5	–	–	1.0271	–	–	–	–	–	1.0282	–
6	–	–	1.0222	–	–	–	–	1.0586	1.0277	–
7	–	1.0264	1.0217	–	–	–	1.0227	–	1.0270	–
8	–	1.0230	1.0208	–	–	–	1.0222	1.0583	1.0262	–
9	–	1.0218	1.0202	–	–	–	1.0220	–	1.0255	–
10	–	1.0213	1.0199	–	1.0298	1.0365	–	1.0580	1.0248	–
11	1.0421	1.0210	1.0195	–	–	–	1.0218	–	1.0237	–
12	1.0415	1.0208	1.0192	1.0345	1.0292	1.0359	–	1.0578	1.0232	0.9014
13	1.0404	1.0203	1.0180	–	–	–	1.0215	–	1.0226	–
14	1.0386	1.0199	1.0156	1.0333	1.0285	1.0342	–	1.0575	1.0212	0.8927
15	1.0370	1.0194	1.0132	–	–	–	1.0211	1.0572	1.0196	–
16	1.0353	1.0166	–	1.0317	1.0274	1.0324	–	1.0561	–	0.8829
17	1.0329	1.0127	–	–	–	–	1.0161	–	–	–
18	1.0304	–	–	1.0286	1.0241	1.0243	–	1.0546	–	0.8714
19	1.0256	–	–	–	–	–	1.0104	–	–	–
20	1.0205	–	–	1.0203	1.0182	1.0137	–	1.0477	–	0.8596
21	1.0158	–	–	–	–	–	1.0000	–	–	–
22	–	–	–	1.0116	1.0091	1.0033	0.9947	1.0396	–	0.8460
23	–	–	–	–	–	–	0.9900	–	–	–
24	–	–	–	0.9999	0.9976	0.9849	–	1.0283	–	0.8355
25	–	–	–	–	–	–	–	–	–	–
26	–	–	–	0.9866	09858	0.9670	–	–	–	0.8237
27	–	–	–	–	–	–	–	–	–	–
28	–	–	–	0.9676	0.9717	0.9503	–	–	–	0.8140
29	–	–	–	–	–	–	–	–	–	–
30	–	–	–	0.9550	09548	0.9305	–	–	–	0.8003
31	–	–	–	–	–	–	–	–	–	–
32	–	–	–	0.9342	–	–	–	–	–	0.7858

Table 2. Lung dose correction factor in dependence on AP and equiv. square side s (proportional sized phantoms in ^{60}Co TBI, chest wall t = 4 cm, $\varrho^{Lg} = 0.30$ g/cm^3)

AP (cm)	s* (cm)	CF(AP/2)	F^{Lg}
12	5.2	1.043	0.8455
	6.9	1.044	0.8463
	9.1	1.044	0.8464
14	6.4	1.076	0.8448
	7.7	1.077	0.8453
	10.3	1.077	0.8456
16	6.8	1.109	0.8434
	8.3	1.110	0.8441
	11.6	1.112	0.8456
18	7.0	1.146	0.8420
	9.0	1.150	0.8449
	12.9	1.156	0.8493
20	7.2	1.184	0.8411
	9.8	1.193	0.8475
	14.2	1.204	0.8553
22	7.6	1.223	0.8377
	10.4	1.235	0.8460
	15.5	1.253	0.8583
24	7.8	1.261	0.8356
	11.1	1.280	0.8481
	16.4	1.303	0.8634
26	8.3	1.307	0.8352
	11.9	1.325	0.8467
	17.5	1.356	0.8665
28	8.4	1.341	0.8289
	12.5	1.374	0.8493
	18.2	1.414	0.8740
30	9.1	1.387	0.8259
	13.2	1.422	0.8468
	19.3	1.472	0.8766
32	9.6	1.429	0.8191
	13.9	1.470	0.8426
	20.4	1.532	0.8781

* s – side of the equivalent square of lung area, as seen from the input direction

References

1. Vrtar M. Local dosimetric functions and lung correction factor under ^{60}Co TBI. *Radiol Iugosl* 1990; **24**:289-96.
2. Vrtar M, Purišić A. Local tissue air ratio in an anatomic phantom in ^{60}Co total body irradiation. *Radiother Oncol* 1991; **21**:157-162.
3. Van Dyk J, Leung PMK, Cunningham JR. Dosimetric consideration of very large cobalt-60 fields. *Int J Radiat Oncol Biol Phys 1980;* **6**:753-9.
4. Podgorsak EB, Pla C, Evans MDC, Pla M. The influence of phantom size on output, peak scatter factor and percentage depth dose in large field photon irradiation. *Med Phys* 1985; **12**:639-45.
5. Quast U. Physical treatment planning of total body irradiation: Patient translation and beam-zone method. *Med Phys* 1985; **12**:567-74.
6. ICRU 1989, Report No 44, Tissue substitutes in radiation dosimetry and measurements. Bethesda MD.
7. Mayneord WV. The significance of the roentgen. *Acta of the International Union Against Cancer* 1937; **2**:271-5.
8. Dutreix A, Bridier A. Total body irradiation techniques and dosimetry. *Path Biol* 1979; **27**:373-8.
9. Marinello G, Barie AM, Bourgeois JP. Measurement and calculation of lung dose in total body irradiation performed with cobalt-60. *J Eur Radiother* 1982; **4**:174-82.
10. Mauceri T, Kase K. Effect of ionisation chamber construction on dose measurements in a heterogeneity. *Med Phys* 1987; **14**:653-6.

Adv Radiol Oncol 1992; 330-4.

Subtotal-skin electron irradiation of the torso

Umek B, Habič M, Jereb B, Štabuc B

The Institute of Oncology, Ljubljana

A patient with multiple skin metastases from breast carcinoma was in addition to chemotherapy treated with radiation therapy. The technique has been developed using 4.5 MeV electron beam from a linear accelerator, and a standard electron applicator, combining multiple fields at increased source-skin distance. The details of the technique and the results of measurements necessary for its clinical application are described.

Key words: skin neoplasms-secondary; breast neoplasms; radiotherapy; electron beam

Introduction

Multiple superficial lesions such as skin metastases, cutaneous lymphoma or mycosis fungoides are often treated with large electron fields. There are several treatment techniques for this purpose, using open electron beams at increased source-skin distance (SSD), arc technique or combination of electron with photon beams.[1-5] None of the described techniques was available at the Institute of Oncology; therefore a new technique was developed using multiple matching electron fields.

Materials and methods

Case report

The patient O.M., a 35 year old woman underwent right radical mastectomy for breast cancer ($T_2N_1M_2$) in June 1981; the histology of the tumour was invasive ductal carcinoma with metastases in the axillary lymph nodes. Postoperative adjuvant chemotherapy with Cytoxan, Methotrexate and 5-Fluorouracyl (CMF - 11 cycles) was completed in July 1982.

In August 1984, the patient underwent radical mastectomy for carcinoma of the left breast, histology was again invasive carcinoma with metastases in the axillary lymph nodes. At the time of diagnosis of the second tumour, she presented with skin metastases spread on the thoracal wall (1 x 1.5 cm in the T 12 and in the lumbal region).

With Nolvadex and Tamoxifen a complete remission was noted after four months. But when recurrent skin and lymph node metastases appeared and were treated with hormones, there was no response. After four cycles of Cytoxan, Adriablastin and 5-Fluorouracyl the patient was in partial remission, but still with multiple residual skin metastases (Figure 5).

Radiation therapy of the whole thoracal skin including the scalp and proximal thirds of both upper extremities was added to chemotherapy.

Radiation treatment was given with 4.5 MeV electrons from linear accelerator Philips SL 75/

Correspondence to: Bogdan Umek, M. Sc., The Institute of Oncology, Zaloška 2, 61000 Ljubljana, Slovenia.

UDC: 616.5-006.6:615.849

20. The largest electron applicator (20 x 20 cm) was mounted on the treatment head and SSD increased to 154 cm, which is near to the lowest possible position of the treatment-couch. In this way, a larger field size (32,5 x 32,5 cm) on the patient's skin is obtained. The patient was treated in the supine position with the arms under the head using four fields. Then she was turned to the prone position and another four fields were applied. In order to match the 50% isodoses from adjacent fields, they were separated by 14 mm gaps on each side (Figure 1). Four of the eight treatment beams were inclined by 30° from the vertical axis in order to avoid underdosage on the lateral sides of the patient. The poles of vertical and inclined fields were changed from treatment to treatment for symmetry. The area of patient's body which was outside the optical border of the treatment fields was shielded with 8 cm thick wood plates (density = 0,6 g/cm^3) as the dose at the border was still 55% of its maximum (Figure 4). Shielding plates were placed on the frame attatched to the treatment-couch. The face was shielded with 3 mm lead. A dose of 300 cGy was given to the points on 100% isodose (Table 1) twice a week to the total dose of 2400 cGy.

The 4.5 MeV electrons were derived by degrading the original 6 MeV beam using a 6 mm perspex absorber placed on the shielding frame approximately 10 cm above the skin surface.

The depth dose profile was measured in a perspex phantom with holes drilled to adequate depths in order to place thermoluminiscent dosimeters (TLDs). Harshaw TLD-100 rods (6 mm x dia. 1 mm) were used, annealed and read-out a Toledo 654 TLD reader.[6]

The dose profile along the horizontal axis in the depth of the maximum dose was obtained with an automatic water phantom RFA-3. The output was defined using a plane-paralell ionization chamber covered with a sheet of perspex equivalent to the depth of the maximum dose. All the measurements were done at SSD = 154 cm.

The dose distribution along the circumference of the patient's body was studied in a body-shaped phantom consisting of ten, 1 cm thick together packed perspex plates. Holes for placing of thermoluminiscent dosimeters were drilled in one of the internal plates of the phantom to adequate depths. Eight TLD rods were placed in the depths of 5 and 10 mm at 30° intervals from vertical axis passing through the center of the phantom (Figure 2). One of dosimeters (No. 9) was placed on the lateral surface of the phantom where the dose maximum was expected. Dosimeter No. 10 measured the x-ray contamination in the middle of the phantom.

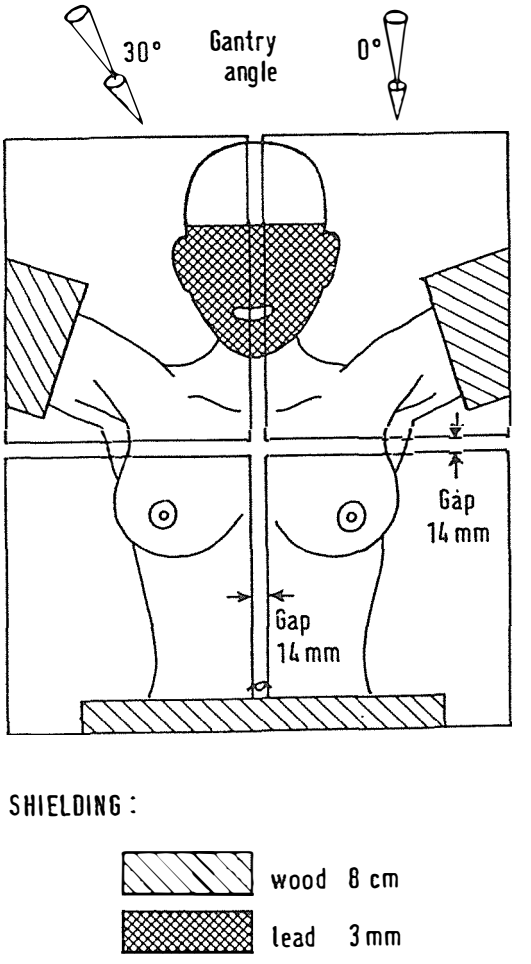

Figure 1. Outline of fields for treatment with 4.5 MeV electrons when patient is in supine position. Half of the beams are angled by 30° from vertical axis.

Table 1. Dose distribution in body-shaped perspex phantom irradiated by 4.5 MeV electrons. Doses are normalised to the depth of 10 mm on vertical axis throught the phantom (see Figure 2).

Depth in perspex (mm)	Angle from vertical axis (degrees)			
	0	30	60	90
5	119	125	109	80
10	100	120	90	48
1	–	–	–	138
100	5.4	X-ray contamination		

Results

The depth-dose curve of 4.5 MeV electron beam is shown in Figure 3. The level of x-ray contamination reaches 1.3% of the maximum dose.

The dose profile in the horizontal plane at the depth of the dose maximum is plotted in Figure 4. As seen from the plot, the dose falls to 50% of its maximum value at the place exceeding the geometrical border of the treatment field. Thus a spacing of 2 x 7 mm between adjacent fields is needed in order to achieve a uniform dose around the gap. It is also seen that the region lying outside the treatment field has to be shielded to the distance at least 10 cm exceeding the geometrical border of the field.

The results of dose distribution measurements are summarized in Table 1. Doses are normalized to the depth of 10 mm, at the point measured by dosimeter No. 2 in Figure 2. The level of X-ray contamination is 5.4%, i. e. four folds the one for X-ray background of a single electron beam.

The appearance of the patient after the treatment is shown in Figure 6. The complete clinical remission lasted 8 months. In December 1986, recurrent disease with metastases in the lung, skeleton, lymph nodes and skin was noted. Brain metastases occurred 2 months later and were the cause of death in May 1987.

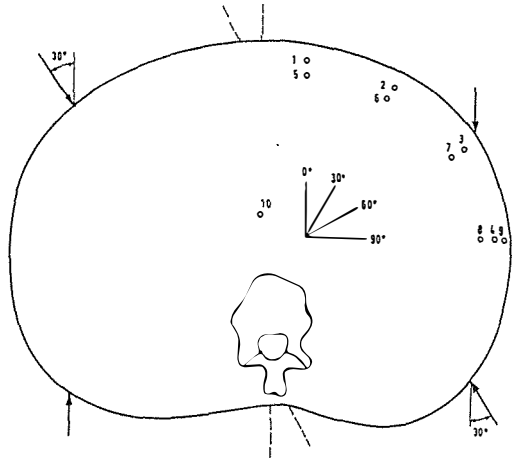

Figure 2. Cross-section of perspex phantom showing field set-up and position of thermoluminiscent dosimeters (1 do 10) during dose distribution measurement. The centers of electron fields are indicated by arrows, field-borders by dotted lines.

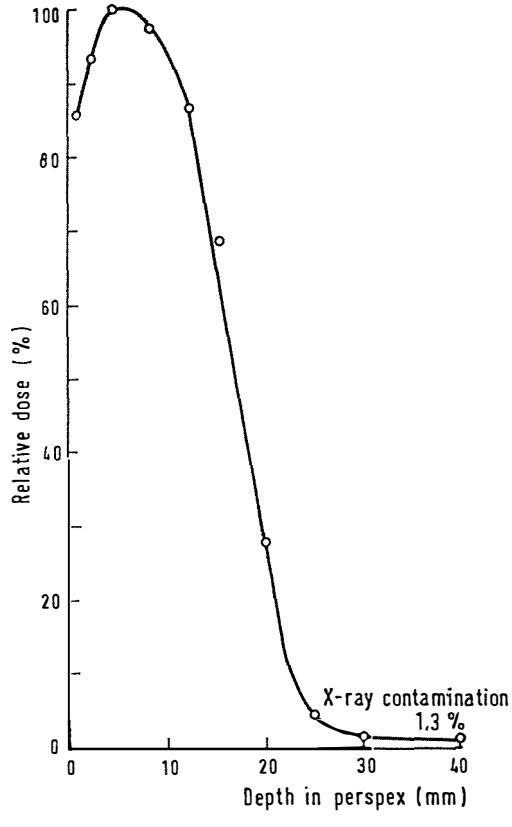

Figure 3. Depth-dose curves for 4.5 MeV electron beam.

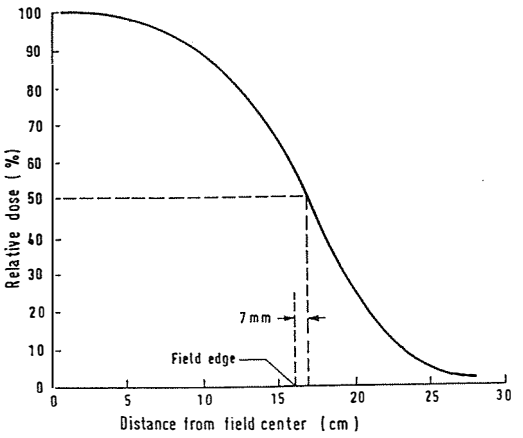

Figure 4. Transverse dose profile fo 4.5 MeV electron beam at the depth of maximum dose.

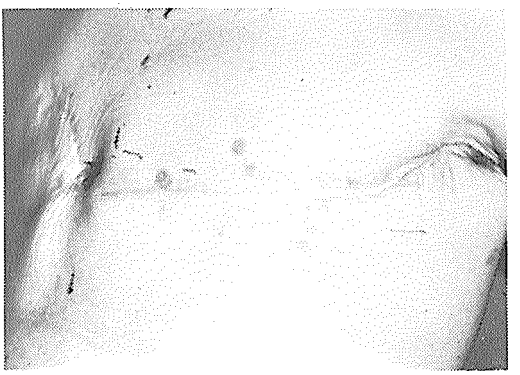

Figure 5. Skin metastases before irradiation.

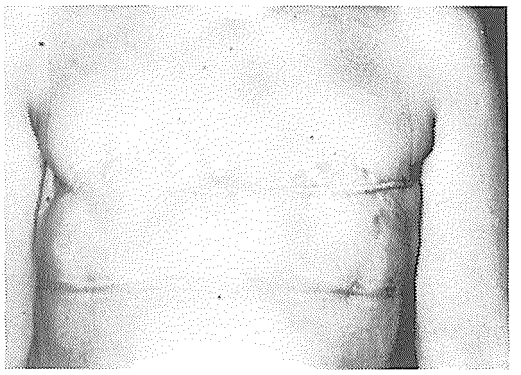

Figure 6. Skin metastases 4 months after completion of radiation therapy.

Discussion

The results of measurements in perspex phantom show that, using the described configuration of beams, depth dose distribution varies along the circumference of the phantom depending on the angles of incident beams. The most unconvenient distribution takes place on the lateral side of the phantom where the dose changes from about 140% at 1 mm depth to 80% of the prescribed dose at 5mm depth of perspex. This could be probably improved by further inclining the angled electron beams, but this would prevent precise matching of treatment fields and would cause problems of shielding of noninvolved areas of the patient's skin.

Comparison of the measured output with the one obtained at standard SSD (95 cm) showed that electrons had not followed the inverse square law, the power law exponent having been increased to 2.33 instead of 2. Measurements also showed that effective SSD for a 20 x 20 cm electron applicator is 18 cm shorter than nominal SSD.

In our opinion, the technique of large matching electron fields is satisfactory from the physical as well as medical point of view. Although time consuming, it could be a good alternative to other more sophisticated methods for treatment of large cutaneous lesions. The number of treatment fields could be further increased or reduced according to the extent of skin lesions. It is comfortable for patient who is laying on the treatment-couch. This fact also simplifies the shielding of uninvolved areas of the patient.

References

1. Edelstein GR, Clark T, Holt JG. Dosimetry for total-body electron-beam therapy in the treatment of mycosis fungoides. *Radiology* 1973; **108:**691.4.
2. Bjarngard BE et al. Analysis of dose distribution in whole body superficial electron therapy. *Int J Rad Oncol Biol Phys* 1977; **2:**319-24.
3. Boyer AI, Eulerton GD, Mira JG. An electron beam pseudoarc technique for irradiation of large areas of chest wall and other curved surfaces. *Int J Rad Oncol Biol Phys* 1982; **8:**1969-74.

4. Villiams PC, Hunter RD, Jackson SM. Whole body electron therapy in mycosis fungoides – a successful translational technique achieved aby modification of an established linear accelerator. *Br J Radiol* 1979; **52:**302-7.
5. Pezner RD et al. The reverse hockey stick technique postmastectomy radiation therapy for breast cancer patients with locally advanced tumour presentation or extensive loco-regional recurrence. *Int J Rad Oncol Biol Phys* 1989; **17:**191-7.
6. Umek B. Fast preparation of thermoluminiscent LiF dosimeters for the use. *Radiol Iugosl* 1988; **22:**93-7.

Adv Radiol Oncol 1992; 335–40.

Scanning slit radiography apparatus with a radiographic grid

Miklavčič L

Ortopedska bolnica Valdoltra, Ankaran

The scanning slit radiography apparatus with a radiographic grid of the invention makes possible the x-ray imaging at an enchanced primary radiation transmission, yet a reduced scatter transmission. By orienting long axes of radiopaque strips obliquely to the sweep of the grid, the strips being separated by air, interspaces can be performed with a sufficient own stiffness so that no aluminum top and bottom covers are needed. The planes of downward lateral faces intersect each other in an upward decentration line and the planes of upward lateral faces intersect each other in a downward decentration line. In a preferred embodiment of the invention, the grid is inclined during the sweep so that the convergent line of the grid continues to pass through the tube focus.

Key words: radiography; technology; radiologic; radiographic image enhancement

Introduction

This article, a part of a patent application.[1] outlines the theory of a particular slit radiographic technique where a new type of an improved grid is used for better suppression of the scattered radiation.

Description of the prior art

In the radiography, especially when performed with X-rays having the energy increasingly above the 50 keV, which is used for medical diagnosing, the Compton scattering of the primary X-rays takes place with increasing probability. The direction of the propagation of secondary radiation. i. e. of scattered radiation, mainly differs from the direction of propagation of primary X-radiation being emitted from the focal spot on the anode of the X-ray tube.

A scatter-removing radiographic grid placed between the object to be imaged and the cassette with the X-ray film prevents the secondary X-radiation from impinging on the film and thus from impairing the contrast of the X-ray image originating just from the primary X-radiation. The radiographic grid was protected by G. Bucky through US patent 1.164.987. It is usually made of strips of a strongly absorbing metal as lead, i. e. of radiopaque strips, between which strips of a weakly absorbing substance as aluminium, i. e. radiolucent strips, are inserted. The long axes of the strips are mutually parallel, however, the strips are differently tilted around the axes so that prolongated strip plains intersect themselves in a convergent line. During an exposure the radiographic grid oscillates within its plane transversely to its strips to prevent an imaging of shadows of the radiopaque strips. Representative parameters of such radiographic grid are: 34

Correspondence to: Dr. Lucijan Miklavčič, Orthopedic Hospital Valdoltra, Jadranska cesta 31, 66280 Ankaran, Slovenia.

UDC: 616-073.755.2

strip pairs/cm: the thickness of aluminium strips is 0.25 mm and of the lead strips 0.05 mm: the ratio of the grid is 10: the grid is stiffened by an aluminium support cover of a thickness of 0.25 mm on its top and bottom: the transmission of the grid is 60% and its focal lenght, i. e. the distance of the convergent line from the grid, equals 1500 mm. It is a disadvantage of such radiographic grids that their transmission for the primary X-radiation is low and lies about 60% and 65%: therefore the patient is exposed to a rather high dose of X-radiation. Furthermore, at the passage of the primary X-radiation across aluminium strips and support covers, the low energy X-radiation is absorbed at a higher rate, whereby the contrast of the X-ray image is impaired. Still another disadvantage of the radiographic grids known in the state of the art exists in that the radiopaque strips are thin and therefore rather translucent for the secondary X-radiation.[2]

In the scanning slit radiography,[2, 3] however, the secondary X-radiation is eliminated by an aft slit, which is swept between the object to be imaged and the cassette with the X-ray film in synchrony with a beam defining fore slit. The images are excellent. However, either the sweep of the fore and aft slit is slow causing an undesiredly long exposure time during which the patient might move or the X-radiation flux density is high, which requires a high X-ray tube loading. When wide body organs or regions, e. g. the chest, are imaged, the width of the aft slit must be increased in order to reduce the exposure time.[4, 5] It is a consequence thereof that more X-ray scatter impinges on the film, which impairs the quality of the image.

Other technical solutions based on a synchronous multiple slit assembly systems may have kinetic artifacts.[5, 6]

Detailed description of the preferred embodiment

A top view of a radiographic grid 1 in the scanning slit radiography apparatus of the invention is shown in Figure 1. A radiopaque frame 11 of the grid 1 is mounted in a carriage 4, which is sweepable along guide bars 21. 21' of a sweeping guide frame 2 (Figure 4). During the X-ray exposure the carriage 4 performs a sweep S. The guiding frame 2 is movably mounted to a transversal guide bar 3, to which a bar 5 carrying an X-ray tube and a collimator (not shown) is fastened (Figure 3). Generally speaking, in each instant the longitudinal axis X of the grid 1 is parallel to the sweep S. In the frame 11 a rectangular aperture 11' is performed. The downward border 11'a and the upward border 11'b, with respect to the sweep S, of the aperture 11' are normal to the axis X.

Radiopaque strips 12 are fastened to the grid frame 11 by means of fasteners 14 (Figure 1, 2). By the radiopaque strips 12 the aperture 11' is separated into air interspaces 13. The long axes A of the strips 12 are mutually parallel. The strips 12, however, are tilted around the axes A differently so that the median planes L of the strips 12 intersect each other at a convergent line CL of the focal plane F of the grid 1 (Figure 3). The projection of the convergent line CL to the plane of the grid 1 is labelled by CL. The point of intersection of the projection CL' with the

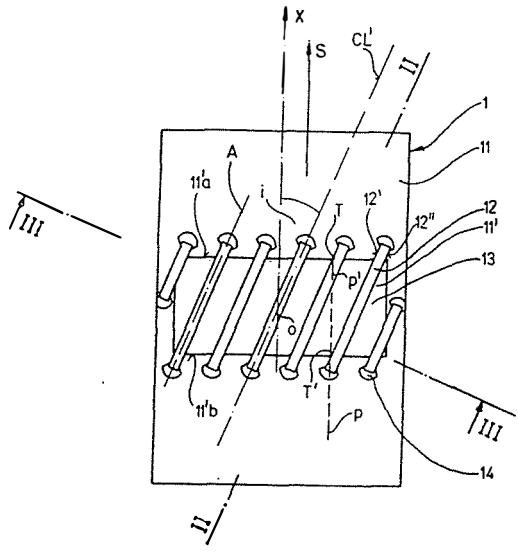

Figure 1. A top view of the construction of the radiographic grid in the scanning slit radiography apparatus of the invention.

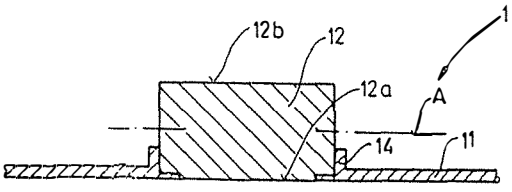

Figure 2. The cross section of the radiographic grid across the line II-II in Figure 1.

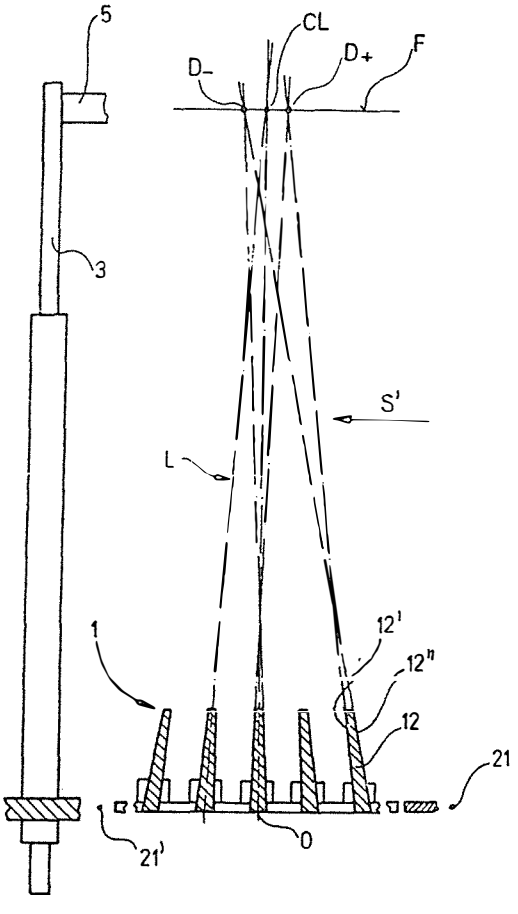

Figure 3. The cross section of the radiographic grid across the line III-III in Figure 1.

grid axis X is situated in the middle point O of the grid 1.

A downward lateral face 12' and the upward lateral face 12'', with respect to the sweep S or, more precisely, with respect to a projection S' of the sweep S onto the plane of Figure 3, of each

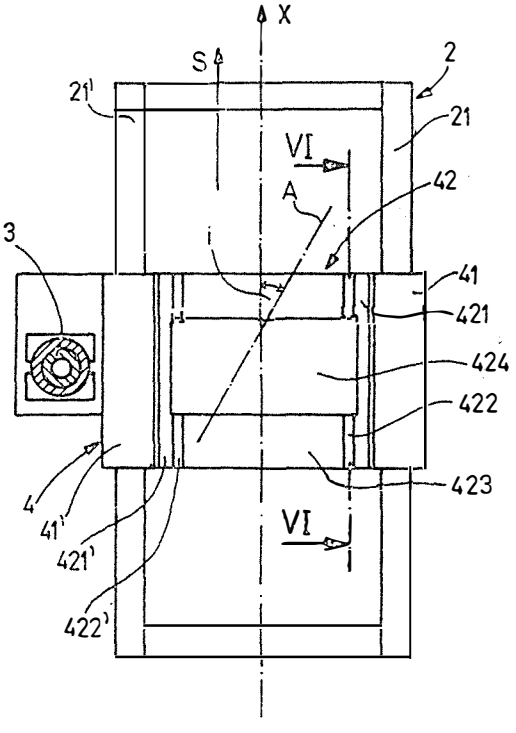

Figure 4. A top view of the scanning slit radiography apparatus with the radiographic grid.

strip 12 are inclined to the medial plane L of the strip 12 so that the strip cross section is trapezial. The inclinations of the lateral faces 12', 12'' are, however, such that the planes of the downward lateral faces 12' of all strips 12 intersect each other in an upward decentrated line D+ and that the planes of the upward lateral faces 12'' of all strips 12 intersect each other in a downward decentrated line D–. The decentrated lines D–, D+ are situated in the focal plane F of the grid 1.

The strips 12 are fastened to the frame 11 so that the angle i between the axes A and the axis X is defined as follows. The point T of intersection of the downward border 11'a with the downward lateral face 12' of any strip 12 is situated on the same line p which is parallel to the axis X, as the point T' of intersection of the upward border 11'b with the downward lateral face 12' of the next strip, which is situated upwaredly with respect to the former strip 12.

Consequently, the points T, T' of intersection are equidistant from the axis X. This condition must be fullfilled for both extreme strips 12 as well.

The guide bars 21, 21' of the guide frame 2 are mutually parallel or, according to the preferred embodiment of the invention, mutually skewed for a small angle 2j. The carriage 4 consists of a holding frame 42 provided to receive the radiographic grid 1 and of sliding shells 41, 41'. The sliding shells 41, 41' are mounted on the guide bars 21, 21' so that they can traslatory sweep along them. In the preferred embodiment, however, uninclinable frame pieces 421, 421' are fastened to the sliding shells 41, 41'. An inclinable frame piece 423, which is provided with a central opening 424 to receive the radiographic grid 1, is pivotally attached to the uninclinable frame pices 421, 421' by means of hinges (422, 422' resp) (Figure 4, 5).

The projections of the guide bars 21, 21' onto the plane CP of the uninclinable pice 423, i. e. of the grid 1, in the middle of the sweep S are mutually parallel. With respect to the plane CP the guide bar 21 rises at the angle j, and the guide bar 21' descends at the angle j (Figure 6). Hence the angles of the hinges 422, 422' being situated in the plane of the inclinable frame piece 423 are inclinated at the angles +j and –j, respectively, with respect to the guide bars 21, 21'. In a small angle approximation the angle 2j of the mutual skewness of the guide bars 21, 21' is determinated by the focal lenght f of the radiographic grid 1, by the decentration e, by the distance w between the hinges 422, 422' and by the lenght s of the sweep S:

$$2\,j = (e * v) / (f * s).$$

In the embodiment of the apparatus of the invention with mutually parallel guide bars 21,

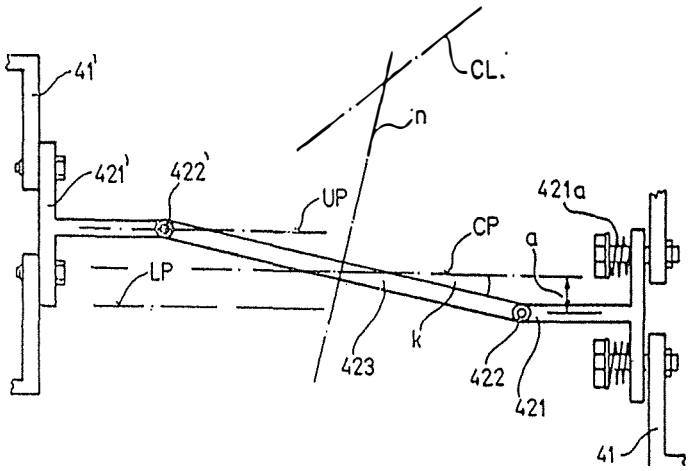

Figure 5. A view in the direction of the sweep of the carriage and partially of a sweep guide within the apparatus of the invention, and

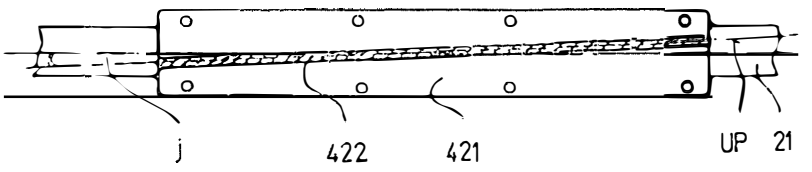

Figure 6. The cross section of the carriage across the line VI-VI in Figure 4.

21', the radiographic grid 1, e. g. provided for the imaging of a complete spinal column onto a film of dimensions 30 cm x 90 cm, has the following design parameters. The aperture 11' of the grid frame 11 determines an X-radiation beam of a height of 150 mm as determined by the distance between the borders 11'a, 11'b and of a width of 300 mm. The sweep lenght s is 1050 mm. The radiopaque strips 12 of a height (h) of 24 mm are made of tantalum: they have a thickness of 0.50 mm at the base line 12a and a thickness of 0.28 mm at the top edge 12b. The width D of t he air interspaces 13 at the level of the base lines 12a is 2.00 mm. The angle i between the strip axes A and the grid axis X is determinated by sin i = 1/60. The ratio h/D of the grid 1 is 12. The primary X-radiation transmission is as high as 80%.

By moving the carriage 4 along the transversal guide bar 3. the focal plane F of the radiographic grid 1 is positioned to include the focus of the X-ray tube. Further, in the middle of the sweep S the middle point O of the grid 1 must be situated just below the focus of the X-ray tube, i. e. the focus will be on the convergent line CL at that moment. In the middle of the sweep S the maximum transmission of the grid 1 is achieved by the convergence of the medial planes L of the strips 12 towards the convergent line CL. At both extreme positions, however, this is accomplished by such an additional inclination of the lateral faces 12', 12'' of the strips 12 that the planes of the lateral faces converge towards decentrated lines D+ and D–. The lines D–. D+ are determined so that at the extreme upward position of the sweep S the tube focus is situated on the downward decentrated line D– of the grid 1, and that at the extreme downward position of the sweep S the tube focus is situated on the upward decentrated line D+ of the grid 1. Thereby is prevented that the upper strip portion would filter the X-ray radiation which would othervise most probably pass a part of the strip height h, i. e. a part of the distance between the base line 12a and the strip upper edge 12b. An extremely exact blurring out of the image of the grid strips 12 is accomplished by the above defined inclination angle i of strip axis A with respect to the grid axis X. Thus the angle i depends on the X-radiation beam height H, which equals the mutual distance of the borders 11'a and 11'b of the grid aperture 11'. By the radiographic grid 1 proposed by the invention excellent diagnostic images of a human spinal column can be achieved also at high anode voltages ranging from 90 to 100 kV. Thereby the dose absorbed by the patient is reduced to 1/3 to 1/4 of the dose that is absorbed when a patient is imaged with a known Pb/Al grid at the anode voltages of 60 to 70 kV. This reduction of the absorbed dose is a consequence of the above indicated advantages of the grid proposed by the invention and of a higher sensitivity of the film-screen combination at this anode voltage.

The preferred embodiment of the apparatus of the invention with mutually skewed guide bars 21, 21' functions as follows. When the carriage 4 performs the sweep S, the uninclinable frame piece 421, 421' translatory rises or descends, respectively, between the lower plane LP and the upper plane UP, which are separated by a distance 2a. In the middle of the sweep S the uninclinable frame pieces 421, 421' are in the same plane CP as there is also the inclinable frame piece 423 with the radiographic grid 1. In this position a normal to the radiographic grid 1 through its middle point O passes through the focus of X-ray tube. When the carriage 4 is sweeped for the lenght s of the sweep S, the inclinable frame piece 423 and thereby the radiographic grid 1 is inclined by rotation around the grid axis X by an angle 2k. During the sweep S the convergent line CL of the radiographic grid 1 moves so that it continues to pass through the X-ray tube focus. As the radiographic grid 1 inclines around the axis X during the sweep S, each point of the convergent line draws an arc of lenght equal to the decentration e of the grid: during the imaging the radiographic grid 1 is continuously centered, which makes possible a still favourable shaping of the cross section of its radiopaque strips 12. Since in each instant the direction of the sweep S coincides with the axis X of the grid 1, the imaging of the strips 12 is completely prevented.

The design parameters of the preferred embodiment of the apparatus of the invention are as follows. For the X-ray imaging on a film 435 mm x 435 mm the height h of the radiopaque strips 12 is 30 mm. The width d of the base line 12a is 0.50 mm and the width D of the air interspace 13 at the base line level is 2.50 mm. The distance H between the downward and the upward borders 11'a 11'b or the grid aperture 11', i. e. the dimensions of the X-ray beam in the direction of the sweep S, is 50 mm and the transverse dimension w of the grid aperture 11' is 435 mm. The grid ratio H/D equals 12, the transverse dimension w of the grid aperture 11' is 435 mm. The grid ratio h/D equals 12. the transmission of the grid for the primary X-radiation equals 83%. for the imaging on the film of the above dimensions the decentartion e = (w/h + 1)(D + d) = 29,10 mm is required. Hence the angle of mutual skewness of the guiding bars 21, 21' equals 1 grade. Therefore the radiographic grid 1 in a complete sweep S is inclined for the angle 2k = 1 grade. The uninclinable frame piece 421 is connected to the sliding shell 41 by a spring 421a to compensate its tiny displacement transversely to the chord of the lenght 2a corresponding to the central angle 2k = 1 grade.

Conclusions

In accordance with the foregoing background discussion, the object of this invention is to provide a scanning slit radiography apparatus with a radiographic grid, which will make possible X-ray imaging with a radiographic grid, which will make possible X-ray imaging with reduced transmission of scattered X-radiation at an enhanced transmission of primary X-ray radiation and with eliminated imaging of the radiopaque strips of the radiographic grid. The construction of the radiographic grid in the scanning slit radiography apparatus proposed by the invention completely prevents the imaging of the grid strips together with as high reduction of the filtration of the primary X-radiation as possible. By orienting the long axes of the strips within the grid obliquely to the sweep, the strips can be performed with an adequate transverse extension and their own stiffness is such that between them air interspaces are possible and no aluminium top and bottom support cover are needed. Thus the patient's exposure to radiation is reduced since the transmission of such grid for the primary X-radiation is high. The portion of low energy X-radiatión in the imaging beam is nearly intact, which has a favourable effect upon the contrast of the image. Another advantage exists in that the construction of the grid allows a greater height of the radiopaque strips and thereby a more complete suppression of the scatter at the area of the X-ray film.

The transmission of the radiographic grid, which during the sweep also changes its inclination so that the convergent line of the grid during the whole sweep passes through the focus of the X-ray tube, is higher than the one of the grid being swept in the known traslatory way, since in this preferred embodiment of the invention the cross section of the radiopaque strips can be changed from a nearly triangular form with an extensive base line to a more pronounced trapezium form with a smaller difference between the lenght of the base line and the thickness of the strip at its top or even to a rectangular form.

References

1. Miklavčič L. Scanning slit radiography with a radiographic grid. European patent application, *Bulletin 1990;* **50:** Publication No. 0 401 527.
2. Barnes GT. Scatter control in imaging recording. In: Taveras JM, Ferrucci JT: eds: *Radiology Diagnosis-Imaging-Intervention.* Philadelphia: J. B. Lippincott Company 1990; 1.
3. Vuorinen P. The roenthenographic slit methods. A survey and analysis of procedures based on the use of a narrow bundle of roentgen rays (scanography). *Acta Radiol.* Suppl 177, Turku 1959.
4. Duinkler S., Vlasbloem H. Apparatus for slit radiography. US Patent No. 4,677,652 Jun 1987.
5. Schultze Kool Lj, Busscher DL, Vlasbloem H, Hermanms J, Merwe PC, Algra PR, Herstel W. Advanced multiple-beam equalization radiography in chest radiology: a simulate nodule detection study. *Radiology* 1988; **169:**35-9.
6. Barnes G.T. Method and Apparatus for reduction of scatter in diagnostic radiology. US Patent No. 4,096,391 Jun. 1978.

Chapter VII. RADIATION PROTECTION

Adv Radiol Oncol 1992; 343–7.

Incidence of structural chromosome aberrations in medical staff occupationally exposed to ionizing radiation

Horvat Đ

Institute for Medical Research and Occupational Health, Laboratory for Mutagenesis, University of Zagreb

In this study occupational exposure to ionizing radiation as a contribution to the presence of permanent somatic cell genome changes in medical staff has been analysed. Control values of medical and technical staff mean »Ø« or pre–exposure mutagenetic data of the persons with similar professions. The total chromosome aberration frequency of control subjects in 16000 checked lymphocytes is lower than 1%. During the occupational exposure in radiological, surgical, orthopedic, urological, gyneacological and nuclear medicine departments, the number of chromosome aberrations is significantly elevated in medical and technical staff. Specific chromosome aberrations – dicentrics and rings and stable aberrations were found in surgeons, while whereas dicentrics and other aberrations were found in radiologists and nuclear medicine specialists. Such aberrations are not present in technical personnel from surgical and urological departments, while other technical profiles have unstable aberrations.

Key words: chromosome aberrations; environmental exposure; hospital departments-staff; radiation effects

Introduction

Analysis of structural chromosome aberrations is a verified test used for determining exposure to numerous clastogens and thus to ionising radiation as well.

The mechanism of origin and reparation of specific radiation induced biological damage is not entirely clear. The basis for an understandable model lies in the assumption that double–strand breaks of the DNA molecules in the cell nucleus are responsible for biological effects such as mutations, chromosomal aberrations or cell reproductive death.[1]

On the other hand, all level mutations, including structural chromosome aberrations, are closely related to the stohastic effects of radiation.

The potentional risk from fractionated low dose radiation during the occupational exposure of medical staff working in radiological departments, surgical, urological, oncologic or nuclear medicine departments have not been sufficiently evaluated.

During the regular dosimetric control only a few of all persons had temporarily registered exposure doses higher than recommended. With regard to the fact that even these doses were received mostly through repeated exposure, it can be assumed that biological effects will be extremely rare, almost negligible.

Correspondence to: Prof. dr. Djurda Horvat, Institute for Medical Research and Occupation Health, Laboratory for Mutagenesis, Trg J. Meštroviča 16, 41000 Zagreb, Croatia.

UDC: 576.312.3:616.001.26-057

If the presence of structural chromosoinal aberrations in the peripheral blood lymphocytes is taken as an indicator of the biologically harmful effect of ionizing radiation, it can be seen that such aberrations were not rare, as well as the fact that their presence was absolutely different from the dosimetric estimation of the exposure dose, in most cases. This statement justifies the use of individual mutagenetic monitoring that has been carried out for the population occupationally exposed to ionizing radiation.[2] If the circulated lymphocyte is assumed as a travelling microdosimeter which motion enables its presence in the circulation as well as in the extravascular spaces, the changes in the cell genome could be a good indicator of exposure. This circumstance is particularly expressed during accidental irradiation.[3] Using the previously prepared calibration (dose–response) curves, it is possible to estimate the irradiation dose with sufficient accuracy on the basis of the specific chromosomal aberration through biological dosimetry.[4]

When the population in question are the medical staff using sources of radiation in their everyday work, accidental irradiations have been rare so far. However, there are some diagnostical or therapeutic procedures during which both the patient and the medical staff are inevitably exposed to radiation.

The aim of this study therefore was the assumption of the biological effect of ionizing radiation, depending on the employment department or the profession of the medical worker. The level of the obligatory training will also be examined.

Subjects and methods

The subjects in this study are employed in a regional medical center in north Croatia. They are not exceptional in any way, so that they can be taken as representative of their profession. The results of the preexposure tests performed in medical staff have been taken as control values, before they start to work with ionizing radiation sources. The »exposed« group consisted of physicians, nurses, RTG–technicians, working in radiological, surgical, orthopedic, urological, gynaecological and nuclear medicine departments.

Before taking the vein blood samples for mutagenic tests, a mutagenic–anamnestic questionnaire was completed for each examinee. The questionnaire consisted of personal data on age, sex, hereditary conditions, alcohohol, smoking and drug dependence, vacinations, diagnostic or therapeutic radiological procedures, and therapy with chemical products.

Notes were made on specific features of the eventual previous working place or ambiental exposure to genotoxica.

The data on recent working place were collected very thoroughly. This included source of radiation, kind of jobs that the examinee was performing, protection measures, and individual dosimetric control.

Information collected through the mutagenic–anamnestic questionaire contributes to the objectivity of the interpretation of suspected or aberrated results.

Persons with acute viral or some other disease caused by biological factors were not examined, and their blood samples for structural chromosome aberration analysis were not taken.

Blood samples for *in vitro* lymphocyte cultures were taken by venopunction. *In vitro* cell cultivation was carried out by standard procedure. An F–10 tissue culture medium (GIPCO) was used, with the addition of 20% inactive calf serum, phytohaemaglutinin (Krka) and BrdU (Calbiochem). After the chromosomal preparation, there were first 200 *in vitro* metaphases analysed per subject.

All present changes in the chromosome structure were noted and categorised as chromatide or chromosome breaks, acentric fragments, dicentric or ring chromosomes, unspecific translocations and symmetric changes. The changes in ploidity, such as tetraploid cells, were also registered.[5] All results were analysed statistically with use of Poisson–based statistical tests.

On the basis of this individual data, the results are presented in Table 1.

Table 1. The incidence of chromosome aberrations in the blood lymphocytes of medical staff occupationally exposed to ionizing radiation.

Department	Number of cells	DISTRIBUTION CHROMOSOME ABERRATIONS PER CELL							%
		Chromatide break	Chromosome break	Acetric	Dicentric	Ring	Sim. exchange	Tetraploid cells	Aberrations
Med. doctors									
Radiological	9400	0.007 ∓0.002	0.004 ∓0.004	0.005 ∓0.006	0.0003 ∓0.001			0.0013 ∓0.002	1.66 ∓0.97
Surgical	1600	0.007 ∓0.005	0.006 ∓0.006	0.007 ∓0.007	0.001 ∓0.003	0.0002 ∓0.001		0.0014 ∓0.003	2.2 ∓0.8
Orthopedic	1600	0.004 ∓0.009	0.003 ∓0.003	0.003 ∓0.003			0.0006 ∓0.002		1.68 ∓0.7
Urological	2200	0.013 ∓0.008	0.006 ∓0.007	0.006 ∓0.005				0.0009 ∓0.002	1.95 ∓1.4
Gineacological	2800	0.006 ∓0.004	0.004 ∓0.016	0.004 ∓0.004				0.0011 ∓0.002	1.3 ∓0.49
Nuclear medicine	2200	0.005 ∓0.004	0.004 ∓0.004	0.008 ∓0.006	0.0005 ∓0.001			0.0009 ∓0.002	1.77 ∓1.19
Control	6800	0.004 ∓0.004	0.002 ∓0.009	0.001 ∓0.002				0.0003 ∓0.0012	0.64 ∓0.2
Tech. personnel									
Radiological	6000	0.008 ∓0.005	0.007 ∓0.006	0.007 ∓0.008	0.002 ∓0.004			0.0003 ∓0.001	2.3 ∓1.27
Surgical	2200	0.008 ∓0.004	0.002 ∓0.003	0.005 ∓0.005					1.45 ∓0.78
Urological	3000	0.008 ∓0.007	0.003 ∓0.005	0.002 ∓0.004					1.36 ∓0.87
Ginecological	11200	0.007 ∓0.005	0.004 ∓0.008	0.007 ∓0.008	0.001 ∓0.002		0.0002 ∓0.0009	0.0009 ∓0.002	2.0 ∓1.36
Nuclear medicine	7400	0.007 ∓0.004	0.006 ∓0.005	0.008 ∓0.012	0.0008 ∓0.002	0.0001 ∓0.0008	0.0001 ∓0.0008	0.0014 ∓0.003	2.14 ∓1.42
Control	9200	0.003 ∓0.003	0.002 ∓0.002	0.001 ∓0.002	0.0001 ∓0.0007			0.0004 ∓0.0007	0.55 ∓0.15

Results

In Table 1 the results are classified according to departments and specific jobs performed by physicians or technical personnel in the »irradiation area«. Within the »exposed« group there were some subjects with elevated number of structural chromosome aberrations and, therefore, their analyses were repeated. As the number of exposed subjects in all departments varied the results were presented through the structural chromosomal damage frequency per analysed cell. Values obtained in the control group, which is actualy »O« or preexposure report, represent a normal population background of the younger generation.

Comparative data analysis of some types of aberrations in the exposed and control samples of a physician has inevitably shown that occupational exposure increases the frequency of aberrations, particularly lesions of the chromosomal type.

The incidence of acentric fragments, which are direct indicators of chromosomal breaks in departments of surgery and urology, is significant at $P<0.001$ or in department of radiology, gyneacology and nuclear medicine at $p<0.01$ in relation to the control sample.

A highly significant difference is present in the incidence of dicentric and ring chromosome.

The presence of dicentrics and rings was evident in exposed persons, while in 6800 examined

pre–exposure metaphases (200 per subject) there were none.

The data are similar for the technical staff, with an obvious difference in chromosome aberration frequency in relation to physicians from the same department.

The total frequency of all registered chromosomal aberrations in the exposed subjects was significantly elevated in relation to the control values.

Discussion

On the whole, these study data could form two separated parts – unexposed control subjects and subjects occupationally exposed to ionizing radiation. The total incidence of chromosome aberrations in the group of examined unexposed subjects was lower than 1%. The dominant types of aberrations are chromatide and chromosome breaks, while acentric fragments are in the minority. A dicentric chromosome was present in only one subject. Rings and translocations were not found in this group. In fact, this group consisted of young physicians before specialisation or soon after it, and technical staff immediately after completed secondary school or college. The obtained results are lower than the data of Bender et al (1990) concerning types of chromosomal aberrations.[8] This is understandable, as Bender's unexposed group of subjects consisted of persons at an average age of 43.7 years, while the average age of our group of subjects was 23.5 years ranging from 18 to 29 years. These results are a very good indicator of so called spontaneous chromosome aberrations in a population without occupational exposure to clastogenic substances. If the chromatide breaks are taken as post G-1 damage of DNA molecules, it can be assumed that only chromosome lesions with acentric fragments be considered as real changes made *in vivo*. They are usually called spontaneous aberrations even though it is more likely that these are the result of numerous environmental genotoxic factors. Obviously the frequency of somatic cell genome changes is not low, compared with the natural and arteficial radiation sources as well as inevitable exposure to chemical genotoxics. Analysing the frequency of chromosome aberrations in medical staff, occupationally exposed to ionizing radiation during many procedures, it has been noted that the number of lympohocyte genome aberrations is greater than in controls. However, these values are very close to the usual background of the middle–aged population in general.[7] After such global evaluation, it is inevitable to focus on to each case of medical and technical personel. It is evident that physicians-surgeons significantly exceed the total chromosome aberration values of the control group, but also all other professions of their colleagues ($p<0.001$). Their mutagenic results present with dicentric and ring chromosomes known as unstable aberrations. Urologists and nuclear medicine specialists follow surgeons with a slightly lower number of total chromosome damage. With regard to the technical staff, the situation is somewhat different. A highly significant difference in the number of total chromosome aberrations in relation to preexposure control values is present in technicians employed in gynecological, radiological and nuclear medicine departments ($p<0.001$).

Such results should be considered from several aspects, the main one being the nature of employment, which is followed by quality, source accuracy, technical protective measures and their application, and very often by the most important factor–professional compliance with the proposed rules and radiological protective measures.

Each of these factors could be thoroughly elaborated. Besides the ionizing radiation sources, we often meet numerous non–ionizing radiation sources, e.g. modern diagnostical–therapeutical devices such as microwave, laser or ultrasound.

It is often impossible to pinpoint occupational exposure to a single physical agent. Usually there is simultaneous exposure to both sources.

The development of medical equipment follows all other branches of technical and technological development. Unfortunately, the training of medical and technical staff has not been organized in the same way.

Acknowledgments

The author acknowledges the excellent technical assistence of Mrs Jadranka Račić and Mrs Jasminka Kapetan.

References

1. Leenhouts HP, Chadwick KH. The molecular basis of stochastic effects. *Health Phys* 1989;**57**:343-8.
2. 1990 Recommendations of the International Commission on Radiological Protection, ICRP Publication 60. Pergamon Press Oxford–New York–Frankfurt–Seoul–Sydney–Tokyo 1990; 59.
3. Kormos C, Koteles GJ. Comparison of cytogenetic tests for monitoring overexposures from ionizing radiation. *Acta Biologica Hungarica* 1990; **41**:115-20.
4. Bender MA, Awa AA, Brooks AL, Evans HJ, Groer PG, Littlefield GL, Pereira C, Preston JR, Wachholz BW. Current status of cytogenetic procedures to detect and quantify previous exposures to radiation. *Mutation Res* 1988; **196**:103-59.
5. Biological dosimetry, Chromosomal aberration analysis for dose assessment, Technical reports series No 260, International Atomic Energy Agency, Vienna, 1986.
6. Bender MA, Preston RJ, Leonard RC, Pyatt BE, Gooch PC. On the distributions of spontaneous chromosomal aberrations in human peripheral blood lymphocytes in culture. *Mutation Res* 1990; **244**:215-20.
7. Horvat D, Brumen–Mahović V, Fucić A, Garaj–Vrhovac V, Kubelka D. Study of possible biological consequences of the Chernobyl nuclear accident. *Arhiv zast majke i djeteta,* 1989; **33**:193-8.

Adv Radiol Oncol 1992; 348-55.

The effect of ionising radiation on the peripheral blood flow of occupationally exposed medical personnel

Brumen V and Bonić I

University of Zagreb, Institute of Medical Research and Occupational Health, Clinical Hospital »dr. Mladen Stojanović«, Zagreb

The aim of this investigation was to point out an interdependent relationship between objective changes in the numerical equilibrium, morphology and function of the peripheral capillary blood flow and occupational chronic exposure to fractionated low doses of ionising radiation. A total of 66 subjects (36 exposed and 30 control persons) was examined. The condition of the blood flow was monitored parallelly by nailfold capillaroscopy, digital thermometry and digital photoplethysmography on both hands. The results showed the incidence of microvascular abnormalities to be significantly higher in the exposed group and pointed out the need for complete diagnostics of peripheral blood flow condition in medical personnel occupationally exposed to ionising radiation, particularly in those whose hands are exposed to the primary beam.

Key words: radiation effects; environmental exposure; blood flow velocity; capillaries;

Introduction

In all environments there is a certain level of radioactivity which originates from natural sources. In the modern world this basic degree of radioactivity is considerably higher due to technological modifiers. Furthermore, some iatrogenous exposure is present in the population, i. e. occupational exposure to sources of ionising radiation.

A specific group of people using radiation sources in their daily work are the medical personnel working in departments for radiological diagnosis and therapy. During the diagnostic procedure efforts are made to ensure that the relevant information is readily obtained even when patients and medical personnel are exposed to minimal doses of radiation. With proper equipment and well trained personnel, this principle has been fulfilled in most cases. As a rule, high doses of radiation are directed to the target tissue during radiotherapy, and at the same time efforts are made to ensure that medical personnel receive as low a dose as possible.

The most widespread aspect of application of ionising radiation in medicine is radiological diagnosis with X-rays. Abundant data exsist in literature on the dose of radiation received by patients during certain radiological examinations, however much less attention is paid to the dose thus received by the professional personnel.

Data are usually given separately for the physicians-specialists, and for the technical personnel,

Correspondence to: Brumen Vlatka, Institute for Medical Research and Occupational Health, University of Zagreb, Laboratory for Mutagenesis, Trg I. Meštrovića 15, 41020 Zagreb, Croatia.

UDC: 616.15-018.5-001.2

who do not usually work with the primary beam of radiation.[1, 2]

The nature of the work of the medical personnel is such that, almost invariably parts of the body are irradiated. Arms are particularly endangered, because they are most frequently in the primary beam, but also the head and the chest.[3, 4, 5] For this reason it is not always opportune to consider the total dose on the film-dosimeter as effective, and it is useful to take into account also biological indicators.[6, 7, 8]

Although the harmful effects of ionising radiation on the human organism have been thoroughly studied and are well known, there are still some aspects of this problem which have not been sufficiently investigated. One of these aspects is the effect of ionising radiation on small peripheral blood vessels. Particularly interesting are the changes in the peripheral blood flow in persons chronically exposed to small doses of radiation.

The aim of this investigation was to prove an interdependent relationship between objective changes in the numerical equilibrium, morphology and function of the peripheral capillary blood flow and occupational chronic exposure to fractionated low doses of ionising radiation.

Subjects and methods

The experimental group consisted of 36 examinees employed in the Department of Radiology in a clinical hospital. The average years of service in a zone of ionising radiation was 18 years (range 2-38 years). The professional structure was as follows: 12 radiologists employed at various diagnostic locations, and 24 radiological technicians.

As smoking can influence vascular status it should be mentioned that within the experimental group there were 16 light smokers (up to 20 cigarettes a day), 2 moderately heavy smokers (20-40 cigarettes a day) whereas there were no heavy smokers (more than 40 cigarettes a day).

In order to achieve as objective an interpretation of findings as possible, it is important to know whether the subject is a chronic alcoholic. All 36 examinees denied alcohol abuse in the case histories.

Data on chemotherapy are also important. During the period of examination one of the examinees in this subgroup was taking diuretics, one analgetics, one antirheumatics and two of them used peroral contraceptives.

The control group consisted of 30 subjects. Persons who had not previously worked in an ionising radiation zone were included in this group, and examinations were carried out within the framework of a pre-exposure analysis prior to starting work with radiation sources. There were 12 general practitioners in the group who were commencing work in corresponding fields of medicine, and 18 technicians due to start work in a zone of ionising radiation.

There were 13 light smokers in the control group and no moderately heavy or heavy smokers. For classification the same criteria were used as in the experimental group.

In case histories all examinees denied alcohol abuse. During the examination one of the examinees was taking analgetic therapy and one analgetics and antibiotics of wide spectra.

In all examinees the condition of the peripheral blood flow was determined by parallel capillaroscopic, photoplethysmographic and thermometric methods. In each examinee nailfold capillaries of both hands (i. e. eponychium) were examined. Capillaroscopy was performed on a Zeiss capillaroscope, under 50-fold magnification. In each subject digital photoplethysmography was performed, also on both hands. The examination was carried out on a plethysmograph Schwarzer. Lastly, digital dermothermometry was done using a »Technoterm« thermometer, type 1200 (measuring probe type 2512). Temperature was taken on each finger at four points: apically (on the finger tip) and at the level of the interphalangeal joints. Temperature differences of 1°C or more between the referent points on the right and on the left hand were considered significant.

In order to reduce the influence of environmental factors, all examinations were carried out in the same room, after a period of adaptation

of the examinee, in optimal temperature conditions (approximately 21°C). All examinees were advised not to consume high caloric food or alcohol on the day before the examination, and to refrain from smoking for 2-3 hours before the examination.

Prior to the examination a detailed case history was taken for each examinee, which included data on personal, family and work history, habits (smoking, drinking) exposure to radiation sources (occupational exposure, diagnostic or therapeutic irradiation in the referent period) or chemical agents (occupational exposure, relevant medical theray).

Capillaroscopic, photoplethysmographic and thermometric findings will be presented comparatively, in order to demonstrate their relation.

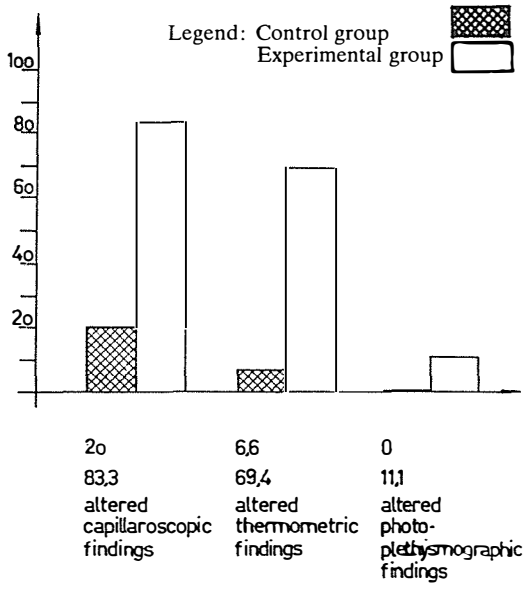

Figure 1. Graphycal presentation of Table 1.

Results

In the medical personnel occupationally exposed to ionising radiation, which was capillaroscopically, photoplethysmographically and thermometrically examined in this study, a high percentage of verified changes in the peripheral blood flow of the hands was seen. The total number and percentage of changed findings are given in Table 1 for each method and presented graphically in Figure 1.

It was particularly interesting to observe a correlation between the findings of certain examinations of the capillary blood flow. The results are shown numerically in Table 2 and graphically illustrated in Figure 2.

In the tested group only 5 examinees (13.8%) had a changed capillaroscopic finding only. The type and scope of the changes found in the microcirculation in such cases did not show »left-right« differences, i. e. the finding was practically symmetric. In 21 examinees (58.3%) the capillaroscopic finding correlated with the thermometric finding, and in 4 examinees (11.1%) both with the thermometric and photoplethysmographic findings. It was observed that the asymmetry of the capillaroscopic finding was accompanied by temperature variation between the right and the left hand. Individual findings in examinees in which a positive correlation was established between the findings of all three examinations are shown in Table 3. These cases can be considered the most characteristic be-

Table 1. Total number and percentage of altered capillaroscopic, thermometric and photoplethysmographic findings.

Group	Number of examinees	Altered capillaroscopic findings		Altered thermometric findings		Altered photoplethysmographic findings	
		No	%	No	%	No	%
Control group	30	6	20	2	6.6	0	0
Exposed group	36	30	83.3	25	69.4	4	11.1

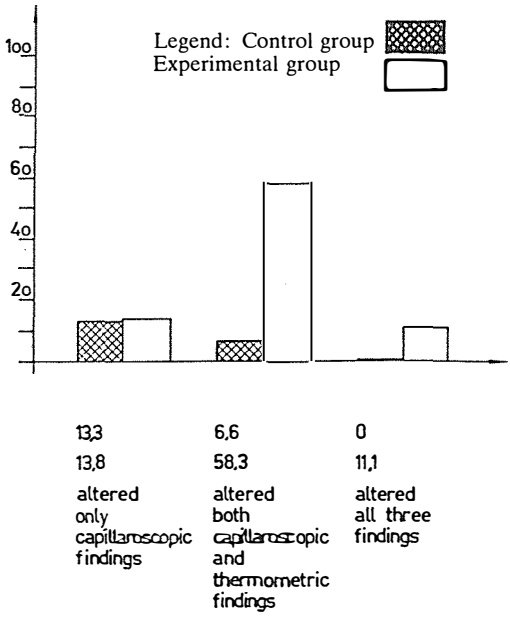

Figure 2. Graphycal presentation of Table 2.

cause the changes in the peripheral blood flow were not noted only in the capillaries, but also in the digital arteriolas.

The capillaroscopically detected changes in the small blood vessels of the periphery were divided into three basic groups: numerical, morphological and functional damages. Numerical damage referred to impaired numerical regularity of the capillaries, i. e. the presence of reduction zones of the capillary numbers. All visible deviations in capillary structure, such as changes in the luminar width (stenosis, dilatations) and in the appearance and continuity of the capillary wall (tortuousness, capillarorhexis, with consequent microhemorrhaging, collaterals) were regarded as morphological damage. Changes in the permeability of the capillary wall (plasmatic and corpuscular extravasations) were considered to be functional damage. The incidence of particular types of damage of microcirculation is shown for the tested and control groups in Table 4.

In the control group changes in microcirculation were found by scopy in 6 examinees (20%). In two examinees (6.6%) changes were accompanied by altered thermometric finding. No case of changed photoplethysmographic finding was found in the control group.

Discussion and conclusion

Apart from direct damage to parenchymal cells, ionising radiation also has a significant vascular effect which modifies the response of tissue to irradiation.

Morphological changes in the blood vessels have been well studied, particularly in the skin. The time needed for them to become apparent probably depends on the time needed to cause the death of the surrounding parenchymal cells. In addition, various vascular structures react differently to radiation, which is associated with the differences in the structure of certain blood vessels.

Although the essence of pathogenetic mechanisms of postirradiational vascular changes, as well as the essence of the reparatory mechanisms of endothelial cells following radiolesions remain unclear, electronic microscopy

Table 2. Correlation between altered capillaroscopic, thermometric and photoplethysmographic findings.

Group	Number of examinees	Only capillaroscopic findings altered		Both capillaroscopic and thermometric finding altered		All three findings altered	
		No	%	No	%	No	%
Control group	30	4	13.3	2	6.6	0	0
Exposed group	36	5	13.8	21	58.3	4	11.1

can provide general information on the nature and origin of capillaroscopically detectable changes in the peripheral blood flow of persons exposed to ionising radiation. The presence of vasodilatations can be explained by the reaction of the skin to radiation, which is basically an

Table 3. Individual findings in examinees in whom the microcirculatory alterations were detected by all three methods.

Examinee		Altered capillaroscopic finding	Altered thermometric finding	Altered photoplethysmographic finding
1	L	Local reduction, local tortuousness, local collaterals	+	Moderate spastic and even initial organic changes of digital arteriolas on both hands
	R	Reduction, tortuousness, local dilatation corpuscular extravasations.	–	
2	L	local dilatation	+	Moderate organic changes of digital arteriolae
	R	Stenoses, local dilatations, local collaterals	–	
3	L	Local reduction, local dilatation, tortuousness	–	Suspected organic changes of digital arteriolas on the left hand.
	R	Dilatations, tortuousness, local collaterals	+	
4	L	Local reduction, stenosis, local dilatation	Bilateral hypothermia	Massive vasospastic changes of digital arteriolae on both hands.
	R	Stenosis, local dilatation, reduction		

Legend: L = left hand
R = right hand
\+ = higher temperature value
– = lower temperature value

Table 4. Distribution of particular types of microvascular damages in exposed and control group.

Group	NUMBER OF EXAMINEES WITH							
	Numerical changes		Morphological changes			Functional changes		
	Unilat.	Billat.		Unilat.	Billat		Unilat.	Billat.
Control group	0	0	Stenosis	1	0	Plasmatic extravasation	0	0
			Dilatation	1	1	Corpuscular extravasation	0	0
			Tortuousness	1	4			
			Collaterals	1	0			
			Capillarorhexis	1	0			
			Microhemorrh.	3	0			
Exposed group	5	4	Stenosis	7	12	Plasmatic extravasation	1	1
			Dilatation	3	25	Corpuscular extravasation	4	0
			Tortuousness	5	25			
			Collaterals	14	10			
			Capillarorhexis	3	0			
			Microhemorrh.	4	2			

inflammatory reaction and can be compared to the reaction in the case of burns.[9] Local hyperthermia of the irradiated area is occasionally macroscopically manifested as erythema. Furthermore, as quickly as 4 to 10 minutes after irradiation scarce oedema of endothelocytes appears in the skin capillaries. The process of hydroscopic damage encompasses a large number of endothelic cells, which leads to partial or complete obturation of the lumen of the small blood vessels.[10,11] These changes are demonstrated capillaroscopically as zones of stenosis of the capillary lumen, i. e. zones of capillary number reduction.

A considerable part of the changes caused by ionising radiation occurs in the form of impairments of the cell membrane. Pathoanatomically, it is a degeneration of the myeline type, leading to fragmentation and destruction of the cytomembrane, and consequently to the cell death.[12,13] Such a finding explains the presence of fragile capillary structures and numerous capillaroscopically visible rexies and microhemorrhaging.

Desquamation of necrotic elements leads to the formation of wide interspaces in the endothelial layer and denudation of the basal layer of the capillary wall. Due to the destruction of the irradiated parenchymal cells chemical mediators are released in the referent zone which increases the permeability of small blood vessels. Of these mediators histamine and serotonin are most important, occurring in the early postirradiational period.[14] In the late postirradiational period a primary role is played by the lysosomal enzymes which release vasoactive peptides from the protein plasm and are responsible for the late vascular changes.[15] These changes result in increased permeability of the capillary wall, which explains the presence of the capillaroscopically detectable plasmatic and corpuscular extravasations in the interstitium.

Since the scope of capillaroscopy is limited because of the frequent non-specific findings, it is recommended that the diagnostics of the peripheral blood flow is complemented and objectivized by plethysmographic and thermometric methods, i. e. thermographic methods.[16, 17, 18] However, there are very few examples in literature of systematic use of all three methods for studying the effect of ionising radiation on the exposed vascular structures.

The majority of authors who have dealt with this problem suggest the use of thermography as a differential method for the detection of temperature changes in the peripheral blood flow. Köteles states that thermography is the best technique for the determination of changes in the extremities in the cases of partial irradiation, even in the early latent period.[18]

The results of this work showed a sufficient number of cases in which capillaroscopic findings correspond to the results of thermometric findings in subjects occupationally exposed to ionising radiation, justifying the use of a simpler thermometric method for following-up the condition of the peripheral blood flow in such population groups.

Plethysmographic techniques are widely used in medical diagnostics but so far they have rarely been used in the follow-up of the peripheral blood flow in subjects occupationally exposed to ionising radiation.

Giménez particularly emphasized the value of plethysmography in partial iradiation of the extremities.[19]

Apart from capillaroscopy and thermometry, all subjects in the study were examined photoplethysmographically. In the majority of the examinees the photoplethysmographic findings were within normal ranges. In order to interpret the obtained results correctly, it is necessary to have a good knowledge of the essence and scope of plethysmographic techniques. This method is relatively simple to perform and one of the most reliable where the digital blood flow is concerned, as it promptly reacts to any change in the flow. However, the changes detected by plethysmography are merely morphological deviations at the level of digital arteriolas, so that the changed findings can be expected only in advanced cases, when vasospastic or even organic changes of the digital arteriolae have already occurred. This is indicated by the case histories of examinees who had a changed plethysmographic finding.

Of the examined personnel from the Institute of Radiology, three radiologists and one radiological technician had plethysmographically detectable marked changes in the peripheral blood flow. They have all worked for many years in a zone of ionising radiation (from 14–34 years) and apart from changes in the peripheral blood flow they also had changes in other organic systems. Thus, in one examinee, a radiologist with 29 years of work service, catarracts were found on both eyes, for which occupational etiology was proved, and he was banned from working in a radiation zone. In the case of another examinee, a radiologist with 14 years of work service, analysis of chromosomal aberrations in a culture of lymphocytes from peripheral blood showed a pathological finding, and for this reason a temporary ban from work followed. In the case of all four examinees leukopenia was regularly found during hematological check-ups.

The results obtained undoubtedly indicate the existence of extensive changes in microcirculation of medical personnel occupationally exposed to ionising radiation and related to this, the need for a continuous follow-up of the condition of the peripheral blood flow in such persons is clearly evident.

Not infrequently the health risks in some professional groups exposed to radiation are judged only, or primarily, on the basis of physical-dosimetric registration of the expositional dose. Physical-dosimetric follow-up and comparison between the registered dose of radiation and the maximum allowed dose for a certain category of exposure are indisputably significant in radiation protection, especially in the case of regimens of homogenous exposure of the entire body. However, such a follow-up should always be closely connected with the so-called »biological monitoring« of exposed individuals or groups, because the biological effects of radiation do not always have a linear dependence on physically measured dose. Furthermore, in some types of radiation, i. e. in some regimens of exposure, estimation of the danger to health for exposed persons, based only on the physically registered dose, may be completely inadequate.

The results of this work indicate the need for complete diagnostics of the condition of the peripheral blood flow in medical personnel occupationally exposed to ionising radiation, particularly those professionals whose hands are exposed to the primary beam. The high percentage of capillaroscopically detectable changes in the microcirculation, and the fact that such changes have been observed in some of the examinees with negative thermometric and photoplethysmographic findings, justify the use of capillaroscopic method in the diagnostics and follow-up of peripheral blood flow condition in all medical personnel occupationally exposed to ionising radiation. The existing legislation treats all medical profiles of personnel who work in a zone of ionising radiation as a unique professional category and envisage the same principles and dynamics for check-ups of their health. However, our study indicates that this is a stratified population group which requires a more comprehensive and frequent examination in some of its segments. In the case of following-up the condition of the peripheral blood flow, the results of this investigation indicate the need, not only for regular capillaroscopic examination, but also thermometric and photoplethysmographic, in those medical profiles in which there is marked exposure of the hands to the primary beam. In order to simplify application, and because of the highly positive correlation of findings with capillaroscopic findings, digital dermothermometry can be carried out regularly in all profiles together with a capillaroscopic examination. Thermometry is necessary in those examinees in whom zones of microvascular reduction and ischemic plaques are optically visible. In certain cases, when thermometric measurement show considerable hypothermia and billateral asymmetry of skin temperature, and extensive morphological changes in the capillary blood flow can be seen capillaroscopically, it is justifiable to assume that changes exist in the digital arteriolas, and to carry out photoplethysmography. This examination is particularly indicated in persons who have been working in a radiation zone for many years, and in all cases where other relevant parameters, i.

e. hematological finding, optical status, biodosimetrical and physical-dosimetrical finding, indicate the probability of considerable irradiation, and the nature of work is such that it requires exposure of the hands to the primary beam of ionising radiation.

Acknowledgment

The authors would like to thank Mrs. Jadranka Račić and Mrs. Verica Butorac for their excellent technical assistance.

References

1. Cool WS. Occupational radiation exposure at U.S. Nuclear Regulatory Commission-licensed facilites 1975 *NUREG*-0419: 1978.
2. Cobb PD, Kase KR, and Bjärngard BE. Radiation exposure of nursing personnel to brachytherapy patients. *Health Phys* 1978; **34:**661.5.
3. Balter S, Mason FS, Brancato R. Radiation exposure to the operator performing angiography with U-arm systems. *Circulation* 1978; **58:**925-32.
4. Lackner K, Ewen K, Felix R. Die Strahlenexposition des Untersuchers bei Angiographie. Fortschr. *Röntgenstr.* 1978; **128:**86-90.
5. Kumazawa S, Numakunai T. A new theoretical analysis of occupational dose distributions indicating the effect of dose limits. *Health Phys* 1981; **41:**465.75.
6. Prêtre S, Donath A, Dutrannois J, et al. Strahlenbelastung und Dosimetrie der beruflich strahlenexponierten Personen in der Schweiz im Kalenderjahr 1977. Eidgenössisches Gesundheitsamt Bern 1978.
7. Purrott RJ, Lloyd DC, Prosser JS, et al. The study of chromosome aberration yield in human lymphocytes as an indicator of radiation doses. In: *A review of cases investigated* 1974; NRPB-R35 1975.
8. Maruyama T, Nishizawa K, Neda Y, et al: Estimates of population doses and risk estimates from occupational exposures in Japan, 1978. Part 1: Determinations of organ or tissue doses and effective dose equivalents. *J Radiat Res 1981;* **22:**182-203.
9. What the general practitioner (MD) should know about medical handling of overexposed individuals, A technical document issued by the International Atomic Energy Agency, Vienna, IAEA.TECDOC-366, 1986.
10. Hopewell JW, Young CMA. Changes in the microcirculation of normal tissue after irradiation. *Int J Rad Oncol* 1978; **4:**53-9.
11. Varabjov EI, Stepanov RP. *Ionizirajuće zračenje i krvožilni sustav.* Energoatomizdat Moskva 1985..
12. Maisin JR, Reyners H, Glanfelici de Reyners E. Changes in the ultrastructure and the permeability of the capillaries after irradiation. In: *Recent Advances Basic Microcirc.* Part 1, Basel 1977; 311-4.
13. Černuh AM, Aljeksandrov PN, Alieksejev OT. *Mikrocirkulacija.* M. Medicina 1975.
14. Van den Brenk HAS, Crowe MC, and Stone MG. Functional integrity and inflammatory reactions of exchanges vessels and lymphatics in x-irradiated tissues. *Br J Exptl Pathol* 1977; **58:**499.
15. Etoh H, Taguchi YH, and Tabachnick J. Movement of betairradiated epidermal basal cells to the spinous-granulosa layers in the absence on cell division. *J Invest Dermatol* 1975; **64:**431.
16. Višnjić V. Vrednost kapilaroskopske metode pri proceni radijacijskog oštećenja. Seminar: Zdravstveni i dozimetrijski nadzor osoba zaposlenih u zoni ionizirajućeg zračenja. Stubičke Toplice 1986; 39-46.
17. Čremosnik-Pajić P. Jedinstveni kriterijum pri oceni uticaja jonizujućeg zračenja na zdravlje i radnu sposobnost, Seminar: Zdravstveni i dozimetrijski nadzor osoba zaposlenih u zoni ionizirajućeg zračenja. Stubičke Toplice 1986; 80-96.
18. Köteles GHJ, Kormos C, Kerekes J, and Sztanyik LB. Further approaches to biological indicators of radiation injury. Seventh International Congress of the International Radiation Protection Association. Radiation protection practice, Sydney 1988, Pergamon Press, Sydney-Oxford-New York-Toronto-Frankfurt. 1988; (III):1149-52.
19. Giménez JC. Predictive value of pletismography in cases of extremities partial external irradiation. In: Kaul A. Neider J, Pénsko J, eds. Radiation-risk-protection-6th International Congress, Berlin (West): Facherband fur Strahlenschutz e. V. 1984; Compacts volume II: 847-50.

Adv Radiol Oncol 1992;356-63.

Biological effect of microwave radiation

Garaj–Vrhovac V

Institute of Medical Research and Occupational Health University of Zagreb

Our study presents the results of structural chromosome aberration analysis in a group of 50 examinees occupationally exposed to microwaves during their work with radar devices and antenna systems. Measurements of electromagnetic field's power density distribution were taken in operating rooms of radar devices. The control group consisted of persons who are not exposed to radiation sources during their work. Results of electromagnetic field's power density distribution measurements at different working places show that during an ordinary working day the examinees stay in zones lower than 5 mW/cm^2. During periodical equipment check–up, values measured at certain working places, amount to 20 mW/cm^2 at times. One part of professionally exposed population shows an increased number of chromosome aberrations. In contrast to control population, in exposed persons the dicentric chromosomes and ring chromosomes were detected. Statistical significance of results is presented by Chi–square test and Fisher's test.

Key words: microwaves–adverse effects; environmental exposure; chromosome aberrations

Introduction

Man is constantly exposed to the electromagnetic field as a constituent element of the biosphere. Natural radiation appears in a wide range of frequencies in which the natural field and radiation strength is very low in comparison with the extent of man–made radiation sources. Sources of non–ionizing radiation are among nowadays well known agents which can even be considered atmospheric pollutants, since they induce changes in the natural electromagnetic field character through the emission of either controlled or non–controlled energy into the environment.[1] The parts of electromagnetic spectrum occupied by the non–ionizing radiation are radiofrequency, infra–red, visible light and ultraviolet radiation.[2]

Technologic development underlies a constant increase in the number of microwave facilities emitting electromagnetic radiation ranging in frequency from 300 MHz to 300 GHz, and with wavelengths from 1 m to 1 mm. Microwave energy is used in different industrial branches and technological procedures for diaelectric heating and other segments of production processes. It is used in medicine for therapeutic and diagnostic purposes and in the treatment of acute and chronic inflammatory processes. Application of microwaves in the treatment of carcinoma is a relatively new method recognized in a progressive clinical treatment.[3] Their therapeutic value is highest in combination with other agents, especially ionizing radiation.[4]

Modern radar equipment used in meteorology, navigation and telecommunication systems also

Correspondence to: Dr Vera Garaj–Vrhovac, Institute of Medical Research and Occupational Health, University of Zagreb, Mutagenesis Laboratory, Trg I. Meštrovića 16, 41000 Zagreb, Croatia.

UDC: 621.317:576.312.54

represents a powerful source of electromagnetic radiation. Due to their increased number and broader application, such sources of microwave radiation represent a potential health risk, especially for the occupationally exposed individuals, but no less for the human population in general.

Some of the harmful effects of radiation on human organism are nowdays well known. It is thus known that in contract with a medium, electromagnetic waves can be reflected, carried through or absorbed by the medium. The amount of electromagnetic radiation absorbed by a living organism is determined by the dielectric properties of the tissue, cells and biomolecules in a solution. Complexity and functional variety of molecular structures, characteristic of biological systems, lead to a different penetration of microwave energy through biologic materials, which explains for the erratic quality of the internal energy depots of biological systems. Electromagnetic energy, which enters biological tissues containing a considerable percentage of water, manifests strong relaxation phenomena of dispersion and conversion into thermal energy, which is responsible for different reactions. There is a possibility of hyperthermic effects, sometimes accompanied by secondary thermal effects on vital organic systems.[5] Some authors even think that those effects are primary and non–thermal ones.[6] Between the thermal and non–thermal effects there is a range of mechanisms of actions, assumed but not as yet explained.

Interactions of weak electromagnetic fields with a biological system are characterised by a strong dependency upon the field frequency and intensity, hence they are often referred to as »window« phenomena.[7]

Biological effects of microwave radiation can be characterised by the physico–chemical changes of tissues and molecules, presenting themselves as the reaction of the organism as a whole. Those are mostly secondary changes caused by the non–functionality of particular organs or organic systems[8,9,10,11] and the data there on are mostly obtained from the experimental animals. Therefore, though often presenting contradictory results, epidemiologic studies on man are of utmost importance. Effects on neurovegetative, cardiovascular and neuroendocrine systems are well known, as well as changes of hematopoiesis and senses.[12,13,14,15,16,17,18,19] In the literature, descriptions of subjective symptoms such as headache, fatigue, emotional instability, can be found. Some authors recognise these as typical, microwave induced functional CNS disorders, i.e. »neurastenic syndrome«.[20]

One of the most sensitive organs is the organ of sight, especially the eye lens. Data on the potential effect of a microwave, having cataractogenic effect and causing impairments of other eye structures, are also often contradictory.[17,21,22,23,24,25,26,27] Majority of authors do not find cataract in persons occupationally exposed to a microwave.[28,29,30,31] Appelton (1974) does not find a specific morphologic characteristic of lens opacity in persons exposed to a microwave in comparison with the control individuals.[32] While the alleged »microwave cataract« does not differ from other types of cataract,[33,34,35] it is argued that changes, if induced by a microwave, are recognizable. For the onset of occupational etiology cataract, the power density strength of microwave radiation at working places should amount to 100 mW/cm^2 or more.[26,27]

There are very few data on the effect of microwaves on man's reproductive system. Changes of spermatogenesis, menstrual cycle in women, decreased fertility rate[36] and congenital anomalies in children are mentioned.[14]

Data on genetic aberrations caused by microwave radiation are scarce and mostly refer to animal cells in a culture.[37,39,40,48] Due to the insufficient knowledge on the mechanism of action of microwave energy in biological systems, results of cytogenetic research are also often contradictory. A special attention is being paid to the research of microwave radiation effect on the induction of chromosome aberrations in human and animal cells.[41,42,43,44]

The aim of our study was to:

- select a group of examinees occupationally exposed to microwave radiation,

- establish the distribution of the electromagnetic field density at particular working places,
- identify structural aberrations of chromosome lymphocytes in the peripheral blood of the examinees, and
- analyse the obtained data statistically in comparison with the control group.

Subjects and methods

A group of 50 workers from the radar equipment and antena system service employed with the District Air-traffica Radar Control Centre was chosen for our study. Out of those, 46 were male and 4 female. The average age of examinees was 39.8 (ranging from 21 to 55 years). They had been employed in the zone of nonionizing radiation for an average of 13.2 years (from 0.5 to 26 years). The power density of the electromagnetic field was measured at different working places of examinees with the RAHAM, model 4A, which measures the frequency range from 0.2 MHz to 26 GHz, power range being between ● and 26 mW/cm^2. Measurements included all of the working places and all of the radar equipment.

The control group consisted of 25 examinees of the same age group who had never worked with sources of radiation. For both the controls and test examinees the data on previous exposure to diagnostic sources of radiation or to a more serious chemotherapy were obtained.

The structural chromosome aberration analysis of the control and test group was performed on the peripheral blood lymphocytes.

For the *in vitro* culture of lymphocytes, the F-10 medium (GIBCO) containing 20% inactivated calf serum was used, with addition of 5 μg/ml BrdU. Fytohemaglutinine (Wellcome) as a mitogenic stimulator was used. The incubation at 37°C lasted for 48 hours. During the 45th hour of incubation, 0.004% colchicine (0.5 ml) was added to the culture. The cells were harvested at 48 h. After hypotonic treatment with KCl (0.075 M) the cells were fixed with methanol-acetic acid (3:1), spread on clear slides, left to dry and stained with 5% Giemsa solution.[45]

Analysis of 200 metaphases, classified as acentric fragments, dicentrics, ring chromosomes and chromosomal and chromatid breaks, was performed for each examinee. The data were statistically analysed by means of Chi-square test and Fisher's test.[46] The results are shown in Tables 1, 2, 3, 4, 5.

Results

The results of measurements demonstrate a general phon of electromagnetic field of the operating rooms during the operation of radar devices. At their working places examinees are exposed to pulse microwaves in the field of 10 μW/cm^2 to 20 mW/cm^2 and frequency of 1250 to 1350 MHz. During their daily routine work examinees stay in the zones of radiation lower than 5 mW/cm^2, but due to the technological process requiring an occasional functioning check-up, those values at certain working places exceed 20 mW/cm^2.

Incidence of chromosome aberrations in the examinees exposed to microwave for the group of 50 persons is presented in Table 1. For comparison, the table contains data on chromosome and chromatid lesions found in the control subjects. The different chromosome changes are presented as a group mean ±SE.

Table 1. Frequency of chromosome aberration after occupational exposure to nonionizing radiation.

Group of workers	Exposed workers	Controls
Number of individuals	50	25
Mean age (years)	39.8 ∓ 7.58	38.2 ∓ 9.42
Total cell examined	10000	5000
Chromatid break	1.22 ∓ 0.55	1.36 ∓ 0.63
Chromosome break	1.36 ∓ 0.76	1.20 ∓ 0.30
Acentrics	2.60 ∓ 1.69	0.12 ∓ 0.30
Dicentric + ring chromosome	0.34 ∓ 1.00	
% aberrations	2.78 ∓ 1.59	1.32 ∓ 0.53

The frequency of chromosomal changes is given per cell ∓ SE.

The percentage of chromosome aberrations in controls is very low. The mean value of all the aberrations amounts to 1.32 ± 0.53. Only acen-

tric fragments, chromatid and chromosome breaks were observed in controls.

The group of occupationally exposed subjects demonstrates a much higher incidence of acentric fragments, and there are also translocations in the from of dicentrics and ring chromosomes. The mean value in this group was 2.78 ± 1.59.

Out of 50 test examinees, there were 8 with a high number of chromosome breaks, accompanied by bigger or smaller acentric fragments and dicentric chromosomes. Distribution of total aberrations per cells, acentrics, chromosome breaks and dicentric is presented in Tables 2, 3, 4 and 5.

Chi-square test was applied to compare the chromosome changes in both group. There were no significant differences ($p > 0.05$)for the field of chromatid breaks and chromosome breaks between the exposed group and the control one.

On the contrary, Fischer's test showed significant difference ($p < 0.02$) for the yield of acentrics and dicentrics between the exposed and control group, while chi-square value for the same case was on the limit ($p = 0.05$).

Discussion and conclusion

Problem of exposure to non-ionizing radiation sources is getting more important in the modern world. Setting standards for limitation of the field strenght during microwave radiation has become a priority task due to an increased application of electronic devices and techniques in various fields of industry, medicine and for military purposes. All of these increase the rate of exposure of general population, and especially of the exposed individuals, to the »pollution« caused by the nonionizing radiation.

Biologically detrimental effect of the forementioned radiation in occupationally exposed persons has not yet been sufficiently explored, and the existing data are often contradictory. According to the existing norms of protection against microwave radiation, which are nowadays being used in certain countires, it can be said that all the values are based on the results of thermal

Table 2. Distribution of total aberrations.

Subjects	Distribution 0	1	2	3	10
13	188	8	4		
21	191	9			
25	193	5	2		
33	191	4	2	3	
39	194	2	4		
42	192	8			
47	188	11	1		
48	179	2	6	3	10

Table 3. Distribution of acentrics.

Subjects	Distribution 0	1	2	3	10
13	193	4	3		
21	197	3			
25	197	2	1		
33	196	1	2	1	
39	197	1	2		
42	195	5			
47	194	5	1		
48	189		3	1	7

Table 4. Distribution of chromosome breaks.

Subjects	Distribution 0	1	2	3	10
13	197	3			
21	197	3			
25	199	1			
33	198	2			
39	199	1			
42	199	1			
47	197	3			
48	198	2			

Table 5. Distribution of dicentrics.

Subjects	Distribution 0	1	2	3
10				
13	199		1	
21	199	1		
25	199		1	
33	199			1
39	198		2	
42	199	1		
47	199		1	
48	193		3	1

effects. Radiation duration has a considerable effect on human health. In this connection, the permissible human exposure time has been sugested and determined.

The American National Standards Institute (ANSI) stipulates conditions of the occupational exposure to frequencies from 300 MHz to 300 GHz, as well as the upper microwave radiation intensity limit to 10mW/cm^2. The total daily duration of exposure has also been limited to 8 hours.[47] These conditions are considered a harmless level of exposure to microwave radiation. It is considered that power density of 100 mW/cm^2 has detrimental effects on human health, while at the power density surpassing 25 mW/cm^2 it is forbidden to stay in the radiation zone.

Russian and East European standards for the occupational exposure in the microwave radiation zone of 300 mMHz to 300 Ghz should not exceed 10 μW/cm^2 in an 8-hours working day, 100 μW/cm^{2}for 2 hours a day and 1 mW/cm^2 for not more than 20 minutes a day.[48] For the general population Russian standards set values of 5 μW/cm^2.[49]

According to our regulation, a standard of 0.1 to 1 mW/cm^2 has been set, but without any real experimental values support. This Yugoslav standard is considered safe enough for all the frequencies, throughout a working day. Though both Russian and American standards stipulate the permissible exposure time, our examinees work in 12-hour shifts.

There are also temporary situations during which radar radiation exceeds even the very liberal American standards, not to mention the Russian ones. As a result of those, there is evidence of structural chromosome aberrations found in our examinees.

Several recent research projects carried out in the last few years on radar centres personnel show their protection as being often inadequate.

Protection of the occupationally exposed personnel is made more difficult due to the fact that there are no personal dosimetres similar to those carried by those working in the zone of ionizing radiation. Prevention of occupational impairments caused by microwave radiation should be based primarily on individual protection measures (protective clothes, protective eyefold etc.) during the direct work with the equipment,

- limited duration of stay in the zone of microwave radiation, and
- periodical medical check-up for all the persons working with microwave radiation sources.

Until recently it has heen argued that thermal effect is the primary effect of microwave elctromagnetic field. But nowadays non-thermal effects are being paid more attention to, since biological consequences (headache, fatigue, memory loss, cardiovascular and various other changes) occur even in low power densities. Our examinees also complained of a series of subjective symptoms like fatigue, neurastenic conditions, headache and others, which can be characterised as »neurostenic syndrome« or »microwave disease« as it is sometimes referred to. Subjective difficulties, headache and exhaustion, as well as the appetite loss, dizziness, emotional instability, have been described by other authors.[20,30,31] Our examinees underwent a series of other analyses which disclosed hematologic changes as a most common findings. From the personal history it could be concluded that some of the examinees had fertility problems, accompanied by the spermiogram changes, which indicated reproductive cells impairments. Similar data were presented by Lancranjan et al, Manikowska et al, Rosenthal and Beering.[36,50,51] However, there are also some contradictory results.[52]

Savitz et al draws attention to an increased risk of leukemia in persons occupationally exposed to the electromagnetic field.[53] Our study also shows that microwave radiation has detrimental effects on cell structures like chromosomes. Chromosome aberrations in occupationally exposed persons range from 1 to 10.5%, and besides structural changes in the number of chromosomes, some of the examinees also show typical structural aberrations. Some of the obtained results show borderline ($p = 0.05$) or increased values ($p > 0.02$) for acentric fragments and dicentric chromosomes.

However, Bauchinger et al, surveying the incidence of chromosome aberrations in persons

occupationally exposed to 50 Hz electromagnetic field, did not find a significant increase in the structural changes in comparison with the control group and a parallel group of subjects exposed to ionizing radiation.[54]

In our examinees, results of structural chromosome aberrations analyses are in correlation with the results of micronucleus test for the same examinees, which confirms, without any doubt, the presence of changes in the cell genome of persons exposed to microwave pulse radiation.[55]

Number and structure of chromosome aberrations can be regarded in the light of the effect of microwave radiation on the DNA molecule structure. Recent studies suggest that micorwave radiation could result in one-strand and double-strand breaks of the DNA molecule,[56] as well as in changes of the deoxiribonucleine acid synthesis and structure.[44]

The analysed mutagenic changes of somatic cells in our examinees can be attached to their occupational exposure to microwaves. According to other authors, consequences of these mutations are related to neoplasms.

Out of 29 epidemiological studies published in the last decade, 22 suggest a relation between various neoplasms and exposure to electromagnetic field.[57]

Therefore, this study, followed by further research of biological effect of microwaves, should shed more light on numerous problems caused by the occupational exposure. Since neither any real national standards nor safety regulations concerning non-ionising radiation have been set in our country, the presented results are our contribution to the notion that protection is a most important in this field, and that our national standards should be set as soon as possible.

Acknowledgment

The author would like to thank Mrs Jadranka Račić for technical assistance.

References

1. Meisel N. Applications industrielles: Les microondes dans les industries alimentaires, Symposium International: Ondes electromagnetiques et Biologie. Jouy-en-Josas France 1980: 93-101.
2. WHO: Nonionizing radiation protection, Copenhagen, World Health Organization Regional, Office for Europe, WHO Regional Publication European Series No 10: 1982; 97-179.
3. Villforth J C. Medical devices nonionizing radiation standards, noionizing radiations: Physical characteristic, Biological effects and Health hazard Assessment, Proceedings of the International Non-Ionizing Radiation Workshop, Melbourne 1988; 427-46.
4. Perez CA. Ocal Hyperthermic and Irradiation in Cancer Therapy. *J of Microw Power* 1981; **16:**205-14.
5. Boysen LE. Hyperthermic and pathologic effects of electromagnetic radiation (350 Mc). AMA *Arch Indust Hyg* 1953; **7:**516-25.
6. Presman AS, Zevitina N. The nonthermal effect of microwaves on the systolic rhythm of animals: The effect of nonpulsed microwaves. *Bull Exp Biol Med* 1962; **53:**41-4.
7. Repacholi MH. Introduction to non-ionizing electromagnetic fields. In Non-ionizing Radiations, Physical Characteristics, Biological Effects and Health Hazard Assessment., MH. Repacholi (Eds) Proceedings of the International Non-Ionizing Radiation Workshop, Melbourne 5-9 April; 1988; 1-15.
8. Baranski S. and Czerski P. Effect of microwaves on the reactions of the white blood cell system. *Acta Physiologica Polonica,* 1972; **23:**685-95.
9. Paulsson LE, Hamnerius Y, Hausson HA, Sjoestrand J. Retional damage experimentally induced by microwave radiation at 55 mW/cm^{-2}. *Acta Ophthalmol* 1979; **57:**183-97.
10. Silverman C. Epidemiologic studies of microwave effects. *Proc IEEE* 1980; **68:**78-84.
11. Smialowicz RJ. et al. Exposure of rats to 425 MHz (CW) radiofrequency radiation: Effects on lymphocytes. *J Microw Power* 1982; **17:**211-21.
12. Baranski S, and Czerski P. *Biological effects of microwaves,* Dowden Hutchinson and Ross, Stroudsburg, PA, 1976; 234.
13. Gordon ZV, Eliseev VV. Sredstva zastiti of SVC-oblucenija i ih effektiv effektivnost, V. kn.: O Biologiceskom dejstvii elektromagnithyh polej i radiocastot. Meditsina Moskva 1964.
14. Marha K, Musil J, Tuha H. *Electromagnetic fields and the life environment.* San Francisco Press 1971; 134.
15. Czerski P. and Piotrowski M. Proposals for specification of allowable levels of microwave radiation. *Medycyna lotnicza,* 1972; **39:**127-39.
16. Siekierzynski M, Czerski P, Milczarek H, Gidynski A, Czarnecki C, Dziuk E. and Jedrzejezak W. Surveillance of personnel occupationally exposed to microwaves. II Functional distrubances. *Aerosp Med* 1974; **45:**1143-45.

17. Siekierzynski M, Czerski P, Gidynski A, Zydecki S, Czarnecki C, Dzivke E, Jedrzejczak V. Health surveillance of personnel occupationally exposed to microwave. III Lens Translucency. *Aerosp Med* 1974; **45:**1146-48.
18. Czerski P. and Siekierzynski M. Analysis of occupational exposure to microwave radiation, In: Michaelson SM, Miller MW, Magin R, Carstensen EL Eds. *Fundamental and applied aspects of non-ionizing radiations.* New York Plenum Press 1975; 367-75.
19. Lin JC, Guy AW. and Caldwell LR. Thermographic and behavioral studies of rats in the near field of 918 MHz radiations. IEEE Trans microwave Theory Tech MTT-25, 1977; 833-6.
20. Silverman C. Nervous and behavioral effects of microwave radiation in humans. *Am J Epidemiol,* 1973; **97:**219-24.
21. Hirsch FG, Parker JT. Bilateral lenticular opacities ocurring in a technician operating a microwave generator. *Arch Indust Hyg Occupat Med* 1952; **6:**512-7.
22. Kurz GH, and Einaugler RB. Cataract secondary to microwave radiation, *Am J Ophthalmol* 1968; **66:**866-9.
23. Appleton B, Mc Crossan GC. Microwave lens effects in human. *Arch Opthalmol* 1972; **88:**259-62.
24. Zaret M. Selected cases of microwave cataract in man associated with concomitant annotated pathologies, Proc, Inter Symp Biol Effects and Health Hazards of Microwave Rad Warsaw 1973.
25. Aurell E. Tengroth B. Lenticular and retinal changes secondary to microwave exposure. *Acta Ophtalmol* 1973; **51:**764-71.
26. Cleary SF. Microwave cataractogenesis, Proceedings of the *IEEE* 1980; **68:**49-55.
27. Hollows FC. and Douglas JB. Microwave cataract in radiolineman and controls. *Lancet* 1984; **18:**80-1.
28. Daily EL. A clinical study of the results of exposure of laboratory personnel to radar and high frequency radio. *US Navy Med Bull* 1943; **41:**1052.
29. Barron CI, Love AA. and Baraff AA. Physical evaluation of personnel exposed to microwave emanations. *J Aviation Med 1955;* **26:**422.52.
30. Đorđević Z. Kolak A. A study of the health status of radar workers. *Aviat Space Environ Med* 1979; **50:**396-8.
31. Đorđević Z. Zdravstveni pregledi radarista. *Vojno sanitetski* pregled 1966; **23:**460.
32. Appleton B. Microwave cataracts. *J Am Med Assoc* 1974; **229:**407-8.
33. Hathaway JA, Stern N, Soles EM, Leighton E. Ocular medical surveillance on microwave and laser workers. *J Occup Med* 1977; **19:**684-8.
34. Schacklett DE, Tredici TJ, Epstein DD. Evaluation of possible microwave induced lens changes in the United States Air Force.*Aviat Space Environ Med* 1975; **46:**1403-6.
35. Zaret MM, Kaplan IT, Kay AM. Clinical micro-wave catarats, *In: Cleary SF ed. Biological effects and health implications of microwave radiation.* Rockville, Maryland, 1970; 82-4.
36. Rosenthal DS. and Beering SC. Hypogonadism after microwave radiation. *J Am Med Assoc* 1968; **205:**245.
37. Huang AT, Engle ME, Elder JA, Kinn JB. and Ward TR. The effect of microwave radiation (2450 MHz) on the morphology and chromosomes of lymphocytes. *Radiat Sci* 1977; *12:*173-7.
38. Alam MI, Barthakur N, Lambert NG, and Kasativa SS. Cytological effects of microwave radiation in Chinese hamster cells *in vitro. Can J Cytol* 1978; **20:**23-30.
39. Baranski S, Czerski P. and Szmigielski S. Microwave effects on mitosis *in vivo* and *in vitro. Genet* 1969; **10:**92-8.
40. Baranski S, Czerski P. Szmigielski S. The influence of microwaves on mitosis *in vivo* and *in vitro. Postery Fiz Medyczniey* 1971; **6:**93-108.
41. Yao KTS. Jiles MM. Effects of 2450 MHz microwave radiation on cultivated rat kongaroo cells, In: Cleary SF ed. *Biological Effects and Health Implications of Microwave Radiation US Dept of Health.* Education and Welfare, 1970; 123-32.
42. Yao KTS. Cytogentic consequence of microwave incubation of mammalian cells in culture. *Genetics* 1976; **83:**84.
43. Stodolnik-Baranska W. The effects of microwaves on human lymphocyte cultures, In: Czerski P, Ostrowski K, Shore ML, Silverman Ch, Suess MJ. and Waldeskog B eds. *Biological effects and health hazards of microwave radiation.* Poslish Medical Publishers, Warsaw, 1974; 1989-95.
44. Garaj-Vrhovac V, Horvat Đ. Koren Z. The effect of microwave radiation on the cell genome. *Mut Res* 1990; **243:**87-93.
45. Biological Dosimetry. Chromosome aberration analysis for dose assessment. Technical Reports series No 260, International Atomic Energy Agency, Vienna, 1986; 59-63.
46. Pavlić I. In: *Statistička teorija i primjena,* Thenička knjiga Zagreb, 1970.
47. ANSI: Safety level of electromagnetic radiation with respect to personnel, New York, Report 95, 1966; 6-9.
48. USSR: Standard for Occupational exposure Gost 12.1.006-76, Occupational safety standards system, electromagnetic fields of radiofrequency, general safety requirements, State standard of the USSR, Moskva, Izdaletstvo Standartov, 1976; 5.
49. USSR: Standard for Public Exposure, SN-1823, 1979; 78.
50. Lancranjan I, Maicanescu M, Rafaila E, Klepsch I, Popescu HI. Gonadic function in workmen with long-term exposure to microwaves. *Health Phys 1975;* **29:**381-3.
51. Manikowska E, Luciani JM, Servantie B, Czerski P, Obrenovitch J, Stahl A. Effect of 9.4GHz microwave exposure on meiosis in mice. *Experientia 1979;* **35:**388-90.
52. Robinette CD, Silverman C, Jablon S. Effects upon health of occupational exposure to microwave radiation (radar). *Am J Epidemiol* 1980; **112:**39-53.
53. Savitz DA. and Colle EE. Leukemia and Occupational Exposure to Electromagnetic Fields: Review of Epidemiologic Surveys. *J Occup Med 1987;* **29:**47-51.

54. Bauchinger M, Hauf R, Schmid E, Dresp J. Analysis of structural chromosome changes and SCE after occupational longterm exposure to electric and magnetic fields from 380 kV systems, Radiat Environ Biophys 1981; **19:**235-8.

55. Garaj-Vrhovac V. Fučić A, Horvat D. Comaparison of chromosome aberration and micronucleus induction in human lymphocytes after occupational exposure to vinyl chloride monomer and microwave radiation. *Period Biol* 1990; **92:**412-16.

56. Sagripanti JL, Swicord ML. DNA structural changes caused by microwave radiation. *Int J Radiat Biol* 1986; **50:**47-50.

57. Szmigielski S. Electromagnetic Fields and Cancer, International Scientific Meeting, »Microwaves in medicine 91« Beograd april 8-11, 1991; Digest of Papers, 34.52.

LIST OF CONTRIBUTORS

Anić P 96
Atanacković M 72
Auersperg M **268**

Baba H 47
Babić M **102**
Bačić S 72
Ban J **241**
Benedik–Dolničar M **196**
Benulič T 7
Bešić N 268
Bešlić Š 41
Bistrović M 241, **311**
Boko H 81, 86, 96, 99
Bonić I 348
Bračko M 275, 280
Breyer B 81
Britton KE **116**
Brkljačić B **86,** 96, 99
Brumen V **348**
Budihna M **236,** 284
Byun HS 25

Cerar O 175
Cijan A 30
Cindro L 167
Clausen M 123
Clemm Ch **202**

Čufer T 268, 275, **280**

Dalagija F **41**
Delić–Brkljačić D 86
Demšar F 66
Dimitrovska A **208**
Dizdarević Z 41
Drinković I 86, **96**, 99
Dujmović I 241

Fink FM 181

Gadner H 181
Garaj–Vrhovac V **356**
Georgieva B 208
Giraldi T **249**
Goehde W 268, 275, 280
Grümayer ER 181

Haas H 181
Habič M 330
Hasuo K 47
Hawliczek R 181
Henze E **123**
Hirakata R 47
Horvat Đ **343**
Hricak H 60

Jarh O 66
Jereb B 167, **175,** 330
Jevtić V **66**
Jovanovski D 208

Karanfilski B **142,** 208
Klun B 167
Kopač Š 167
Korbelik M 261
Kos–Golja M 66
Košmelj K 275, 280
Kovačević D 60
Kragelj B 167
Kralj Z 81
Kranjec I **30**
Krepler R 181
Krmpotić T 99
Krošl G **261**
Kuang LR 25
Kuroiwa T 47

Ladenstein R **181**
Lamovec J 275, 280
Lawrence D 22
Lešničar H **284**
Lietzenmayer R 123
Lincender L **51**
van Lingen A 135
Lovrenčić M **35**

Mahon T **22**
Marotti M **60**
Masuda K 47
Matovinović D 102
Mihajlović L 81
Miklavčič L **335**
Milas L **229**
Milčinski M 123
Miletić Z 241
Mirić S **90**
Mitrović M 72
Mizushima A 47
Moult RG 25
Mutz I 181

Nešković
–Konstantinović Z **221**
Nikolova L 208
Novaković S **214**

Odak D 96, 99
Ogrizović N 221
Onitsuka H 47

Papa J **56**
Pavčnik D **15,** 30
Perissin L 249
Peters AM **111**
Petrič–Grabnar G **167**
Pichler E **81**
Ploier R 181
Podgoršak EB 151, **301,**
Pogačnik A 275, 280
Poleksić Lj **72**

Rapozzi V 249
Roos JC **135**
Rozman B 66

Sabljak I 90
Serša G 214
Sorić J 241
Souhami L **151,** 301
Stanovnik M 268
Stare J 167, 175
Stöllingere O 181

Škrbec M 167
Škrk J 236
Štabuc B 175, 330
Šušnjar S 221

Tansey W 25
Tasić S 221
Teule GJJ 135

Thun–Hohenstein L 181
Tulzer W 181

Umek B 167, **330**
Urban C 181
Us–Krašovec M 175, 268, **275,** 280

Velkov K 208
Vidjak V 86, 96, **99**
Vrtar M **323**
Vuletić L 221

Wallace S 15, 25

Zdravković Đ 72
Zorzet S 249

Župančić N 167

Yamashita Y 25
Yang DJ **25**
Yasumori K **47**
Yoshida K 47

THIS BOOK WOULD NOT HAVE BEEN POSSIBLE WITHOUT THE VALUABLE HELP OF OUR SPONSORS:

Institut za onkologiju i radiologiju, Beograd

Institut za radiologiju i onkologiju UMC, Sarajevo

Inštitut za diagnostično in intervencijsko radiologijo, UKC Ljubljana

Klinička bolnica »Dr Mladen Stojanović«, Zagreb

Klinički zavod za dijagnostičku i interventnu radiologiju, KBC REBRO, Zagreb

Klinika za nuklearno medicino, UKC Ljubljana

KODAK, Paris, France

Medicinska fakulteta, Ljubljana

Medicinski centar »ZAJEČAR«, Zaječar

Mestni sekretariat za izobraževanje, raziskovalno dejavnost in šport – Enota za raziskovalno dejavnost, Ljubljana

Ministrstvo za znanost in tehnologijo Republike Slovenije, Ljubljana

NYCOMED AS, Oslo, Norway

Onkološki inštitut, Ljubljana

Papirnica Vevče d.o.o., Ljubljana

SMELT International Group, Ljubljana

Zavod za onkološku zaštitu, Kladovo

ADVERTISEMENTS IN THIS ISSUE HAVE BEEN CONTRIBUTED BY THE FOLLOWING COMPANIES:

ANGIOMED
Karlsruhe, Germany

BAYER PHARMA d.o.o.
Ljubljana, Slovenia

BYK GULDEN
Konstanz, Germany
Representative Office FABEG
Zagreb, Croatia

FOTOKEMIKA s.p.o.
Zagreb, Croatia

GENERAL ELECTRIC – CGR
Representative Office
Zagreb, Croatia

KRKA p.o.
Novo mesto, Slovenia

LECLERC & CO
Schaffhausen, Switzerland

LEK d.d.
Ljubljana, Slovenia

MEDITRADE–KODAK
Ljubljana, Slovenia

POLYSTAN–BENELUX
Medical Products
Almere–Haven, The Netherlands

SALUS d.d.
Ljubljana, Slovenia

SANOLABOR p.o.
Ljubljana, Slovenia

SIRION s.r.l.
Medical Supplies
Gorizia, Italy

SKB Banka D.D.
Ljubljana, Slovenia

TOSAMA p.o.
Domžale, Slovenia

Abaktal®

(pefloxacin)

tablets 400 mg
ampoules 400 mg

A new potent drug against infections

- May be given orally and parenterally
- Effecive in life-threatening infections caused by nosocomial strains resistant to many drugs
- May be given to patients hypersensitive to penicillins and cephalosporins
- Its favourable pharmacokinetic properties allow twice-a-day dosage
- Is very well tolerated

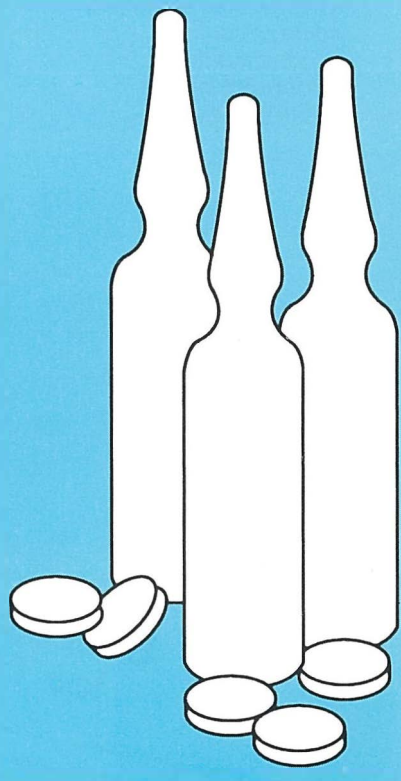

Contraindications

Pefloxacin is contraindicated in patients with known hypersensitivity to quinolones, in pregnant women, nursing mothers, children under 15 years of age, and patients with inborn glucose-6-phosphate dehydrogenase deficiency.

Precautions

During pefloxacin therapy exposure to strong sunlight should be avoided because of the risk of photosensitivity reactions. In patients with a severe liver disorder dosage of pefloxacin should be adjusted.

Side effects

Gastro-intestinal disturbances, muscle and/or connective tissue pains, photosensitivity reactions, neurologic disturbances (headache, insomnia), and thrombocytopenia (at doses of 1600 mg daily) may occur.

Dosage and administration

The average daily dosage for adults and children over 15 years of age is 800 mg.
Oral: 1 tablet twice daily after meals.
Parenteral: the content of 1 ampoule 400 mg diluted in 250 ml of 5 % glucose as a slow 1-hour infusion twice daily. The maximum daily dosage is 8 mg of pefloxacin per kg bodyweight. In severe hepatic insufficiency pefloxacin is administered only once daily (jaundice), once every 36 hours (ascites), and once every 48 hours (jaundice and ascites).

lek Pharmaceutical and Chemical Works Ljubljana

Klimicin®

(Clindamycin)

Klimicin is an effective bactericidal or bacteriostatic as evidenced by the MIC/MBC ratio.

It stimulates the action of polymorphonuclear leukocytes (PMN) principal factors in host immune system.

PMN leukocyte.

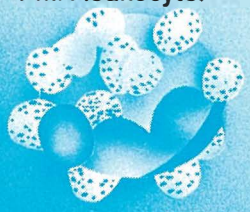

Succesful and reliable treatment for life-threatening infections

Aerobes

Streptococcus spp. (including Streptococcus pyogenes), except Enterococcus

Pneumococcus spp.
Staphylococcus spp. (including B-lactamase producing strains)

Anaerobes

Bacteroides spp. (including Bacteroides fragilis)
Fusobacterium spp.
Propionibacterium
Eubacterium
Actinomyces spp.
Peptococcus spp.
Peptostreptococcus spp.
Clostridium perfringens

Contraindications: In patients hypersensitive to lincomycin and clindamycin.

Precautions: Klimicin should be prescribed with caution to elderly patients and to individuals with a history of gastrointestinal disease, particularly colitis.

Side Effects: Gastrointestinal disturbances (abdominal pain, nausea, vomiting, diarrhea). When significant diarrhea occurs, the drug should be discontinued or continued only with close observation of the patient. The posibility of pseudo-membranous colitis must be ruled out.

Lek, Pharmaceutical and Chemical works Ljubljana

NYCOMED
Contrast Media

Periferna i visceralna arteriografija

OMNIPAQUE™

joheksol

neionsko kontrastno
sredstvo
gotovo za upotrebu

GLAVNE PREDNOSTI OMNIPAQUEA U PERIFERNOJ I VISCERALNOJ ARTERIOGRAFIJI

- dobra opća podnošljivost
- nikakvi ili klinički beznačajni učinci na hemodinamičke i kardiovaskularne parametre
- značajno smanjena učestalost i težina subjektivnih reakcija bolesnika u usporedbi s konvencionalnim ionskim kontrastnim sredstvima
- nikakav učinak na enzime jetre i gušterače
- izuzetno rijetka pojava alergijskih reakcija
- visokokvalitetni angiogrami

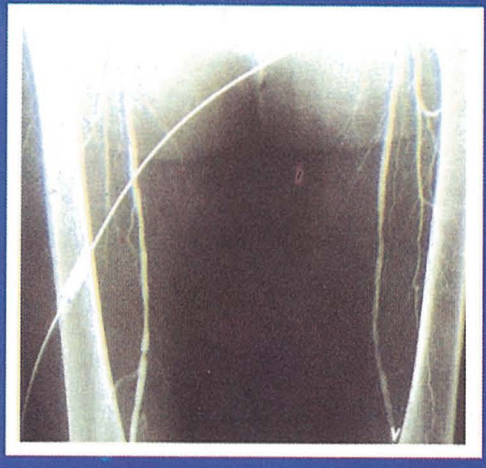

IZ NYCOMEDA – INOVATORA U PODRUČJU KONTRASTNIH SREDSTAVA

Omnipaque je zaštićeno ime

SIGURNIJE KONTRASTNO SREDSTVO U DIJAGNOSTIČKOJ RADIOLOGIJI

Proizvođač Nycomed A/S Oslo, Norveška

Isključiva prava prodaje u Jugoslaviji ima firma
LECLERC & CO. Schaffhausen/Švicarska.

Zastupstvo za Jugoslaviju ima:
REPLEK-MAKEDONIJA,
91000 Skopje, Jurij Gagarin bb, 091/237-266, 237-272, 232-222, 232-350
Zastupstvo 091/233-138, Telex 51431

NYCOMED
Contrast Media

Kardioangiografija

OMNIPAQUE™

joheksol
neionsko kontrastno sredstvo gotovo za upotrebu

Glavne prednosti Omnipaquea u kardioangiografiji

- vrlo dobra podnošljivost nakon aplikacije u koronarne arterije
- nikakvi ili klinički beznačajni učinci na krvni pritisak, akciju srca i EKG parametre
- smanjena učestalost i intenzitet subjektivnih reakcija bolesnika u usporedbi s konvencionalnim ionskim kontrastnim sredstvima
- izuzetno rijetka pojava alergijskih reakcija
- visokokvalitetni angiogrami

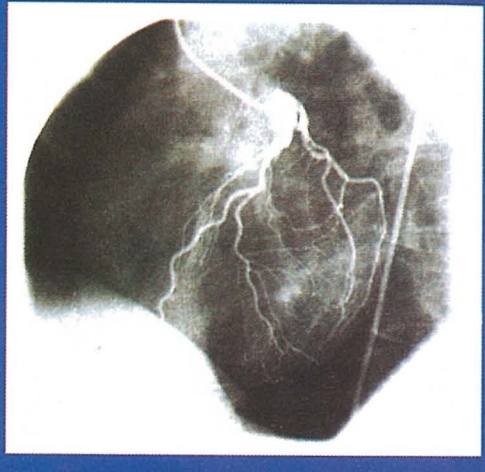

IZ NYCOMEDA – INOVATORA U PODRUČJU KONTRASTNIH SREDSTAVA

Omnipaque je zaštićeno ime

SIGURNIJE KONTRASTNO SREDSTVO U DIJAGNOSTIČKOJ RADIOLOGIJI

Proizvođač Nycomed A/S Oslo, Norveška

Isključiva prava prodaje u Jugoslaviji ima firma LECLERC & CO. Schaffhausen/Švicarska.

Zastupstvo za Jugoslaviju ima:
REPLEK-MAKEDONIJA,
91000 Skopje, Jurij Gagarin bb, 091/237-266, 237-272, 232-222, 232-350
Zastupstvo 091/233-138, Telex 51431

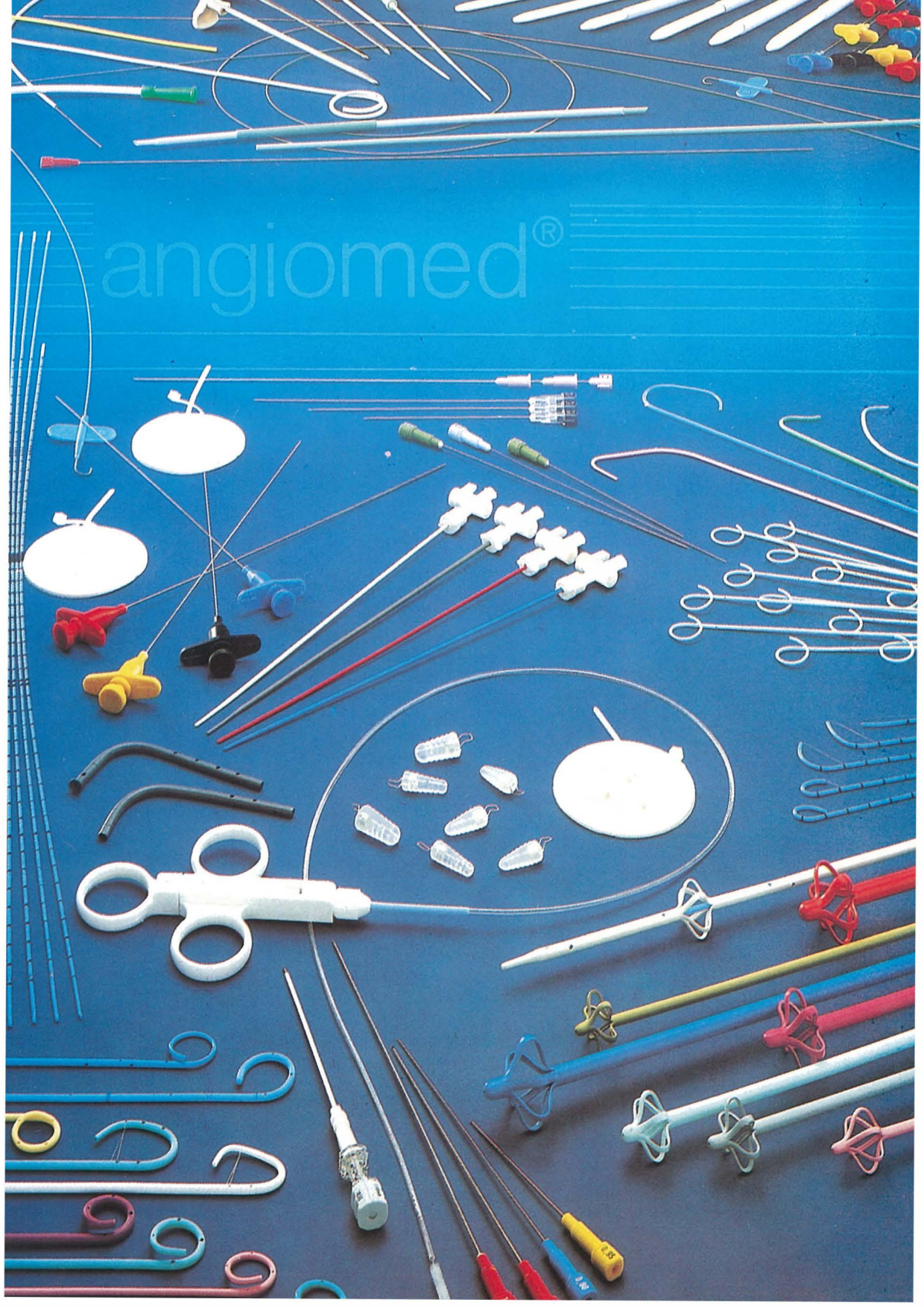
angiomed®

Corso Italia 112
34170 Gorizia - ITALY
P. Iva 00380480319

SIRION s.r.l.
medical supplies

☎ (0481) 32073
☎ Fax (0481) 534753
Tx 461240 - SIRION - I

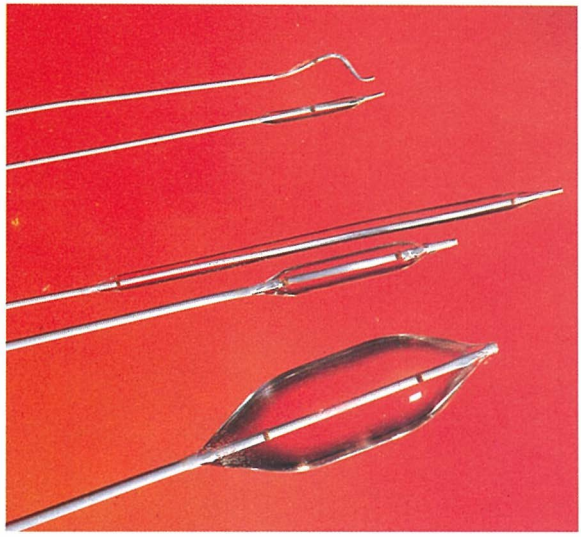

January 1989
BALT offer for Transluminal Angioplasty the thinnest,
most flexible and, at the same time, the most resistant device

CRISTAL BALLOON

January 1889
VAN GOGH painted "Man with a pipe"
He. too. believed in the value of his work.

BALT EXTRUSION

10, rue Croix-Vigneron - 95160 Montmorency - France - Tél. (33/1) 39 89 46 41 - Télex 699 965 F - Fax (33/1) 34 17 03 46

© Eastman Kodak Company, 1990

Kodak systems provide dependable performance for advanced diagnostic imaging. Our quality components are made to work together from exposure to viewbox.

Kodak X-Omat processors are the most respected in the field. Kodak X-Omatic cassettes are known the world over for unexcelled screen-film contact and durability. Kodak multiloaders have earned an enviable reputation for reliability. The Kodak Ektascan laser printer is changing the look of digital imaging. The list goes on. There are quality Kodak products throughout the imaging chain.

Equally important, they are made to work together to achieve remarkable performance and diagnostic quality. Contact your Kodak representative for more information.

ADVANCED DIAGNOSTIC IMAGING SYSTEMS. KODAK

Quality imaging worldwide

Kodak

danes najuspešnejši kinolonski preparat

Cenin®/Ciprobay®

ciprofloksacin

širokospektralni kemoterapevtik

- **hitro baktericidno delovanje na gram pozitivne in gram negativne mikroorganizme kakor tudi na problemske klice**
- **izrazito delovanje na psevdomonas**
- **hiter terapevtski uspeh zaradi visoke učinkovitosti**
- **dobra prenosljivost**
- **samo dvakratna dnevna uporaba, kar pomeni veliko olajšanje v klinični in splošni praksi**
- **prednost tudi zaradi oralnega zdravljenja na domu**

Kontraindikacije: preobčutljivost za ciprofloksacin; otroci in mladi v dobi rasti; nosečnost, dojenje; previdnost pri starejših bolnikih in poškodbah osrednjega živčevja.

BAYER

Bayer-Pharma Jugoslavija
Ljubljana

PROIZVODNI PROGRAM ZA MEDICINU

- **MEDICINSKI RENDGEN FILMOVI**
  (PROIZVEDENI U SURADNJI)
  FOTOKEMIKA - KODAK):
  SANIX RF-4
  SANIX ORTHO-4
- **FILM ZA MAMOGRAFIJU:**
  SANIX M
- **ZUBNI RENDGEN FILM:**
  SANIX DENT-20
  STATUS-d
- **FILMOVI ZA NUKLEARNU MEDICINU, CT I ULTRAZVUK:**
  SANIX FNM-4
- **FILMOVI ZA KORONAROGRAFIJU**
  35 mm: SANIX KOR-17
  SANIX KOR-21
- **KEMIKALIJE ZA STROJNU I RUČNU OBRADU MEDICINSKIH MATERIJALA**
- **EFKE EKG PAPIR:** -001
  -002
  -003
- **POLAROID:** -CRNO-BIJELI 667
  -KOLOR 339
- **KONTRASTNA SREDSTVA ZA RENDGENOLOŠKE PRETRAGE GASTROINTESTINALNOG SUSTAVA**

Micropaque suspenzija

Micropaque colon

Micropaque H. D. oral

Co_2 granulat Nicholas

FOTOKEMIKA

generalni zastupnik za Jugoslaviju
tvrtke Nicholas Kiwi, Geneva

generalni zastupnik tvrtke Nicholas

Nicholas

Poduzeće za proizvodnju i promet fotografskih materijala i opreme s.p.o. ZAGREB,
Hondlova 2 Tel. 041 231-833, Telex: 22-214 FOKEM, Telefax: 041 232-653

General Electric GR

REPRESENTATIVE OFFICE
Gundulićeva 23/II – 41000 Zagreb – CROATIA
Tel: +38 41 437 159 – Fax: +38 41 425 512

We bring technology to life

Visoko aktivni virostatik s selektivnim delovanjem na viruse:
Herpes simplex tip 1, tip 2 in Varicella zoster

VIROLEX® (aciklovir)
tablete

VIROLEX® (aciklovir)
injekcije za infuzijo

VIROLEX® (aciklovir)
krema

VIROLEX® (aciklovir)
mazilo za oči

- **visoka selektivnost**
- **neznatna toksičnost**
- **hitro zaustavi razmnoževanje virusa**
- **preprečuje diseminacijo virusne infekcije**
- **hitro odpravlja simptome infekcije**
- **učinkovita profilaksa**

Podrobnejše informacije in literaturo dobite pri proizvajalcu.

KRKA
tovarna zdravil, p. o., Novo mesto
s sodelovanjem firme The Wellcome Foundation Ltd., London, Anglija

pbn medicals

Trocar drainage catheter sets

A simple, safe technique for percutaneous nephrostomy, abscess and other fluid collection drainage.

A full range of drainage products;

- Available from 4 upto 14 french
- Variaty of materials
- 2 standard lengths, 20 and 30 cm.
- Available with string safity lock

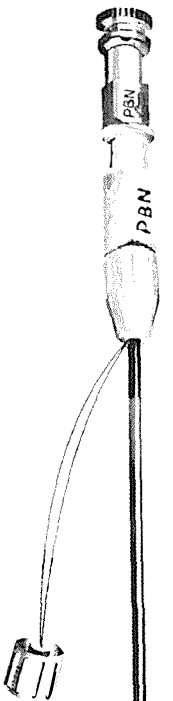

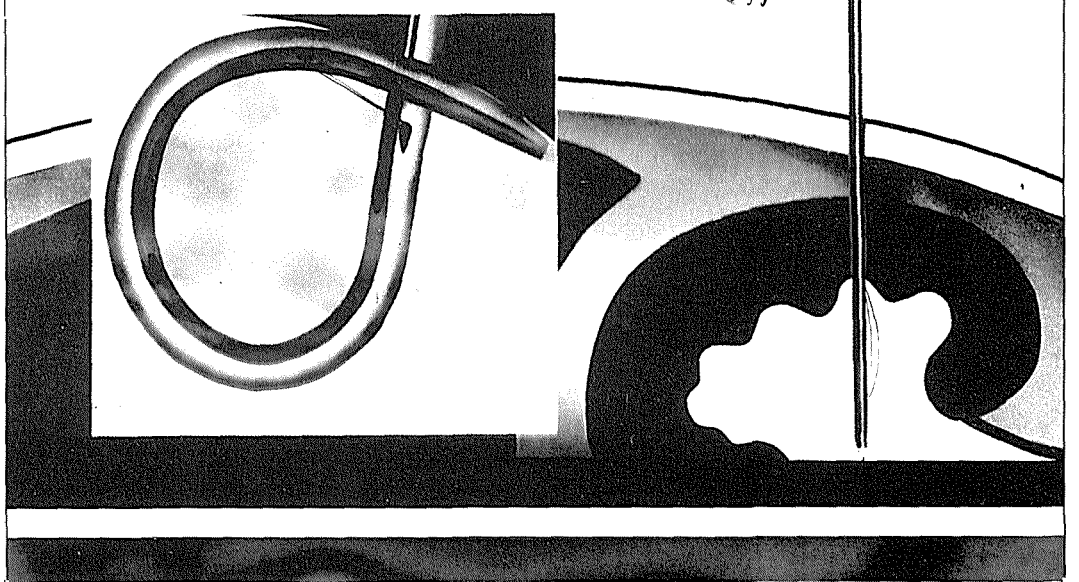

POLYSTAN BENELUX

Address ; De Steiger 172
P.O. Box ; 50045 1305 AA Almere-Haven
The Netherlands

Phone ; 036-5312844
Telex ; 76200 polyb nl
Fax ; 036-5313194

SALUS

LJUBLJANA D. D.

61000 LJUBLJANA, MAŠERA-SPASIĆEVA ul. 10

Telefoni: n.c. (061) 181-144 – direktor: 182-069 – prodaja: 181-031, 181-130, 182-001, 181-041 – Fax: 181-022

OSKRBUJE lekarne, bolnišnice, zdravstvene domove ter druge ustanove in podjetja s farmacevtskimi, medicinskimi in drugimi proizvodi domačih proizvajalcev, s proizvodi tujih proizvajalcev pa s pomočjo lastne zunanjetrgovinske službe.

Proizvaja: ALLIVIT PLUS®
Kapsule česna z dodatkom zdravilnih zelišč.

Prodajna in dostavna služba posluje vsak dan neprekinjeno od 7. do 16. ure, razen sobote.

SANOLABOR

IZVOZNO UVOZNO PODJETJE ZA PROMET Z MEDICINSKIMI INSTRUMENTI, APARATI, OPREMO ZA BOLNICE, LABORATORIJE IN LEKARNE

LJUBLJANA, Cigaletova 9
Telefon: (061) 317-355
Telex: 31-668 sanlab yu
Telefax: 325-395

Predstavništvo:
ZAGREB, Koturaška 73
Telefon: (041) 614-877
Telefax: (041) 513-385

Iz prodajnega programa trgovine na debelo nudimo široko izbiro domačega in uvoženega blaga po konkurenčnih cenah in sicer:

- rentgenske filme in kemikalije proizvajalcev »Fotokemika«, »KODAK«, »3 M – TRIMAX«, »AGFA GEVAERT« in drugih ter kontrastna sredstva firme »NICHOLAS«,
- medicinske instrumente, specialno medicinsko in sanitetno blago, potrošno blago za enkratno uporabo,
- medicinske aparate in rezervne dele zanje ter bolniško in drugo opremo,
- tekstilne izdelke, konfekcijo in obutev za potrebe zdravstvenih, proizvodnih in varstvenih organizacij,
- laboratorijske aparate, opremo, laboratorijsko steklovino, reagente, kemikalije in pribor,
- aparate, instrumente in potrošno blago za zobozdravstvo

V Ljubljani imamo dve prodajalni:

- na Cigaletovi 9 prodajamo izdelke iz asortimana trgovine na debelo, s posebnim poudarkom na izdelkih za nego bolnikov, ortopedskih pripomočkih in ostalemu blagu za široko potrošnjo vsak dan od 9^h do 18^h, ob sobotah od 9^h do 13^h.
- v prodajalni na Njegoševi 15 nudimo opremo, instrumente in potrošne materiale za zobozdravstvene ordinacije in tehnike vsak dan od 8^h do 15^h, ob sobotah od 8^h do 12^h.

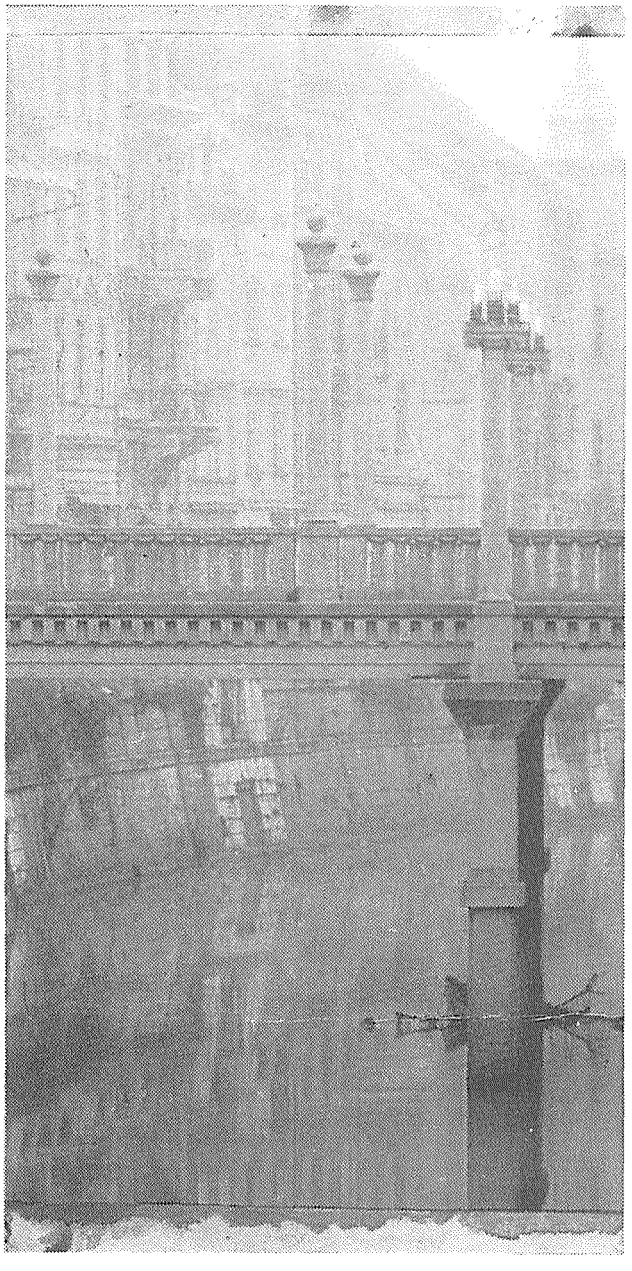

WHENEVER YOUR DREAMS OVERSTEP REALITY
YOU ALSO NEED A RELIABLE BANK.

RELIABILITY IS OUR STRENGTH.

SKB BANKA D.D.
Trg Ajdovščina 1, 61000 Ljubljana

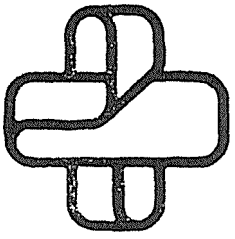

TOSAMA

Tovarna sanitetnega materiala p.o.
61230 Domžale p.p. 128
Vir, Šaranovičeva 35
telefon: (061) 714-611
telefax: (061) 714-660
telex: 39-804

IZDELUJE:

SANITETNI PROGRAM

- tkane, rezane, elastične povoje
- mavčne in sadrona povoje
- sanitetno mrežo Virfix
- konfekcionirano gazo
- konfekcionirano vato
- celulzno vato in izdelke
- obliže
- sanitetne torbice, omarice
- avtomobilske in motorske apoteke

PROGRAM IZDELKOV ZA OSEBNO HIGIENO

- higienski vložki VIR
- higienski tamponi VIRTAMP
- higiensko in cika–cak vato
- Jasmin vato
- Jasmin blazinice
- bebi palčke

OTROŠKI PROGRAM

- tekstilne plenice
- nočne plenice TOSAMA
- hlačne plenice SAMO Super
- bebi plenične predloge
- povijalne rutice
- zaščitne hlačke

PROGRAM MEDICINSKE PLASTIKE

- Virkol vrečke
- urinske vrečke

VIRTEKS PROGRAM

- posteljno perilo
- zdravniške maske
- kape–bolniške, ortopedske, zdravniške
- operacijski plašči, halje, predpasniki
- prevleke za obuvala
- rute za operirance
- operacijska pregrinjala

INKO PROGRAM

- Inko podloge
- Inko povijalne rute
- Inko hlačke
- podloge za bolnike

PROGRAM IZDELKOV ZA DOM

- večnamenska krpa Bistrica
- polirna vata
- vrteks – vrtnarska vlaknovina

BYK GULDEN
KONSTANZ/SR NEMAČKA

RENTGENSKA KONTRASTNA SREDSTVA:

HEXABRIX
– kontrastno sredstvo niskog osmoaliteta, smanjene toksičnosti i gotovo bezbolan u primeni.

INDIKACIJE:
Sva arteriografska ispitivanja, zatim cerebralna angiografija, i flebografija, kao i selektivna koronarografija.

PAKOVANJA:

Hexabrix amp. (5 amp. x 10 ml)
Hexabrix amp. (20 amp. x 20 ml)
Hexabrix boč. (2 boč. x 50 ml)
Hexabrix boč. (1 boč. x 100 ml)
Hexabrix inf. (1 boč. x 200 ml bez pribora za infuziju)

DIMER X ampule 5 x 5 ml
– kontrast za lumbosakralnu mielografiju

TELEBRIX
– kontrast za urografije, angiografije, periferne i selektivne arteriografije.

PAKOVANJA:

Telebrix 300 amp. (20 amp. x 30 ml sa špricom)
Telebrix 300 amp. (20 amp. x 30 ml bez šprica)
Telebrix 380 amp. (20 amp. x 30 ml sa špricom)
Telebrix 380 amp. (20 amp. x 30 ml bez šprica)
Telebrix 380 za inf. (2 boč. x 50 ml)
Telebrix 300 za inf. (2 boč. x 50 ml)
Telebrix 30 za inf. (1 boca x 100 ml)
Telebrix 45 za inf. (1 boca x 250 ml)

Byk Gulden
Predstavništvo:
Hotel »Slavija lux« A-158
Beograd, Svetog Save 2
tel. 434-712 fax. 431-517

FABEG
Inostrana zastupstva
Beograd, Kosovska 17/VI
telefoni: 321-440 i 321-791